AN INVESTIGATION OF SHEAR STRESS DISTRIBUTION BY DIE-ROTATION, IN BAR-DRAWING

by D. Rothman B.Sc.

Submitted in fulfillment of the requirements
for the degree of Doctor of Philosophy

University of Aston in Birmingham
October 1970

Faculty of Engineering
Department of Mechanical Engineering

Supervisor : Dr. D.H. Sansome

SUMMARY

A review was made of theories of axisymmetric drawing, and their treatment of friction as an independent parameter was noted. Experimental methods for determining friction in the drawing process were reviewed, and the rotating- die technique was selected as the most suitable. The possibility of using this technique to verify postulated distributions of shear stress* was noted.

An experimental programme was initiated in which mild steel bars of 1.1/16, 1.1/8, 1.1/4, 1.5/16 in. nominal diameters were drawn down to 1 in. over the speed ranges 5 to 15 ft./min. and with die speeds of 14.5 and 28.5 rev/min., the lubricant being soap over a phosphate coat. Contrary to the literature of the subject, it was found that the bar twisted during die-rotation and failure to anticipate this feature, coupled with the poor condition of the test material, made it possible to calculate only values of mean coefficient of friction.

A second test programme was performed, again with mild steel but using the speed ranges 1 to 15 ft/min. and 5 to 50 rev/min. The rotational speed of the bar was measured and both soap and oil were used as lubricants. Although the results of these tests were closely repeatable by the standards of conventional studies of friction, they were insufficiently so to enable the distribution of shear stress to be deduced. However, it was shown that knowledge of the distribution was unnecessary for accurate determination of coefficient of friction, and these values were found to be 0.020/0.025 for soap and 0.04/0.06 for oil. It was also shown that the chief source of error in a simple method of analysis was failure to recognise plastic torsion of the drawn bar, but that such analyses could neverthless give quite accurate results over a wide range of parameters.

---

*at the die/workpiece interface

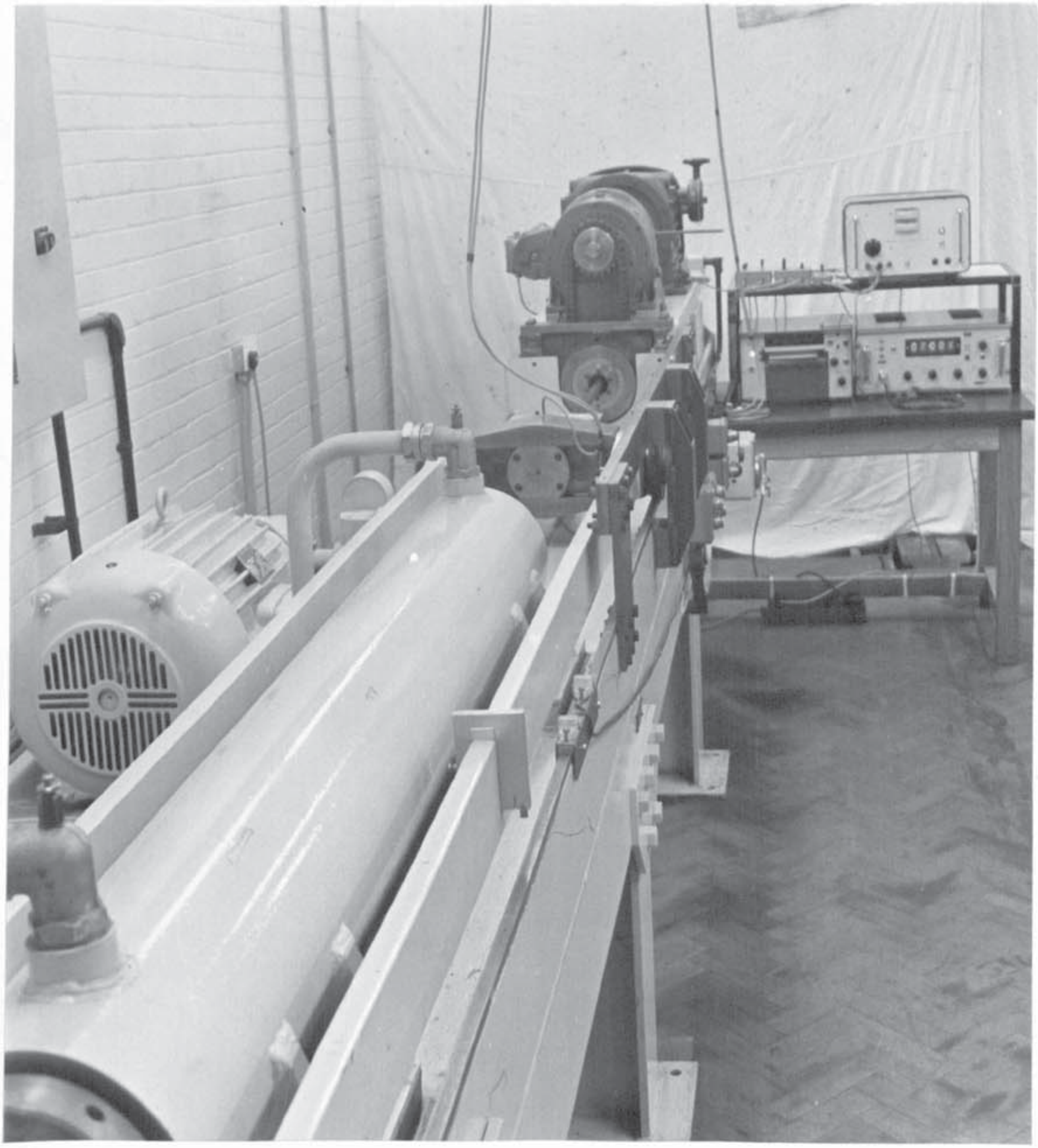

FRONTISPIECE

CONTENTS

TITLE OF SECTION | PAGE NO

TITLE OF SECTION PAGE NO

NOTE ON THE SYSTEM OF TEXTUAL CROSS-REFERENCE

The system which has been used for numbering sections of this thesis is conventional, and individual sections may be located from the Table of Contents. Diagrams have been given two-part reference numbers, the first part of which indicates the number of the section containing the diagram, and the second part the position within the section. The prefix A shows that the section referred to is an Appendix. An identical system has been used for numbering tables and equations.

Bracketed numerals which appear in the text designate references listed at the end of the thesis

NOMENCLATURE

Symbols as used in Section 2

μ	:	coefficient of friction
α	:	semi-angle of die
A_1	:	cross-sectional area after drawing
A_2	:	cross-sectional area before drawing
A_s	:	surface area
P	:	drawing force
P_i , P_f , P_r	:	components of drawing force due to loss-free deformation, friction at die/workpiece interface, and redundant deformation
Q	:	total normal force at interface
F	:	total shear force at interface
P_o	:	$Q \sin \alpha$
P_F	:	$F \cos \alpha$
S	:	die-splitting force
Y	:	yield stress
k	:	yield stress in shear
c	:	shear factor
r	:	proportional reduction in area
ϕ	:	redundant work factor

Symbols as used elsewhere

Experimental Parameters

P	:	drawing force
P_R	:	drawing force with die-rotation
T	:	torque
V	:	drawing speed
v	:	axial velocity at any point
V_s	:	velocity towards apex of die, at any point
R	:	rotational speed of die
R_B	:	rotational speed of bar
S_D	:	circumferential velocity of die
S_B	:	circumferential velocity of bar
A	:	cross-sectional area

A_s	:	curved-surface area
d	:	diameter
θ	:	swing of velocity/friction vector away from apex of die
ϕ	:	helix angle
σ	:	direct or normal stress
τ	:	shear stress
x	:	axial distance from apex
k	:	velocity coefficient

<u>Subscripts</u>

1, 2	:	refer to die exit and entry respectively
r	:	refers to cross-section which bisects curved-surface area
a, b, c, d, e, f,	:	refer to particular instants during the drawing tests (see Figure 10.12)
bc, cd, de	:	refer to periods between those instants

<u>Superscripts</u>

^ , ' , " ,	:	refer to instants shortly after c

<u>Symbols not affected by above suffices</u>

$\Delta_P, \Delta_T, \Delta_R, \Delta_V$	:	galvanometer deflection corresponding to experimental parameters
δ	:	a small increment
Q	:	total normal force on die surface
F	:	total friction force on die surface
P_F	:	component of drawing force due to the friction at interface
$P_{F(P)}$, $P_{F(T)}$	:	P_F when calculated from measurements of P and T
P_o	:	component of drawing force due to die-pressure
τ_T , τ_P	:	τ when calculated from measurements of P and T
n	:	coefficient describing distribution of shear stress
I_1 , I_2 , I_3	:	integrals defined in section 3.2

A, B, C, D, E, F	:	mathematical constants defined in section 3.2
A, B	:	also used to identify grid markings, section 10.4

1. INTRODUCTION

It will be realised that there is no fundamental difference between the processes of wire-drawing and bar-drawing provided that both are axisymmetric, and in this work the terms have to some extent been treated as being interchangeable. The division between bar and wire is one of dimension only, and is both arbitrary and variable. In practice the processes differ considerably with regard to design of machinery and drawing speeds, but the mechanics of deformation are identical in both.

Metalworking theories present the working load for an operation in terms of the geometrical parameters of the process, the yielding characteristics of the material being worked, and the frictional boundary conditions. For bar-drawing the geometry is virtually fixed by the dimensions of the workpiece and tools, the material properties are usually determined in a uniaxial tension test, and the frictional boundary conditions are usually assumed to be adequately described by a constant coefficient of friction. Although some workers describe this, with justice, as Amontons friction, normal usage attributes it to Coulomb, and the latter description has been adopted here.

The Coulomb Law of Friction, which has long been substantiated for lightly loaded sliders, is explained on the basis that the true area of contact of such bodies is much less than the apparent, and increases as the load increases. This leads to proportionality of load and true area of contact, and hence to constancy of true contact stress. An upper limit to this situation must be reached in metalworking operations, where a workpiece undergoing heavy deformation must always conform closely to the tool surface. Thus there are strong grounds for doubting the applicability of Coulomb's Law to metalworking, and even if it does apply, there remains the question of what value to ascribe to the coefficient.

The lubrication regime in conventional low speed drawing is generally accepted as highly complex, being predominantly boundary but with possible contributions from hydrodynamic lubrication and solid friction. Furthermore, contact pressures are extremely high, and surface conditions change significantly throughout a single pass. It is clear that these conditions are too complex for analysis by current lubrication theory, although the particular case of full thick-film lubrication has received considerableattention. It is therefore necessary to resort to experiment to determine the magnitude of μ, the coefficient of friction. It may be noted that although there is no reason for presupposing μ to be constant, it is still useful to specify friction conditions in the familiar form, and this author does not agree with Hockett (1) when he calls for a redefinition of μ in terms of surface conditions and material and lubricant properties. Thus although the basis for that suggestion is unquestionably sound, it would seem preferable to retain the definition of μ as the ratio of shear to normal force, or more properly the ratio of the stresses, provided that μ be considered merely as whatever value this ratio happens to take, rather than as an immutable material property.

It does not seem to be possible to adapt conventional friction testing apparatus to adequately simulate metalworking conditions, so friction must be studied in the process itself. A serious obstacle to doing this in conventional wire-drawing is that there are more unknown than measurable quantities, and for a fundamental determination of μ it becomes necessary to modify the process. This generally introduces considerable experimental difficulty, and such investigations have been confined to slow drawing speeds or relatively soft materials, or both. In spite of these difficulties the general range of values is fairly well agreed, being quoted by Wistreich (2) as being 0.01 to 0.05 for solid lubricants and 0.08 to 0.15 when drawing with liquid lubricants, although the latter range appears to be rather high in the light of more recent results. It will be shown in section 2 that, even without the latter point, these ranges can lead to significant indeterminacy, particularly with regard to relatively recent attempts to improve the understanding of the mechanics of the process.

The object of studying friction in metalworking processes can be seen as being twofold. Firstly it is desirable to establish the friction forces in specific cases, so that the correct boundary conditions may be combined with the appropriate theoretical analyses of the process, the validity of which may thereby be checked. Given a theory which has been rigorously validated in such specific cases, its primary use would be the prediction of behaviour in other situations. Unfortunately, the pertinent friction conditions would not in general be reliably predictable from lubrication theory. So the second object of friction studies is to establish a body of information on behaviour in metalworking conditions, initially to furnish the deformation theories with the boundary conditions necessary for their application, and later on, it is hoped, to verify lubrication theories when they become sufficiently developed to deal with metalworking conditions.

The research described herein was initially designed as a phenomenological study of the friction conditions in a series of bar-drawing experiments; that is, the magnitude of the friction forces was to be measured without particular regard to how they arose, together with any parameters needed to check current theories of drawing. In this form the work was intended to achieve the former of the above mentioned objectives, and to a very limited extent the latter. However, sometime after the rotating-die technique had been adopted as a suitable experimental method, it became apparent that the scope of this technique had not been recognised. The emphasis of the work then shifted away from the checking of theories of drawing, and towards the full exploitation of the technique. The experimental work therefore fell into two distinct groups, which have been termed Series I and Series II. The value of Series I was limited by the relatively small range of experimental parameters, by non-uniformity of the test material, and by the development of a feature of drawing with a rotating-die which had not been mentioned in the literature. The results were therefore calculated according to the more or less pre-existing analysis given in section 3.1. Series II was designed to make full use of the analysis which has been developed in Section 3.2, and also to overcome the shortcomings of Series I. It therefore constituted by far the most significant part of the experimental work.

2. REVIEW OF LITERATURE

Reviews of both the theory and mechanics of drawing have appeared in the literature, and will be referred to where appropriate, so it would be to some extent merely repetitive to attempt to construct such a detailed review here. In view of the fact that this investigation was concerned primarily with establishing the behaviour at the interface between workpiece and die, rather than with the internal mechanics of deformation, such a review would also be inappropriate.

It is nevertheless necessary to discuss the above subjects in order that the central but equivocal role of friction may be appreciated, and this is done in sections 2.1 and 2.2, in so far as is relevant to this investigation. However a comprehensive review of the literature of friction determination in drawing has not, to this author's knowledge, been published, and this field is covered in detail in section 2.6. Some aspects of the literature which were of secondary importance to this investigation are discussed in the later sections.

The basic postulates of the Theory of Plasticity are not discussed here, as they have been dealt with comprehensively in standard text-books (23, 24, 25 29, 38).

2.1 BASIC THEORIES OF DRAWING

Substantial reviews of the theory of axi-symmetric drawing have been published by MacLellan (3) and Johnson and Sowerby (4), and some such work is also contained in Wistreich's general review (2). Plane-strain theories of drawing have been discussed by Green (5). Reviews of the same subjects were published contemporaneously with the former and latter of these by the German workers Siebel (6) and Pawelski (7).

2.1.1 Energy Solution

It is not clear who originated this approach, but it was probably Siebel, and that worker certainly presented it in the most highly developed form (6).

The assumption is that the work expended in drawing may be divided into three components of drawing force, bearing in mind that work done per unit drawn length is equal to the drawing force. Thus P_i represents the component due to the ideal loss-free reduction, P_f the component due to friction at the die/workpiece interface, and P_r arises from redundant deformation. P_i may be simply derived from the equivalent stress-strain curve, and if it is assumed that the corresponding die-pressure is unaltered by the introduction of Coulomb friction,

$$(P_i + P_f) = A_1 Y(1 + \mu \cot\alpha) \ln (A_2/A_1) \qquad (2.1)^*$$

where A_2 and A_1 are initial and final cross-sectional areas, and Y is the mean yield stress. Siebel then assumed that the boundaries of the deformation zone were two spherical caps, and that movement within the zone was towards the apex of the die. He evaluated P_r by considering that it arose from shearing at these boundaries, and the complete expression for drawing force became

$$P = (P_i + P_f + P_r) = A_1 Y [(1 + \mu \cot\alpha) \ln (A_2/A_1) + \tfrac{2}{3}\alpha] \qquad (2.2)$$

In fact Siebel made the further assumption that $\tan\alpha = \alpha$, but this can be disregarded for the practical range of die-angles. The original aspect of the work arose when he pointed out that the addition of P_r destroyed the equilibrium of forces between die and workpiece, and he then went on to deduce the distribution of stress throughout the deformation zone. Confusion over the symbols which were used has prevented this author from following the derivation, but it appears to involve arbitrary assumptions regarding the form of distribution, after which the magnitudes were adjusted to restore equilibrium.

2.1.2 Equilibrium Solution

Sachs (9) assumed that plane cross-sections of the workpiece remained plane as they passed through the die, and that the distribution of stress was uniform on such planes. This enabled him to express the longitudinal stress on a plane element of the deforming material in terms of the stresses at the die surface. These he described by Coulomb friction and the yield criterion, considering the case of constant yield stress and taking the surface of the die as a principal plane. Summation through the die gave the drawing force.

$$P = A_1 Y \left(1 + \frac{\tan\alpha}{\mu}\right) \left(1 - \left(\frac{A_1}{A_2}\right)^{\mu \cot\alpha}\right) \qquad (2.3)$$

Davis and Dokos (10) extended the solution to the case where the material work-hardened linearly. Atkins and Caddell (11) have recently considered work-hardening according to a power law, and have shown that for the practical range of parameters it makes little difference whether the law is included formally

---

* This expression has also been proposed by Sachs and van Horn (8) for the total drawing force.

into the differential equation before solution, or whether the mean yield stress is used in the solution of equation (2.3). The latter always underestimates the drawing force; if required it would be possible to correct these values from curves which those authors present. They have also given a method for incorporating an empirically determined redundant deformation factor into the solution (see section 2.2).

Körber and Eichinger (12) used a method for evaluating P_r which was closely similar to Siebel's, the only difference being in their choice of yield criterion. They then added this term directly to the Sach's solution, equation (2.3), but did not take further action to restore the equilibrium of forces on the die.

2.1.3 Kinematically Admissible Solutions

As implied by the name, this group of solutions is concerned with the movement of the material through the deformation zone. In particular, they consider only those modes of deformation which conform to the external boundaries without violating the incompressibility and continuity criteria, and the primary concern of the solutions is the deduction of such admissible velocity fields. The results are normally presented graphically and as they are specific to the particular geometry under consideration, they are not given here.

2.1.3.1 The Method of Characteristics. With this method both stress equilibrium and flow equations are considered. No assumptions regarding the distribution of stresses are made directly, but the starting point for the deformation pattern often implies such an assumption. The method is strictly valid only for conditions of plane strain, in which situation the basic differential equations become hyperbolic. These equations may then be solved by what is known to mathematicians as the method of characteristics (13, 14). The characteristics are orthogonal sets of curves which in these problems coincide with the directions of maximum shear stress, and give the method the more usual name of slip-line field solutions. Prager's geometrical method (15) may be used to build up a field once an arbitrary starting point has been selected. Except for certain geometrically convenient situations this can be extremely laborious, particularly so because the validity of the field cannot be verified until it has been completed. Once a valid field has been constructed, the working forces may be deduced directly from the associated stress plane. However, the solution also gives a direct method of determining redundant deformation.

The first application of the method to drawing was by Hill and Tupper (16), who presented it at the time as a theory of wire-drawing, but it is now known(17) that such a direct transposition is not valid. Hill and Tupper analysed the case of frictionless drawing, but gave two methods for considering Coulomb friction. The simplest was to assume that die-pressure was unaltered by friction, and this led to a multiplying factor of $(1 + \mu . \cot \alpha)$ as in equation (2.1). The rigorous allowance for μ can be extremely lengthy, because the angle subtended by the slip-lines at the surface of the die is dependent on the die-pressure as well as the value of μ. It is therefore necessary to construct the entire field before the initial selection of geometry can be checked. This has been done by Green and Hill (18), and they summarise their findings as a modification to the factor given above.

$$\frac{P\text{ (with friction)}}{P\text{ (without friction)}} = (1 + \mu \cot \alpha) - \mu(0.2 + 0.08r \cot^2 \alpha) \qquad (2.4)$$

The case where full, or sticking, friction obtains may be studied with relative ease, for it is known that the slip-lines must then subtend 0° and 90° at the surface of the die, but this situation is manifestly not applicable to the drawing process. A large number of slip-line solutions have been published, and apart from the fact that many are for extrusion and in a range of parameters which is of no interest for drawing, the fundamental inapplicability to axisymmetric conditions has been indicated earlier. This is not to say that they are without consequence for axisymmetric drawing, and this is discussed in section 2.1.4.

The equations for axisymmetric deformation are not directly soluble by the method described above, but application of the Haar-von Kármán hypothesis renders the stress equilibrium equations hyperbolic once more. The characteristics of the equations again coincide with the directions of maximum shear stress, but the relations are more complex. Shield (19) has solved some problems in this way and Mróz (20) has presented a geometric method analogous to that of Prager. However, the only applications to drawing of which this author is aware are related to the prediction of ideal die-profiles, which are intended to induce no redundant deformation into the workpiece. This work has been reported by Richmond and Morrison (21) and commented on by Hill (22), and is a development of earlier work on ideal die-profiles for plane strain drawing which is quoted therein. The basic requirement for deformation to be homogeneous is that streamlines should everywhere be aligned with the directions of principal stress, and this implies that at any point the velocities along both families of slip lines are equal. It is clear that the surface of the die must be a streamline, so the condition cannot be met there except for the frictionless situation which was considered. The solutions are nevertheless of great interest, although a further practical limitation for drawing is that all the forms so far proposed have zero entry angle.

2.1.3.2 Upper-Bound Solutions. Strictly speaking the terms upper-bound and kinematically admissible are interchangeable, but the former has come to imply the class of solutions described here, as opposed to slip-line solutions. The upper-bound theorem has been reported (23) as being developed by Hill and also by Drucker, Greenberg and Prager at about the same time. It states that if a kinematically admissible velocity field can be deduced for a deformation process, then the associated rate of work will always be greater than that for the actual velocity field; where the actual field is that which is also statically admissible. The working forces associated with the assumed deformation pattern, can of course be deduced from the power and the velocity field.

Some original work in which Johnson applied the method to plane-strain extrusion has been reviewed by Johnson and Mellor (23). The basic assumption was that the deformation zone was built up of triangular elements which were chosen to be similar in general appearance to the zones deduced by slip-line solutions. However, the material was considered to be rigid both inside and outside these triangles, and all deformation took place by shear at the boundaries. The upper bound inequality could then be readily evaluated in terms of the energy expended in shear at these boundaries, and in overcoming friction at the die/workpiece interface. In the first instance friction could be either zero or full sticking friction ($\tau = k$). Coulomb friction could be allowed for by the now familiar technique of assuming that the mean die-pressure associated with the frictionless condition was unaffected by the introduction of μ , but the result would no longer be a true upper-bound. The alternative was to introduce a constant, c, such that $\tau = ck$, and the solution could then proceed as for sticking friction.

Thomsen, Yang and Kobayashi (24) have reviewed some more recent work by Kudo. Kudo developed a similar technique to that of Johnson at about the same time. He considered the deformation zone to be built up of unit rectangular deforming regions, which were themselves composed of triangular regions. As with Johnson's method, deformation was considered to be by shear at the boundaries, and a solution was effected by optimising the geometry. Kudo extended the method to the solution of axisymmetric problems by considering unit cylindrical regions, which were again subdivided into sections which were triangular on the plane of symmetry. In this case it was necessary to consider the energy expended by deforming the material within the individual regions as well as by shearing at the boundaries.

A very large volume of literature incorporating the upper-bound theorem has been published in recent years; but it is neither possible nor desirable to review it here, particularly so because, as discussed later, the approach has considerably more significance for extrusion than for drawing. One body of work which requires mention by virtue of its distinctive nature is due to Avitzur and associates, and this has been comprehensively reviewed by Avitzur (25). The feature of this work is that it deals with a deformation zone which is assumed to lie between spherical caps centred on the virtual apex of the die, a zone which is very similar to that considered by Siebel (6).

With regard to friction it may further be noted that as the upper-bound theorem is concerned with power dissipation and not stresses, there is no direct way in which Coulomb friction can be considered. Some work which does appear to deal with that situation, for instance reference (26), in effect assumes uniform die-pressure and therefore restates the problem in terms of constant shear stress. However Collins (27) has recently presented a method for dealing with Coulomb friction which involves a redefinition of the velocity boundary conditions required to satisfy kinematic admissibility. It leads to solutions which can be significantly in error compared with exact solutions, but does seem to provide a better correction factor than the $(1 + \mu \cot \alpha)$ term, when the exact solution for the frictionless condition is known.

2.1.3.3 Flow in a Converging Conical Channel. Shield (28) has produced solutions to the above problem for material obeying the von Mises and Tresca yield criteria, each with its associated flow rule. For the latter the Haar-von Kármán hypothesis was also made, and for both the frictional condition was assumed to be that of constant shear stress. Several reviewers have remarked that ignorance of the end effects limits the utility of the analysis for wire-drawing, and Ford and Alexander (29) in particular have noted weaknesses for this application. However, as for slip-line solutions, the results are of qualitative interest (2). The principal interest that the work has for this review is that it has been used as a basis for determining friction (see section 2.6).

2.1.4. Discussion

The upper-bound theorem referred to earlier has its counterpart lower-bound theorem which is reported (23,25) as implying that among all possible statically admissible stress fields which could cause deformation, the actual one will be that which would require maximum power, a statically admissible stress field being one which satisfies the equilibrium criterion. From this point in time it is possible to categorise all genuine theories of wire-drawing as either upper or lower-bound solutions of varying degrees of exactness, except that a truly exact solution would be both. It is also possible to see that there are no solutions at all; in the sense that it is not possible to start with the independent parameters and work directly forward to a unique solution. That this is so with regard to the slip-line and upper-bound methods is manifest in the manner of their application, but a muliplicity of statically admissible stress-fields is not so readily arrived at, and it is only against the background of the limit theorems that the equilibrium method of solution can be truly evaluated. That the equilibrium solution is not kinematically admissible is readily apparent. Thus the evaluation is in terms of a distribution of stresses, which must be related to a distribution of strain increments through the flow rule. The summation of the strain increments in turn gives rise to the velocity field, but as only the yield criteron and not the flow rule is considered in the solution, it would be highly coincidental if the resulting velocity field were valid. In comparison with this, the other assumptions which the equilibrium approach uses are minor.

In the simplest case, where P_i only is derived, the energy solution avoids the mechanics of the process and redefines the problem in its own terms. However in the presentation given by Wistreich (2) it becomes obvious that where friction and redundant work are negligible, the energy and equilibrium approaches are identical, and not merely in the result but also in their formulation of the problem. It may be added that as the various components, P_i, P_f, P_r, are merely additive with the energy solution, there is no theoretical way in which interdependence can be incorporated.

Only when it comes to the question of redundant work does Siebel's solution take cognizance of the actual problem, and then it is in a manner equally as arbitrary as the equilibrium method. That particular expression for P_r and the energy solution can easily be separated. Wistreich (2) suggested simply multiplying equation (2.1) by a redundant work factor, and the generality of the energy approach has been discussed by Thompson (30). Similarly Siebel could have added the P_r term to Sachs' basic equation and performed the same manipulations to derive a distribution of stresses. Of course he was prevented from doing this by Sachs' formal assumption of uniform stress over the cross-section, but as noted above this assumption was implicit in the derivation of P_i. Sachs was certainly aware of both the existence and the general dependence of redundant work (8), and the further existence of optimum die-angles, but was apparently not prepared to make arbitrary assumptions to evaluate it. It is therefore difficult to find any fundamental justification for Wistreich's (2) preference of Siebel's solution to the Sachs' and van Horn energy solution or the Sachs' equilibrium equation, so selection between the theories must be on the pragmatic grounds of which best predicts drawing force, and this is clearly dependent on how well Siebel's term for P_r represents reality. Whitton (31) has shown that there is little to choose as P_r is overestimated at one end of the range of drawing geometries and underestimated at the other.

Another feature which that publication shows very clearly, is that for the practical range of geometries the basic homogeneous frictionless deformation force, P_i, is the largest proportion of calculated drawing force in all these analyses, and that over most of the range it is much the largest. A further point is that they all give quite good predictions of actual drawing force, except with the combination of high die-angle and low reduction, when the proportional error can be significant with theories which disregard redundant work. However, in that situation the drawing force is relatively small, so the absolute error in predicted values is also small. This situation is at first sight surprising in view of the failure of the simple theories to take account of the way in which metal actually deforms, and it is useful to consider the difference between extrusion and drawing in order to find the explanation.

Theoretically the two processes differ only in the hydrostatic stress, and it is fundamental to Plasticity that this would not affect either the yield or flow behaviour of the material. Practically there are considerable differences, and the major one is that the drawing process is restricted by the requirement that the drawn material be able to withstand the drawing force. This ensuresthat drawing is in practice carried out under conditions which minimise the drawing force; that is with small die-angles and efficient lubrication, and these conditions are of course those which most closely represent those assumed by the simple theories. It is therefore unsurprising that the simple solutions give quite good approximations for drawing force. An alternative way of looking at this is first to note that the upper-bound technique shows that the calculated working load is by no means critically dependent on the choice of deformation zone. In these terms it is evident (7) that over a wide range of geometries the kinematically admissible fields are not significantly different from those assumed in the equilibrium method. This leads to the same conclusion as previously. That this certainly would not apply to extrusion may be established by considering the application of the simple theories to geometries where $\alpha = 90^{\circ}$. The failure of the equilibrium solution is immediately obvious, and that of the Siebel type of deformation zone equally so when one considers the observed phenomenon of dead-metal zones. The obvious conclusion is that accurate prediction of drawing force is not a suitable criterion for evaluation of the fundamental validity of a theory.

The pragmatist may therefore ask why, if good estimates of drawing force are available from simple solutions, it is necessary to consider the slip-line and upper-bound methods. The answer is that in part it is not necessary and that they are most directly useful when applied to extrusion, but that even in pragmatic terms they have importance for axisymmetric drawing. Thus studies of drawing have tended to move away from the simple prediction of drawing force, and have concentrated on establishing the magnitude of the various components more accurately so that the process may be optimised. In particular there is a growing body of literature concerned with the undesirable phenomena of bulge formation, central fracture and redundant deformation, all of which are of practical interest. The great advantage that the kinematically admissible solutions have is that they do consider the modes in which it is possible for metal to flow, and are hence more likely to give the correct result to the above problems than the simple approaches. In this context it may be noted that although slip-line solutions are not directly applicable to axisymmetric drawing, it has been shown (2) that the deformation zone in the latter corresponds in general form to the deductions of the former. One must therefore wonder why Avitzur (see section 2.1.3.2) has done so much work with a velocity field which although admissible is unrealistic.

Slip-line methods have great value in addition to the solutions which they yield directly. Thus although they may not be applied directly to the axisymmetric situation, theories which do treat that case may be modified for the plane-strain case, and checked against the slip-line solution.

Although the three components of drawing force, P_i , P_f , P_r , are not simply additive as assumed by Siebel, it is still meaningful and indeed useful to consider the problem in those terms. In spite of considerable confusion regarding the applicability of an isotropic yield criterion to material in the work-hardened condition*, there seems to be no real dispute over the use of an equivalent stress-strain curve obtained in uniaxial tension to the case of wire-drawing. A qualification to this is that even laboratory metalworking processes are usually performed at much higher strain-rates than are tension and compression tests; and there is growing awareness (33) that in spite of the low strain-rate sensitivity of commonly drawn metals at ambient temperatures, the large difference in strain-rate can lead to significant errors in the stress-strain curve. In principle this presents little problem so values of P_i are easily determined. This leaves the two quantities P_f and P_r , and much work has centred on their evaluation.

As indicated earlier, Siebel's form of the energy solution does give a value to P_r , while the equilibrium solutions ignore it. The kinematically admissible solutions inherently allow for redundant deformation, and redundancy factors may be deduced from the solutions. There are also experimental methods for determining these factors, and the subject of redundant deformation and redundant work is discussed in section 2.2.

The treatment of friction in the theories of drawing is straightforward in that it is considered to be an independent parameter, described either by the coefficient μ or directly by the shear stress τ , the former being the preferred method where available. In either case it is assumed that the value is known. It is possible to deduce friction conditions from plasticity theory for some idealised surface conditions, but not realistically for boundary lubrication. The theory of friction and lubrication is also unable to supply quantitative data, so it is necessary to deduce μ empirically. The subject is discussed fully in

* The literature of this topic is much too large to be given here, but see for example reference (32) and others quoted therein.

section 2.3, but it may be noted here that inability to measure μ directly has led many workers to select values which gave their theories the best correlation with measured drawing force. This does not apply to the comparisons made by Whitton which were discussed earlier, for he was able to use values of μ derived objectively by Wistreich (17).

For straightforward estimation of drawing force to probably better than $\pm$ 20%, an energy method seems to be the simplest currently available. Thus the P_i term would be calculated from the stress-strain curve of the material to be drawn and the geometry, and the friction and redundancy terms could be taken from the literature, which is discussed in the following sections. If the proposed draw had a large redundancy factor it might also be necessary to modify the mean yield stress accordingly.

2.2 REDUNDANT DEFORMATION

The energy approach discussed in section 2.1.1 assumed that the drawing force could be separated into three components such that

$$P = P_i + P_f + P_r$$

and that although these were influenced by the yield strength of the material, they were otherwise independent. Although this assumption is invalid, it can be useful to consider just such a separation, and provided that the quantities are re-defined slightly, the relationship becomes valid. P_i retains its original significance as the area under the stress-strain curve corresponding to the external strain, and P_f is still the component of drawing force required to overcome the shear stress at the die/workpiece interface. However, P_r is now defined as

$$P_r = P - P_i - P_f$$

where P and P_f are assumed to be measured and P_i is calculated from the stress-strain curve. P_r becomes a component of drawing force which, as it arises from neither homogeneous deformation nor friction loss, must be caused by inhomogeneous deformation. The fact that P_f and P_r will in general be interdependent does not destroy the validity of the concept. Both P and P_i may be readily obtained, which in practice leaves two unknowns, and obviously measurement of either automatically leads to the other.

Until recently the situation was clear. Inhomogeneity of deformation was expressed as a redundant work factor ϕ , which was used to multiply the expression for drawing force with homogeneous deformation. For the expression given in equation (2.1), the drawing force with redundant deformation became

$$P = A_2 Y \phi (1 + \mu \cot \alpha) \ln (A_2 / A_1) \tag{2.5}$$

The fact that ϕ operated on the friction term should not be taken as necessarily implying that P_r was dependent on P_f , as the possibility that ϕ varied with μ was recognised. In this context it may be noted that statements in the literature that redundant work was or was not dependent on μ can be ambiguous. For instance if a particular statement meant that ϕ was independent of μ , it follows with equation (2.5) and most others that P_r was dependent. It will be clear that for given values of P, P_i , P_f and P_r , the calculated value of ϕ was dependent on the particular theoretical expression which was to be corrected, and four methods were available for its evaluation. For the plane-strain frictionless case (5) the drawing force could be calculated by slip-line methods, and its ratio to $A_1 Y \ln (A_2/A_1)$ became ϕ . Clearly this could have also been done using the other theories, but the exercise would have been pointless as the equilibrium solutions would merely have given $\phi = 0$, and Siebel's solution predicted P_r directly. Secondly, P and P_f could be measured (17), the corresponding value of μ calculated, and values put into an expression such as equation (2.5). The resulting value of ϕ would clearly give correct values of P for the conditions of the test and the theory selected for correction, however incorrect the basic theory, but the method was rare because of the difficulty of measuring P_f. Thirdly, P could be measured under conditions where P_r was considered to be negligible, and the corresponding value of P_f and hence of μ was calculated. P was then measured again under conditions where P_r was not negligible, and by taking the previous value of μ , P_f and then P_r and then ϕ could be calculated. In this case the value of ϕ would again be affected by the particular theory which was to be corrected, but its validity would also be subject to the accuracy of the original assumptions that P_r was negligible in certain cases and that μ was constant between tests. The fourth method involved performing stress-strain tests on drawn material and comparing the resulting curve with that for undrawn material. It was observed that if the curve for the former was plotted from a base corresponding to the equivalent drawing strain, $\ln (A_2/A_1)$, it rose above that for the latter. It was then moved in the direction of increasing strain until the two curves fitted. The amount by which the curve had been moved was taken to be the average redundant strain, and P_r was calculated as the area above it.

Atkins and Caddell (11) have recently drawn a distinction between redundant work factors and redundant deformation factors. They pointed out that the first three methods gave rise to work factors, in that ϕ was a coefficient which was used to make calculated forces agree with measured ones, and that as indicated earlier, the value was specific to the theory which was being corrected. However, the fourth method gave deformation factors, in that it indicated the mean redundant strain suffered by the material, and this value was independent of any theory.

Since then further definitions of redundancy factors have been reported (4) and this field is in a state of flux. According to Johnson and Sowerby (4) two papers on this subject are to be published shortly, one of them being a critical review, and in this situation it would be pointless to attempt a further evaluation here. For this reason again, references have not been quoted in the preceeding discussion, and the interested reader should consult references (11) and (4) for additional sources.

Although there is no doubt that the deformation factor described above is fundamentally more valid than the work factor, there seems to be no objection to use of published values of the latter (2, 34) for the prediction of drawing force, provided that they are combined with the appropriate analyses. Alternatively, values of deformation factors (11,35) may be used if it is desired to use the energy solution. In this connection it may be further noted that Atkins and Caddell (11) have developed the equilibrium approach so that account may be taken of both strain-hardening (see section 2.1.2) and redundant deformation. Both are assumed to develop monotonically through the deformation zone, and to exhibit no discontinuity at either entry or exit section.

2.3 DISCUSSION OF FRICTION

As indicated in section 1, there are fundamental grounds for supposing that the classical concept of Coulomb friction may not be applicable to metal-working situations. It is nevertheless valid to describe frictional conditions in terms of μ, provided that it is regarded merely as a ratio of stresses which has no fundamental significance. Not only is this valid, but it has definite advantages. Thus although μ may not be a constant, the friction force does seem to be strongly dependent on applied pressure, and it provides a convenient method for describing and comparing the results of experimental investigations.

However, the concept of stress is equally as abstract as that of μ, so the definition $\mu = \tau / \sigma$ is unhelpful although valid. If the stresses are assumed to be uniform over a small element δA_s of a surface area A_s, then a mean coefficient of friction may be defined as

$$\mu = \frac{\int_0^{A_s} \frac{\tau}{\sigma}\, dA_s}{A_s} \tag{2.6}$$

Alternatively the mean coefficient of friction may be defined in terms of the total forces F and Q which arise from the stresses τ and σ.

$$\mu = \frac{F}{Q} = \frac{\int_0^{A_s} \tau\, dA_s}{\int_0^{A_s} \sigma\, dA_s} \tag{2.7}$$

It is clear that the two results are identical when either σ or τ/σ are constant, but not in the general case. It might be supposed that it would be necessary to distinguish symbolically between the two, and also between these and the basic definition of τ/σ. However measured values of μ almost invariably refer to equation (2.7) for metalworking generally, and invariably so when numerical values are given in this thesis. The theories of drawing consider μ at individual points, so values derived from comparison of experimentally and theoretically determined drawing force (see section 2.6) refer to equation (2.6); but no dichotomy is introduced because the theories regard μ as constant. Therefore no symbolic distinction is made between the two definitions, and the basic definition is also not distinguished, because as observed earlier it has no real significance. One further usage of the symbol μ may be noted, and that is where it is used to indicate friction conditions generally. Thus, expressions such as "determination of μ" should in the first instance be understood as referring to friction generally, whatever form it happens to take, but in practice it will usually revert to evaluation of the mean.

It was indicated in section 1 that the range of values of μ obtaining in wire-drawing was broadly agreed, and the results of some investigations have been summarised in Tables 2.1(a) and 2.1(b). Similar tables have been published by Wistreich (2) and Gerds and Boulger (39), but more prominence has

TABLE NO. 2.1(a)

Ref. no.	Material	Lubricant	μ	Reduction of Area (%)	Drawing Speed (ft/min)	Drawn Diameter	Material of Die	Semi-Angle of Die	Type of Derivation
62	65/35 Brass	Soap R.O.D. Emulsion Castor oil Oil - Daq Hypoid 90	0.03 - 0.06 0.06 - 0.08 0.07 - 0.08 0.09 - 0.10 0.10 - 0.11	27 → 48	3.5	0.064 in.	Tungsten Carbide	$3° \rightarrow 6°$	Theoretical:- Sachs Davis & Dokos Hill & Tupper & Back-Pull
63 & 65	Steel (.58c)	Large range of coatings & lubricants	0.02 - 0.08		100	4 mm.			Theoretical:- Siebel
67	Steel (.1c)	Lime + Rapeseed Oil	$\left.\begin{matrix}0.01\\0.04\end{matrix}\right\}$	25 20	15	5 → 25 mm. 40 mm.	tool steel		Theoretical:- $P_r \rightarrow 0$
68	Aluminium (type 1100)	Soap	0.035	50			Steel ($58R_c$)	3°	Theoretical:- $P_r \rightarrow 0$
34	Steel (.1c)	Soap	0.03	50	7.5	all below ½ in.	tool steel	2°	Theoretical:- $P_r \rightarrow 0$
		Mineral oil + 5% oleic acid	0.045						
		Amarine N.D.L. + Sulphur All grit-blasted	0.07						
	60/40 Brass	Mineral oil + 5% oleic acid	0.06						
	Copper	All lubricants	0.10						

Ref. no.	Material	Lubricant	μ	Reduction of Area (%)	Drawing Speed (ft/min)	Drawn Size	Material of Die	Semi-Angle of Die	Type of Derivation
44	Steel (·144 C)	grit-blasted + soap	0·025/0·05	15 & 30	½	below ½in (thick)	tool steel	$0 \rightarrow 10°$	Split-Die (plane-strain)
		mineral oil + 5% oleic acid	0·07/0·12						
75	Steel (St 37)	lime + rapeseed oil	0·06 0·02	3 35	5	5 mm. (thick)		$3° \rightarrow 12°$	Split-Die (plane-strain)
		mineral oil	0·11 0·06	3 35					
17	Copper	Soap	0·02/0·03	$5 \rightarrow 45$	6	0·1in	tool steel	$2° \rightarrow 16°$	Split-Die
37	Aluminium	white lead + machine oil	0·08 0·04	4 20	$10 \rightarrow 15$	0·225in	tool steel	10°6'.	Split-Die
	Zinc		0·02 0·07	4 20					
82	60/40 Brass	Rapeseed oil	0·07 0·05	$7 \rightarrow 59$	0·3	3mm.	carbide	$2° \rightarrow 30°$	Rotating-Die

TABLE NO. 2.1(b)

been given here to fundamental investigations. Wistreich (2) has suggested that likely ranges of μ are 0.01 to 0.05 for soap and 0.08 to 0.15 for oil; but since then more data has become available and taking account of the short-comings of many of the methods of derivation (see section 2.6), this author suggests 0.02 to 0.05 for soap and 0.06 to 0.12 for oil.

It will be observed that the range of parameters covered in the tests is large, and comparison of results between investigations is extremely difficult, indeed, so is comparison of results obtained within a single investigation. The reason for this is that the parameters of the drawing process are rarely separable, but are closely interlinked. So much so that it becomes difficult to follow the classic experimental method of varying only individual parameters, in fact with regard to the study of friction it seems to be impossible. Thus a feature of experimental results which is frequently discussed is whether or not μ is pressure dependent, in other words whether or not Coulomb's Law applies, and support for both viewpoints appears in the literature. Quite apart from the question of the validity of the results on which such conclusions are based, it would seem essential that for a serious study of this topic tests were performed in which μ was determined with the normal pressure as the only variable. With conventional friction testing such as pin-on-disc techniques this would be a simple matter, but it cannot be done directly in the drawing process. One method which has been used is to vary the die-angle with which a particular draw is effected, but this could clearly affect the amount of lubricant drawn into the die. An alternative method is to perform geometrically identical draws with material of differing yield strength, but differences in the behaviour of the lubricant could then be expected where the lubrication regime was boundary, and this is thought to apply at least in part to most drawing operations (see section 2.4). A more reasonable approach is to use the same material but in differing states of hardness, and even here it is not entirely certain that the results would be directly comparable. The danger that the pre-treatments might lead to variations in surface texture could in principle be overcome, but the angle of incidence between ingoing material and die is not a function solely of external geometry, but is also influenced by features such as 'bulging' and 'sinking-in'. Furthermore it is not clear that ~~the behaviour of~~ the surface asperities of the previously hardened material would behave in the same way as those of an annealed specimen. This line of argument could be extended to the interdependence of other features which could affect friction conditions, but the object has been simply to demonstrate that there is little conclusive evidence on which the mechanics of friction in drawing might be formulated. This should become even clearer when the methods available for its study have been described.

At first sight it might appear that the previously quoted ranges of values within which μ probably lies are narrow enough for practical purposes. The danger here is one of thinking that because μ is small relative to unity, large percentage variations become unimportant. It can be readily shown that because of the small values of α generally used in drawing dies this is not so. Considering equations (3.1) to (3.3) and Figures 3.1 and 3.2, equation (3.2) may be re-written in terms of the components of drawing force P_o and P_F

$$\mu = \frac{P_F}{(P - P_F)} \tan \alpha = \frac{P_F}{P_o} \tan \alpha \qquad (2.8)$$

P_o should not be confused with the quantity P_i used earlier, although P_F and P_f do have the same significance. A die semi-angle of 7° was used in the experimental part of this investigation, and Figure 2.1(a) was drawn from equation (2.8) using this value. This shows the relationship between μ and P_F/P, and it will be seen that at a value of 0.05, friction accounts for 30% of the total drawing force, and at 0.12 the proportion rises to fully 50%. It should be noted that this relationship is absolutely valid. Although the actual values given to μ on this curve depend on its definition as F/Q, the values of P_F/P corresponding to the physical conditions represented by particular values of μ when defined thus, do not.

This is not to say that if an operation subject to a value of μ of 0.12 were to be rendered frictionless, there would necessarily be a corresponding fall in drawing force of 50%. However, if the assumption is made that the die-pressure is independent of μ, and it will be recalled that this is equivalent to introducing the $(1 + \mu \cot \alpha)$ term to allow for friction (see section 2.1), then Figure 2.1(b) may be drawn. This shows the increase in drawing force attributable to an increase in μ, and although it probably overestimates the dependence of P on μ, it is unlikely that it does so seriously.

It can be seen from this figure that the ranges of values previously quoted for μ correspond to a range of indeterminacy of drawing force of 20% for soap

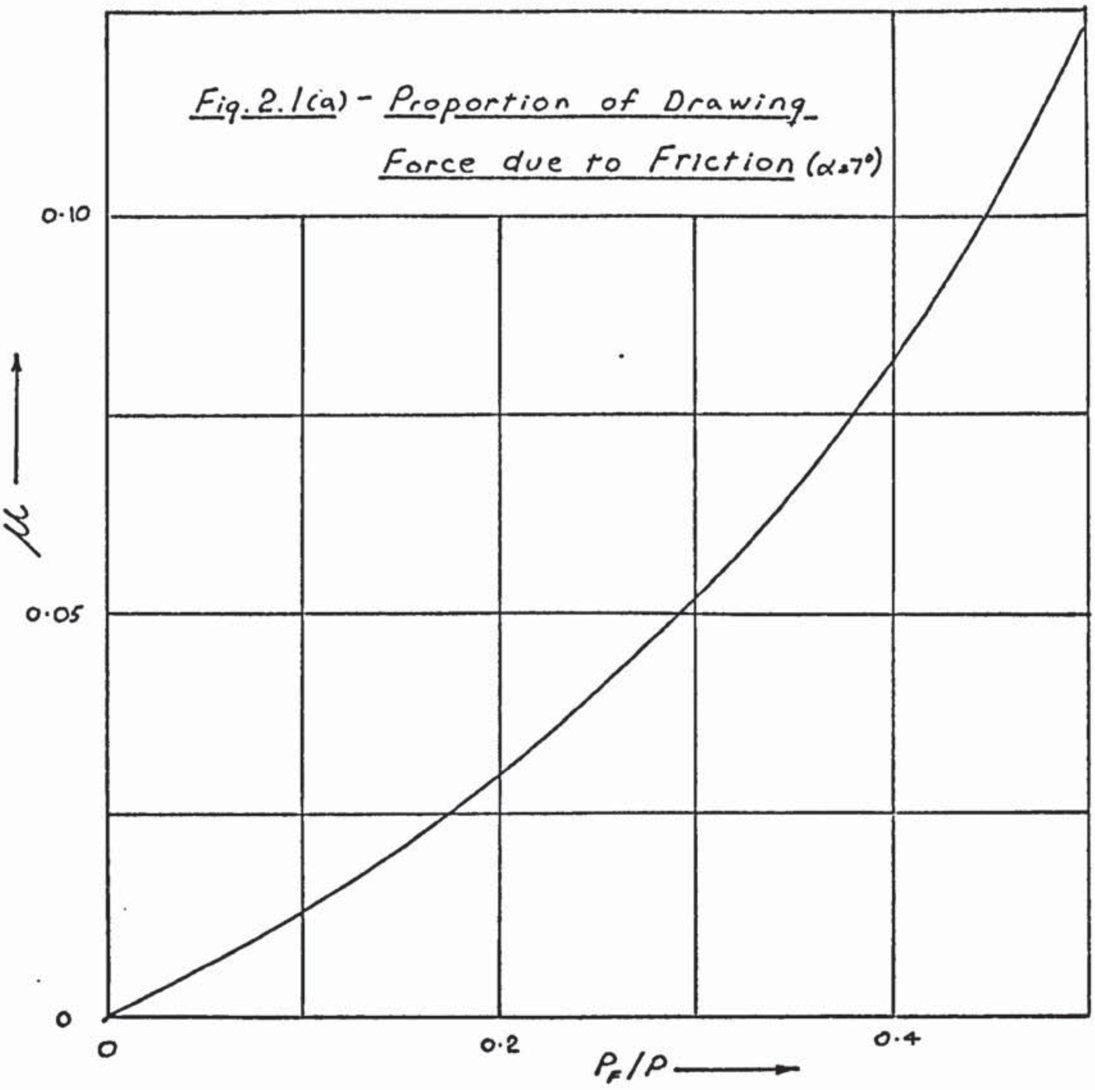

Fig. 2.1(a) - Proportion of Drawing Force due to Friction (α=7°)
0.10
0.05
0
μ
0
0.2
0.4
P_F/P

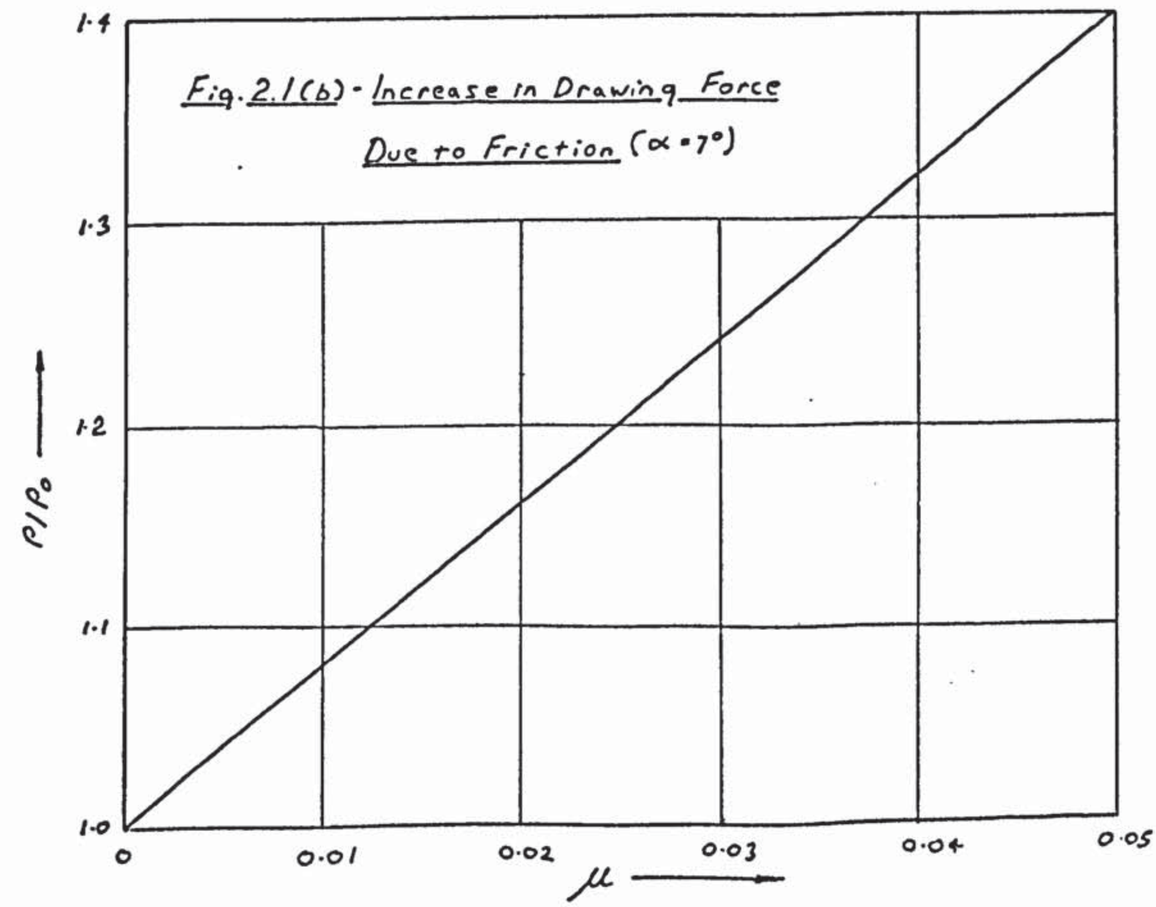

Fig. 2.1(b) - Increase in Drawing Force Due to Friction (α=7°)
1.4
1.3
1.2
1.1
1.0
P/P_0
0
0.01
0.02
0.03
0.04
0.05
μ

and 30% for oil. Thus even in the pragmatic terms of predicting drawing force it would be desirable to be able to specify μ more closely. In terms of the other theoretical objectives discussed in section 2.1.4, and of reaching full understanding of the basic mechanics of the process, it becomes even more important. In this context it seems that what is really required is an experimental method of determining shear and normal stresses throughout the deformation zone, rather than simply μ. If this could be done there would be a scund basis on which to evaluate theories of drawing.

The general situation with regard to studies of friction in metalworking has been admirably described by Wistreich, and the following quotation is from a summary made by Capus (40) of his remarks.

> ." In investigations of the subject of friction there was danger that the conceptual model was oversimplified: many of the generalizations drawn from experiment or theory were quite unwarranted. The coefficient of friction (μ) was but a ratio of forces, an index of the condition of a complex system at the time of observation. As such, it was highly specific to the place and circumstances in which it was measured. In applying the coefficient of friction in metalworking problems there was a tendency to regard it as a material property, which it was not.- - - - - - -
>
> In the measurement of μ the soundest course in Dr. Wistreich's view was the direct measurement of the relevant tangential and normal forces in the very process under investigation: it was experimentally the most difficult and therefore had been used least.
>
> Dr. Wistreich claimed that all other methods invo ked mathematical models of the process with varying degrees of verisimilitude, the coefficient of friction being extracted as the residue that could not be accounted for in any other way. Just how good such a method was depended not only on the accuracy of the mathematical model, but also on what part friction played in the model and - equally - how it was affected by errors in the measured parameters.
> - - - - - - - - - he did not wish to decry such indirect methods, which usually had the virtue of great experimental simplicity. His criticism was that, in his view, investigators rarely carried out a critical analysis of their mathematical model to establish the degree

of confidence to be attached to the resulting values of μ. During his own lifetime the coefficient of friction had been reduced by a factor of 10 – representing refinement in the mathematical model rather than improvement in the frictional conditions! "

2.4 THEORY OF FRICTION AND LUBRICATION IN DRAWING

Although the investigation described here was not aimed directly at achieving an understanding of the mechanics of friction (see section 1), it seemed wise to take account of the very considerable quantity of work which had been done on friction phenomena in general. The acknowledged authorities on friction (41) were consulted, together with some other work (42), and in addition specialist papers on lubrication in drawing (43,44,45) and on friction and lubrication in metalworking generally (46, 47, 48, 49) were studied. A number of the latter group (48,49) were found to be concerned almost entirely with simulative tests, which are discussed in the next section. The general impression obtained was that although the mechanisms were quite well understood qualitatively, friction and lubrication theory could give little quantitative assistance when it came to ascribing the value of μ to be expected from a particular combination of drawing parameters. The exception to this was the case of drawing with thick-film or hydrodynamic lubrication, which is a technique developed from the work of Christopherson and Naylor (50). This was regarded as being inapplicable to conventional drawing, and the literature was not studied in depth.

With regard to conventional drawing, the consensus of opinion was that the lubrication regime was boundary, with a certain amount of the dry friction often associated with that state, and in addition it was possible for hydrodynamic effects to appear at unusually low speeds. It was also possible to induce extra throughput of lubricant by grit-blasting the surface of the workpiece (43, 44). The point here was that once the lubricant entered the deformation zone it was forced to proceed irrespective of how high the working pressure became, and that as the high points of the asperities were smoothed out, the lubricant which was trapped in the troughs would be squeezed out to cover a larger proportion of the surface. It seems likely that some such mechanism would operate even where the surface had not been artificially roughened.

2.5 SIMULATIVE TESTS

The existence of these was briefly referred to in the previous section, but there are in fact a wide variety of them available. Their common basis is that some metalworking operations, notably that of simple compression, are more readily analysed and controlled and have fewer variables than processes such as wire-drawing and extrusion.

It is well known that friction between test piece and platens produces inhomogeneous deformation in the compression test , and raises the load required to produce a given strain. Provided that the stress-strain curve of the material is known, it is possible to deduce the coefficient of friction from a comparison of load/deflection curves obtained experimentally with those predicted theoretically (51). A fundamental drawback is that the stress-strain curve will itself have been derived from a compression test, and will therefore have ~~been~~ some inherent friction error. In practice a variety of techniques are available for reducing this error, and these are the selection of suitable initial geometry, incremental loading and relubrication with P.T.F.E., and extrapolation of results to infinite aspect ratio. It therefore seems likely that where the inverse geometry is chosen for the friction test, and where a high friction condition is being studied, little error would result. However this might not be the case where friction was low, as it would be expected to be in any test which adequately simulated wire-drawing.

Developments of this concept have been aimed at removing the need to know the stress-strain behaviour of the material, and a group (52 - 55) of methods relies on measurement of change of geometry during compression.

It may be noted that the compression process is non-steady state, and that it is generally difficult to deduce variations in μ throughout the duration of the test with these methods. Male (54) and Shutt(55) appear to have done so with some success, but the methods which they have used assume that the situation at a given instant is unaffected by the previous history. It seems unlikely that this is strictly true in compression testing, but in practice the error thus introduced may be small.

Vershchagin et al (56) have used a technique of contra-rotation of the compression platens with simultaneous measurement of applied load and torque. This experimental technique had earlier been used by Bridgeman (57) and Boyd and Robertson (58), but the particular application used by those workers was irrelevant to the topic being discussed here. Lauterbach et al (59) used a similar system, but in their investigation the specimen was totally enclosed. Shaw et al (60) rotated a Brinell hardness test specimen under the indenter. A modification to the rotational technique was made by Ling and Peterson (49), who compressed a thin foil between one wide and one narrow anvil. The narrow anvil indented the foil, and the tangential force required to slide the narrow anvil and foil over the wide anvil was measured. In the two latter investigations it appears that the deformation was first imparted to the specimen, and friction measurements were then made, rather than being made continuously during the progress of deformation. However the published accounts are not completely unambiguous on this point.

The most fundamental study of friction in plastic compression was made by Pearsall and Backofen (61), with the pin-load cell technique. They used two pins, inclined at differing angles to the surface of the platens. This enabled them to measure the distribution of both shear and normal stress across the test piece. They found that μ varied from point to point at each strain increment, and also from increment to increment at each point.

Although these simulative tests are of great interest to metalworking generally, and to forging particularly, this author considers that the results are not directly applicable to drawing because the conditions are dissimilar between the two, and this opinion has also been expressed in the literature (40). Thus compression testing is a non-steady but slow speed process, while wire-drawing is relatively high speed but steady-state. Apart from speed effects, the greatest difference is probably that with a single exception (49) deformation in the simulative tests takes place over a particular portion of surface, but in drawing, fresh surface and fresh lubricant is continuously drawn into the deformation zone. Even with the exception the authors do not report that speed of displacement was used as a variable parameter, or that it was other than very small.

The difference in conditions is well illustrated by one of the above mentioned techniques (55), which is based on measurement of the diameter at which sticking friction occurs. This situation is clearly not representative of drawing conditions. In this situation it seems best to regard any correspondence which may exist between values of μ obtained in compression tests and those in drawing tests as fortuitous. This does not deny the possibility that there may in fact be a correlation, but there is at present little evidence on which one might be formulated.

2.6 DETERMINATION OF FRICTION IN DRAWING

Where neither the theory of friction and lubrication nor simulative tests are able to furnish suitable values of μ , it clearly becomes necessary to measure it in the process itself, and this presents considerable difficulty. The basic problem is that in conventional axisymmetric drawing, the resultants of both the pressure and friction forces (Q and F, see Figure 3.2) are axial and directly additive. Resolution of forces gives

$$P = Q \sin \alpha + F \cos \alpha \tag{2.9}$$

in which there are two unknown forces, Q and F, which cannot be separated merely by measuring the drawing force P. The basis of the most frequently used methods is merely that another relationship must be established before the two can be separated. As discussed in section 2.1.4, the coefficient of friction is an abstract quantity which must be interpreted in terms of some physical and mathematical model before it can be evaluated, and the methods which are described below use a variety of such models to derive the additional relationship which is required. However, this author sees a clear distinction between those methods, such as thesplit-die technique, which are based on a simple model involving only the static equilibrium of forces, and others which use a model founded on the Theory of Plasticity, particularly so where the theory is applied in an arbitrary and incomplete manner.

In the following review, the parameters and results of the various investigations are not described, except where it is necessary to do so to make a specific point. The reasons for this have been outlined in section 2.1.4, and those results which seem to this author to be of most interest have been summarised in Table 2.1.

2.6.1 Comparative Studies

Methods described in this section ignore equation (2.9), and derive a completely separate relationship wherein μ is the only unknown. Thus the theories of drawing yield solutions of the general form

$$P = f(A_1, r, Y, \alpha, \mu) \tag{2.10}$$

and although the kinematically admissible solutions do not give such direct results, they do consider the same parameters. Values of A_1, r, and α are geometrically defined, and Y may be measured in a uniaxial tension test. If P is then measured, μ may be evaluated according to whichever particular form of equation (2.10) is preferred. Within this general approach there are a number of variations.

2.6.1.1 Directly from Theory :- This group of investigations followed the approach described above exactly, and they are well illustrated by Sachs' original study(9).

This led him to equation (2.3) in which he inserted values measured experimentally, and thereby calculated a value of μ of 0.21, which is much higher than is normally accepted nowadays. One of the justifications put forward for this technique is that it frequently appears to give the same value of μ over a range of tests, and this coincides with classical ideas of the nature of friction. The fact that often it only appears to do so is related to the point made in section 2.3 about the possibility of overlooking proportionally large variations in μ. This is also shown by Sachs' results. Thus he plotted three experimental points, corresponding to different reductions of area, against theoretical curves for different values of μ. These points appeared to lie closely about a curve corresponding to the value of 0.21 quoted above, but as far as can be judged from Sachs' presentation, the small deviations from the curve actually correspond to a range of 0.17 to 0.26. However no criticism is made of the adoption of a mean value, for this was certainly preferable to the interpretation of the results as showing a specific relationship between μ and reduction of area.

Many investigators have used this approach, frequently in order to obtain verification of a theory which they had developed, as described above for Sachs. It would be tedious to quote all these, but the method has also been used for comparative evaluation of lubricants, and was particularly popular with German workers in the 1950's who naturally favoured the use of Siebel's theoretical expression. Some such investigations which appear to be of value by virtue of their breadth of coverage are listed (62 - 66), and some of their results appear in Table 2.1. It is obvious that if the values of μ which those investigations obtained are put back into the theoretical expressions which were used in their derivation, good predictions of drawing force should be possible, provided that the experimental parameters are also similar.

It is clear that when μ is derived in this manner it is no more than a coefficient of compensation for shortcomings of the original theory, and it has no fundamental significance. This is not to deny that such studies were worthwhile when fundamental determinations were not possible, or even when these are possible, but are complicated and difficult to apply to realistic metalworking situations. However the results should be interpreted merely as giving information about drawing force, in an abbreviated manner, rather than describing behaviour at the die/workpiece interface. The most telling comment on this method of derivation was made by Wistreich (40) and has been quoted in section 2.1.4.

2.6.1.2 Allowing for Redundant Work:- As discussed in section 2.2, the unknowns of the drawing process may be regarded as being friction and redundant work, and measurement of either is sufficient to define both in terms of drawing force. It is well known (8, 2, 31) that the equilibrium solutions fail to take account of redundant work, and that Siebel's solution overestimates it (31) over a wide range of conditions. Attempts to derive μ from these or similar equations by the method described in the previous section, will therefore result in over or underestimates, the size of which will be related to the difference between the actual and theoretical magnitudes of redundant work. It is universally accepted that redundant work is least with small die-angles and large reductions of area, and it may be supposed that the equilibrium solutions would be most reliable for those conditions. Several investigators (34, 67, 68) have taken advantage of this, and have used the method described in the previous section, but in this region where it is probably most reliable. In fact these investigations were concerned primarily with evaluating redundant work, and this was done by assuming that values of μ were constant between different reductions of area. This may well be true, but this approach cannot be used to confirm it. However redundant work has been discussed in section 2.2, and is of no concern here.

This approach is the same as that described in section 2.6.1.1, but as it has been applied more realistically it seems likely that the results will also be more realistic. However, it should be noted that even if the basic assumption that redundant work is negligible at low die-angles and high reductions is correct, the resulting values of μ will still be dependent on the basic validity of the theory from which they are derived. The parameters and results of the above mentioned investigations are given in Table 2.1, but only for the low α and high r tests.

The converse approach of determining redundant deformation factor (see section 2.2) and thereby deducing P_f has not, to this author's knowledge, been used.

2.6.1.3 Optimum Die-Angle:- It is well established (2,8,38) that for any proposed combination of geometry, material, and lubricant, there will be an optimum die-angle which will give the minimum drawing force. This arises because the components of drawing force, P_f and P_r, have opposed dependencies on die-angle. Evans and Avitzur (69) have carried out drawing tests to determine the value of this optimum, and have interpreted their results in terms of both μ and the shear factor c. Their analysis depends on a theoretical prediction of redundant work, and for this they have used the theoretical treatment of Avitzur (see reference (25) and also sections 2.1.3.2 and 2.1.4). It is therefore not clear where their investigation differs in principle from the general approach discussed in section 2.6.1.1, except in being considerably more inconvenient experimentally. Furthermore it has been shown (17) that although a definite minimum does occur, drawing force is by no means critically dependent on die angle, and the selection of the minimum value must therefore be somewhat arbitrary.

It must be added that the authors do not share these reservations about their investigation, for they are sufficiently confident of their results to quote derived values of μ to four significant figures.

2.6.1.4 Measurement of Distortion :- Where a theory of drawing can be used to predict the inhomogeneity of deformation, comparison with measured inhomegeneity may be used to determine friction. In principle this is identical with the previous techniques in that the validity of some theory must be assumed, and the accuracy of the results are clearly dependent on that validity.

The inhomogeneity produced by axisymmetric deformation can be expressed as the distortion of an orthogonal grid imposed on a meridian plane. The measurement of such distortion has been used very extensively for the study of extrusion, under the title of Visioplasticity (24), but not as far as this author is aware for the purpose of determining friction. The method seems to have been but little applied to drawing, and then only to tube-drawing (70). This is probably associated with the very much greater difficulty of preparing suitable drawing specimens.

The only application of the technique of distortion measurement to the measurement of friction in drawing, of which this author is aware, was made by Wells (71), who used Shield's theory (28) to evaluate the results. Quite apart from the question of the applicability of that theory, which is discussed in section 2.1.3.3, the method seems to have involved considerable practical problems. Considering a grid-line cut across the meridian plane, Shield's theory predicted that the departure from linearity, measured as the distance of the mid-point from a straight line between the ends, which would be caused by drawing through a frictionless die of the geometry used by Wells, would be about 10^{-4} in. Measured values were about 10^{-3} in. This clearly presented a considerable metrological problem, but values of μ of 0.03 to 0.18 were found, and as this covered a range of lubrication conditions from full hydrodynamic to dry friction, it appears that the investigation was fairly successful, but the absolute accuracy of the results is of course unknown.

2.6.1.5 Back-Pull :- The basis of this system is that when back-pull is applied to the material being drawn, the required drawing force increases, but it does so by less than the amount of the back-pull. The explanation seems to be that the addition of back-pull reduces the die-pressure necessary to cause deformation, and that this in turn reduces the shear stress at the die/workpiece interface. Lunt and MacLellan (72) derived an expression for the 'back-pull factor' which involved μ but not the yield strength of the workpiece.

This technique for the determination of μ appears to be more fundamental than the others so far considered in section 2.6, and it is not in fact certain that it should be grouped here. In the late 1940's the method was considered to be a solution to the longstanding friction problem (3) and several investigations (36, 62) were subsequently carried out. However it seems to have fallen into disrepute, and Wistreich (2) has summarised the weaknesses. For this reason the method was not considered further, but it may be noted that Pawelski and Lueg (67) have used a variation of this technique which involved 'back-push'.

2.6.2 'Steckel-Drawing'

According to brief reports available from some sources, Ya Veiler et al carried out a substantial amount of work on friction and lubrication in wire-drawing, in the U.S.S.R. in the 1950's. Fortunately this has been reviewed by Likhtman et al (73). According to those authors, and Likhtman was associated with the original publications, the work was in fact strip-drawing. The system which was used was to initially draw through freely rotating rolls, and then to fix the rolls. The friction force on the tools was taken as being the difference between the two forces.

This work, and the technique, were not further considered.

2.6.3. Split-Die Technique

This method was first suggested (3) and used (17, 36) for axisymmetric drawing, but it is instructive to consider the plane-strain case first. When drawing through wedge-shaped dies there is a side thrust on the dies which tends to force them apart. If the magnitude of this force, at right angles to the direction of drawing, is denoted by S, then resolution of forces in this direction gives

$$2S = Q \cos \alpha + F \sin \alpha \qquad (2.11)$$

Q and F are the total normal and friction forces on both dies. Resolution in the longitudinal direction yields equation (2.9) again, for a drawing force P. This gives the extra relationship which was sought, and if P and S are measured, then μ may be easily evaluated as F/Q.

This technique has been used extensively in conditions of zero or low reduction of area and relatively low die-pressure, which probably simulate conditions in deep-drawing well, but are of no interest here. Another investigation (43) did use substantial reductions, but the authors pointed out that their method of calculation of μ relied on an approximate theoretical solution and the results could only be regarded as comparative. The reason for this was that they used cylindrical dies, and with those the distribution of stresses must be known before the reaction forces can be resolved into their components.

Rogers and Coffin (74) used the split-die technique with wedge-shaped dies, and were therefore able to make use of the exact analysis associated with equations (2.11) and (2.9). However the primary area of interest in their investigation was the subject of structural damage, such as the formation of central cracks, and the effect of hydrostatic pressure. Their results are therefore of very limited interest as a study of friction, and are not quoted here.

Green (5) showed that the derivation of μ was critically dependent on accurate measurement of the experimental parameters, particularly of α, and two major investigations (44, 75) which were made using the split-die technique took account of this factor in different ways. Lancaster and Rowe (44) used the plug-bar technique, in which two strips were drawn simultaneously through the dies, separated by the plane-strain equivalent of a tube drawing plug-bar. By measuring the pull on the plug-bar as well as the drawing force and die-splitting force, it was possible to evaluate μ between die and strip and also between strip and plug-bar. The latter corresponded to $\alpha = 0$, so the sensitivity of the evaluation to errors in α was eliminated. Pawelski (75) used inductive probes to detect elastic movement of the dies during drawing, and was therefore able to correct for this factor. Both of these investiations must be regarded as significant fundamental contributions. The only adverse criticism which this author has is of Pawelski's conclusions regarding the dependence of μ on die-pressure. He made no allowance for bulging, but most of the high end of the pressure range which he claims to have covered, was in a range of reductions where this feature could have been expected to reduce the actual pressure below that derived by considering only the reduction of area and die angle. Of course this would not affect the magnitudes of the derived values of μ, but merely their dependence on die-pressure. The results of these investigations are summarised in Table 2.1.

In order to apply this technique to axisymmetric drawing it is necessary to use a die which is in two pieces, split along a meridian plane and then clamped together, and this is in fact the form in which MacLellan (3) first suggested the technique. The equation for μ becomes slightly different from that for plane strain because of the altered geometry. If S is the splitting force, then

$$\mu = \frac{P - \pi S \tan\alpha}{P \tan\alpha + \pi S} = \tan\left[\tan^{-1}\left(\frac{P}{\pi S}\right) - \alpha\right] \qquad (2.12)$$

It should be noted that both of these forms of the equation have been incorrectly reproduced in the literature (3, 17), although both authors used the correct forms in their experimental work. The first application of the method (36) was unsuccessful, and the explanation given by the author was that lubricant penetrated the split and gave rise to additional forces of unknown magnitude. Wistreich (17) used the method successfully in what is probably the single most authoritative investigation of wire drawing. In this application he followed the general approach used earlier (36), in which the die was first held together with a force greater than the expected splitting force. The holding force was applied through a compression spring, and this was gradually released until the two halves of the die started to separate, at which point the holding force was taken as being equal to the splitting force.

Although this investigation was completely satisfactory the technique was rather cumbersome, and as equilibrium was lost as soon as the dies started to separate (36), it could not be adapted for continuous measurement. A further problem with continuous measurement is that the two halves must be held tightly together if lubricant and metal are not to penetrate the split and alter both the process and the measurements. This implies that the holding force must always exceed the splitting force, and unfortunately the system then becomes statically indeterminate. In that situation the splitting force would have to be deduced from the elastic strain in the die, and the considerable problem of calibration, which is discussed in the next section, arises. Nevertheless Yang (37) has used this system, although he did not indicate the method of calibration.

2.6.4 Measurement of Hoop-Strain

This method of determination makes use of the same analysis as the split-die technique, but it uses a conventional one-piece die, and deduces the splitting force from measurement of the hoop strain in the casing. The dominating problem with this technique is that of calibration. Two investigations (76, 77) are known to this author, the first being of wire-drawing, and the second of axisymmetric plug-drawing. In both, the calibration procedure involved admitting hydraulic pressure to a sealed portion of the die. The maximum pressures which were used were 10^4 and 12×10^3 lbf/in^2 respectively, and substantial extrapolation was necessary. Apart from this difficulty there are two fundamental sources of error. Firstly, a hydrostatic calibration involves the assumption that the die-pressure in drawing is uniformly distributed, and secondly, the nature of the pressure seals which must be used make it extremely difficult to ensure that the calibration pressure is applied over the correct part of the die. Indeed, it becomes extremely difficult to determine just where it is applied, and for the calibration to be made in terms of splitting force it is clearly necessary to know the area of application.

Majors (76) used a very low angle die, $\alpha = 1^\circ$, and although this clearly eased the problem of calibration, it would seem to make his results unrepresentative. One source (78) indicates that Kanaev and Ya Veiler (79) have also used this technique, but this author has been unable to check that report.

Kenny (80) has published a theoretical method of calibration for dies used in the tube sinking process, but this has not to this author's knowledge been applied experimentally.

2.6.5 Rotating-Die Technique

Die-rotation has been used industrially from time to time for such things as evening out die wear, and removing the tendency of wire to 'cast', but this aspect is of no consequence here.

The method by which die-rotation may be used to measure friction is described in detail in section 3 , so a brief explanation suffices here. In conventional drawing the path through the die of a particle at the surface of the bar is directed towards the virtual apex. Introduction of die-rotation gives such a particle a circumferential component of velocity relative to the die, so that its resultant relative velocity swings away from the apex. The direction of the friction vector will therefore also swing round, and will in fact account for the torque which die-rotation would be expected to require. However, provided that the magnitude of the friction vector remains unchanged, there will be an accompanying reduction in drawing force. The die-pressure, being by definition normal to the plane in which these velocity changes take place, will not be affected by them from the point of view of the dynamics of the situation, but the change in conditions may of course produce a change in the deformation behaviour of the material. However, if this does not happen, and this point is discussed at length in section 10, it should be possible to deduce the friction conditions either from measurement of torque or of reduction in drawing force.

The method was brought to this author's attention by the work of Moore and Wallace (81) who studied tube-sinking. They used a modified version in which the die was oscillated around its longitudinal axis, but they pointed out that continuous rotation was a more suitable experimental technique. Research uncovered a substantial history of the technique. The original and in many ways the most thorough application was by Linicus and Sachs (82), but they measured only the reduction in drawing force. The analysis which they used is presented in section 3.1, with a slight modification for an inconsistent treatment of the velocity at the surface of the bar, and an equally slight extension to allow evaluation from measurement of torque. Their results are given in Table 2.1. In the same year Greenwood and Thompson (83) discovered that die-rotation caused a reduction in drawing force, and later published a full account of their work (84), which did not include evaluation of friction. They claimed forcefully that their results disproved the basis of Linicus and Sachs' analysis, but their approach was completely empirical and they showed little appreciation of the mechanics of die-rotation. This author finds, with a single exception, none of their results inconsistent with the basic mechanism proposed by the originators of the technique. The exception was one test which showed a slight increase in drawing force with die-rotation.

Since then several workers (85, 86, 87) have observed reductions in drawing force associated with die-rotation, but have not evaluated friction from them. The last of these three publications includes a diagram which seems to show an increase in drawing force with die-rotation, for some speed parameters, but does not discuss it in the text.

Nishihara et al (88) performed rotating-die tests, and evaluated friction from measurements of both reduction in drawing force and torque. They used a die with a curved profile, and the object was to obtain a value of μ with which to check their theory of drawing with curved dies. In their analysis they assumed a distribution of die-pressure which was predicted by their theory, and constant μ. These assumptions were similar to those made by Linicus and Sachs, but they also introduced a theoretically predicted magnitude of die-pressure, in terms of the yield strength of the workpiece, into the analysis. It is extremely tempting to do this, as this author found when developing the analysis given in section 3.2, but it must destroy all merit which the rotating die technique has. For it adds the shortcomings of the theoretical derivations described in section 2.6.1, to the possible disturbance of the process caused by die-rotation.

Rothman and Sansome (89) have modified the original analysis slightly and determined μ from measurements of both torque and reduction in drawing force. This work is in fact that comprising the Series I tests described in section 9, and will be discussed there.

Intuitive considerations suggest that die-rotation might cause some permanent torsion of the workpiece. The only reference to this in the literature is by Lietzmann and Eichner (87) who said that metallographic tests on cross-sections of wire drawn with rotating dies showed no movement of material in the circumferential direction.

2.6.6 Die-Pressure

Several investigations have been concerned with evaluating die-pressure rather than friction, but in terms of finding an extra quantity so that equation 2.9 may be evaluated, there is clearly no difference.

Photoelastic techniques have been used (90, 91) for plane-strain drawing. The former deduced only die-pressure, but the latter studied shear stress as well. However, the materials which must be used for photoelastic investigations render them without interest as a source of practical metalworking friction information, although they are of obvious interest in the wider context.

Veys (92) has used a development of Majors (76) method of measuring hoop strain. For this he used a thin-walled die, with a series of steps on the outside. Each of these steps had a backing ring pressed onto it, and these rings were separated by P.T.F.E. sheets. The hoop strain could be measured at the periphery of each ring. The biggest practical problem was the liability of the die to fracture, and the biggest technical problem that of calibrating the strain measurements. In fact a theoretical calibration was used. The material was copper, and lubricants were sodium stearate and also graphite in tallow. Derived values of μ were generally between 0.02 and 0.03, but the extreme range included some slightly negative values.

The pin-load cell technique has been applied to axisymmetric drawing by Gokyu et al (93) and Pawelski and Armstroff (94). The former used a conventional system with a number of pins positioned normal to the surface, and determined distribution of die pressure, but did not calculate μ from the results. The method used by the latter precluded the possibility of measuring shear stress directly by the Pearsall and Backofen (61) method, for the pins did not contact the workpiece but measured the deflection of thin parts of the wall of the die. This clearly had advantages from the point of view of removing several problems normally encountered with pin-load cell techniques. The investigation was primarily concerned with tube drawing, but values of μ were derived for steel bar with rapeseed oil, and these ranged between 0.015 and 0.04, the smaller values occurring at larger reductions.

2.6.7 Selection of Experimental Technique

Of the methods which are available for the evaluation of friction in drawing, only the last four have any pretence of being fundamental. The pin-load cell technique, as applied by Pearsall and Backofen (61) to plastic compression, is clearly the only system which is available for the determination of both shear and normal stresses, and where it can be made to work satisfactorily it is definitely the preferred method. However it seems that the technique can involve substantial experimental difficulties, and although not rejected out of hand, it was decided to avoid it if possible.

The hoop strain method has some advantage over the other systems, in that as it in no way interferes with the inside of the die, the experimental technique cannot alter the conditions being studied. However, the experimental difficulties are again considerable. The split-die technique has been applied with the most notable success (17), and although this has not been remarked in the literature, it is not in principle limited to a split along the meridian plane. Thus the split could be made in any plane, or in two planes, and in this way a complete pressure distribution could be built up. Of course in practice the range of possibilities would be very limited, and even the straightforward application has been criticised by Wistreich (2) who may be regarded as the authority on the subject. Thus he considers it to be limited to slow speed drawing, dry lubricants, and also to be difficult experimentally. It may be added that in view of the substantial weakening of the die arising from the split, it is probably only possible to draw materials which are much softer than the die, if fins are to be avoided.

To summarise the attributes of these three methods, it may be said that they are all absolutely sound theoretically, but that in practice two of them can be difficult to apply without disturbing the quantities being measured, and all three present substantial technical problems.

The rotating-die technique shares the advantage of the hoop-strain method that it uses a conventional die, and it is therefore unlikely to be limited as to material. Furthermore the experimental methods are quite straightforward; speed, drawing force and torque are all parameters which may be measured with relative ease.The drawbacks of the method are twofold. Firstly it is clear that rotation of the die could alter the quantities being measured, and secondly, although the requisite data is easily obtained the subsequent analysis is not fundamentally sound. Thus, if the die was in fact cylindrical and there was no change in longitudinal speed as the material passed through the die, then there would be no problem, and whatever the distribution of shear and normal stresses, it would be possible to calculate a valid mean μ as for the split-die technique. In fact it is necessary to assume some form of distribution for the velocity and stresses before the data can be evaluated. At first sight this might appear to over-ride any benefits accruing from experimental simplicity. However, there is another advantage that the rotating-die technique has, which although obvious, has not hitherto been specifically pointed out in the literature. Thus for any given test, friction may be evaluated independently from measurements of either torque and reduction in drawing force, and in particular, this may be done at an infinite number of rotational speed to drawing speed ratios. If the assumptions made in the analysis are correct, then all these evaluations should yield a unique value of μ, or of shear stress if friction conditions be assumed in that form.

Originally this was seen as a method of compensating for any change in conditions due to rotation. It seems clear that such change would be least at low rotational speeds, and it was thought that results over a range of speeds could be extrapolated to zero. However, it was later realised that if rotation did not alter the magnitude of the shear stress significantly, then it would be possible to check the validity of various assumed distributions. Another feature of the rotating die-technique which seemed to be of some interest for its own sake, was that of the reduction in drawing force.

The conclusion of the review was that the rotating-die technique had significant potential advantages over the other methods, and that these appeared to have been neither fully exploited nor realised in the past. It was therefore selected as the basis of the investigation described herein.

The method of analysis which is described in section 3 falls into two parts. The first corresponds closely with that used by Linicus and Sachs (82) and aims to derive a mean value of μ . The significance of the points made above is that if the assumptions of the analysis are correct, then all tests should give the same result. However, it is shown in section 3.2 that the analysis contains an implicit assumption which would change the derived values, even if the explicit assumptions were correct. The analysis in that section was developed to overcome this problem, and to facilitate the evaluation of shear stress directly.

2.7 PROFILE OF DRAWING DIE

It was necessary to specify a die-profile for the experimental work, and as discussed in section 4.3, this was done with reference to the literature. The conical form was selected because most of the theories treated this case, and the die-angle was chosen from data given by Wistreich (2).

Most industrially used drawing dies have a parallel, or land, at the minimum section, and this created a problem. Theoretical solutions for such dies are available (25, 36, 37), but Wistreich (2) argued that one of these is unsatisfactory. The others post-date his comments, but his most cogent argument must apply to them also. This was that it has been observed that the drawn material can be sufficiently smaller than the die-throat for it to lose contact in the parallel . It may be noted that this was also observed in the tests performed during this investigation (see section 8 and Table 10.5) It was therefore decided to use a die with the minimum possible parallel.

2.8 TENSILE TESTS

In order to use measured values of friction to check theories of drawing, it is also necessary to know the equivalent stress-strain curve of the test material. The most suitable test for axisymmetric drawing is the uniaxial tension test, but it is not possible to use this to large strains because of the onset of instability and subsequent fracture.

There are two commonly used correction factors for this region, one due to Bridgman (95) and the other to Davidenkov and Spiridonova (96), although it seems that the latter was in fact suggested by Siebel much earlier. The two were compared, and over the strain range which was of interest in this investigation, up to about 0.55, there was only 0.15% difference between them. The Bridgman correction is the more awkward to apply, as it is sensitive to round-off errors in the calculation, and it is also critically dependent on accurate measurement of the relative radii. Thus, incorrect measurement can lead to a correction of the wrong sign. It was therefore decided to adopt the Siebel correction

$$\frac{\sigma^*}{\sigma} = \frac{1}{(1 + a/4R)}$$

In this, σ and σ^* are respectively the measured and corrected direct stresses, a is the radius of the minimum section, and R is the radius of curvature of the neck. This correction factor was used for the tensile tests described in section 10.8.

3. DETERMINATION OF FRICTION BY THE ROTATING DIE TECHNIQUE

Conventional stationary-die drawing is represented in Figure 3.1, in which the normal and shear stresses, σ and τ, are shown acting at the periphery of an element δA_s of the curved surface area of contact, A_s, between bar and die. The drawing force P may be expressed as the summation of the stresses on all such elements throughout the die, as follows

$$P = \int_{x_1}^{x_2} \sigma \sin \alpha \; dA_s + \int_{x_1}^{x_2} \tau \cos \alpha \; dA_s \qquad (3.1)$$

If P_o is defined as the portion of the drawing force arising from the summation of the normal stress, and if τ / σ is assumed constant throughout the die, then equation (3.1) transforms very simply to

$$\mu = \frac{(P - P_o)}{P_o} \tan \alpha \qquad (3.2)$$

which is the basis for the rotating die technique. It should be noted that the only assumption made in this derivation was that μ was constant. It should also be noted that P_o is not necessarily the same as the drawing force in the hypothetical frictionless condition.

If the die were to be rotated at infinite speed, then the velocity vector relative to the die, represented by V_s in Figure 3.1, of a particle at the die surface, would swing round to the circumferential direction. The component of shear stress along the axis of the bar would then vanish, and provided that the normal stress had not been altered in magnitude by die-rotation, the measured drawing force would become equal to P_o. μ could then be calculated from equation (3.2). Infinite die-speeds are clearly not possible, but by using low drawing speeds it would be possible to come close to the full 90° swing of the velocity vector, and therefore of the friction vector. However it is to be expected that die-rotation would in fact have some effect on the magnitudes of the stresses. Several possible mechanisms for such an effect may be postulated (see Section 10.6.4.4), and although magnitudes cannot be predicted, it seems clear that they would be greatest at the highest rotational speeds, and for the greatest swing of the friction vector. Such a realisation of the technique would therefore be suspect.

The more attractive and practicable system which was used, was to measure the reduction in drawing force produced by some intermediate swing of the friction vector, and then to deduce P_o analytically. The following section deals with this analysis, although it was not in fact necessary to deduce P_o directly.

3.1 APPROXIMATE ANALYSIS FOR COEFFICIENT OF FRICTION

Referring to Figure 3.2, Q and F are representations of the resultant normal and shear forces acting on the die in the non-rotational situation, and d_r is the diameter of the section at which they act. The assumption of constant μ ensures that they do act at the same section, although this is not strictly necessary for the analysis.

Equating forces gives :- $P = Q \sin\alpha + F \cos\alpha$ (3.3)

By putting $\mu = F/Q$ and noting that $Q \sin\alpha = P_o$, equation (3.2) may again be arrived at. This shows that even if μ was not constant through the die, equation (3.2) would give a meaningful average value.

Figure 3.3 is a view normal to the die surface, showing the velocity and friction vectors at d_r, during die rotation. V_s is the velocity at that diameter in the absence of die-rotation, and S the circumferential velocity relative to the die. If AC represents the friction vector F in the absence of die-rotation, then rotation of the die causes F to swing round to AD. Provided that there is no directionality in the surface finish, AD will oppose the resultant velocity vector, and provided the magnitudes of F and Q are unchanged by rotation, there will be a reduction in drawing force corresponding to BC cos α.
The drawing force with rotation will be given by

$$P_R = Q \sin\alpha + F' \cos\alpha$$

$$= Q \sin\alpha + F \cos\alpha . \cos\theta \qquad (3.4)$$

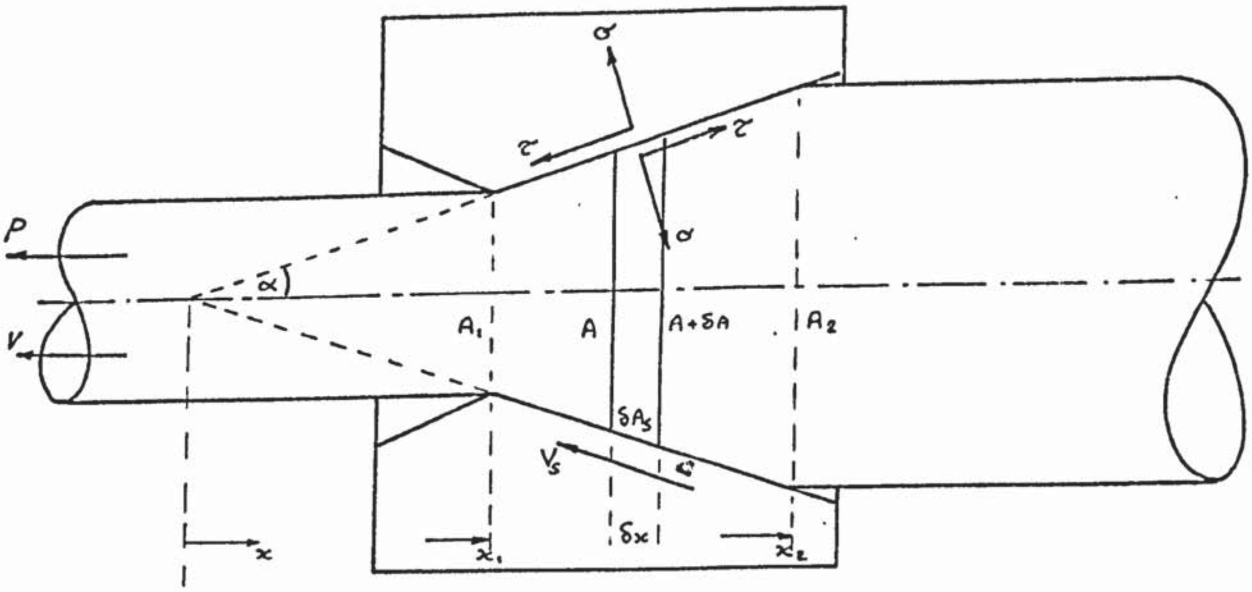

Fig. 3.1 - Representation of Stresses at the Die/Bar Interface

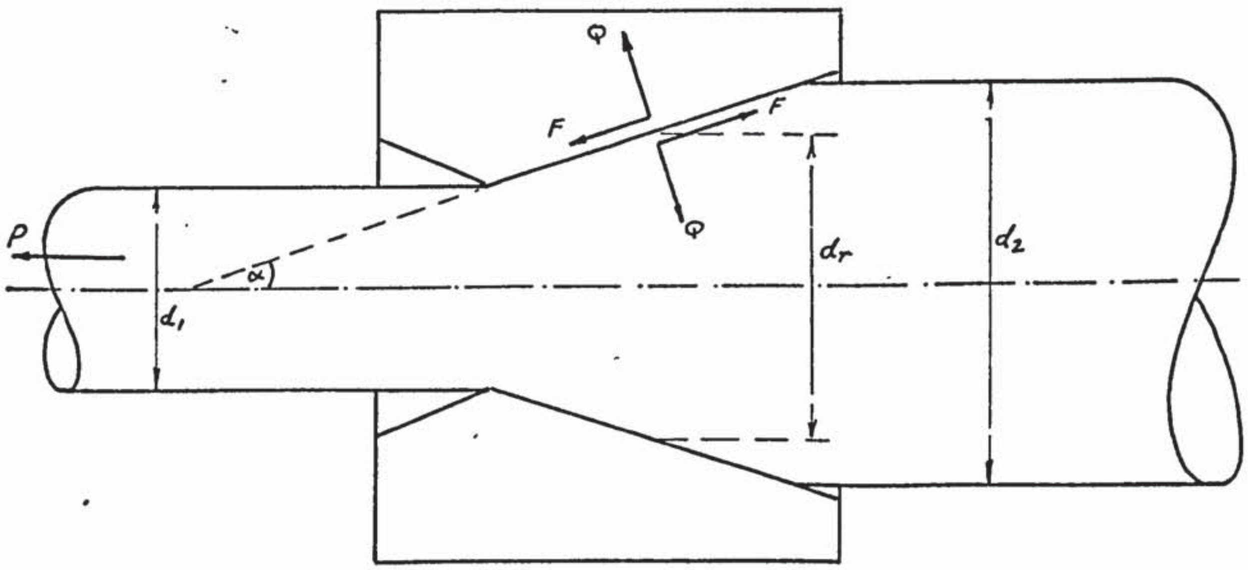

Fig. 3.2 - Representation of Forces at the Die/Bar Interface.

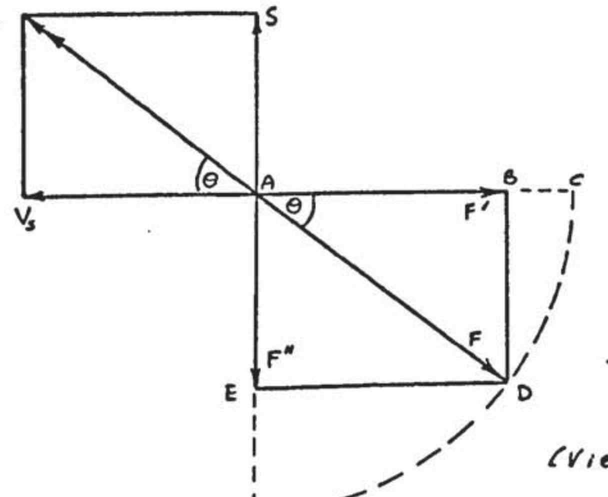

Fig. 3.3 - Velocity & Friction Vectors with Die-Rotation

(View normal to die surface - Q direction in Fig. 3.2)

Combining with equation (3.3) gives

$$\mu_P = \frac{F}{Q} = \frac{(P - P_R)}{(P_R - P\cos\Theta)} \tan\alpha \qquad (3.5)$$

where the subscript P indicates calculation from measurement of drawing force reduction.

Thus far the analysis has followed closely the gist of the original . It is a simple matter to extend it slightly by considering the torque during rotation. This will correspond to AE and will be given by

$$T = \frac{F''}{2} d_r = \frac{F}{2} d_r \sin\Theta \qquad (3.6)$$

Combining with equation (3.3) gives

$$\mu_T = \frac{F}{Q} = \frac{2T\sin\alpha}{(P d_r \sin\Theta - 2T\cos\alpha)} \qquad (3.7)$$

In order to evaluate these equations it is necessary to estimate V_s and S at d_r. Following the original work, the assumption is made that the shear stress is uniform over the contact surface. This leads to d_r being the diameter of a section which bisects the curved surface area of contact A_s.

Thus $$\frac{A_s}{2} = \frac{A_2 - A_r}{\sin\alpha} = \frac{A_r - A_1}{\sin\alpha} \qquad (3.8)$$

where A_1, A_2, and A_r are the cross-sectional areas at the relevant points. This leads to

$$d_r = \sqrt{\frac{(d_1^2 + d_2^2)}{2}} \qquad (3.9)$$

which allows S to be calculated in terms of the rotational speed of the die.

$$S = \pi R d_r \qquad (3.10)$$

For some unexplained reason, Linicus and Sachs (82) then took V_s as being the same as the drawing speed V. However it is more consistent to evaluate V_s at d_r. This may be done by considering continuity of the workpiece through the die, together with the assumption of a radial flow field between spherical caps.

Thus $$V_s = V\left(\frac{d_1}{d_r}\right)^2 \qquad (3.11)$$

It is known that $$\theta = \tan^{-1}\left(\frac{S}{V_s}\right) \qquad (3.12)$$

so equations (3.5) and (3.7) may now be solved to give μ_P and μ_T for any set of experimental parameters. It was however noted that as $\cos\theta \longrightarrow 1$, $P_R \longrightarrow P$, and equation (3.5) becomes indeterminate. Even where $\cos\theta \longrightarrow 0$, P_R would still be the greater proportion of P, and for sensible results to be obtained it was recognised that measurements would have to be of very high accuracy, particularly measurements of P and P_R.

3.2 DETERMINATION OF DISTRIBUTION OF SHEAR STRESS

A number of significant assumptions were made in the foregoing analysis. The basic one was that die-rotation did not alter the stresses at the bar/die interface, and a group of them concerned the distributions of velocities and stresses through the die. None of these have been validated, as far as this author is aware, and this clearly detracted from the importance of the rotating die technique. However, it has an extremely attractive feature, in that tests may be performed over a wide range of speed parameters, and the analysis made from both force and torque measurements. In fact this feature constitutes a self-checking mechanism, so that provided that the basic assumptions were correct, a unique value of μ would be expected to emerge whatever speed parameters were used.

This is the principle underlying the postulated use of the rotating-die technique to deduce the distribution of shear stress. The distribution can not be calculated directly from experimental results, but various models may be checked for correspondence with reality over a wide range of tests. However, it was recognised that even if the explicit assumptions made in the simple analysis were correct, a test to test variation in the calculated values of μ would appear. This would be caused by the implicit assumption that the resultant forces always act at the same section, diameter d_r. It will be clear that for any finite die-speed, θ will vary throughout the die and will always be greatest at die-entry. Therefore for an analysis to be valid, even within the assumption of uniform distribution of shear stress, account would have to be taken of this variation.

When this variation of θ was first comprehended, it was thought of as producing a test to test change in the diameter at which the resultant torque would act, and the dependence of this diameter on the speed parameters of the test was seen as a way of checking the postulated distribution of shear stress. However, the position at which this resultant acts would be very difficult to deduce experimentally, and indeed, the entire concept of the distributed shear stress as acting at a resultant diameter seems to be tenuous. A more reasonable approach was thought to be to compare theoretical predictions of torque and reduction of drawing force with measured values, for a range of speed parameters and distribution models.

An attempt was therefore made to produce a valid analysis for uniform shear stress, using the distribution of velocity given by the continuity condition, as for equation (3.11). The form of integral which was obtained offered little hope of an analytical solution, and graphical or numerical solutions were contemplated. It was decided to hold these in abeyance until some experimental work had been done, in order to determine the range of parameters of interest, and thereby to save labour. It eventually transpired that a linear approximation could validly be used for the distribution of velocity within the die (see Section 10.4), and an analytical solution thereby became possible. This is now given, with some of the experimental findings regarding the distribution of velocities being presented at this stage as assumptions.

3.2.1 Velocity Equations

The distribution of velocity is illustrated in Figure 3.4, with the virtual apex of the die being taken as the origin in all cases. The peripheral speed of any point on the die surface relative to earth, S_D, is given in terms of the rotational speed of the die by

$$S_D = \pi d R = 2\pi x \tan\alpha . R$$

It is assumed that, in general, the free end of the bar will rotate at a speed R_B under the applied torque. The drawn end cannot rotate, and this leads to Figure 3.4(d). The peripheral speed S_{B2} of the bar at inlet is given by

$$S_{B2} = 2\pi x_2 \tan\alpha . R_B$$

It is further assumed that the variation between S_{B2} at x_2 and zero at x_1 is linear, as in Figure 3.4(e). Therefore the peripheral speed S_B at a general position x, is

$$S_B = S_{B2}\frac{(x-x_1)}{(x_2-x_1)} = 2\pi x_2 \tan\alpha . R_B \frac{(x-x_1)}{(x_2-x_1)}$$

The pheripheral speed of a point on the die surface relative to a corresponding point on the bar, S, may now be written.

$$S = S_D - S_B$$

$$= \frac{2\pi R\tan\alpha}{(x_2-x_1)}\left[x(x_2-x_1) - x_2\left(\frac{R_B}{R}\right)(x-x_1)\right]$$

Re-arranging and substituting constants C and D leads to

$$\left.\begin{aligned} \frac{S}{R} &= \frac{Cx + D}{(x_2-x_1)} \\ \text{where} \quad C &= 2\pi\tan\alpha\left[x_2 - x_2\left(\frac{R_B}{R}\right) - x_1\right] \\ \text{and} \quad D &= x_1 x_2\left(\frac{R_B}{R}\right)2\pi\tan\alpha \end{aligned}\right\} \quad (3.13)$$

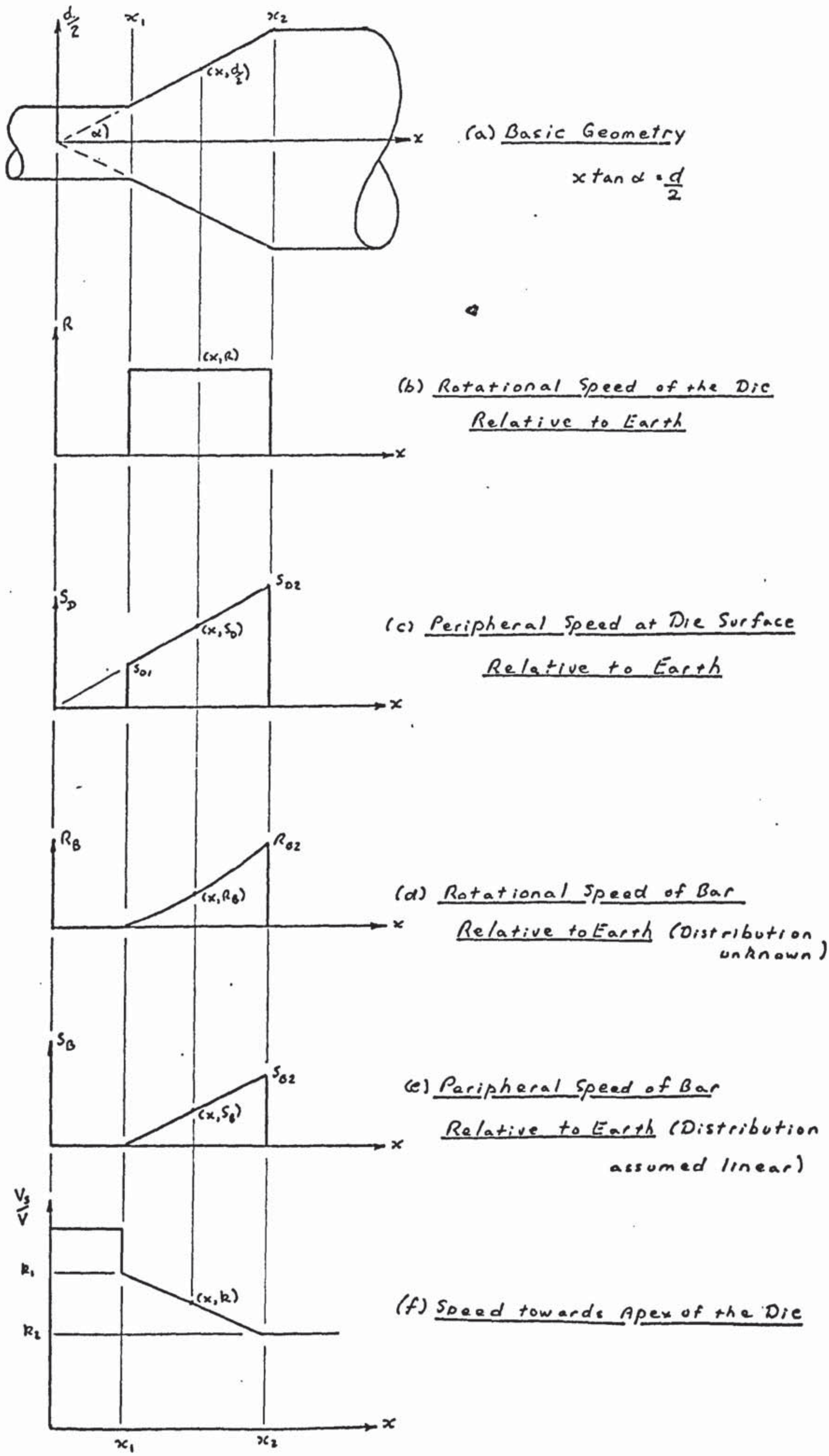

Fig. 3.4.- Distribution of Speed through the Die

By expressing the values of the surface speed V_s towards the apex of the die, at x_1 and x_2, as proportions of the drawing speed, and by assuming a linear variation between them, the distribution shown in Figure 3.4(4) is obtained. The value of the coefficient k at a general point x is given in terms of the particular values k_1 and k_2 by the linear equation

$$k = \frac{k_1(x_2 - x) + k_2(x - x_1)}{(x_2 - x_1)}$$

which leads to :-

$$\left.\begin{aligned} \frac{V_s}{V} = k = \frac{(A - Bx)}{(x_2 - x_1)} \qquad & \text{where} \quad A = (k_1 x_2 - k_2 x_1) \\ & \text{and} \quad B = (k_1 - k_2) \end{aligned}\right\} \quad (3.14)$$

Using equations 3.14 and 3.13, the swing of the friction vector Θ (see Figure 3.3) at a general point x can now be defined as

$$\tan\Theta = \frac{S}{12V_s} = \frac{R(Cx + D)}{12V(A - Bx)} \qquad (3.15)$$

where the conversion factor for the system of units used in the experimental work has been included.

3.2.2 Stress Equations

Referring to Figure 3.1, the rate of change of cross-sectional area with increasing x may be easily derived.

$$A = \frac{\pi d^2}{4} = \pi x^2 \tan^2\alpha$$

$$\frac{dA}{dx} = 2\pi x \tan^2\alpha$$

The elemental change in curved surface area, δA_s, can be put in terms of the associated change in cross-sectional area, δA.

$$\delta A_s = \frac{(A + \delta A) - \delta A}{\sin\alpha} = \frac{\delta A}{\sin\alpha}$$

Equation (3.1), for the non-rotational situation, can now be re-written.

$$P = P_o + \int_{x_1}^{x_2} 2\pi \tan\alpha \, . \, \tau \, x \, dx \qquad (3.16)$$

The drawing force with die-rotation may be deduced in the same way that equation (3.4) was derived, using Figure 3.3, but recalling that stresses at any position, x, are being considered.

Thus $$P_R = P_o + \int_{x_1}^{x_2} 2\pi \tan\alpha \, . \, \tau \, x \cos\theta \, . \, dx$$

Eliminating Po leads to

$$\frac{P - P_R}{2\pi \tan\alpha} = \int_{x_1}^{x_2} \tau \, x \, dx - \int_{x_1}^{x_2} \tau \, x \cos\theta \, dx \qquad (3.17)$$

Similarly the torque may be written

$$T = \int_{x_1}^{x_2} \tau \frac{d}{2} \sin\theta \, . \, dA_s$$

$$= 2\pi \frac{\tan^2\alpha}{\cos\alpha} \int_{x_1}^{x_2} \tau \sin\theta \, . \, x^2 \, dx \qquad (3.18)$$

It is now necessary to assume some form of distribution of shear stress. The model chosen is that of a linear variation of τ with x. The end values are defined as τ_1 and τ_2, at x_1 and x_2. A coefficient n which describes the variation through the die is defined as

$$n = \frac{\tau_2}{\tau_1}$$

The shear stress at a general position x can now be written .

$$\frac{\tau}{\tau_1} = \frac{x(n-1) + (x_2 - n x_1)}{(x_2 - x_1)}$$

$$\text{or} \quad \frac{\tau}{\tau_1} = E + Fx \qquad \text{where} \quad E = \frac{(x_2 - n x_1)}{(x_2 - x_1)} \quad \text{and} \quad F = \frac{(n-1)}{(x_2 - x_1)} \qquad (3.19)$$

Replacing for τ in equations (3.17) and (3.18)

$$\frac{P - P_R}{2\pi \tau_1 \tan\alpha} = \int_{x_1}^{x_2} (E + Fx)\, x\, dx - \int_{x_1}^{x_2} (E + Fx)\, x \cos\theta.\, dx \qquad (3.20)$$

$$T = 2\pi \tau_1 \frac{\tan^2\alpha}{\cos\alpha} \int_{x_1}^{x_2} (E + Fx)\, x^2 \sin\theta.\, dx \qquad (3.21)$$

Using equation (3.15), the equations may be put in forms ready for integration.

$$\left.\begin{aligned} \frac{P - P_R}{2\pi \tau_1 \tan\alpha} &= \int_{x_1}^{x_2} (E + Fx)\, x\, dx \\ &\quad - \int_{x_1}^{x_2} \frac{(E + Fx)\, 12 V (A - Bx)\, x\, dx}{\sqrt{\{R^2 (Cx + D)^2 + 144 V^2 (A - Bx)^2\}}} \end{aligned}\right\} \qquad (3.22)$$

$$\frac{T \cos\alpha}{2\pi \tau_1 \tan^2\alpha} = \int_{x_1}^{x_2} \frac{(E + Fx)\, R\, (Cx + D)\, x^2\, dx}{\sqrt{\{R^2 (Cx + D)^2 + 144 V^2 (A - Bx)^2\}}} \qquad (3.23)$$

For convenience the integrals will be termed I_1 , I_2 and I_3 .

$$\text{Thus} \quad (P - P_R) = 2\pi \tau_1 \tan\alpha \left[I_1 - I_2 \right] \qquad (3.24)$$

$$\text{and} \quad T = 2\pi \frac{\tan^2\alpha}{\cos\alpha} . \tau_1\, I_3 \qquad (3.25)$$

I_1 may be solved directly. I_2 and I_3 must first be expanded, so that they become the sums of a series of integrals of the form

$$\int_{x_1}^{x_2} \frac{x^m\, dx}{\sqrt{(a + bx + cx^2)}}$$

where m takes whole values up to 4 for I_3, and up to 3 for I_2. These are standard forms which may be found in tables of integrals (97). The solutions then become perfectly straightforward, but exceptionally laborious. They are given in section 3.2.4, together with the definitions of the various constants which have been used to shorten the presentation.

If τ_P and τ_T are defined as values of τ_1, calculated from equations (3.24) and (3.25) respectively,

$$\tau_P = \frac{(P-P_R)}{2\pi \tan\alpha\,[I_1 - I_2]} \qquad (3.26)$$

$$\text{and} \qquad \tau_T = \frac{T\cos\alpha}{2\pi \tan^2\alpha \,.\, I_3} \qquad (3.27)$$

Each of these equations contains the unknowns τ and n, so if the two lines of analysis are to be independent, another relationship is required. For this it is noted that provided that conditions are unchanged by die-rotation, the correct value of n is that value which gives unique values of τ_P and τ_T over the whole range of speed parameters. Changes in conditions which may be caused by die-rotation could become apparent in various ways. Non-correspondence of τ_P and τ_T is one obvious way, another being the possibility that values might be level over some portions of the R/V range, but not others. However, direct comparison of τ vR/V curves obtained with different values of n would be awkward, because the level as well as the slope of the curve would change with each value. It is better to transpose the calculations into terms of P_F, the proportion of drawing force due to shear stress. Referring to equation (3.16).

$$P_F = \int_{x_1}^{x_2} 2\pi \tan\alpha \,.\, \tau x \, dx$$

$$= \int_{x_1}^{x_2} 2\pi \tan\alpha \,.\, \tau_1 (E+Fx)\, x \, dx$$

$$= 2\pi \tan\alpha \,.\, \tau_1 \, I_1 \qquad (3.28)$$

Replacing for τ_1 from equation (3.26), and expressing P_F as a proportion of the total drawing force

$$\frac{P_{F(P)}}{P} = \frac{(P - P_R)}{P} \cdot \frac{l_1}{(l_1 - l_2)} \qquad (3.29)$$

Where $P_{F(P)}$ indicates P_F calculated from measurements of drawing force reduction. $P_{F(T)}$ may similarly be established from equation (3.27).

$$\frac{P_{F(T)}}{P} = \frac{T}{2240.P} \cdot \frac{\cos\alpha}{\tan\alpha} \cdot \frac{l_1}{l_3} \qquad (3.30)$$

a conversion for the units used in the experimental work having been made. The advantage of plotting P_F/P versus R/V is that solution of equations (3.29) or (3.30) for a range of values of n leads to a directly comparable family of curves. l_1, l_2 and l_3 contain only geometrical and speed parameters, and the coefficient n, so it should be possible to solve the equations to predict the form and spread of the family of curves corresponding to an assumed range of n. The method for doing this is given in section 3.2.3.

The form of equation (3.29) is similar to that of (3.5), and a similar caution applies. Thus $l_2 \longrightarrow l_1$ as $P_R \longrightarrow P$, and a high accuracy of measurement would therefore be required for sensible results. The best possible accuracy of measurement, and repeatability of experimental conditions is also required for maximum resol~~tuion~~ution between various values of n. Thus, given perfect repeatability and accuracy, it would theoretically be possible to distinguish between linear and other more complex forms of distribution of τ. However, the practical possibility of doing this seems remote.

3.2.3 Theoretical Model for Form of Results

The basis of the method for determination of distribution of shear stress, defined by the coefficient n, is that only the correct value of n would lead to the calculation of a unique value of P_F over the R/V range. It is therefore of interest to predetermine the variation in calculated values which would result from an incorrectly assumed value of n.

Assuming that the correct distribution for an arbitrarily chosen set of conditions is defined by $n = a$, and that the corresponding correct values of the associated parameters are denoted by the superscript a, then from equation (3.28)

$$\tau_1^a = \frac{P_F^a}{2\pi \tan\alpha . I_1^a}$$

Combining this with equations (3.26) and (3.27), and noting that

$$\tau_P^a = \tau_T^a = \tau_1^a$$

gives $$(P^a - P_R^a) = P_F^a \frac{[I_1^a - I_2^a]}{I_1^a}$$

and $$T^a = P_F^a \frac{\tan\alpha}{\cos\alpha} . \frac{I_3^a}{I_1^a}$$

$(P^a - P_R^a)$ and T^a correspond to values of reduction of drawing force and of torque which would be observed experimentally. Consider now that such values have actually been measured, but that in the absence of foreknowledge of the correct value of n, some incorrect distribution denoted by $n = n$ has been assumed. The values of parameters calculated with this incorrect value are denoted by the superscript n. From equations (3.29) and (3.30).

$$P_{F(P)}^n = (P^a - P_R^a) \frac{I_1^n}{(I_1^n - I_2^n)} = P_F^a \frac{(I_1^a - I_2^a)}{I_1^a} . \frac{I_1^n}{(I_1^n - I_2^n)}$$

and $$P_{F(T)}^n = T^a \frac{\cos\alpha}{\tan\alpha} . \frac{I_1^n}{I_3^n} = P_F^a . \frac{I_3^a}{I_1^a} . \frac{I_1^n}{I_3^n}$$

Re-arranging,

$$\frac{P_{F(P)}^n}{P_F^a} = \frac{I_1^n}{I_1^a} . \frac{(I_1^a - I_2^a)}{(I_1^n - I_2^n)} \qquad (3.31)$$

and $$\frac{\rho^{n}_{F(T)}}{\rho^{a}_{F}} = \frac{l_1^{n}}{l_1^{a}} \cdot \frac{l_3^{a}}{l_3^{n}} \qquad (3.32)$$

If some value of n were now to be assumed as representing reality, equations (3.31) and (3.32) could be solved for a range of speed parameters, and of incorrect values of n. This would yield a family of curves similar to that which it is expected would be obtained experimentally. Unfortunately l_2 and l_3 contain R_B , which is a dependent speed parameter influenced by the magnitude of τ . It is therefore not possible to solve equations (3.31) and (3.32) independently of experimental data. The apparently simple alternative of putting $R_B = O$ is not available, because the solutions for l_2 and l_3 become invalid in that condition.

Of course it would be possible to obtain a separate solution for the case where $R_B = O$, and this would in fact be very much simpler. However, measured values of R_B became available at about the same time that the above analysis was completed, and in that situation it became pointless to derive the extra solution. Evaluation of equations (3.31) and (3.32) using experimentally measured speed parameters is described and discussed in sections 10.6.6 and 10.7.3.

3.2.4 Solutions of Integrals

$$I_1 = \left[\frac{E}{2}(x_2^2 - x_1^2) + \frac{F}{2}(x_2^3 - x_1^3) \right]$$

$$I_2 = \frac{12V}{j}\left[\sqrt{X}\left\{ AE + \frac{(AF-BE)}{2}\left(x - \frac{3h}{2j}\right) - \frac{BF}{3j}\left(x^2 j - \frac{5hx}{4} + \frac{15h^2}{8j} - 2g\right)\right\} \right.$$

$$\left. + \left\{ (AF-BE)\left(\frac{3h^2}{4j} - g\right) - AEh - \frac{BFh}{2j}\left(3g - \frac{5h^2}{4j}\right)\right\} \frac{1}{2\sqrt{j}} \sinh^{-1}\left(\frac{2jx+h}{\sqrt{q}}\right) \right]_{x_1}^{x_2}$$

$$I_3 = \frac{R}{j}\left[\sqrt{X}\left\{\frac{DE}{2}\left(x - \frac{3h}{2j}\right) + \frac{(EC + DF)}{3j}\left(x^2 j - \frac{5hx}{4} + \frac{15h^2}{8j} - 2g\right)\right.\right.$$

$$\left.+\frac{FC}{4j}\left(x^3 j - \frac{7}{6}hx^2 + \frac{35h^2 x}{24j} - \frac{3}{2}gx - \frac{35h^3}{16j^2} + \frac{55hg}{12j}\right)\right\}$$

$$+\left\{\frac{DE}{2}\left(3h^2 - 4gj\right) + (EC + DF)h\left(3g - \frac{5h^2}{4j}\right)\right.$$

$$\left.\left.+\frac{FC}{8j}\left(\frac{35h^4}{4j} + 12g^2 j - 30gh^2\right)\right\}\frac{1}{4j\sqrt{j}}\sinh^{-1}\left(\frac{2jx + h}{\sqrt{q}}\right)\right]_{x_1}^{x_2}$$

$$A = k_1 x_2 - k_2 x_1$$

$$B = k_1 - k_2$$

$$C = 2\pi \tan\alpha . \left\{ x_2 - x_2 \left(\frac{R_B}{R} \right) - x_1 \right\}$$

$$D = x_1 x_2 \left(\frac{R_B}{R} \right) 2\pi \tan\alpha$$

$$E = \frac{(x_2 - n x_1)}{(x_2 - x_1)}$$

$$F = \frac{(n-1)}{(x_2 - x_1)}$$

$$X = (g + hx + jx^2)$$

$$= \left[R^2 (Cx + D)^2 + 144\, V^2 (A - Bx)^2 \right]$$

$$g = (R^2 D^2 + 144\, V^2 A^2)$$

$$h = 2(R^2 CD - 144\, V^2 AB)$$

$$j = (R^2 C^2 + 144\, V^2 B^2)$$

$$\sqrt{q} = \sqrt{4gj - h^2} = 24\, VR [BD + AC]$$

4. GENERAL SPECIFICATION OF PARAMETERS FOR RESEARCH PROGRAMME

The initial terms of reference for this research were to study friction in drawing, and a conclusion of the review work was that the rotating-die method would be a rewarding technique. Three criteria were used when specifying the experimental parameters. Firstly the general scale of the tests, on rod as opposed to wire, was determined by the equipment available, which was a thirty tonf. hydraulic drawbench. Secondly it was decided to make the tests as representative of industrial conditions as reasonably possible, in order to enhance their practical utility. Thirdly, as wide a range of test conditions was to be covered as was practicable.

Judicious application of these criteria led to complete specification of the test conditions. However, for a variety of reasons which will become apparent, the first series of tests was not entirely satisfactory. Furthermore, the first series was initiated before the possibility of using the rotating-die technique to deduce the distribution of shear stress had been realised. A second, more comprehensive and more closely controlled, series was therefore performed. The second series used slightly different material and conditions, but the same experimental equipment. For this reason, only the general criteria used for the design of the equipment and specification of material are given here. Details of the actual parameters used are given in sections 8, 9 and 10.

4.1 TEST MATERIAL

Considerable quantities of both ferrous and non-ferrous metal are drawn commercially, so either choice would have met the second criterion. However, there were two indications for a ferrous metal.

(a) The split-die technique has only been applied to axisymmetric drawing with aluminium and copper, and it was wished to gather some fundamental data relating to steel.

(b) Had either aluminium or copper been selected, it would have been necessary to use excessively large diameters in order to work the drawbench over a realistic range. The use of high strength non-ferrous alloys was precluded by their general inability to withstand heavy reductions.

Having decided on ferrous material, a low-carbon steel was chosen on the grounds of availability, workability, and the relatively low rate of work-hardening. It was felt that the latter point would ease the problem of defining a mean yield stress when checking the drawing theories.

It is fundamental to the method described for deducing distribution of shear stress (section 3.2) that all tests be made on material which is highly uniform from test to test. From the point of view of checking theories of drawing, it is also desirable to have material which, in the absence of the rigid/perfectly plastic ideal, is at least isotropic and homogeneous. Provision of uniform test material seems to be a recurring problem in Applied Plasticity, particularly when, as here, the sizes and quantities required preclude laboratory processing but are small by industrial standards. Compromise was inevitably necessary, and the method for obtaining the best uniformity was thought to be to require all barstock to be from the same cast, and to be in the drawn and then annealed condition. The latter conditions are to some extent mutually defeating, and in any case it was not found to be possible to satisfy all three conditions simultaneously. Added complications were the unusual length of tag required, and that for the largest reduction the tags had to be work hardened.

4.2 LUBRICANT

Two situations are to be distinguished when considering the selection of lubricant. The first is the case where material is being 'broken-down', and the object is maximum reduction. Here it is usual to use a 'good' lubricant, that is, one which gives a thick film and a low value of μ. For mild steel the best such lubricant is considered to be soap used over a surface preparation such as a phosphate coat.

The second situation is where rod is being given a light 'finishing-pass'. In this case a thick lubricant film is undesirable, as one object is to improve the surface finish. So an oil oubricant is used, and unfortunately a relatively high value of μ results.

It was decided to perform tests with both soap and oil, to cover the range of industrial and experimental variables. However, there was some danger that the oil lubricant might break down completely when drawing the heavy reductions, and it was thoughtadvisable to use both soap and oil in conjunction with a surface treatment. The size and quantity of the barstock made treatment difficult, and it was necessary to use industrial facilities for this.

4.3 DRAWING DIE

The conical die-form was selected, as the large majority of theoretical analysis is for this shape, and it is also widely used industrially. In selecting the angle of the die-cone, it was noted firstly that for any given drawing reduction there is an optimum angle which gives a minimum drawing force, and secondly that this optimum value changes with reduction. However drawing force is relatively insensitive to die-angle over quite a wide range, and the optimum angle is not critically dependent on reduction. Hence it is possible to specify a single die which will give close to optimum drawing force for a wide range of reductions.

Furthermore, the magnitudes of optimum angles are generally agreed, so it would have been pointless to have performed tests over a range of die-angles. Consultation with the manufacture of the die, and study of the literature led to the specification of a die semi-angle of 7°.

Dies which are used industrially invariably have their cone-flank blended into a 'parallel' or'land' at the die-throat, to increase the working life of the die. However there is no satisfactory theoretical analysis of the effect of this parallel, and it was thought that to have followed industrial practice on this point would have jeopardised the possibility of obtaining any useful results at all. It was therefore decided to study the analytically simpler case of a die without parallel.

Tungsten carbide was chosen for the die material, as this is representative of industrial practice, and its high resistance to wear is experimentally convenient.

4.4 SIZE OF TEST MATERIAL

Calculations of drawing force, and information supplied by the manufacturer of the die, indicated that 45% reduction of area was a reasonable maximum to aim for, and four or five different reductions were considered adequate to cover the range 0 — 45%. Considerations of economy and experimental convenience indicated that it would be better to obtain the various reductions by drawing differing sizes of stock through one die, rather than by having a single diameter of stock and a number of dies.

The range of usable drawing forces was set at 2 to 30 tonf. by the hydraulic drawbench. Calculations of drawing force were made using Siebel's formula. For this purpose, values of μ of 0.05 for soap and 0.1 for oil were assumed (2), and mean yield stresses for mild steel were taken from data given in reference (77). On this basis the diameter of the die-throat was selected as one inch, and this enabled nominal sizes of 1.1/16, 1.1/8, 1.3/16, 1.1/4 and 1.5/16 in. diameter to be specified for the stock. Stock was obtained in the longest lengths conveniently available, to reduce the amount of tagging required, and to increase uniformity between tests.

4.5 DRAWING SPEED

The test speeds were selected to cover as wide a range of swing of friction vector θ, and hence of force reduction, as possible. Clearly θ could have been varied by altering rotational speed at constant drawing speed, or vice versa, or by altering both speeds simultaneously. As the object was to evaluate friction in the non-rotational case, it was decided to run the tests at constant drawing speed.

For the greatest realism, the drawing speed should have been the maximum possible with the drawbench, which was nominally 15 ft/min. However, some reduction in this figure was anticipated with the higher drawing forces, and 13 ft/min. was fixed as the test speed. Due partly to the difficulty of setting the drawing speed accurately to a pre-determined value, and partly to a desire to cover the widest range of parameters, tests were eventually run over the entire speed range, but the figure of 13 ft/min. was used for the design calculations.

4.6 ROTATIONAL SPEED AND POWER

To have covered the entire 0 to 90° range for θ would have required infinite power. From section 3.1

$$\text{Torque} \propto \sin\theta$$

$$\text{and } \tan\theta \propto \text{Rotational Speed}$$

$$\text{Therefore Power} \propto \sin\theta \, \tan\theta$$

$$\text{Furthermore} \quad \text{Force-Reduction} \propto (1 - \cos\theta)$$

These relationships are illustrated in Figure 4.1. It is clear that in terms of the extra increment of θ obtained for a given increment of power, it becomes experimentally unprofitable to go much above 60°. The force-reduction curve tends to linearity in this region, so this argument also applies to the force-reduction available for a given power. Of course θ does not take a unique value throughout the die, but the model described in Section 3.1

was used for the design calculations. The data used was as for sections 4.4 and 4.5.

Selection of values of θ up to between 45° and 60° led to a specification for a drive which could deliver 5 H.P. at a maximum speed of 50 rev/min. Calculations showed that this might not be sufficient power for the highest speed tests on the largest size barstock, when using oil lubricant. It was decided not to go to a higher power drive, as the next step was to $7\frac{1}{2}$ H.P., and the small number of tests which were involved did not justify the considerably greater cost and difficulty of assembly. Furthermore, it was felt that in view of the additional torque loading on the tag, it might well prove impossible to perform those tests at all.

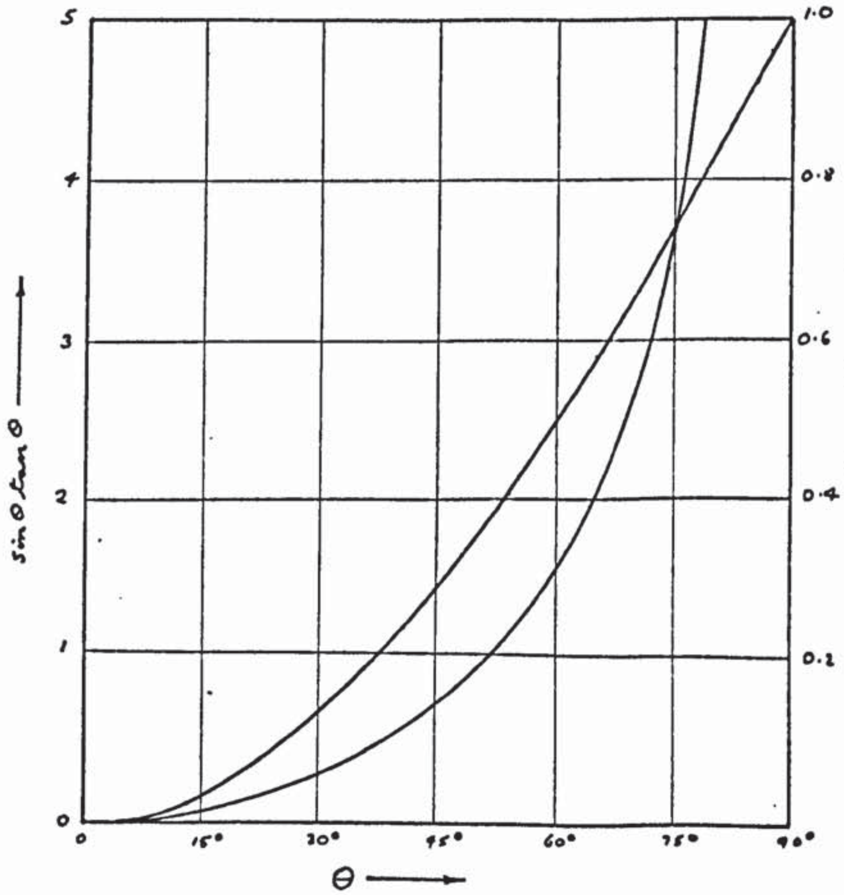

Fig.4.1- Relationship between Swing of Friction Vector (θ) and Reduction in Drawing Force (1- cos θ), and Power Required for Die-Rotation (sin θ. tan θ).

5. MODIFICATIONS TO THE DRAWBENCH

A Brookes hydraulic tube-drawing bench of 30 tonf. capacity and 54 in. stroke was used for the drawing tests. As supplied, the drawbench had no instrumentation other than a pressure gauge in the pump delivery line, and no provision for die-rotation. The drawing speed control was also found to be unsuitable for experimental purposes.

5.1 HYDRAULIC SYSTEM

The speed control dial was graduated from 0 to 15 ft/min., but at drawing loads below 2 tonf. the control valve was inoperative, and the minimum available speed was then 11 ft/min. Even at higher loads it was not possible to draw at less than 5 ft/min.

A needle valve was fitted in the oil return line from the hydraulic ram (see Plate 3). It was thus possible to create a back-pressure in the cylinder, which simulated a working load, and enabled the bench to be run over the 5 to 15 ft/min. range without drawing rod. However, some back-pressure was developed even with the valve fully open, thus reducing the load capacity. To overcome this an enlarged valve seating was fitted. It was later realised that by suitable manipulation of this valve, in conjunction with the pressure relief valve in the pump delivery line, it would be possible to draw over the entire 0 to 15 ft/min. range. To make this technique work (see Appendix 2) it was necessary to refit the original seating and accept the reduction in load capacity. This was only significant at the higher speeds, and even then did not limit the tests described here.

The hydraulic cushioning system, originally built into the ram, was removed to increase the useful working stroke.

5.2 ROTARY DRIVE

For experimental flexibility an infinitely variable speed drive was preferred, and these are generally either constant power or constant torque devices. For this application maximum torque would always occur at maximum speed, so either type could have been used. The speed range was specified in Section 4.6 as 0 to 50 rev/min. with a 5 H.P. drive, and several possible systems were compared. The Carter hydraulic gearbox was selected as the most suitable from all aspects, this gearbox comprising a complete hydrostatic system in a single casing.

The complete rotary drive arrangement is illustrated in Figure 5.1 and Plates 1 and 2. Details of the equipment are given in Appendix 1. It will be seen that the components of the drive were mounted in line on a fabricated bed, which was in turn mounted on two box sections above the end of the drawbench. The barstock ran between the box sections on roller supports, and then into the thrust block. The fabricated bed provided a reference plane for alignment of the drive components, and was bolted down at the front end, to the top of the die support pillars built into the drawbench. The final drive to the thrust block was taken vertically down by chain, adjustment of chain tension being by shims under the front end of the fabricated bed.

5.3 THRUST BLOCK

The manufacturing and assembly drawings for the thrust block appear in Appendix 6.1, and it is partly shown in Plates 1 and 2. As its principal purpose was to allow the die to be rotated under load, the thrust bearing was the definitive component. A taper roller bearing was used (see Appendix 1), and was selected with a safety margin on its rated brinelling load. The normal industrial ratings for a 3,000 hour useful life were considered irrelevant.

The thrust bearing was a shrink fit over the hollow central drive shaft, and abutted the flange at the upstream (i.e. bar inlet) end of the shaft. This shaft was located in the thrust block housing, at the upstream end by the main thrust bearing, and at the other end by a second taper roller bearing fitted in the rectangular end plate. This bearing was required to take little load, its principal functions being to preload the main bearing, and to carry the journal load due to the chain drive. The chain drive entered the thrust block through two holes in the housing, and went to a chain wheel mounted on the hollow shaft between the bearings.

The hollow cylindrical die housing was bolted and dowelled to the flange of the central shaft, and the die butted against the flange. The three jack screws spaced around the die housing were used to centralise the die, the torque drive being supplied by the key. One of the jack screws also held the key down. The die housing was made slightly shorter than the die, so that the latter could be located axially by the retaining plate. The bolts holding the retaining plate to the die housing must not be overtightened, or the flange of the hollow shaft will be distorted.

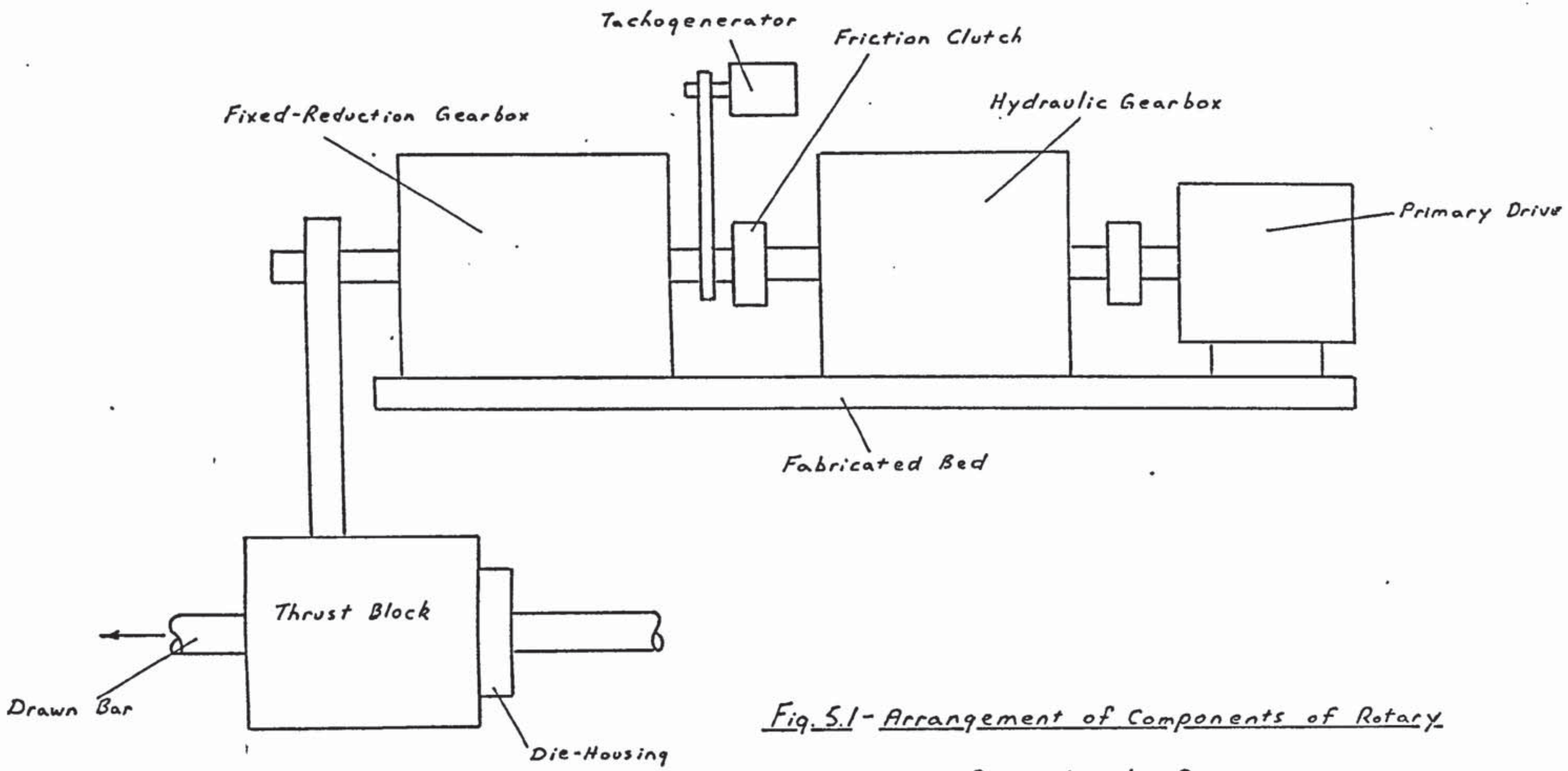

Fig. 5.1 - Arrangement of Components of Rotary Drive to the Die

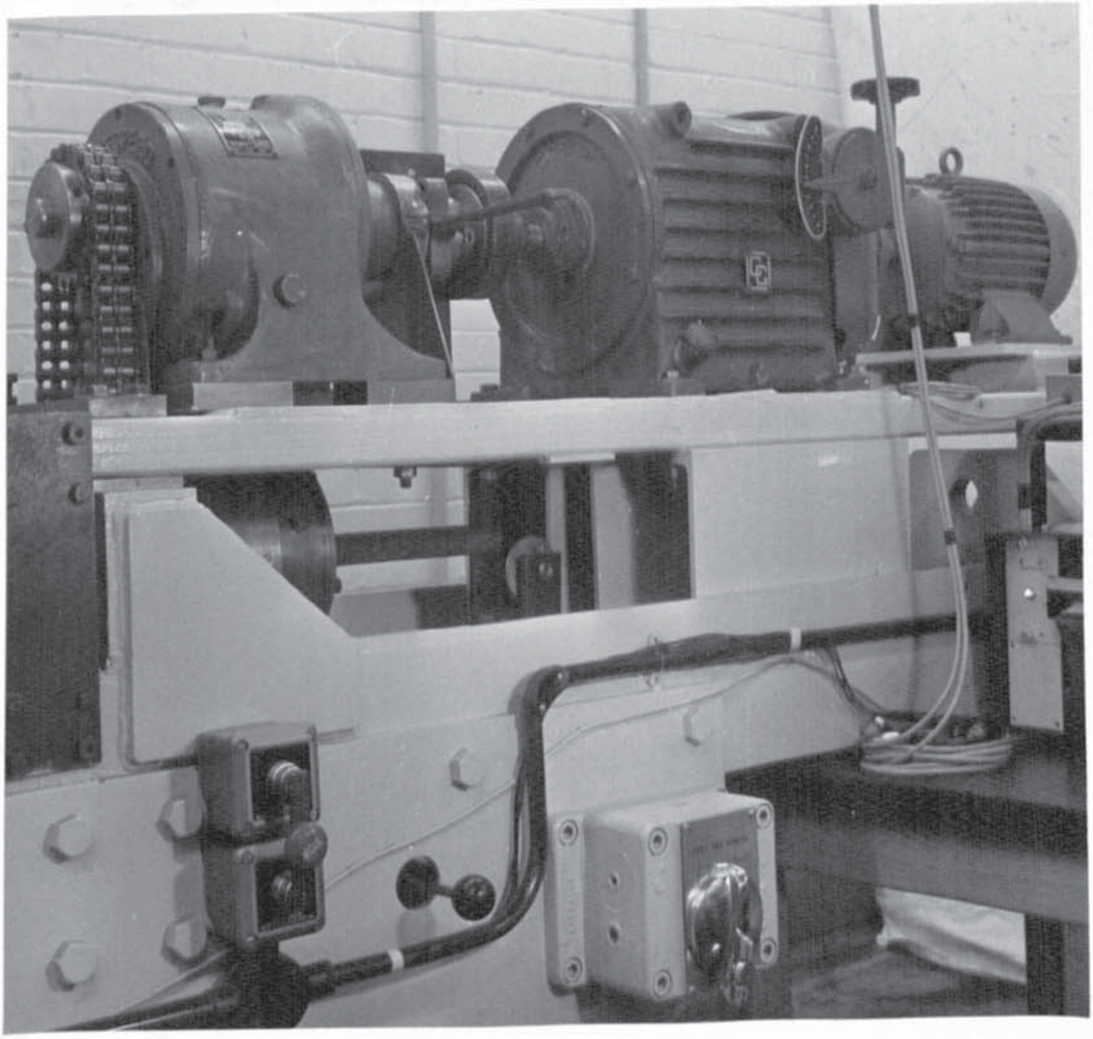

Plate 1 :- ROTARY DRIVE

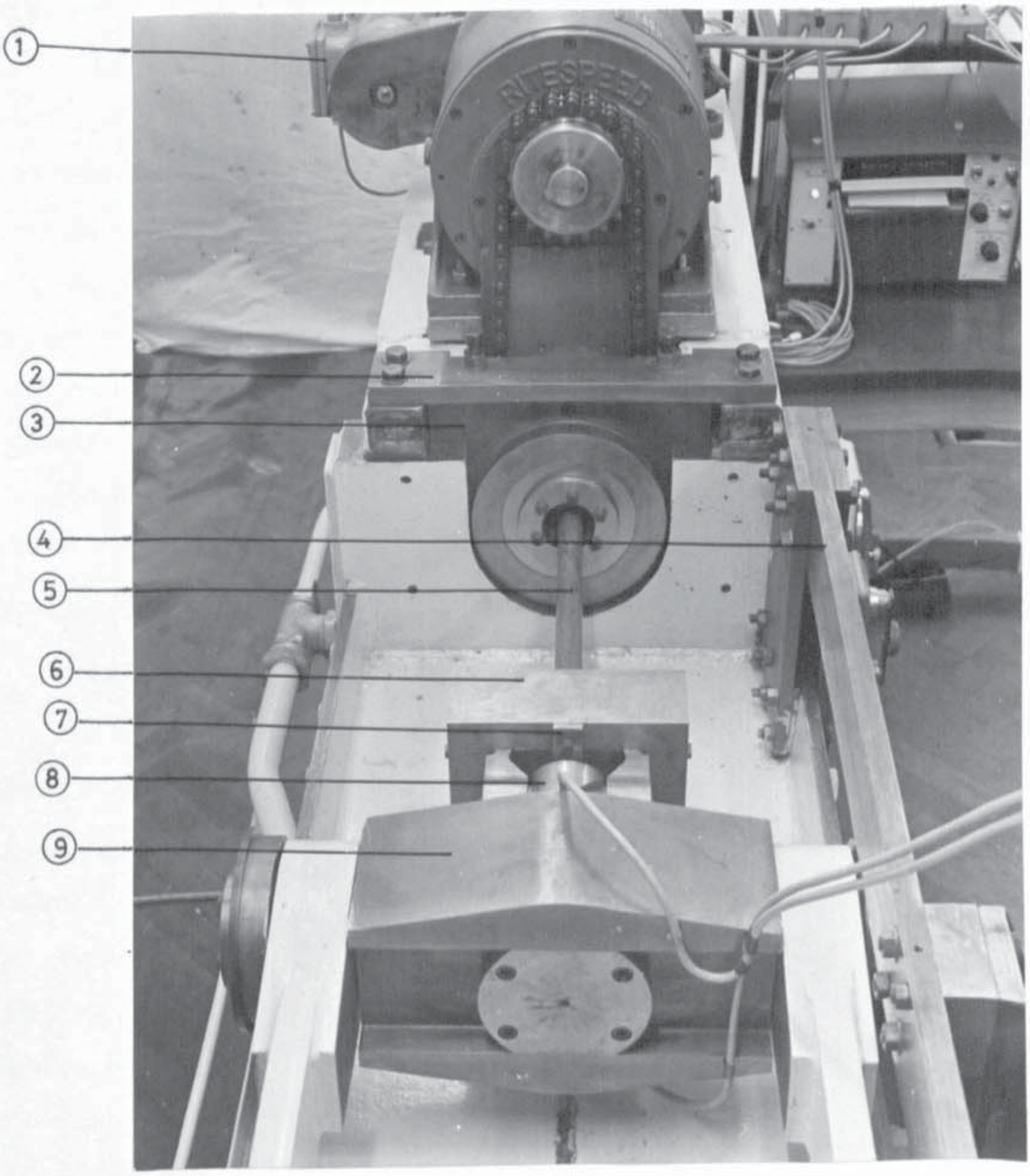

(1) Tachogenerator
(2) Clamping Strip
(3) Front Plate of Thrust Block
(4) Torque Rail
(5) Drawn Bar
(6) Jaw-Housing
(7) Heel-Plate
(8) Load-Cell
(9) Cross-Beam

Plate 2:- OPERATIONAL AREA

The rectangular end plate was similar in size to the original die holder supplied with the drawbench, and this allowed the original clamping strips to be used to locate the complete thrust block. These clamps located the thrust block in the horizontal plane only, and a strip with two jack screws was fixed across the top of the die support pillars to oppose the chain tension (see Plate 2). An external reservoir was connected to the oil sump in the thrust block, in order to increase its effective volume.

The only drawback with this design of thrust block was that unusually long tags, about 14 in., were necessary on the barstock, as they had to pass through the complete unit before reaching the jaws. However, the alternative arrangement would have produced a cumbersome and unsatisfactory design.

The bore of the hollow shaft was made as large as possible with the particular choice of thrust bearing, to increase the versatility of the equipment for possible future investigations.

5.4 LOAD-CELL ASSEMBLY AND TORQUE-RAIL

The original cross-beam was integral with the jaw-holder, and was replaced with this unit so that torque and drawing force could be measured at the tag. Careful design was necessary to avoid shortening the working stroke. The assembly is shown in Plate 2, and the manufacturing drawings are in Appendix 6.2. The load-cell also appears in Plate 4. In this section the load-cell is treated simply as a mechanical link, the design as a force/torque transducer being described in Section 6.

The cross-beam was free to pivot in the ends of the tie-bars, and ran on the original flanged wheels. As a corollary to the provision of die-rotation, it was necessary to restrain one of these wheels so that it did not lift off its track. The torque-rail (see Plate 2) was designed to do this. It was positioned on assembly to have a small running clearance, and then dowelled so that if necessary it could be removed without losing the setting.

The load-cell passed through the cross-beam from the rear, and was bolted to it by the flange. Drawing force and torque were both taken directly by the flange. Connection of the load-cell to the jaw assembly was via a trunnion pin through a cross-hole in the load-cell, and this was parallel to the axis of the cross-beam. The load-cell was therefore free to pivot at both ends, about an axis transverse to that of the drawbench. A further degree of freedom arose from side clearance between the flanged wheels and the track. The ideal of having crossed pivot joints at each end of the load-cell could not be achieved without seriously reducing the working stroke.

Shortly after the load-cell was first subjected to its maximum design load of 30 tonf., a faint crack was noticed inside the cross-hole. The load-cell was then cycled a number of times to 35 tonf., and a close watch was thereafter kept on the crack. It never showed any sign of spreading after its first appearance, and it was concluded that it was merely a surface crack caused by the hardening and grinding processes.

5.5 JAW ASSEMBLY

This can be seen in Plate 2, and the manufacturing drawings appear in Appendix 6.2. The jaw design followed the general pattern of the wedge type found in tensile testing machines. The wedge angle was made larger than usually found in testing machines, partly to reduce the possibility of the jaws locking, and partly to reduce the load on the jaw housing. The conventional type of vee-slot used within jaws, was considered to be unsuitable for resisting torque loading and for drawing with large reductions of area. The gripping part of the jaws was therefore made circular in section, and the jaws were suitable for only the one size of bar. The bore through the jaws was tapered slightly from end to end, to bite deepest at the more lightly stressed end of the tag. The teeth themselves were of buttress thread form, and were also slotted longitudinally to give individual teeth points. This form was completely successful, and once the jaws bit, no slippage in either direction was ever observed.

The jaw side plates fitted over the ends of the trunnion pin where it protruded from the cross-hole of the load-cell. They carried the drawing force and torque reaction, and provided the wedge angle for the jaws. The side plates fitted inside the rectangular housing, which resisted the splitting force on the jaws and held the side plates in alignment against the torque reaction, but did not carry any direct drawing force. The housing carried an internal triangular guide plate which separated the two halves of the jaws. Originally there was no provision for preloading the jaws and they would not bite, so the heel-plate shown in Plate 2 was added. One end of this bore on the housing, and the other on the jaws. It drove both halves into the wedge simultaneously, and thus performed the function of the cross-linkage usually found with testing machine jaws. The lack of such a linkage caused no trouble, except occasionally with unduly ragged tags. The restricted space which was available made the heel-plate awkward to use, and it also had a short life because of the recoil of the machine on completion of a drawing operation. It is recommended that an alternative arrangement be developed for any future work but care must be taken not to weaken the housing significantly.

The jaw assembly pivoted on the trunnion pin, and a wheel was therefore attached to support it when not drawing bar. The height of the wheel was such that it lifted clear of the bed of the drawbench during the working stroke, and did not interfere with the self-alignment of the load-cell. Slight warping of the trunnion pin took place under load, and thereafter it could be readily removed and refitted in only one alignment, which was indicated by dots stamped on one end of the pin and on a side plate. Future refitting of the pin should commence with these dots in conjunction, and the pin should be driven straight in. Loosening the bolts holding the side plates to the jaw housing was found to ease this operation.

6. INSTRUMENTATION OF DRAWBENCH

Four parameters were to be measured in the drawing tests. These were drawing speed and force, and rotational speed and torque. Although it was envisaged that measurements would be made under essentially steady state conditions, data recording was to be continuous. A policy decision to use direct current transducers was made, to reduce cross-coupling effects in the wiring, and continuously screened cable was used throughout.

Numbers of carbon resistors were used for current limiting and galvanometer damping purposes. It was established that some early trouble with signal drift was due to self-heating of these resistors, although they were being operated within their rated load. They were therefore replaced by metal oxide resistors, which have much better temperature stability, and requisite values of resistance were built up from numbers of resistors, in order to reduce generation of heat in individual components.

6.1 SPEED MEASUREMENT

Rotational speed may be easily measured by using a tachogenerator, but linear speed is more difficult. The common system of measuring position and differentiating with respect to time was rejected, mainly because of the limited accuracy that could be expected of available equipment. Velocity transducers are available, and although they usually have much shorter strokes than needed here, it would have been possible to overcome this by using a cam arrangement. However, the manufacturers of the only such transducer then known to the author claimed only 10% reliability for their calibration figures, and this referred to possible variations in output from point to point of the working stroke. To have achieved high accuracy it would have been necessary to calibrate at different parts of the stroke, and to have recorded position during the drawing tests. It was therefore decided to make a linear to rotary conversion, and to use tachogenerators for both speed measurements.

D.C. tachogenerators are inherently subject to two types of distortion of output signal. Brush noise is random, and as it is of high frequency it may be easily filtered out. There is also some regular A.C. component, or ripple, superimposed on the D.C. signal. The ripple has the same frequency as the rotational speed, or some whole multiple thereof, and arises from non-uniformity in the windings or magnetization of the poles, and bearing eccentricity. The magnitude also varies with operating speed. The overall effect was of differing importance between the two measuring systems.

6.1.1 Rotational Speed

A one to one chain drive, taken from the input shaft of the fixed reduction gearbox (see Figure 5.1) was used to drive the tachogenerator. There was therefore ample power available to drive a large marine tachogenerator (see Appendix 1) and the operating speed was relatively high, being about 1,400 rev/min. at maximum speed. As a result, ripple on the recorded data was both small in amplitude, being equivalent to a few thicknesses of the recording line, and of short period. It was therefore easy to ascribe a mean value to the signal, and ripple was no problem here.

The voltage output from the tachogenerator was too high to pass directly to the recording galvanometer, and an additional resistance load was used (see Figure 6.1). It will be seen that a three position switch was incorporated in the circuit, enabling the resistance load to be varied. The purpose was to increase the galvanometer deflection at the lower speeds, but this facility was not needed in practice, and the maximum resistance load was always used. The resistance was arranged on each side of the capacitor to maximise the noise suppression obtained with the given capacitance, and this arrangement also served to limit the start-up current. It was verified that the time-constant of the circuit was small compared with the dynamic response required.

6.1.2 Drawing Speed

The basic problem with the proposed system for measurement of drawing speed, lay in arranging for the tachogenerator to be driven at a usefully high speed. The maximum speed with the arrangement used was about 100 rev/min., and at this relatively low speed, both ripple and brush noise can limit the utility of tachogenerators. Tachogenerators which can adequately measure very low speeds are available, but they are both large and expensive. In principle the drive could have been geared up once the linear to rotary conversion had been made, but in view of the magnified inertial effect, this would have required a positive drive such as chain or rack and pinion. Assessment of the available tooth pitches and pinion sizes led to the conclusion that even with a large step-up ratio, no greater speed would have been obtained than with the simple string and pulley system used. In addition the periodic fluctuations which were to be expected with small pinions, could have been

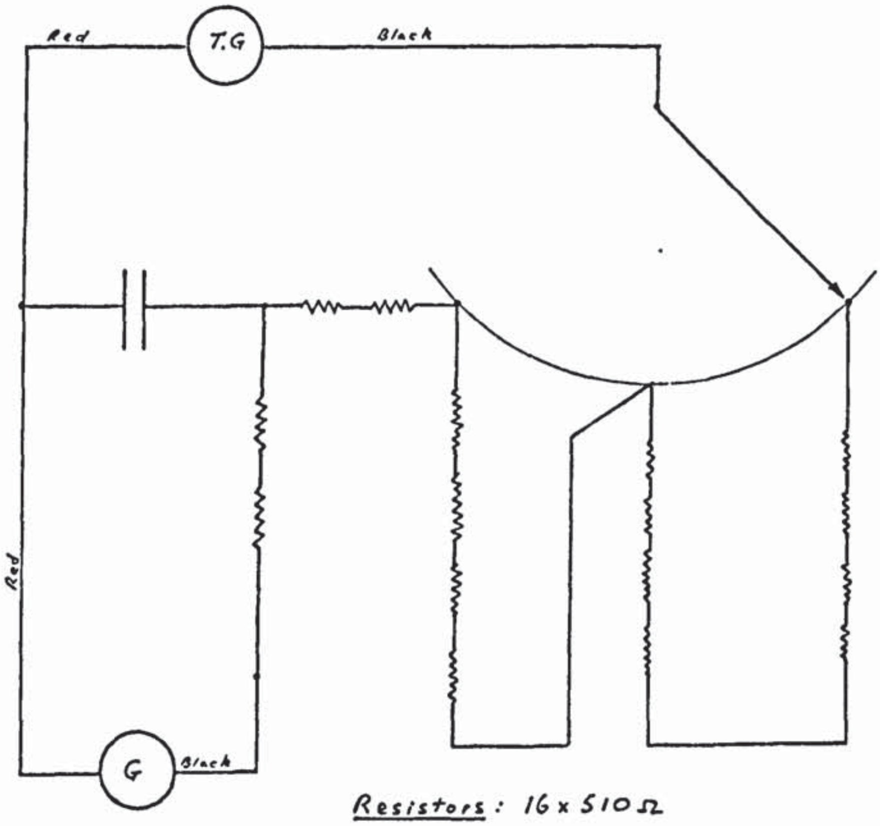

Resistors: 16 x 510 Ω

Capacitor: 10 μF., 35 volts max.

Fig. 6.1 - Circuit Diagram for Measurement of Rotational Speed

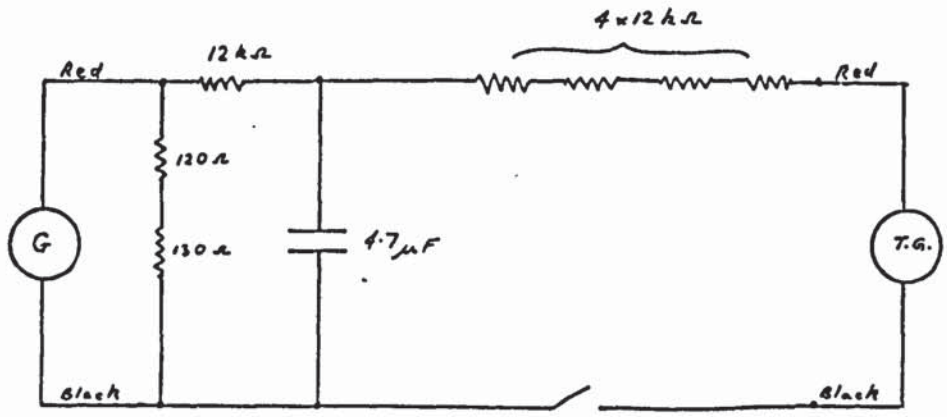

Fig. 6.2 - Circuit Diagram for Measurement of Drawing Speed

easily mistaken for genuine speed variations.

A low inertia aircraft tachogenerator (see Appendix 1) was used, with the arrangement shown in Plate 3. The unit was originally mounted directly on the drawbench, near the die. In this position the output was markedly affected by vibration from the rotary drive to the die, and by electromagnetic noise from the drive motor of the hydraulic system. The final location, as shown, was on a free standing pillar, which required careful positioning to align the string.

The lower limit on pulley size was not set by string slippage as had been anticipated, but by variations in string diameter and groove depth. Thus a much smaller pulley than was finally used could drive the tachogenerator, but variations in these quantities distorted the output signal. This effect was particularly marked with conventional drive cords, which are usually braided. Many types of 'string' were tried, both metallic and non-metallic, and glass fibre yarns were found to give the best results. Of these the best was 'Radiospares Special Drive Cord'. This is a loosely spun yarn, with a braided nylon sheath. The sheath had to be stripped from the core, and this was a delicate operation, but it was useful as it could be left on at the end connection points, where it protected the fragile yarn. The yarn was susceptable to fraying during use, and it was replaced between the two test series.

As with the rotational speed system, some additional load was incorporated in the output circuit, and brush noise was suppressed capacitively (see Figure 6.2). However ripple was not insignificant. This component was about 5%, measured peak to peak, of the D.C. signal level, and had twice the frequency of the operating speed of the tachogenerator. This meant that with the relatively few revolutions made by the tachogenerator during the stroke of a drawing test, ripple could be mistaken for genuine speed fluctuations. The method used to overcome this problem was thought to be novel.

If a tachogenerator with zero inherent ripple were to be driven by an elliptical pulley from a constant velocity source, then the signal would have the form described above. It follows that the inherent ripple of the real tachogenerator could be apparently removed by driving it through an elliptical pulley, mounted in suitable angular relation to the rotor shaft. In practice the differences between the axes of the ellipse were small, and the profile was constructed from circular arcs, by mounting the pulley on a

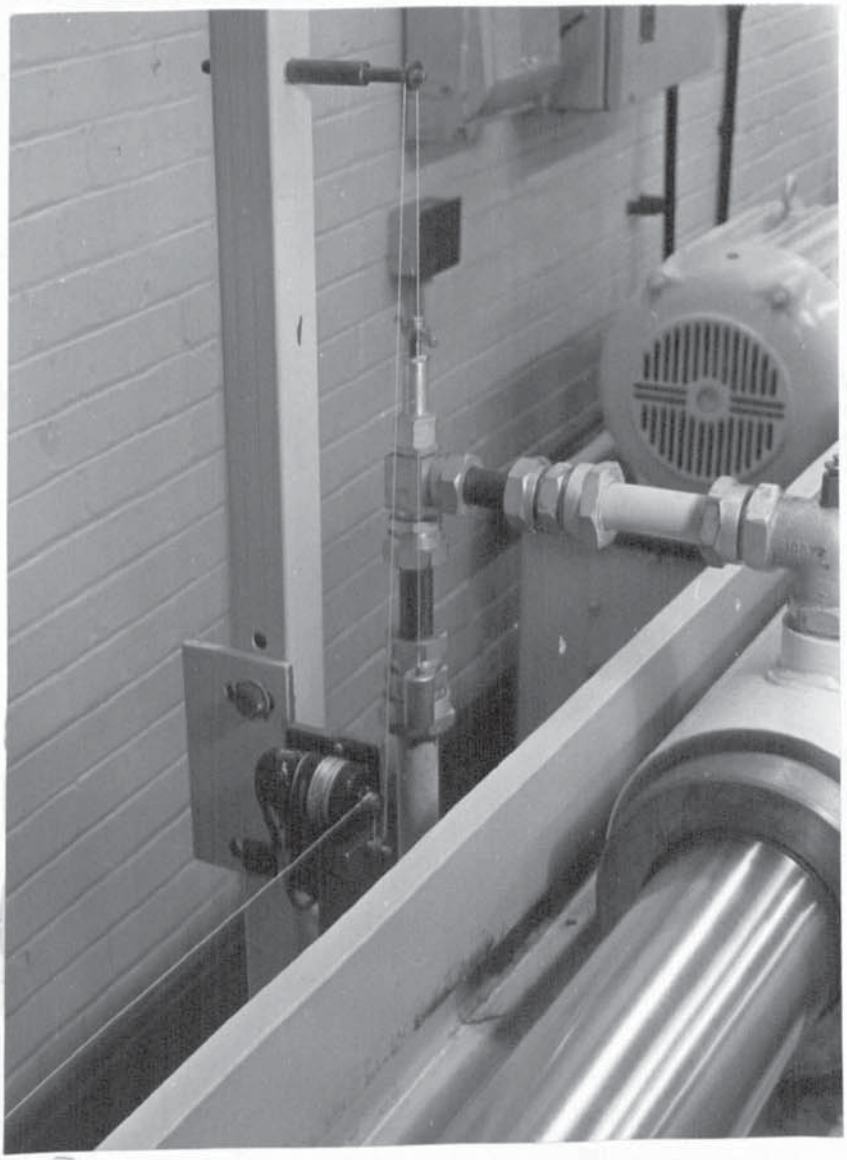

Plate 3 :- ARRANGEMENT OF DRIVE TO DRAWING-SPEED TACHOGENERATOR

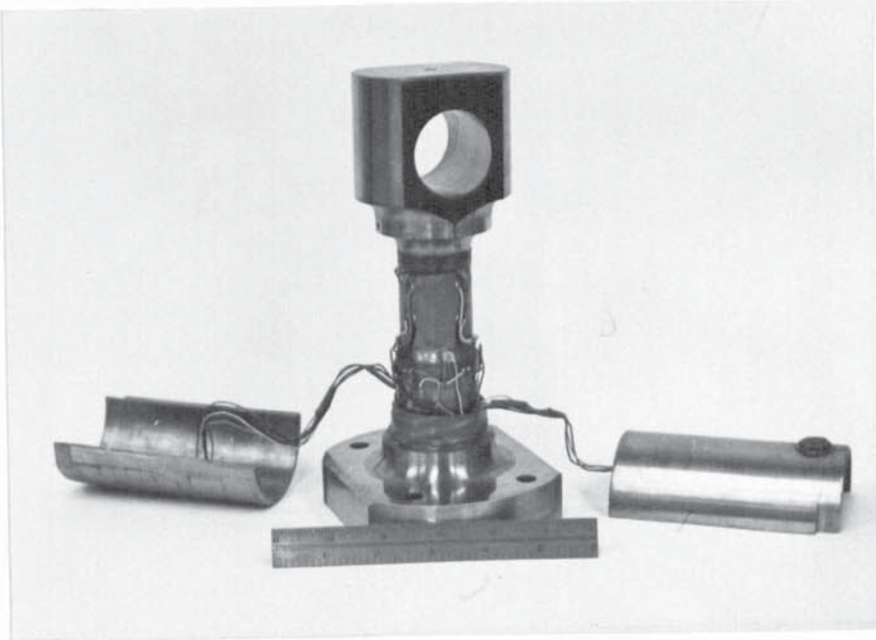

Plate 4 :- LOAD-CELL

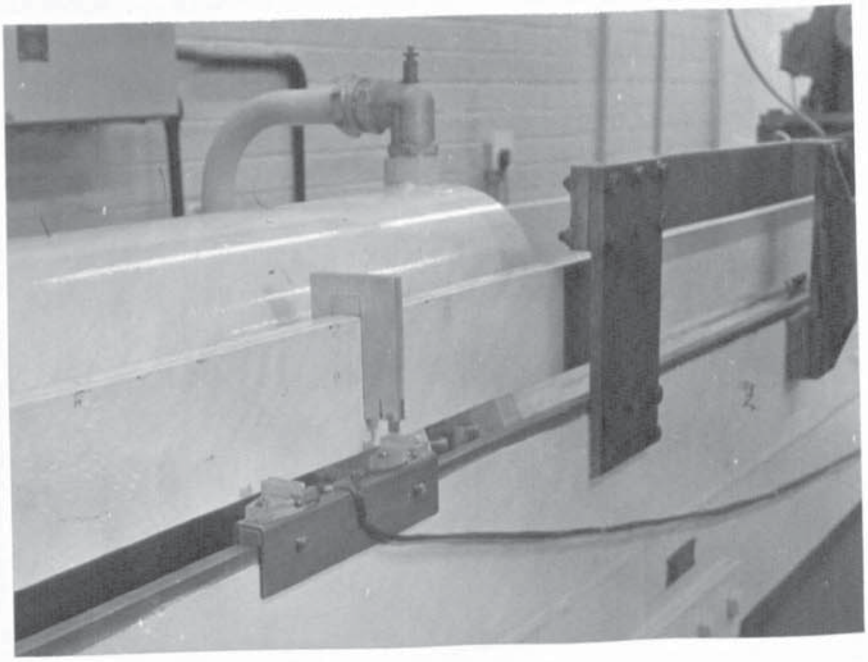

Plate 5 :- CALIBRATION OF DRAWING SPEED

spigot held offset in a four-jaw chuck. Quite a good first approximation to the required ovality was obtained, by considering the correction needed, but the final form was the result of considerable experimentation. It is represented in Figure 6.3, together with an accurate profile. The latter should be interpreted as showing the variation in radius of the pulley, measured at the bottom of the groove, around the periphery of the pulley. The groove itself was of vee-form, with an included angle of 60^{o} and tip radius of 0.012 in.. The optimum angular location of the pulley, relative to the shaft, was found by trial and error, and it should not be disturbed. It should also be noted that with the pulley set in this position, the ripple correction is only effective when the tachogenerator is mounted in the attitude shown in Plate 3.

Ripple correction was virtually perfect at the start of a drawing stroke, the amplitude being little more than the thickness of the writing line. Some decrease in the effectiveness of the correction was observed throughout the stroke. This change was probably caused by the increase in the active length of drive cord, which made it less stiff, and therefore less able to transmit the pulsating force necessary for the cyclic acceleration of the tachogenerator.

The tachogenerator signal was modulated by vibration of the drawbench. The magnitude was only significant when the speed of the rotary drive to the die matched a resonant frequency of the cantilevered end of the drawbench, and this occurred at between 30 and 40 rev/min. The resulting signal noise was of higher frequency than the original ripple, but was not so much higher that it could be filtered electrically. In appearance it was spiky and close packed on the record trace, and mean values could be selected readily.

6.2 LOAD-CELL

Drawing force and rotational torque were measured at the tag end of the bar, with a combined force/torque load-cell. The disposition of the unit as a mechanical component has been discussed in Section 5.4 and is shown in Plate 2. Advantages of this arrangement were that slip-rings were not required, measurements were not subject to friction effects, a single load-cell sufficed, and alignment problems were minimised.

The load-cell was designed and built to be a high accuracy permanent installation. Material and heat treatment are described on the manufacturing drawing in Appendix 6.2, and the unit is shown in Plate 4 prior to being water-proofed. The two diameters of the mid-section carried the separate

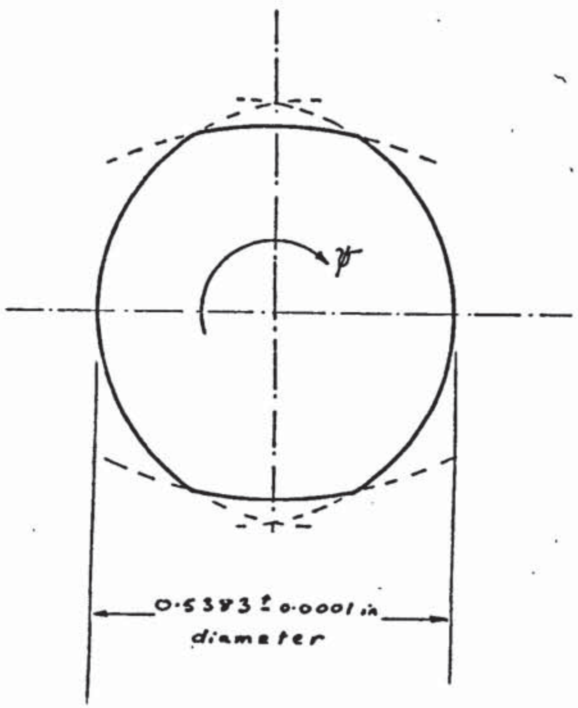

(a) End View of Pulley.

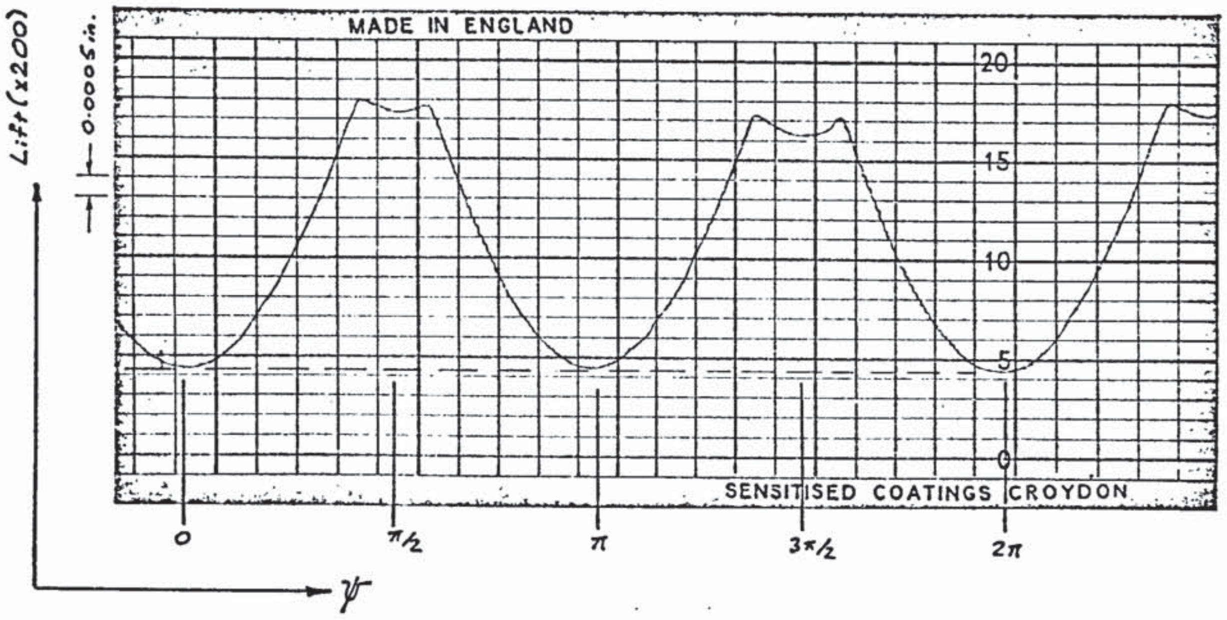

(b) Development of Periphery of Pulley

i) 'Lift' is change in radius above base value indicated in (a).

ii) ψ measured clockwise, viewing tachogenerator from shaft end.

iii) Origin for ψ taken from radius through pulley clamping screw.

Fig. 6.3 - Profile of Pulley for Tachogenerator Drive

force and torque bridges, both of which were four-arm, fully balanced and compensated for temperature and bending (99). Alignment and positioning of the gauges, and the internal wiring of the bridges, are shown schematically in Figure 6.4, and the complete circuit diagram in Figure 6.5.

A nominal maximum of 0.1% strain in the active direction of the gauges, under maximum combined loading, was used as the design criterion for the load-cell diameters. If stability of the gauge bonding material is taken as the limiting factor, it would have been better to have used 0.1% strain in the direction of maximum principal strain, and this would have resulted in both sections having the same diameter. However, the criterion which was used led to a maximum principal strain under combined loading of about 0.16% on the torque bridge section, which had the smallest diameter, and this value is not regarded as being unduly high. Specific design figures are given in Appendix 1, together with details of the gauges. The diameters of the load-cell were large enough for it to be unnecessary to use a hollow section.

Metal foil gauges were used, and the manufacturers recommendations regarding surface preparation, choice of adhesive and application of gauges, curing, and soldering of leads, were followed scrupulously. As the gauges used are no longer commercially available, details of these procedures are not given here. The bridges were completed within the load-cell, and the leads firmly secured and soldered to two separate gold-plated socket connectors. It was necessary to mount these flush with the surface of the load-cell cover pieces (see Plate 4), because of the small clearance available when fitting the load-cell to the cross-beam.

The linear gauges used for the force bridge were taken from a single batch, with a manufacturer's tolerance of $\pm$ 0.5% on resistance. As expected the completed bridge was slightly out-of-balance, and this was corrected using a resistance in parallel with one arm. This resistance comprised a small trimming resistor for datum adjustment, and a large fixed value to obviate the possibility of short circuiting the arm. In practice, the former was never re-adjusted once it had been set.

The torque gauges were also taken from a batch matched for sensitivity, but the variation in resistance values was much larger, being about 5% overall. The manufacturers recommended a technique for polishing individual gauges to increase their resistance, prior to the connection of leads. This was so

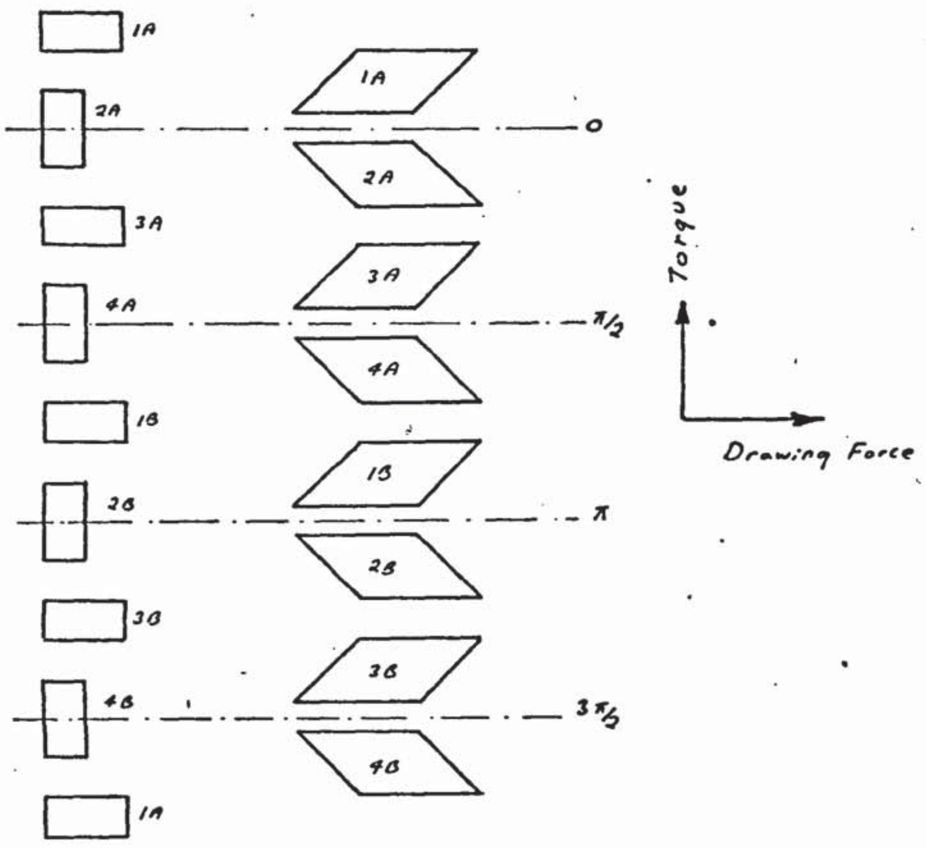

(a) Development of Surface of Load-Cell

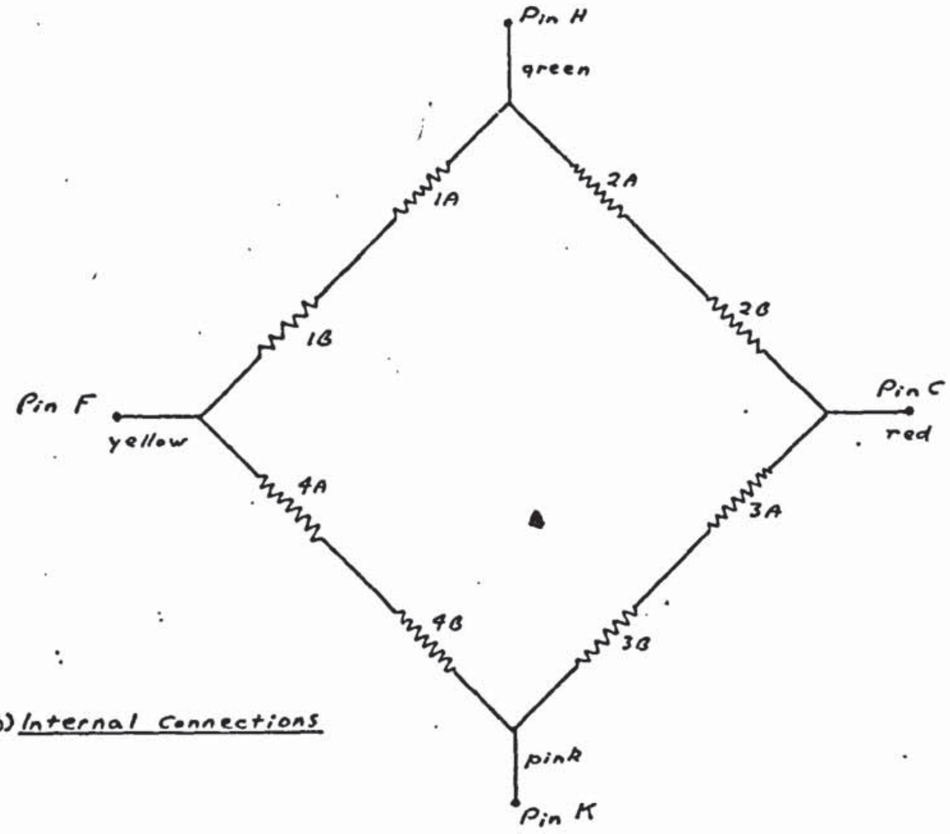

(b) Internal Connections

Fig. 6.4 - Alignment of Strain Gauges and Internal Wiring of Drawing Force and Torque Bridges

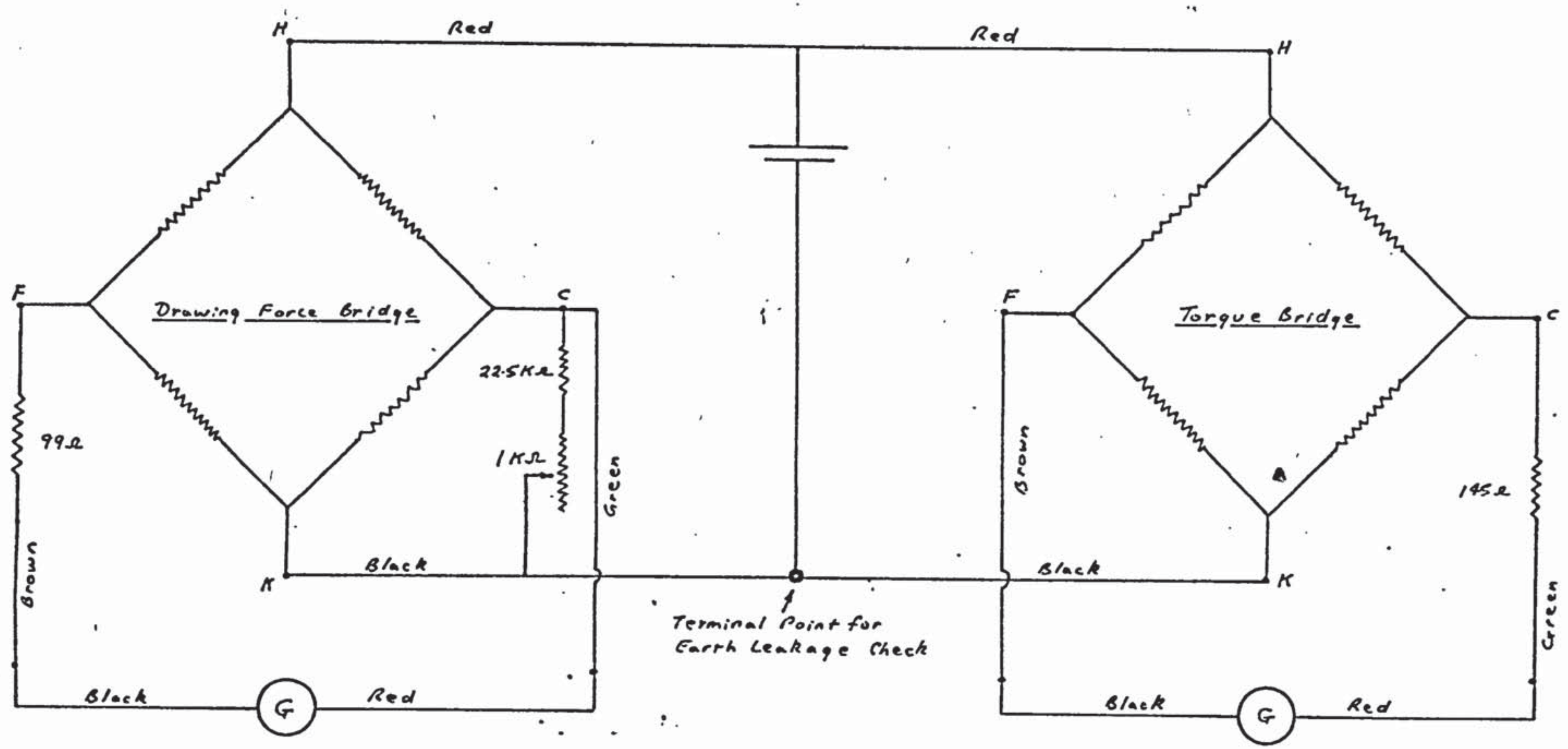

Fig. 6.5 - Circuit Diagram for Load-Cell (Further details given in Appendix I)

successful that the residual out-of-balance would have required a parallel resistance of several megohms to remove it, and the torque bridge therefore had no external trimming.

Water-proofing was done after a final curing operation, by packing the load-cell cover pieces with Di-Jell. This was used in preference to more modern techniques because, if necessary, it could be easily removed without damaging the gauges. An external terminal post was provided for each bridge to facilitate checking of the earth-leakage resistance, and this was found to be always in excess of 200 megohms. Should this fall significantly at any time in the future, the load-cell should be re-cured at 80°c for about twelve hours. The Di-Jell should first be removed, care being taken not to contaminate the electrical contacts.

The load-cell functioned with complete reliability throughout all tests.

6.3 DATA RECORDING

This was done with a ten-channel, continuous writing, ultra-violet galvanometer recorder (see Appendix 1). Test results were expected to be taken under steady-state conditions, so the dynamic response of the galvanometers was not critical. However it was considered to be desirable to use the stiffest galvanometers reasonably possible, to reduce signal noise. Ample signal was available from the rotational speed transducer to drive a high resonant frequency fluid-damped galvanometer, but those used with the load-cell and drawing speed transducer had no inherent damping. The manufacturers recommended circuit matching for damping these galvanometers to give optimum dynamic response, and although this was not critical for these tests, it was done again to reduce signal noise.

6.4 LOAD-CELL SUPPLY VOLTAGE

The choice of supply voltage had to be high enough to give a useful signal, and low enough to avoid heating the gauges significantly. As discussed above, it was possible to use galvanometers of high sensitivity, so the usable range of voltages was wide and the figure of 7 volts was selected. With this value it was possible to use galvanometers which were not the most sensitive available, and the power consumption was less than a third of that which could have been used without exceeding the manufacturers recommended figure of 0.5 watts/in^2. The load-cell also provided a substantial heat sink so thermal drift of the output was never observed.

A single stabilised voltage unit (see Appendix 1) was used to supply both bridges.

7. CALIBRATIONS

The high degree of repeatability required has been discussed in Section 3. Although the exact analysis given in that section was not available at the time of these calibrations, it was clear that variations of the order of 0.1% f.s.d. could be significant, particularly with regard to measurement of load reduction. This seemed to be roughly the limit that could possibly be achieved with the available equipment, and it was therefore taken as a general target figure for each parameter. The chief obstacle was found to be with the data recording system, and considerable effort was devoted to improving this.

7.1 LOAD-CELL SUPPLY VOLTAGE

Stability of supply voltage was critical with the continuous deflection measuring system used, and it was also desired to use the load-cell supply as a reference for calibration of the galvanometers, as discussed in Section 7.3. This voltage was therefore checked frequently during calibrations and drawing tests, with a digital voltmeter. Owing to shortage of equipment, two different meters were used at various times, but they were calibrated against each other as well as against their own internal standard cells. Drift of the supply voltage was found to be very slight. It was not always possible to set it to exactly 7 volts, and variations of up to about 5 millivolts were tolerated, but were corrected for at the stage of data measurement.

7.2 ULTRA-VIOLET RECORDER, GALVANOMETERS, AND SENSITIVITY DRIFT

With the U.V. recorder used (see Appendix 1), the maximum useable deflection was about five inches, so great care was needed when taking measurements from the record charts. In all cases zero positions were set up before and after a signal recording, and datum lines were ruled across between them. The deflection of the signal from the datum was measured with a finely divided steel rule and magnifying glass. A needle was used to locate the centres of the signal and zero traces, and also to rule the datum. By making multiple measurements on the same signal, it was established that repeatability within $\pm$ 0.003 in. could generally be obtained. The simpler method of measuring from the imposed grid lines was not used, as this would have involved two separate measurements.

One problem which was never satisfactorily resolved was that with the particular recorder used, the paper sometimes tended to ride up off its backing roll. This was not allowed to proceed unchecked, as significant error could have resulted from the change in optical path length.

Calibrations were performed on the complete transducer/galvanometer/recorder arrangement, with the same components as used in the drawing tests. The calibrations were performed with the galvanometers in the same channels in the magnet block, and from the same zero positions, as were used in the drawing tests. The former was to overcome the effects of variations in magnetic field across the block, and the latter to overcome non-linearity in the optical system. These details are given in Appendix 1.

During calibration, a drift in the sensitivity of the force measuring system was observed. This was traced to the recorder, and it is now certain that it was due to long term heating of the magnet block and/or galvanometer by the ultra-violet lamp. This only became apparent because the force calibration was spread over a long period, but the other galvanometers exhibited the same behaviour once it had been recognised. A short term zero drift also occurred each time the lamp was switched on. This was due to thermal warping of the optical system and soon stablised, and in any case zero drift was automatically compensated for by the method of measurement described above.

The form of the drift in sensitivity was a monotonic decrease of about 2%, which took eight to ten hours to stabilise. The manufacturers had been unaware of this behaviour, but performed independent tests which verified both the magnitude of the drift and that the magnet-block/galvanometer-assembly was the source. The drift was unacceptably large for the tests envisaged, and the prospect of performing calibrations with lamp burning time as an additional variable was rejected. The solution of leaving the lamp on permanently was also unacceptable, on economic grounds. Although they had been unaware of the drift problem, the manufacturers did produce temperature stabilised magnet blocks for other purposes, and one of these was fitted. The stabilisation temperature for the new block was $45^{\circ}c \pm 2^{\circ}c$, and the time was claimed to be 20 minutes. As expected the magnitude of the drift increased, but the stabilisation time did not decrease significantly. However, it was found that the drift could be stabilised by leaving the heater of the magnet block switched on permanently, it being necessary to switch the lamp on only when required for recording.

7.3 CALIBRATION OF GALVANOMETERS

Although the heated magnet block removed the large repeatable drift which had been detected, there remained a much smaller apparently random change, which amounted to about ½% over the entire duration of the test programme. No pattern was evident in this change, not even between the galvanometers themselves. It is now thought that the cause was variation in contact resistance at the galvanometer pins, and that this was probably accentuated by the use of the heated block. Striking evidence in support of this is that at intervals of roughly a few weeks, the apparent sensitivity of any particular galvanometer could suddenly become extremely erratic, always in the direction of reduced sensitivity, and sometimes to such an extent that the signal virtually disappeared. Rotation of the galvanometer in the block and manipulation of the contact pin, would restore normal behaviour. The pins were spring-loaded, and it is not clear which end caused the trouble.

A standard procedure was adopted to check the galvanometers before use. They were first manipulated as described above to clean the contacts, and their sensitivity was then checked against a calibrating voltage. This was derived from the load-cell supply voltage, through a set of fixed resistors. These calibrating resistors were built into the instrumentation circuit of the drawbench, and were checked regularly and found to be completely stable within the resolution of the Wheatstone Bridge used. Details are given in Appendix 1, together with a caution on their use.

The procedure described above gave day to day information on the sensitivity of the galvanometers, and it was therefore possible to correct for the small random variations which were found. This was done by relating the calibration curves for the transducer/recorder assembly to arbitrarily chosen galvanometer sensitivities, as measured with the calibrating voltage. Test data were then corrected according to the actual galvanometer sensitivity at the time of the test, as described in Section 10.6.4.

7.4 CALIBRATION OF TRANSDUCERS

All four transducers were calibrated before the Series I drawing tests (see Section 9). The speed transducers could be calibrated while on the drawbench, and they were both re-calibrated just before the start of Series II. The load-cell had to be removed for re-calibration, and this was done at the conclusion of the Series II drawing tests. The reference sensitivities for the calibration curves were selected before the full range of the random changes were known, and they were therefore not necessarily mean values. This has no importance, as they merely provided an arbitrary reference for the calibration data.

It will be clear, from the description in Section 7.2 of the method used to take data from the record charts, that physically large calibration curves, or mathematical expressions thereof, would be required if accuracy was not to be lost. The curves were highly linear, but nevertheless could not be expressed to the accuracy required as straight line equations. A compromise between the two methods was adopted, and the curves were drawn as the deviation from some arbitrary straight line. The method required little extra labour for conversion of data, and achieved the accuracy of conventional calibration curves of much larger scale.

The curves are given in Figures 7.2 to 7.5. Only the final calibration is given for the drawing speed, as the first one was done using a different drive string for the tachogenerator, and covered only a limited range of speeds. The initial and final curves for torque and rotational speed were closely repeatable. The drawing force calibration showed some change, and general scatter, at the top end of the range, but this corresponded to higher forces than were actually used in the drawing tests.

The methods used to obtain the calibration curves are described in the following sections.

7.4.1 Rotational Speed

For this calibration a magnet was mounted on the die housing, and a reed switch on a stand on the bed of the drawbench. The stand was positioned so that when the die rotated, the magnet operated the reed switch each time it passed. The switch closure was used to gate clock pulses from a crystal oscillator timer/counter (see Appendix 1), and thereby time the period of revolution. The circuit used is shown in Figure 7.1(a), but this was not a permanent installation on the drawbench. One or more periods of revolution could be timed, but as the counter was much more accurate than required, the preferred method was to time a single period repetitively, to ensure that stable running had been achieved before taking a U.V. record trace. Trigger point variations can cause significant error with period measurement of small numbers of cycles, but this did not apply here, because the pulse rise time was very short compared with

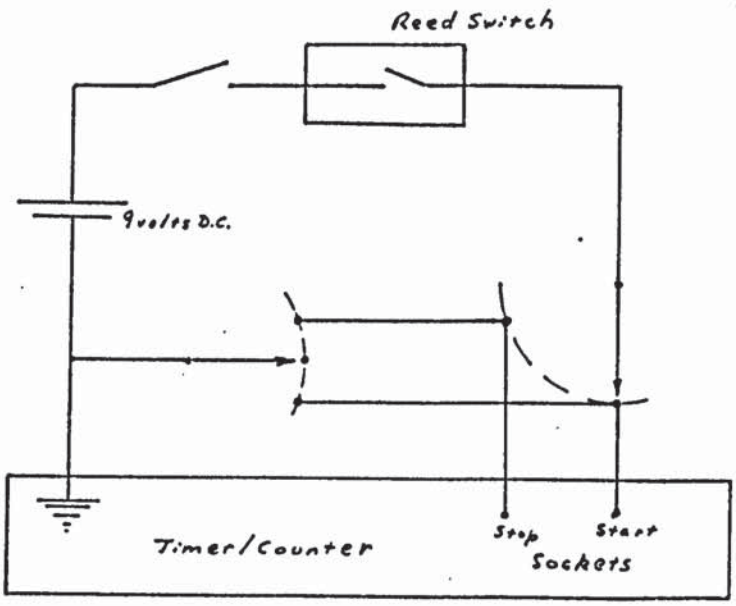

Fig. 7.1(a) - Circuit for Calibration of Rotational Speed Transducer

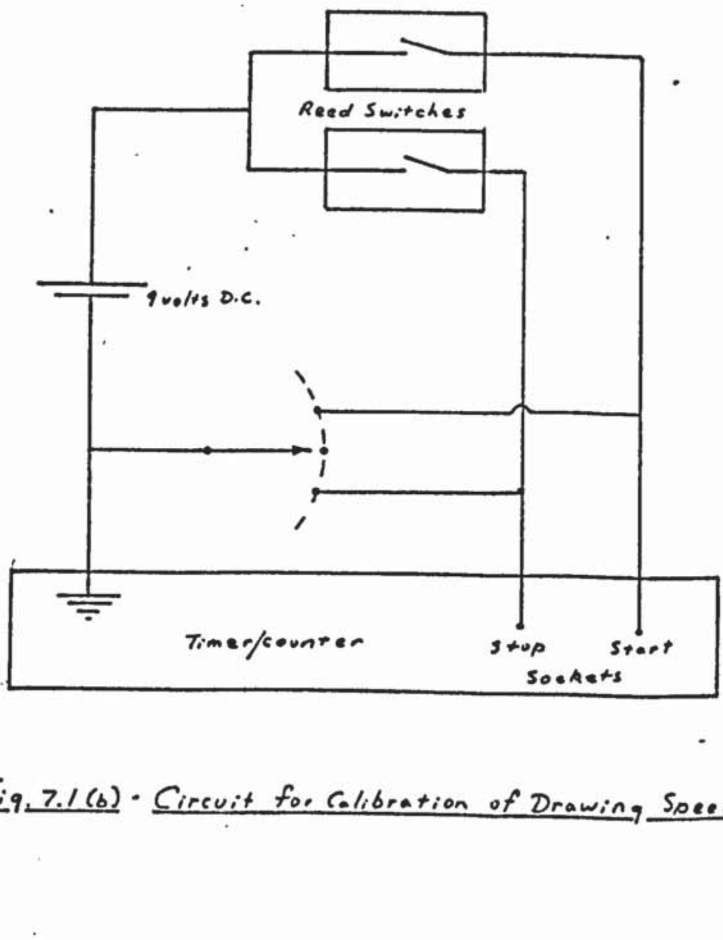

Fig. 7.1(b) - Circuit for Calibration of Drawing Speed Transducer

the period being measured.

7.4.2. Drawing Speed

A similar system to that described above was used, but the problem was complicated by the need to define a reference distance. Two reed switches were used, as indicated in Figure 7.1(b). They were mounted at a nominal separation of six inches, on a sub-assembly which could be clamped to a side rail of the drawbench (see Plate 5). The operating magnet moved with the hydraulic ram. The sub-assembly or the magnet, or both, could be moved to make the reference length coincide with any part of the working stroke.

The main problem was that the distance traversed between closure of the two switches was not necessarily the same as the physical distance between them, even if that could be defined accurately. Furthermore, the operating distance could change whenever either the switches or the magnet were re-positioned. It was therefore necessary to measure the distance in situ.

For this operation an Avometer was used to indicate the points of closure of the switches. By reducing to a minimum the setting of the relief valve in the hydraulic supply, and depressing the control handle for the ram very gently, it was possible to traverse the ram very slowly, or in short steps. Using a combination of dial-indicator and slip gauges, it was then possible to determine accurately the distance between the closure points of the reed switches. The time interval between the two closures was measured with the same timer/counter as before, and a U.V. record trace was taken simultaneously.

7.4.3. Drawing Force

Calibration of the load-cell under direct force was done in a 50 tonf. capacity universal testing machine (see Appendix 1). Special adaptors were required, and the arrangement is shown in Plate 6. Readings were taken for both increasing and decreasing load, and full use was made of the more sensitive ranges of the machine.

7.4.4 Torque

Torque calibration was done on a torque testing machine (see Appendix 1). One of the adaptors used for the drawing force calibration was dual purpose, but a separate adaptor was required for the flanged end of the load-cell. The arrangement is shown in Plate 7. Torque was applied in one sense only, anti-clockwise viewing the load-cell from the flanged end. As with the drawing force calibration, readings were taken with ascending and descending increments,

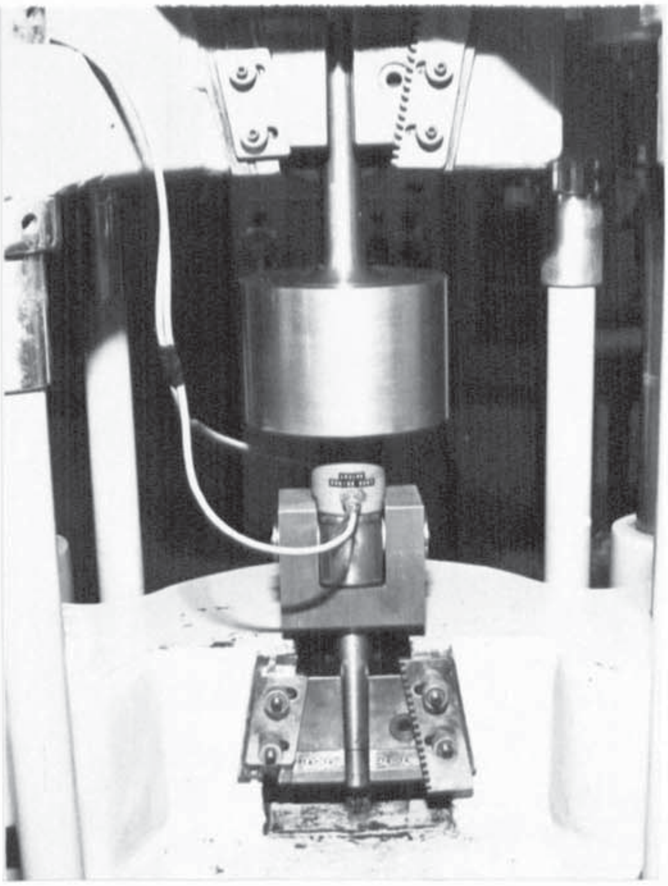

Plate 6 :- CALIBRATION OF DIRECT FORCE BRIDGE

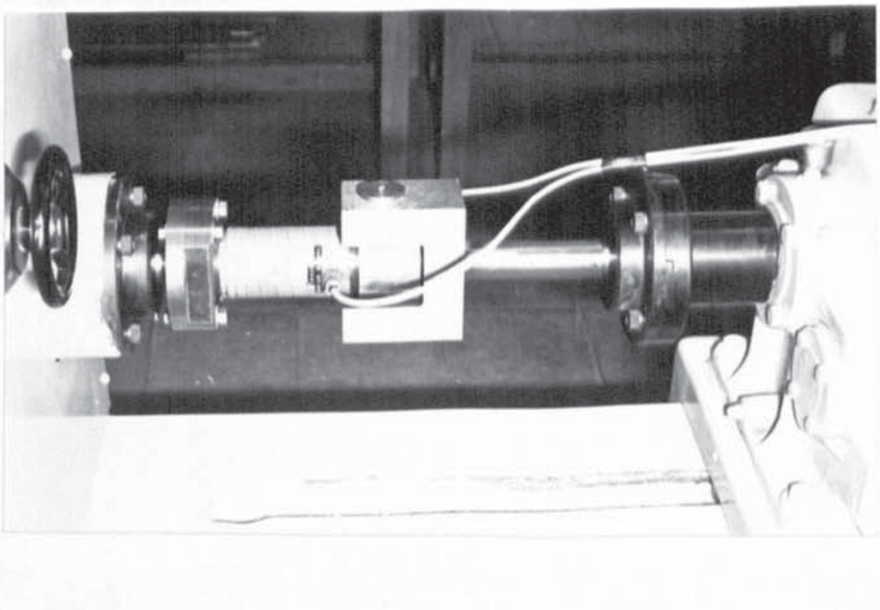

Plate 7 :- CALIBRATION OF TORQUE BRIDGE

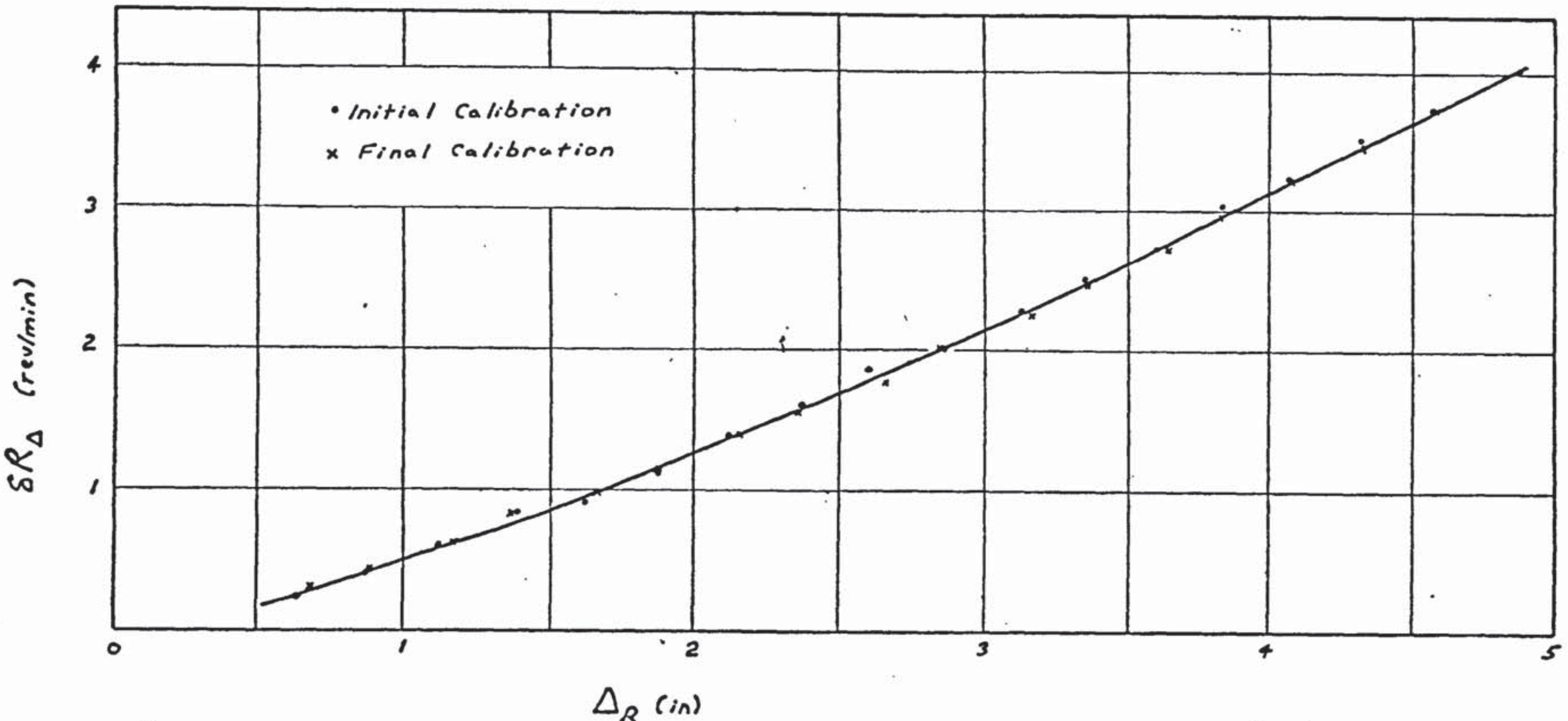

Rotational Speed (R rev/min) = $11.\Delta_R + \delta R_\Delta$

Fig. 7.2 - Calibration Curve for Rotational Speed Transducer

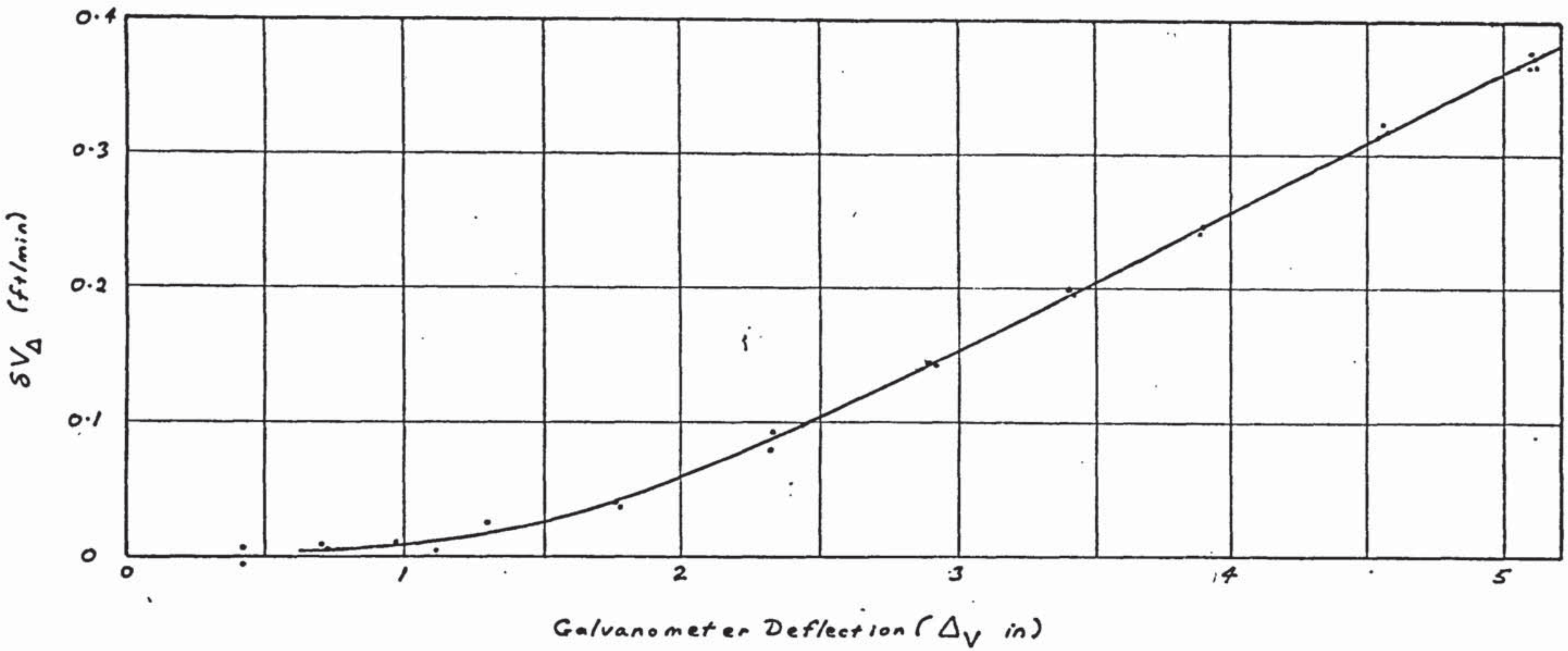

Drawing Speed (V ft/min) = $3.\Delta_V + \delta V_\Delta$

Galvanometer no. V1688

Data corrected for calibrated deflection of 4·520 in.

Fig. 7.3 - Calibration Curve for Drawing Speed Transducer

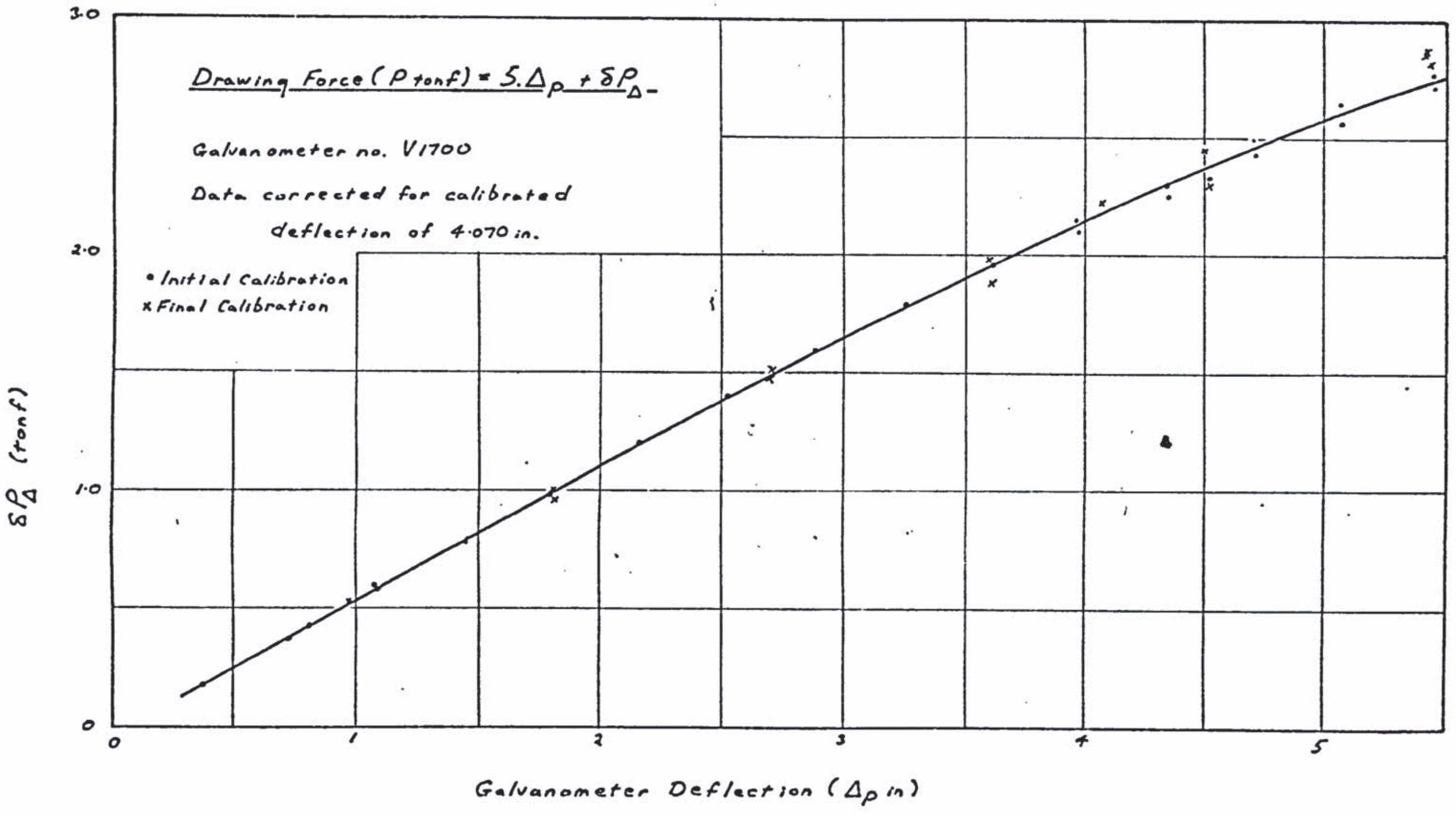

Fig. 7.4- Calibration Curve for Drawing Force Transducer

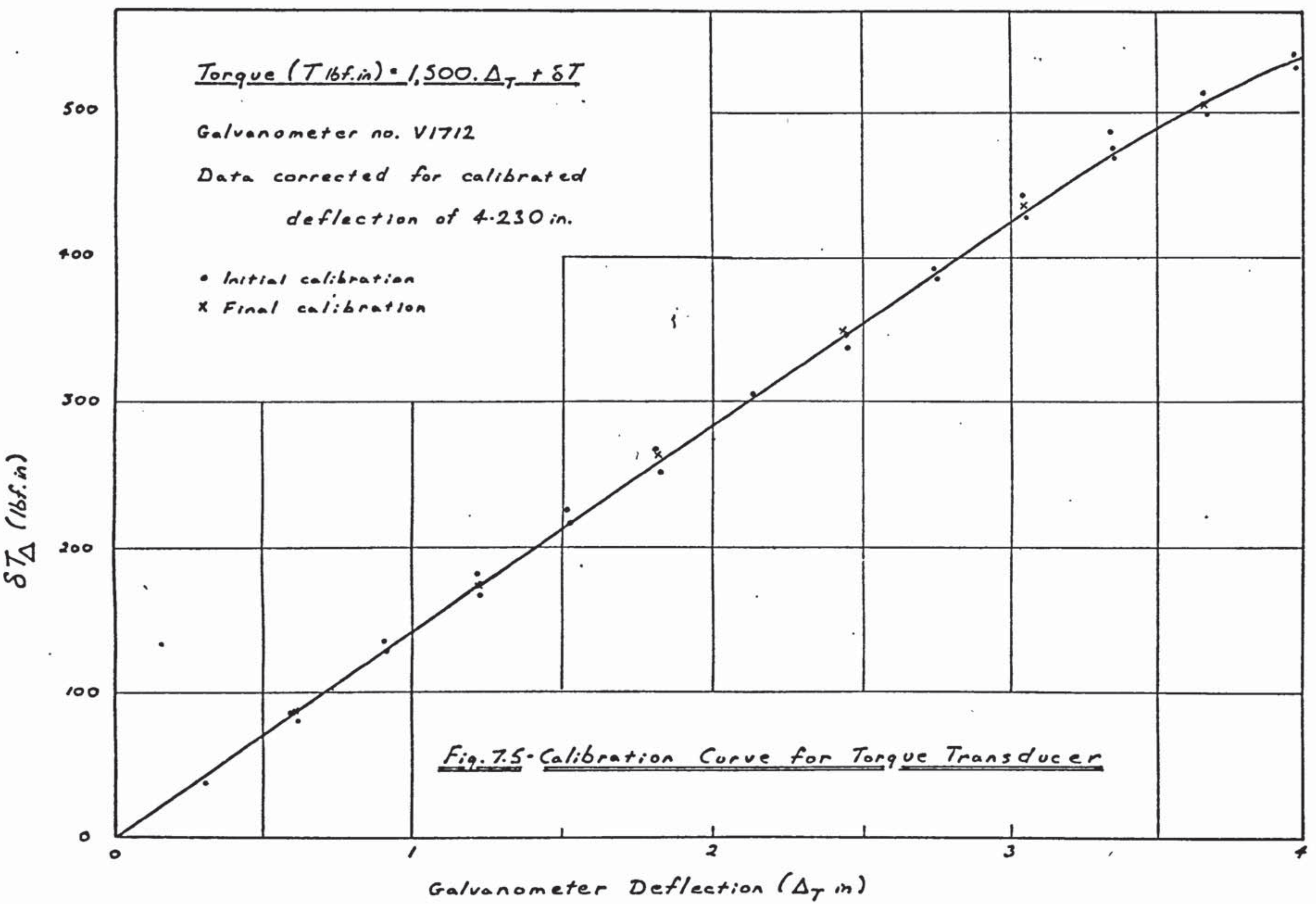

Fig. 7.5 - Calibration Curve for Torque Transducer

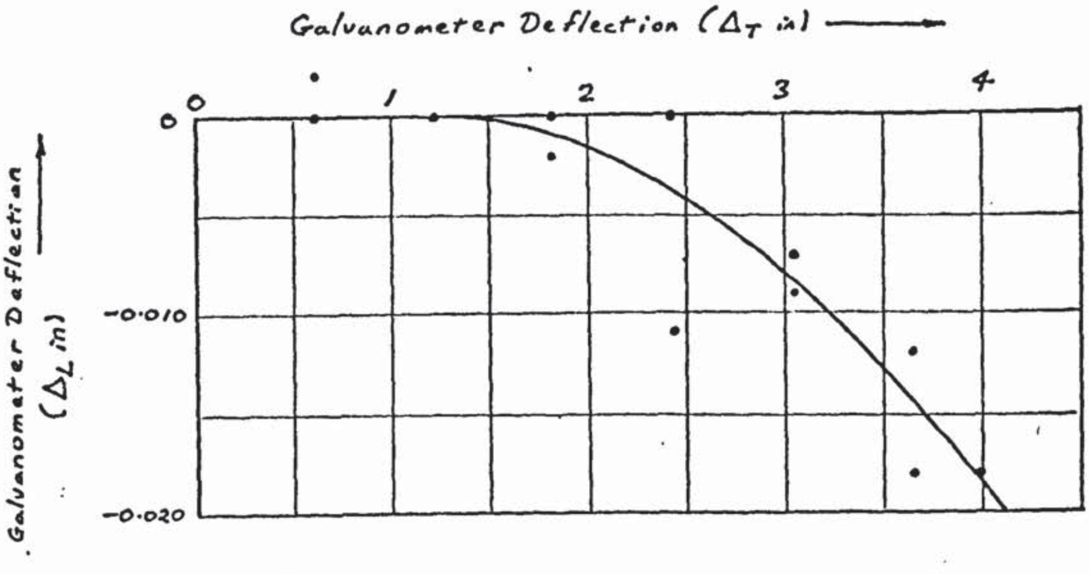

Fig. 7.6(a) - Sensitivity of Drawing Force Bridge to Torque

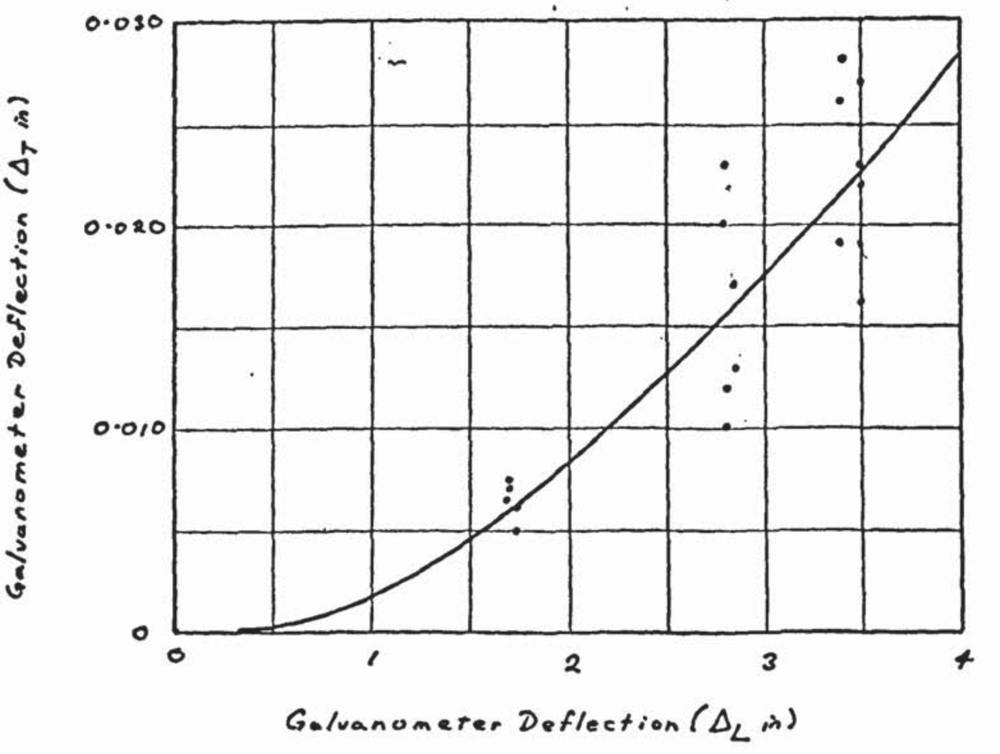

Fig. 7.6 (b) - Sensitivity of Torque Bridge to Drawing Force

and the more sensitive ranges of the machine were used where possible.

7.4.5 Cross-sensitivity

The carriage on the torque testing machine was free to move axially and it was therefore possible to establish the sensitivity of the force bridge to torque, concurrently with the torque bridge calibration. This was slight and is shown in Figure 7.6(a).

During direct calibration of the force bridge, considerable deflections of the torque galvanometer were observed. However, no repeatable pattern could be established, either from test to test, or between increasing and decreasing loads within one test. As the torque bridge functioned satisfactorily under torque loading, it was concluded that the method of application for the direct force was producing genuine torque loadings. However, these torque loadings were not large enough to have affected the drawing force calibration.

The cross-sensitivity of the torque bridge to direct force (see Figure 7.6(b)) was finally established from measurements made of behaviour during drawing tests, and is discussed in Section 10.6.4.

7.4.6 Sensitivity to Bending

At one time it was thought that bending might have been the cause of the apparent sensitivity of the torque bridge to force loading, and the sensitivity to bending was therefore checked directly. The arrangement shown in Figure 7.7 was used for this. The maximum bending moment that was applied,

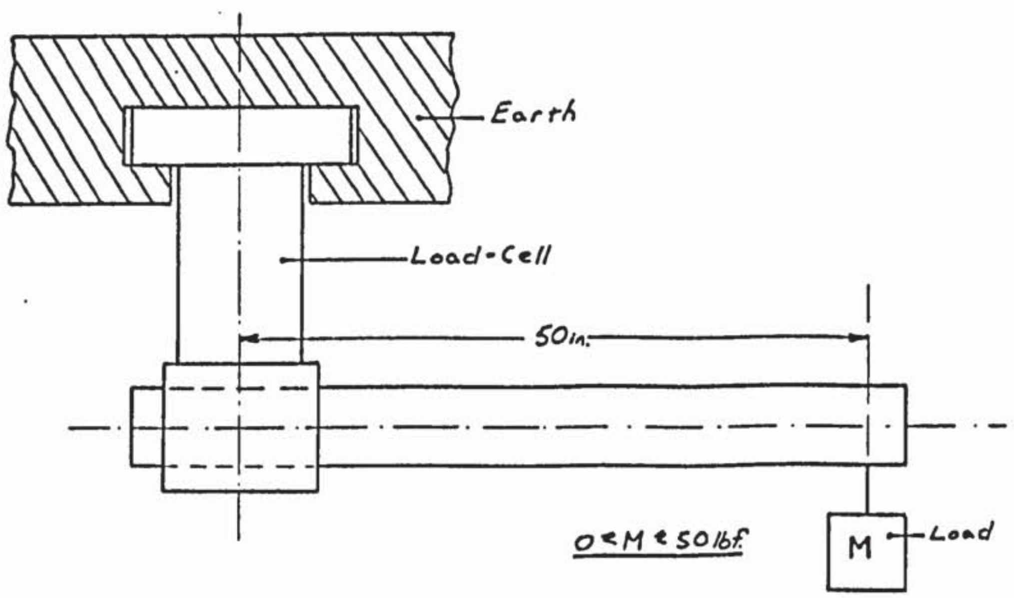

Fig. 7.7. - Arrangement for Determination of Sensitivity of Load-Cell to Bending

corresponded to a maximum principal strain of about 0.05% in the smaller of the two sections. The associated deflections of the load-cell galvanometers did not exceed 0.010 in., and bending sensitivity of the load-cell was subsequently ignored.

8. DRAWING DIE

Two tungsten carbide dies were obtained to the general specification described in Section 4.3 and extensive measurements were made to check their form. One was found to deviate appreciably from specification and was never used, all drawing tests being performed with the other die (see Appendix 1). Details of only this die are given here.

Radial reference lines, permanently numbered one to eight, were scribed on the die casing at intervals of 45°. Profile measurements were made at all these reference positions, but in view of the high degree of uniformity found, die form can be adequately specified by a flank profile at one reference position, together with throat diameter measurements, and eccentricity profiles at different positions through the die. Throat diameter and flank profile were measured with a high accuracy optical machine (see Appendix 1), before and after the drawing tests and at the same reference position. The values are listed in Table A7.1. The profile was plotted to a large scale which it is not practicable to reproduce here, but the throat section is shown in Figure 8.1. The origin for the measurements was arbitrary, and the ordinate was adjusted so that its origin coincided with the throat. Measurements along the abscissa were adjusted so that profiles before and after drawing coincided. This procedure was valid for expressing the profile geometrically, but the measurements have no value for assessing die wear. No deviation from the 7° degree flank angle was detectable outside the region shown in Figure 8.1, except close to the inlet position for the largest size bar, where the die opened out slightly too early. The maximum deviation there was 0.0025 in.

Eccentricity profiles, at three positions through the die, were taken on a Talyrond machine (see Appendix 1). Profiles taken after the drawing tests are shown in Figure 8.2, with values of total departure from roundness before and after. A discrepancy will be seen between the value given for eccentricity before drawing, and the equivalent value which can be deduced from the throat diameter measurements in Tables A7.1. This was not noticed until after the drawing tests, but it is unimportant with regard to the effect on the geometrical parameters.

Measurements of surface finish were made prior to the drawing tests on a Talysurf machine. This was done with the die mounted on an adjustable

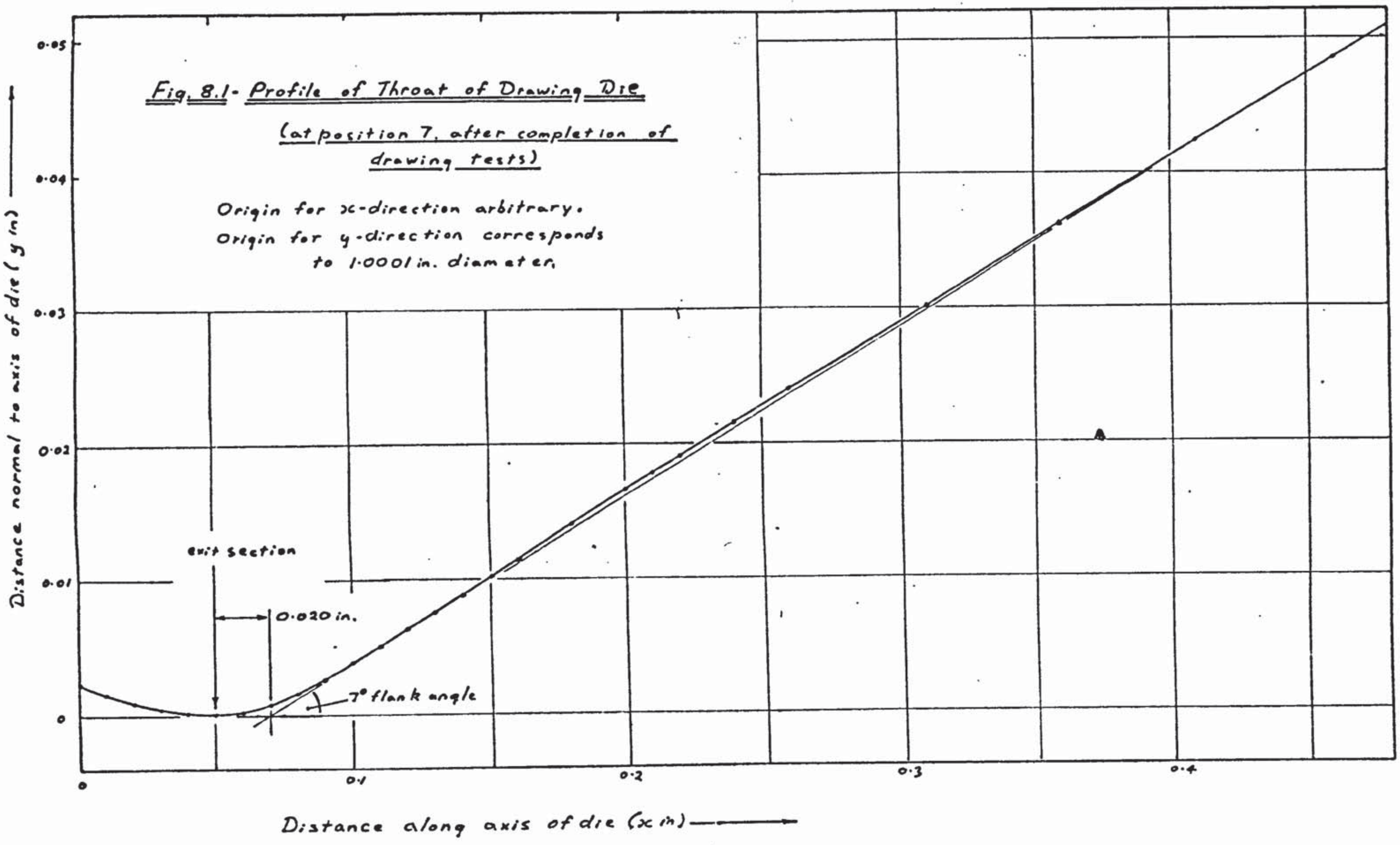

Fig. 8.1 - Profile of Throat of Drawing Die (at position 7, after completion of drawing tests)

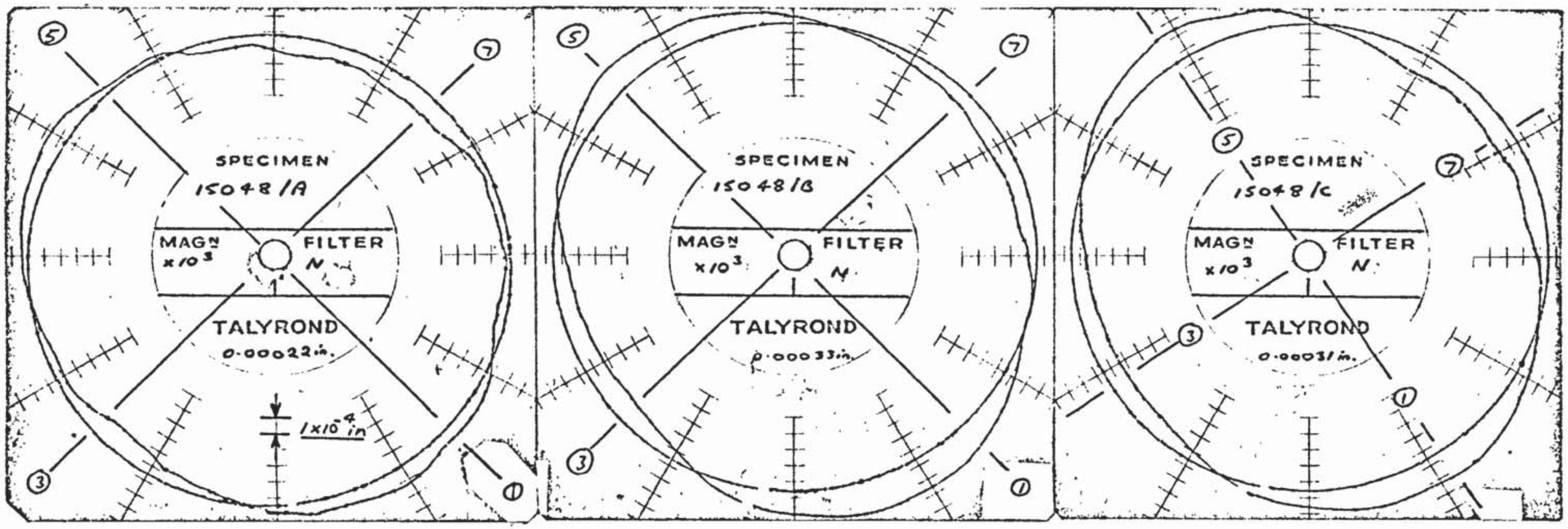

Position A

Position B

Position C.

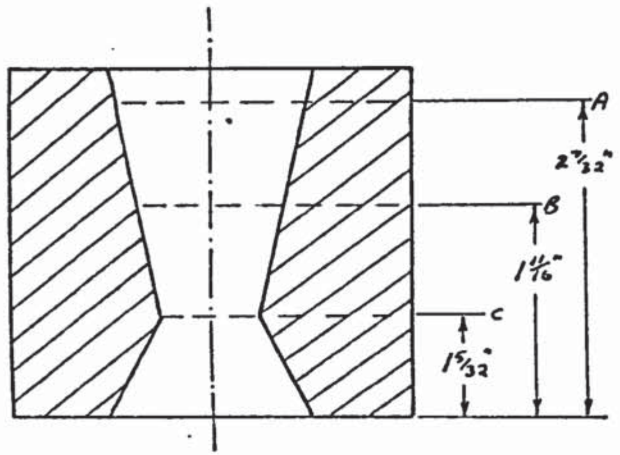

Position in Die	Total Indicated Run-Out (in x 10^{-3})	
	Before Drawing	After Drawing
A	0·28	0·22
B	0·36	0·33
C	0·39	0·31

Fig. 8.2 - Out-of-Roundness Profiles at Three Positions in the Die

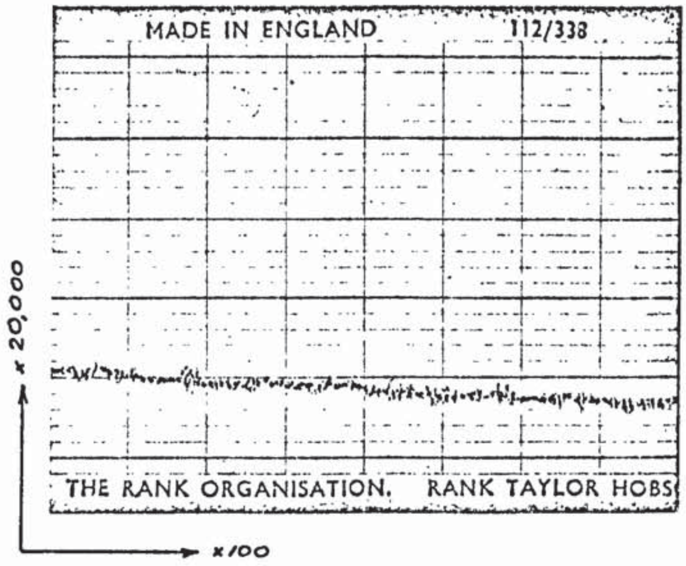

(a) Drawing Die

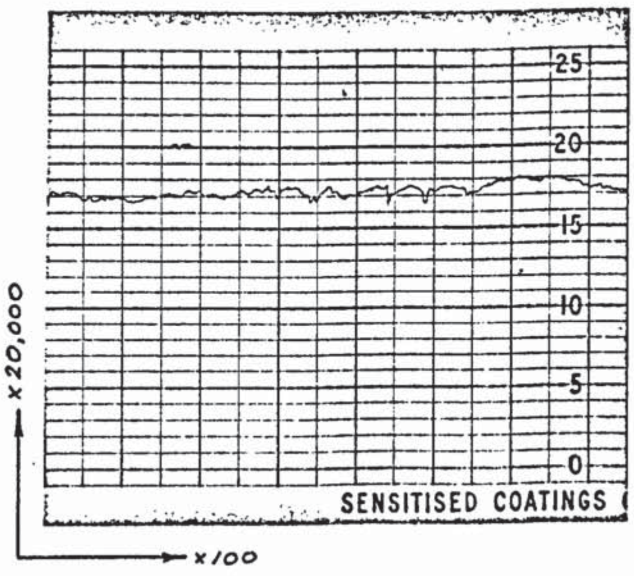

(b) 1 microinch C.L.A. standard specimen

Fig. 8.3- Comparison of Surface Profile of Drawing Die with Standard Specimen

angle plate inclined at 7° to the vertical. In order to obtain sensible readings it was necessary to use the shortest meter cut-off lengths (98), and to use an external glass datum plate rather than the radiused skid which is normally used. Meter readings were about 2 microinches C.L.A. However the method of mounting the die made the readings susceptible to vibration. Figure 8.3 shows a section of a typical trace and the effect of vibration is clearly seen. Comparing the record for the die with that of the standard specimen, it appears that the actual finish was no worse than 1 microinch C.L.A. Measurements were not repeated after the drawing tests due to shortage of time, but visual inspection suggested that little change had taken place.

9. PRELIMINARY TEST SERIES - SERIES I

9.1 INTRODUCTION

A batch of material was obtained to the general specification of Section 4.1, with all bars in the annealed condition and from the same cast. Unfortunately, due to a misunderstanding on the part of the supplier, the material had been rolled instead of drawn immediately prior to annealing. It was clear that because of unevenness in this material, results could not be expected to be of sufficient repeatability to enable distribution of shear stress to be deduced; although it should be noted that the possibility of using the rotating-die technique for this purpose had not been realised at the time that this material was acquired.

In view of the delay involved in re-ordering material, it was decided to go ahead with tests using this batch, partly to test the equipment and refine the experimental techniques, and partly to obtain results using the simpler analysis in Section 3.

The main utility of this series of tests was the revelation of some unexpected features of the rotating-die technique, and exposure of weaknesses in the scope and method of performing tests. The results of Series I tests are now considered to be limited and incomplete compared with those of Series II, the main test series, and they may also be unrepresentative. However they are thought to be reliable within their recognised limitations, and they have already been reported (89). They are given here for completeness, and to indicate the line of development of this research. Many features, which can be more profitably discussed with reference to Series II, have been mentioned only briefly in this section.

9.2 TEST MATERIAL AND LUBRICATION

In addition to the ovality and rolling flash to be expected from the rolling treatment, many of the bars in this batch had surface damage over much of their length. This took the form of diametrically opposed pairs of 1/4 in. wide longitudinal or helical flats. Many individual measurements of diameter were made, but, as little importance is attached to the results of this series generally, it would be pointless to include all of them here, and they can in any case be adequately summarised as follows. The bars were non-circular by about 0.010 in. total run-out, in addition to which there was rolling flash of up to 0.020 in. on diameter. These figures varied along the length of each bar, and from bar to bar. However, as far as can be judged from the many measurements taken, the cross-sectional area was sensibly constant along each bar and between bars of the same nominal diameter. The actual effective diameters are given in Table 9.1. There was no material of 3/16 in. diameter

Nominal Bar Diameter (in.)	Actual Bar Diameter (in.)	Reduction of Area (%)
1.1/16	1.072 $\pm \frac{1}{2}$%	13
1.1/8	1.133 $\pm \frac{1}{2}$%	22
1.1/4	1.256 $\pm \frac{1}{2}$%	36

TABLE 9.1

with this batch, and the 1.5/16 in. size has not been included because, as discussed in Section 9.3 it was not possible to perform a coherent series of tests on that size. The material was mild steel to specification En 2A, and lengths of bar were random between eight and twelve feet.

Tensile tests were performed on full diameter undrawn sections of the barstock, as part of the series described in Section 10.8. The data are given in Table A7.2 and the stress-strain curves in Figure 9.1. Specimens of the two smaller sizes of bar were taken from undrawn remnants of bars used in the drawing tests, but for the 1.1/4 in. size it was necessary to use a specimen from a bar which, although supplied as part of the batch, was not used in the drawing tests reported here.

Surface treatment and lubrication of the material for the drawing tests was done by the Pyrene company. The material was pickled, phosphated and soap-dipped, according to one of the 'Borderlube' processes of the company, but precise details of the treatment were never made available. The condition of the bars prior to drawing may not have been representative of this treatment, because traces of mill scale were still apparent, and because there was a considerable time delay before the drawing tests. However, the material

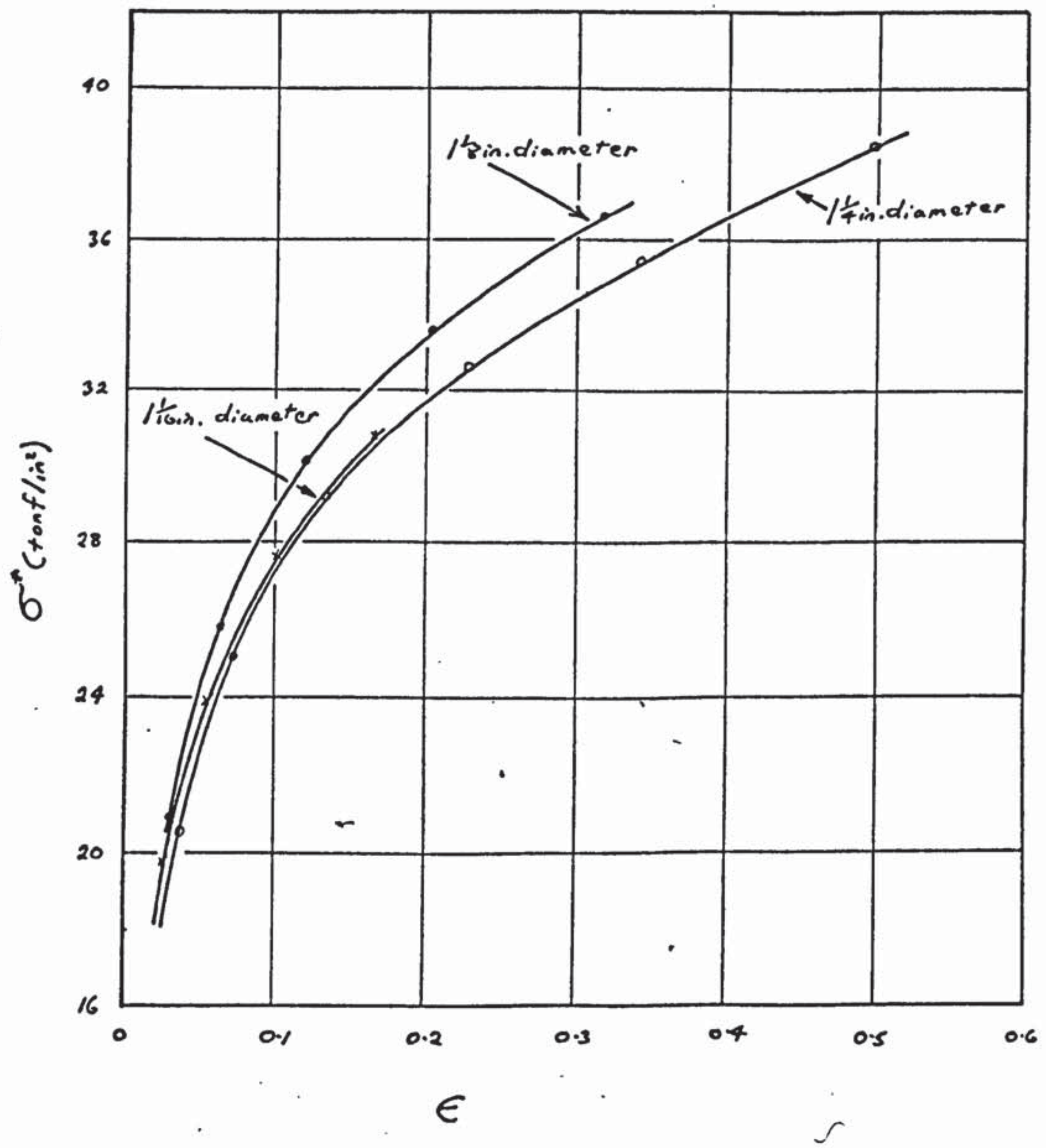

Fig. 9.1 - True Stress-Strain Curves for Material used in Series 1

was stored in dry conditions, and no visual evidence of corrosion was found. The soap deposit appeared to be patchy, being powdery white in some places, and apparently absent in others. Pyrene claimed that the active part of the deposit would not be visually evident, and that the powdery deposits were simply surplus.

No tests using oil lubrication were done in this series, and no surface finish measurements were made.

9.3 DRAWING TESTS

Some exploratory tests were made, during which it was found that although drawing speed was constant throughout a particular test, it was difficult to set it to a pre-determined value. Setting of rotational speed was comparatively precise and repeatable, so a procedure was adopted in which tests were run in sets, each set being performed at nominally constant rotational speed but covering the range of drawing speeds. The exploratory tests were also used to study long term changes during the test. These are described fully in Section 10.6.4. The main conclusion was that drawing force became virtually stable after a very short length of bar had been drawn, and on this basis a standard format was adopted for subsequent tests. The exploratory tests did not constitute a coherent group, and are not reported here. Most of them were performed on the large size bars, and insufficient of the 1.5/16 in. size was left for the standardised tests.

Individual tests, within a particular set at constant rotational speed, were performed consecutively and on a single bar. The sequence usually used was 5, 10, 15 ft/min., and then 5, $7\frac{1}{2}$, $12\frac{1}{2}$ ft/min.. The purpose of this sequence is discussed in Section 10.6.1. Each individual test comprised a section of bar drawn without die-rotation, then one with, and another without. Drawing was not stopped between the three sections, and the duration of each section was timed to be four inches, that is twelve inches total per test. Control of the section lengths was difficult at the higher drawing speeds.

During this series a method for drawing at speeds less than 5 ft/min. was discovered, but this could only be done while the die was rotating. To do this the pressure relief valve in the oil delivery line was unscrewed while drawing with die rotation. When the pressure setting fell below the current drawing pressure, the drawing speed would fall until equilibrium was re-established, with an increased swing of the friction vector. Further reduction in pressure produced a further fall in drawing speed, until the swing of the vector reached 90^{o}. This was an experimentally haphazard technique, with which the drawing speed and drawn length could not be predicted.

9.4 RESULTS

Interpretation and conversion of data from the record charts is discussed in Section 10.6.4. Values taken for this series of tests were of rotational and drawing speed during the die-rotation period, torque and drawing force at the start and finish of die-rotation, and drawing force just before die-rotation and at the very end of the test. These values are given in Tables A7.3 to A7.5, in which coupled values indicate a range of uncertainty.

In order that directly comparable experimental results could be plotted, corrections were applied for variations in drawing force and rotational speed between tests in the same sets. Thus a mean value for drawing force, prior to die-rotation, was taken for each size of bar, it having first been checked that variations were random. Values of torque and drawing force obtained in each test were corrected linearly, according to the variation of the initial drawing force in that test, from the mean for that size of bar. Variations in rotational speed from the nominal value were partly random, arising from day to day errors in re-setting the value, and partly systematic with increasing torque loading. Correction factors for these variations were obtained by plotting the torque and drawing force dependence on rotational speed, at nominally constant drawing speed. Corrected values are listed in Tables A7.3 to A7.5 and are plotted in Figures 9.2 to 9.4. It will be seen from the tables that the corrections were always small and often negligible, so errors in the corrections are likely to be insignificant.

Coefficients of friction μ_T and μ_P were calculated according to Section 3.1 , for conditions at the start of die-rotation, and are listed in the tables and plotted in Figure 9.5. Some of the extreme values of μ_P calculated for test conditions which gave very small load reductions, have not been plotted as they were not considered to represent reality. This is discussed further in Section 10.7.

Various markings on the surface of the original bars were distinguishable after drawing, and from their appearance it was clear that the bar had been twisted helically as it passed through the rotating-die, but no reliable

Fig. 9.2 - Increase of Drawing Force with Drawing Speed, at Constant Speed of Die Rotation

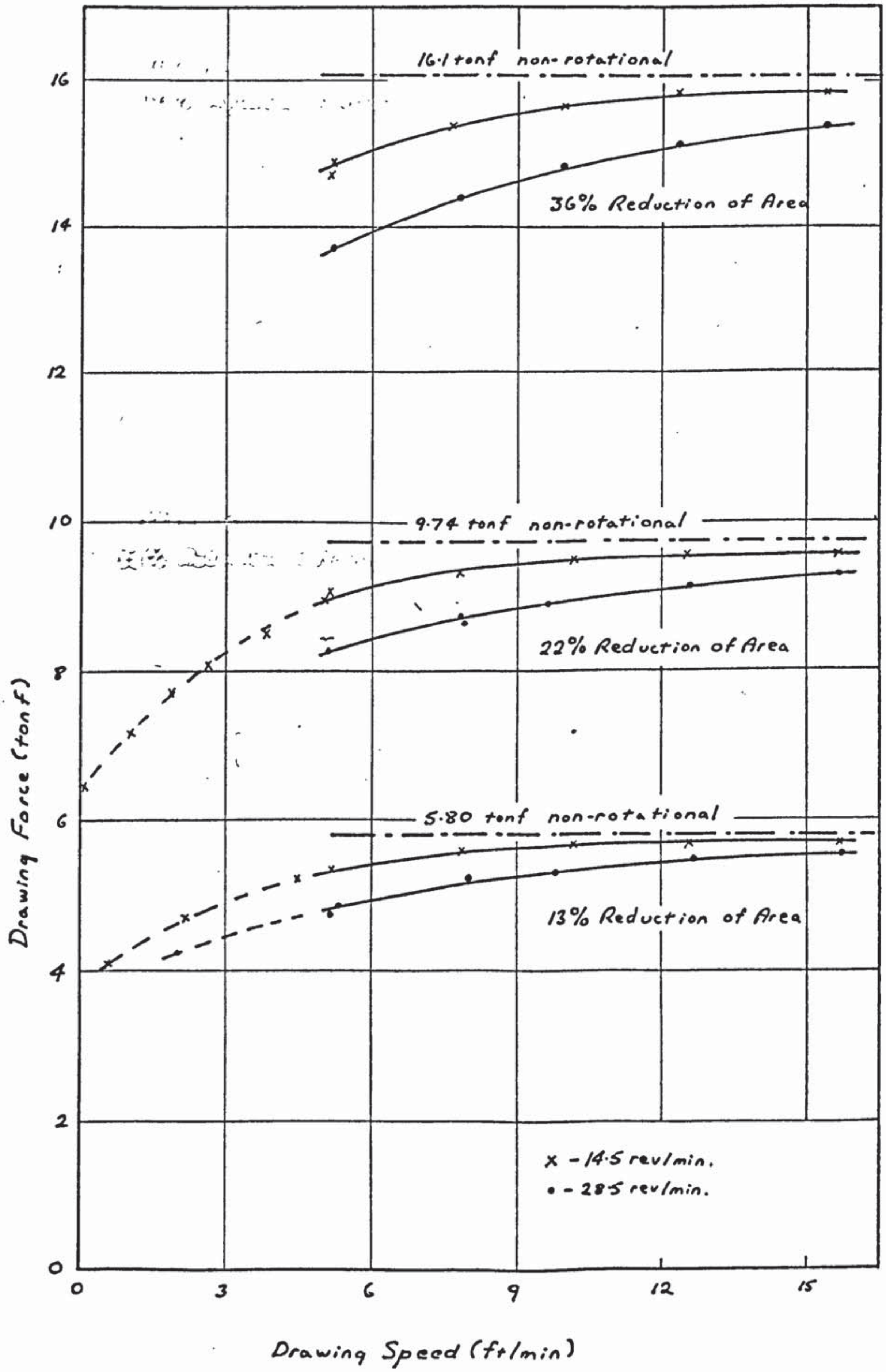

Fig. 9.3 - Effect of Drawing Speed on Torque Required to Rotate the Die at 14·5 rev/min.

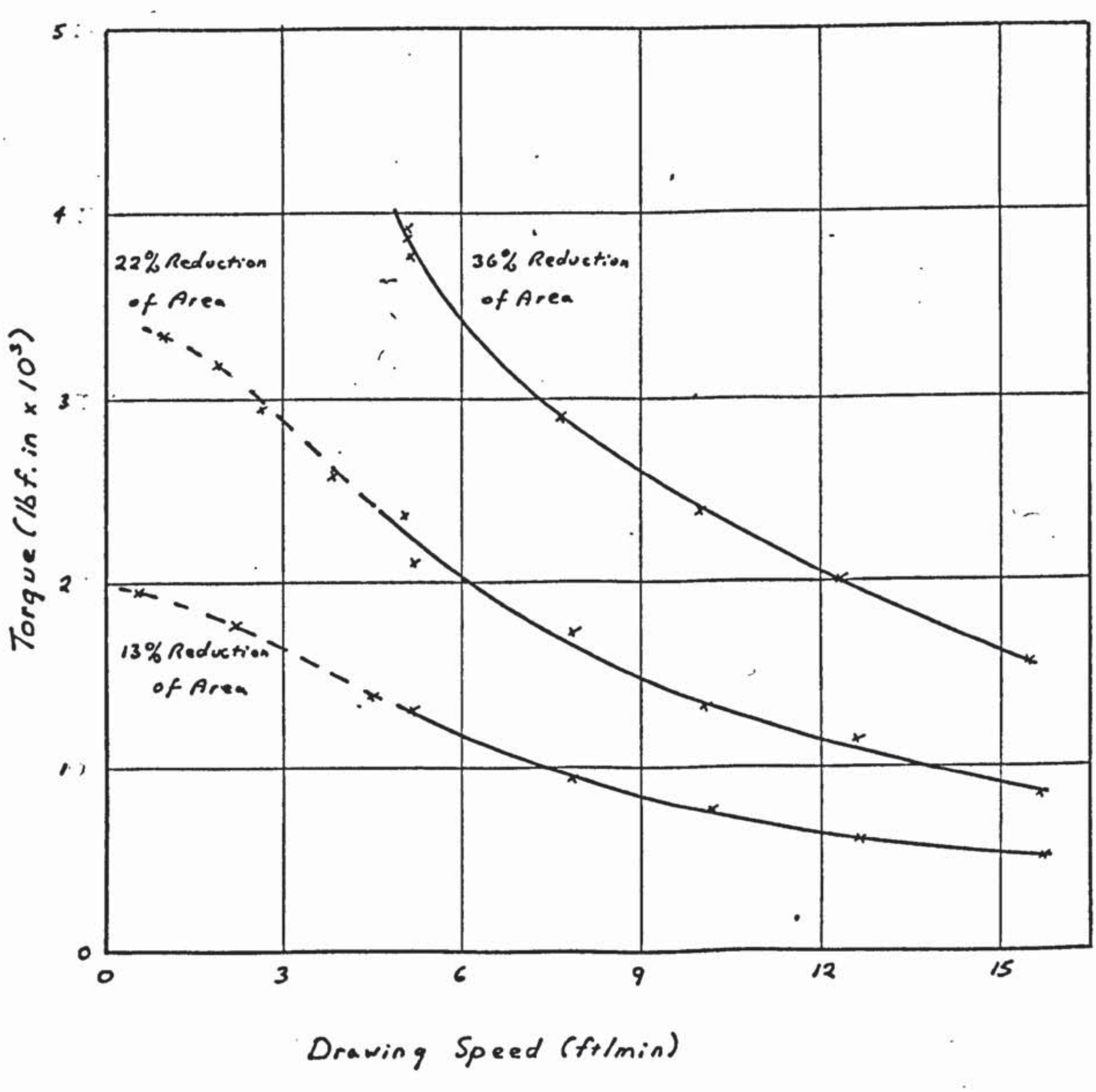

Fig. 9.4 - Effect of Drawing Speed on Torque Required to Rotate the Die at 28·5 rev/min.

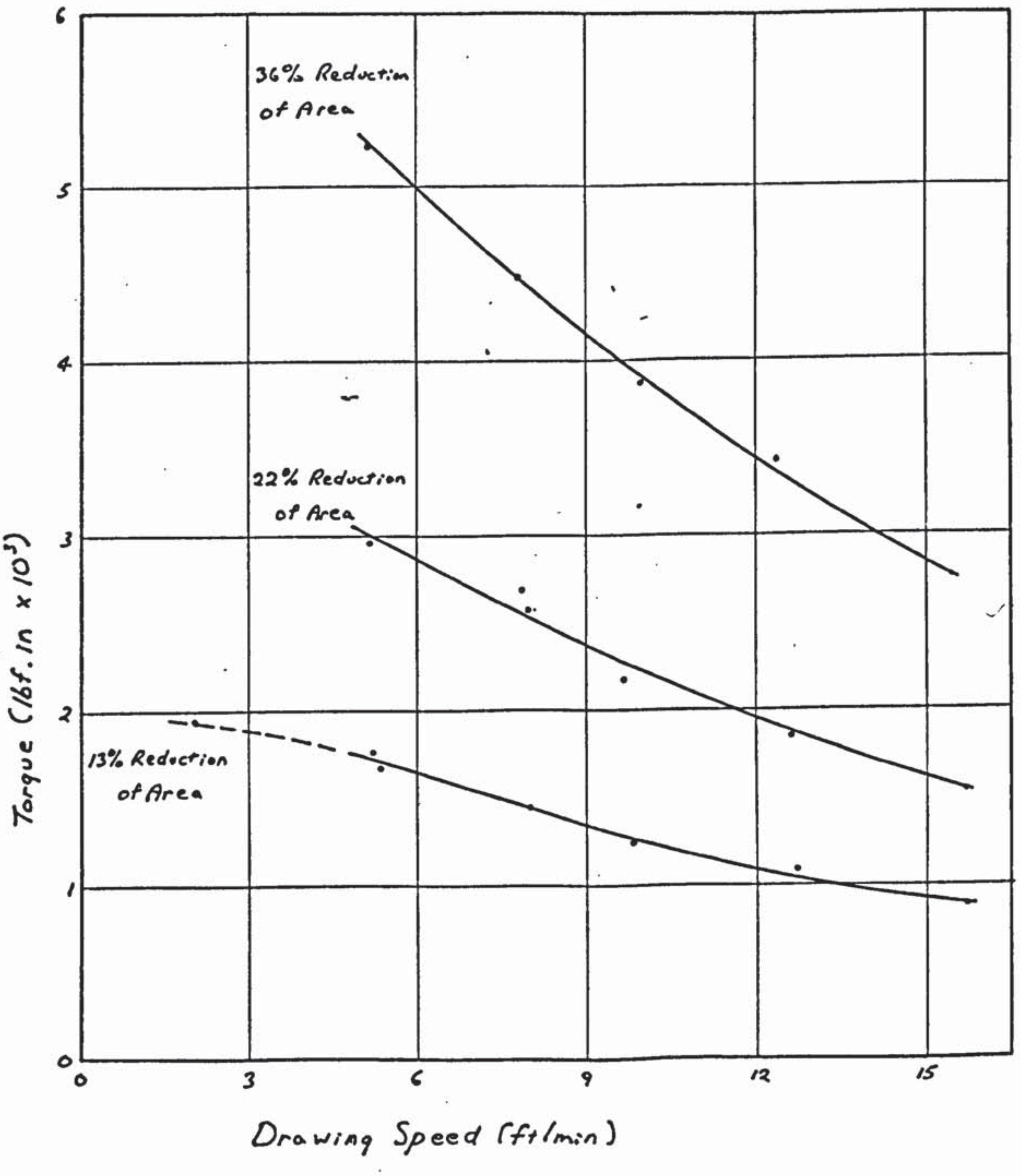

Fig. 9.5- Calculated Coefficients of Friction

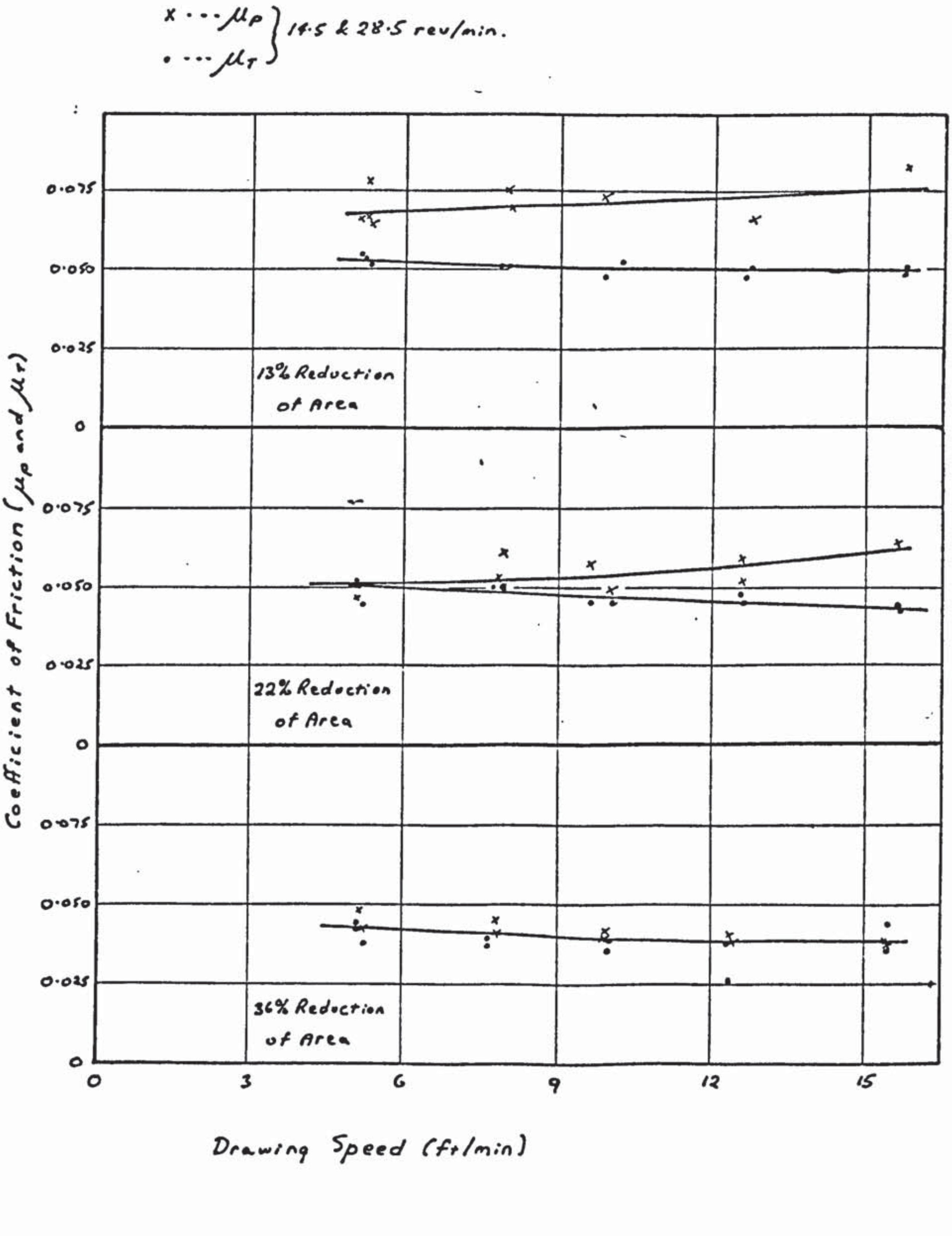

measurements of the twist were possible.

9.5 DISCUSSION OF RESULTS

Two peculiarities were not recognised at the time that these results were analysed, one being of the rotating-die technique in general, and the other of the equipment used here. They are discussed in detail in Section 10.6.4. Both of these features were relatively unimportant over the 5 to 15 ft/min. range, and it will be shown that the lower speed tests are not comparable anyway.

One effect was that of a surge in drawing speed at the start of die-rotation, but the results given here are not subject to error caused by non-recognition of this factor. The other feature was that the twist observed in the drawn bar implied rotation of the free end of the bar. This had the effect of reducing the relative rotational speed between die and bar, and is now thought to account for the reduction in torque observed in the early stages of die-rotation. The maximum error in values of μ_T given here, which result from non-consideration of this factor, are an over-estimate of about 10%; μ_P being unaffected. This magnitude relates only to results obtained under conditions of high reduction of area, and high R/V ratio. The good agreement of μ_T with μ_P found in this range (see Figure 9.5) must therefore be regarded as being fortuitous.

From the point of view of a possible comparison between experimentally and theoretically determined curves, it was clear that the 0 to 5 ft/min. range of drawing speeds was of great interest. However the data obtained in that range were not directly comparable with the other results, as the higher drawing speed data corresponded to conditions at the start of die-rotation, whereas the low speed results were taken after some indeterminate period of die-rotation. They were therefore probably lower than they would have been under directly comparable conditions. The good agreement obtained by back-extrapolating the lower curves in Figures 9.3 and 9.4 is not in conflict with this argument, as that size of bar showed no change in torque and drawing force reduction during the die rotation period.

9.6 CONCLUSIONS

Values of μ deduced for conditions in these tests were between 0.04 and 0.07, with a weighted mean of 0.05. The main value of the Series I tests lay in the revelation of necessary modifications to the test programme. These were as follows :

a) The drawbench was to be modified so that straightforward drawing at speeds below 5 ft/min. was possible.

b) Regulation of the length of bar drawn in each section of the tests was to be done directly, instead of by timing.

c) Measurements of the speed of rotation of the free end of the bar, during die-rotation, were to be made.

d) Errors arising from the use of an assumed velocity field at the die/bar interface were to be removed, by measuring the actual velocity field.

e) Material for Series II was to be of better uniformity than used here.

10. MAIN TEST SERIES - SERIES II

10.1 TEST MATERIAL

A second batch of material was obtained, from a different supplier, for this series. This had been cold-drawn and had good dimensional uniformity (see Section 10.5). Although this was satisfactory, it was necessary to accept some departures from the general specification discussed in Section 4.1. These were firstly that the material was in the normalised condition, instead of being annealed, and secondly that it was not all from the same cast. However, all bars of the same nominal diameter were from the same cast. The material was once again mild steel, but of slightly higher carbon content than that used in Series 1. The chemical composition and details of heat treatment are given in Table 10.1. Further departures relating to particular sizes of bar were that the 1.5/16 in. size had been reeled after being normalised, and that the 1.1/8 in. size was pitted by corrosion. The reeling process could be expected to have work-hardened the bar, and to have done so variably from point to point.

10.2 SURFACE TREATMENT AND LUBRICATION

The batch of material was made up into two equal bundles, and spacing rings were used to separate the bars within each bundle from each other. They were taken to an industrial tube works for treatment, where they were both pickled and phosphated, and one bundle was then soap dipped. Precise details are given in Table 10.2.

On their return there was some doubt as to the amount of soap deposited on the one bundle, and there were also some patches of grease and grit, and bare patches, on the bars. Some preliminary rotating-die drawing tests were therefore done on the soap-dipped bars. These were done consecutively on a single 1.3/16 in. size bar. The experimental details and evaluation of results were as for Series I tests, and the results are given in Table 10.3.

The first test was done on the bar as returned from the tube works, but a section free from obvious contamination was selected. The whole bar was then washed down with trichloroethylene to remove grease, grit, and soap, and the second test was done with no lubricant other than the phosphate coat. For the third test, fresh soap was applied in the laboratory as described later in this section. The fourth test was also done with laboratory applied soap, but the bar was first abraded down to the bare metal, using 220 grit emery

Nominal Bar Diameter(in)	Element (%)				
	C	Mn	Si	S	P
1.1/16	0.12	0.59	0.21	0.05	0.01
1.1/8	0.14	0.58	0.29	0.03	0.01
1.3/16	0.12	0.57	0.19	0.04	0.01
1.1/4	0.15	0.60	0.22	0.04	0.01
1.5/16	0.15	0.62	0.26	0.03	0.01
Condition :-	Nomalised (Heated at 900°c for 50 mins., air cooled)				

TABLE 10.1

Treatment	Time (Mins)	Temperature (° c)	Details
Pickle	20	78	7% H_2SO_4
Cold Rinse	-	-	Water
Drain	½	-	-
Hot Rinse	-	-	Water & Paroxite RC to pH9
Drain	1	-	-
Phosphate	14	63	18% Bonderite 188x
Hot Rinse	-	-	Water
Drain	-	-	Until dry
Soap Dip*	7	50	9% TD 20

* N.B. See Section 10.2

TABLE 10.2

Nominal Bar Diameter = 1.3/16 in. Drawing Speed = 5 ft/min. Rotational Speed = 15 rev/min.		
Condition of Bar	μ_T	μ_P
1) As treated at tube works	0.048	0.041
2) De-greased, no lubricant	0.072	0.065
3) De-greased, re-soaped	0.025	0.023
4) Phosphate coating removed, then re-soaped	0.022	0.020

TABLE 10.3

cloth in the circumferential direction.

Conclusions drawn from the results were, firstly that the phosphate coating was in itself quite a good lubricant; and secondly that the industrially applied soap gave reasonable results, but that much better results were possible using the laboratory technique. The results obtained with the abraded bar were somewhat surprising, and it was tempting to conclude that occasional bare patches in the phosphate coating would not affect results, and even that the phosphate coating was superfluous. However, it is well known that shot blasting of drawing stock is one method of inducing good lubrication (44), and it may be that the method of abrasion used had a similar effect. So the surface was not necessarily representative of naturally occurring bare patches. On the basis of these results, it was decided that all tests would be done using laboratory applied lubricant.

The soap used was commercial sodium stearate powder, originally supplied for the soap-box type of lubrication used with bull-block wire-drawing. The powder was dissolved in water at about 80°c, to give a 10% solution by weight; the solution then being decanted to remove the insoluble impurities. The solution was stirred continuously during cooling, until it coagulated abruptly at 28°C. At room temperature it was a soft jelly which could be brushed onto the barstock.

Industrial practice is to dip bars in hot soap solution, most of which drains off when the bar is removed, and only a thin film remains. The problem with using this method for experimental work was that, to ensure a uniform repeatable coating, at the very least a system for rotary drying of the bars would have been required. The alternative was to ensure that a surplus of lubricant was always available at the die inlet. The bar would then carry into the die as much as it could, and thereby create its own uniform coating, provided that the other parameters were constant. Soap-box drawing was not considered sufficiently reliable for these tests, and in any case the use of the rotating die would have made this difficult. It may of course be that the films produced by industrial hot dipping do constitute a surplus relative to the quantity which can enter the die, but the results described above do not support this. It was therefore decided to use thick coatings of soap.

Prior to the drawing tests, the bars were washed down with trichloroethylene and left to dry for about four hours. A heavy layer of soap was then brushed on. This was very uneven but always complete, and after a further half-hour another thick coat was applied. Before being drawn the bars were then left for at least twelve hours. A number of variations were tried concurrently with the tests described earlier. These varied from a single thick coat dried for four hours, up to multiple coats dried for twenty four. Variations in results were small, and could not be correlated with the type of soap application used. In view of the much rougher surface of the 1.1/8 in. size bars (see Section 10.3), they were given an extra coat. All final coats were very uneven, and the term 'thick coat' could not be defined precisely. However, it is known that 85 gms. of soap were used to cover about 60 ft^2. of bar surface. During the drawing tests it was seen that soap was continuously rejected at the die inlet, so it was concluded that the aim of providing a surplus had been achieved.

The lubricant used in the oil drawing tests was Shell Vitrea 75. This is a straight mineral oil with viscosity of 24 centistokes at 100°c and 1,300 centistokes at 20°c. Surface-active lubricants were deliberately avoided, partly because high friction forces were specifically desired in these tests, and partly because such lubricants might have been more affected by increased heat generation during die-rotation. The particular choice of oil was made because it was closely comparable with an oil used in a separate investigation (34). Bars which were to be drawn with oil were degreased a few hours beforehand. Immediately prior to being drawn they were loaded onto the support rollers at the rear of the drawbench, and brushed liberally with oil. The oil was sufficiently viscous to drain off slowly compared with the duration of a set of tests. As with the soap lubricated tests, surplus lubricant was seen to be rejected at the die inlet, and all round the circumference of the bar. A further check was carried out. A 1.3/16 in. size bar was loaded and lubricated in the normal way, and was then drawn without die-rotation at about 13 ft/min. After about seven inches had been drawn, a copious supply of oil was abruptly squirted into the mouth of the die for a few seconds. No change in drawing force that could be related to the extra oil supply was observed.

10.3 SURFACE FINISH

Measurements were made of the surface finish of the test material using a Talysurf (see Appendix 1). Values obtained were extremely variable from point to point, and also depended on the meter cut-off length used (98).

Variations appeared to be random, so the minimum cut-off was used in order to obtain the range of values. Measurements were made very simply in the longitudinal direction of the bar, and many such readings were taken. The technique for measurement in the circumferential direction was extremely lengthy, and only a few such readings were taken. Measurements were made on the undrawn remnants of fourteen of the bars used in drawing tests, three each of the 1.1/8, 1.3/16, 1.1/4 and 1.5/16 in. sizes, and two of the 1.1/16 in. At least six readings were taken at different positions on each bar, and more where atypical distributions were found. Occasional values which lay grossly outside the band width for a particular set of readings were discarded, but otherwise the limits of values obtained on individual bars are shown in Table 10.4, and typical profiles in Figure 10.1. Corrosion pitting of the 1.1/8 in. size bars was clearly reflected in the high figures for that size. No circumferential measurements were made on these bars as it was thought that pickling would have removed any directionality caused by the earlier mechanical working.

All lubricant was washed off the bars before the measurements were made, but the phosphate coating was still present. It is not clear what significance should be attached to values obtained in the presence of such a coating, but repeated readings taken over the same track gave the same results. It seems therefore that a stable surface was being measured, be it metal or phosphate.

A set of measurements was also made on bars which had been drawn. For this a total of ten bars was used, two bars of each original size, one drawn with oil and the other with soap, and readings were taken on sections drawn with and without die rotation. Other details are as for the measurements made on the undrawn stock, and the results are also given in Table 10.4 and profiles in Figure 10.2. The general variability of readings swamped any variations which may have resulted from differences in the speed parameters with which the bars had been drawn. Circumferential measurements were made on two bars, the same portions being used as were used for the longitudinal measurements.

10.4 DISTRIBUTION OF VELOCITY AT THE DIE SURFACE

In order to describe the swing of the friction vector mathematically (see Section 3), it was necessary to determine the surface speed of the bar throughout the die. This was done by partly drawing bars which had grids engraved on their surfaces. The required distribution was then deduced from the progressive change in grid spacing through the die. The usual problems

		Nominal Diameter of Bar (in)				
		1.1/16	1.1/8	1.3/16	1.1/4	1.5/16
Undrawn Bars		50/60	115/150	40/70	50/70	30/55
Undrawn Bars		30/70	130/175	40/65	45/65	30/60
Undrawn Bars		-	125/150	45/70	45/70	35/60
Bars drawn with soap	without die rotation	40/55	55/70	30/50	30/50*	30/40
Bars drawn with soap	with die rotation	30/45	50/70	30/50	30/50	20/40
Bars drawn with oil	without die rotation	25/35	45/70	20/40	25/30+	12/25
Bars drawn with oil	with die rotation	20/40	50/70	15/35	20/45	15/30
		Surface roughness measured longitudinally (microinches C.L.A.)				

Corresponding circumferential * 40/55
Values + 40/70

TABLE 10.4

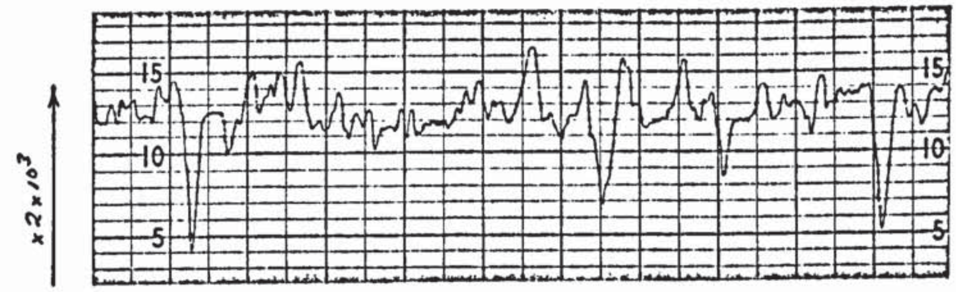

$1\frac{1}{16}$ in. diameter - 52 microinch C.L.A.

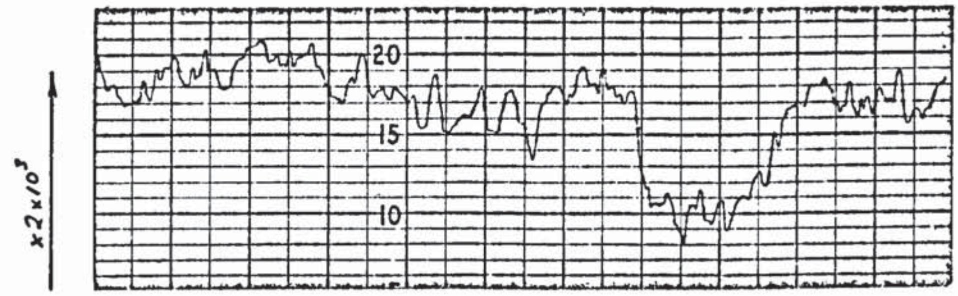

$1\frac{3}{16}$ in. diameter - 52 microinch C.L.A.

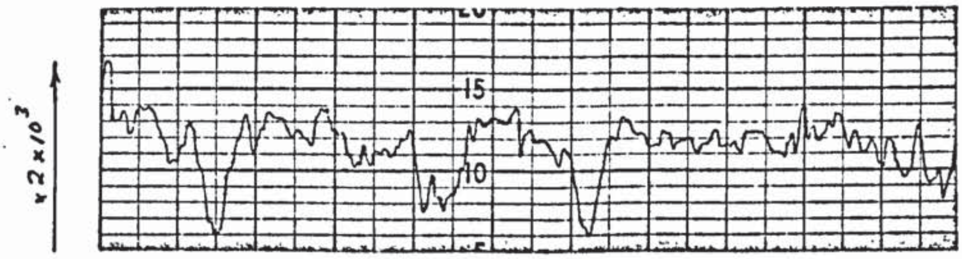

$1\frac{1}{4}$ in. diameter - 56 microinch C.L.A.

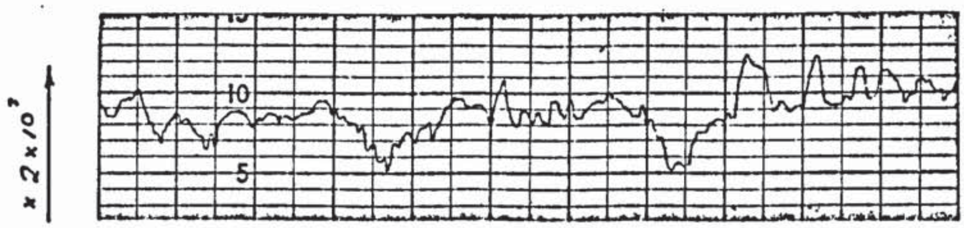

$1\frac{5}{16}$ in. diameter - 38 microinch C.L.A.

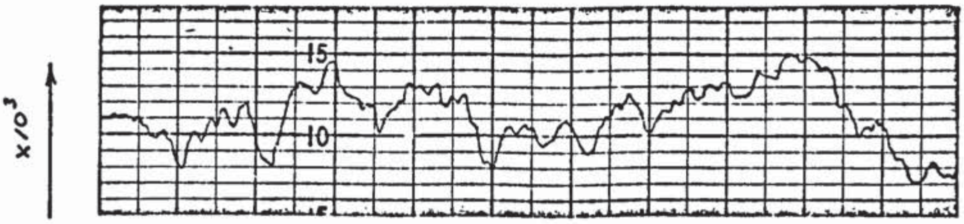

$1\frac{1}{8}$ in. diameter - 116 microinch C.L.A.

Fig. 10.1 - Typical Surface Profiles of Test Material Before being Drawn.

(Horizontal axis x20 on all)

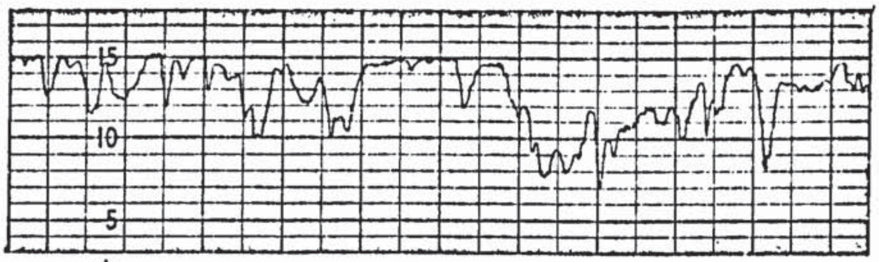

1⅛ in. diameter - 60 microinches C.L.A.
Drawn with oil.

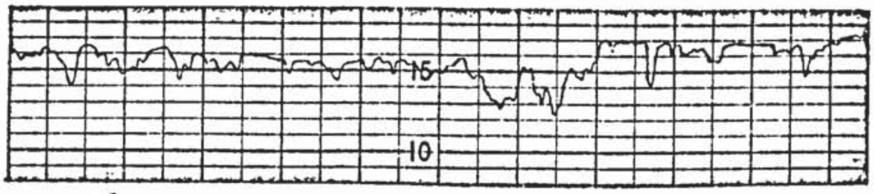

1 3/16 in. diameter - 28 microinches C.L.A.
Drawn with oil.

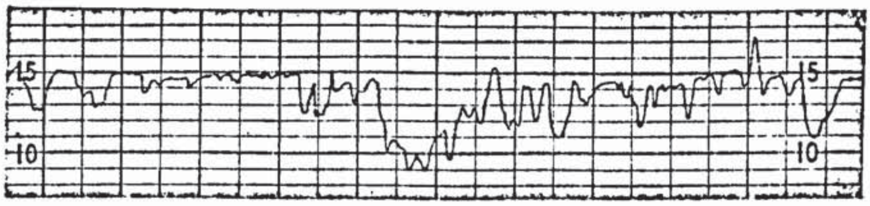

1¼ in. diameter - 32 microinches C.L.A.
Drawn with oil.

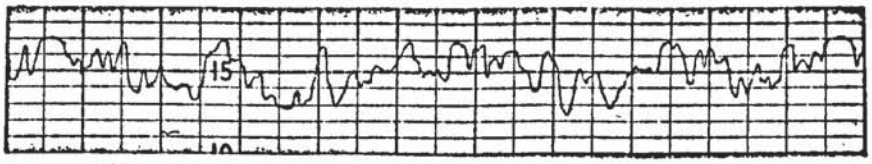

1 1/16 in. diameter - 36 microinches C.L.A.
Drawn with soap

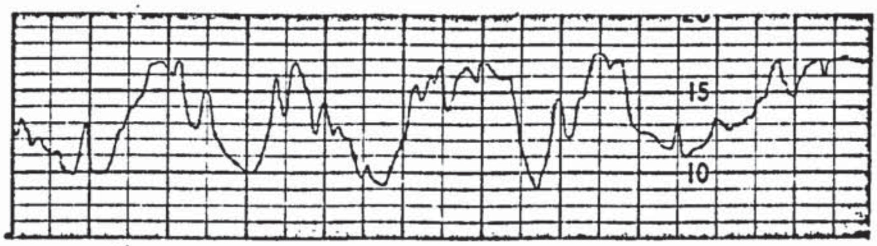

1⅛ in. diameter - 64 microinches C.L.A.
Drawn with soap

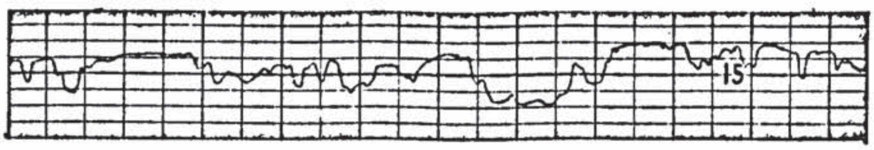

1 5/16 in. diameter - 20 microinches C.L.A.
Drawn with soap

Fig 10.2 - Typical Surface Profiles of Test Material After being Drawn.

Horizontal axis × 20 on all.
Vertical axis × 2×10^3 on all

involved with this type of work were greatly eased by the presence of the phosphate coating, on which clearly defined grids were easily cut, and which retained them during drawing.

The equipment used both to cut and to measure the grids was an optical measuring machine (see Appendix 1), with Tracelet attachment. The use of this equipment for engraving plane grids has been described elsewhere (100), but circumferential grids were needed here. The arrangement is illustrated in Figure 10.3.

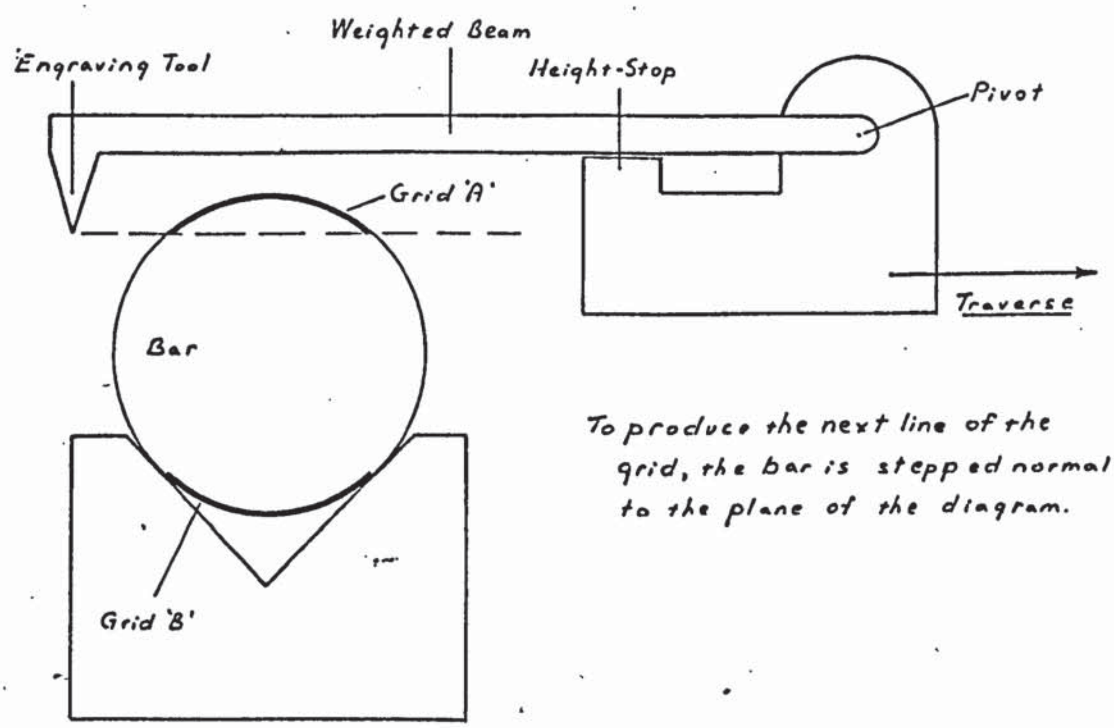

Fig. 10.3. - Mode of operation of 'Tracelet' Mechanism.

The bar was mounted on the table of the machine, with its axis parallel to that of the table. The Tracelet, which was simply a weighted and pivoted single point engraving tool, was attached to the head of the machine. Traversing the head produced one line of the grid, and the bar was re-positioned for the next line with the table traverse. This gave a parallel grid, which was all that was required. The method produced a grid over only a part of the periphery of the bar, so two opposed grids were cut, grids A and B, to correct for any asymmetry in the drawing operation. No longitudinal datum was available, so it was not possible to ensure that the grids were exactly opposite each other. A grid-spacing of 0.050 in. was used, except for the 1.1/16 in. size bar, for which 0.025 in. was chosen. The machine was extremely accurate, and it was not thought necessary to check the grid-spacing after it was cut.

An Avery tensile testing machine (see Appendix 1) was used for the drawing operation, as this had to be done slowly to ensure that drawing could be stopped with the grid spanning the die. Tests were first done on two sections of 1.3/16 in. bar, one drawn with soap and the other with oil. No difference between the two velocity profiles could be detected. Therefore only one test was performed on each of the other sizes of bar, and soap was used. Passage of the 1.1/16 in. bar through the die was so seriously asymmetric that no meaningful measurements could be made on its grids. The results for the other sizes are given in Tables A7.6 to A7.10, and the manipulations on the results for grid A are described below. Grid B measurements were treated identically.

Each grid-line was given a reference number, n, starting from the drawn end of the grid, and its position relative to the measuring machine scale is given under the heading A_n. The grid-spacing at any position is then δ, where

$$\delta = A_{(n+1)} - A_n$$

It should be noted that this is the grid-spacing measured along the axis of the bar, and within the zone of contact it is the cosine component of the real grid-spacing. The axial velocity v at any point, is conveniently expressed as a proportion of V, the exit or drawing velocity. To do this it is necessary to know δ_1, the grid-spacing after exit, and to use the fact that the average velocity between two grid lines is proportional to the spacing of those lines. By assuming volumetric constancy,

$$\frac{v}{V} = \frac{\delta}{\delta_1} = \frac{\delta}{\delta_2} \cdot \left(\frac{d_1}{d_2}\right)^2$$

where δ_2 is the original grid-spacing, and d_1 and d_2 are the diameters at exit and entry. As this defines the average velocity between grid-lines, it is most properly related to the mid-point, and this is given by $(A_n + \delta/2)$.

This would enable the velocity profile to be plotted, but only relative to the arbitrary datum of the machine scale. Thus no direct comparison between results for A and B grids, or between different bars could be made. Nor would the precise location of the die relative to the profile be known. The best reference position would be the exit plane, but neither entry nor exit planes were clearly defined under the microscope of the measuring machine. For the first two tests, on 1.3/16 in. bar using oil and soap, these positions were estimated using a rule and magnifying glass, and the measurements were not considered reliable to better than ± 0.010 in. The conclusion that there was no difference in velocity distribution between the two tests, was reached by noting that the form of the two curves was identical. For the two test conditions to have given the same velocity profiles but different velocity distributions, the effective entry and exit planes relative to the die would have had to be different, and this is extremely unlikely.

To accurately locate the entry and exit planes, measurements were made with the grid-lines viewed in profile as in Figure 10.4. Measurements were made in both axes, and the profile was plotted. These profiles were compared with the known profile of the die (see Section 8). Point Z in Figure 10.4

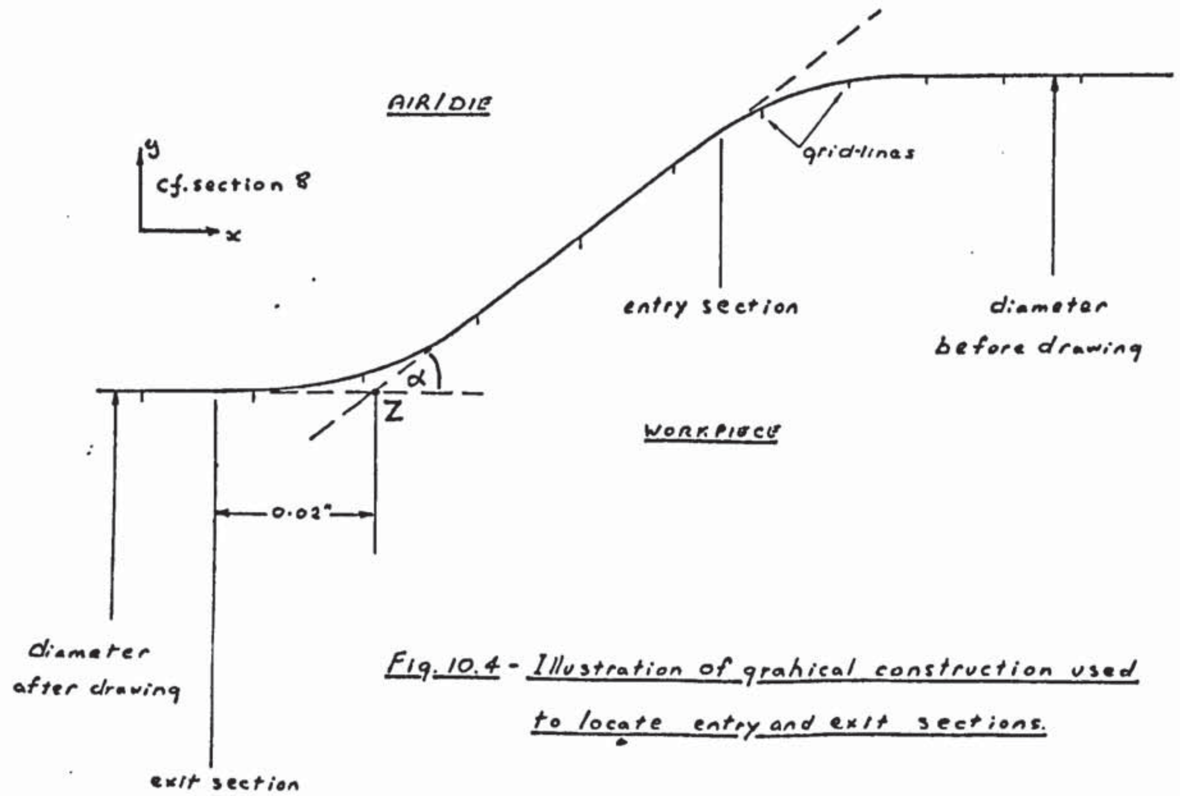

Fig. 10.4 - Illustration of grahical construction used to locate entry and exit sections.

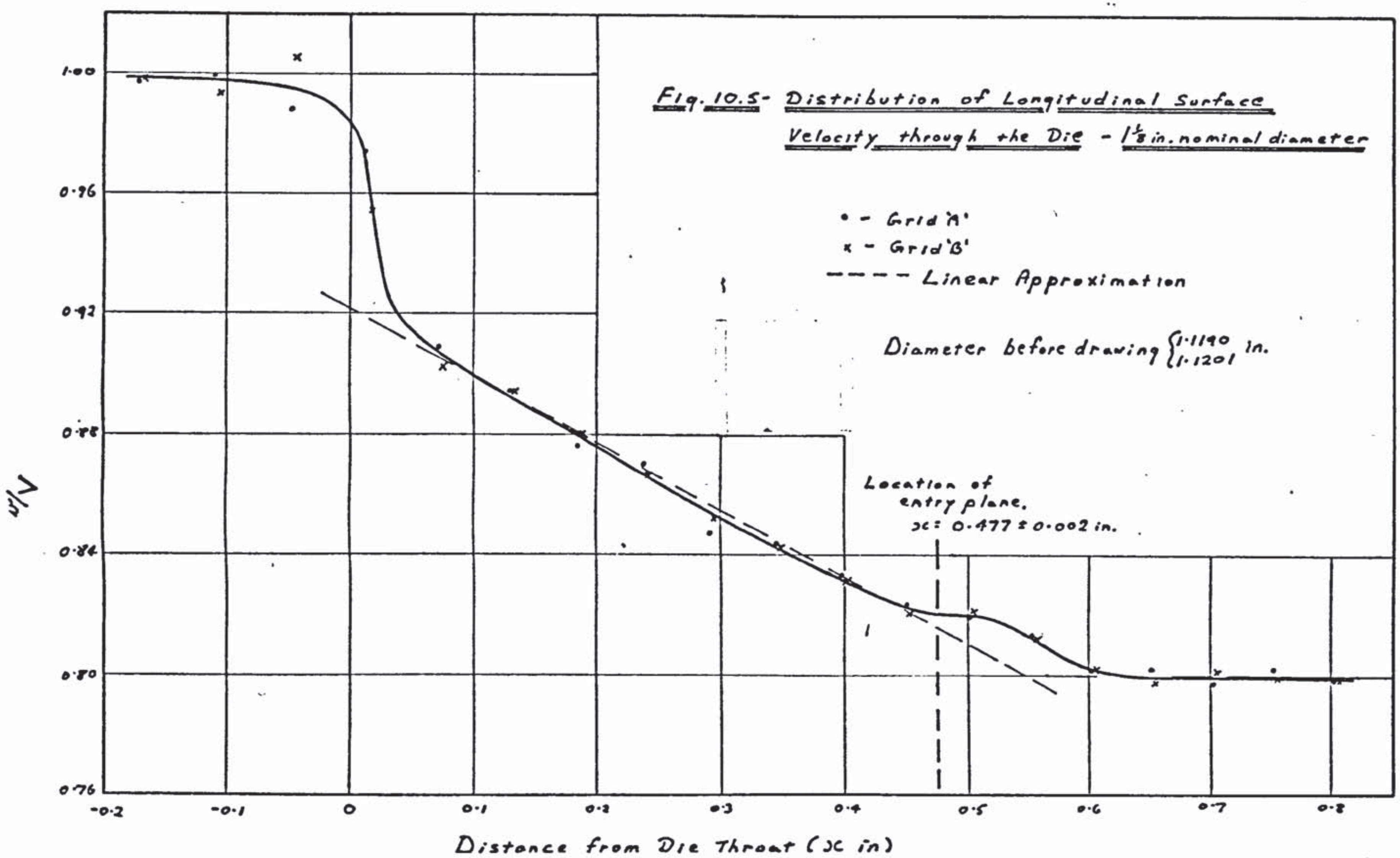

Fig. 10.5 - Distribution of Longitudinal Surface Velocity through the Die - $1\frac{1}{8}$ in. nominal diameter

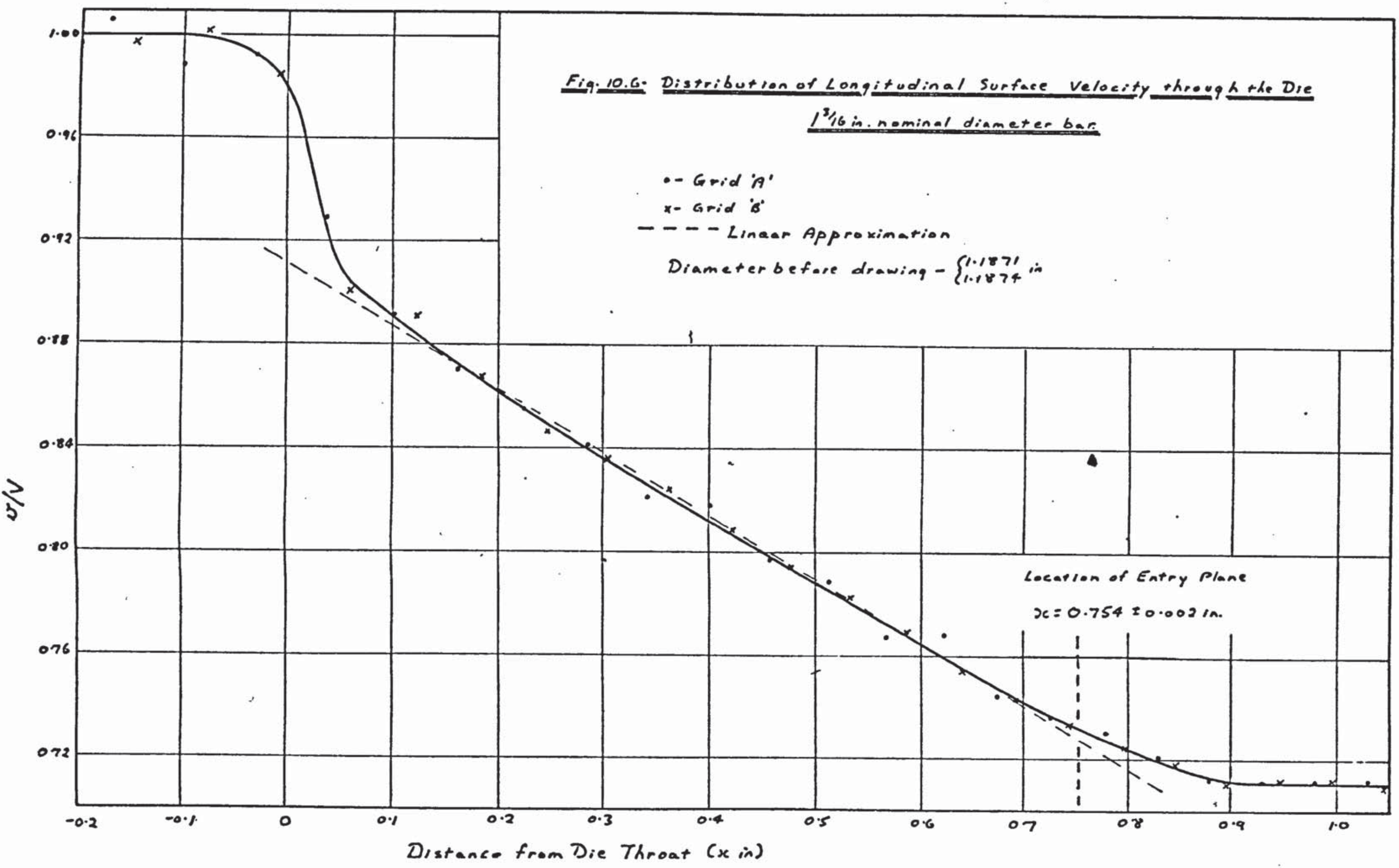

Fig. 10.6 Distribution of Longitudinal Surface Velocity through the Die
$1\frac{3}{16}$ in. nominal diameter bar.

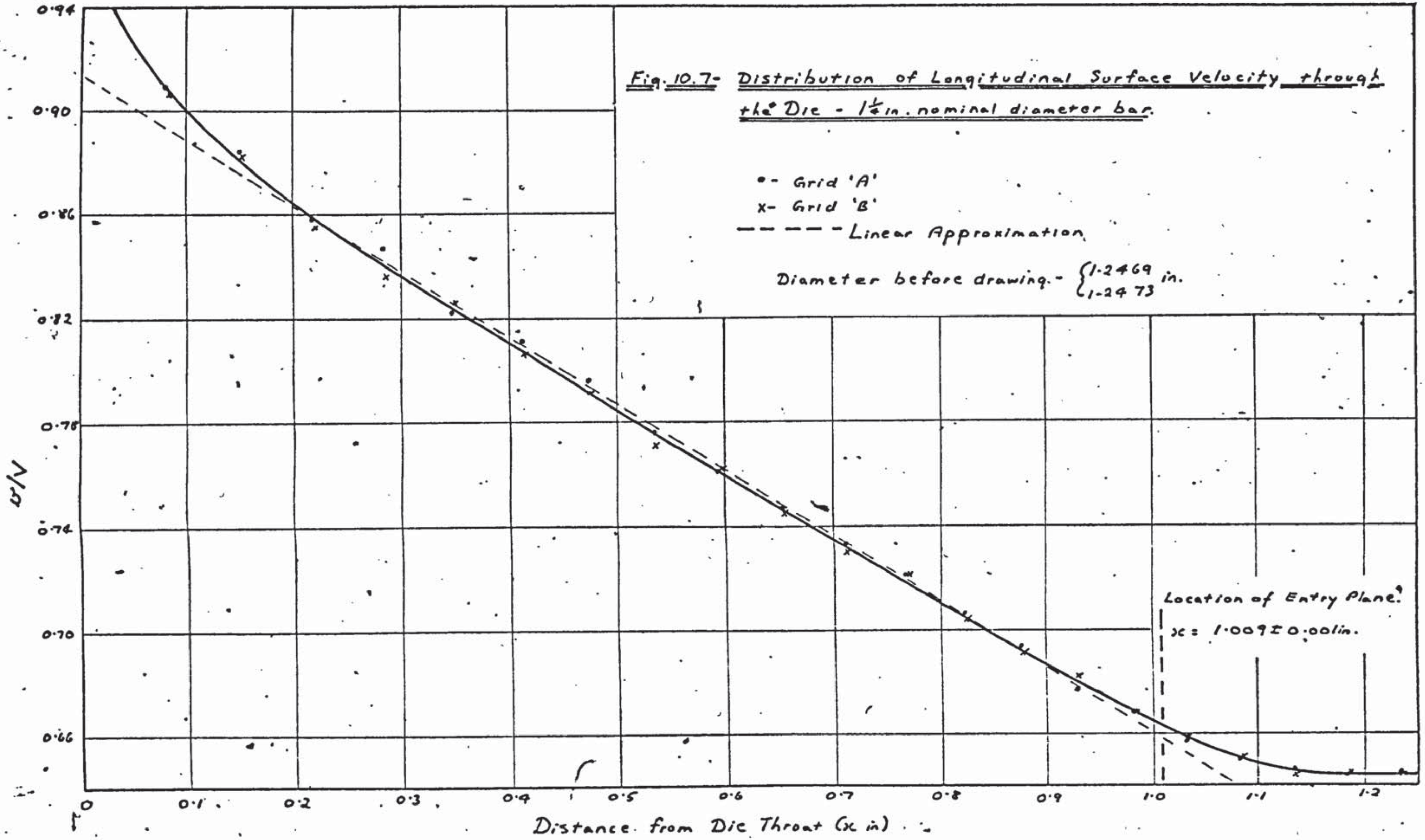

Fig. 10.7- Distribution of Longitudinal Surface Velocity through the Die - $1\frac{1}{4}$ in. nominal diameter bar.

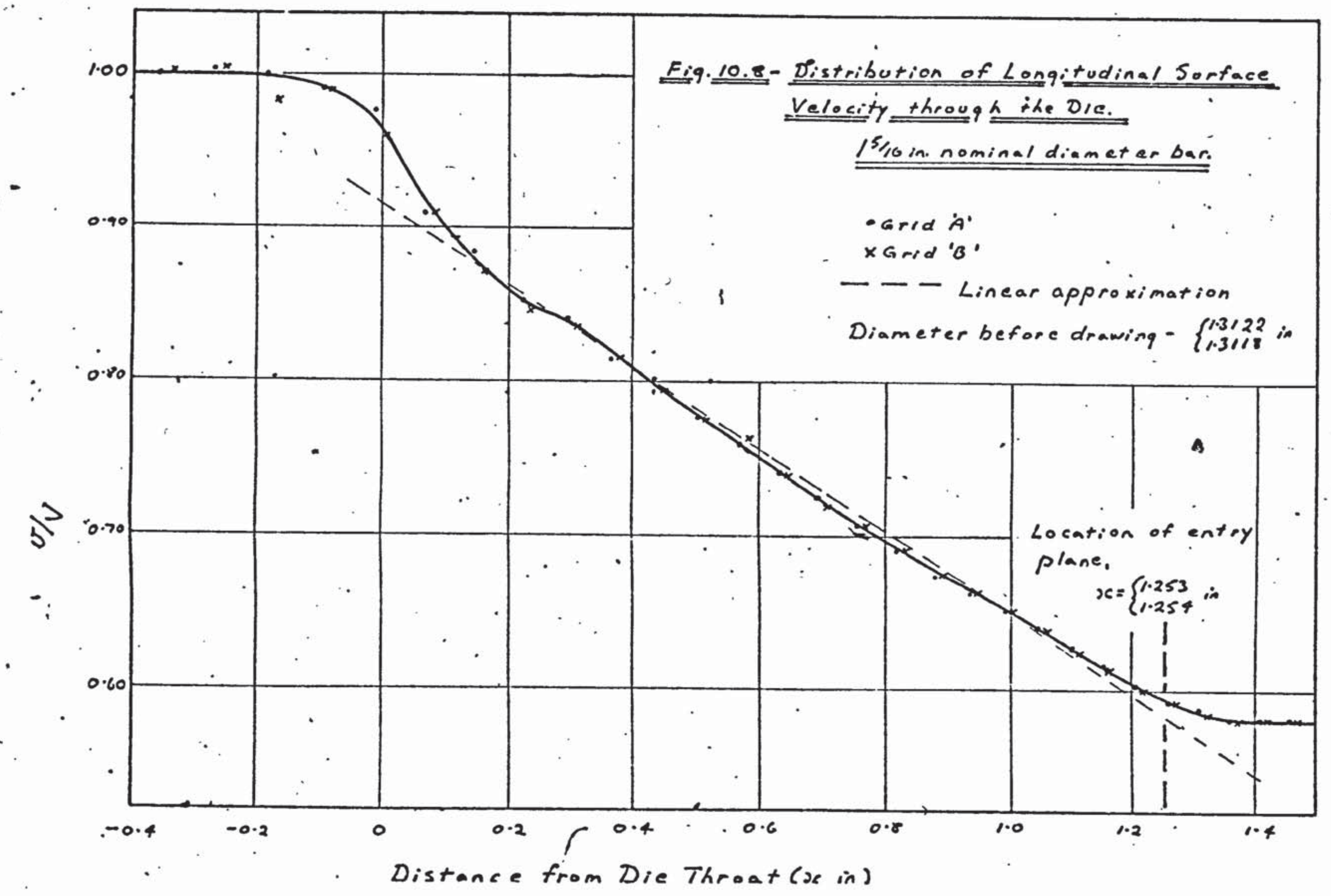

Fig. 10.8 - Distribution of Longitudinal Surface Velocity through the Die.
1 5/16 in. nominal diameter bar.

was specifically located by the intersection of the 7° flank angle with the surface of the completely drawn part of the bar, and the exit plane was taken to be at the throat, which was a known distance from Z (see Figure 8.1). Location of the entry plane was more difficult, as it involved estimating the position at which the two surfaces diverged. However, in view of the high accuracy of the measuring machine, these figures were thought to be reliable to $\pm$ 0.002 in.. This technique gave the location of the entry and exit planes relative to the earlier grid measurements, and these values are included in Tables A7.7 to A7.10. The method could not be used on the first test specimen, 1.3/16 in. bar drawn with soap, as this had been destroyed when the test was repeated with oil.

With the new information, the exit plane was made the datum for the velocity profile, and the values of $(A_n + \frac{\delta}{2})$ were modified accordingly. The final velocity distribution curves are plotted in Figures 10.5 to 10.8, together with the linear approximations used in Section 10.5. An interesting feature of the curves is that the bar clearly started to deform before making contact with the die. The extreme roughness of the 1.1/8 in. bar was probably the cause of the anomaly at the entry section in Figure 10.5. Apart from this, no discontinuity can be seen at the entry sections, but marked discontinuities are apparent at the exit sections. As the grid method gave average velocities between points, discontinuities may have been even sharper than is evident.

The main conclusion which can be drawn from these tests, is that the use of a linear relationship, for the increase of speed as the bar passes through the die, is justified. The selection of specific values of the coefficients k_1 and k_2 is discussed in Section 10.5

10.5 GEOMETRICAL PARAMETERS

The analysis described in Section 3 required that the die/workpiece contact region be described mathematically. The parameters required were the die angle, and the location of the entry and exit planes relative to the apex of the die cone. In addition the coefficients k_1 and k_2, which defined the distribution of velocity through the die, were needed. These were all dependent on the entry diameter of the workpiece.

10.5.1 Diameter of Bar

Many measurements of diameter were made around and along each bar, both before and after being drawn. In view of the small variations found

Nominal Diameter (in)	Actual diameter before drawing (in)			Diameter after drawing (in)		Reduction of Area (%)
	Mean	Ovality	Variation	Soap	Oil	
1.1/16	1.0575	± 0.0004	± 0.0011	1.0000 ± 0.0005	1.0000 ± 0.0005	10
1.1/8	1.1230	± 0.0005	± 0.0033	1.0010 ± 0.0005	1.0008 ± 0.0004	21
1.3/16	1.1867	± 0.0003	± 0.0017	1.0007 ± 0.0004	1.0004 ± 0.0004	29
1.1/4	1.2462	± 0.0003	± 0.0012	1.0002 ± 0.0005	0.9994 ± 0.0006	36
1.5/16	1.3124	± 0.0003	± 0.0008	0.9984 ± 0.0010	0.9964 ± 0.0011	42

TABLE 10.5

between bars of the same nominal size, the measurements made on bars used in the main drawing tests have been summarised as shown in Table 10.5. For the purpose of ascribing values to the other geometrical parameters, the exit diameter of the bar was assumed to be that of the die throat. In spite of the relatively large difference between this, and the measured diameter of the 1.5/16 in. bar after drawing, the only analytical errors resulting from this assumption were due to the elastic strains in the die.

10.5.2 Effective Die-Angle

Although the die form was very close to the ideal, there was a slight parallel (see Section 8). Allowance for this was made by using an equivalent die-angle for each size of bar. This was obtained from a large scale plot of the die profile, and the procedure is illustrated in Figure 10.9. Values are listed in Table 10.6.

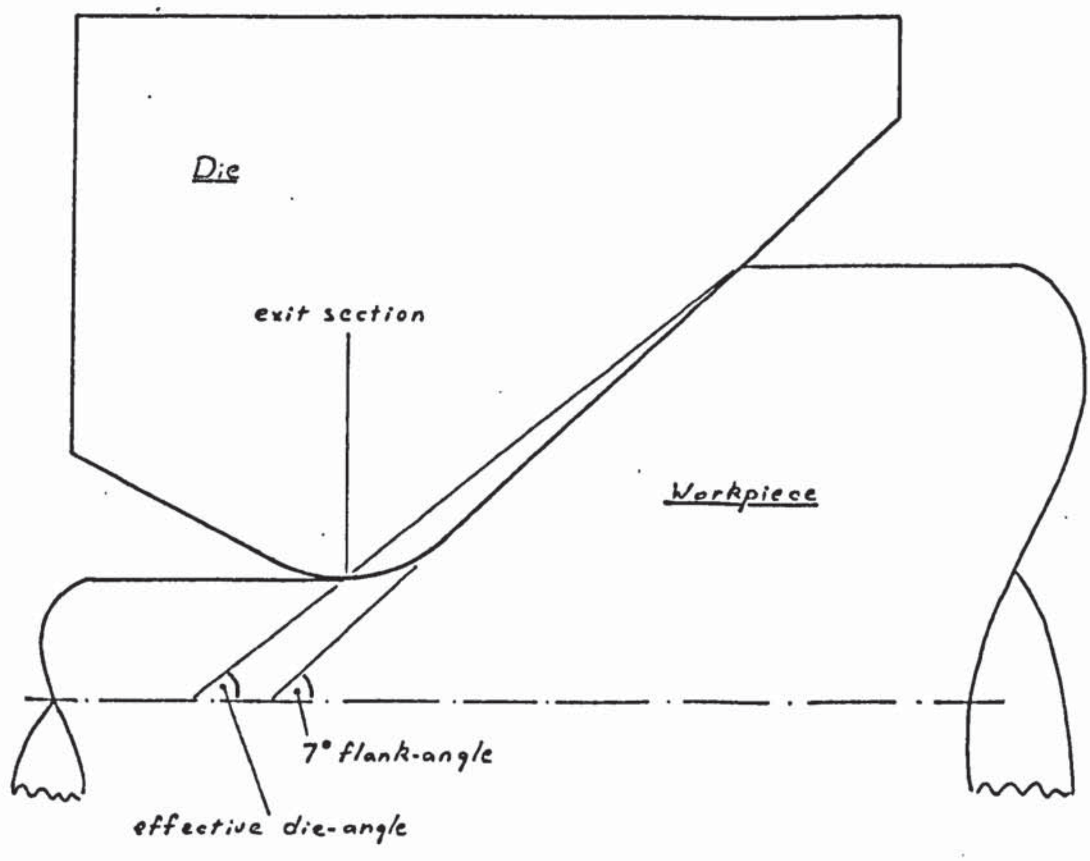

Fig. 10.9 - Graphical construction to find effective die-angle

10.5.3 Position of Entry and Exit Planes

The value of x_1 , the distance between the apex of the die-cone and the exit plane, was obtained trigonometrically for each size of bar, using the equivalent die-angles referred to above, together with the diameter of the die-throat. The corresponding values of x_2, the distance to the entry plane, could not be obtained in the same way, because the velocity distribution tests of Section 10.4 had shown that the diameters of the bars decreased before reaching that plane. However, some trouble had been taken during those tests to measure the actual distance between the two planes, so x_2 could be obtained by addition. The diameters of some of the bars used in those tests were at the extremes of the ranges shown in Table 10.5. In fact the 1.1/8 in. size was slightly outside the range. Therefore the locations of the entry plane found in those tests, were corrected according to the deviation of the diameters of bar used in those tests from the mean values of Table 10.5, before making the addition to find x_2. The values deduced for x_1 and x_2 are shown in Table 10.6.

The location of the entry plane for the 1.1/16 in. size was obtained by extrapolation from the data known for the other sizes. The extrapolation was quite a long one, so to reduce errors it was first noted that due to the early onset of deformation, measured values of bar/die contact length were always slightly less than calculated values. Extrapolation of this difference gave less scope for error.

10.5.4 Velocity Coefficients

Values of k_1 and k_2, the coefficients used to describe the distribution of velocity at the bar/die interface, were obtained from large scale versions of Figures 10.5 to 10.8, using the corrected values of die/bar contact length. As taken from the curves, values referred to the axial direction, and were divided by $\cos \alpha$ to obtain k_1 and k_2. The final values are given in Table 10.6. Values for the 1.1/16 in. size were once again obtained by extrapolation. A similar technique to that described in Section 10.5.3 was used for k_2. For k_1 an additional point on the extrapolation curve was obtained, by assuming that k_1 must equal unity at zero reduction of area.

Nominal Diameter (in)	Die-Angle (tan α)	Location of Entry and Exit Planes		Velocity Coefficients	
		x_1	x_2	k_1	k_2
1.1/16	0.1147	4.358	4.581	0.958	0.918
1.1/8	0.1187	4.211	4.702	0.928	0.819
1.3/16	0.1196	4.181	4.933	0.919	0.733
1.1/4	0.1201	4.163	5.168	0.921	0.664
1.5/16	0.1223	4.088	5.341	0.922	0.587

TABLE 10.6

10.6 DRAWING TESTS

10.6.1 Parameters of the Test Programme

i) Figures given in this sub-section are nominal values which were aimed for during the tests, and they should not be treated as experimental data.

ii) The terms 'set of tests' and 'group of tests' have been used in a specific way, which is defined in the text. Briefly, one set comprises two groups.

A method for operating the drawbench at speeds below 5ft/min. had by this time been developed, and is described in Appendix 2. The general system of performing tests in definite sets was similar to that used in Series I. For Series II each set comprised eight individual tests, which spanned the range of drawing speeds. They were performed at a nominally constant rotational speed, and consecutively on a single bar. It was possible to perform four tests in quick succession, before exhausting the stroke of the drawbench. Each set was therefore split into two groups of four, and the sequence 1, 5, 10, 15 ft/min. and then 1, 3, 7½, 12½ ft/min. was used. Performing the tests in ascending speed order was a token in the direction of achieving steady-state temperature conditions, as was the repetition of the 1 ft/min. test. The two groups were interlinked so that if progressive changes had been observed, distinction could have been made between speed or temperature effects, and changes in material properties along the bar.

Sets of tests were performed at five rotational speeds over the range 5 to 50 rev/min., and were done with both oil and soap lubrication. All of the soap lubricated tests were done first, with the object of obtaining as much data as possible before any possible damage to the die. Many of the soap lubricated tests on 1.1/16 in. bar showed considerable asymmetry, the die/bar contact length varying by as much as two to one around the periphery, and the oil lubricated tests on this size were curtailed when the first set showed the same behaviour. It was not possible to cover the full range of speed parameters when using oil with the larger sizes of bar, as this would have entailed exceeding the limiting design torque for the equipment. This arose because the original programme specification was for high drawing speed tests only. It was occasionally possible to perform two sets of tests on a single bar, with these shortened sets, and a number of tests which gave equivocal results were repeated.

Procedure within tests was closely similar to that for Series I. A section of bar drawn without die-rotation was followed by one drawn with, and then another without. Each section was of four inches drawn length. This applied to all tests except those at 1 ft/min., for which the sections were three, two and two inches long. The latter lengths were adopted partly to save stroke, partly because it was thought that conditions would stabilise rapidly at the very slow drawing speed, and partly because the bar surface appeared to become unduly hot during the die-rotation period.

10.6.2 Experimental Procedure and Observations

The lamp of the ultra-violet recorder, the load-cell supply voltage, and the digital voltmeter, were always switched on well before drawing tests were to be performed. The load-cell supply voltage was checked immediately to confirm that it was near the correct value, and after a minimum period of one hour it was re-checked accurately. The galvanometers were then calibrated by the procedure given in Section 7.3 .

The hydraulic system and rotary drive were switched on just before the drawing tests began, and they were cycled over their speed ranges to clear them of air. The rotary drive was left at the setting required for the following tests, this being done from the control scale rather than with the speed transducer. The die was wiped out with a clean dry rag but was not degreased.

The following description is for drawing tests using soap, additional points relating to oil lubricated tests being given later. The bar was loaded onto the support rollers, having previously been prepared as described in Sections 10.2 and 10.6.3. The rotary drive was switched off and a short length of record chart was run to give datum positions, after which the rotary drive was switched on again, but was left de-clutched. The bar was rolled forward into the die, and the ram, which had been left partly extended, was retracted to bring the jaw assembly over the tag. It was usually necessary to lift the jaw assembly off its supporting wheel before this could be done. After some manipulation the jaws could be pushed forward into the wedge, and the heel plate fitted and tightened. This part of the operation could be awkward when the tag was bent or uneven.

A few inches of bar were drawn to engage the full diameter in the die, and this was done abruptly to make the jaws bite. The drawing speed control was then set to the desired value and the stroke measuring scale adjusted as described later. The time and exact supply voltage were noted, the recording chart started, and drawing commenced. Drawing and recording were stopped when the test length had been drawn, the clutch of the rotary-drive having meanwhile been engaged and disengaged at the appropriate points. The drawing speed was re-set, the stroke scale re-adjusted, recording re-started, and the next test performed. Four such tests were performed at different drawing speeds (see Section 10.6.1) and as rapidly as possible. The heel-plate was then removed, the ram inched in reverse to disengage the jaws, and then run forward again to free the tag completely. The rotary drive was switched off and another short length of chart was run to set up the final data. The chart speeds used were 0.15 in/sec with drawing speeds up to $7\frac{1}{2}$ ft/min., and 0.5 in/sec above.

The drawn length of bar was cut off by hand, and stamped with the reference number (see Appendix 3) of a test which had been done on it. Only one such reference was necessary, as the boundaries between test lengths were clearly marked by an indented ring. The second group of tests in that set were then performed, the new section of drawn bar was cut off, and the undrawn part of the bar was then pushed out using the reverse stroke of the ram. Some of the larger sizes of bar could easily be withdrawn by hand.

For tests using oil, the oil was applied to the bar (see Section 10.2) just before the initial datum record was made. It was brushed onto the full length of bar to be used in the set of tests. Whenever possible during the set, the bar was rotated through 180° to allow the oil to re-distribute itself. The interval between starting the first and second groups of tests was eleven to twelve minutes when using oil. The larger part of this was taken up with cutting off the drawn section, and during this period it was possible to turn the bar frequently.

Two systems were used for monitoring the length of bar drawn during tests. With one, a scale was taped to the tag, and its movement past a fixed pointer was observed. This was not possible for the first test in a group, as there was then insufficient tag visible. The alternative was to watch the movement of the assembly past a fixed scale*.

External forces made it necessary to complete the drawing tests within a limited period, and it was therefore not possible to fully evaluate the test data as it was acquired. A compromise was therefore adopted. Rough measurements of torque and load reduction, and a few accurate measurements, were made on each chart as soon as possible, and the records were then stored away. This was done after each set of tests when using oil, and after each group when using soap. The measurements of torque and load reduction were not converted, but were plotted as galvanometer deflections against the nominal speed parameters. As deviations from these parameters were fairly small and repeatable, this gave a good quick check on the quality of the data as it was obtained. Thus it was possible to repeat some tests where equivocal results had been found and spare material was available, and it was also possible to avoid others which would have overstressed the equipment. The purpose of the accurate measurements was to detect any dimensional change in the charts during storage.

The barstock was not perfectly straight, and tended to move about on the support rollers while being drawn. The rollers had some degree of freedom, but imposed some restraint on the bar. More seriously, the stock passed through a two inch diameter hole at the rear of the drawbench, and would sometimes press hard against this. However after a few feet had been drawn the end of the bar would abruptly come free, and as no related discontinuity could be seen on the record charts, it was concluded that the effect of the restraint was insignificant.

At the end of the programme of drawing tests measurements of angle of twist and of diameter were made on all drawn material. These were described in Sections 10.6.3 and 10.5.1.

10.6.3. Twist of Bar During Die-Rotation

Two of the conclusions drawn from Series I (see Section 9.6) were that die-rotation caused the free end of the bar to rotate, and that this speed should be measured. Direct measurement posed several problems, but it was realised that a definite relationship existed between the speed and the final twist in the drawn bar. This relationship and its derivation are given in Appendix 4.

The method used to measure the angle of twist involved scribing a longitudinal line on the bar prior to drawing. The obvious way to do this would have been to use a height marking gauge, with the bar laid on a surface table. This could not be done because the bars were not perfectly straight, and the plane of bending usually varied along the bar. A conveniently simple adaptation of this method was used, and is illustrated in Figure 10.10. This amounted to using a small portable surface table in the form of an angle plate. Bending was usually not noticeable over the ten inch length of the angle plate, and where it was the bar was rotated until the plane of bending was parallel to the plane of the plate. A high speed steel turning tool held against the plate was used as a scriber. The dimensions of this tool had no fundamental importance, but it was thought best to arrange for a radius from the centre of the bar to roughly bisect the point of the tool, as in Figure 10.10. A series of longitudinally overlapping lines were scribed, but no attempt was made to link individual lines together.

After the bar had been drawn, the helix angle was measured by developing the surface of the bar. Such a development is shown in Figure 10.11(a). A magnified representation is shown in Figure 10.11(b) to illustrate the points of interest. The linear portion of the helix was connected to untwisted sections of the bar by curved regions. As expected, the length of these curved regions corresponded roughly to the interval for a given particle to traverse the die, but it will be realised that the junction points between curved and linear regions could not be accurately defined. It was not necessary to develop the entire curve for ϕ, the helix angle, to be measured. A strip of tracing paper with one edge trimmed straight was wound round the bar, and adjusted so that the edge overlay itself. Two points were marked on the paper, just within the curved ends of the helix. The inclination to the reference edge, of a line between the two joints, was measured with a vernier protractor. The overall

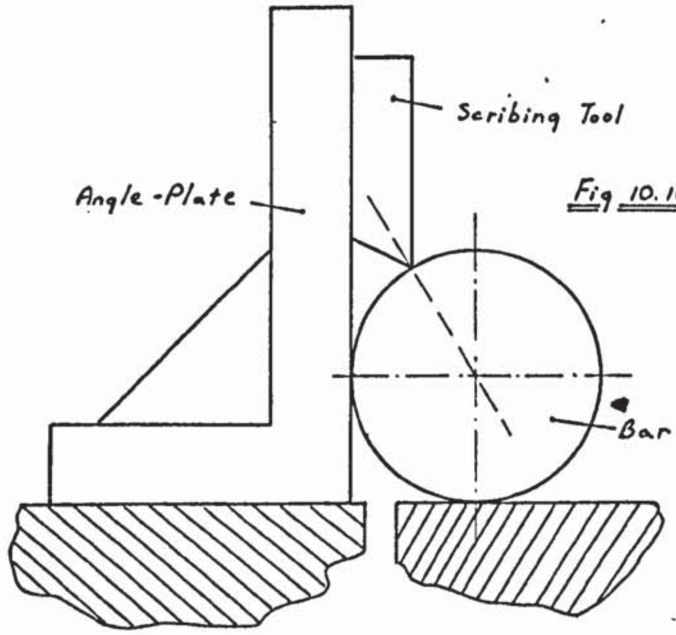

Fig 10.10 - Arrangement used for Scribing Longitudinal Lines on Test Material.

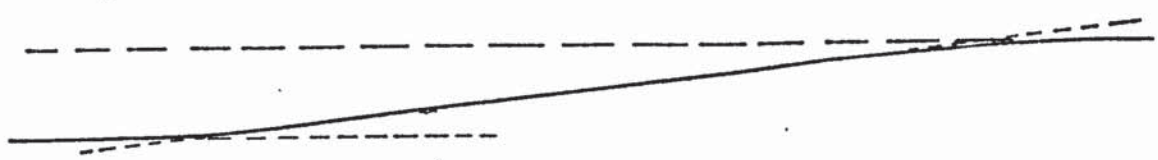

Fig. 10.11 (a) - Development of Surface of Drawn Bar, (Test no. 94) Showing twisting caused by Die-Rotation

Direction of Drawing

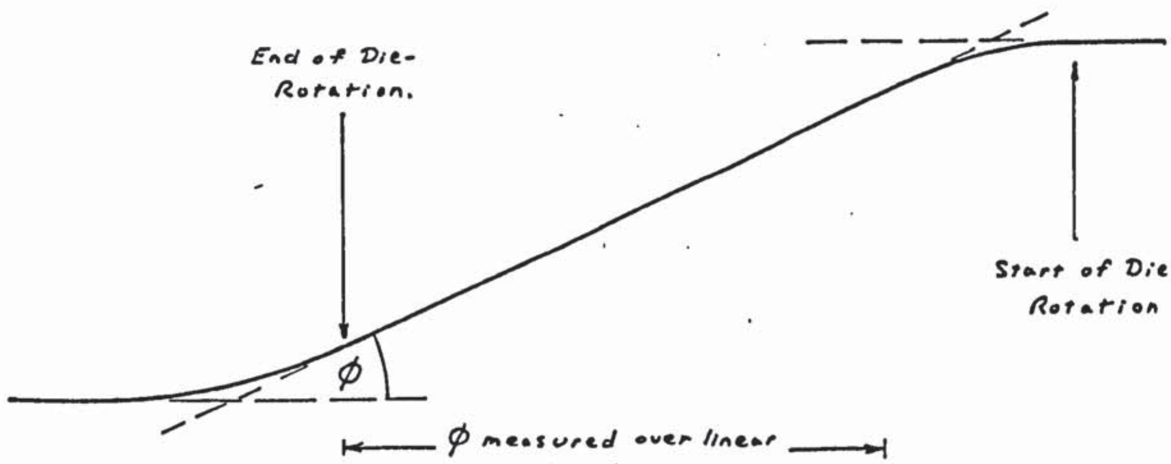

Fig. 10.11(b) - Magnified Representation of Fig. 10.11(a)

accuracy of the technique was estimated at $\pm 1/4^{\circ}$.

Some obvious limitations were found. Firstly, no sensible measurements could be made on bars drawn at 1 ft/min., because in those tests the whole die-rotation period covered only two inches; and secondly, any small changes in ϕ which may have occurred during the 'linear' part of the helix could not be detected.

Measured values of ϕ are given and discussed with the main body of the test results.

10.6.4 Interpretation of Test Records

The original analysis (see Section 3) assumed that conditions would be essentially steady-state when drawing with a rotating-die, and that the test parameters would take unique values throughout each section of the test. The measuring and recording systems were designed specifically for these conditions. Behaviour in many of the tests was of this form, but many others showed considerable point to point variations. However, it was clear that these variations were systematic, and to have treated them as being random would have destroyed the utility of the work. It was therefore necessary to arrive at some hypothesis to explain the variations, so that a rational system for the selection of data could be established. To avoid the possibility that data might have been selected to support the hypothesis, both the hypothesis and the system were produced before any calculations were made with the data. This was done simply by reviewing the forms of the record traces, and noting the associated experimental conditions. Thus this sub-section must partially arrogate the function of Section 10.7.

A clear indication of the general explanation for the variations was that the features to be discussed were also found to be present in the Series I records, but there they were of much smaller magnitude and had either been missed completely or partially misinterpreted. The aspect of Series II which magnified them was the tests at low drawing speeds, and a representation of records of such tests is shown in Figure 10.12. Reference is made in the following discussion to the form of records obtained in Series I, where they differed from Series II records, and where a line of argument followed on from one developed earlier.

Random fluctuations are not considered except where specifically mentioned.

10.6.4.1 Speed Records :- The rotational speed traces followed closely the ideal form that had been hoped for, except that rise and fall times were of course finite. Rise time increased with torque, and also with the distance between jaws and die. The former was consistent with behaviour expected of the friction clutch, and the latter with elastic wind-up of the drawn part of the bar. Speed was steady after the initial rise, except occasionally at very high torques where the drive was working near its design limit.

The drawing speed traces showed substantial transients. However, V_c and V_e were equal and V_{cd} was steady. Differences between V_c and V_{cd} were always small, and were only detectable below 5 ft/min. This difference had been anticipated and was a function of the control system at low speeds (see Appendix 2). The size of the velocity jump at t_c and t_d was largest at high R/V ratios where, amongst other effects, load reductions were greatest. This behaviour was analogous to the yield point behaviour of 'soft' tensile testing machines. When the demanded drawing force fell at t_c, the energy stored in the machine frame and hydraulic system produced the surge in drawing speed, and conversely at t_d. The jump could be of first order magnitude compared with V_{cd}, and was highly transient as indicated. The nature of the drive to the drawing speed transducer suggested that no significance could be attached to indicated values of V at or near $\hat{V}$.

10.6.4.2 Secondary Features of Drawing Force and Torque Records :- These are dealt with first in order to clarify the general picture. The initial peak of P_b needs no comment, but occasionally, atypical behaviour was observed at that point when drawing with oil. This was probably associated with temporary thick-film lubrication, caused by elastic kick-back of the drawbench after the preceeding test, which allowed oil to run into the die, and is of no interest here. The negative blip in torque at t_d only occurred with very high values of T'_{cd}, and was small even then. It seemed likely that it could have been caused by overshoot when the bar unloaded, and it was ignored as such an elastic double kick-back was actually observed.

In general, the torque and drawing force traces showed some small deflections, P_a and T_a, as soon as the jaws were tightened, and did not return to their zero positions until the jaws had been disconnected at t_f. This behaviour was to be expected in view of the friction in the two drive systems. Values of T_{bc} and T_{de} sometimes varied during a test. It seemed likely that any initial stray torque load caused by tightening the jaws, would be released once the material started to flow at t_b. Similarly, residual frictional torque remaining after t_d would be released throughout t_{de}. Values of T_{bc} and T_{de} were therefore thought to reflect the cross-sensitivity of the torque bridge to direct load, and it was from these measurements that Figure 7.6(b) was obtained. Considerable scatter is shown in that diagram, and this seemed to be associated with bars which drew asymmetrically. There was no anomaly between this observation and the very low bending sensitivity of the load-cell (see Section 7.4.6), as it was possible for a bent bar to impose a genuine torque on the load-cell. This apparent variability in the cross-sensitivity caused no problem, as it could be overcome by suitable choice of datum (see Section 10.6.4.6)

10.6.4.3 Primary Features of Drawing Force and Torque Records :- During Series I, values of P_{bc}, had been observed to fall slightly during t_{bc}, and P_{de} to rise slightly during t_{de}, when drawing the larger size bars; the final value, P_e, being always equal to or slightly less than P_c. These changes were not observed in Series II tests using soap, in which these values were essentially stable. They may have occurred in the tests using oil, but random fluctuations were larger in those tests, so no firm conclusion could be reached. Series I also showed steady decreases in P_{cd} throughout t_{cd} in some tests and this behaviour was found in Series II as well.

P changed abruptly at t_d, but then rounded off gently to P_{de}. At t_c, P fell sharply and then levelled off sharply. However, after the first well defined levelling point there was, in some cases, a further slight fall before joining P_{cd} in the region of t_c' and t_c'' . The location of these instants is described later.

The torque traces showed the largest changes during individual tests, and the widest variations in form from test to test, of all the measured parameters. The long and short term changes shown in Figure 10.12 could appear together, separately, or not at all. In addition, the initial peak of $\hat{T}$ could

Fig. 10.12 - Representation of Test Record Chart

Sequence of Operations	
Time Instant	Operation
t_a	jaws connected
t_b	drawing started
t_c	rotation started
t_d	rotation stopped
t_e	drawing stopped
t_f	jaws disconnected

Datum lines indicated thus —·—·—·—

Equal time lines indicated thus - - - - - - - -

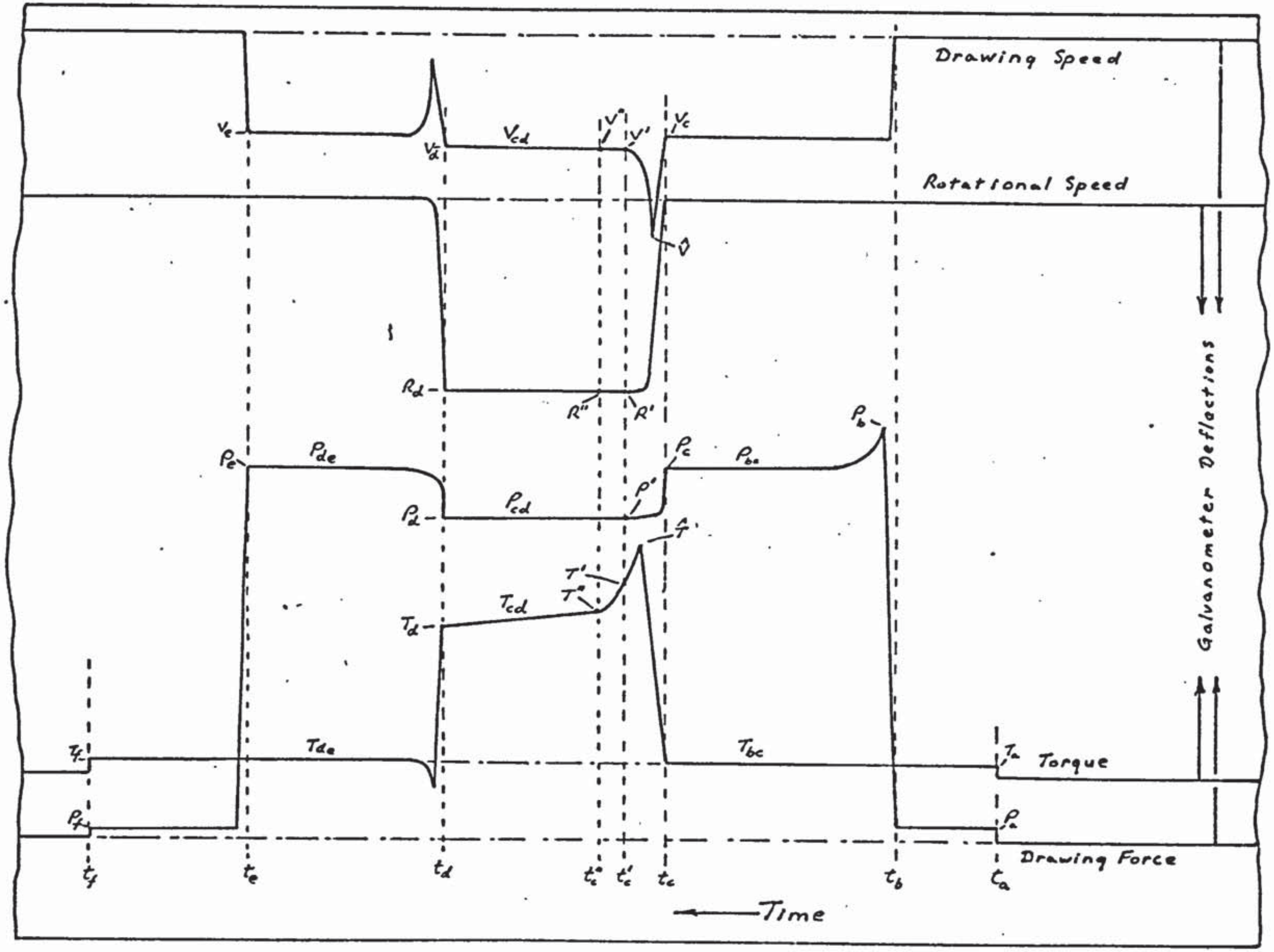

be much sharper than indicated, or much more rounded. Rounding of the initial value of torque seemed to be associated with high torques when an initial peak was present, and with longer distances between jaws and die when such a peak did not occur. This part of the assessment of the record charts was confused by the fact that the latter condition always occurred with the higher drawing speeds, and hence lower torques, and vice versa for the former condition.

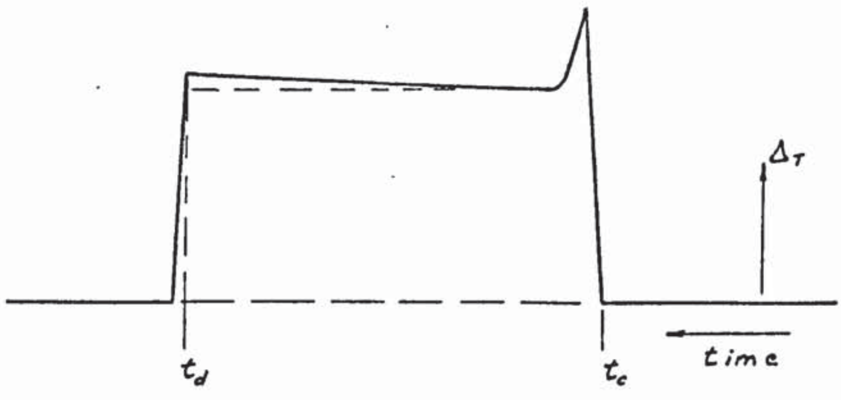

Fig. 10.13 - Form of Torque Record sometimes obtained when drawing with Soap

Another form which was sometimes observed, but only in tests using soap, is shown in Figure 10.13. The rise after the initial dip was of significant magnitude only at the larger reductions and R/V ratios.

10.6.4.4 Discussions:- The only one of the types of trace discussed above which was not found at all in Series I, was that of Figure 10.13. Other differences were simply that the relative magnitudes of the variations, and in particular of $\hat{V}$ and $\hat{T}$, were much less. As a much smaller range of speed parameters was covered, and random fluctuations were greater, it had not been possible to obtain a clear picture of the pattern of behaviour. Such variations as were observed in Series I had been explained in terms of heating effects as follows.

It seemed likely that deformation and lubrication regimes would have become stable after only a short length was drawn. The slight fall in P_{bc}

experienced during t_{bc} could then only be attributed to increased temperature, and as would have been expected it was greatest at large reductions of area. There was no possibility that an interval sufficient to achieve a stable temperature could have been used, and it was for this reason that standard lengths were specified for each section of the test. The behaviour of P_{cd} and P_{de} was seen to accord with the above hypothesis, bearing in mind the increased heating due to die-rotation.

Heat due to plastic deformation would have been generated throughout the body of the workpiece, and, as individual elements spent little time in the die, the temperature of the deforming zone of metal could be expected to have stabilised rapidly. If this was the case, then the heating effect referred to above must have been that the increasing temperature of the die reduced friction forces. This hypothesis was not unreasonable in terms of the effect of temperature on lubricant behaviour, and also accorded with the observation that decreases in torque between t_c and t_d were much greater than the accompanying decreases in drawing force.

Although steady long term decreases in torque and drawing force were satisfactorily explained by the arguement given above, the highly transient torque peaks which became apparent during Series II suggested that another factor was present. Three other possible mechanisms were considered.

i) Change in lubrication conditions caused by die rotation:- Rotation of the die caused a change in the direction and speed of relative movement between bar surface and die, and it is quite possible that this altered the rate of lubricant intake. However this could have caused only a progressive change in torque, as the full effect would not have been felt until the new thickness of film became established over the whole contact region. A non-rotational test performed during but separate to Series I, involved drawing a bar with a coating of P.T.F.E. over a well defined portion of its length. The progress of the start and finish of this section through the die was clearly reflected by the drawing force record. It therefore seemed that a change in condition of lubrication could not explain the sharp initial torque peak. It is possible that such a change caused some of the behaviour observed later in the t_{cd} period, such as that shown in Figure 10.13, but attempts to relate the path length through the die to specific points on the record were foiled by the indeterminacy of the velocity jump at t_c.

ii) Change in die-pressure caused by altered stress system :- *
Die-rotation changed the direction of the friction vector, and therefore altered the stress system at the die surface. The mode of deformation and the die-forces causing it could thereby have been changed. However, there is evidence that variations of μ between zero and normal cold-drawing values have little effect on the mode of deformation (34) or the pressure forces in the die (44,75,18). Additional confirmation of the former point was given by some of the tests described in Section 10.4. It was therefore a reasonable assumption that changing the direction of the friction vector would also have had little effect on the pressure forces. It was also to be expected that changes in die-pressure would have been reflected at least as much in the drawing force trace as in the torque trace, and this was not so with these results.

iii) Plastic rotation of the bar :-
As described in Section 10.6.3, bar drawn with die-rotation showed signs of plastic twisting. This must have resulted from rotation of the bar as it passed through the die, and this implied rotation of the free end of the bar. Such rotation was seen during Series II tests, and the twist of the drawn bar was measured. The angle of twist was found to be proportional to torque, and equivalent to substantial rotational speeds (see Section 10.6.6). The relative rotational speed between die and bar was therefore less than the measured speed of the die.

This plastic twist was used to explain the initial sharp torque peak by considering the onset of die-rotation. The bar twisted in response to the applied torque, so there must have been an instant when the die was rotating at some speed, but the bar had not yet responded. After some indeterminate

* N.B.- see also APPENDIX 8

interval both die and bar would have then reached their steady speeds. In the interim it is likely that the friction vector would have overshot its steady state position. Considering the shape of helix shown in Figure 10.11, it might be thought that the bar would not have reached its steady rotational speed until some particle had traversed the length of the rotating die. However the helix corresponded to the accumulated circumferential strains as the bar passed through the die, whereas the rotational speed of the free end was the sum of the instantaneous strain rates through the die. The bar could therefore have reached its steady speed very rapidly.

This argument qualitatively explained the transient behaviour of the torque trace in the region of $\hat{T}$, but an anomaly was apparent in the drawing force trace. If overshoot of the friction vector caused the peak in the torque trace, then the load trace should have showed a corresponding transient dip. However the elasticity of the drawbench did not allow an instantaneous reduction in load (see Section 10.6.4.1), but caused a surge in drawing speed at t_c. Provided that the duration of the surge was comparable with the stabilisation time for the friction vector, then the otherwise expected dip in force could have been masked. This was so as far as could be judged from the records. This raised the additional point that the surge in drawing speed should have had its own effect on the swing of the friction vector, and a very small number of records did show kinks in the rising torque or falling load near t_c, which might have been caused by this. However the transients were so many and rapid that data could not be considered reliable over this short interval, and no firm conclusions could be reached.

The hypothesis presented above may be simply summarised. It was proposed that initial sharp peaks, found in torque records of tests at high R/V ratios, were caused by the onset of plastic torsion of the workpiece. Smaller long term changes in torque and drawing force were the result of temperature changes, together with a possible contribution from changes in conditions of lubrication.

The research programme was intended as a study of friction in conventional rod-drawing. Therefore the various changes observed during the die-rotation period were of direct interest only in so far as they represented real changes in conditions due to die-rotation, which could have been misinterpreted as applying to conventional drawing. At the conclusion of Series I, those mechanisms which were recognised as being capable of altering conditions were thought to be responsible for only very small changes, or for long term changes. It followed that data taken early in the die-rotation period would be representative of non-rotational conditions. This would also have been true with regard to the rapid short term changes observed in Series II, provided that data could have been taken early enough, but this was not possible (see also Section 10.6.4.5). However, the mechanism which was proposed above as being the cause of the short term changes in observed parameters was a simple mechanical one, which did not imply any change in frictional conditions at the surface of the die. Data was therefore taken where it was judged that the initial transients had passed, but that the long term changes had not yet become significant.

10.6.4.5 Selection of Data from Records :- It should first be noted that the range of uncertainty, of the value of parameters at the start of die-rotation, was large only with the high R/V ratio tests introduced in Series II. These constituted a small proportion of the test programme, in terms of the range of values of Θ , the swing of the friction vector. Therefore they had little intrinsic value, but were of interest in that by revealing the mechanism of the transient behaviour, they allowed more representative values to be taken over the rest of the range.

Referring again to Figure 10.12, it would at first sight seem best to have carried out the analysis using values of $\hat{T}$, as this had a clearly defined value and would not have suffered heating effects. However, the very short rise times of torque and rotational speed, coupled with the surge in drawing speed, made it impossible to specify the relevant speed parameters reliably. There was also no certainty that $\hat{T}$ corresponded to an instant before the bar had started to rotate. Therefore the analysis was carried out on data corresponding to the first instant when the bar reached its steady rotational speed.

This value of torque, T", was taken at its first steady value, and corresponding values of R" and V" were taken at the same instant t_c'' . Where the torque curve showed a long term change as in Figure 10.12, T" was taken at the change of slope, which was usually well defined.

The form of the drawing force trace has been described in Section 10.6.4.3, and its anomalous behaviour after t_c in the previous section. On this basis P' was taken at the first steady value of drawing speed, at t_c' . In the majority of cases t'_c and t''_c corresponded closely, but at high R/V values t'_c tended to precede t''_c. Values R', V' and T' were taken at t'_c in these cases. It was not necessary to define two separate values P' and P", as changes between the two points were not detectable.

It was not clear which of the two positions corresponded to the instant when the bar first reached its steady rotational speed. Instant t''_c had the more consistent basis for selection, but it was also possible that some longer term effect could have occurred between the two.

10.6.4.6 Measurement and Conversion of Data:- As in the calibration tests, all data was measured relative to datum lines ruled across from start to finish of the test. Datum lines for the speed parameters were as indicated in Figure 10.12, but tests were performed in groups of four without intermediate uncoupling of the jaws, so the drawing force datum had to be ruled from start to finish of the whole group. This system was also used for the torque datum for a time, but variations in the apparent cross-sensitivity of the torque bridge (see Section 10.6.4.2) caused concern. The datum for torque measurements was therefore changed to a line ruled between T_{bc} and T_{de} as in Figure 10.12, and all measurements given in the tabulated results were converted for this datum. This was used because it was thought that any stray torque loadings due to friction in the thrust bearing would have been relaxed during the t_{bc} and t_{de} sections of the test, and variations due to bending of the drawn bar would be automatically compensated for.

When data was taken from the charts, it was compared with the accurate measurements made at the time of the drawing tests (see Section 10.6.2). Spread of the charts was very variable, up to a maximum of about 0.015 in. over the full width, and corrections were made as the measurements were taken. Tabulated data has therefore already been corrected, for this factor.

Conversion of the speed data was straightforward. Referring to test no. 47 (table A7.13).

The basic deflection of the rotational speed galvanometer	= 1.015 in.
The sensitivity of that galvanometer to the standard signal, measured prior to the test	= 4.586 in.
The sensitivity relating to the calibration curves (see Figure 7.2)	= 4.605 in.

The correction factor for this deviation would have been

$\times \left(\frac{4.605}{4.586}\right)$, but a more convenient form was used.

Thus $\Delta_R = 1.015 + (4.605 - 4.586)\left(\frac{1.015}{4.586}\right) \qquad = 1.019$ in.

Referring to Figure 7.2,

$$R = 1.019 \times 11 + 0.51 \qquad = 11.72 \text{ rev/min.}$$

Drawing speed data were corrected and converted in indentical manner. Non-rotational drawing force data were also handled in the same way, except that an additional correction was made for variations of the supply voltage from nominal, but this was almost always completely negligible. Drawing force with die-rotation required an additional correction for the cross-sensitivity of the force bridge to torque. This was obtained from Figure 7.6(a) and was once more usually negligible.

The torque measurements were inherently corrected for cross-sensitivity to drawing force, by the choice of datum. A slight correction was necessary for the change in drawing force at the start of die-rotation, and this could be made using Figure 7.6(b), but once again it was almost invariably negligible.

10.6.5 Experimental Results

Measurements of galvanometer deflections, at the different instants discussed in section 10.6.4 and illustrated in Figure 10.12, are listed in Tables A7.11 to A7.20. Occasional question marks indicate that representative values could not be selected, either because of random fluctuations, or in the case of values at t''_c , because the torque trace showed no definite break between $\hat{T}$ and T_d. Arrows indicate unchanged values. The associated data which is required for the corrections and conversions described in section 10.6.4.6 is included. However, the magnitudes of the various long and short term changes may be assessed directly from the galvanometer deflections, as the conversions are linear to quite a high degree.

Data which was of direct consequence for the purpose of this investigation was corrected and converted, and is listed in Tables A7.21 to A7.30. The subscripts and superscripts which were used to denote values taken at different instants have been dropped, it being understood that values just before and after the start of die-rotation were the only ones of interest. Thus values of P refer to instant t_c , while values of the speed parameters R and V, and of torque and reduction in drawing force, refer to t_c' and t_c''. Where a particular test has two rows of data, the first, reading from top to bottom, shows values at t_c' and the second t_c''. A single row of data indicates that there was no change between the two instants, or that t_c'' could not be defined. Values of torque and reduction in drawing force have been listed in non-dimensional form. This was done by expressing them as proportions of the drawing force prior to die-rotation. As indicated in the table heading, the characteristic throat diameter was used for the conversion of torque. The object of non-dimensionalising the results in this way was to make at least a first order correction for test to test variations in material properties. This form of the data was used only for plotting the graphs, and not in the calculations described in the following section.

The dependence of torque and reduction in drawing force on the speed parameters has been plotted in Figures 10.14 to 10.31, for the different bar sizes and for soap and oil lubrication. Values of torque correspond to t_c'. Plotting directly against the R/V ratio would have led to overemphasis of the low drawing speed tests, so the more meaningful base of Θ was adopted. No attempt was made to derive mean values of Θ, but Θ_1 was used and the values are included in the tables. The advantage of using Θ_1 was that it was not necessary to take account of the rotational speed of the bar for its evaluation.

Values of ϕ, measured as described in section 10.6.3, have also been listed in the tables. The relationship between ϕ and T for different bar sizes has been plotted in Figures 10.32 to 10.36, points for both oil and soap appearing in the graphs. In these graphs, deviations from the best straight line usually fall within the $\pm\frac{1}{4}^{\circ}$ accuracy estimated for the measurement of ϕ. Therefore values of R_P were calculated (see Appendix 4.1) using measured values of T and the derived T versus ϕ relationships, rather than directly from measured values of ϕ. R_B was taken as the sum of R_P and R_E (see Appendix 4). In fact, values of R_E were small throughout the range, but this was not immediately obvious from the form of the equation. Once R_E had been calculated it was large enough, at up to three to four per cent of R_P to be included. A similar solution was derived for the effect of elastic tension on the longitudinal velocity, but it was immediately apparent that this was insignificant, and this correction was not adopted. Values of R_B/R are included in Tables A7.21 to A7.30, and their dependence on Θ_1 has been plotted in Figures 10.37 to 10.41.

10.6.6 Calculated Results

Even though analytical solutions had been obtained for the equations derived in section 3.2, they were of such complexity that it was necessary to use a digital computer to process the experimental results. The computer programme is given in Appendix 5. Values of $P_{F(P)}/P$ and $P_{F(T)}/P$ were calculated according to equations (3.29) and (3.30) for various values of n. Solutions for n = 1.0 are given in Tables A.7.31 to A7.40, and for n = 0.25 and n = 4.0 in Tables A7.41 to A7.50. The dependence of the former on Θ_1 is plotted in Figures 10.42 to 10.51, but values at t''_c have been omitted in order to reduce the confusion. Results were obtained for other values of n, but it is neither possible nor desirable to include all of them. μ_P and μ_T may be calculated from equation (3.2) once $P_{F(P)}/P$ and $P_{F(T)}/P$ are known, bearing in mind that $P_F = (P - P_o)$. These values, calculated for n = 1, are included in Tables A7.31 to A7.40. Also given in those tables are values of μ_P and μ_T calculated according to the analysis of section 3.1, in which R_B was ignored.

In order that the magnitudes of the test to test variations, as shown in Figures 10.42 to 10.51, might be compared directly with the variations caused by changing n, the analysis of section 3.2.3 was used. For this it was assumed that n = 1 was the correct value. Values of $(I_1 - I_2)/I_1$ and I_3/I_1 obtained with n = 1 are listed with the other data in Tables A7.31 to A7.40. These values were punched onto the programme data cards, and a slight modification was made to the programme so that equations (3.31) and (3.32) could be solved. The resulting values of $P^n_{F(P)}/P^a_{F(P)}$ and $P^n_{F(T)}/P^a_{F(T)}$ for n = 0.25 and n = 4.0 are listed in Tables A7.41 to A7.50, and the relationships between some of these values and Θ_1 are shown in Figures 10.52 to 10.55.

Some trouble was taken to check both that the computer evaluated results represented sensible solutions of the equations, and that the equations themselves had been correctly derived. Initially, manual solutions of equations (3.29) and (3.30) were attempted. It became apparent that rounding-off the intermediate results to five or six significant figures could lead to errors of first order magnitude in the final result, particularly when solving for I_3. This raised the possibility that the computer solutions might be subject to similar errors, although the I.C.L.1900 which was used works to ten or eleven significant figures. To check this, a number of tests were selected which spanned the range of parameters, and these were evaluated with a programme which called for 'double precision' operation. The computer works to about twenty significant figures in this mode. The results obtained on double precision were identical with those on normal operation, to the four or five significant figures of print-out which were specified. Subsequent evaluations were therefore performed on normal operation.

However, this still left the problem of checking the programme itself, and the solutions of I_2 and I_3. Graphical solutions may be obtained with great simplicity, but equally great labour, from equations (3.20) and (3.21), in conjunction with manual solutions of equation (3.15). This was done for test number 305, using $n = 1$. The graphical and computer solutions were within 0.4% of each other, and it was concluded that the derivations of I_2 and I_3, and the computer programme were correct.

10.7 DISCUSSION

A substantial discussion of some aspects of the results of the drawing tests has already been given in section 10.6.4.

10.7.1 Distribution of Velocity

Models of the distribution of radial and circumferential velocities at the die/bar interface were presented as assumptions in the analysis of section 3.2. This analysis was performed after the experimental results became available, so it is unsurprising that the assumptions corresponded well with reality. The variation of V_s through the die is shown in Figures 10.5 to 10.8, and it is clear that deviations from the assumed linear distribution were very small indeed. These relationships are of interest in their own right, in that they could be used to check various theoretical models for the deformation zone, but this would be outside the area of direct interest here. These distributions are regarded as being completely reliable as the experimental measurements were of much greater accuracy than is represented graphically, but they were obtained with a stationary die, and their applicability to drawing with a rotating-die must be questioned.

A similar argument to that used in section 10.6.4.4 with regard to the possible effect of die-rotation on die-pressure applies here. In that discussion it was pointed out that variations of μ between zero and maximum normal cold-drawing values are thought to have little effect on die-pressure or the mode of deformation, and that some tests performed in section 10.4 supported the latter point. It seems reasonable to extrapolate this, and to postulate that changing the direction of the friction vector would also have little effect. Indeed, it is very difficult to imagine a mechanism by which die-rotation could alter the distribution of V_s.

This conjecture would have been avoided had it been possible to perform the tests of section 10.4 with a rotating-die. Such tests were in fact contemplated as a method of determining the distribution of circumferential velocity; in which case an orthogonal grid would have been used. These were not performed, partly because there was no way of stopping both drives either instantaneously or simultaneously. However, this would not have affected the measured distribution of V_s, provided that die-rotation itself did not affect it. Nevertheless, practical problems of time and of engraving a sufficiently long grid precluded the repetition of the tests with die-rotation.

Another way in which some indication of the distribution of circumferential velocity could have been obtained, would have been by studying the form of the transition regions of ϕ, at the start and finish of die-rotation (see Figure 10.11). However, this was not considered to be worthwhile, partly because of the great difficulty of making measurements of sufficient accuracy to give sensible results, partly because there was no method of either starting or stopping the rotary drive instantaneously, and partly because there seemed little likelihood that the assumed distribution was seriously in error. The basic assumption made in section 3.2, that the free end of the bar had some unspecified rotational speed, is in fact self-proving, and the method that was used to determine it (see Appendix 4) was limited only by the accuracy with which ϕ could be measured. It was also known that the drawn end of the bar could not rotate, so the only assumption which was really made about the distribution of S through the die, was that it was linear. When it is considered that the allowance for plastic torsion was only a correction to the speed parameters, albeit a significant one, and that the end points on the distribution curve were known accurately, it seems unlikely that significant error could have resulted from any possible variation from linearity.

Furthermore, any errors which may have resulted from incorrectly assumed distributions of velocity would, with a single exception, have had a comparable effect on the results of all tests on a given size of bar. These errors would therefore have manifested themselves as a systematic bias, which would have led eventually to a slight error in the deduced value of n, but would not have interfered with the method of deduction. The exception arises from small bar to bar and test to test variations in diameter. To allow for this, each test should have had its own value of x_2 and k_2. The small range of variation of bar diameter (see Table 10.5) did not seem to justify the large amount of extra labour and computer time which would have been involved. The fact that the results for the 1.1/8 in. group, which had much the widest spread of diameters, showed no greater scatter than the others is taken as evidence that no significant error was introduced.

10.7.2 Rotation of Undrawn Bar

This rotation, and the associated helical twist in the drawn bar, are of considerable interest independently of the direct effect on the circumferential velocity. This feature of drawing with a rotating-die has not, as far as this author is aware, been reported hitherto; and the sole reference to it which appears in the literature states in effect that it was not found (87).

Figures 10.32 to 10.36 show a linear relationship between helix angle and torque, and although the proportionality is dependent on the initial bar size, it is independent of lubricant. Torque is a function of process geometry, independent speed parameters, and shear stress. It follows that it should be possible to deduce friction forces from measurement of ϕ, or of R_B, independently of measurements of torque and drawing force. This is discussed further in section 12.

Figures 10.37 to 10.41 show the dependence of R_B on the independent speed parameters. Extrapolation of these curves through the short distance to the R_B/R ordinate leads to a highly anomalous situation, in which R_B/R seems to have a positive finite value, even though R approaches zero and $R > R_B$. Fortunately a few of the curves show a slight hook which indicates that they probably do pass through the origin. Values of R_B may be plotted in a variety of forms, and various mathematical manipulations may be performed; but the fundamental significance of these cannot be appreciated in the absence of an analytical solution for R_B.

However, an important conclusion may be drawn from Figures 10.37 to 10.41. Most of the graphs which have been presented here have been plotted to an apparently dimensionless base of Θ_1. The general base of Θ was chosen because it was more significant and representative than R/V, and the particular one of Θ_1 because it could be conveniently calculated without allowing for R_B. However, it is clear that torque and reduction in drawing force are influenced by R_B, even though that quantity is itself a dependent parameter. Put another way, Θ is a quasi-dimensionless parameter which is implicitly dependent on the shear stress to some extent. This could have had serious consequences for the intended method of deducing n, and in fact for any comparison of data based on the R/V ratio. Fortunately, Figures 10.37 to 10.41 show that for a particular bar size the error introduced by this effect is a function only of R/V and the friction conditions. Therefore Θ_1 may validly be used as a basis for comparison between results obtained with the same friction conditions.

Although of great interest, rotation of the undrawn bar was a nuisance as it seriously complicated the theoretical analysis, and intruded an extra dependent parameter into the solution in an unfortunate position. A partial solution to this problem would be to constrain the undrawn end of the bar, so that its speed was predetermined, preferably at zero. This would not reduce the number of dependent parameters, as an extra torque would be introduced. However, this torque would be more susceptible to dynamic measurement than R_B, and it would probably appear in the equations in an analytically less embarassing place. This would also give the possibility of making some interesting additional measurements, and these are discussed in section 12.

One additional detrimental effect which was caused by the plastic torsion of the bar, was that the swing of the friction vector actually produced by a given R/V ratio was less than otherwise expected. This effect is illustrated in section 10.7.4.

10.7.3. Further Discussion of Initial Torque Peak

The form of the test records has been discussed in section 10.6.4. where the presence of large and highly transient peaks at the start of the torque trace was noted. The hypothesis was presented that these peaks were caused by the onset of plastic torsion, which produced a rotational speed at the free end of the bar and thereby reduced the swing of the friction vector. The observation that the largest values of ϕ coincided with the largest peaks, seemed to be in agreement with the hypothesis.

When measured values of ϕ were converted to equivalent values of R_B (see Appendix 4), it became apparent that the largest values of the one did not necessarily correspond to the largest values of the other. This can be seen in the tabulated data (Tables A7.21 to A7.30), and the resulting dependence of R_B/R on Θ_1 is shown in Figures 10.37 to 10.41. These curves show that in spite of the observed correlation between ϕ and the torque peaks at high values of Θ_1, the largest values of R_B/R occurred at the other end of the range. In fact, R_B/R became negligible in the region which showed the largest peaks. The inevitable conclusion is that the hypothesis is incorrect.

A variety of other mechanisms which might have led to the peaks were discussed in section 10.6.4.4. The only one which was thought capable of producing the rapid transients which were observed, was that of a reduction in die-pressure, caused by the changed stress system.* This possibility was dismissed on convincing evidence, and it may now be added that in order to explain the peaks, the reduction in die-pressure would have had to be as much as 40% in some cases. This is inconceivable.

The only other possibility that occurred to this author was that the phenomenon was connected with the surge in drawing speed which was observed at the onset of die-rotation. This surge has been discussed in section 10.6.4.1, and the effect was that of a rapid acceleration when the demanded drawing force fell. It is quite conceivable that this was accompanied by an increase in the demanded torque, but this cannot be quantified in the absence of any reliable data for this short interval.

The practical implications of this modification to the hypothesis are slight; the only consequence being that data at t'_c comes to be regarded as being more representative than that at t''_c. It might be expected that although the original hypothesis was incorrect, the same mechanism should have applied at low values of Θ_1, where R_B/R was significant. However, the argument hinged on the rate at which the onset of plastic torsion could follow the swing of the friction vector, and this is unknown. It may be further noted that tests at low Θ_1 tended to occur at the end of the drawing stroke, where elastic torsion of the drawn bar would have slowed down the rate of relative acceleration of the die.

---

* N.B.- see also APPENDIX 8

10.7.4 Theoretical Model for the Form of Results

These families of curves were calculated according to section 3.2.3 for an assumed value of n = 1, and using the experimentally measured speed parameters. Some of them are shown in Figures 10.52 to 10.55, and they exhibit a variety of interesting features.

The curves for $P_{F(P)}/P_F$ all come to unity at $\pi/2$. This indicates that at infinite R/V the correct value of P_F should be obtained, irrespective of the assumed value of n. This corresponds with the disappearance of I_2 in that situation, and the physical significance is of course that at infinite R/V, P_o and hence P_F can be measured directly. The torque curves do not do this, and consideration of the limiting value of I_3, and of the physical significance, indicate that there is no reason why they should.

The behaviour of the curves at low Θ_1 is not so readily explained. An intuitive approach suggests that they should return to the n = 1 line. Unfortunately it is not possible to examine the limiting values of I_2 and I_3 because the factor R_B/R appears, and as discussed previously, this becomes indeterminate as $\Theta_1 \rightarrow 0$. Data listed in Tables A7.41 to A7.50 for $P^n_{F(P)}/P^a_{F(P)}$ should be treated with care in this region. These values were derived using values of $(I_1-I_2)/I_1$ listed in Tables A7.31 to A7.40, and it will be seen that these were not accurately determined at low values of Θ_1. This caution does not apply to corresponding data for $P_{F(T)}$.

The differences which occur between the curves for oil and soap illustrate very well the point made in section 10.7.2 about the quasi-non-dimensionality of Θ_1. They also show the effect of the reduced swing of the friction vector associated with the higher values of R_B.

Of particular importance are the magnitudes of the changes due to incorrectly assumed values of n. The changes are largest with the largest bar sizes, even expressed proportionately, and are larger with respect to $P_{F(P)}$ than $P_{F(T)}$. The largest variation between the curves for n = 0.25 and n = 4.0 is about 18%, Figure 10.54. However, it should be noted that this occurs at low Θ_1, when the observed reduction in drawing force would be at a minimum, and the effective accuracy of measurement likewise. It was always understood that analysis from torque measurements would be the most reliable and at first sight the corresponding variation in Figure 10.55 seems to be about 16%. However, the band in the middle where the curves do not meet the n = 1 line must be regarded as wasted, as it is only by point to point variations within a single curve that the correct value of n could be assessed. Thus, no matter how widely spaced the curves were, it would be impossible to assess the correct value of n if they were parallel. The strictures on required accuracy made in section 3 may now be quantified. Referring again to Figure 10.55, an increase of 4% in the level of the calculated value of $P_{F(T)}$ as Θ_1 goes from 0.1 to 1.5, indicates n = 4.0, while an increase of 2% indicates n = 2.0; these figures assuming that n = 1 be correct. Thus, large variations in the deduced values of n would be caused by systematic changes in $P_{F(T)}$ of the order of only 1%, and this is for the largest size bar, where the technique is most sensitive.

10.7.5 Comparison of Theoretical and Experimental Results

The experimental curves for $P_{F(T)}$ and $P_{F(P)}$ are plotted in Figures 10.42 to 10.51. These data were evaluated for n = 1, and only points corresponding to t'_c have been plotted. Obviously the correct value of P_F was not known, and $P_{F(T)}$ and $P_{F(P)}$ have therefore been expressed as proportions of the non-rotational drawing force as in equations 3.29 and 3.30. The curves are nevertheless comparable with Figures 10.52 to 10.55, the points of interest being the shape and slope.

Such a comparison makes it immediately obvious that general experimental scatter was of much greater magnitude than the systematic changes which were being sought. Furthermore, where individual sets of tests did give results which showed little scatter, the systematic changes were usually much larger than could have been corrected for by assuming an even remotely reasonable value of n. Either of these circumstances would have made it impossible to use the method proposed for determining the correct value of n. Plotting points for different values of n in Figures 10.42 to 10.51 would merely have added to the confusion, but data for n = 0.25 and n = 4.0 are given in Tables A7.41 to A7.50, and the reader may easily verify the above conclusion. Values at t''_c were considered, and it was found that the slope of some of the $P_{F(T)}/P$ curves was thereby reduced at high values of Θ_1, but for others it was increased. Therefore no conclusions regarding the relative merits of data at t'_c and t''_c could be reached on this basis. Variations between these values were within the general spread and again it would have been confusing to plot them.

The conclusion is that distribution of shear stress cannot be reliably deduced from these results. However, the results can be usefully interpreted in terms of coefficient of friction but some features of Figures 10.42 to 10.51 will be discussed before this is done.

10.7.5.1 Torque Results (Figures 10.42 to 10.46) :- In spite of the general scatter, the curves do show some definite grouping by rotational speed, the effect appearing to be too systematic to have been caused by bar to bar variations. In general the effect of increasing the rotational speed seems to have been to have reduced $P_{F(T)}/P$ at corresponding values of Θ_1. The conclusion reached in section 10.7.2, that Θ_1 was in fact a valid base for comparison of results obtained under different speed conditions, can now be seen to be of some importance. In the light of that conclusion the speed shift can only be interpreted as being the result of a change in shear stress with speed, but not necessarily of rotational speed, as a change with drawing speed could also explain the grouping. However, the fact that the slope of the $P_{F(T)}/P$ versus Θ_1 curve sometimes changes sign from one size of bar to another, or from one lubricant to another, or even in some cases during one set of tests, indicates that more than one factor influenced the shear stress.

There seems to be little possibility of reaching any firm conclusions regarding the source of these groupings, and it will in any case be shown later that they are of small consequence in terms of determining coefficient of friction. However, some further points of interest may be noted, by comparing these figures with the experimental results plotted in Figures 10.14 to 10.22. The separate groupings are clearly indicated in those figures, but only for sets of tests at the higher rotational speeds. Most of the curves show very little scatter at the lower values of Θ_1. However, it will be recalled that the method of analysis is equivalent to the extrapolation of results obtained at arbitrary values of Θ_1, to deduce data corresponding to $\Theta_1 = \pi/2$. Therefore a given magnitude of absolute variation becomes more significant as Θ_1 decreases.

The theoretical model for the behaviour of the $T/(d_1 P)$ versus Θ_1 curve indicates that it should be of sinusoidal form, and therefore have zero slope at $\Theta_1 = \pi/2$, provided that the magnitude of the shear stress is unaltered by die-rotation. In fact the curves in Figures 10.14 to 10.22 do not show this behaviour, although those at high rotational speeds come closer than those at low speed. It cannot be accepted that conditions at high rotational speed conform to stationary-die drawing more closely than those at low rotational speed, and the possibility again presents itself that the shear stress was detectably dependent on drawing speed. However, no firm conclusion can be reached.

10.7.5.2 Drawing Force Results (Figures 10.47 to 10.51) :- It is apparent that the scatter on these curves is much greater than that for the corresponding torque results, and this was to be expected from the magnitudes of the galvanometer deflections which led to them. Relatively little evidence of systematic grouping according to rotational speed could be seen, either on these curves, or on the experimental results plotted in Figures 10.24 to 10.31. The dominant feature of the former group of curves is the tendency to high values of $P_{F(P)}/P$ at low Θ_1

The first question which arises is whether or not these high values do represent reality. Typical curves in Figures 10.47 to 10.51 cover a range of values of $P_{F(P)}/P$ of 0.1 or greater. Reference to Figure 2.1 shows that this should be accompanied by a change in non-rotational drawing force of 10 to 15%. No such variations were observed, either from test to test, or between values measured before and after die-rotation within one test. In order to provide a possible explanation for the initial high values, and the subsequent fall with increasing Θ_1, it is first necessary to point out that the variations correspond to very small changes in experimental measurements. Reference to Figures 10.23 to 10.31 shows that the drawing force was reduced by only a few per cent at values of Θ_1 up to 0.5. In terms of % f.s.d. on the test records, the deflection was even smaller. Two possible sources of the variations become apparent. Either small errors in the measurements made on the test records, or small changes in die-pressure caused by die-rotation, could have had significant effect on the calculated values of $P_{F(P)}/P$. The former could certainly explain the very large and highly erratic variations which are seen at very low Θ_1 with the smaller size of bars, but would fail to explain the much more systematic and well defined relationships observed with the larger bars.

Die-rotation introduces a shear stress into the circumferential direction, which then ceases to be a principal direction, and it seems certain that this will reduce the normal stress. This argument is not at variance with the one presented in section 10.6.4.4, because that discussion was concerned with variations an order of magnitude larger than those of interest here. Where the reduction in drawing force due to die-rotation is only a few per cent, it is clear that even very slight reductions in normal stress would significantly increase the calculated value of $P_{F(P)}/P$. This behaviour is also reflected in the primary experimental results, plotted in Figures 10.23 to 10.31. These curves should have the form of $(1 - \cos \Theta)$, which would have zero slope at the origin, but it is evident that this is not so. The general conclusion which may be drawn is that values of $P_{F(P)}/P$ obtained at low Θ_1 should be ignored. It may be further noted that values at higher Θ_1 approach the corresponding values of $P_{F(T)}/P$ quite closely.

A few of the curves in Figures 10.47 to 10.51 do show some evidence of grouping by rotational speed, and it would be possible to follow the same line of discussion set out in the previous section. However, this would still be conjectural, and it has been omitted as it would have added nothing.

10.7.6 Coefficient of Friction

It was established in section 10.7.3 that calculated values of P_F are highly insensitive to the assumed value of n. This had such serious consequences for the proposed method of deducing the distribution of shear stress that it failed completely. However, the corollary is that values of P_F, and hence of μ, may be reliably calculated without knowledge of the correct value of n. In this situation the assumption of uniform distribution of shear stress (i.e. n = 1) becomes reasonable rather than arbitrary. The calculation of μ_P and μ_T from values of $P_{F(P)}/P$ and $P_{F(T)}/P$ was part of the computer programme, and values for n = 1 are listed in Tables A7.31 to A7.40. However, it is possible to derive representative values very simply without scanning the tables. The ranges of values of $P_{F(T)}/P$ and $P_{F(P)}/P$ which have been plotted in Figures 10.42 to 10.51 have been listed in Table 10.7. Some values which are obviously unrepresentative have been omitted, but the ranges cover the very large majority of values of $P_{F(T)}/P$. Values of $P_{F(P)}/P$ at low Θ_1 were discounted in the discussion of section 10.7.5, and these have not been included. The associated values of μ_P and μ_T were obtained directly from Figure 21.

Lub.	Diameter of Bar (in)	$P_{F(T)}/P$	μ_T	$P_{F(P)}/P$	μ_P
Soap	1.1/16	0.200 0.225	0.030 0.035	0.195 0.240	0.029 0.039
	1.1/8	0.140 0.165	0.020 0.024	0.125 0.150	0.017 0.021
	1.3/16	0.150 0.180	0.021 0.025	0.130 0.165	0.018 0.024
	1.1/4	0.150 0.175	0.021 0.026	0.125 0.170	0.017 0.025
	1.5/16	0.150 0.180	0.021 0.025	0.120 0.170	0.016 0.025
Oil	1.1/16	0.350 0.380	0.066 0.074	0.390 0.420	0.078 0.090
	1.1/8	0.250 0.280	0.041 0.048	0.250 0.300	0.041 0.053
	1.3/16	0.290 0.330	0.050 0.060	0.260 0.330	0.043 0.060
	1.1/4	0.270 0.310	0.045 0.055	0.200 0.350	0.048 0.066
	1.5/16	0.260 0.300	0.043 0.053	0.250 0.360	0.041 0.069

TABLE 10.7 *

It is considered that ranges of μ_P do not represent genuine variations of friction conditions, but arise from the sensitivity of the derivation to slight errors and fluctuations. These values are therefore of direct interest only in that they roughly corroborate values of μ_T, but even if values of μ_P are considered, the spread of results for each bar size is unusually narrow. Considering values of μ_T alone, the repeatability can only be described as excellent compared with the variation in values usually obtained in studies of friction.

It should be recalled that the results of the 1.1/16 in. size are questionable because of the high degree of asymmetry that was developed when drawing those bars, and also because some of the geometrical and velocity distribution

* N.B.- see APPENDIX 8

parameters were not directly available. It is also unfortunate that results for the 1.1/8 in. size are not directly comparable with the others, due to the much rougher surface of those bars. Nevertheless, values of μ_T for the four largest reductions are very close to each other with soap lubricant, but rather less so with oil. The actual values, 0.020 to 0.025 for soap, are at the bottom end of the accepted range, but compare very well. The values of 0.04 to 0.06 are rather lower than is usual for oil, and are more or less at the top end of the range for soap. This could easily be the result of using the oil over a phosphate coating.

10.7.7 <u>Comparison of Approximate and Exact Solutions</u>

Values of μ_P and μ_T calculated using the solution of section 3.1, are listed in Tables A7.31 to A7.40 for comparison. It can be seen that the simple solution always underestimates the 'true' value, and an interesting situation therefore arises with regard to values of μ_P at low θ_1. In that situation values calculated using the 'exact' solution are known to be seriously in error (see section 10.7.5) and it transpires that the approximate solution gives more representative results.

Values of μ_T compare quite well for soap, the difference increasing from a few per cent with the smallest bar size, up to a maximum of about 20% with the 1.5/16 in. size. The difference for oil covers the range of 3% to 25% up to the 1.1/4 in. size, but then jumps to 50% for the 1.5/16 in. size. For the simple solution to underestimate μ, it must in effect overestimate the value of θ corresponding to a particular set of test parameters. This implies that the major source of error is the failure to take account of the rotation of the free end of the bar, and this is supported by the observation that the greatest errors occur at low values of θ_1, where R_B/R_D is greatest.

10.7.8 <u>Drawing Force without Die-Rotation</u>

There was some suggestion in section 10.7.5 that shear stress might have been reduced by increasing drawing speed. Values of drawing force prior to die-rotation (see Tables A7.21 to A7.30) were scanned for evidence. Such effect as was observed was in the form of a fairly regular increase in P throughout each group of tests. If the initial test in each group is ignored, the increase is of about 3 or 4%. However, this increase cannot be used to indicate speed effects on either friction or yield strength, because values of P from each group within a set of tests were interlinked in such a way as to indicate a systematic change in yield strength along the test bars. The small and rather variable changes involved cannot be satisfactorily represented graphically.

10.7.9 Assessment of Theories of Drawing

In order to make use of the measured values of μ to evaluate the various theories of drawing, it is first necessary to derive the equivalent stress-strain curve for the material being drawn. This was done in the series of tests described in section 10.8.

Although all the information necessary to check the theories was collected, and is presented in this thesis, it has not proved possible to actually do this in the time available. It may however be noted that, as the values of μ obtained here correspond well with previously accepted values, it is unlikely that any significant differences from previous evaluations would have been found.

10.8 STRESS-STRAIN TESTS

A series of uniaxial tension and compression tests were made to determine the stress-strain relationship of the undrawn test material. No tests were made on bar in the drawn condition, as the only use foreseen for the results of such tests was the evaluation of redundant deformation by the method of curve matching (see section 2.2). This was considered to be outside the scope of this investigation, and the results would in any case have been subject to ageing of the drawn material.

Tests fell into two broad groups. Firstly tests were made on the undrawn remnants of the individual bars used in drawing tests, to determine the properties of parts of the bars actually used in those tests. Secondly tests were made on some complete bars which were surplus to the requirements of the drawing programme. The object of these tests was to determine how nearly isotropic and homogeneous the material was within a particular bar and hence to deduce how representative the results of the first group of tests were, of the properties of those parts of the bars which had been drawn.

All tests, both tension and compression, were incremental. Stress and strain were deduced from measurements of diameter, the minimum section being used for the tensile tests, and the maximum section for the compression tests. Although it was not possible to perform them at strain-rates comparable with those of the drawing operations, attempts were made to maintain a constant strain rate throughout themselves. The conventional problems found in tension and compression testing were eased here, as it was necessary to go up to true strains of only about 0.55 to exceed the equivalent strain for the drawing tests with maximum reduction. This is easily attained in tensile tests at atmospheric pressure, and compression tests may reasonably be conducted to this figure without remachining the specimen.

Unfortunately it has not proved possible to fully evaluate the data from all the tests in the time available, and only the most pertinent tests, those of the following section, are reported here.

10.8.1 Tension Tests on Undrawn Material from Stock used in Drawing Tests

It is clear that the tensile test is the uniaxial test most closely related to rod-drawing, and that it should be performed on the full section and along the axis of the rod. One such test was done on the undrawn remnant of every bar used in the Series II drawing tests, and also on some material from Series I. The test pieces were fifteen inches long, and the central part was polished down by about 0.005 in. to promote necking in that region. Testing was done on a 50 tonf. Denison machine (see Appendix I), with the test pieces gripped so that the initial jaw separation was eight inches.

Systems of stepping through pre-determined load or deflection increments, which can be used in incremental compression testing, cannot be applied satisfactorily to tensile testing because of the effects of instability. Another difficulty was that it was necessary to keep a check on the progress of each test, so that the machine controls could be set to give constant strain rate. The adopted procedure involved preparation of a diameter/true-strain curve for each size of bar, before the test. The first increment was from zero to slightly above the initial yield load, where the bar was abruptly off-loaded. It was not possible to time this increment, as the interval was very short, and it was also desired to record the yield-point load. However the machine speed setting was as for the succeeding increment. Values of yield point are not considered reliable as the load pointer indicated serrated yielding.

When the bar was off-loaded care was taken that the jaws did not disengage completely from their serrations. The diameter of the bar was then measured while unloaded. The next few strain increments were made to predetermined load points, the step being timed from when the increasing load passed the previous maximum until the release valve was opened. At each off-load point the strain increment and mean strain-rate were quickly estimated from the diameter/true-strain curve. On the basis of how the particular test was proceeding, and of past experience of the machine controls, the speed setting was altered to maintain the mean strain-rate at about 2×10^{-3}/sec over the succeeding increment. The setting was not altered during the loading cycle. The method was fairly successful after it was realised that the rapid traverse valve, which also provided the rapid off-loading facility, had to be closed very firmly before each loading cycle. As instability was approached it became impossible to use load increments, and time increments were used instead, the other details being unchanged.

Once into instability, strain-rate varied appreciably throughout a given increment, even though the mean strain-rate between increments was held fairly steady. Continued use of time increments could therefore lead to large deviations from the intended strain increment. To overcome this, a micrometer was set to a slightly larger diameter than that corresponding to the total strain required after the next step, and it was held against the bar during straining. The loading cycle was interrupted as soon as was conveniently possible after the micrometer slipped over the bar. When off-loaded, the actual bar diameter was measured with a ball-ended micrometer.

When using time and diameter increments to pre-determine the duration of the loading cycle, the start of the deformation period was found by observing the 'break' in the movement of the load pointer. The pointer moved rapidly during the period that load was increasing without deforming the bar; the start of deformation being indicated by sudden deceleration of the pointer, caused by the related increase in demanded oil supply to the hydraulic ram.

At the end of the test the radius of curvature of the neck was measured. This was done by matching the neck with such machined cylinders and discs as were available. It will be clear that this procedure was somewhat haphazard, and usually required interpolation between available radii. To overcome this, the correction factor (see Section 2.8) obtained from each test was plotted in Figure 10.56. It will be seen that the curve was not assymptotic to unity, and this is thought to be due to the initial radius produced by polishing. Correction factors applied in evaluating the results of these tests were taken from Figure 10.56, related to a datum of 0.998, and corrections were not applied at strains below 0.25. The results are given in Tables A7.51 to A7.55.

GRAPHICAL RESULTS

Fig. 10.14 - Relationship between Swing of Friction Vector (Θ_1) and Demanded Torque.

Bar size :- $1\frac{1}{16}$ in
Lubricant :- Soap & Oil

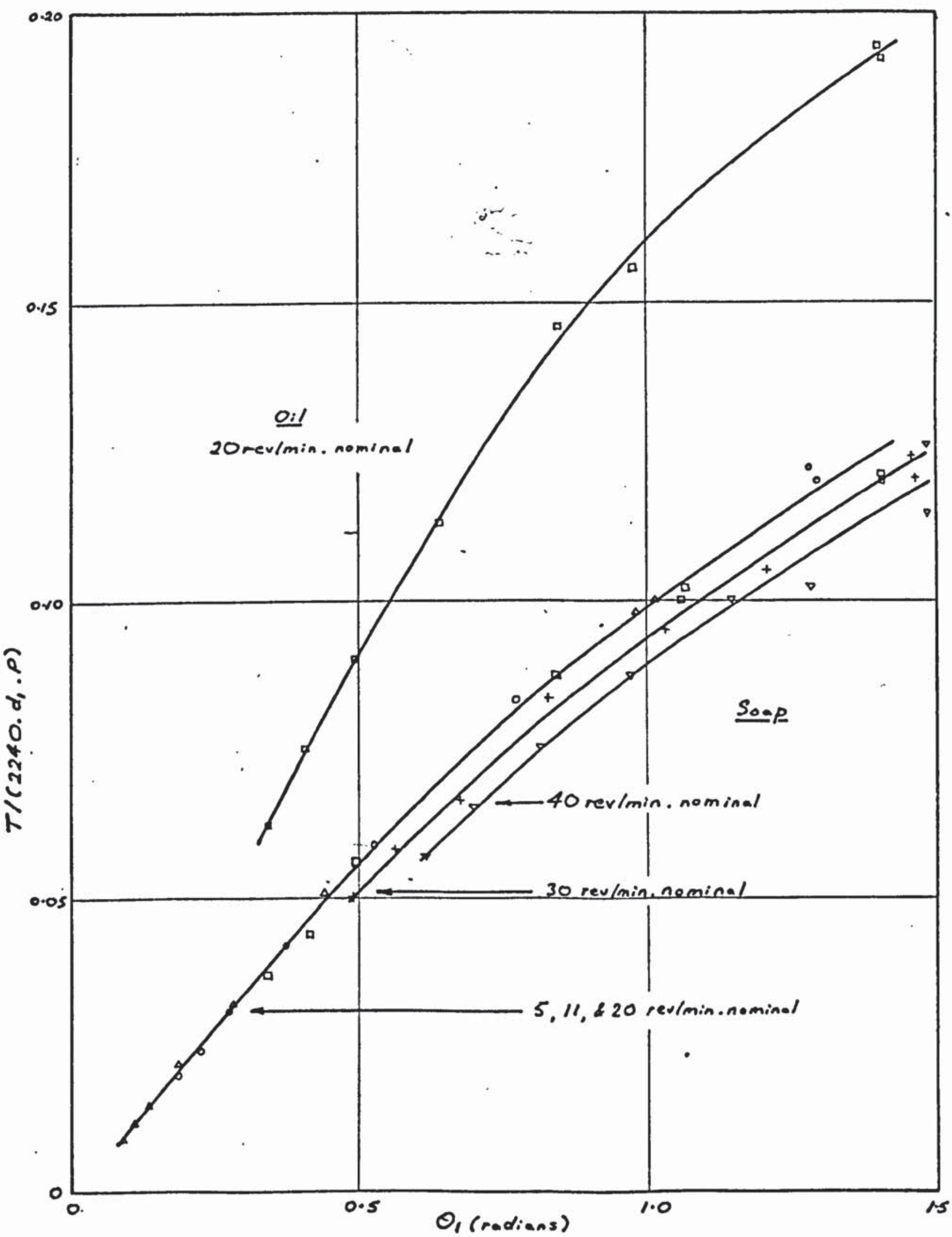

Fig. 10.15. Relationship between Swing of Friction Vector (θ_1) and Demanded Torque

Bar size :- $1\frac{1}{8}$ in.
Lubricant :- Soap

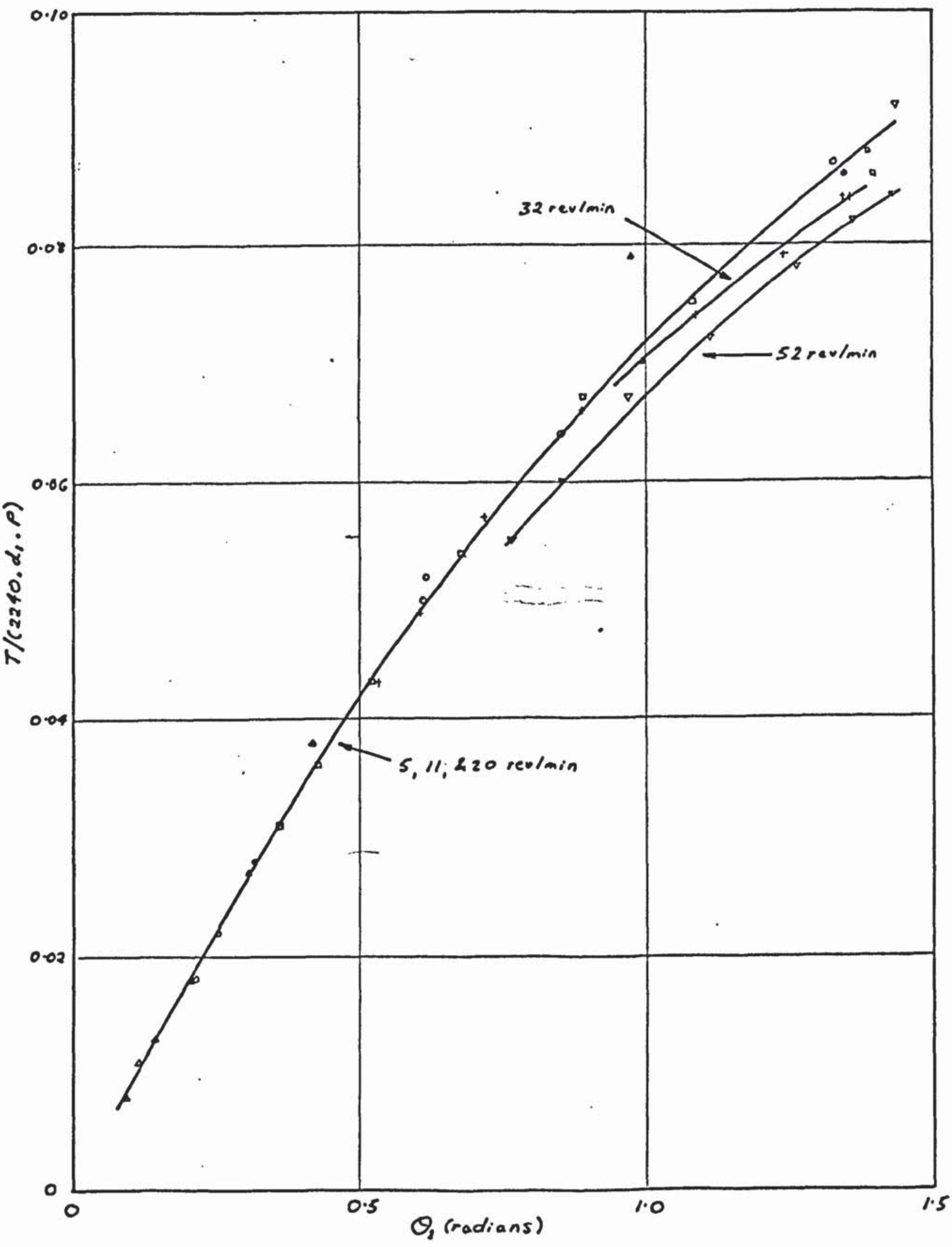

Fig. 10.16 - Relationship between Swing of Friction Vector (Θ_1) and Demanded Torque

Bar Size :- $1\frac{1}{8}$ in.

Lubricant :- Oil

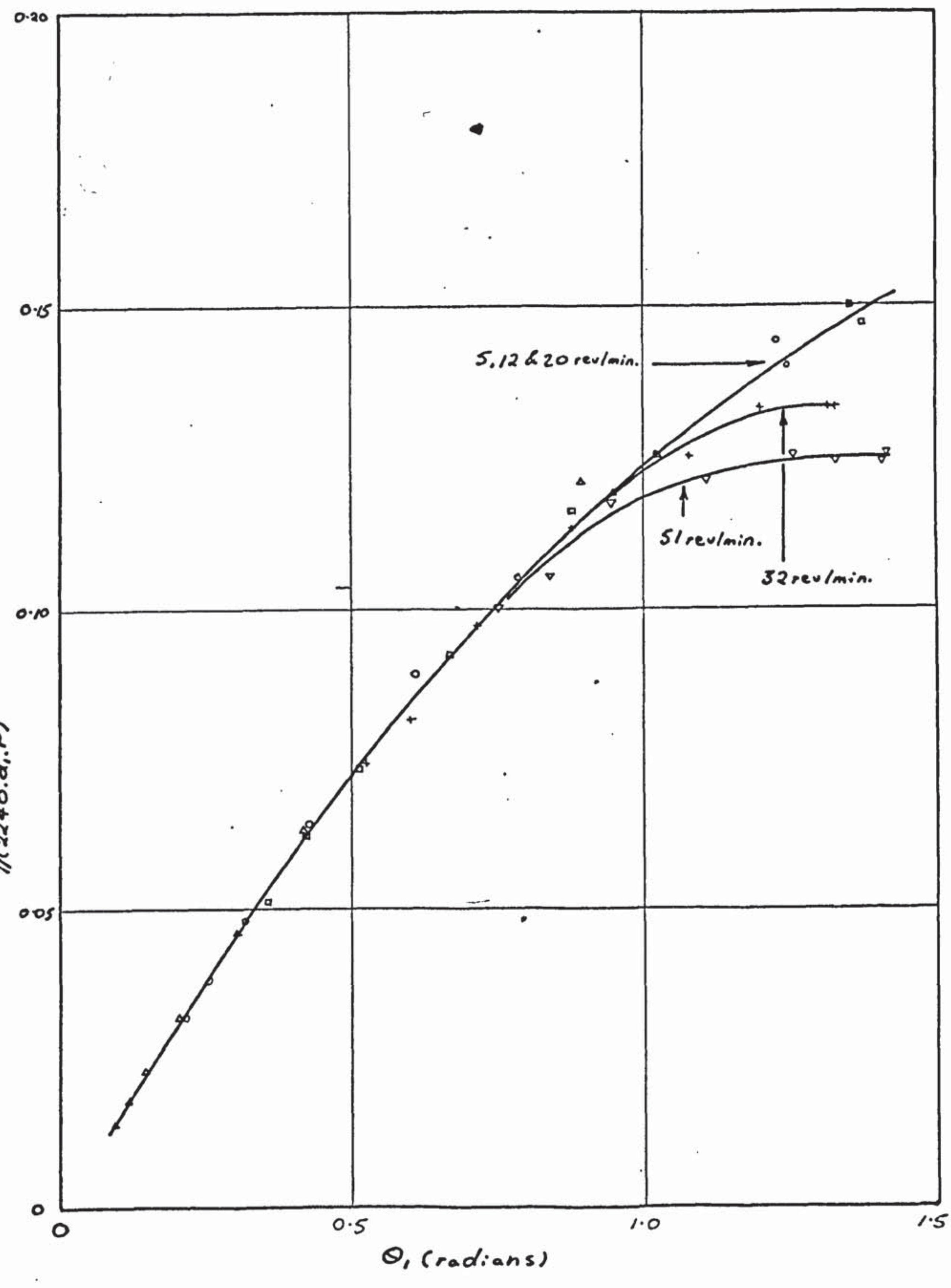

Fig. 10.17 - Relationship between Swing of Friction Vector (θ_1) and Demanded Torque

Bar size:- $1\frac{3}{16}$ in.

Lubricant:- Soap

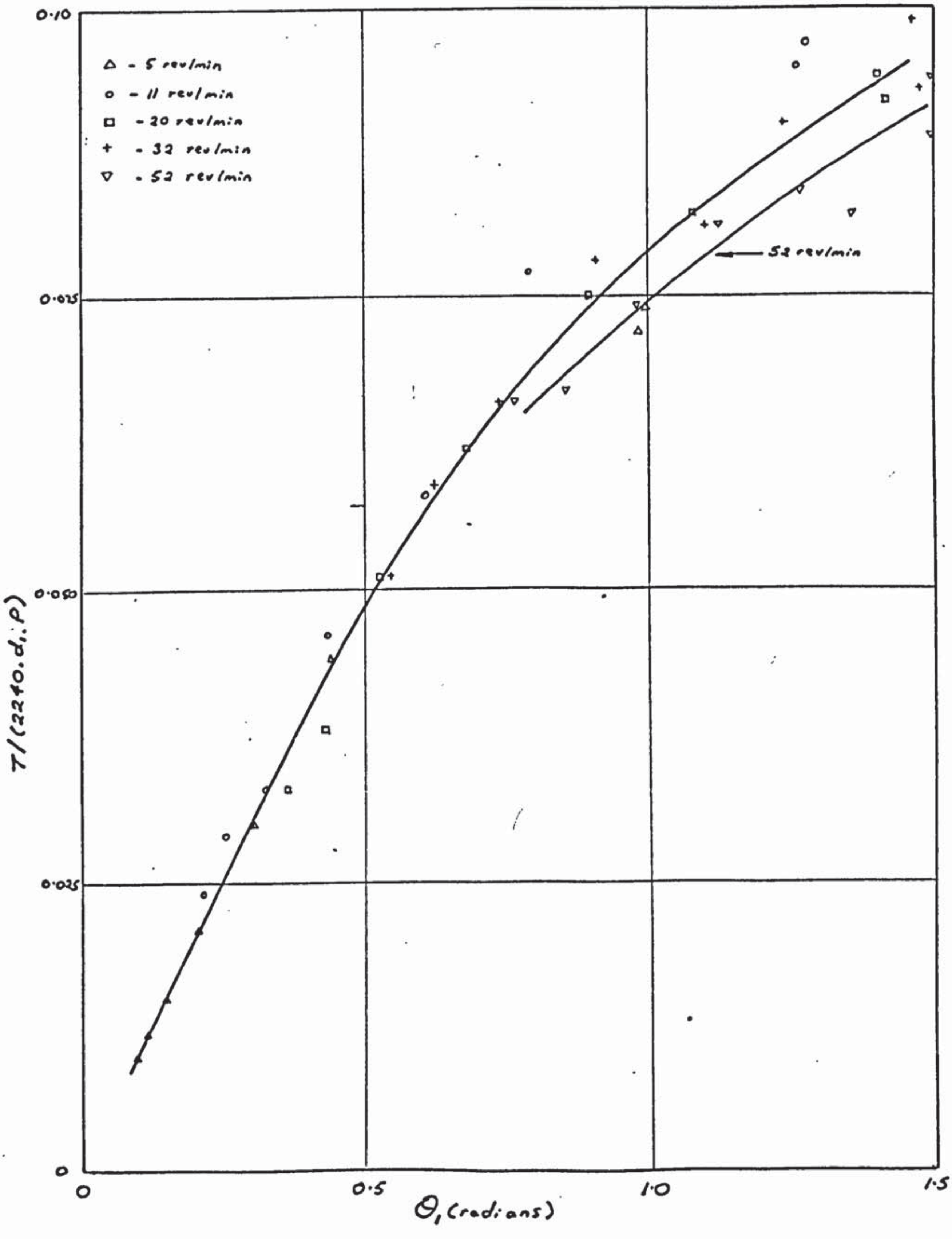

Fig. 10.18. - Relationship between Swing of Friction Vector (θ_1) and Demanded Torque

Bar Size:- $1\frac{3}{16}$ in.

Lubricant:- Oil

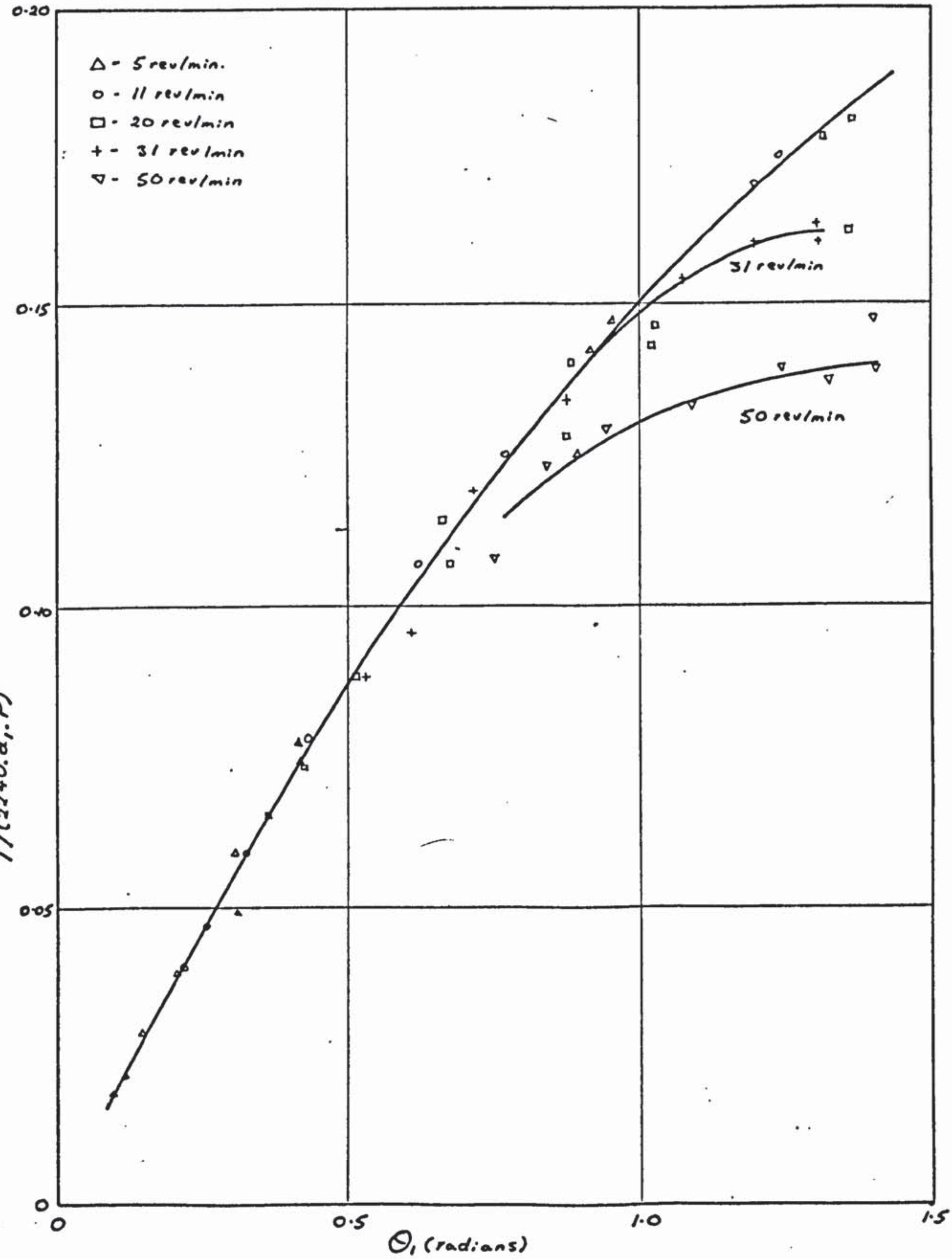

Fig. 10.19 - Relationship between Swing of Friction Vector (θ_1) and Demanded Torque

Bar Size:- $1\frac{1}{4}$ in.
Lubricant:- Soap

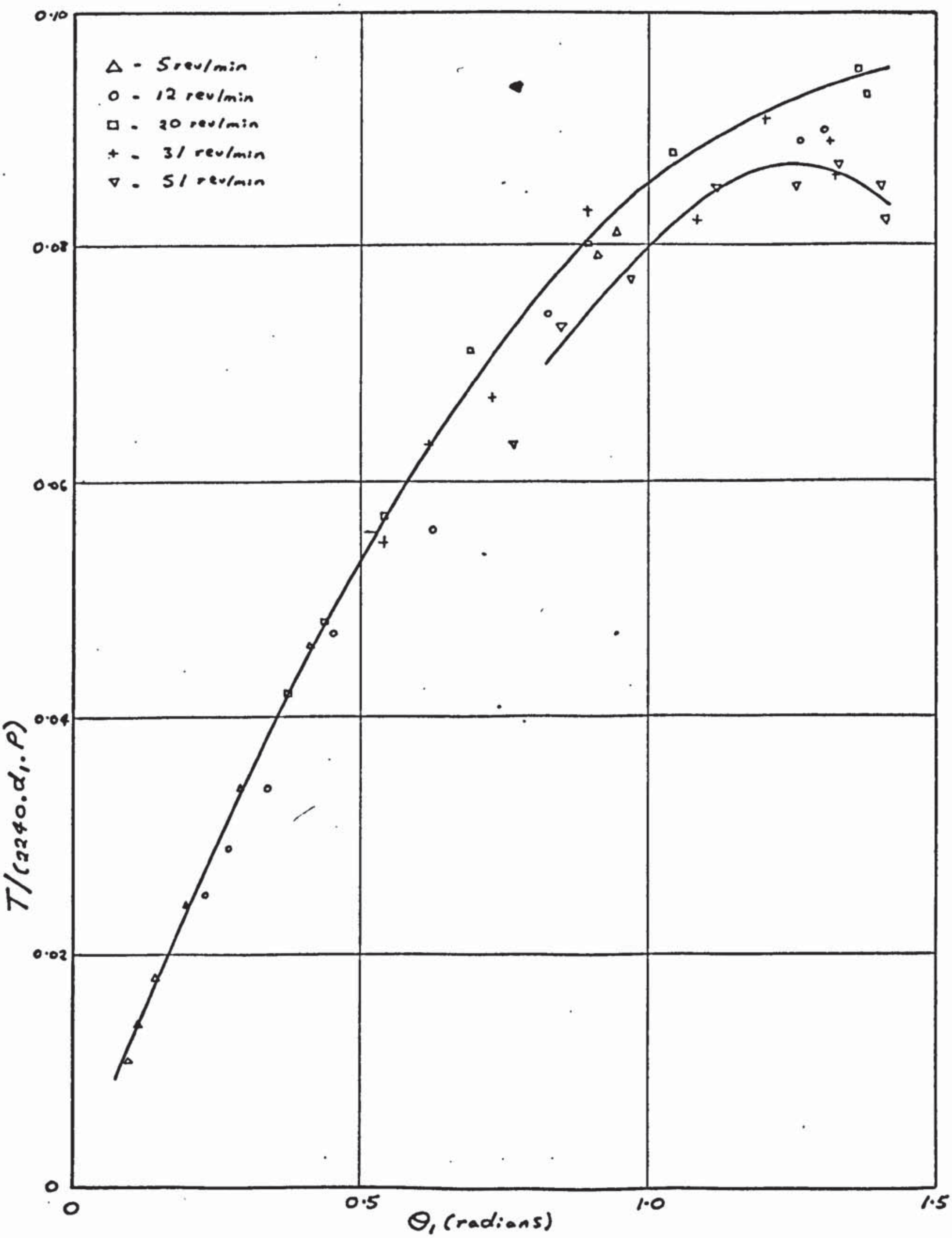

Fig. 10.20 - Relationship between swing of Friction Vector (θ_1) and Demanded Torque

Bar size :- $1\frac{1}{4}$ in.

Lubricant :- Oil

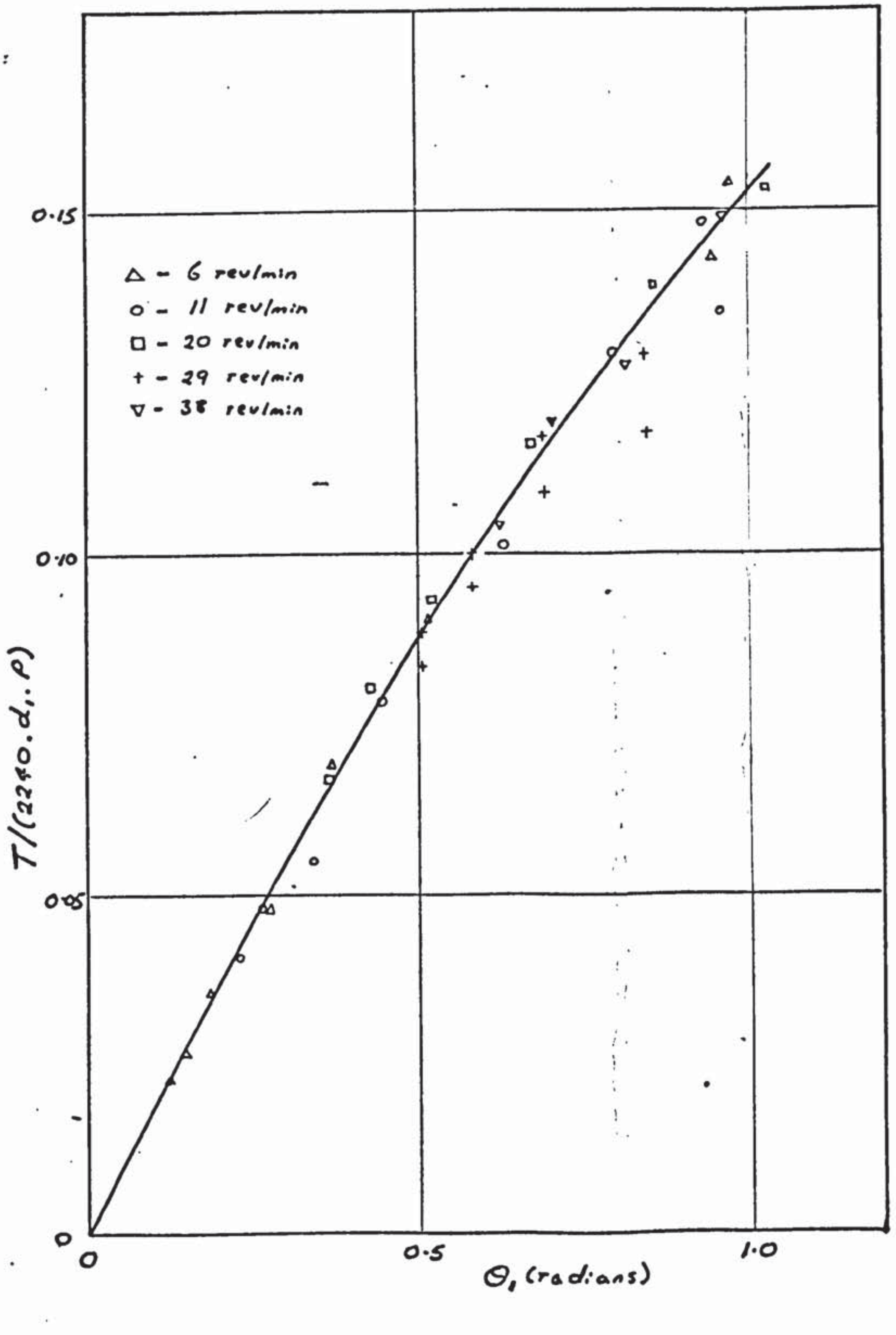

Fig. 10. 21- Relationship between Swing of Friction Vector (θ_1) and Demanded Torque

Bar size:- $1\frac{5}{16}$ in.
Lubricant:- Soap

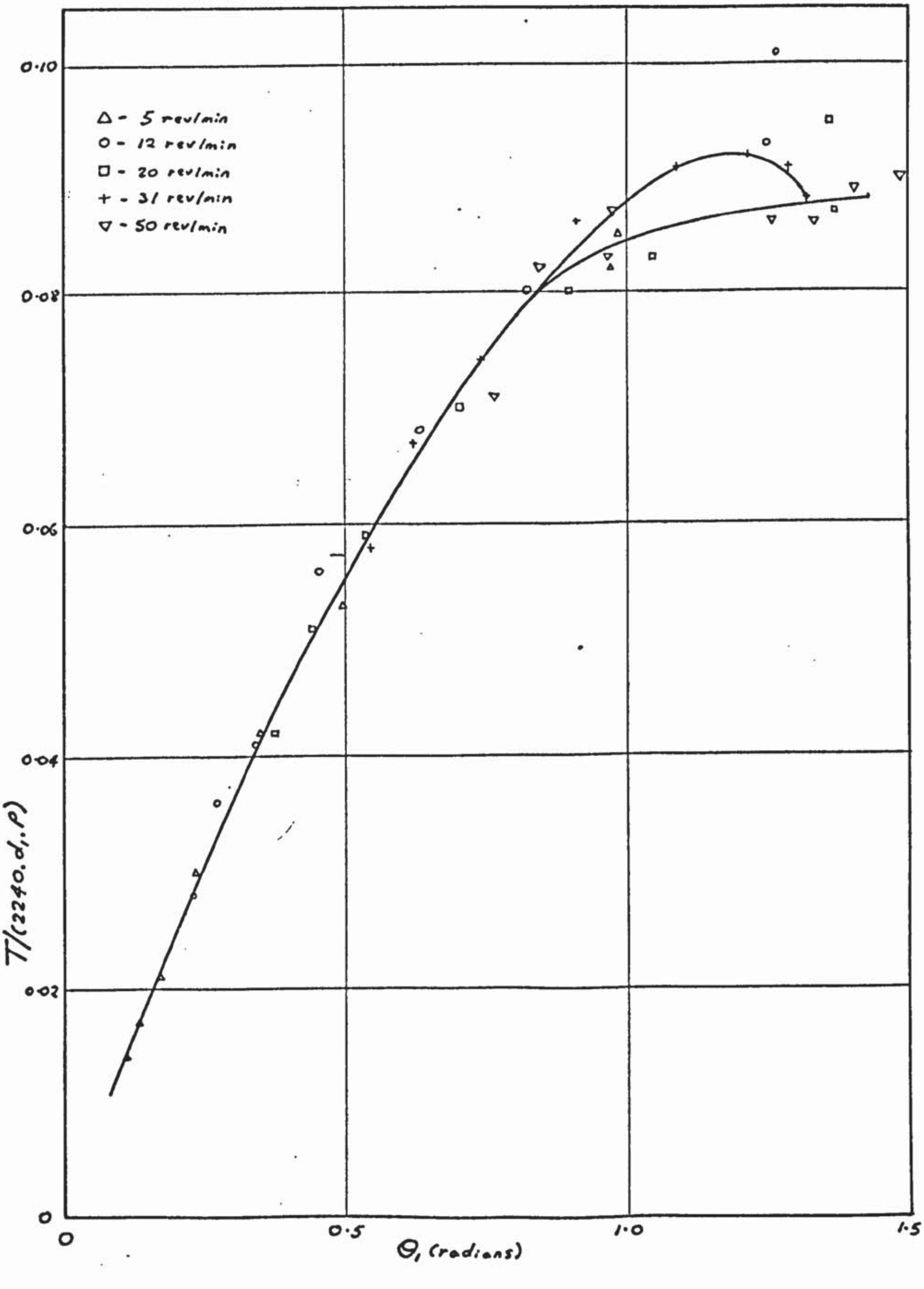

Fig. 10.22 - Relationship between Swing of Friction Vector (θ_1) and Demanded Torque

Bar Size:- $1^{5}/_{16}$ in.

Lubricant:- Oil

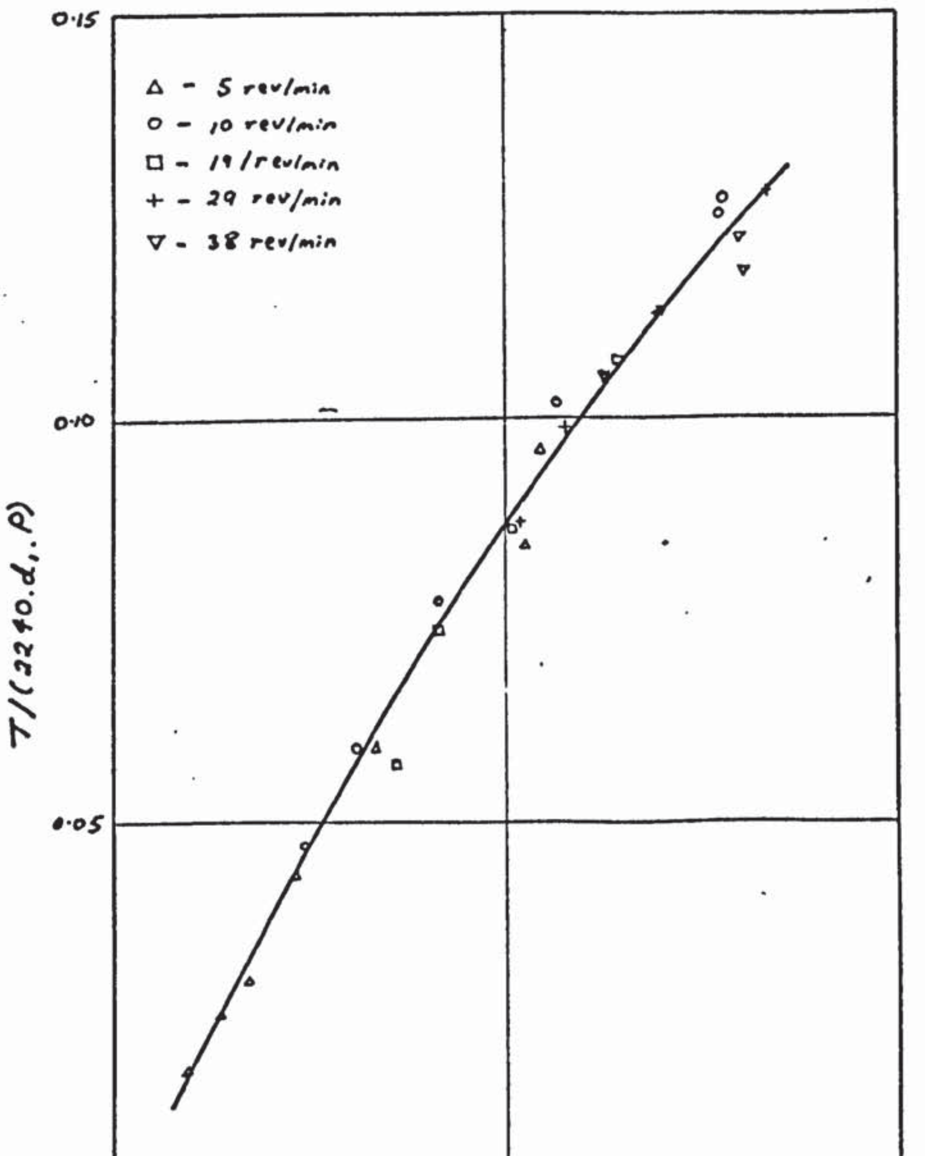

Fig. 10.23 - Dependance of Reduction in Drawing Force on Swing of Friction Vector (Θ_1)

Bar Size:- $1\frac{1}{16}$ in.

Lubricant:- Oil & Soap

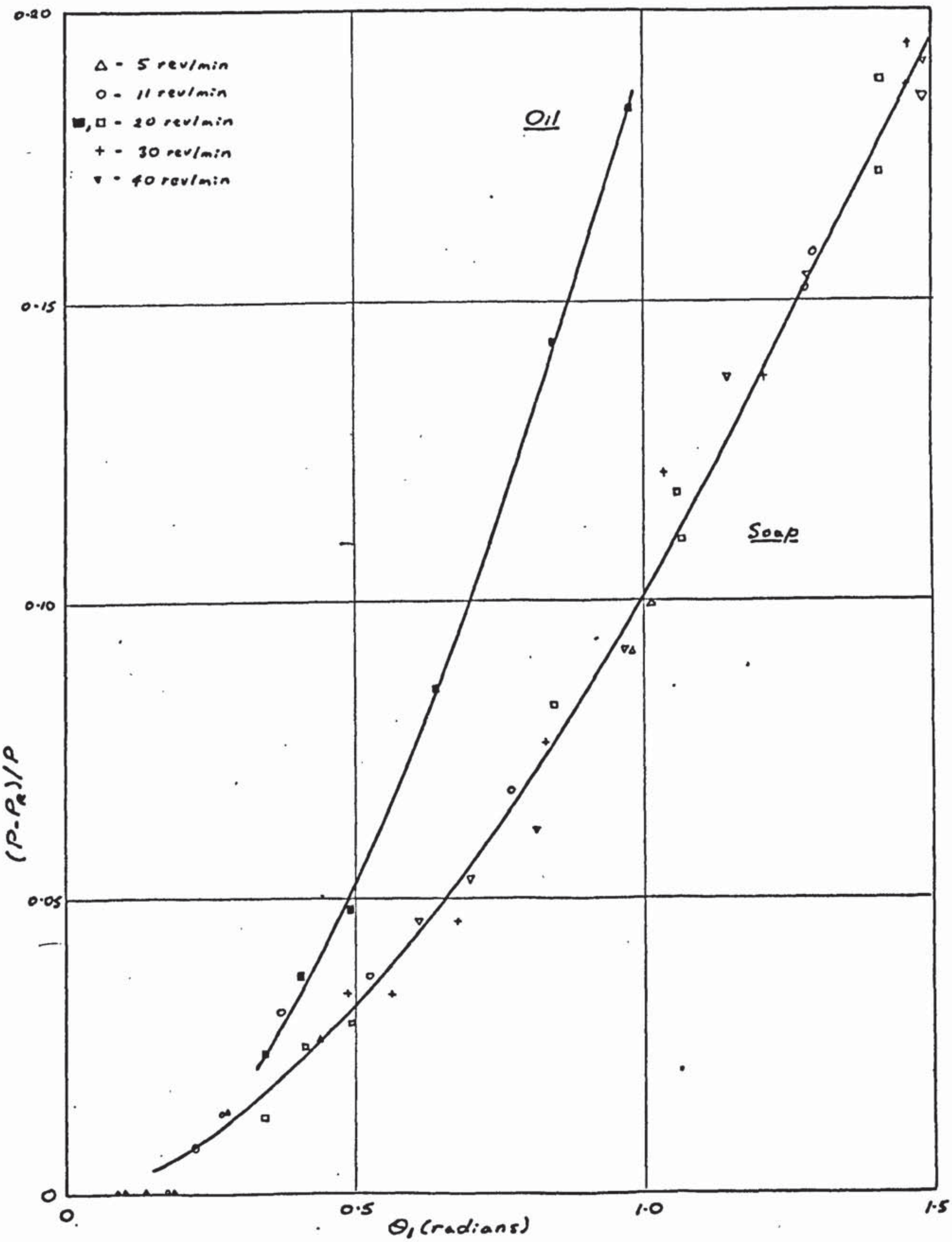

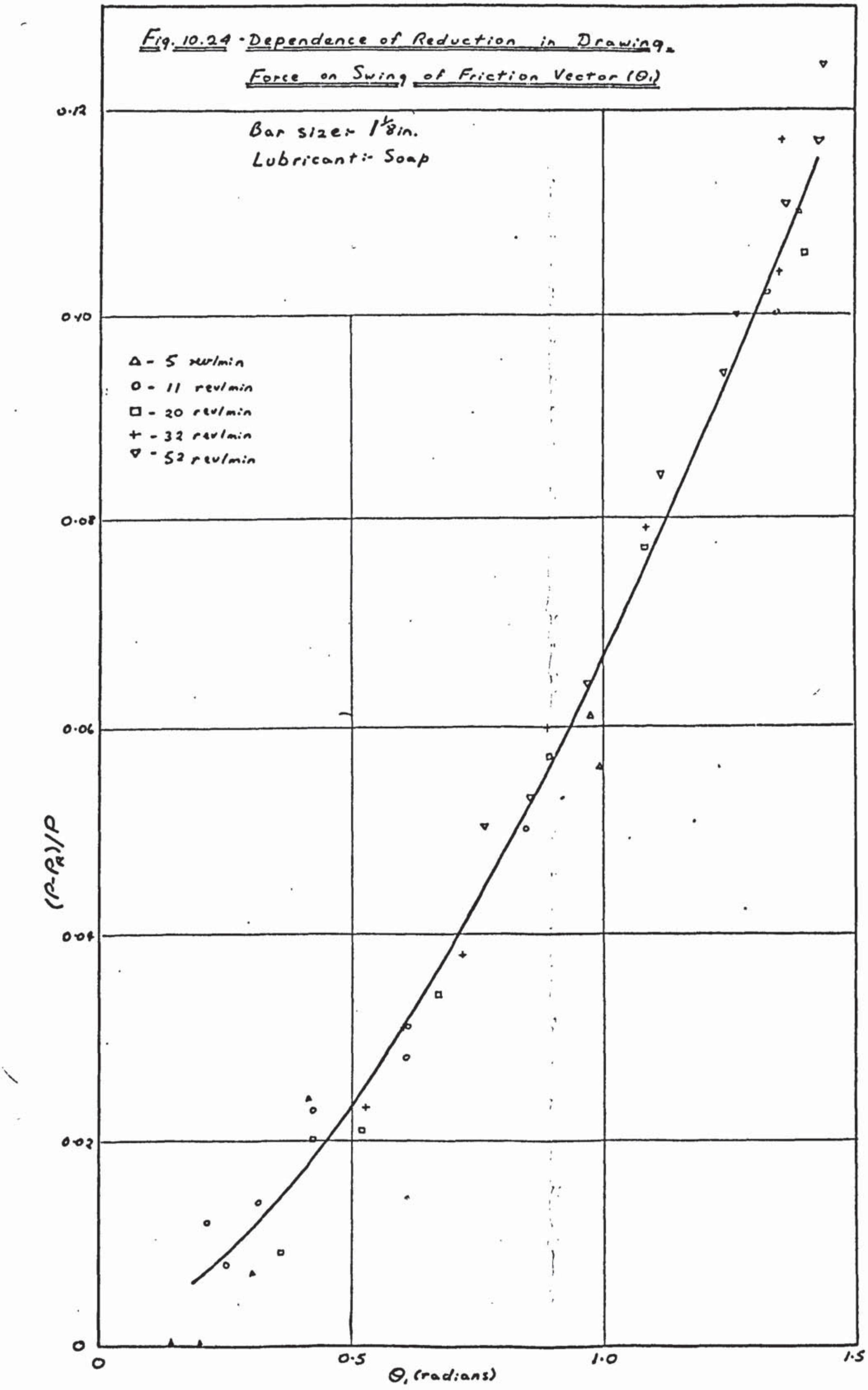

Fig. 10.24 - Dependence of Reduction in Drawing Force on Swing of Friction Vector (θ_1)
Bar size:- $1\frac{1}{8}$ in.
Lubricant:- Soap
Δ - 5 rev/min
○ - 11 rev/min
□ - 20 rev/min
+ - 32 rev/min
▽ - 52 rev/min
0.12
0.10
0.08
0.06
0.04
0.02
0
$(P-P_R)/P$
0
0.5
1.0
1.5
θ_1 (radians)

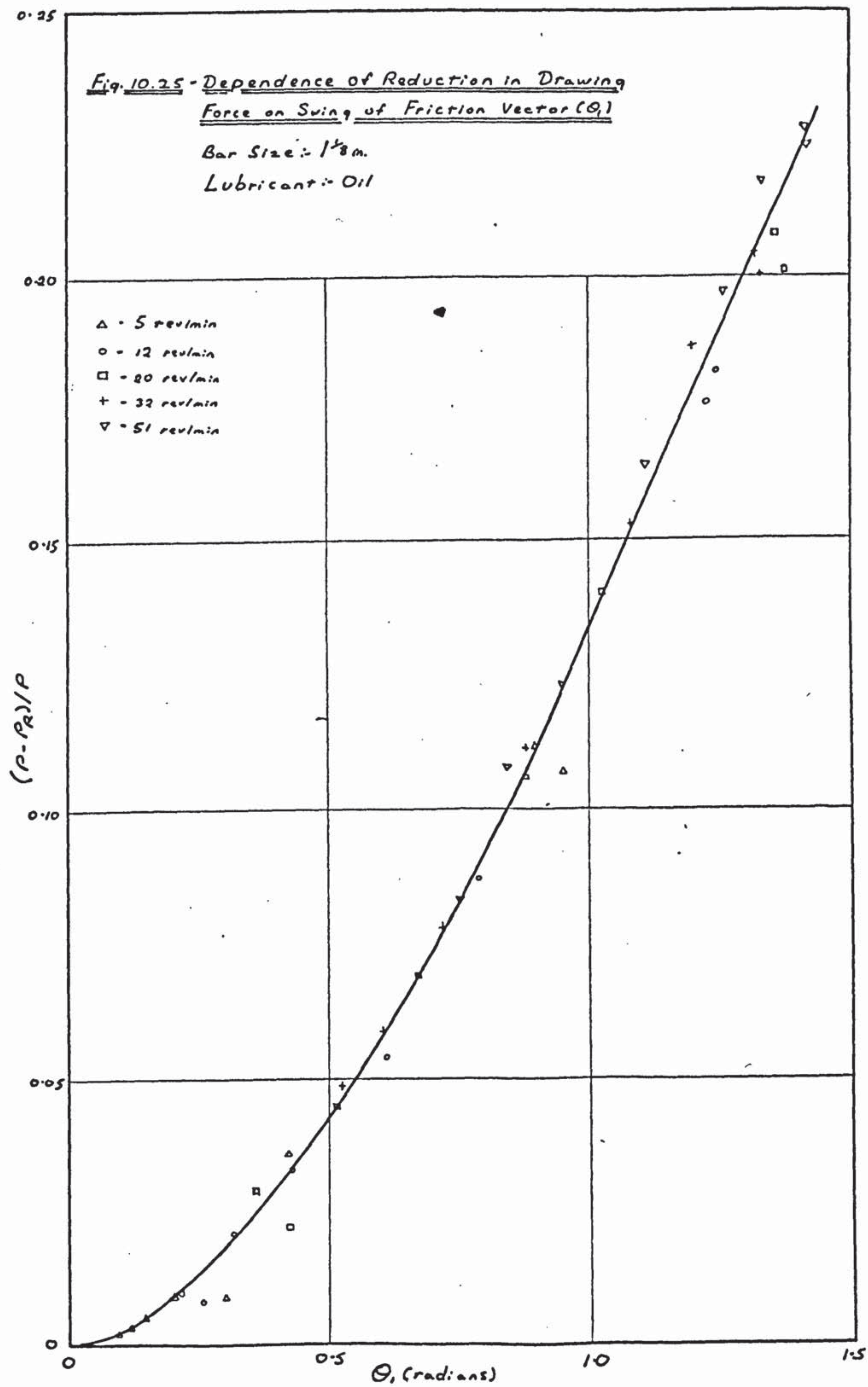
Fig. 10.25 - Dependence of Reduction in Drawing Force on Swing of Friction Vector (θ_1)
Bar Size :- 1⅛ in.
Lubricant :- Oil
△ - 5 rev/min
○ - 12 rev/min
□ - 20 rev/min
+ - 32 rev/min
▽ - 51 rev/min
$(P-P_R)/P$
θ_1 (radians)
0
0·05
0·10
0·15
0·20
0·25
0
0·5
1·0
1·5

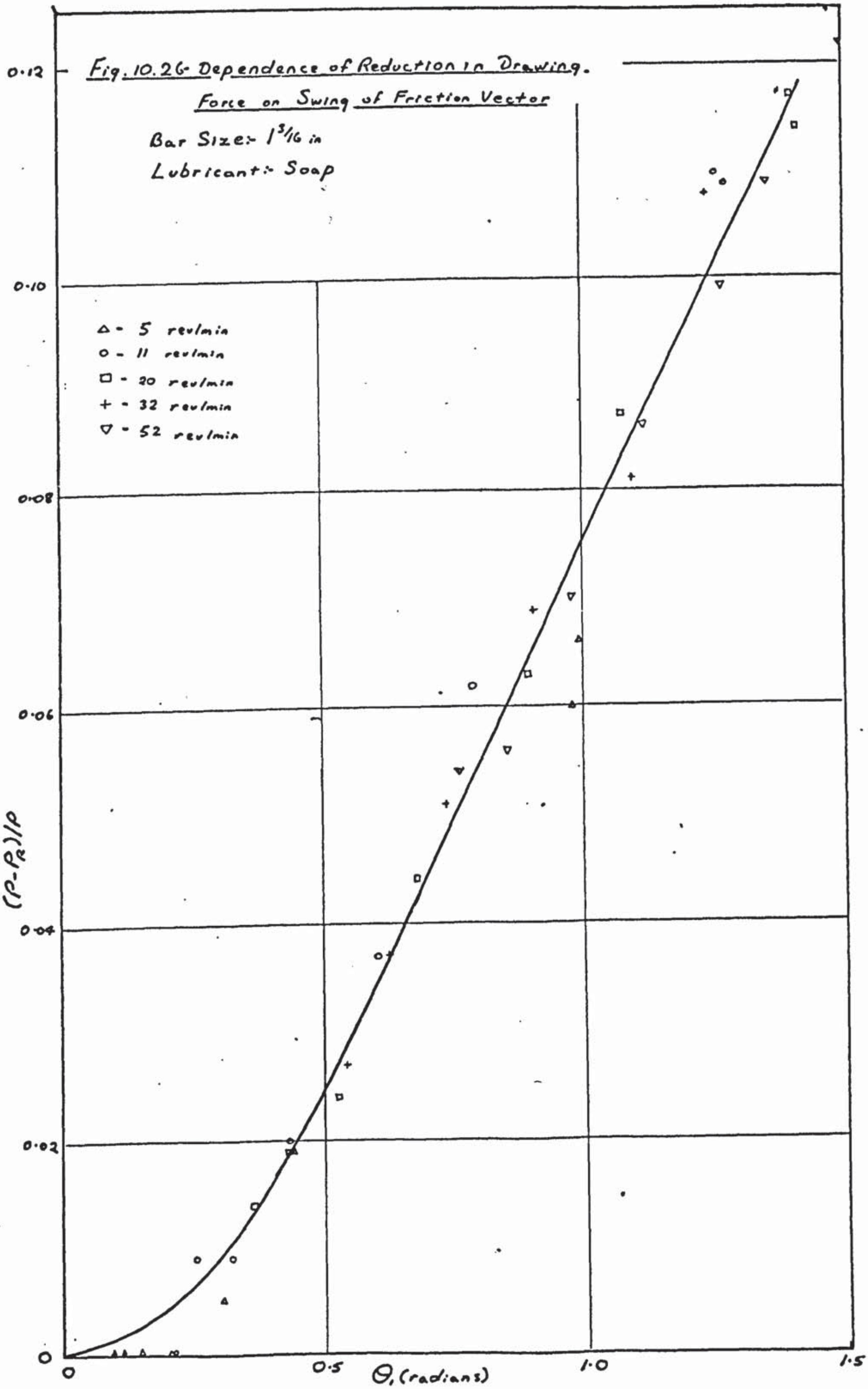

Fig. 10.26 Dependence of Reduction in Drawing Force on Swing of Friction Vector
Bar Size:- 1 3/16 in
Lubricant:- Soap
△ - 5 rev/min
○ - 11 rev/min
□ - 20 rev/min
+ - 32 rev/min
▽ - 52 rev/min
0.12
0.10
0.08
0.06
0.04
0.02
0
(P-P_R)/P
0
0.5
1.0
1.5
θ, (radians)

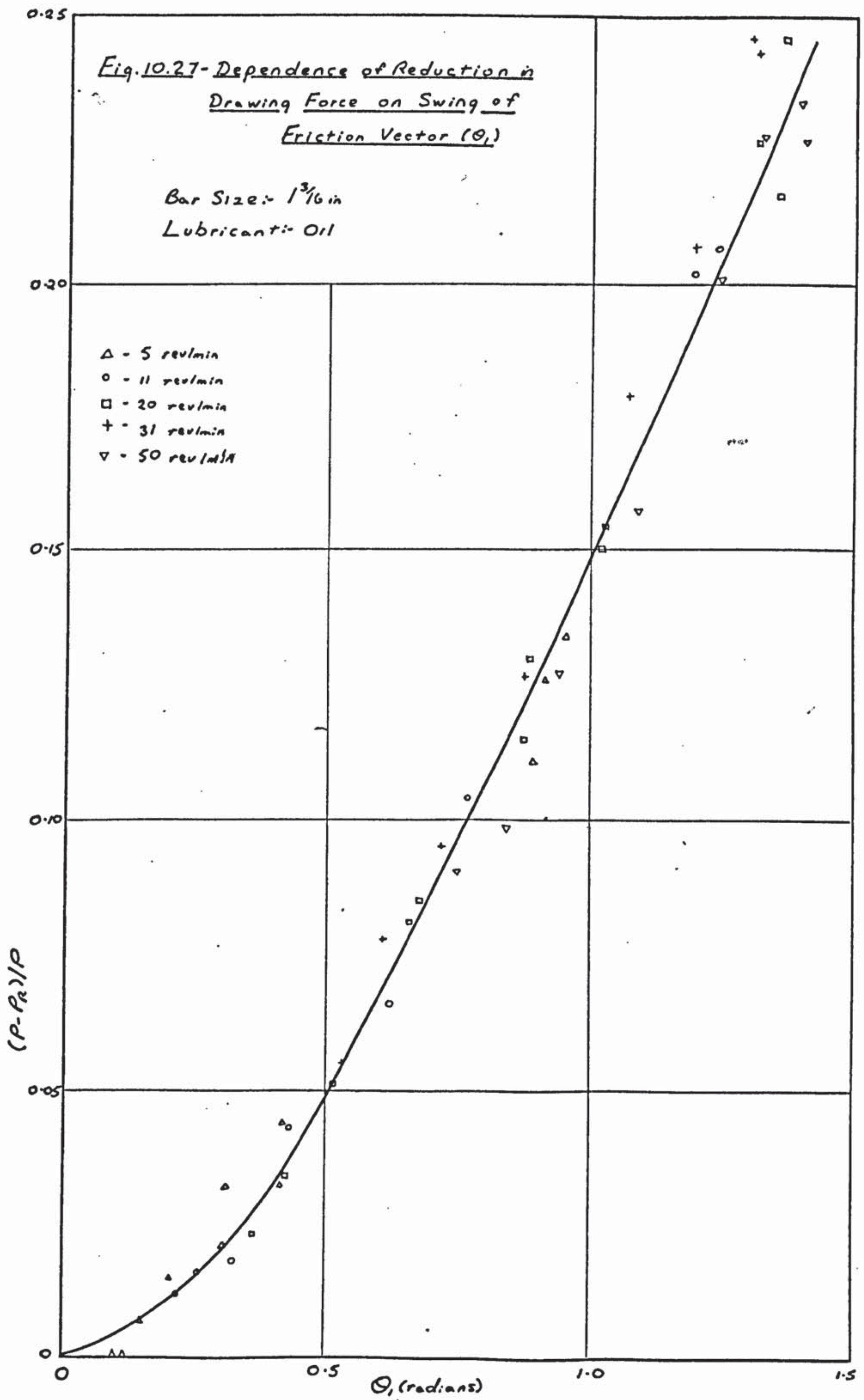

Fig. 10.27 - Dependence of Reduction in Drawing Force on Swing of Friction Vector (θ_1)
Bar Size:- $1\frac{3}{16}$ in
Lubricant:- Oil
△ - 5 rev/min
○ - 11 rev/min
□ - 20 rev/min
+ - 31 rev/min
▽ - 50 rev/min
0.25
0.20
0.15
0.10
0.05
0
$(P-P_R)/P$
0
0.5
1.0
1.5
θ_1 (radians)

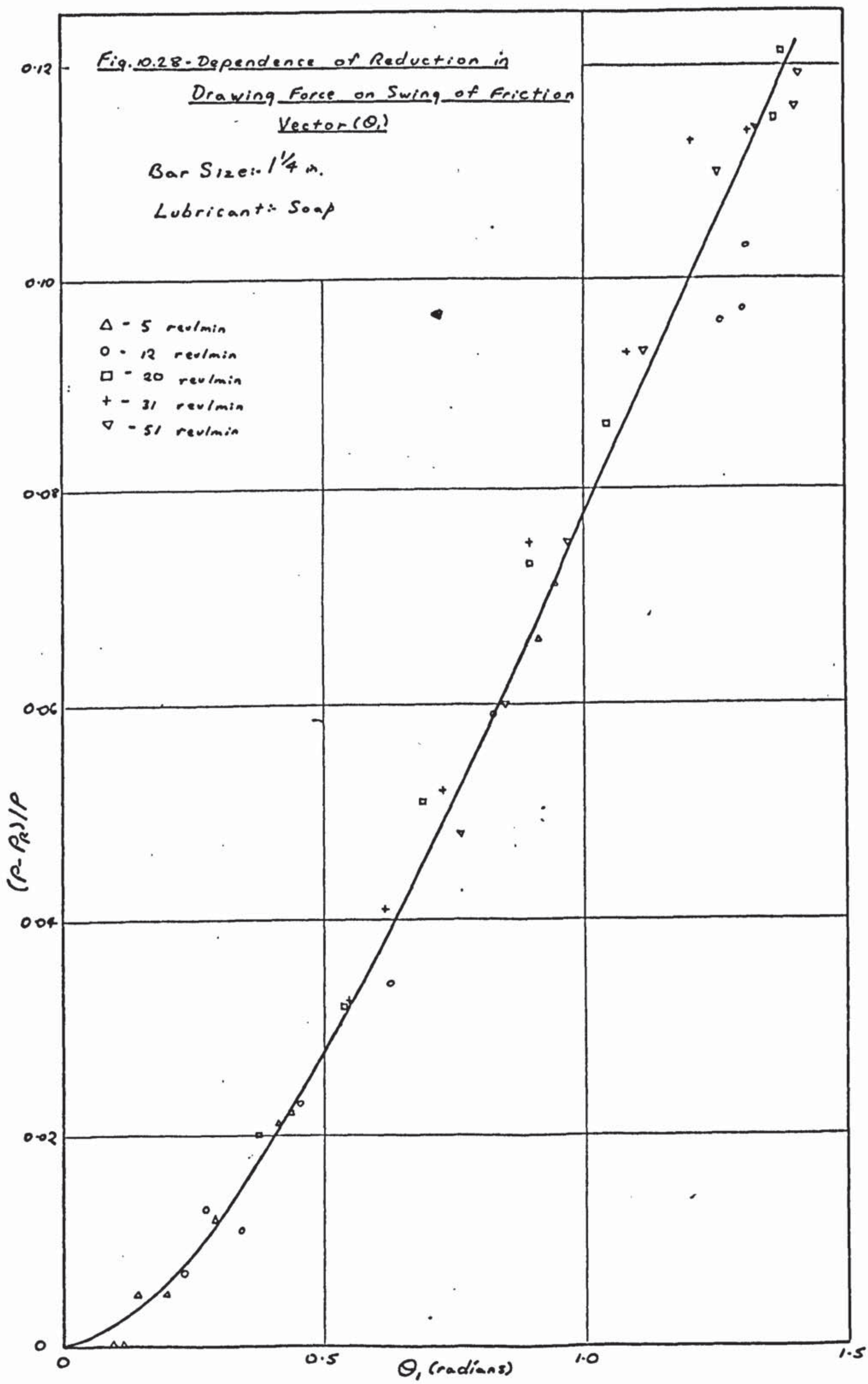

Fig. 10.28 - Dependence of Reduction in Drawing Force on Swing of Friction Vector (θ_1)
Bar Size:- $1\frac{1}{4}$ in.
Lubricant:- Soap
△ - 5 rev/min
○ - 12 rev/min
□ - 20 rev/min
+ - 31 rev/min
▽ - 51 rev/min
$(P-P_R)/P$
θ_1 (radians)
0
0·02
0·04
0·06
0·08
0·10
0·12
0·5
1·0
1·5

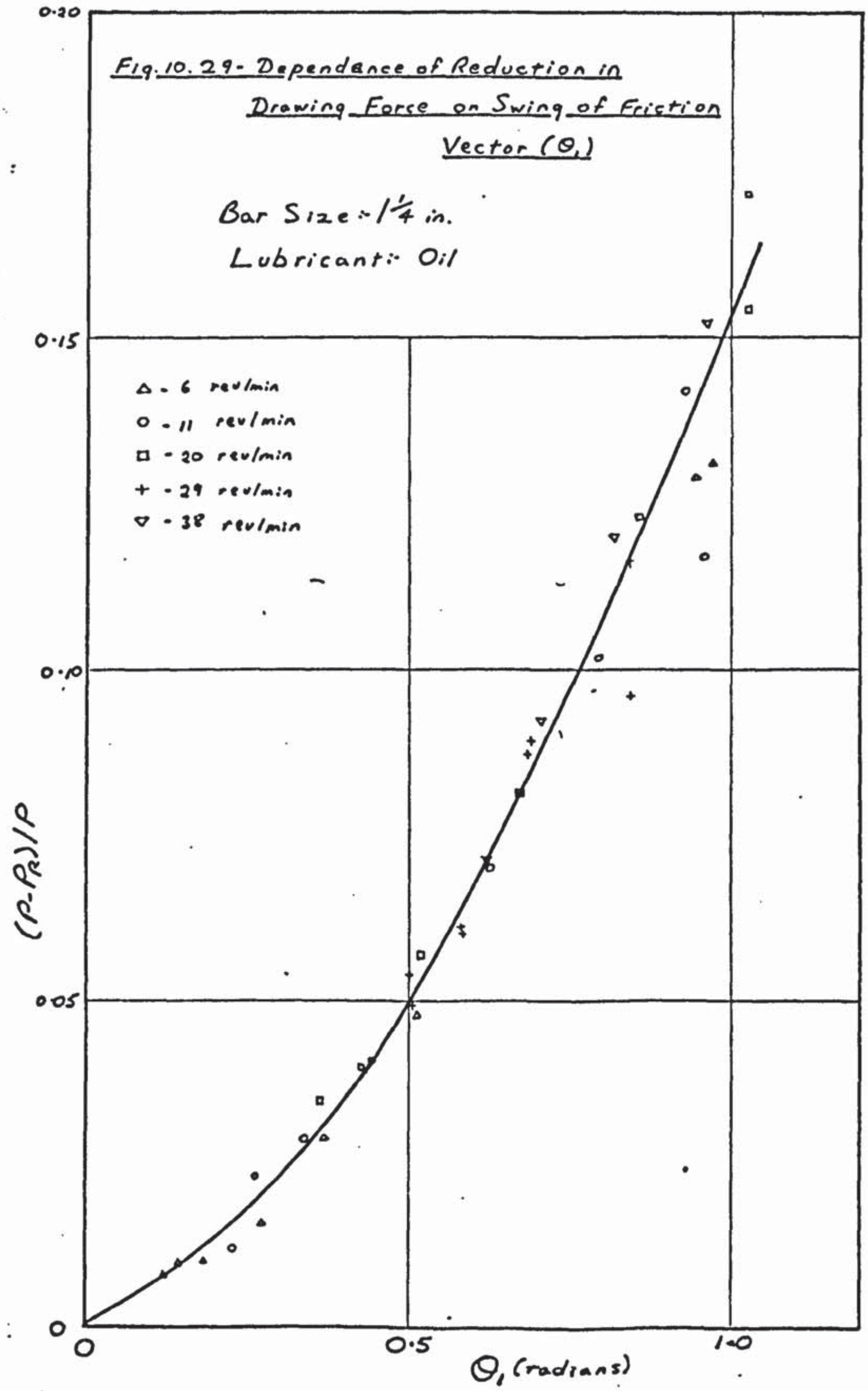

Fig. 10.29 - Dependance of Reduction in Drawing Force on Swing of Friction Vector (θ_1)

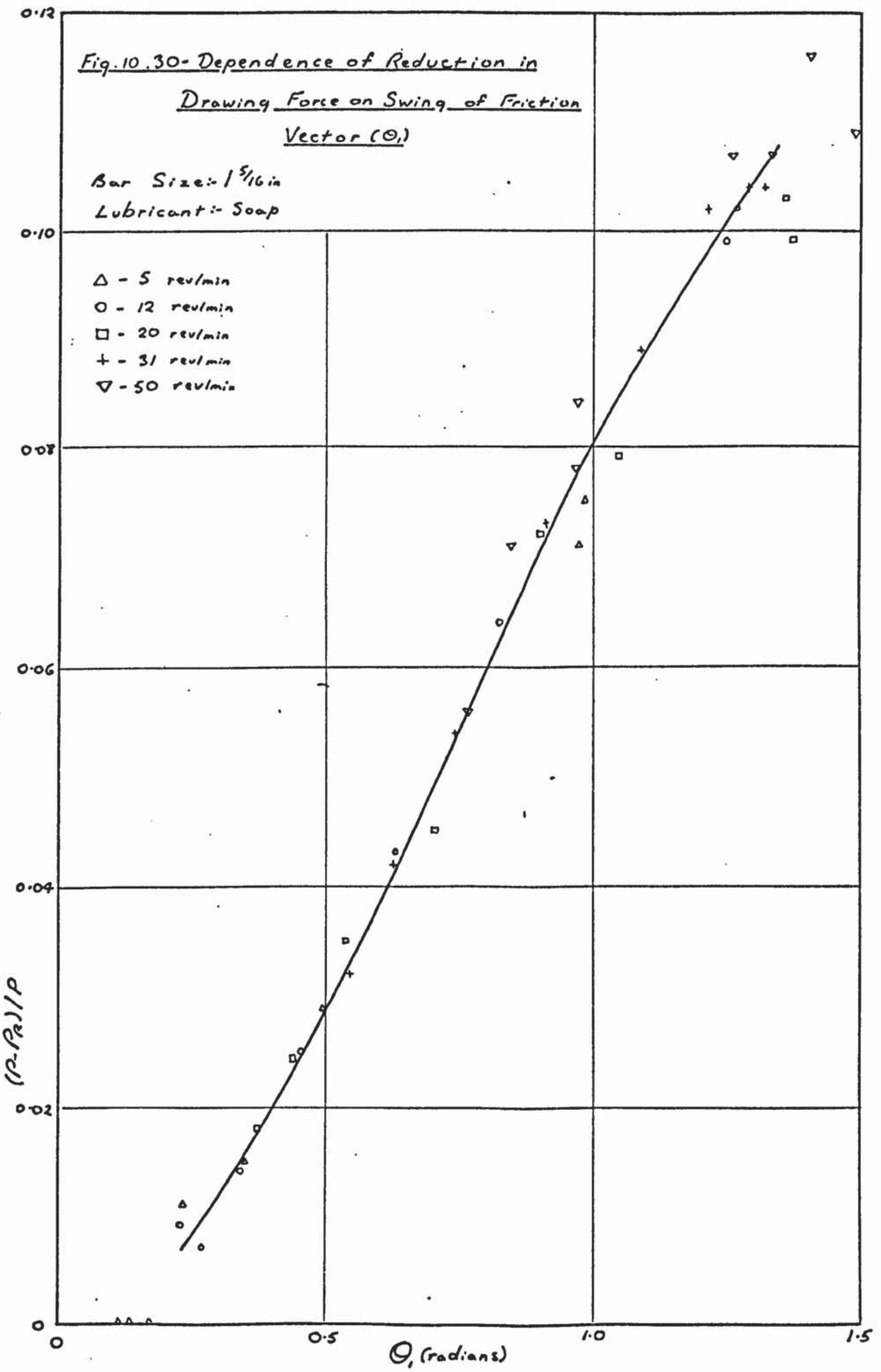

Fig. 10.30 - Dependence of Reduction in Drawing Force on Swing of Friction Vector (Θ_1)
Bar Size:- 1 5/16 in
Lubricant:- Soap
△ - 5 rev/min
○ - 12 rev/min
□ - 20 rev/min
+ - 31 rev/min
▽ - 50 rev/min
0·12
0·10
0·08
0·06
0·04
0·02
0
$(P-P_2)/P$
0
0·5
1·0
1·5
Θ_1 (radians)

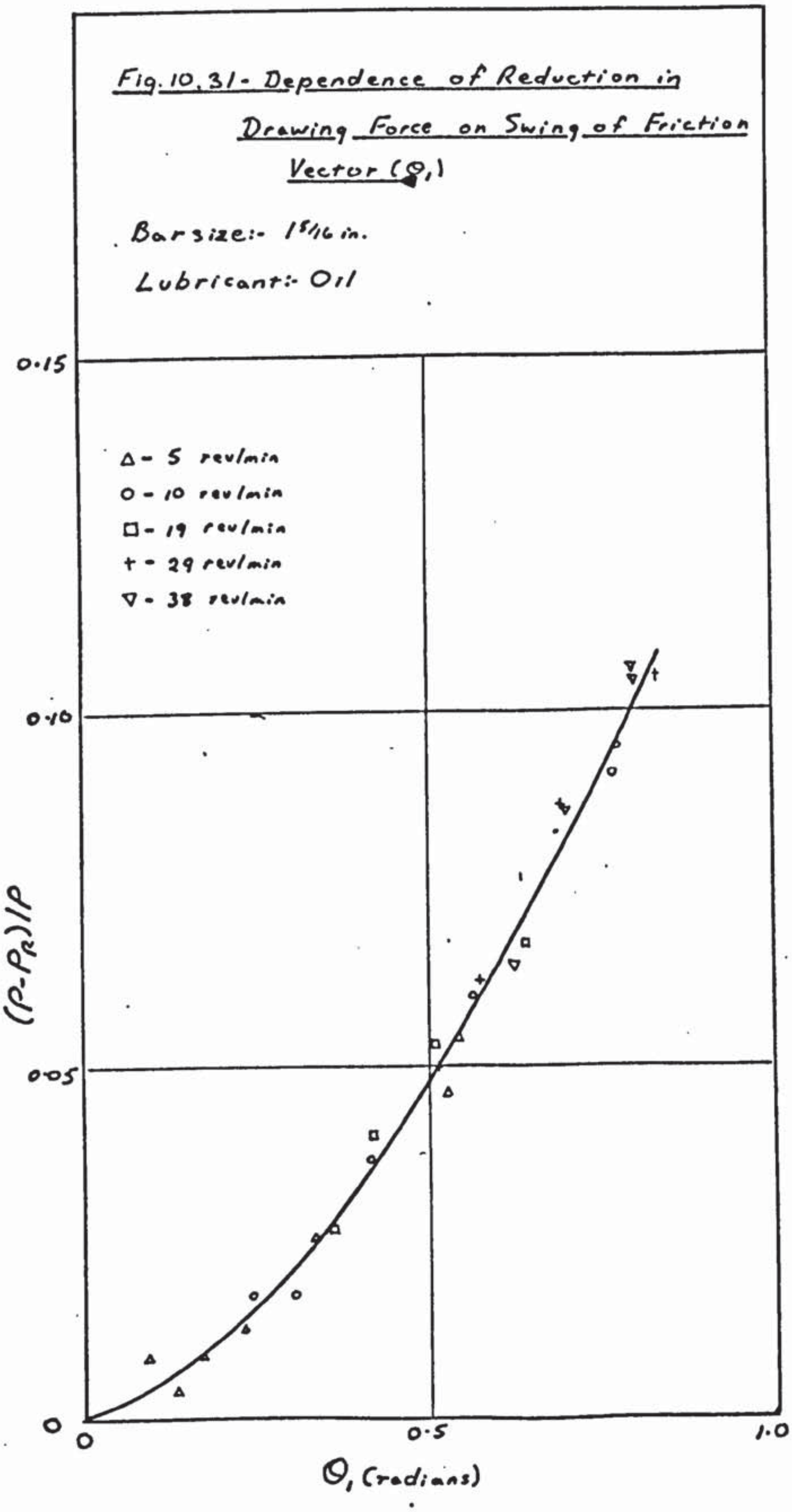

Fig. 10.31 - Dependence of Reduction in Drawing Force on Swing of Friction Vector (θ_1)
Barsize:- 1 5/16 in.
Lubricant:- Oil
△ - 5 rev/min
○ - 10 rev/min
□ - 19 rev/min
+ - 29 rev/min
▽ - 38 rev/min
0.15
0.10
0.05
0
0
0.5
1.0
$(P-P_R)/P$
θ_1 (radians)

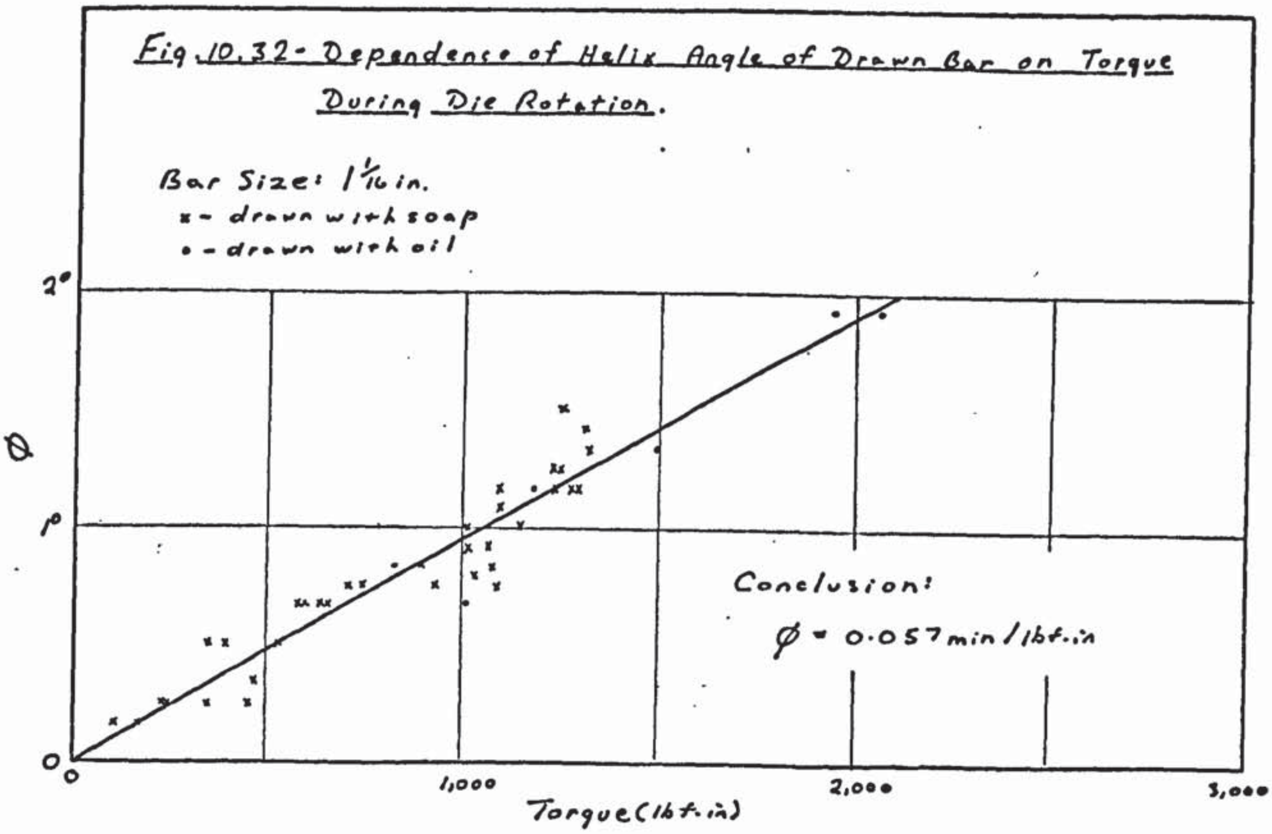

Fig. 10.32 - Dependence of Helix Angle of Drawn Bar on Torque During Die Rotation.
Bar Size: $1\frac{1}{16}$ in.
x - drawn with soap
• - drawn with oil
Conclusion:
ϕ = 0.057 min/lbf.in
2°
1°
0
ϕ
0
1,000
2,000
3,000
Torque (lbf.in)

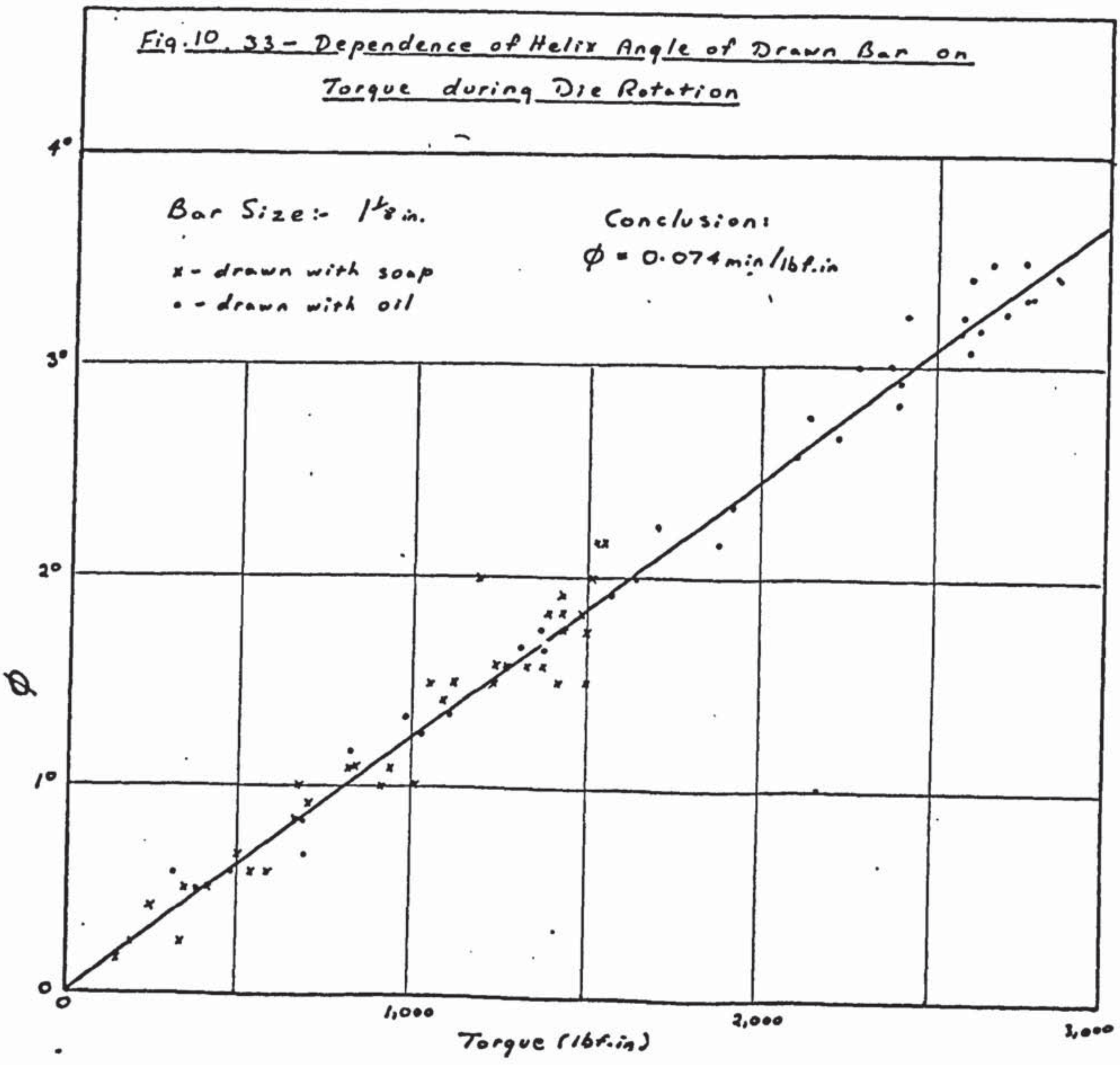

Fig. 10.33 - Dependence of Helix Angle of Drawn Bar on Torque during Die Rotation
Bar Size:- $1\frac{1}{8}$ in.
x - drawn with soap
• - drawn with oil
Conclusion:
ϕ = 0.074 min/lbf.in
4°
3°
2°
1°
0
ϕ
0
1,000
2,000
3,000
Torque (lbf.in)

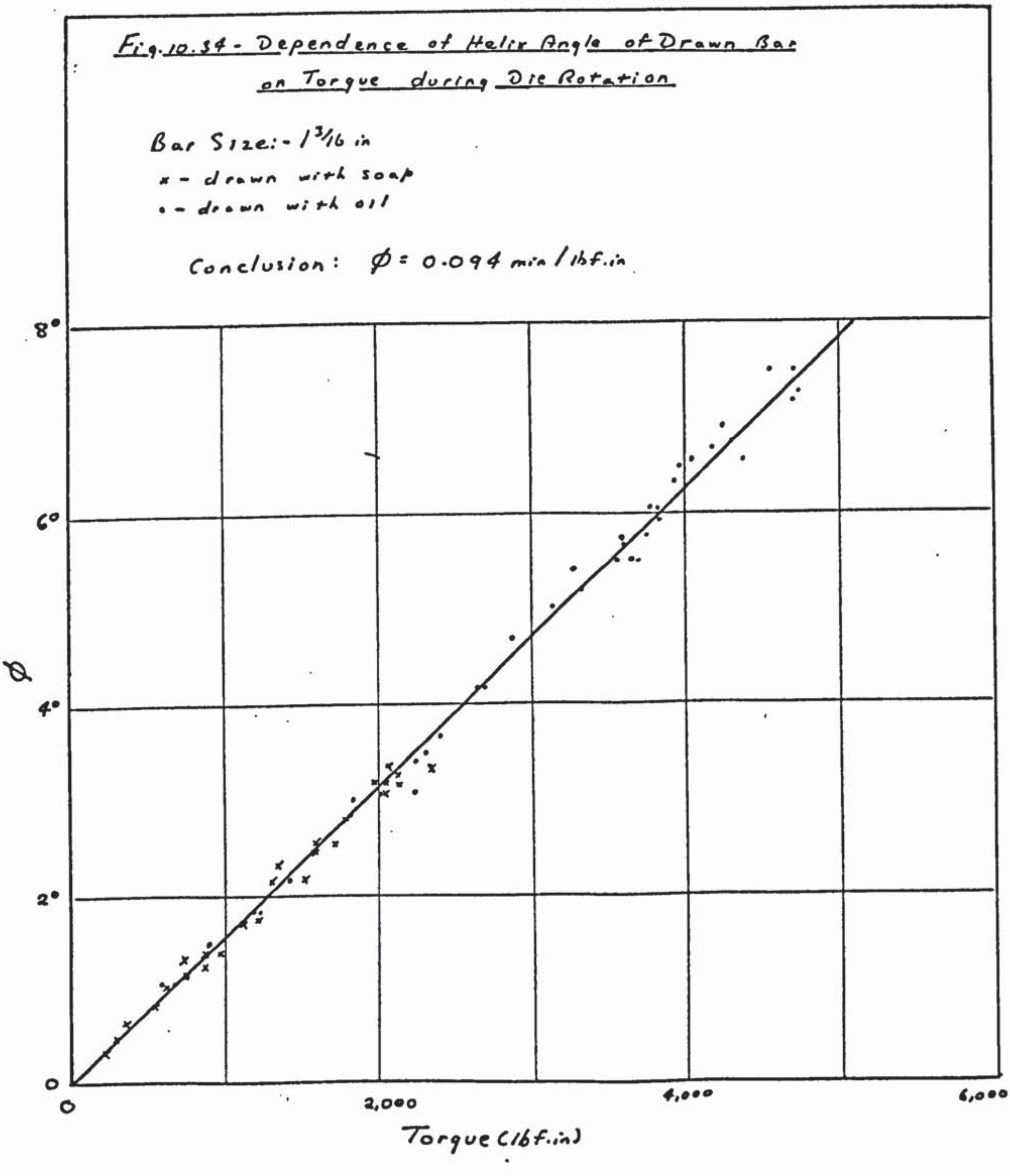

Fig. 10.34 - Dependence of Helix Angle of Drawn Bar on Torque during Die Rotation
Bar Size:- 1 3/16 in
x - drawn with soap
• - drawn with oil
Conclusion: ϕ = 0.094 min / lbf.in
8°
6°
4°
2°
0
ϕ
0
2,000
4,000
6,000
Torque (lbf.in)

Fig. 10.35 - Dependence of Helix Angle of Drawn Bar on Torque during Die Rotation

Bar Size - $1\frac{1}{4}$ in

x - drawn with soap

• - drawn with oil

Conclusion:

ϕ = 0·106 min/lbf.in.

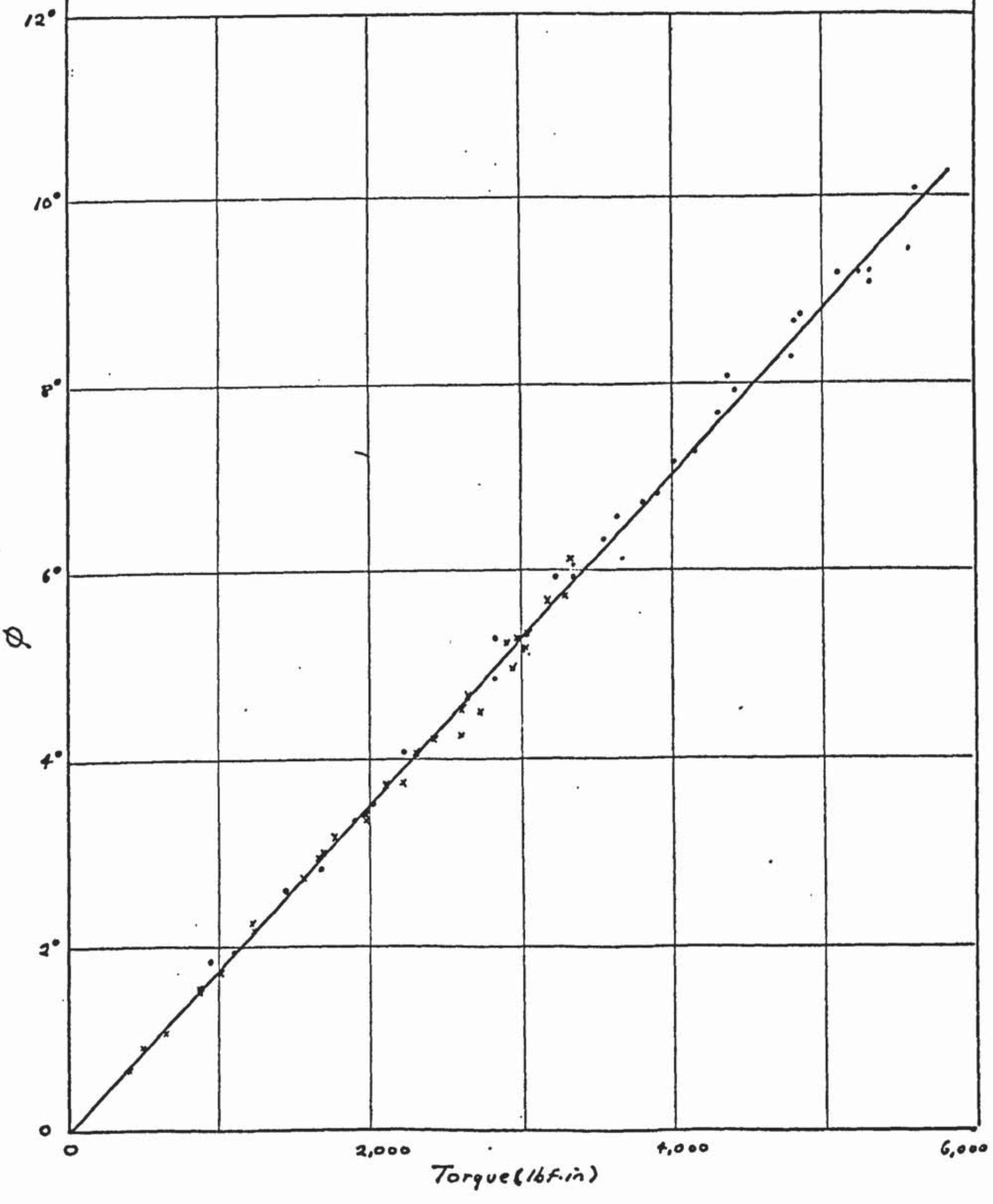

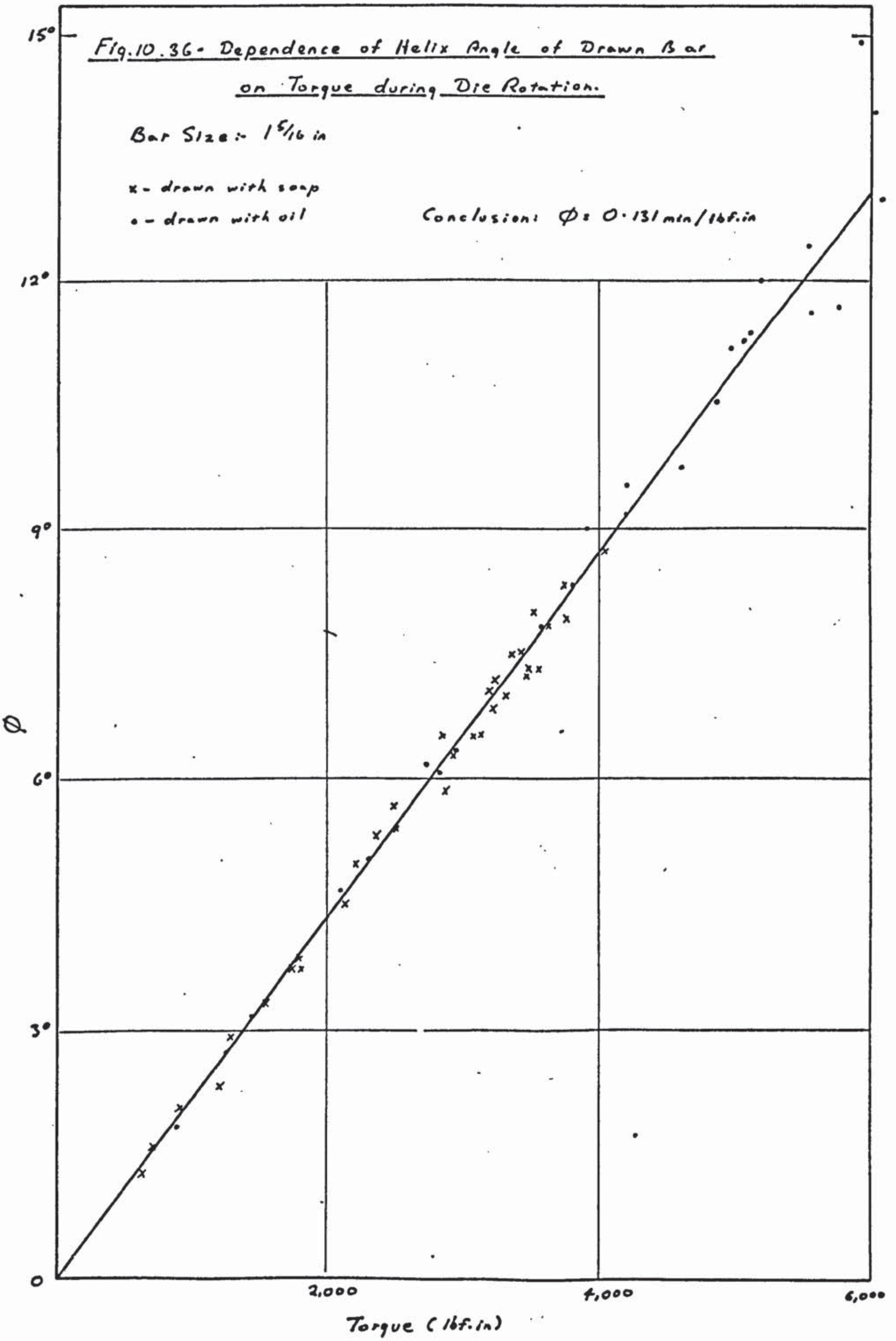
Fig. 10.36 - Dependence of Helix Angle of Drawn Bar on Torque during Die Rotation.
Bar Size :- 1 5/16 in
x - drawn with soap
• - drawn with oil
Conclusion: Φ = 0·131 min/lbf.in
15°
12°
9°
6°
3°
0
Φ
2,000
4,000
6,000
Torque (lbf.in)

Fig. 10.37 - Influence of Speed and Friction Parameters on Rotational Speed of the Undrawn Bar

Bar size :- $1\frac{1}{16}$ in.

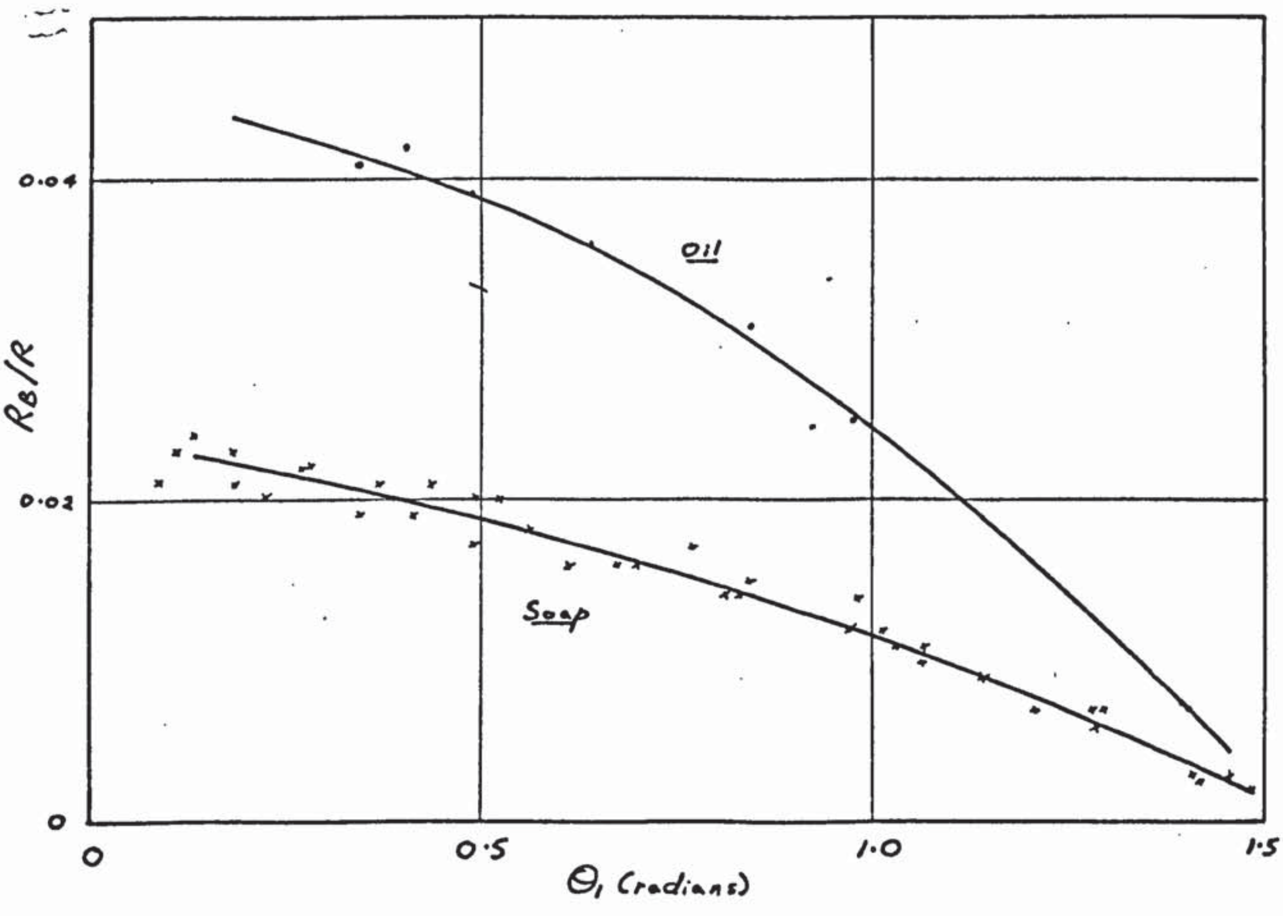

Fig. 10.38 - Influence of Speed and Friction Parameters on Rotational Speed of the Undrawn Bar

Bar Size:- $1\frac{1}{8}$ in.

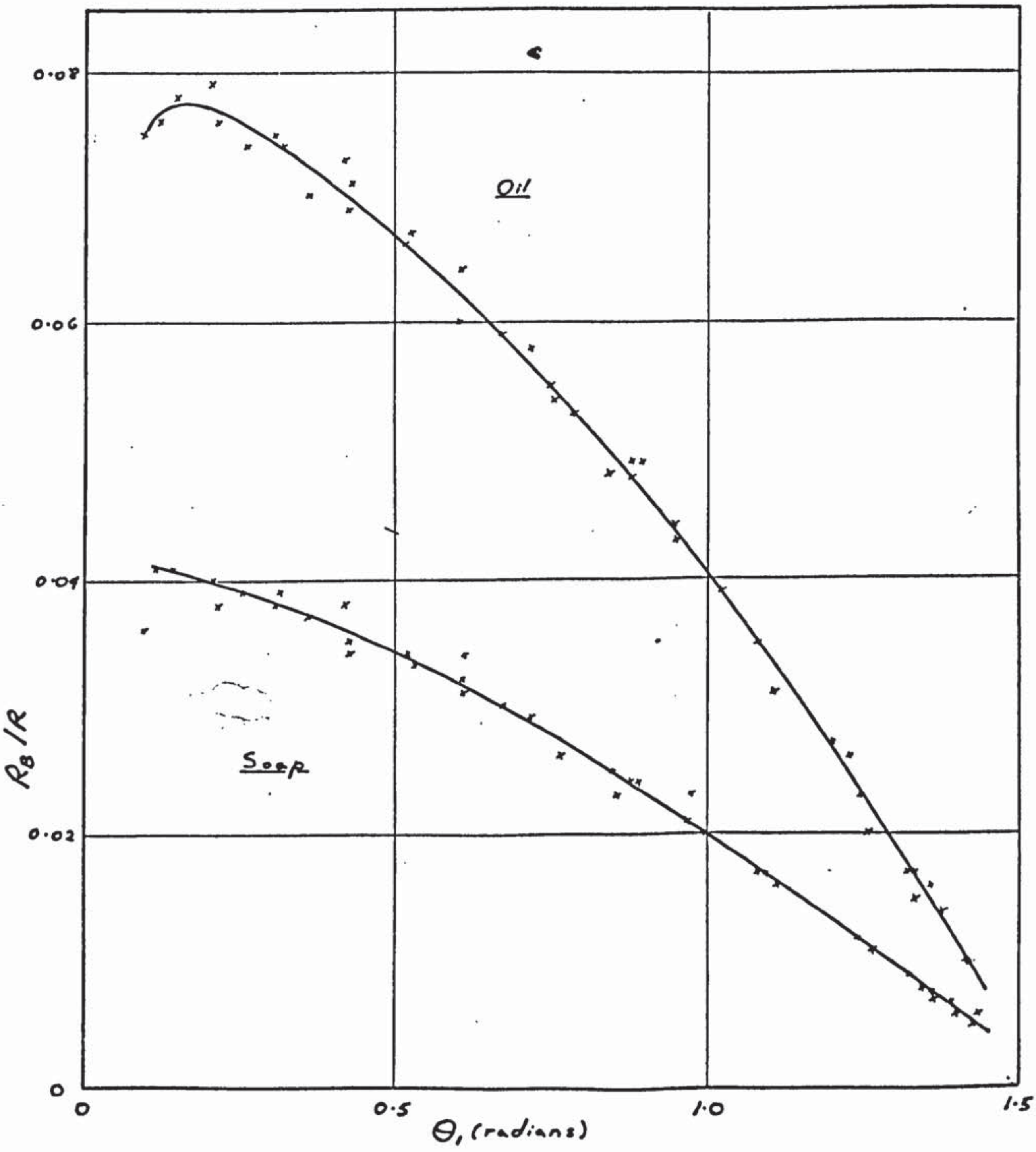

Fig. 10.39. Influence of Speed and Friction Parameters on Rotational Speed of the Undrawn Bar

Bar Size:- $1\frac{3}{16}$ in.

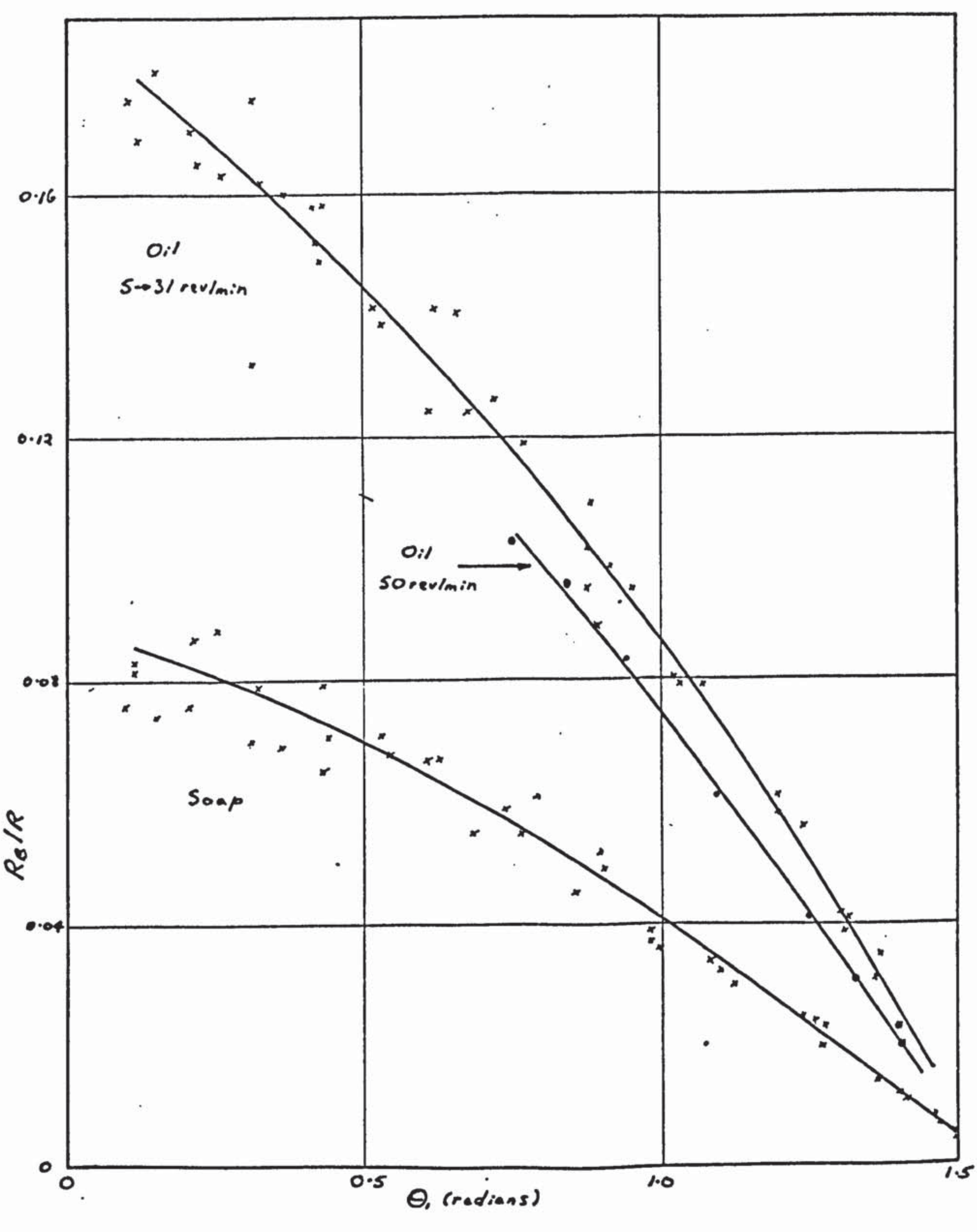

Fig. 10.40 - Influence of Speed and Friction Parameters on Rotational Speed of the Undrawn Bar

Bar Size:- $1\frac{1}{4}$ in

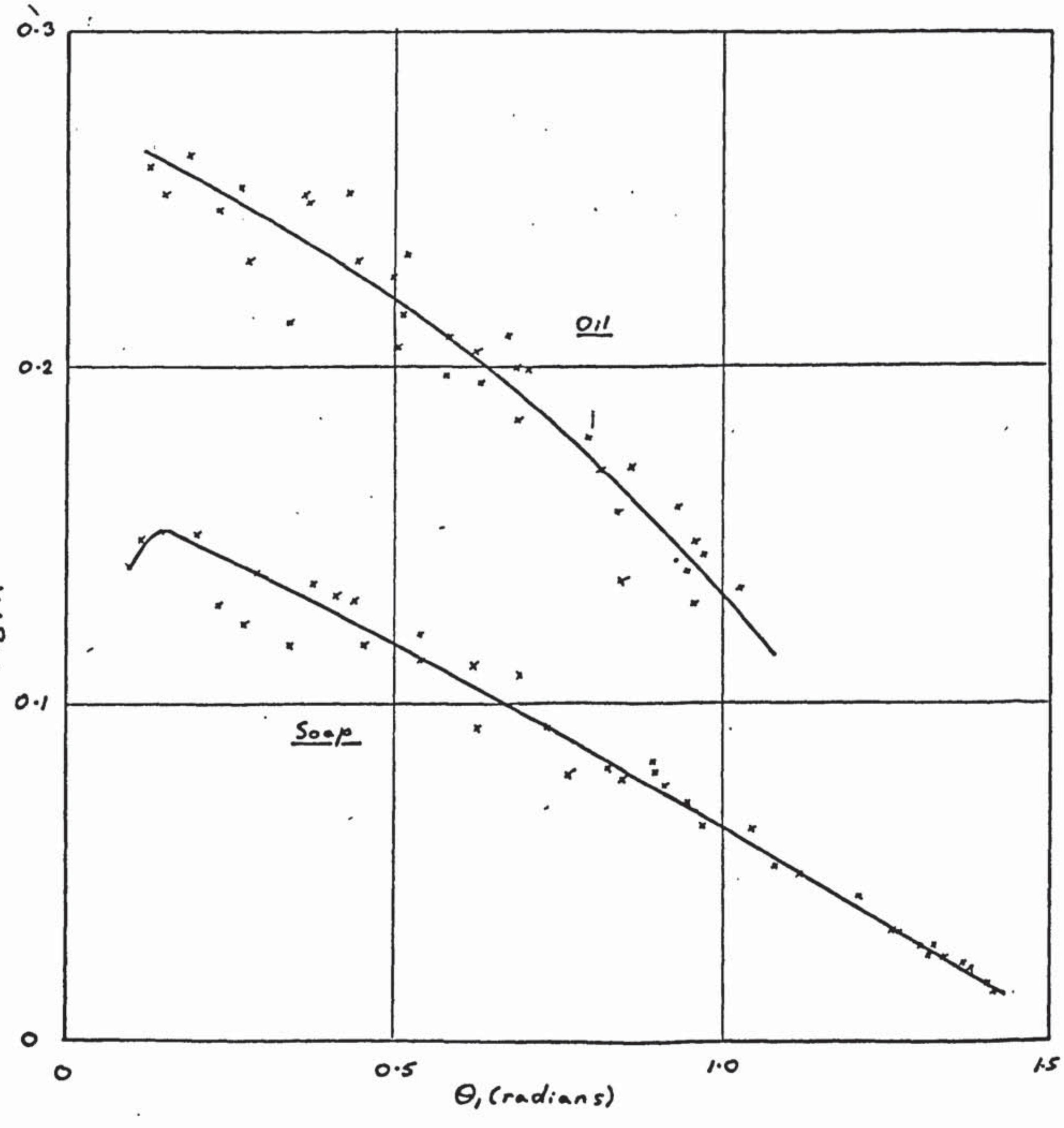

Fig. 10.41. Influence of Speed and Friction Parameters on Rotational Speed of the Undrawn Bar.

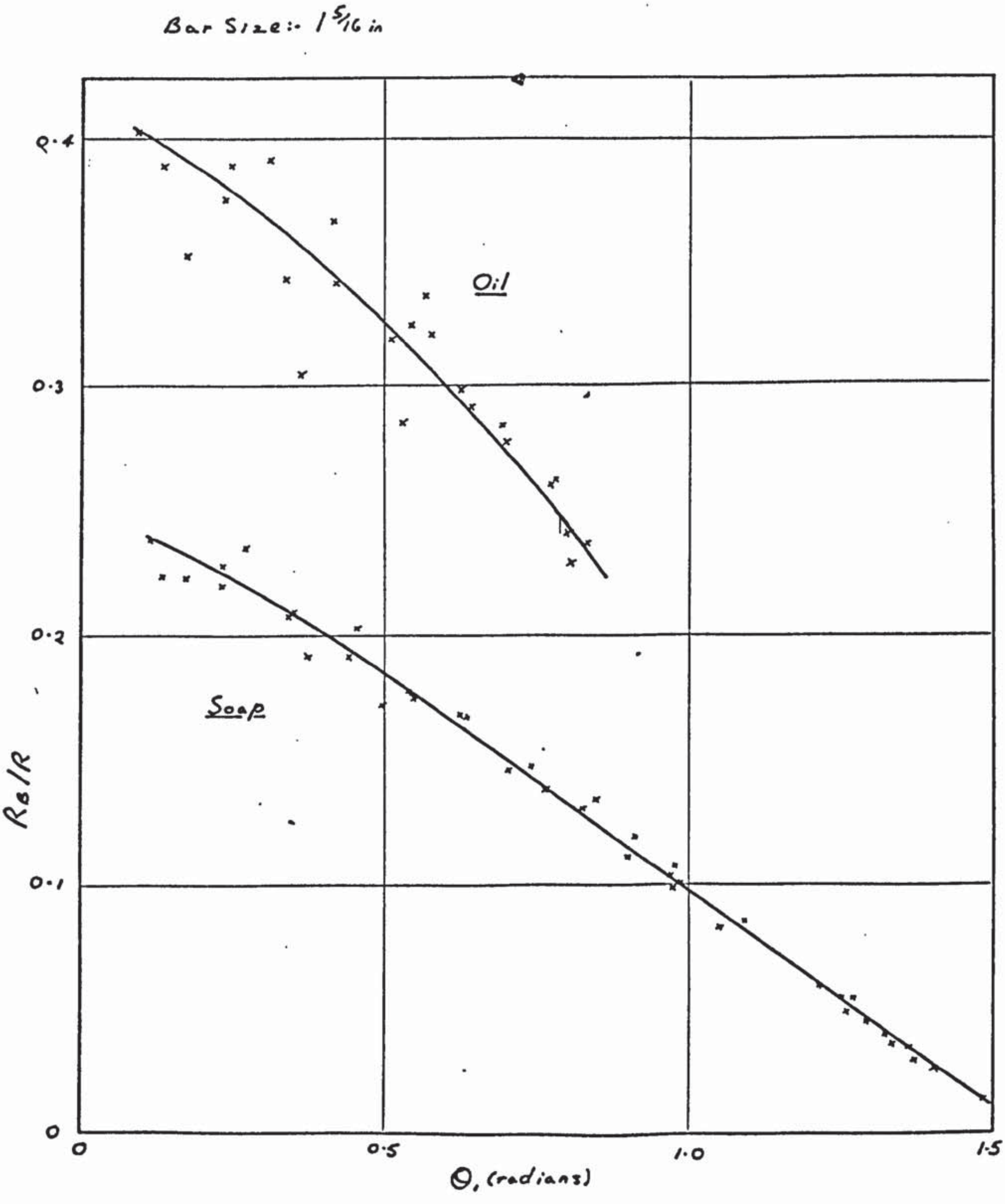

Fig. 10.42 - Component of Drawing Force due to Friction,

Calculated from Torque measurements,

assuming $n=1$

Bar Size: $1\frac{1}{16}$ in.

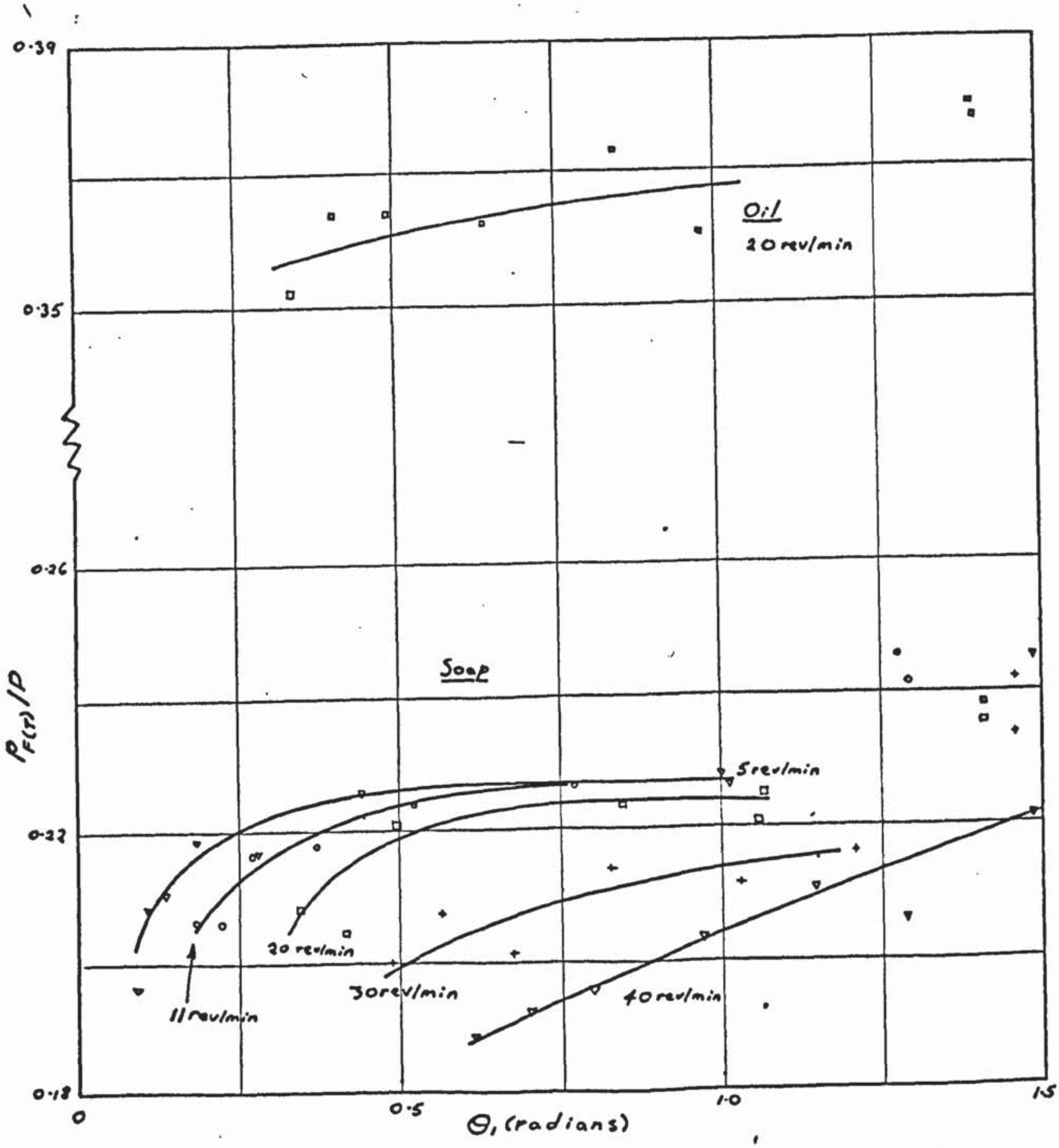

Fig. 10.43 - Component of Drawing Force due to Friction. Calculated from Torque measurements, assuming n = 1.

Bar Size: $1\frac{1}{8}$ in.

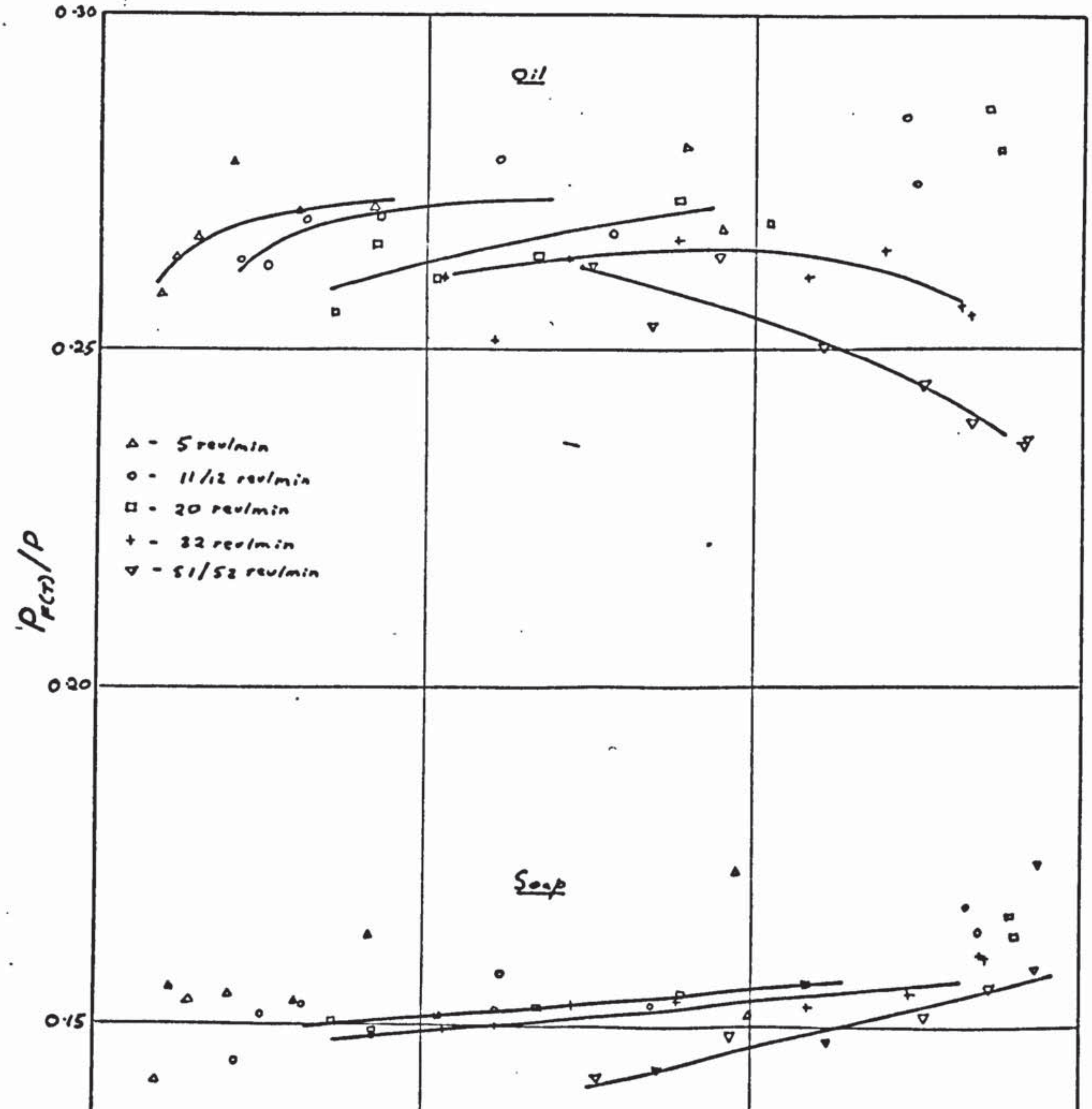

Fig. 10.44. Component of Drawing Force due to Friction. Calculated from Torque measurements, assuming n=1

Bar Size: $1\frac{3}{16}$ in

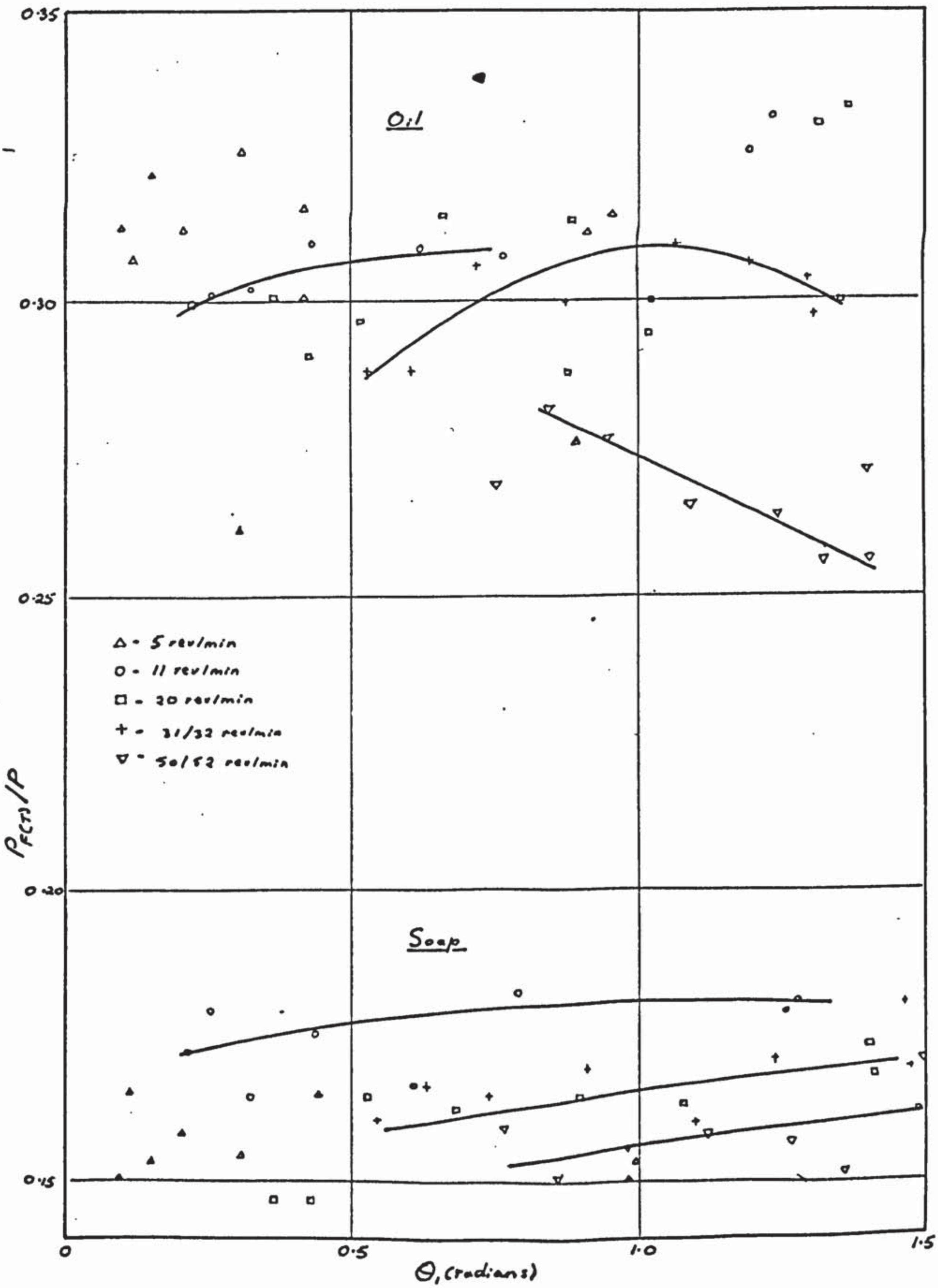

Fig. 10.45 - Component of Drawing Force due to Friction.
Calculated from Torque measurements,
assuming n=1

Bar Size: 1¼ in

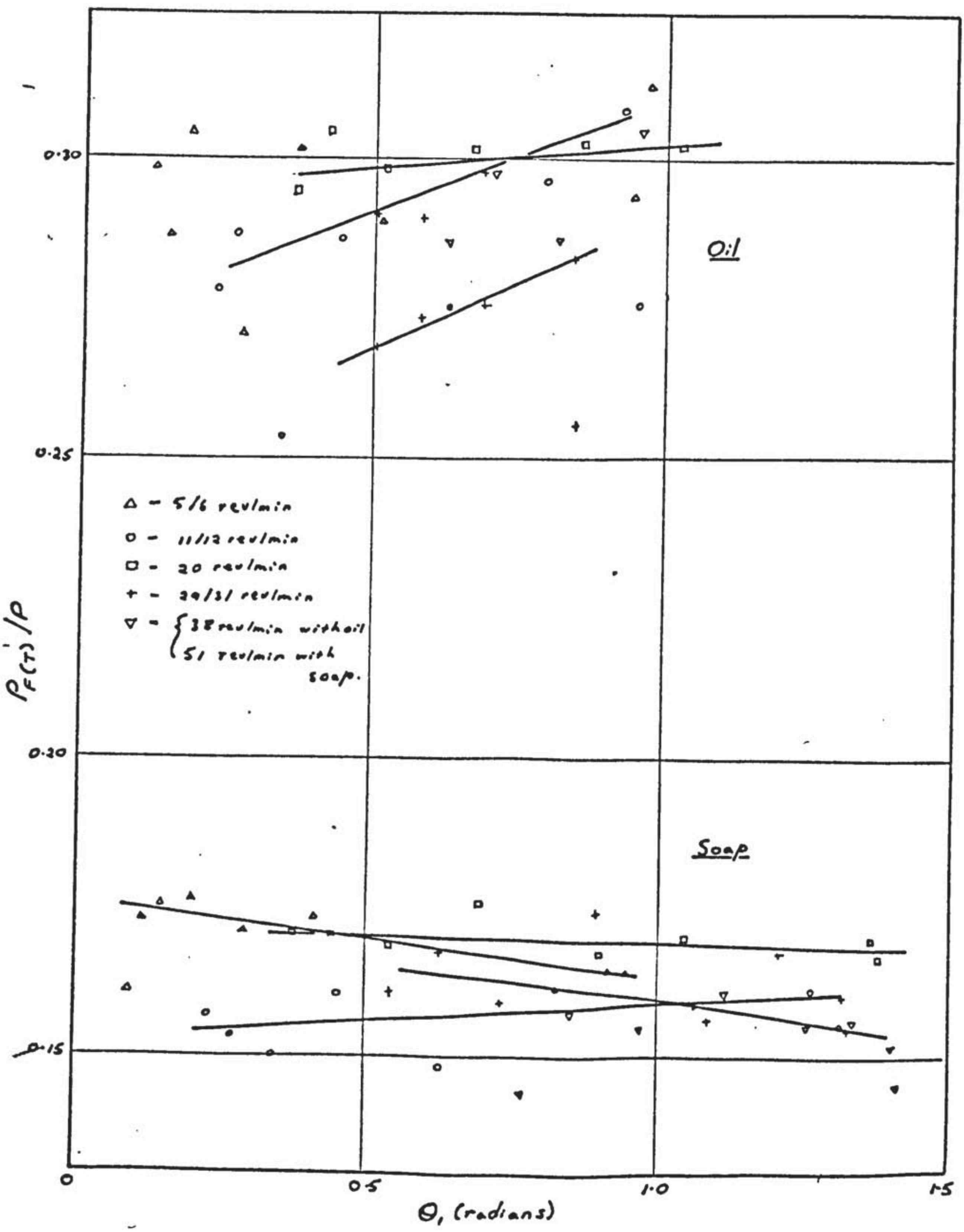

Fig. 10.46 - Component of Drawing Force due to Friction.
Calculated from Torque measurements,
assuming n=1

Bar Size: $1\frac{5}{16}$ in

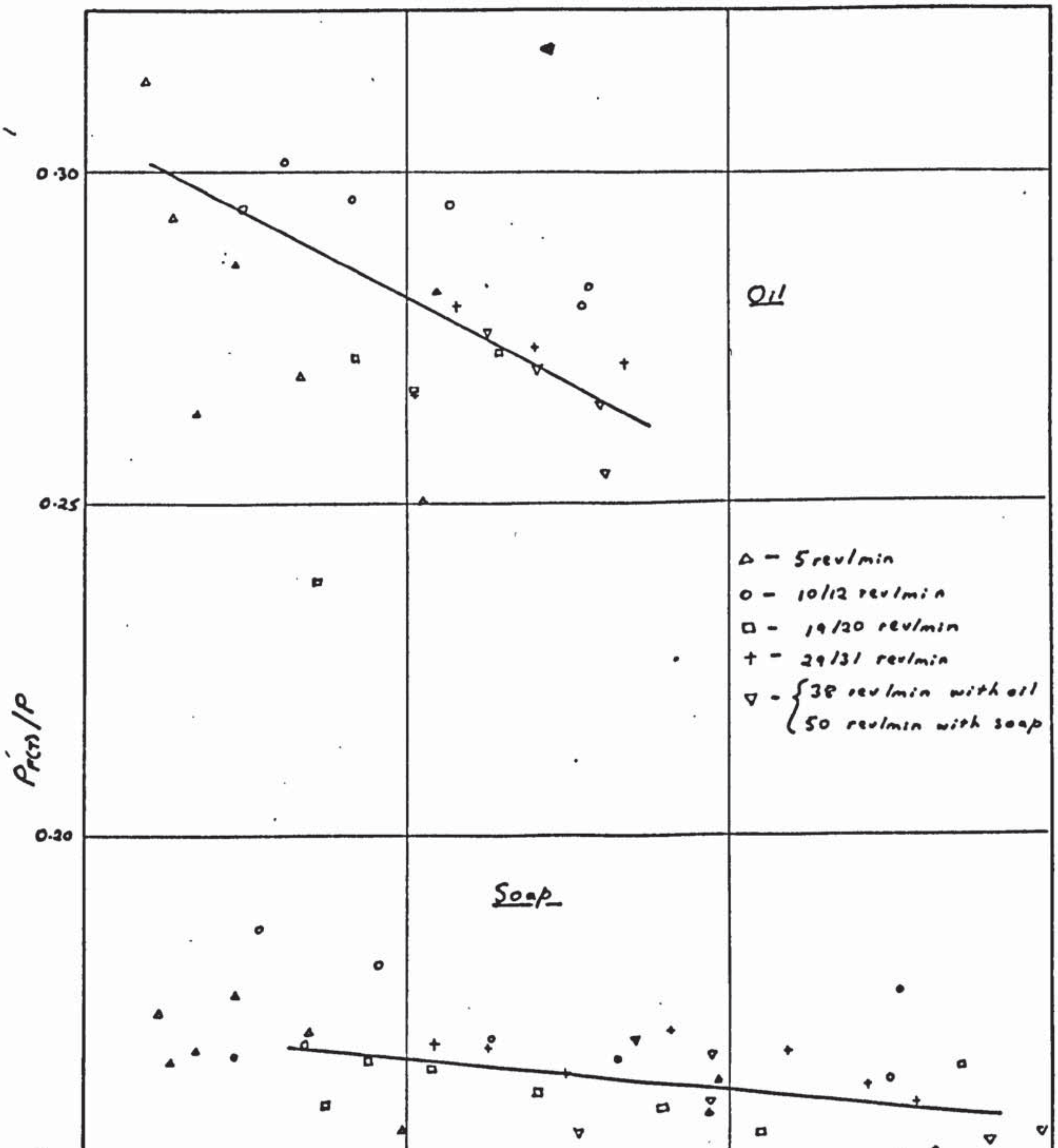

Fig. 10.47 - Component of Drawing Force due to Friction.
Calculated from Reduction in Drawing Force,
assuming n=1.

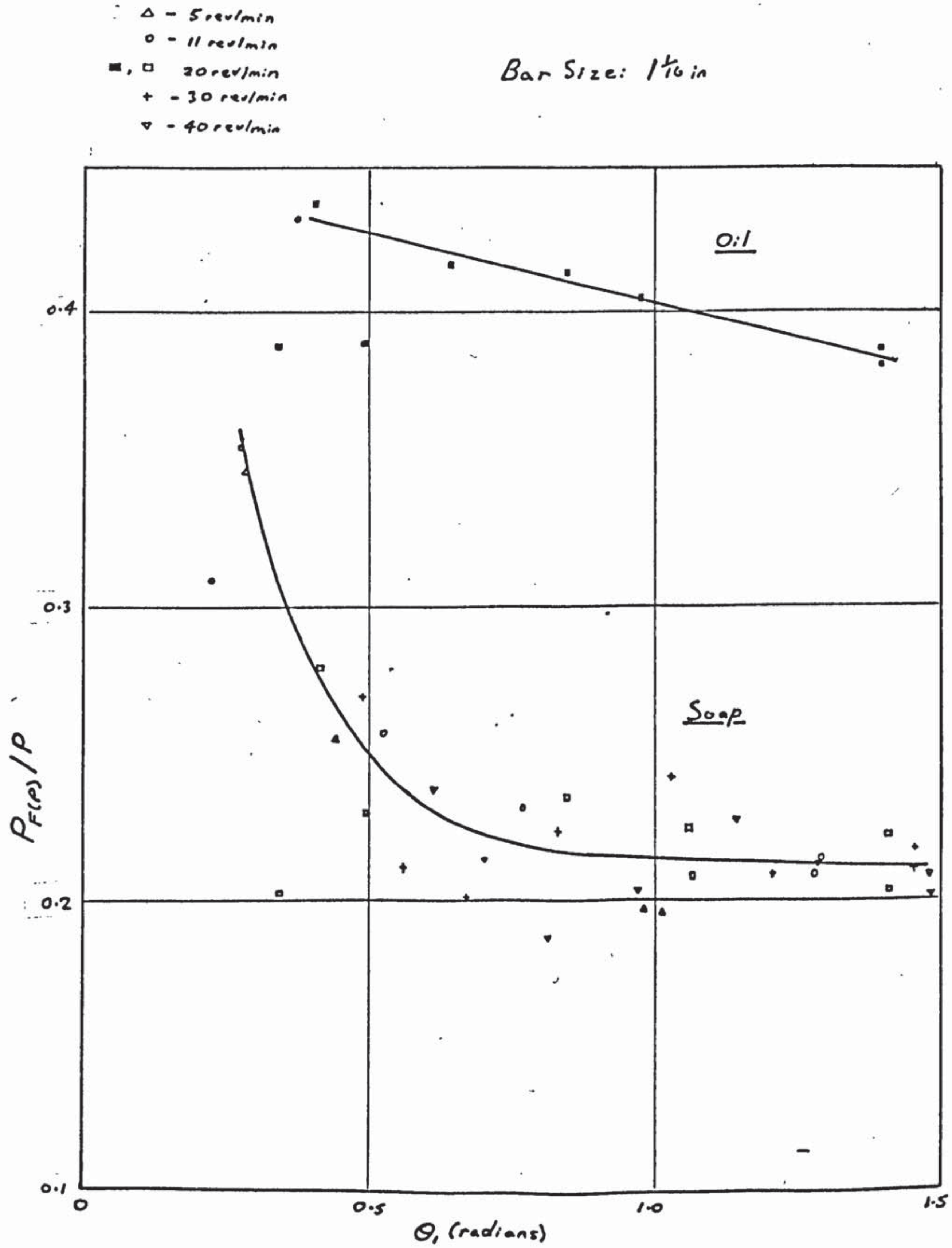

Fig. 10.48 - Component of Drawing Force due Friction.
Calculated from Reduction in Drawing Force,
assuming n=1.

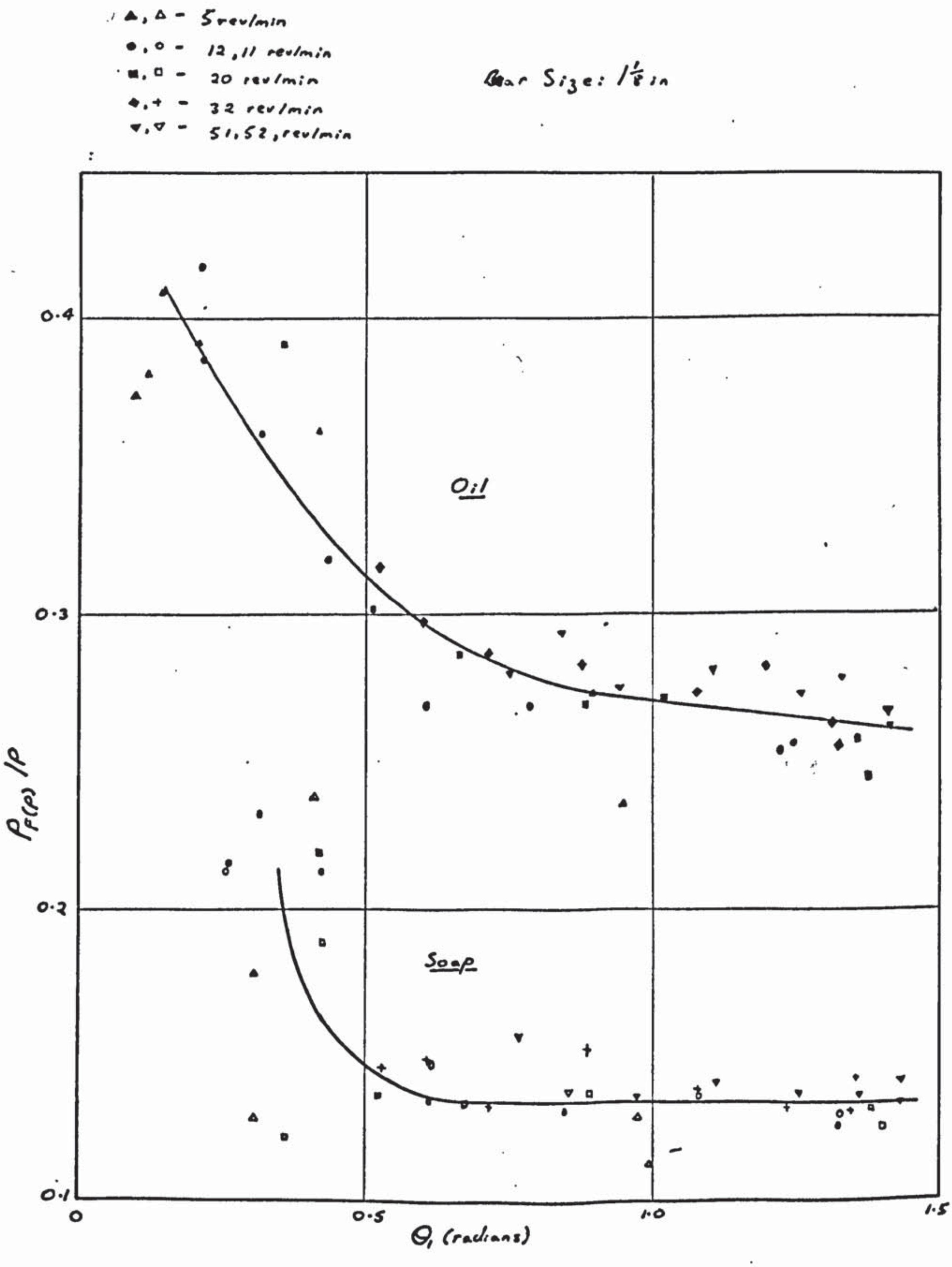

Fig. 10.49 - Component of Drawing Force due to Friction.
Calculated from Reduction in Drawing Force,
assuming n=1

▲, △ - 5 rev/min
●, ○ - 11 rev/min
■, □ - 20 rev/min
◆, + - 31, 32 rev/min
▼, ▽ - 50, 52 rev/min

Bar Size: $1\frac{3}{16}$ in

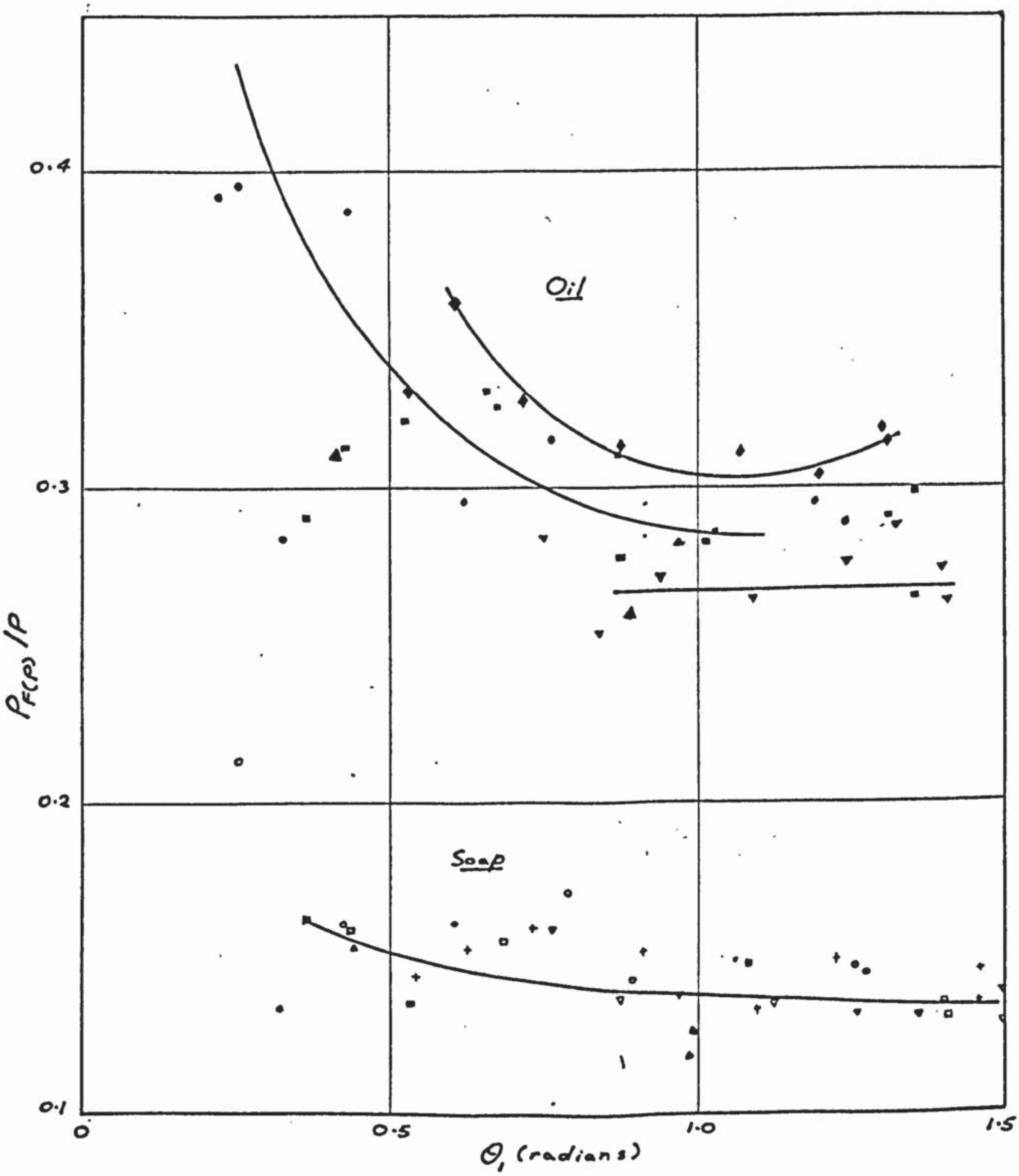

Fig. 10.50 - Component of Drawing Force due to Friction. Calculated from Reduction in Drawing Force, assuming n=1.

Bar size: $1\frac{1}{4}$ in

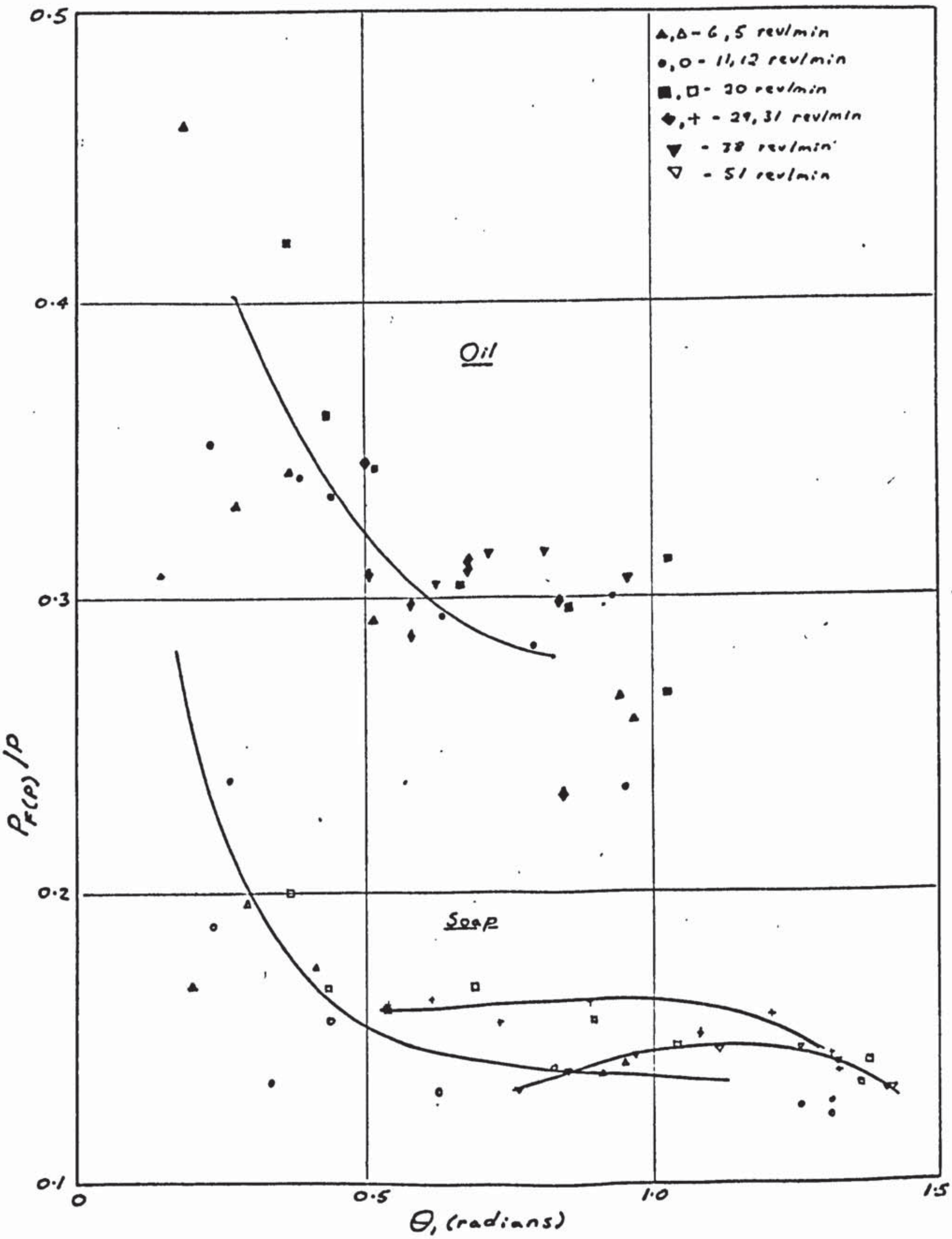

Fig. 10.51 - Component of Drawing Force due to Friction.
Calculated from Reduction in Drawing Force,
assuming n=1.

Bar size: 1 5/16 in

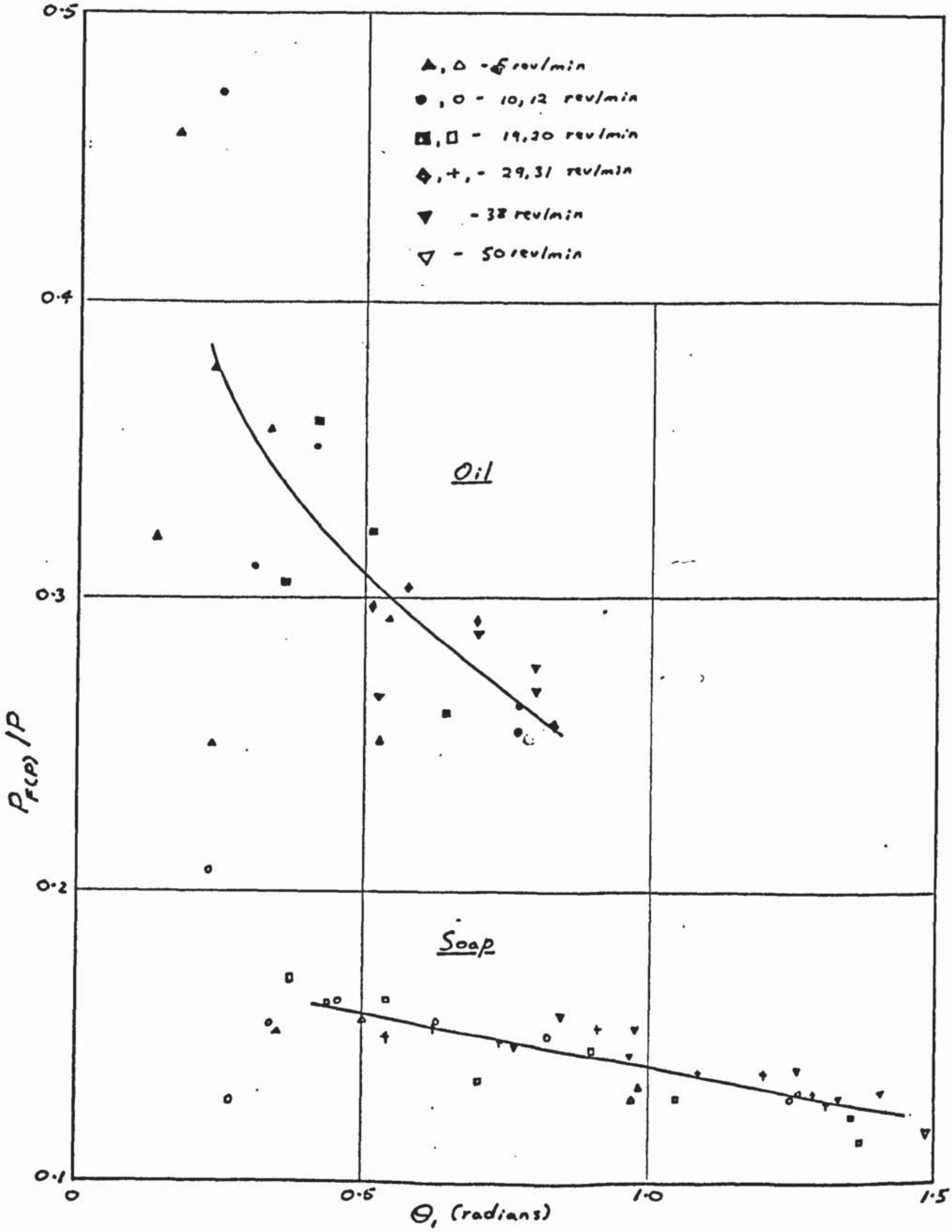

Fig. 10.52 - Error in Calculated Values of $P_{F(P)}$, Caused by Incorrectly Chosen Value of 'n'. Assuming that n=1 is correct.

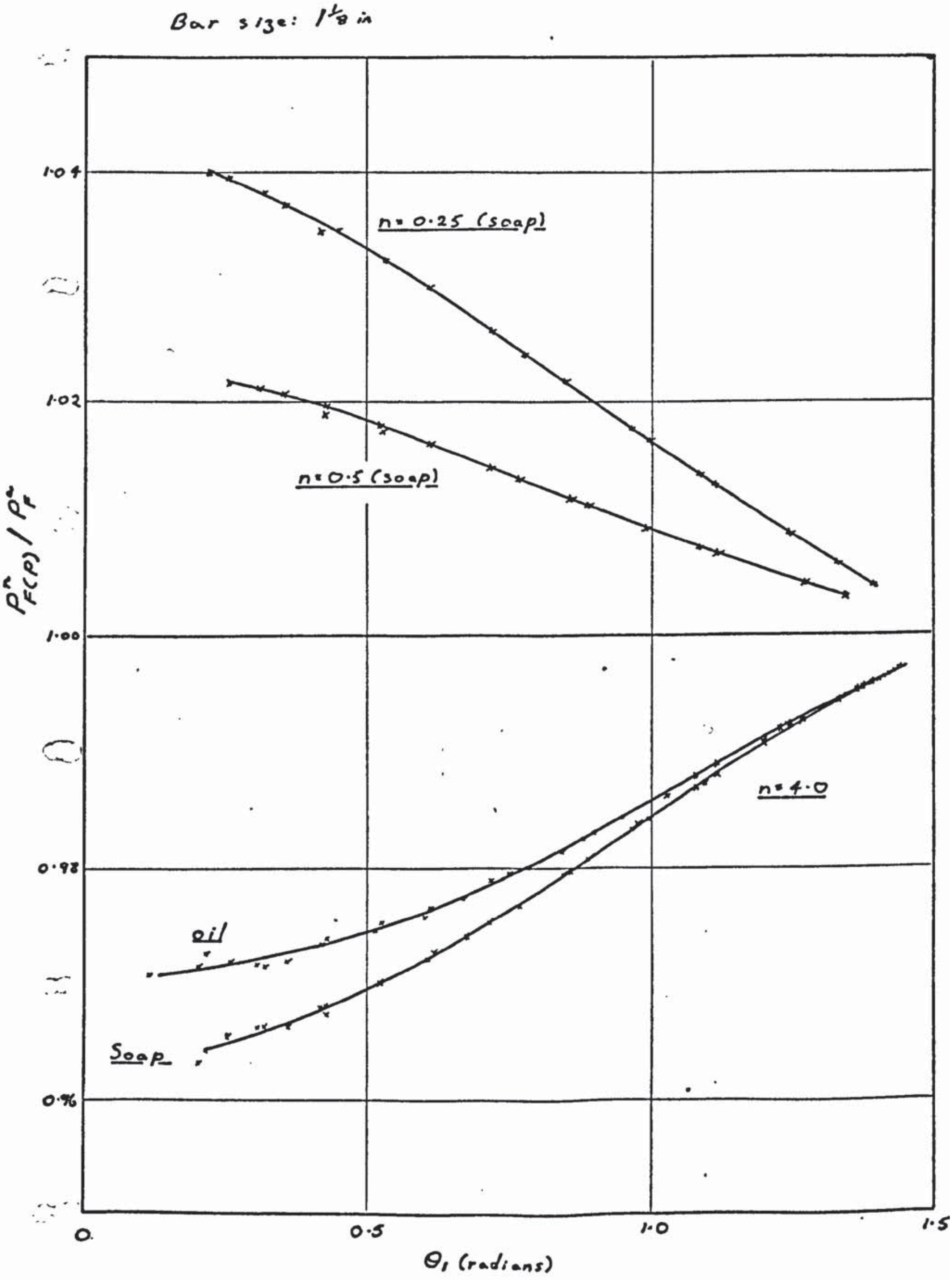

Fig. 10.53 - Error in Calculated Values of $\rho_{F(T)}$, caused by incorrectly chosen values of 'n'; assuming that n=1 is correct.

Bar size: $1\frac{1}{8}$ in

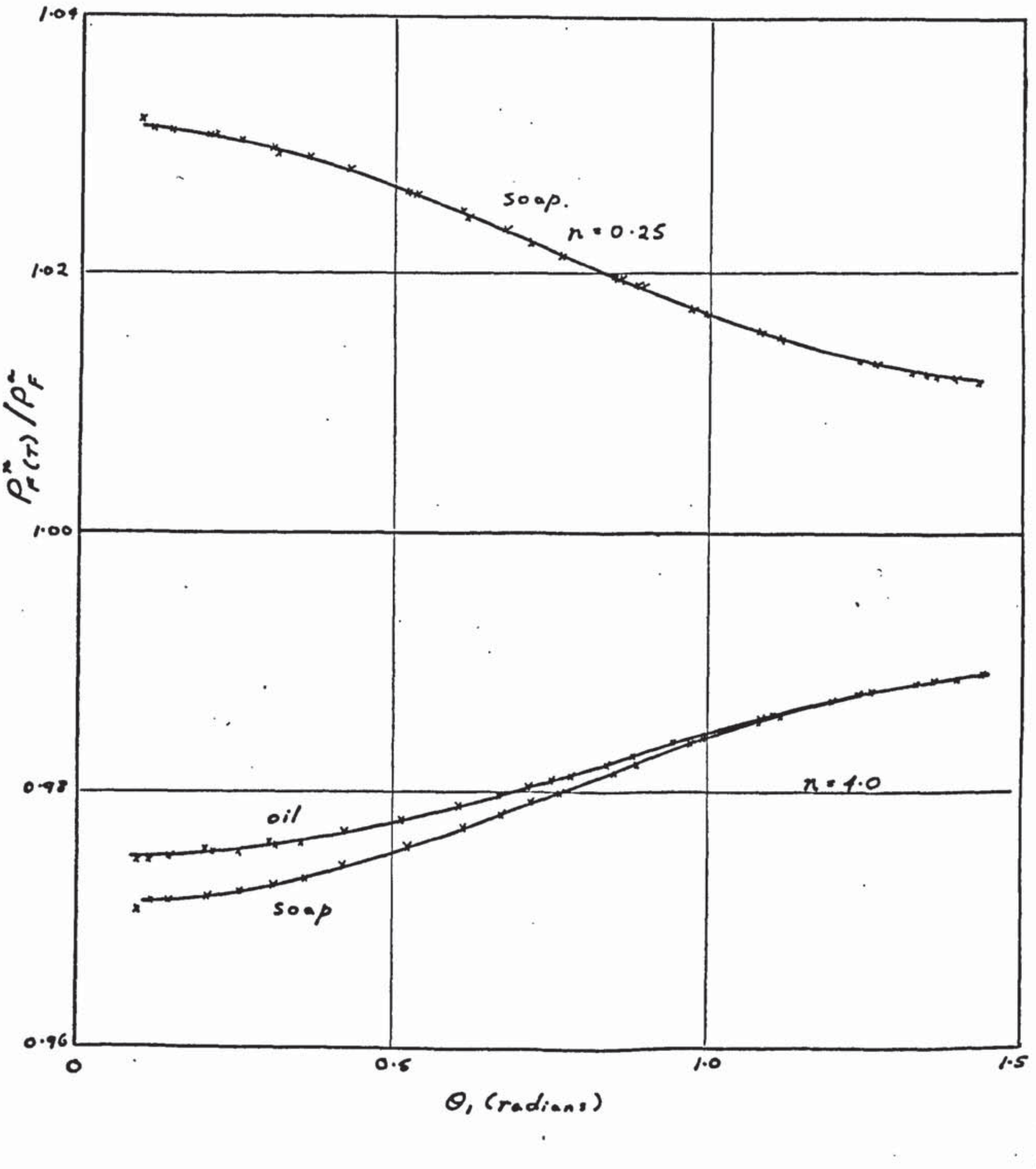

Fig. 10.54 - Error in Calculated Values of $P_{F(P)}$, caused by incorrectly chosen value of 'n', assuming that n=1 is correct.

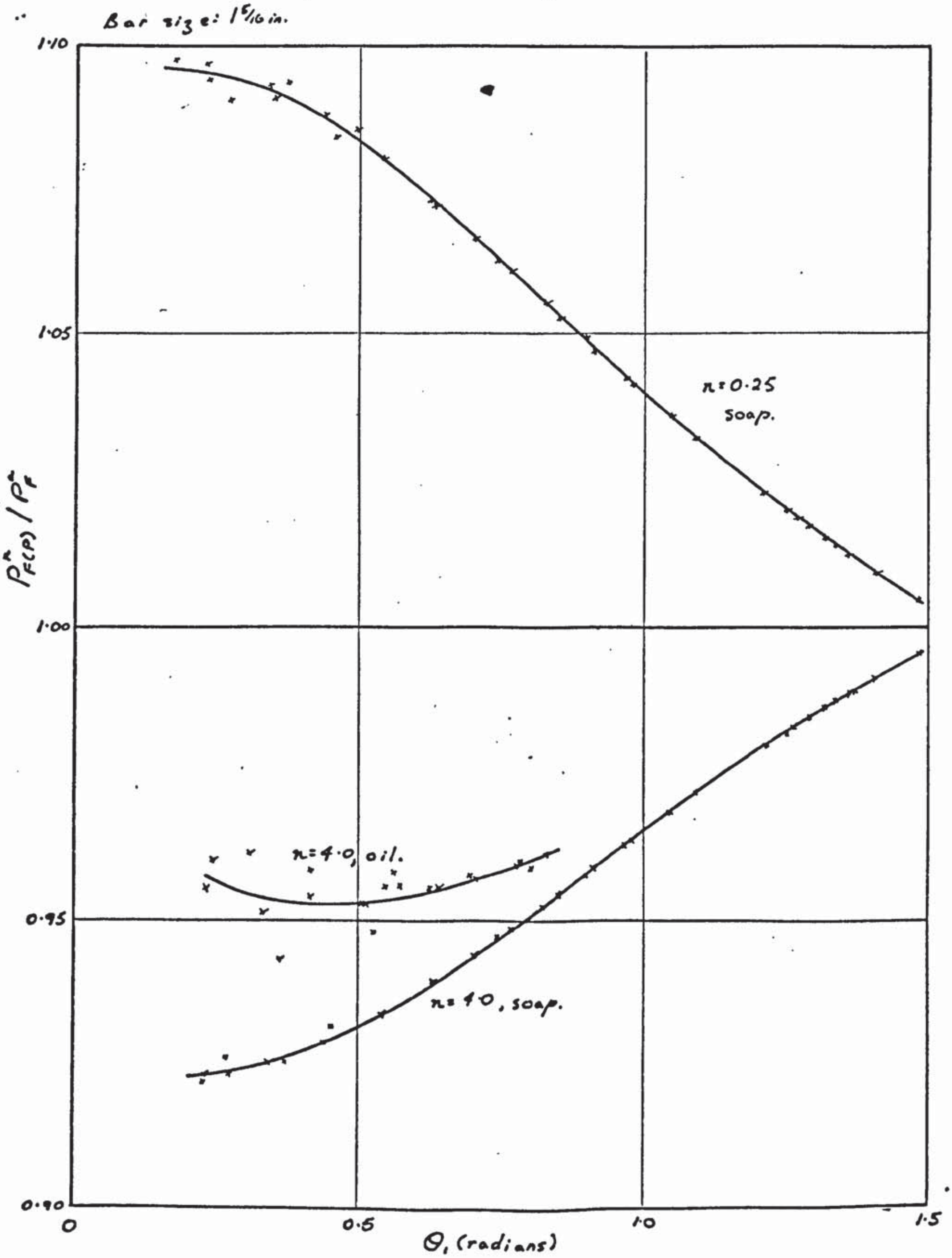

Fig. 10.55.- Error in Calculated Value of $P_{F(T)}$, caused by incorrectly chosen values of 'n', assuming that n=1 is correct.

Bar size: 1 5/16 in

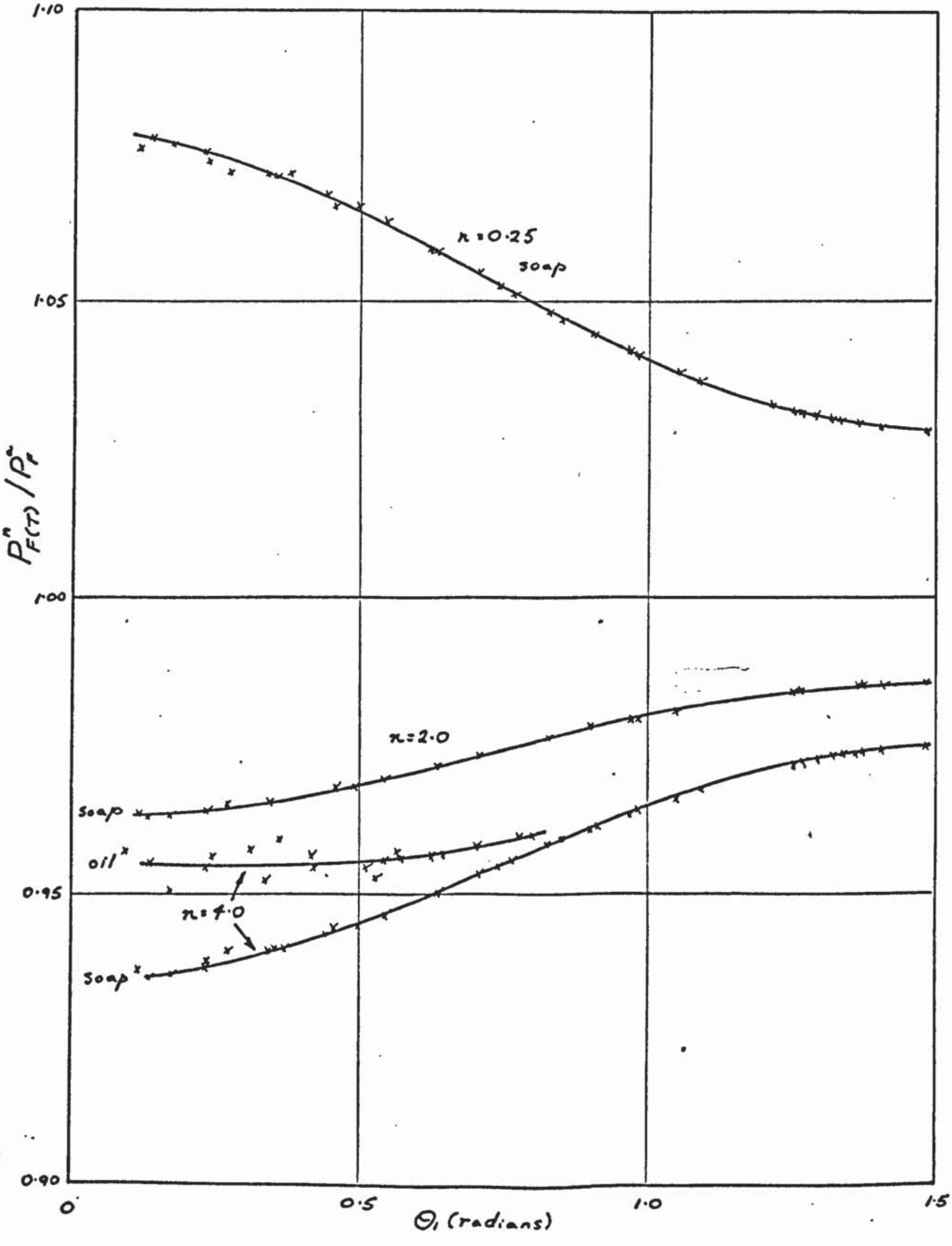

Fig. 10.56 - Values of Necking-Correction Factor obtained in Tensile Tests

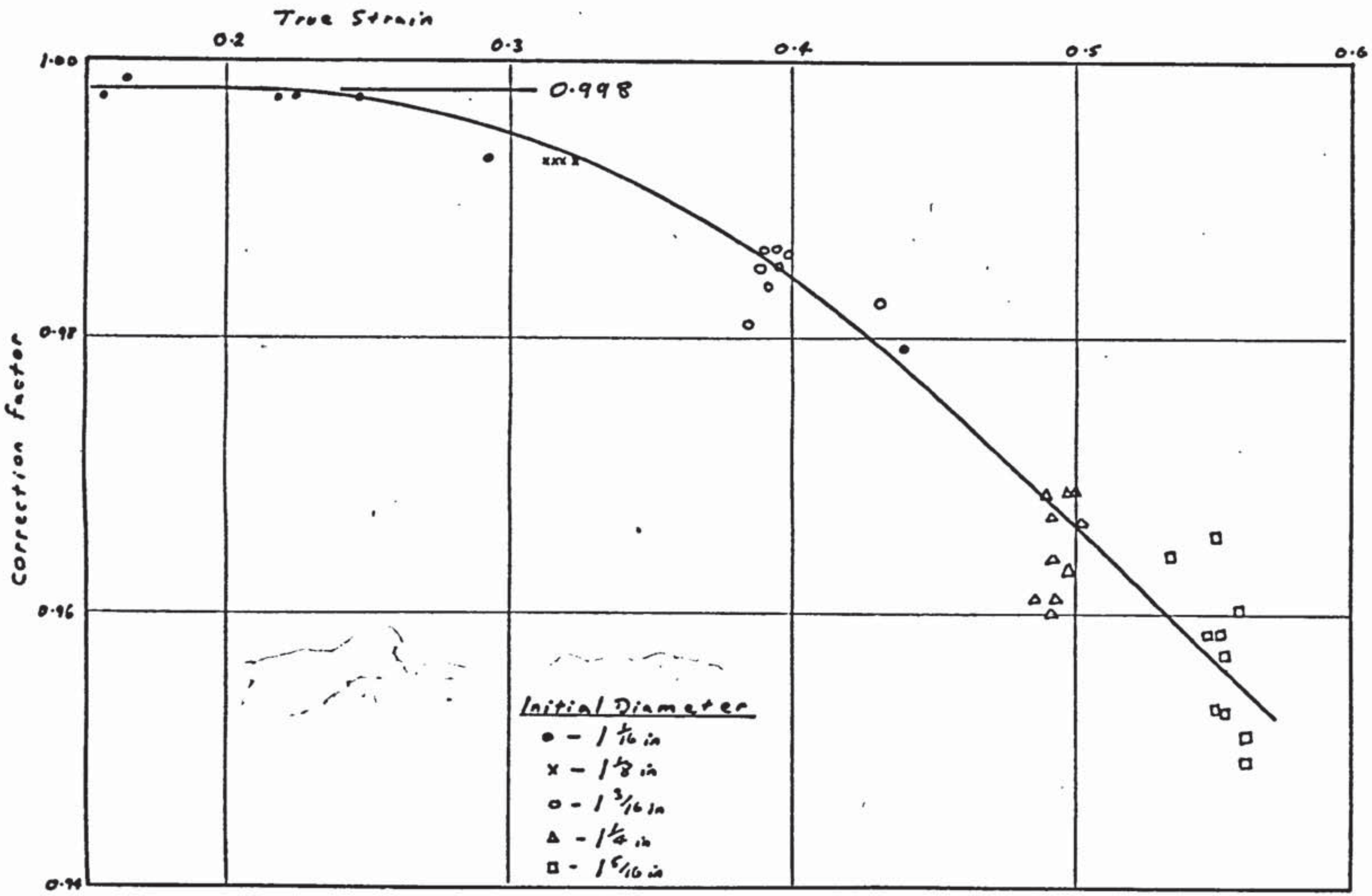

11. CONCLUSIONS

(1) The method which was proposed for this determination was theoretically sound, but required a very high degree of repeatability of experimental conditions and of accuracy of measurement for its successful application.

It was not possible to determine the distribution from the results obtained in this investigation, partly because the repeatability criterion was not sufficiently well satisfied, and partly because the shear stress itself appeared to be slightly dependent on the speed parameters.

It now seems unlikely that the method could ever be used to reliably determine the distribution of shear stress, but it is possible that this author is unable to be completely objective on this point.*

(2) The assumption of an arbitrary distribution of shear stress did not introduce significant error into the calculated values of friction force at the surface of the die, and the analysis for the determination of distribution of shear stress could therefore be modified to give reliable values of coefficient of friction, without knowledge of the correct distribution of shear stress.

(3) Although not previously recognised in the literature of the rotating-die technique, rotation of the drawing die produced a helical twist in the drawn bar, and caused the undrawn end of the workpiece to rotate at speeds of up to 30% of the speed of the die. Failure to include this feature in the analysis could have led to significant errors in tests where the angular swing of the friction vector was small.

The velocity towards the apex of the die increased linearly with axial displacement through the die, and there was no discontinuity at the inlet. There was an abrupt increase in velocity where the workpiece left the die.

Error arising from uncertainty as to the variation of angular swing of the friction vector, from point to point through the die, was negligible in this investigation.

(4) Evaluation of coefficient of friction from measurements of torque was always to be preferred to evaluation from reduction in drawing force. This was so fundamental that values obtained from the latter source could be regarded as superfluous.

(5) The use of a drawbench of relatively low stiffness caused some transient behaviour at the start of the die-rotation, which was difficult to explain but did not lead to significant error.

---

*N.B. - see also APPENDIX 8

(6) The coefficient of friction for the tests using soap lubricant was 0.020 to 0.025 for reductions of area of 21% up to 42%, and corresponding values for the tests using oil were 0.040 to 0.060. Values for the 10% reduction of area were 0.030 to 0.035 for soap, and 0.065 to 0.075 for oil, but these values are not regarded as being reliable. The spread of values was narrow by conventional standards for studies of friction, indicating firstly that in spite of conclusion no.(1) test conditions were good, and secondly that the rotating-die technique is an experimentally precise one.

The values of coefficient of friction which were obtained here compare well with accepted values. They are at the low ends of the ranges, and this reflects careful surface preparation for the tests using soap, and the presence of the phosphate coat for the tests using oil.

Values for the range of reductions of area of 29% to 42%, support the commonly held view that coefficient of friction is independent of reduction. Values obtained at 21% reduction are also in agreement, but these values are not directly comparable because the material for those tests had a much rougher surface.

(7) Although the simple Sachs type of analysis for the rotating-die technique is theoretically unsound, it gave results which were of adequate accuracy over most of the range of experimental parameters. The major source of error with that analysis was its failure to recognise the plastic torsion of the workpiece which was observed.

(8) Rotation of the drawing die had no significant effect on measured values of surface finish.

12. SUGGESTIONS FOR FURTHER WORK *

12.1 FURTHER INTERPRETATION OF THE RESULTS PRESENTED HERE

(1) The inclusion of the stress-strain data described in section 10.8 makes it possible to fulfil one of the original objects of the investigation, that of checking the theories of drawing. In addition to a straightforward comparison of experimental and theoretical values of drawing force, values of die-pressure and redundant work factors could be easily calculated.

(2) It would be useful to express the correlation between results obtained with the approximate and exact solutions more succinctly than has been done here. One obvious method would be to plot the ratio of the two values against θ_1.

As the largest source of error with the approximate solution was its failure to allow for the rotation of the undrawn end of the bar, there is a good chance that a very simple correction would significantly improve the accuracy. An obvious method for doing this would be to subtract the bar speed corresponding to the location of the resultant cross-section from the speed of the die.

(3) The problems raised by the rotation of the free end of the bar have been discussed in section 10.7.2, and it could greatly simplify the exact solution if an analytical derivation of R_B in terms of the independent parameters could be obtained. This would also clarify some of the odd features described in section 10.7.2 and 10.7.4. The linear relationship which was observed to exist between R_B and T also suggests that such a derivation might make it possible to determine μ independently of measurements of torque or drawing force.

A possible method of obtaining a solution for R_B would be to use a minimum energy hypothesis. Thus, the faster the bar rotates the less the work that is done in rotating the die; but the reduction in drawing force is then smaller, and the direct work becomes greater. Similarly, at low speeds of bar rotation the reduction in drawing force is maximised, but so is the rotational work. It may be postulated that the rotational speed of the bar will be such as to minimise the total expenditure of energy, and it should then be possible to deduce R_B in terms of μ or of P_F/P.

12.2 NEW INVESTIGATIONS

(1) It is unfortunate that the tests at the two smallest reductions of area were not directly comparable with the larger sizes, particularly so in view of the significantly higher values of μ which were obtained at 10%. This is

* N.B.- see also APPENDIX 8

in a region where redundant deformation is regarded as being significant, and an increase in μ in that range could obviously have some importance for evaluations which are based on the assumption that μ is independent of reduction. It would therefore seem to be desirable to check this feature.

(2) For any fundamentally new investigations using the rotating-die technique, it would seem preferable to constrain the undrawn end of the bar so that it could not rotate. The possibility of doing this was considered briefly in the course of this investigation, and it was apparent that to do so in an experimentally viable manner would have presented a substantial design problem. The main source of difficulty would have been the length and non-linearity of the test material, but this could have been overcome.

Some advantages of adopting this procedure have been mentioned in section 10.7.2, and it may be further noted that potentially interesting measurements could be made by abruptly freeing the undrawn bar, and noting the accompanying changes in measured parameters. It is to be expected that the jump in drawing speed when this is done would be considerably less than the main transient at the start of die-rotation, and it may therefore be possible to separate the effect of the onset of rotation of the bar.

(3) It may be noted, with regard to the speed transient, that the 'soft' type of machine which was used in this investigation was unsuitable in principle. However, if the suggestion that the torque transient resulted from the speed transient be accepted as correct, then little practical difficulty would result from continued use of the drawbench.

(4) In its existing form the equipment could be used to derive data relating to a range of lubricants and materials. This might normally be considered as being outside the scope of academic research, but it could be done so easily and directly that it would seem to be worth doing before the equipment is broken down or converted.

(5) It is suggested that for any future investigation of friction, close attention be paid to the external uniformity of the test material. This would probably mean relaxing the requirement for uniformity of material composition and processing, but variations within a particular material specification should be unimportant, as the analysis allows for variations in non-rotational drawing force.

(6) Discussions with people involved in the industry have given this author the impression that, in the manufacture of bar, the drawing process tends to be used mostly as a finishing operation. This is not true of the manufacture of tube, where multiple passes over large reductions of area are common. The

greater industrial importance of tube-drawing was always recognised, but solid bar was selcted in the first instance to ease the experimental problems involved in developing the technique, and to check the theories of drawing.

The existing equipment could be used directly to investigate friction in tube-sinking, although it might in that case be thought desirable to increase the drawn diameter. For plug-bar drawing there is a variety of possibilities. Friction at the die/tube interface could again be determined readily, it being necessary only to add the plug-bar to the drawbench. The rotation of the undrawn part of the tube, which would be expected to accompany die-rotation, might be sufficient to allow friction at the plug/tube interface to be determined without provision of a drive to the plug-bar. Provision of such a drive would involve major modifications to the equipment, but it might be possible simply to split the existing drive. Clearly, a variety of combinations of experimental conditions would be possible if such a drive were to be installed, the basic conditions being, fixed, driven, freely rotated, and contra-rotated. The implications of these has not been considered.

(7) Drawing of solid section is of basic importance in the wire-drawing industry, and although there is a noted dearth of knowledge of the effect of high drawing speeds on the coefficient of friction, there appears to be no fundamental objection to using the rotating-die technique at high drawing speeds. Analysis from measurements of reduction in drawing force would probably become impracticable, but this would be no detriment to the technique.

13. ACKNOWLEDGEMENTS

The author's thanks are due primarily and principally to Dr. D.H. Sansome, for his close interest and support throughout this investigation.

It would be invidious to select among the many research associates, both inside and outside the Department, who showed interest and discussed the various problems which arose, except for Mr. R.M. Spiers and Mr. G.R. Dawson who were the author's closest colleagues during the early and late stages of the research, and Dr. O.K. Jones who wrote the original computer programme from which that given in Appendix 5 was developed.

The equipment aspects made considerable demands on the technical staff of the Department. In particular the author would like to thank Mr. E. Denchfield, Mr. J. Hirons, Mr. H. Pratt, and Mr. G.M. Jones, whose help was always available when most needed, and Mr. A. Evitts who produced the photographs which appear here.

The staff of the Metrology Laboratory of the Production Engineering Department were unfailingly helpful throughout the metrological aspects of the work.

Outside the University, Mr. J. Paul of Southern Instruments Limited co-operated closely during the considerable problems which were encountered with the recording equipment, and Mr. B. Cope of Phoenix Steel Tube Company arranged for the treatment of the material used in Series II.

With regard to final production of the thesis, the author is indebted to Mrs. W. Croft for her considerable effort in typing from the manuscript at very short notice, to Miss C. Clarke for proof-reading and logistical support in the final stages, and to Mr. S. Birchall and the Special Publishing Services Section of the Aviation Division of Smiths Industries Limited, for help with aspects of the reproduction.

APPENDIX 1 - DETAILS OF EQUIPMENT *

1) HYDRAULIC DRAWBENCH

Manufacturers	:	Brookes (Oldbury) Ltd.
Primary drive	:	40 H.P., 1440 rev/min.
Hydraulic Delivery	:	25.2 gallons/min. at 1440 rev/min. and 100 lbf/in^2.
Nominal speed range	:	0 to 15 ft/min.
Stroke	:	54 in.
Maximum working pressure	:	2,000 lbf/in^2, giving 30 tonf. drawing force.

2) ROTARY DRIVE

The components are listed in sequence from the power input end (see Figure 5.1).

i) 5 H.P. induction motor, 1430 rev/min.

ii) Disc-type flexible coupling, Fenner size no. 5¼.

iii) Carter hydraulic infinitely variable speed gear, size 3A 5 H.P.

iv) Crofts type 4½ 'RO' friction clutch coupling. Maximum start-up power, 10 H.P. at 1400 rev/min.

v) Crofts no. 5 CFRT Ritespeed reduction gearbox. Ratio 20·7:1 Input shaft 3.1/8 in. longer than standard.

vi) Duplex chain sprocket, 21 tooth. Renold no. 213621

vii) Duplex chain, ¾ in. pitch x 58 pitches. Renold no. 114066.

3) THRUST BLOCK

Power Input	:	Triplex chain sprocket, 25 tooth, Renold no. 21367. One row of teeth has been machined off.
Main thrust bearing	:	Timken taper-roller bearings, no. 98400/98788
Secondary thrust bearing	:	Timken taper-roller bearing, no. 495/493.

* This appendix is intended to supplement the descriptions already given in the main body of the thesis. Information which has already been given, or which is readily available from manufacturers literature, has not been repeated here.

3) THRUST BLOCK Continued

Bearing preload	:	0.001/003 in.
Lubrication	:	Shell Alvania Grease EP2 for the bearings. Mineral oil, S.A.E. 30, for the chain. Fill the reservoir to 3.15/32 in. above the bed of the drawbench.

4) SPEED TRANSDUCERS

Rotational Speed	:	Smiths type G.D.C. 1 tachogenerator Serial No. E1965. Nominal output 25 volts D.C./1,000 rev/min., armature resistance 39 ohms, maximum load current 100 milliamps.
Drawing Speed	:	Sperry Mark 1 D.C. tachogenerator Serial no. L1982. Nominal output 20 volts/1,000 rev/min. armature resistance 300 ohms, maximum load current 4 milliamps. String tensioning weight 113 gm.

5) LOAD-CELL

Drawing Force Bridge	:	Saunders-Roe metal foil strain gauges, type '½ in. linear', gauge resistance 75 ohms. Two gauges per arm, bridge resistance 150 ohms. Strain in Active direction at 30 tonf.* = 1.07×10^{-3} Strain in 'Passive' direction at 30 tonf.* = 0.32×10^{-3}
Torque Bridge	:	Saunders-Roe metal foil strain gauges, type '1 in. torque', gauge resistance 25.85 ohms.

5) LOAD-CELL Continued

Torque Bridge : Two pairs of gauges per arm, bridge resistance 103.4 ohms.

Strain in Active directions at 500 lbf.ft* $= \pm 0.51 \times 10^{-3}$

Maximum Principal Strain at 500 lbf.ft. and 30 tonf.* $= 1.62 \times 10^{-3}$

Voltage Supply : Thorn Electronics stabilised power supply type VP21 3 - 30 volts D.C., 0 - 1 amp.

6) DATA-RECORDING

This was done with a Southern Instrument ten-channel, direct writing, ultra-violet, galvanometer recorder. The type and reference numbers of the galvanometers are given in Table A1.1, together with details of their operating positions within the recorder.

Parameter	Galvanometer	Channel	Datum Position+
Drawing Force	V1700	2	0.3 in.
Rotational Speed	MA129	4	3.6 in.
Drawing Velocity	V1688	6	3.7 in.
Torque	V1712	8	0.6 in.

+ Measured from left-hand side of chart.

TABLE A1.1

The galvanometers were calibrated using the circuits shown in Figure A1.1. These circuits were built into the instrumentation of the drawbench, and if they are used in the future, care should be taken not to connect the low resistance circuit to the V-type galvanometers. It is also necessary to reverse the polarity of the voltage supply when calibrating galvanometer V1688.

* Taking Young's Modulus as 13.5 tonf./in^2.

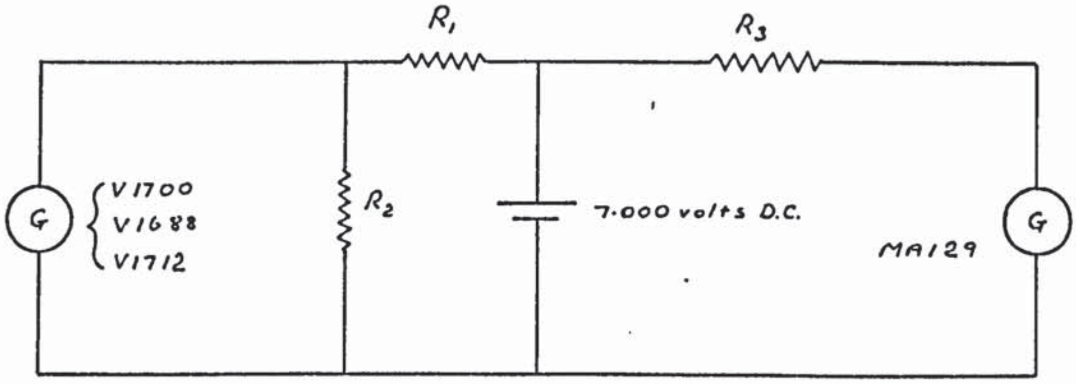

$(R_1 + R_2) = 224,500 \pm 200$ ohms (measured) $R_3 = 1,593 \cdot 3$ ohms (measured)

$R_1 = 4 \times 56$ Kilohms (nominal)

$R_2 = 250$ ohms (nominal)

Fig. A1.1 - Circuits for Calibration of Galvanometers

7) CALIBRATION METERS

Digital Voltmeters	:	i) Digital Measurements, type DM2001 Mk. 2
		ii) Solartron, type LM1420.2
Time/Counter	:	Advance Electronics, type TC4A.

8) DRAWING DIE

Two tungsten carbide dies, reference numbers 15048 and 15049 were obtained from Wire Drawing Dies (Manchester) Ltd., a subsidiary of Sir James Farmer Norton & Co. As explained in Section 8, only the former was used.

9) TESTING MACHINES

i) Torque Calibration	:	Avery 15,000 in. lbf. torque testing machine, type 6609 CHG, machine no. E55703/1
ii) Drawing Force Calibration	:	Denison 50 tonf. universal testing machine, model T42/B4 machine no. 25011.

9) TESTING MACHINES Continued

iii) Tensile and Compression
Tests on Full Diameter Bar : As above

iv) Tensile and Compression
Tests on Small Diameter
Specimens : Amsler 15 tonf. tensile testing
machine no. 8306.

v) Velocity Distribution Tests : Avery 30 tonf. universal testing
machine , type A806/1474
machine no. E4484/245

10) METROLOGICAL EQUIPMENT

i) Société Genevoise
D'Instruments De Physique
Universal Measuring
Machine MU-214B : used for measurement of die-profile
and for determination of
velocity distribution over bar/
die contact region

ii) Taylor-Hobson Talyrond
Model 1 : used for measurement of eccentricity
of drawing die

iii) Taylor-Hobson Talysurf
Model 3 : used for measurement of surface
finish of bar and of drawing die.

APPENDIX 2 – SPEED CONTROLS

A2.1 ROTATIONAL SPEED

The speed control knob of the Carter gear was fitted with a speed setting indicator, graduated in equal increments from 0 to 10. The relation between this setting and the rotational speed of the die, under no-load conditions, is given in Figure A2.1.

A2.2. DRAWING SPEEDS ABOVE 5 ft/min.

The drawing speed control knob of the drawbench carried a pointer over a scale graduated from 0 to 15 ft/min. Speeds above 5 ft/min. could be obtained by using this control, provided that the working load was sufficient to generate a pressure of greater than about 50 lbf/in^2 in the hydraulic system. The relationship between set speed and actual speed, at a working pressure of 500 lbf/in^2, is shown in Figure A2.2.

A2.3 DRAWING SPEEDS BELOW 5 ft/min.

The hydraulic system is illustrated in Figure A2.3. Speed control was effected by the flow control valve, which bled off a proportion of the fixed delivery of the pump, depending on what drawing speed was required. At low drawing speeds the valve would have been required to discharge the greater part of the pump delivery without appreciable pressure drop, and it appeared that it could not do this. Fundamentally the best solution would have been to have fitted a larger capacity flow control valve, or an additional one. However practical considerations made an alternative solution attractive.

It was realised that reduced speeds could be obtained by using the pressure relief valve to bypass some of the pump delivery. For this system to work it was necessary to have a large rate-sensitive load in the circuit, and this was already present, in the form of the needle valve which had been fitted in the oil return line from the ram (see Section 5.1). The flow-rate through this valve was directly proportional to the drawing speed, and it was first necessary to establish the pressure-drop/drawing-speed relationships for the valve at different settings. This was done very simply using the pressure relief valve, and the data are given in Table A7. . These relationships were not of direct interest, but were cross-plotted to give Figure A2.4.

In order to draw at speeds below 5 ft/min. the drawing force was first estimated, and the equivalent hydraulic pressure calculated. A throttle setting

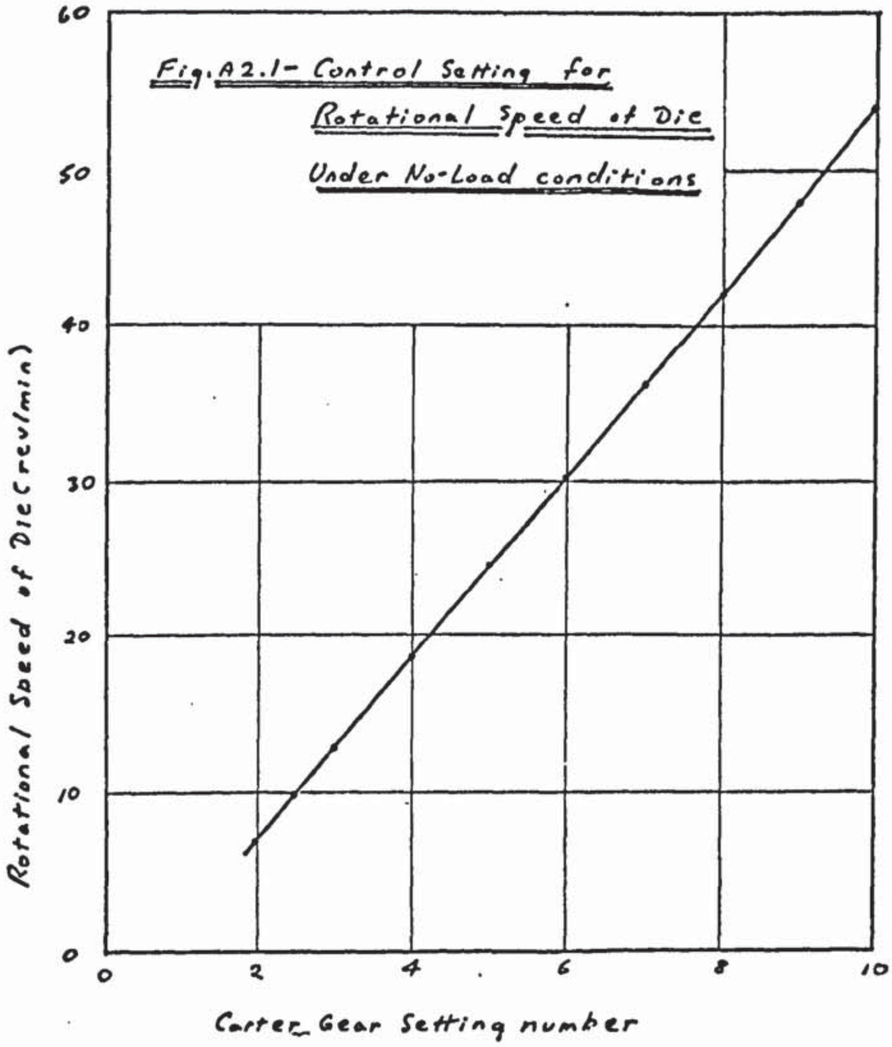
Fig. A2.1- Control Setting for
Rotational Speed of Die
Under No-Load conditions
Rotational Speed of Die (rev/min)
Carter Gear Setting number
0
10
20
30
40
50
60
0
2
4
6
8
10

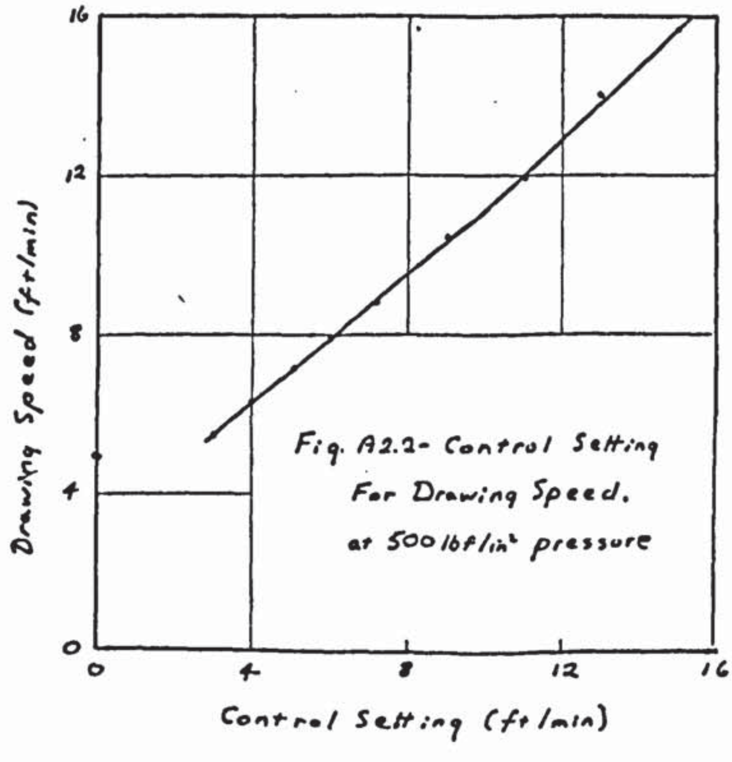
Fig. A2.2- Control Setting
For Drawing Speed.
at 500 lbf/in² pressure
Drawing Speed (ft/min)
Control Setting (ft/min)
0
4
8
12
16
0
4
8
12
16

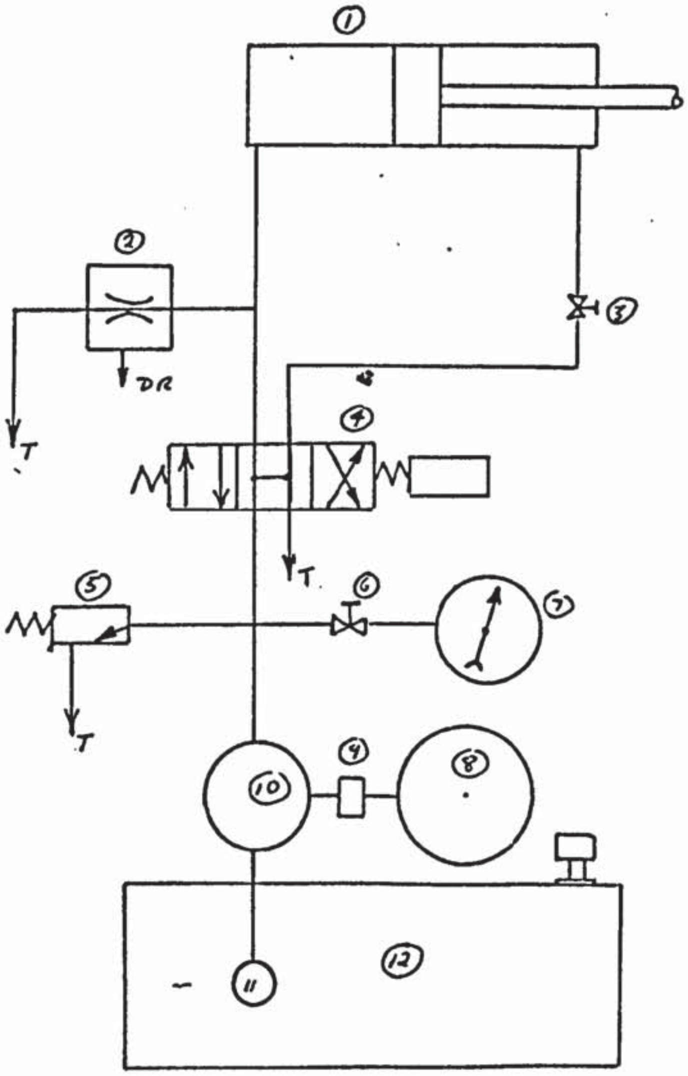

1 - Hydraulic Cylinder
2 Flow Control Valve
3 Needle Valve
4 Manual Forward/Reverse Valve
5 Relief Valve
6 Instrument Valve
7 Pressure Gauge

8 Electric Motor
9 Coupling
10 Pump
11 Oil Strainer
12 Tank Unit

T:- Tank Return
DR:- Drain

Maximum Working Pressure = 2,000 lbf/in²

Fig. A2.3- Hydraulic Circuit of Drawbench

Fig. A2.4 - Setting of Needle Valve Required to Produce a Given Pressure Drop, at Different Drawing Speeds.

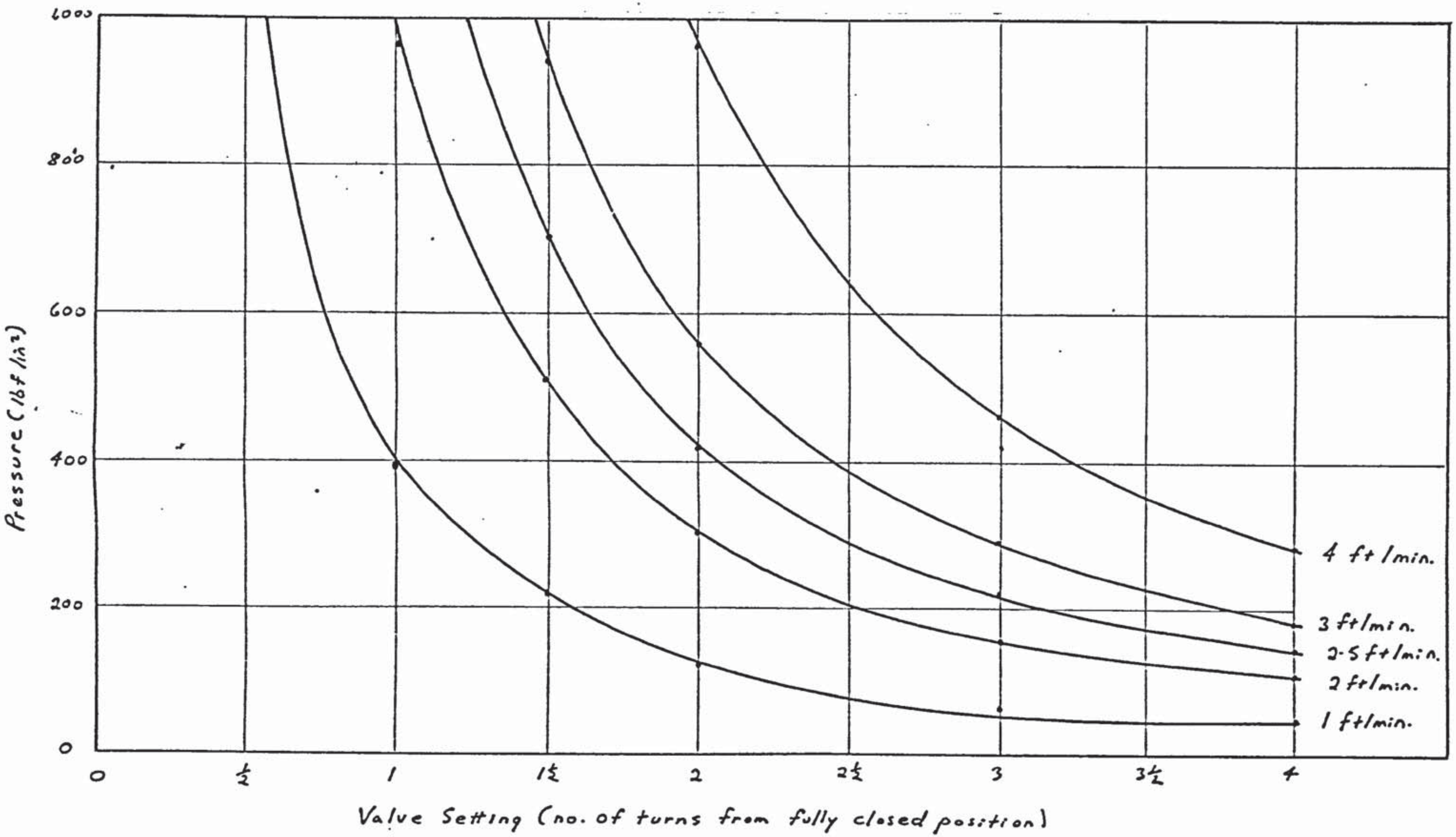

and pressure drop, corresponding to the required drawing speed, were then selected from Figure A2.4. The relief valve was then set to the sum of this pressure and the estimated drawing pressure, and the required drawing speed followed automatically. It will be apparent that an infinity of combinations of pressure drop and throttle setting could have been chosen from Figure A2.4. However, an increase in drawing speed would be expected when the drawing force decreased at the start of die rotation, and to minimise this change, the smallest practicable throttle openings were used. The limit on this optimisation was set by the maximum working pressure of the hydraulic system, and by the fact that at high pressures the relief valve would sometimes vent erratically. It was therefore found to be best to keep the relief pressure setting below 1,800 lbf/in^2. Apart from this the system worked very well indeed.

It is fundamental to the derivation and usage of Figure A2.4 that the conventional speed control knob should be at its minimum setting when operating at less than 5 ft/min.

APPENDIX 3 – EXPLANATION OF BAR AND TEST REFERENCE NUMBERS

Throughout this thesis, groups of bars have been referred to by their nominal diameter prior to being drawn, even where this differed significantly from the actual value (see Section 10.5). Each bar which was used in Series II has also been given an individual three part reference. The purpose of this is partly to facilitate cross-reference between data from the tension and compression tests with that from the drawing tests, and partly to indicate the grouping of tests.

The first part of the reference is a letter, S or O, which indicates which of soap or oil were used in the drawing tests done on that bar. The second symbol is a number, from 1 to 5, which indicates which group of nominal diameters the bar belonged to. The sequence was taken in ascending order, 1 corresponding to 1.1/16 in. and 5 to 1.5/16 in. nominal diameter. The last symbol is an arbitrarily chosen number, ranging from 1 to the number of bars in that group. It serves simply to distinguish the bar, and the associated data, and carries no implication of sequence. Thus bar number S3/2, was a 1.3/16 in. nominal diameter bar, on which some drawing tests using soap were performed, and which bore the number 2.

Each drawing test performed in Series II has also been given an individual number, ranging from 1 up to the total number of tests performed. These numbers were allotted in time sequence. As well as indicating the order in which tests were performed, they have been used to cross-reference different presentations of the results of the drawing tests.

The presentation of Series I results which has been adopted does not require any cross-reference, so although one was used during the experimental work, it has been omitted to avoid confusion.

APPENDIX 4* - ROTATION OF UNDRAWN BAR

A4.1 PLASTIC ROTATION

The problem was to deduce the rotational speed of the undrawn section of the bar from measurements of helix angle in the drawn section, and is illustrated in Figure A4.1. The bar is shown as approaching the die with longitudinal speed v and a steady rotational speed R_P. At exit, the longitudinal speed is V and the rotational speed is zero. Consider the longitudinal line PQ, where the length of the line is such that

$$PQ = vt$$

where t is the time taken for a particle to pass through the die. The angular position of points P and Q is denoted by Θ_P and Θ_Q, with the datum for these values being taken at the instant that P reaches the die. Conditions after an interval t are denoted by P', Q', Θ'_P, and Θ'_Q. The angular displacement, Θ'_P, suffered by point P need not be evaluated. The corresponding displacement of point Q is given by

$$\Theta'_Q = 2.\pi.tR_P$$

The positions of points P and Q after a further interal t are indicated by P" and Q". The distance moved by point P is given by

$$P'P'' = Vt$$

but the angular position is unchanged. The angular position of Q" is Θ''_Q, and by noting that the displacement suffered by Q as it traverses the die must be the same as that suffered by P when it traversed the die,

$$\Theta''_Q = \Theta'_P + \Theta'_Q$$

Thus the angular position of Q" relative to P" is simply Θ'_Q, and, considering a plane development of the surface, the distance between P' and Q" is given by

$$P'Q'' = \frac{d_1 \Theta'_Q}{2}$$

---

* Some of the symbols used in this appendix do not conform to the system prevailing in the rest of the thesis. These symbols are defined as they are introduced.

The helix angle, ϕ , may now be described.

$$\tan \phi = \frac{P'Q''}{P'P''} = \frac{\pi}{V} \cdot d_1 R_P$$

Transposing, and modifying for the system of units used in the body of the thesis,

$$R_P = \frac{12}{\pi d_1} V.\tan \phi \text{ (rev/min)}$$

A4.2 ELASTIC ROTATION

The undrawn end of the bar also had a component of rotational speed, R_E, caused by the increasing length of drawn bar under *elastic torsion*. The resulting angular displacement of the free end, θ , during an interval t, is given in terms of the change in length l of the drawn section, by

$$\frac{T}{J} = \frac{C\theta}{l} \quad \text{where } J = \text{polar moment of area and } C = \text{shear modulus.}$$

Expressing l in terms of the drawing speed,

$$\frac{\theta}{t} = \frac{TV}{CJ}$$

But θ may also be determined from the required rotational speed thus

$$\theta = 2\pi R_E t$$

Taking the units of C as lbf/in^2, this leads to

$$R_E = \frac{192TV}{\pi^2 C d_1^4} \text{ (rev/min)}$$

A4.3 COMBINED ROTATION

Although the magnitude of R_E is easily calculated, the nature of the correction which should be made for it is not obvious. However, it is known that the bar can have no rotational speed as it leaves the die, and also that a cross-section of the bar undergoes continuously increasing torque as it passes through the die. It therefore seemed reasonable to assume a linear variation between R_E at entry and zero at exit. This is the same form as was assumed for R_B in section 3.2, and leads to

$$\underline{\underline{R_B = R_P + R_E}}$$

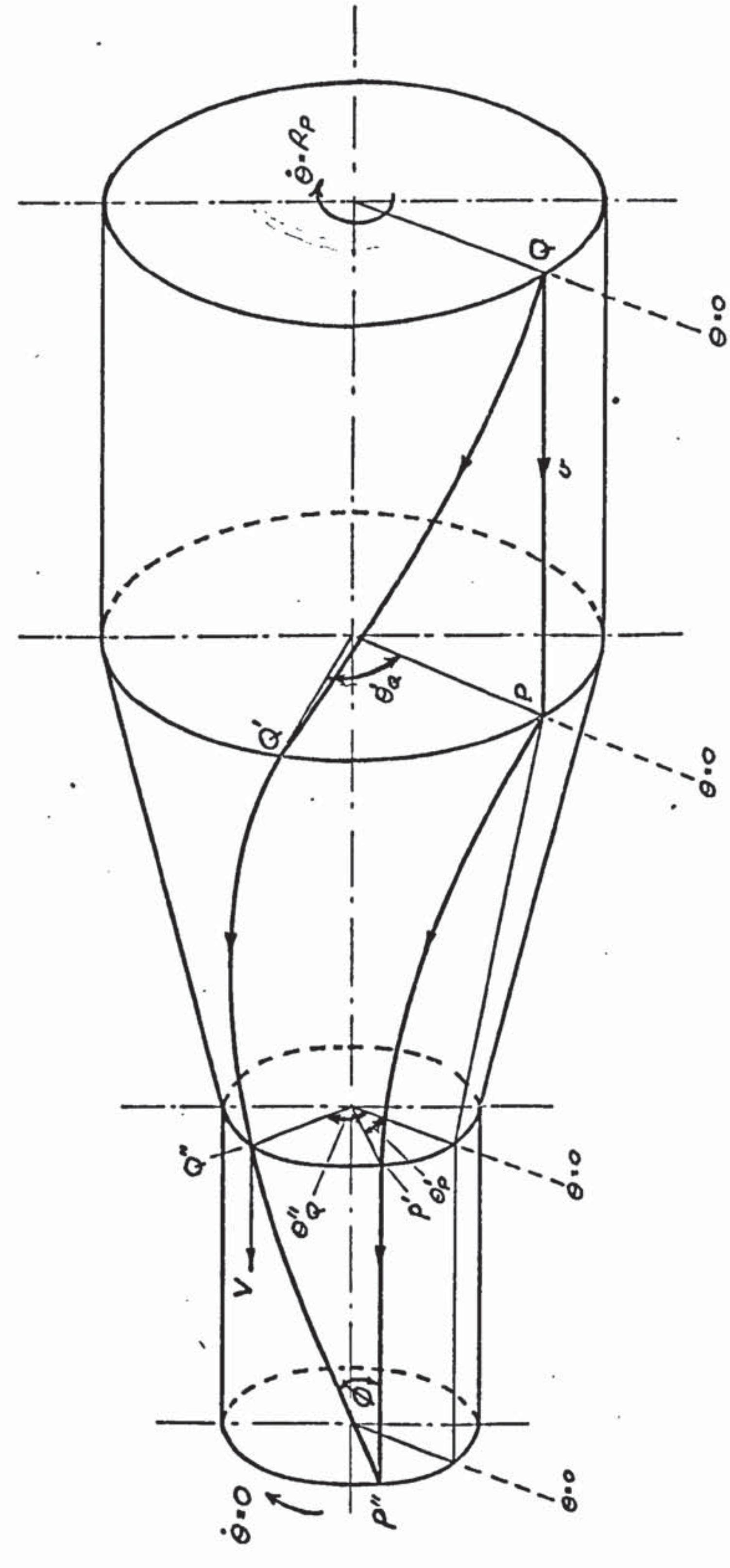

Fig. A4.1- Trajectories of Particles at the Surface of the Bar, as they Traverse the Die.

APPENDIX 5 - COMPUTER PROGRAMME *

The programme which was used for the solution of equations (3.29) and (3.30) is given on the following pages. The language is Fortran, and the correlation between labels used in the programme and the nomenclature used elsewhere, is given below

Programme Label	Symbol	Programme Label	Symbol
P	P	TA	$\tan \alpha$
PR	P_R	CA	$\cos \alpha$
K1	k_1	SX (1)	x_1
K2	k_2	SX (2)	x_2
V	V	T (1)	T'
RD (1)	R'	T (2)	T''
RD (2)	R''	MUP	μ_P
RP (1)	RB'	MUT	μ_T
RP (2)	RB''	N	n
INT1	I_1	INT2	I_2
INT3	I_3	THETA 1	θ_1
PFPP	$P_{F(P)}/P$	PFTP	$P_{F(T)}/P$

'NSER' - The number of groups of results being run through, results being grouped by undrawn bar size.

'SREF' - A number, 1 to 5, indicating the group of bar size.

'NTEST'- The number of tests within the group.

'REF' - The test reference number.

* See section 13

```
      MASTER(ZSHE)
      INTEGER•SREF,REF
      REAL•N,INT1,INT2,INT3,K1,K2,INT3L,MUP,MUT
      DIMENSION•T(2),RD(2),RP(2),SH(2),X(2),SX(2),W(2),U(2)
    1•FORMAT(F4.1)
    2•FORMAT(I1)
    4•FORMAT(I1,2F6.4,2F6.3,2F5.3)
    5•FORMAT(I3)
    6•FORMAT(3H1N=,F4.1,4X,6HSERIES,I2)
   61•FORMAT(43HO••TAN•••••COS•••••SX(1)••SX(2)•••K1•••••K2,9X,
     1•33HINT1••••••INT3LIM••••••GROUP(T)LIM)
    7•FORMAT(1HO,2F8.4,4F7.3,3F12.4///)
    9•FORMAT(I3,2F6.2,F6.0,F7.3,2F6.2,F6.0,2F6.2)
   19•FORMAT(1H+,3X,2F7.2,F8.3)
   20•FORMAT(1H+,25X,4F9.4)
   21•FORMAT(52HOREF••••RD••••VEL•••THETA1••••INT2•••GROUP(P)••PFP/P,5X,
     1•3HMUP,17X,30HINT3•••GROUP(T)••PFT/P•••••MUT/)
   22•FORMAT(1H+,72X,4F9.4/)
   28•FORMAT(1H•,I3,2F7.2,F8.3)
      READ(1,1)N
      READ(1,2)NSER
      DO 3 I=1,NSER
      READ(1,4)SREF,TA,CA,SX(1),SX(2),K1,K2
      READ(1,5)NTEST
      C1=3.14159265/(12.0*K1)
      A=K1*SX(2)-K2*SX(1)
      B=K1-K2
      CT=2240.0*TA/CA
      F=(SX(2)-N*SX(1))/(SX(2)-SX(1))
      F=(N-1.0)/(SX(2)-SX(1))
      INT1=.5*E*(SX(2)**2-SX(1)**2)+F*(SX(2)**3-SX(1)**3)/3.0
      INT3L=E*(SX(2)**3-SX(1)**3)/3.0+F*(SX(2)**4-SX(1)**4)/4.0
      GTLIM=INT3L/INT1
      WRITE(2,6)N,SREF
      WRITE(2,61)
      WRITE(2,7)TA,CA,SX(1),SX(2),K1,K2,INT1,INT3L,GTLIM
      WRITE(2,21)
      DO•8•J=1,NTEST
      READ(1,9)REF,P,PR,T(1),V,RD(1),RP(1),T(2),RD(2),RP(2)
      IF(T(2))10,11,10
   10•M=2
      GO•TO•12
   11•M=1
   12•DO•13•L=1,M
      C=2.0*3.14159265*TA*(SX(2)-SX(2)*RP(L)/RD(L)-SX(1))
      D=2.0*SX(1)*SX(2)*RP(L)*3.14159265*TA/RD(L)
      G=RD(L)*RD(L)*D*D+144.0*V*V*A*A
      H=2.0*(RD(L)*RD(L)*C*D-144.0*V*V*A*B)
      AJ=RD(L)*RD(L)*C*C+144.0*V*V*B*B
```

```
      RQ=24.0*V*RD(L)*(B*D+A*C)
      RDV=RD(L)/V
      THETA1=ATAN(C1*RD(L)/V)
      RPRD=RP(L)/RD(L)
      PPR=P-PR
      IF(PR)24,25,24
   24•IF(L-2)26,25,25
   25•WRITE(2,19)RD(L),V,THETA1
      GO•TO•27
   26•WRITE(2,28)REF,RD(L),V,THETA1
   27•DO•14•N1=1,2
      S=(2.0*AJ*SX(N1)+H)/RQ
      SH(N1)=ALOG(S+SQRT(1.0+S*S))
   14•X(N1)=SQRT(G+H*SX(N1)+AJ*(SX(N1)**2))
      IF(L-2)23,16,16
   23•IF(PR)15,16,15
   15•DO•17•N1=1,2
      Z=A*E+.5*(A*F-B*E)*(SX(N1)-1.5*H/AJ)
      Z=Z-B*F*(SX(N1)**2*AJ-1.25*H*SX(N1)+1.875*H*H/AJ-2.0*G)/(3.0*AJ)
      Y=(A*F-B*E)*(.75*H*H/AJ-G)-A*E*H-B*F*H*(3.0*G-1.25*H*H/AJ)/(2.*AJ)
   17•W(N1)=12.0*V*(X(N1)*Z+Y*SH(N1)/(2.0*SQRT(AJ)))/AJ
      INT2=W(2)-W(1)
      PFP=PPR*INT1/(INT1-INT2)
      PFPP=PFP/P
      GP=(INT1-INT2)/INT1
      MUP=PFP*TA/(P-PFP)
      WRITE(2,20)INT2,GP,PFPP,MUP
   16•DO•18•N1=1,2
      Z=(SX(N1)**3)*AJ-7.0*H*(SX(N1)**2)/6.0+35.0*H*H*SX(N1)/(24.0*AJ)
      Z=Z-1.5*G*SX(N1)-35.0*H*H*H/(16.0*AJ*AJ)+55.0*G*H/(12.0*AJ)
      Y=(SX(N1)**2)*AJ-1.25*H*SX(N1)+1.875*H*H/AJ-2.0*G
      Y=(E*C+D*F)*Y/(3.0*AJ)
      Y=Y+.5*D*E*(SX(N1)-1.5*H/AJ)
      Y=X(N1)*(Y+F*C*Z/(4.0*AJ))
      Q=.5*D*E*(3.0*H*H-4.0*G*AJ)
      Q=Q+(E*C+D*F)*H*(3.0*G-1.25*H*H/AJ)
      Q=Q+.125*F*C*(8.75*(H**4)/AJ+12.0*G*G*AJ-30.0*G*H*H)/AJ
   18•U(N1)=RD(L)*(Y+Q*SH(N1)/(4.0*AJ*SQRT(AJ)))/AJ
      INT3=U(2)-U(1)
      PFT=T(L)/CT*INT1/INT3
      PFTP=PFT/P
      GT=INT3/INT1
      MUT=PFT*TA/(P-PFT)
   13•WRITE(2,22)INT3,GT,PFTP,MUT
    8•CONTINUE
    3•CONTINUE
      STOP
      END
```

N.B: blanks indicated thus: •

APPENDIX 6.1 - MANUFACTURING DRAWINGS

Thrust Block Assembly

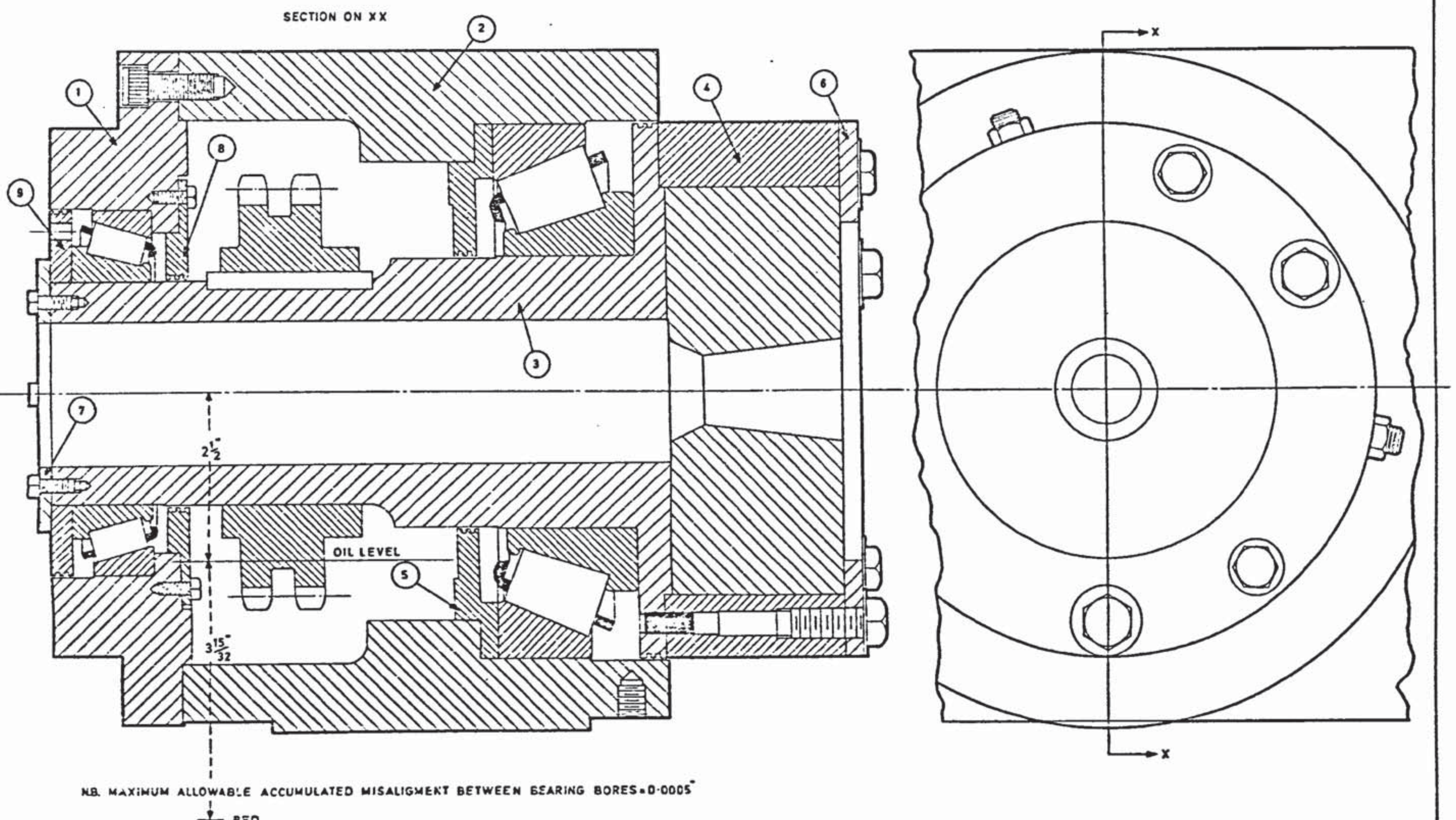

N.B. MAXIMUM ALLOWABLE ACCUMULATED MISALIGMENT BETWEEN BEARING BORES = 0·0005"

ARRANGEMENT OF THRUST BLOCK FOR HYDRAULIC DRAWBENCH-L82		No1 END PLATE SHEET 1	No5 PRIMARY BEARING SEAL SHEET 5
		No2 CASING SHEET 2	No6 DIE RETAING PLATE SHEET 6
DRAWN- D ROTHMAN	FULL SIZE- THIRD ANGLE PROJECTION	No3 SHAFT SHEET 3	No7 END PLATE SHEET 6
DATE- 4-8-56		No4 DIE HOUSING SHEET 4	No8 SECONDARY BEARING SHEET 7
	SHEET No.8 OF 8 SPS/10921	No9 SPACER SHEET 7	

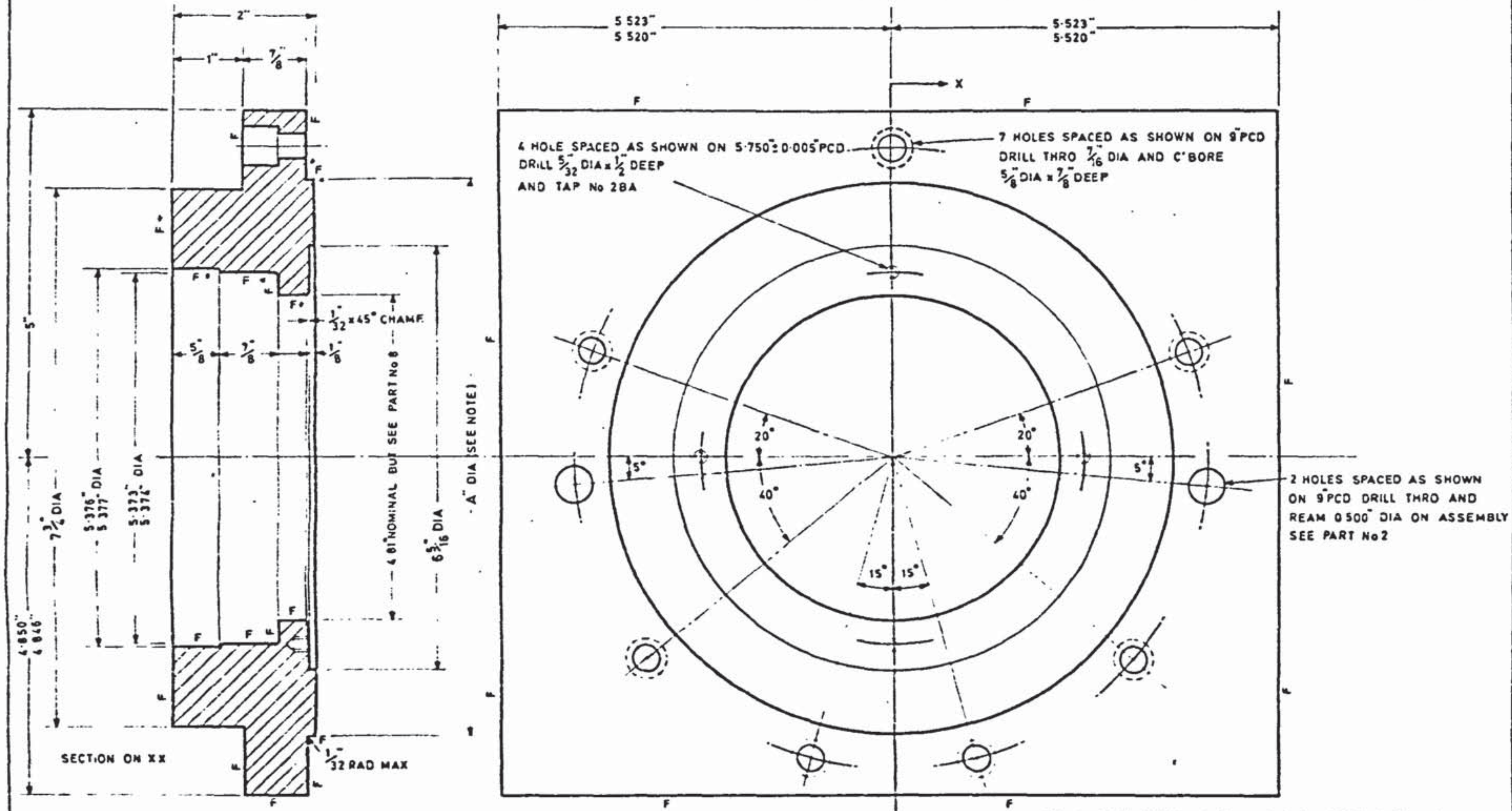

NB A = 8·00" NORMAL BUT MAX CLEARANCE TO PART No 2
IS 0·0002" ON DIA

FULL SIZE - THIRD ANGLE PROJECTION	TITLE - END PLATE FOR THRUST BLOCK HYDRAULIC DRAWBENCH - L82
MATERIAL - MILD STEEL	DRAWN - D ROTHMAN — DATE 28 7 66
FRACTIONAL DIMENSIONS ± 0·010"	SHEET 1 OF 8 — PART No 1 — SPS/10914

FINISH MACHINE AT F

FACES MARKED BY ASTERISK TO BE CONCENTRIC AND PARALLEL AND/OR SQUARE
AS APPLICABLE SEE NOTE ON SHEET 8

HALF FULL SIZE - THIRD ANGLE PROJECTION	TITLE:- CASING FOR THRUST BLOCK HYDRAULIC DRAWBENCH - L. 82
MATERIAL - MILD STEEL	
FRACTIONAL DIMENSIONS ± 0·010"	DRAWN D. ROTHMAN DATE 28·7·66
	SHEET 2 OF 6 PART No. 2 SPS/10915

FINISH MACHINE AT F
ALL FINISH MACHINED SURFACES TO BE CONCENTRIC AND PARALLEL AND/OR SQUARE AS APPLICABLE SEE NOTE ON SHEET 6.

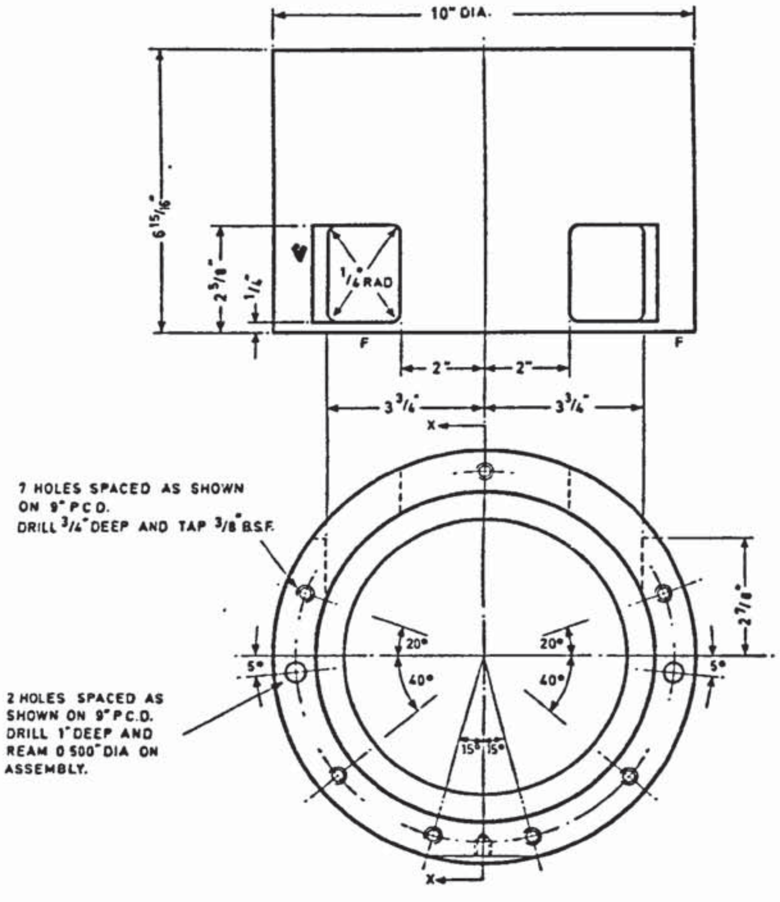

N.B. A" = 8" ± 0·010" BUT SEE PART No. 1

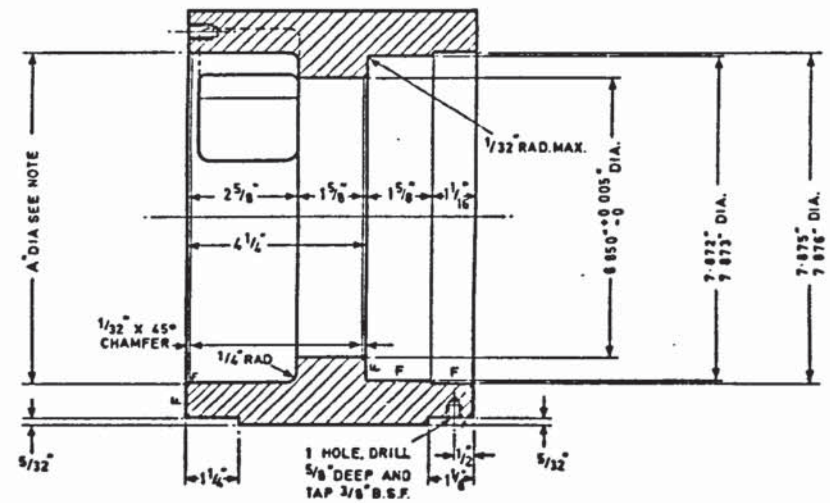

SECTION ON X X

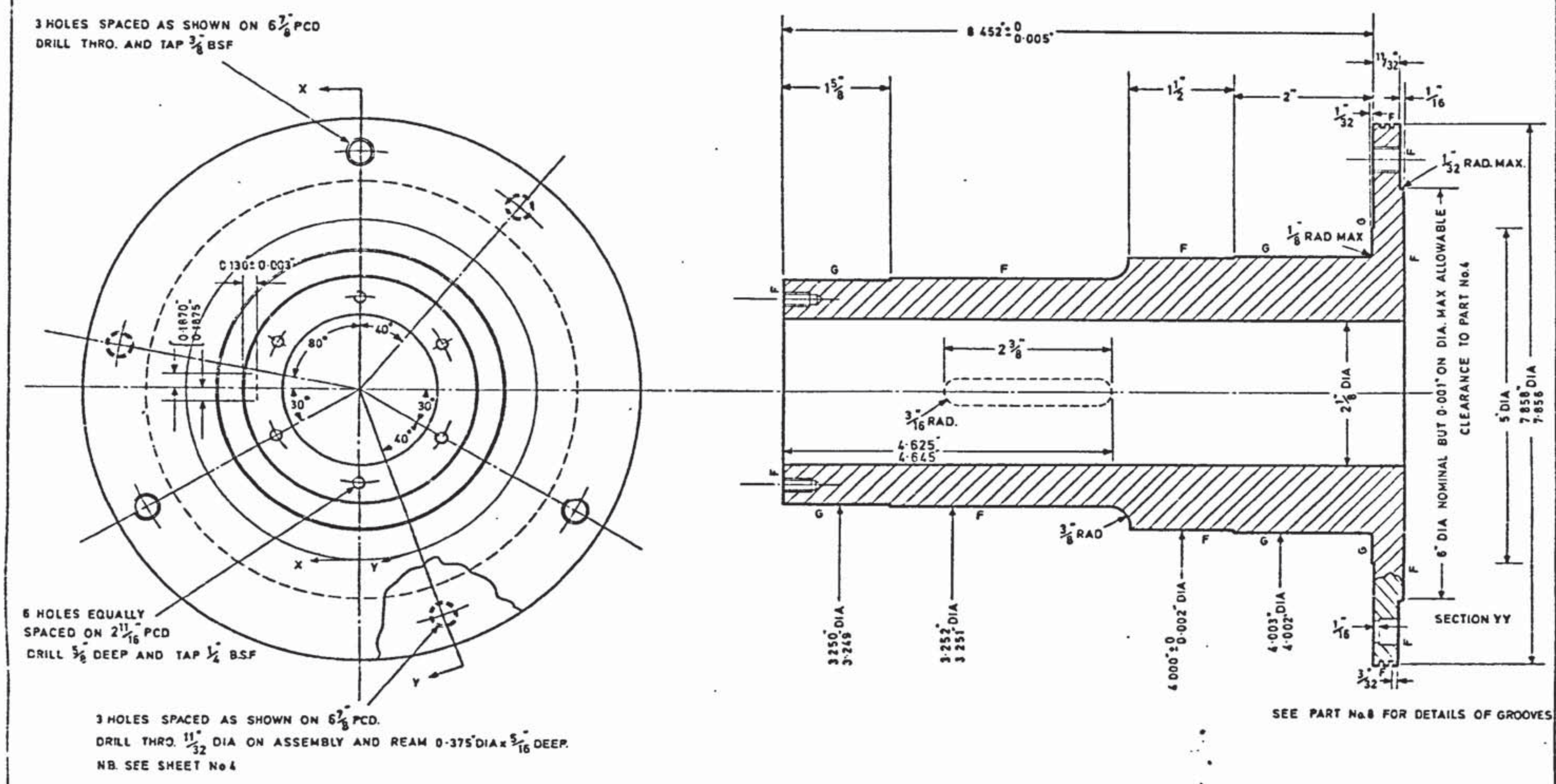

FULL SIZE - THIRD ANGLE PROJECTION	TITLE - THRUST BLOCK SHAFT HYDRAULIC DRAWBENCH - L82
MATERIAL - MILD STEEL	DRAWN - D. ROTHMAN DATE - 30.7.66
FRACTIONAL DIMENSIONS ± 0.010	SHEET No. 3 OF 8 PART No. 3 SPS/10516

GRIND AT G
FINISH MACHINE AT F
ALL SURFACES REQUIRING GRINDING OR FINISH MACHINING
TO BE CONCENTRIC AND PARALLEL
AND/OR SQUARE AS APPLICABLE

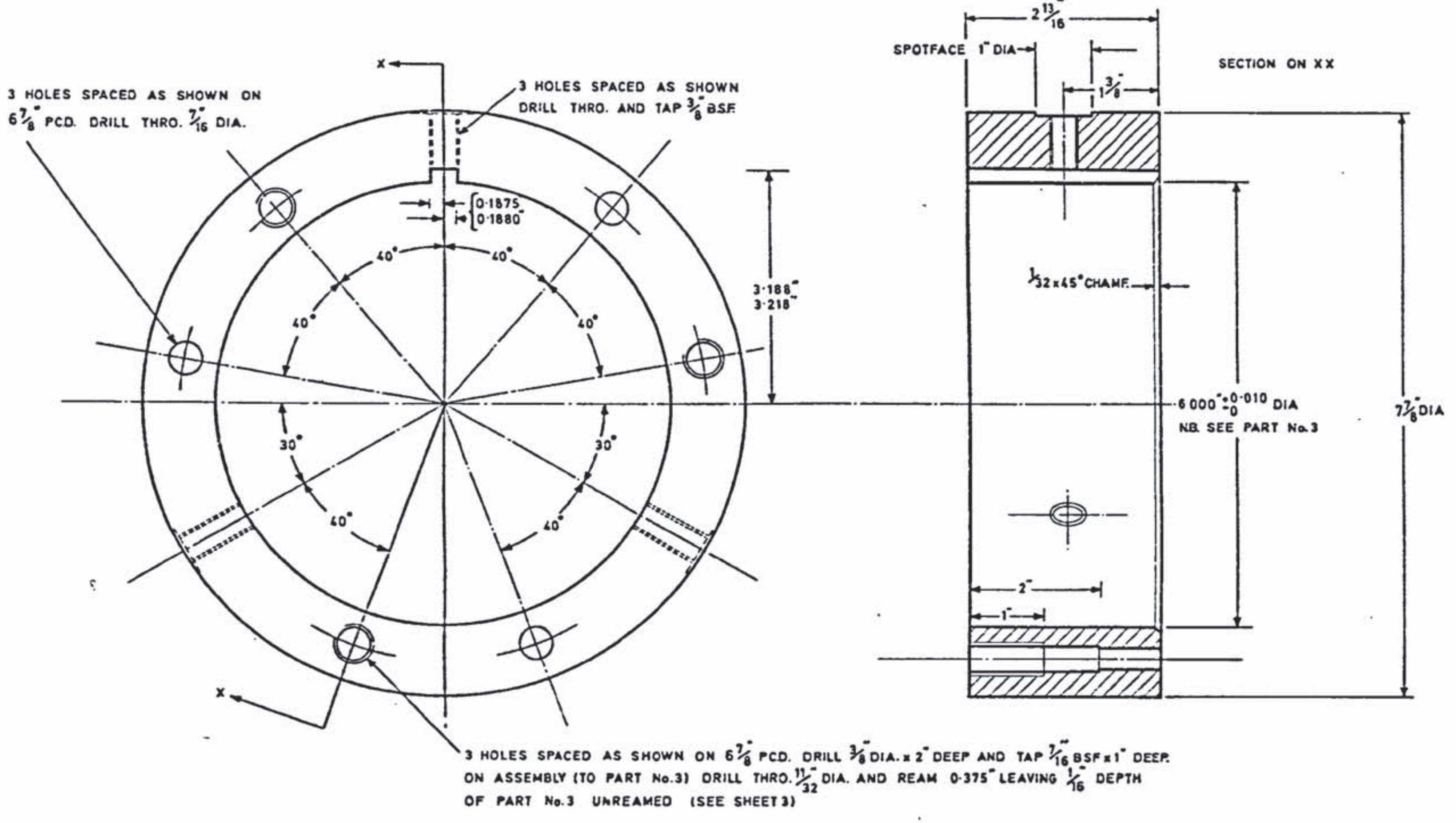

FULL SIZE - THIRD ANGLE PROJECTION	TITLE - DIE HOUSING THRUST BLOCK FOR HYDRAULIC DRAWBENCH - L82	
MATERIAL - MILD STEEL	DRAWN BY D. ROTHMAN	DATE - 1·8·66
FRACTIONAL DIMENSIONS ± 0·010"	SHEET 4 OF 8 PART No. 4	SPS/10917

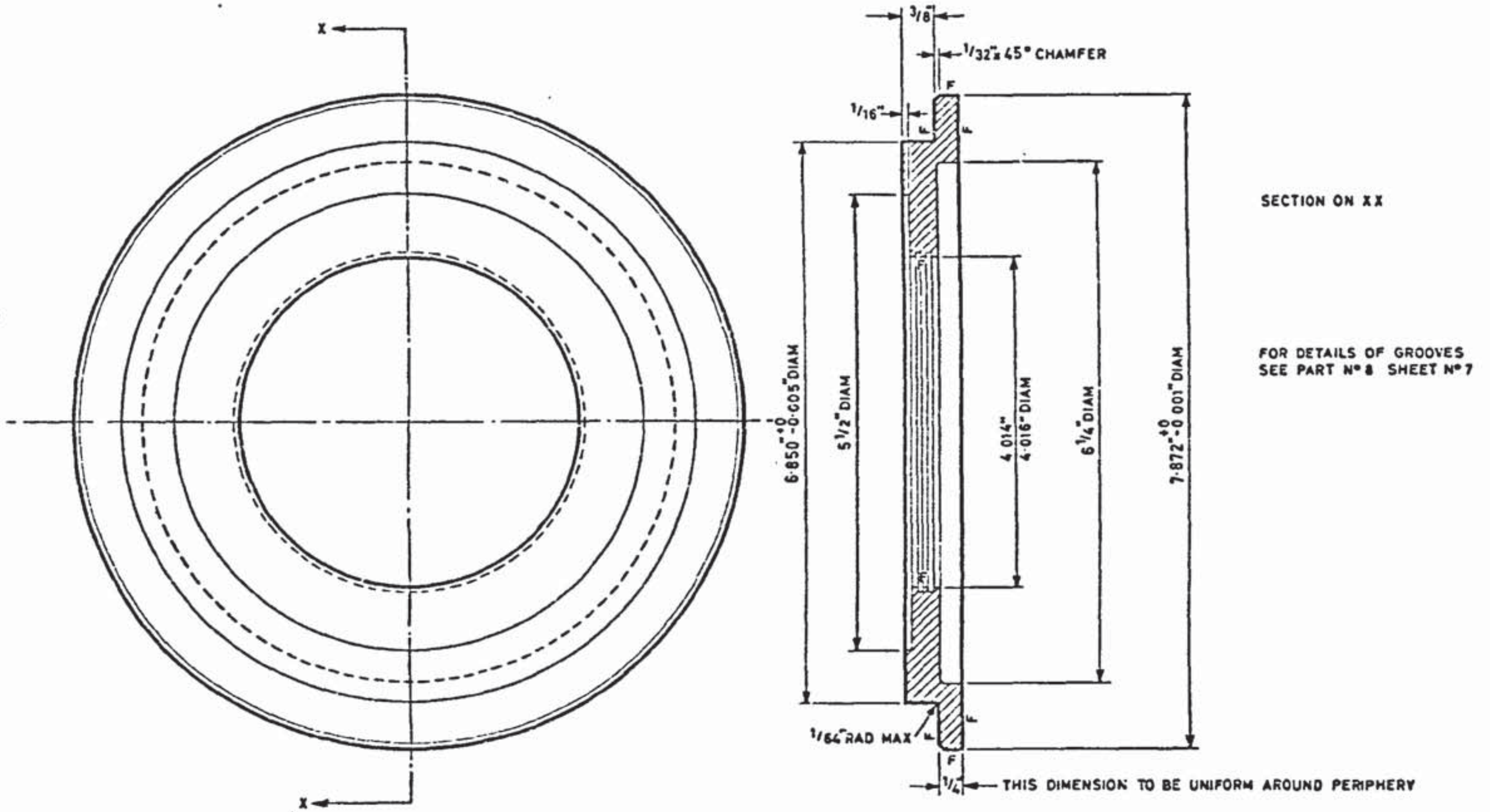

FULL SIZE - THIRD ANGLE PROJECTION	TITLE PRIMARY BEARING SEAL THRUST BLOCK ASSEMBLY FOR HYDRAULIC DRAWBENCH. L82	
MATERIAL - MILD STEEL	DRAWN - D ROTHMAN	DATE 2·8·66
FRACTIONAL DIMENSIONS ±0·010"	SHEET N° 5 OF 8 PART N° 5 SPS/10918	

FINISH MACHINE AT F

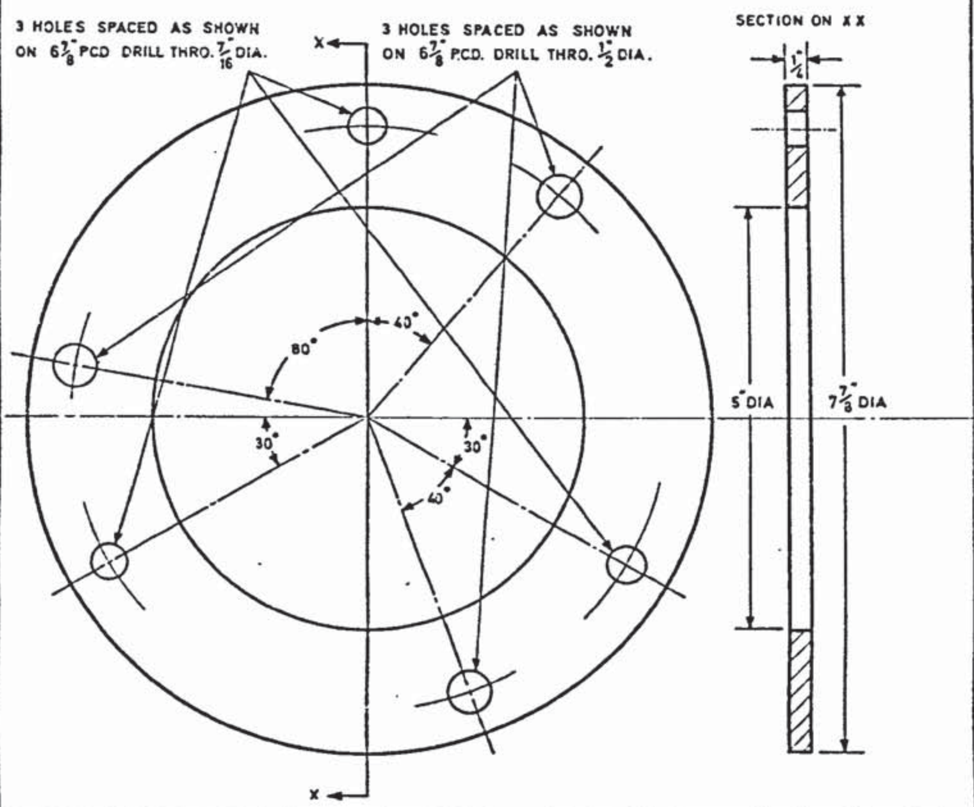

TITLE - DIE RETAINING PLATE. THRUST BLOCK ASSEMBLY FOR HYDRAULIC DRAWBENCH - L82 PART No 6

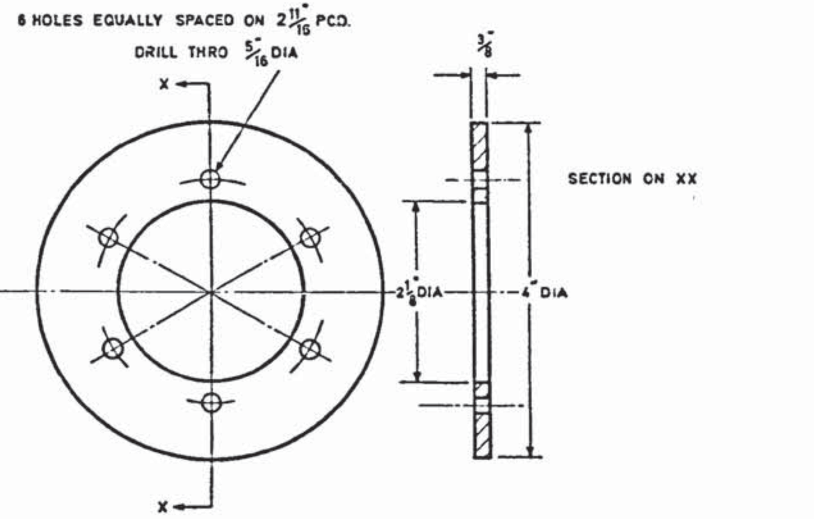

TITLE - END PLATE. THRUST BLOCK ASSEMBLY FOR HYDRAULIC DRAWBENCH - L82 PART No. 7

FULL SIZE - THIRD ANGLE PROJECTION	DRAWN D. ROTHMAN
MATERIAL - MILD STEEL	DATE - 1.8.'66
FRACTIONAL DIMENSIONS ±0·010	SHEET No. 6 OF 8 SPS / 10919

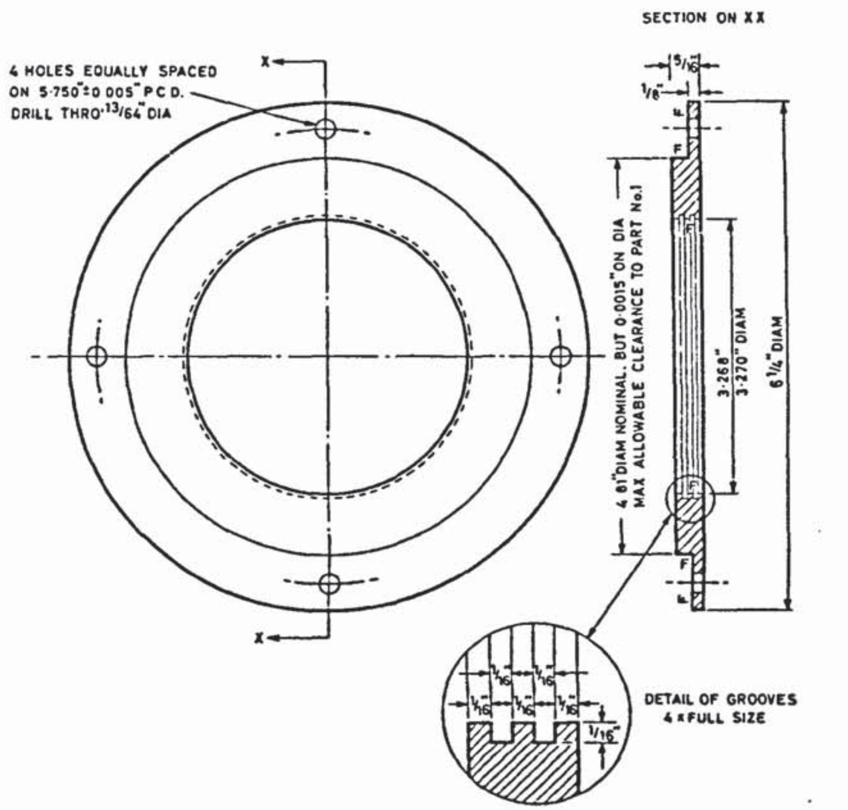

TITLE SECONDARY BEARING SEAL.
THRUST BLOCK ASSEMBLY FOR HYDRAULIC DRAWBENCH - L 82

PART N° 8

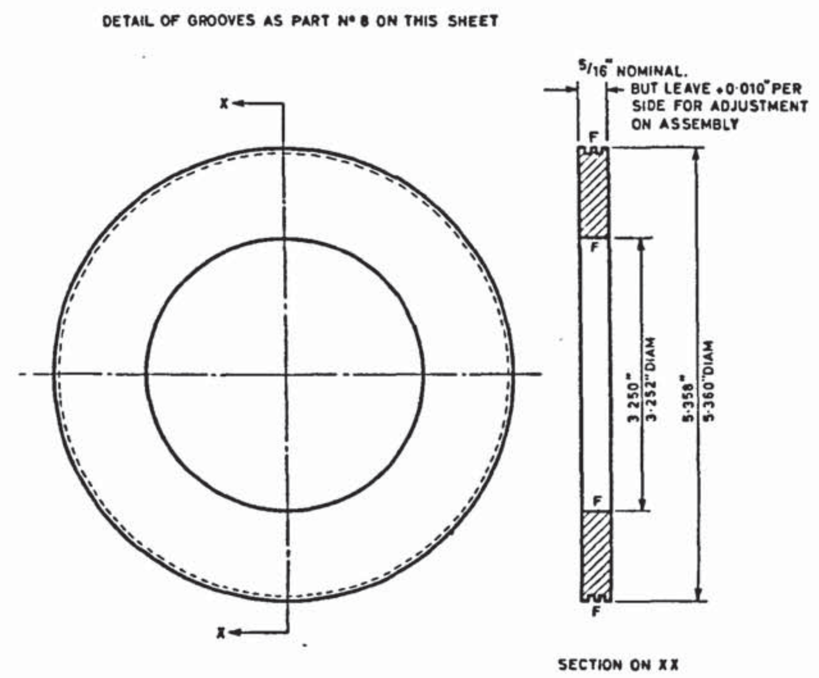

TITLE. SPACER.
THRUST BLOCK ASSEMBLY FOR HYDRAULIC DRAWBENCH - L82

PART N° 9

FINISH MACHINE AT F

FULL SIZE - THIRD ANGLE PROJECTION	DRAWN - D ROTHMAN
MATERIAL - MILD STEEL	DATE - 2·8·66
FRACTIONAL DIMENSIONS ±0·010" UNLESS OTHERWISE STATED	SHEET N° 7 OF 8 SPS/10920

APPENDIX 6.2 - MANUFACTURING DRAWINGS

Load-Cell and Jaw Assembly

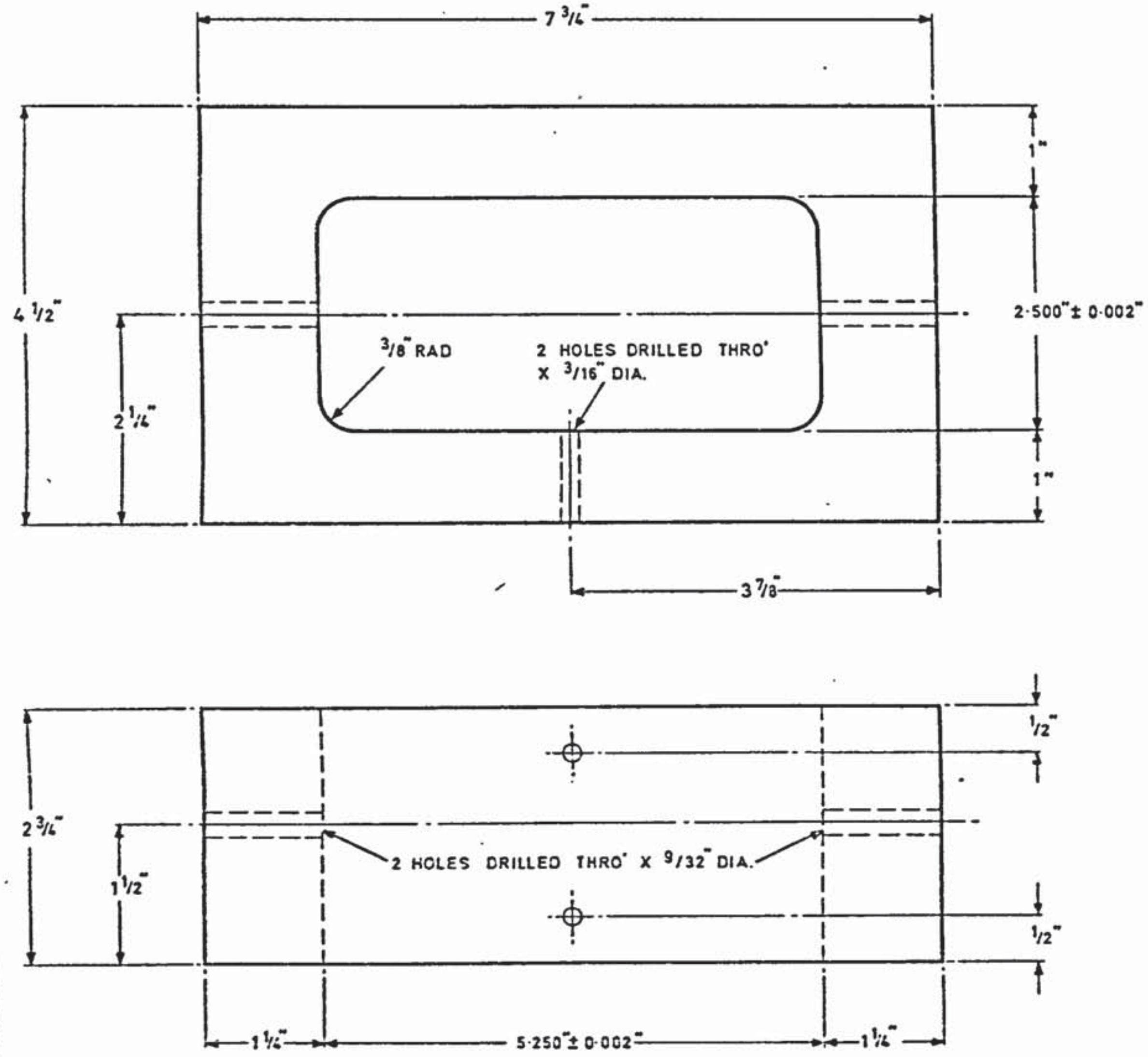

TITLE JAW HOUSING FOR ROTATIONAL ROD-DRAWING RIG-L. 82	
DRAWN - D ROTHMAN	DATE 6·7·66
SHEET No. 1 OF 6 COMPONENT No. 1 1. OFF	
FULL SIZE - THIRD ANGLE PROJECTION	
MATERIAL - MILD STEEL	
SPS/10908	

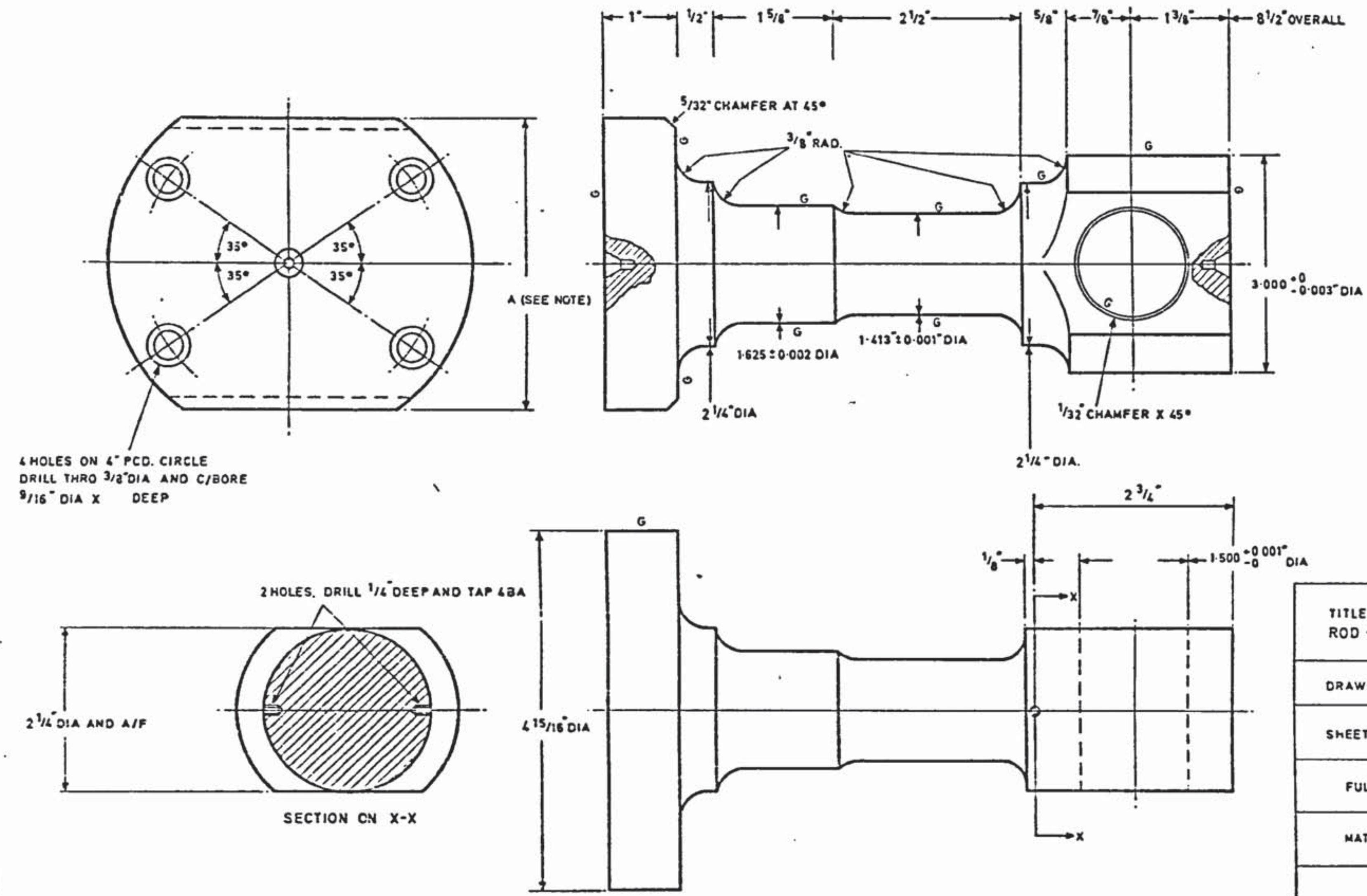

NB.

1. DIMENSION A TO MATCH COMPONENT No. 4 SHEET No. 4 NOMINAL SIZE 4·000" MAX. CLEARANCE = 0·001" EACH SIDE.
2. HEAT TREATMENT OIL QUENCH FROM 820/850°C AND TEMPER AT 240/260°C TO GIVE BRINELL HARDNESS No. 420 MIN.

TITLE LOAD CELL FOR ROD - DRAWING RIG L 82	
DRAWN - D. ROTHMAN	DATE 8 7 66
SHEET No 2 OF 6 COMPONENENT No 2 1 OFF	
FULL SIZE - THIRD ANGLE PROJECTION	
MATERIAL - VIBRAC 45 (EN 26)	

SPS/10909

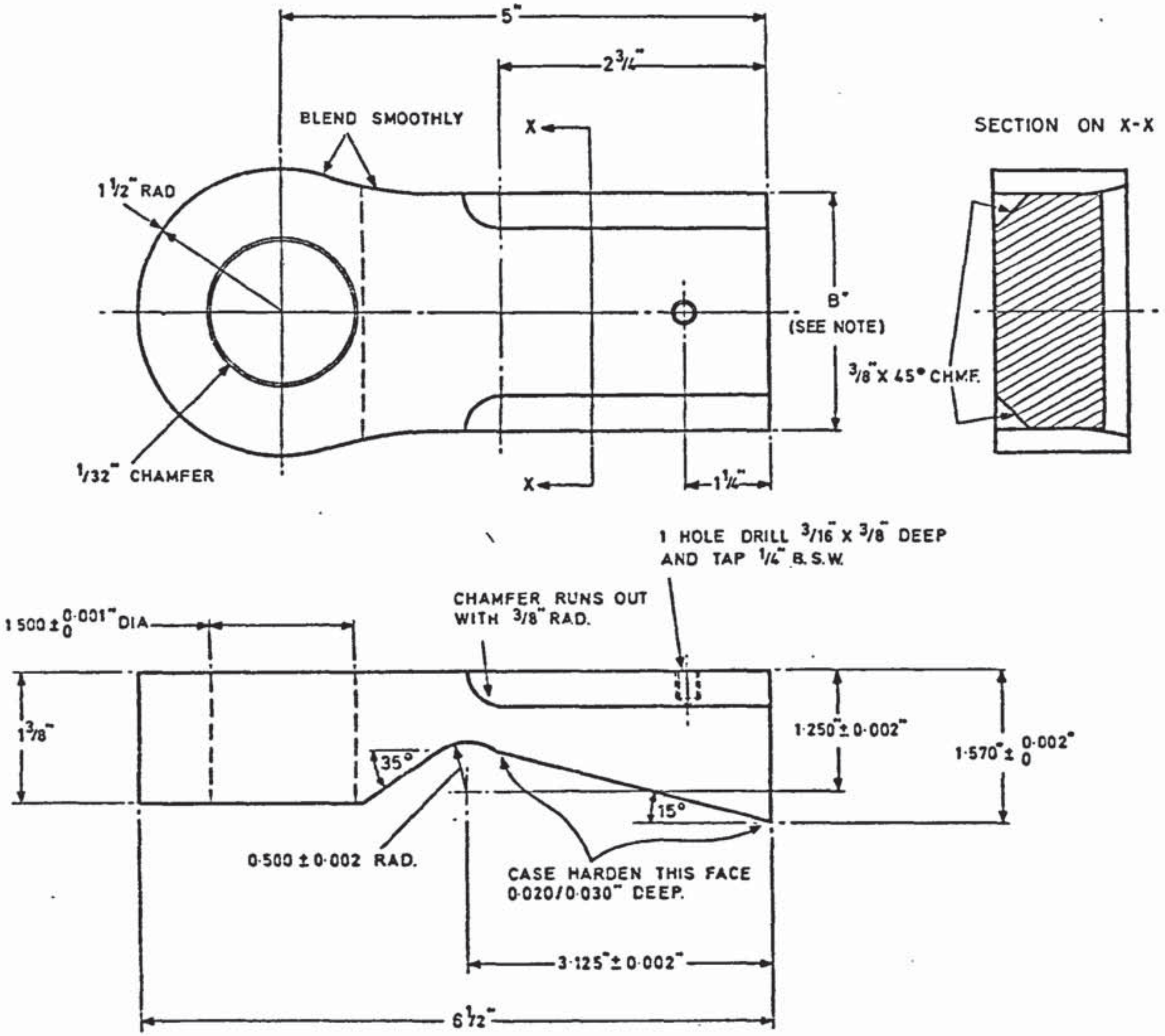

N.B

1. DIMENSION B" IS 2·500" NOMINAL, TO MATCH COMPONENT No. 1, SHEET No. 4, CLEARANCE 0·002" MAX.
2. BORE TO BE CENTRAL W.R.T. B" DIMENSION.

TITLE TIE-BAR FOR ROD-DRAWING RIG L. 82	
DRAWN - D ROTHMAN	DATE 6·7·66
SHEET No. 2 OF 6 COMPONENT No. 3 2. OFF	
FULL SIZE - THIRD ANGLE PROJECTION	
MATERIAL - EN. 32	
SPS/10S1G	

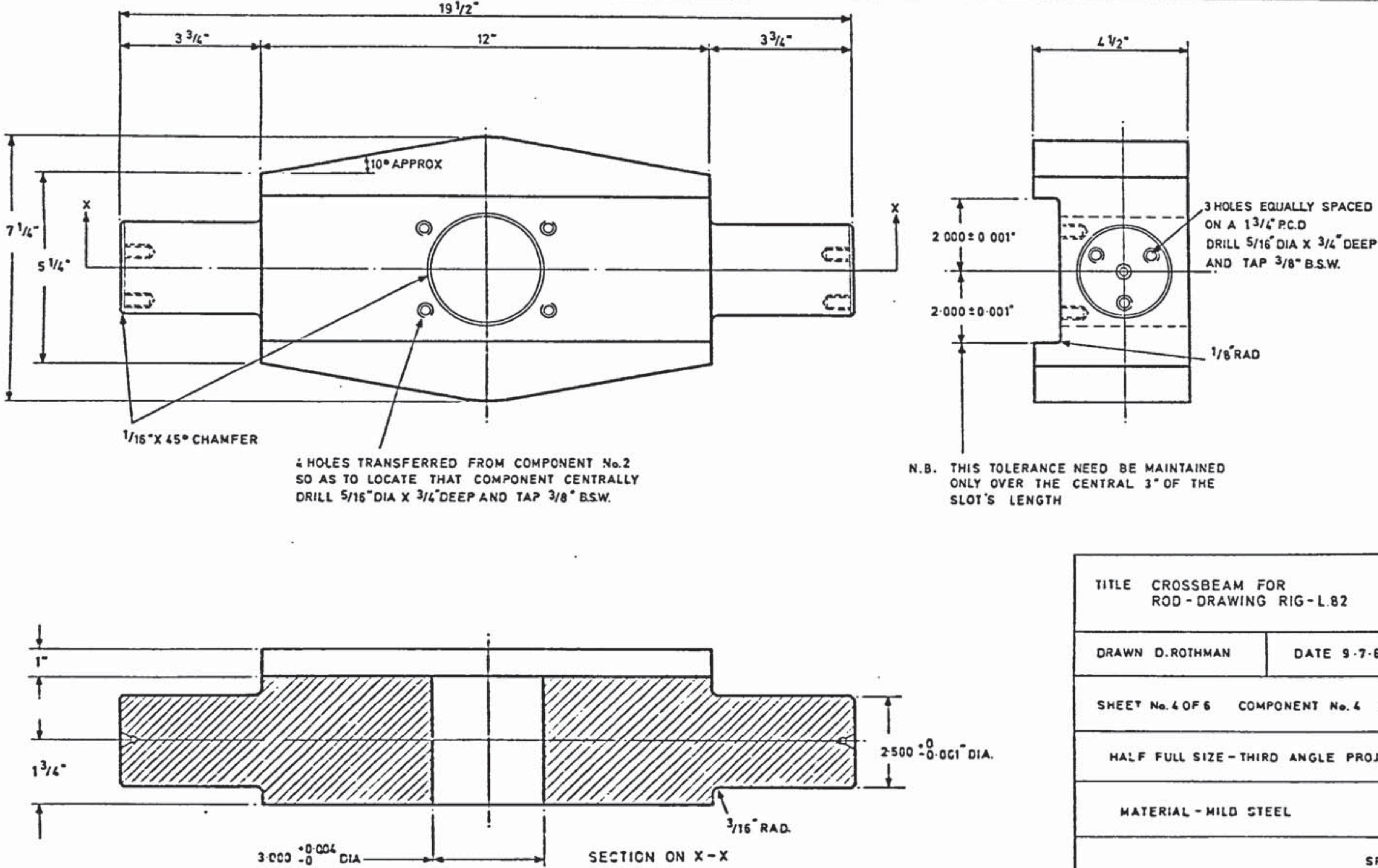

TITLE CROSSBEAM FOR ROD-DRAWING RIG-L.82	
DRAWN D. ROTHMAN	DATE 9-7-66
SHEET No. 4 OF 6 COMPONENT No. 4 1 OFF	
HALF FULL SIZE – THIRD ANGLE PROJECTION	
MATERIAL – MILD STEEL	
SPS/10911	

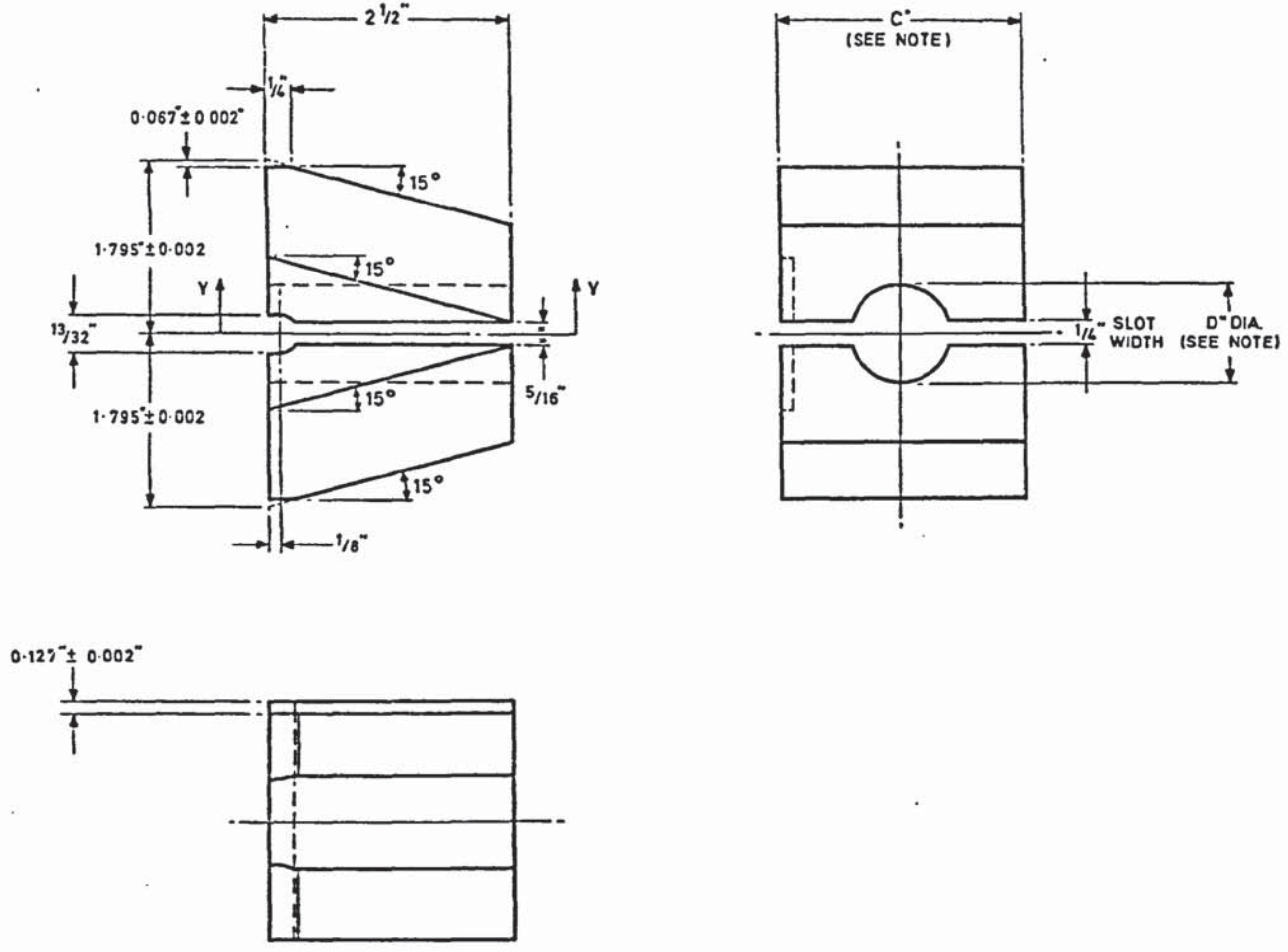

VIEW ON Y-Y

NB

1. D" DIMENSION TO BE 1·000" ± 0·002" AT FRONT END TAPERING TO 0·980" ± 0·002" AT BACK.
2. C" DIMENSION TO BE 2·500" NOMINAL AND CENTRAL W.R.T. BORE; TO MATCH COMPONENT No. 1. MAX. CLEARANCE 0·0015"
3. BORE TO BE SERRATED PRIOR TO CARBURISING; 8 T.P.I. BUTTRESS THREAD, SLOTTED LONGITUDINALLY WITH 45° POINT TOOL, AT 15° CIRCUMFERENTIAL SEPERATION.

TITLE JAWS FOR ROD-DRAWING RIG L.82	
DRAWN - D. ROTHMAN	DATE 11 · 7 · 66
SHEET No 5 OF 6 COMPONENT No. 5. 1 PAIR OFF	
FULL SIZE - THIRD ANGLE PROJECTION	
MATERIAL - EN. 33	
HEAT TREATMENT - CASE HARDEN 0·020"/0·030" DEEP	
SPS/10912	

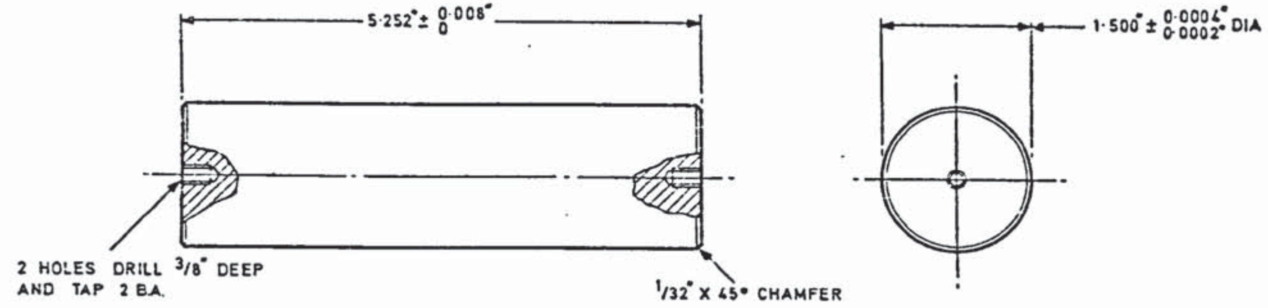

TITLE PIN FOR ROD-DRAWING RIG L.82

DRAWN - D ROTHMAN	DATE
SHEET No. 6 OF 6 COMPONENT No. 6 1 OFF	
FULL SIZE - THIRD ANGLE PROJECTION	
MATERIAL - EN 8 (TENSILE RANGE P)	
HEAT TREATMENT - TO SUIT TENSILE RANGE P IF NOT SUPPLIED IN THAT CONDITION.	

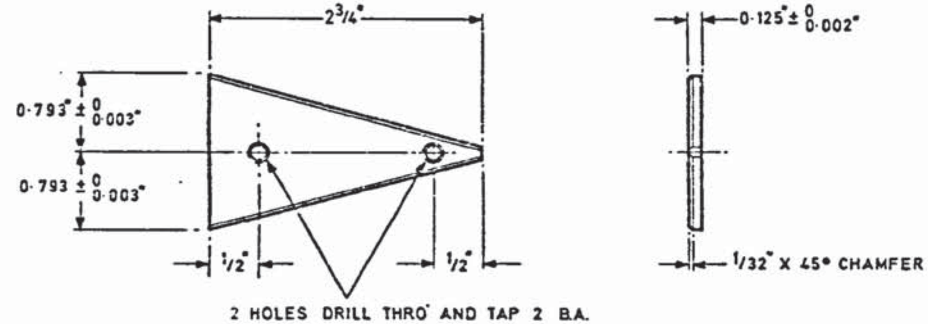

TITLE JAW SEPARATING PLATE FOR ROD-DRAWING RIG L.82

DRAWN - D ROTHMAN	DATE
SHEET No. 6 OF 6 COMPONENT No. 7 1. OFF	
FULL SIZE - THIRD ANGLE PROJECTION	
MATERIAL - MILD STEEL	
HEAT TREATMENT - CASE-HARD ON WORKING EDGES	

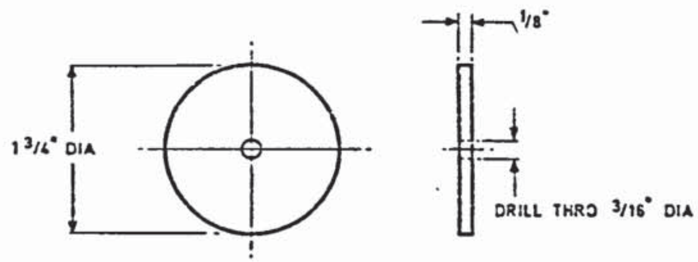

TITLE END-CAP FOR ROD-DRAWING RIG L 82

DRAWN - D ROTHMAN	DATE
SHEET No. 6 OF 6 COMPONENT No. 8 2. OFF	
FULL SIZE - THIRD ANGLE PROJECTION	
MATERIAL - MILD STEEL	

SPS/10913

APPENDIX 7-TABLES OF RESULTS

TABLE No. A7.1

PROFILE OF. DRAWING DIE

(at position 7)

Before Drawing		After Drawing	
Distance along axis (x. in $\times 10^{-3}$)	Distance normal to axis. (y. in $\times 10^{-3}$)	Distance along axis. (x. in $\times 10^{-3}$)	Distance normal to axis. (y. in $\times 10^{-3}$)
0	2.53	0	2.33
10	1.70	10	1.55
20	1.04	20	0.90
30	0.57	30	0.42
40	0.20	40	0.08
50	0.00	50	0.00
60	0.04	60	0.18
70	0.38	70	0.71
80	1.12	80	1.58
90	2.13	90	2.64
100	3.30	100	3.83
110	4.53	110	5.05
120	5.78	120	6.28
130	7.09	130	7.53
140	8.39	140	8.82
150	9.72	150	10.13
200	16.19	160	11.44
250	22.38	180	14.03
300	28.46	200	16.57
350	34.63	210	17.77
400	40.76	220	19.02
450	46.85	240	21.49
500	52.98	260	23.95
550	59.06	310	30.03
600	65.23	360	36.11
650	71.30	410	42.27
700	77.35	460	48.37
750	83.44	510	54.51
800	89.49	560	60.64
850	95.50	610	66.76
900	101.62	660	72.81
950	107.64	710	78.81
1,000	113.74	760	84.89
1,050	119.86	810	90.88
1,100	126.02	860	96.93
1,150	132.28	910	103.00
1,200	138.69	960	109.06
1,250	145.14	1,010	115.15
1,300	151.99	1060	121.30
1,350	159.82	1,110	127.48
1,400	173.48	1,160	133.76
		1,210	140.13
		1,260	146.70
		1,310	153.65
		1,360	162.37
		1,410	178.63

Before Drawing	
Reference Position	Throat Diameter (in)
1/5	1.00020
3/7	1.00001

After Drawing	
Reference Position	Throat Diameter (in)
1/5	1.00038
2/6	1.00018
3/7	1.00009
4/8	1.00027

TENSILE TESTS ON SERIES I MATERIAL   TABLE No. A7.2

(SEE SECTION 10.0)

diam. of bar	ε true strain	$\dot{\varepsilon}$ $(\times 10^{-3} sec^{-1})$	σ (tonf/in²)	σ^* (tonf/in²)	Ref. no. of bar	ε true strain	$\dot{\varepsilon}$ $(\times 10^{-3} sec^{-1})$	σ (tonf/in²)	σ^* (tonf/in²)
1.1/16 in.	0		17.3	17.3					
	0.0265		19.77	19.77					
	0.0545	1.9	23.92	23.92					
	0.1014	2.4	27.60	27.60					
	0.1655	2.1	30.74	30.74					
1.1/8 in.	0		19.4	19.4					
	0.0296		20.88	20.88					
	0.0640	2.2	25.78	25.78					
	0.1203	2.3	30.13	30.13					
	0.2037	2.2	33.63	33.63					
	0.3170	2.1	36.83	36.66					
1.1/4 in.	0		17.9	17.9					
	0.0382		20.53	20.53					
	0.0725	2.1	25.04	25.04					
	0.1345	1.8	29.19	29.19					
	0.2263	1.7	32.61	32.61					
	0.3420	1.3	35.70	35.45					
	0.4983	2.4	39.70	38.52					

TABLE No. A7.3

SERIES I DRAWING TESTS ON 1.1/16 in. DIAMETER BAR

Mean Non-Rotational Drawing Force taken as 5·80 tonf.
Nominal Rotational Speeds taken as 14·50 and 28·50 rev/min.

Rotational Speed (rev/min)	Drawing Speed (ft/min)	Measured Values: Drawing Force (tonf), Without Rotation, Before	After	With Rotation, Start	End	Torque (lbf.in), Start	End	Adjusted Values: Drawing Force, With Rotation, Start	End	Torque, Start	End	Coefficient of Friction, μ_P	μ_T
14·82	5·21	5·89	–	5·42	→	1350	→	5·35	→	1320	→	0·066	0·055
14·82	4·61	"	–	5·27	–	1420	–	5·21	–	1390	→	0·075	0·053
14·76	2·19	"	–	4·76	–	1830	–	4·71	–	1790	→	0·066	0·052
14·71	0·57	"	–	4·13	–	2000	–	4·10	–	1970	→	0·063	0·051
14·92	7·89	5·81	5·70	5·49	→	980 920	→	5·54	→	960 900	→	0·075	0·053 0·048
14·83	10·18	5·90	5·94	5·66 5·75	→	770 830	→	5·55 5·74	→	740 800	→	0·160 0·019	0·049 0·065
14·93	12·64	5·76	5·76	5·62	→	610 620	→	5·66	→	590 600	→	0·169	0·047 0·048
14·86	15·73	5·89	5·76	5·77	5·69	520	480	5·68	5·73	510	→	0·190	0·050
28·86	5·22	5·97	–	4·88	→	1880 1760	→	4·75	→	1820 1700	→	0·078	0·057 0·052
28·86	1·99	–	–	4·26	–	2000	–	4·26	–	1940	→	0·065	0·051
29·07	5·34	5·75	5·77	4·84	→	1620 1710	→	4·89	→	1630 1720	→	0·064	0·049 0·053
29·09	7·99	5·87	5·79	5·17	→	1400 1490	→	5·15	→	1380 1470	→	0·071	0·048 0·053
29·12	9·82	5·79	5·74	5·25	→	1230 1270	→	5·29	→	1210 1250	→	0·073	0·047 0·049
29·24	12·71	5·82	5·83	5·48	→	1070 1130	→	5·47	→	1060 1120	→	0·066	0·049 0·053
29·13 29·30	15·74	5·86	5·75	5·59	5·47	920	860	5·53	→	890	830	0·083	0·048

TABLE No. A7.4

SERIES I DRAWING TESTS ON 1.1/8 In. DIAMETER BAR

Mean Non-Rotational Drawing Force taken as 9·74 tonf.
Nominal Rotational Speeds taken as 14·50 and 28·50 rev/min.

Rotational Speed (rev/min)	Drawing Speed (ft/min)	Measured Values						Adjusted Values				Coefficient of Friction	
		Drawing Force (tonf)				Torque (lbf.in)		Drawing Force		Torque			
		Without Rotation		With Rotation				With Rotation					
		Before	After	Start	End	Start	End	Start	End	Start	End	μ_P	μ_T
14·53	5·05	9·78	–	9·01	8·81	2370	2260	8·97	8·77	2360	2250	0·052	0·052
14·53	3·84	"	–	8·51	–	2580	–	8·48	–	2570	–	0·068	0·049
14·35	2·65	"	–	8·11	–	2950	–	8·08	–	2950	–	0·063	0·035
14·28	1·90	"	–	7·74	–	3190	–	7·72	–	3200	–	0·062	0·051
14·28	1·02	"	–	7·18	–	3380	3310	7·17	–	3370	3300	0·062	0·051
14·68	5·16	9·47	9·43	8·80	8·75	2000 2050	→	9·06	9·01	2050 2100	→	0·046	0·043 0·045
14·63	7·82	9·66	9·76	9·25	9·31	1700	→	9·33	9·31	1710	→	0·053	0·049
14·79	10·16	9·63	9·57	9·38	→	1310	1270	9·49	→	1310	1270	0·049	0·045
14·69	12·52	9·82	9·77	9·64	9·56	1160	1130	9·56	9·48	1140	1110	0·052	0·048
14·89	15·67	9·73	–	9·58 9·47	→	890 870	→	9·60 9·49	→	870 850	→	0·066 0·206	0·043 0·042
28·57	5·15	9·87	–	8·40	8·21	3110	2900	8·29	8·10	2970	2860	0·051	0·050
28·57	0:08	"	–	6·53	–	3170	–	6·44	–	3130	–	0·064	0·045
28·75	7·95	9·95	9·68	8·80	8·60	2630	2280	8·63	8·43	2570	2270	0·061	0·050
28·62	7·83	10·04	9·83	9·02	8·77	2760	2540	8·76	8·63	2640	2470	0·050	0·053
28·86	9·62	9·60	9·55	8·75	→	2150	2070	8·89	→	2170	2090	0·057	0·045
28·96	12·59	9·84	9·66	9·22	→	1950 1810	→	9·14	→	1910 1770	→	0·059	0·047 0·042
29·03	15·68	9·72	9·64	9·26	→	1600 1530	→	9·29	→	1580 1510	→	0·064	0·045 0·042

TABLE No. A7.5

SERIES I DRAWING TESTS ON 1.1/4 in. DIAMETER BAR

Mean Non-Rotational Drawing Force taken as 16·08 tonf.
Nominal Rotational Speeds taken as 14·50 and 28·50 rev/min.

Rotational Speed (rev/min)	Drawing Speed (ft/min)	Measured Values: Drawing Force (tonf), Without Rotation, Before	Measured Values: Drawing Force (tonf), Without Rotation, After	Measured Values: Drawing Force (tonf), With Rotation, Start	Measured Values: Drawing Force (tonf), With Rotation, End	Measured Values: Torque (lbf.in), Start	Measured Values: Torque (lbf.in), End	Adjusted Values: Drawing Force, With Rotation, Start	Adjusted Values: Drawing Force, With Rotation, End	Adjusted Values: Torque, Start	Adjusted Values: Torque, End	Coefficient of Friction μ_P	Coefficient of Friction μ_T
14·05	5·17	15·91	15·79	14·77	14·66	3660	3510	14·89	14·78	3760	3600	0·037	0·041
13·95	5·12	16·15	—	14·83	14·78	3800	3750	14·72	14·67	3860	3800	0·044	0·042
13·94 } 14·12	5·12	16·09	15·76	14·84	14·62	3860	3600	14·88	14·64	3910	3650	0·037	0·043
14·35	7·66	15·86	15·70	15·15	14·96	2830	2680 } 2630	15·37	15·18	2890	2740 } 2690	0·037	0·039
14·47	9·97	15·98	15·78	15·52	15·38	2360	2270	15·62	15·48	2380	2290	0·036	0·038
14·51	12·31	15·95	15·74	15·70	15·42	1980	1830	15·83	15·55	2000	1850	0·026	0·038
14·66	15·46	16·02	15·80	15·77	15·58	1570	1500	15·83	15·64	1570	1500	0·044	0·036
27·62 } 27·92	5·14	16·24	16·05	13·77	13·59	5190	4510	13·72	13·51	5220	4490	0·042	0·048
27·86 } 28·22	7·79	16·30	15·88	14·54	14·29	4470	4000	14·39	14·12	4480	3970	0·041	0·045
28·10 } 28·45	9·95	16·16	16·07	14·85	14·72	3830	3670	14·80	14·65	3860	3660	0·040	0·042
28·18 } 28·36	12·34	16·27	16·10	15·27	15·08	3430	3210	15·11	14·90	3430	3190	0·039	0·041
28·55	15·43	16·06	15·98	15·36	15·29	2750	2670	15·38	15·31	2760	2680	0·038	0·037

Undrawn Diameter : 1·1190/1·1201 in

Drawn Diameter : 1·0007/1·0010 in

Initial grid spacing (δ_2) = 0·050 in.

Final grid spacing (δ_1) = 0·06256 in

Lubricant: SOAP

TABLE NO. A7.6

(SEE SECTION 10.4)

grid no. n	A_n (in)	δ (in)	$\frac{v}{V}\left(=\frac{\delta}{\delta_1}\right)$	$A_n+\delta/2$	$A_n+\delta/2-11{\cdot}042$	grid no. n	B_n (in)	δ (in)	$\frac{v}{V}\left(=\frac{\delta}{\delta_1}\right)$	$B_n+\delta/2$	$B_n+\delta/2-11{\cdot}121$
1	10·40044	·06268	1·002	10·526	− 0·516	1	10·48443	·06253	0·999	10·609	− 0·512
5	10·65116	·06259	1·000	10·682	− 0·360	5	10·73455	·06257	1·000	10·766	− 0·355
6	10·71375	·06240	0·997	10·745	− 0·297	6	10·79712	·06230	0·996	10·828	− 0·293
7	10·77615	·06213	0·993	10·807	− 0·235	7	10·85942	·06262	1·001	10·891	− 0·230
8	10·83828	·06240	0·997	10·869	− 0·173	8	10·92204	·06241	0·998	10·953	− 0·168
9	10·90068	·06253	0·999	10·932	− 0·110	9	10·98445	·06215	0·993	11·016	− 0·105
10	10·96321	·06182	0·988	10·994	− 0·048	10	11·04660	·06290	1·005	11·078	− 0·043
11	11·02503	·06091	0·974	11·055	+ 0·013	11	11·10950	·05967	0·954	11·139	+ 0·018
12	11·08594	·05687	0·909	11·114	0·072	12	11·16917	·05646	0·902	11·197	0·076
13	11·14281	·05593	0·894	11·171	0·129	13	11·22563	·05591	0·894	11·254	0·133
14	11·19874	·05478	0·876	11·226	0·184	14	11·28154	·05507	0·880	11·309	0·188
15	11·25352	·05440	0·870	11·281	0·239	15	11·33661	·05416	0·866	11·364	0·243
16	11·30792	·05296	0·847	11·334	0·292	16	11·39077	·05333	0·852	11·417	0·296
17	11·36088	·05280	0·844	11·387	0·345	17	11·44410	·05270	0·842	11·470	0·349
18	11·41368	·05209	0·833	11·440	0·398	18	11·49680	·05202	0·831	11·523	0·402
19	11·46577	·05150	0·823	11·492	0·450	19	11·54882	·05128	0·820	11·574	0·453
20	11·51727	·05122	0·819	11·543	0·501	20	11·60010	·05136	0·821	11·626	0·505
21	11·56849	·05086	0·813	11·594	0·552	21	11·65146	·05080	0·812	11·677	0·556
22	11·61935	·05013	0·801	11·644	0·602	22	11·70226	·05017	0·802	11·727	0·606
23	11·66948	·05017	0·802	11·696	0·653	23	11·75243	·04989	0·797	11·777	0·656
24	11·71965	·04984	0·797	11·745	0·703	24	11·80232	·05011	0·801	11·827	0·706
25	11·76949	·05019	0·802	11·795	0·753	25	11·85243	·05000	0·799	11·877	0·756
26	11·81968	·04992	0·798	11·845	0·803	26	11·90243	·04990	0·798	11·927	0·806
27	11·86960					27	11·95233				

Position of Entry Plane : A_2 = 11·517

Position of Exit Plane : A_1 = 11·042

Position of Entry Plane : B_2 = 11·600

Position of Exit Plane : B_1 = 11·121

Undrawn Diameter = 1·1874/1·1871 in

Drawn Diameter = 1·0010/1·0007 in

Initial grid spacing (δ_2) = 0·050 in.

Final grid spacing (δ_1) = 0·07036 in

Lubricant: SOAP

TABLE NO. A7.7

(SEE SECTION 10.4)

grid no. n	A_n (in)	δ (in)	$\frac{v}{V}\left(=\frac{\delta}{\delta_1}\right)$	$A_n + \delta/2$	$A_n + \delta/2 - 7.180$
6	6·73643	·07038	1·000	6·772	−0·408
7	6·80681	·07065	1·004	6·842	−0·338
8	6·87746	·06980	0·992	6·912	−0·268
9	6·94726	·07096	1·009	6·983	−0·197
10	7·01822	·07076	1·006	7·054	−0·126
11	7·08898	·07016	0·997	7·124	−0·056
12	7·15914	·06485	0·922	7·192	+0·012
13	7·22399	·06265	0·890	7·255	0·075
14	7·28664	·06221	0·884	7·318	0·138
15	7·34885	·06060	0·861	7·379	0·199
16	7·40945	·05953	0·846	7·439	0·259
17	7·46895	·05853	0·832	7·498	0·318
18	7·52751	·05707	0·811	7·556	0·376
19	7·58458	·05648	0·803	7·613	0·433
20	7·64106	·05556	0·790	7·669	0·489
21	7·69662	·05476	0·778	7·724	0·544
22	7·75138	·05379	0·764	7·778	0·598
23	7·80517	·05275	0·750	7·832	0·652
24	7·85792	·05195	0·738	7·884	0·704
25	7·90987	·05138	0·730	7·936	0·756
26	7·96125	·05073	0·721	7·987	0·807
27	8·01198	·05012	0·712	8·037	0·857
28	8·06210	·05003	0·711	8·087	0·907
29	8·11213	·05013	0·713	8·137	0·957
30	8·16226	·04993	0·710	8·187	1·007
31	8·21219				

Position of Entry Plane: A_2 = 7·92 ± 0·01

Position of Exit Plane: A_1 = 7·18 ± 0·01

grid no. n	B_n (in)	δ (in)	$\frac{v}{V}\left(=\frac{\delta}{\delta_1}\right)$	$B_n + \delta/2$	$B_n + \delta/2 - 7.270$
13	6·88046	·07017	0·997	6·916	−0·354
14	6·95063	·07039	1·000	6·986	−0·284
15	7·02102	·07010	0·996	7·056	−0·214
16	7·09112	·07033	1·000	7·126	−0·144
17	7·16145	·07045	1·001	7·197	−0·073
18	7·23190	·06729	0·956	7·266	−0·004
19	7·29919	·06266	0·891	7·331	+0·061
20	7·36185	·06232	0·886	7·393	0·123
21	7·42417	·06075	0·863	7·455	0·185
22	7·48492	·05970	0·848	7·515	0·245
23	7·54462	·05869	0·834	7·574	0·304
24	7·60331	·05776	0·821	7·632	0·362
25	7·66107	·05634	0·801	7·689	0·419
26	7·71741	·05592	0·795	7·745	0·475
27	7·77333	·05448	0·774	7·801	0·531
28	7·82781	·05442	0·773	7·855	0·585
29	7·88223	·05327	0·757	7·909	0·639
30	7·93550	·05198	0·739	7·961	0·691
31	7·98748	·05174	0·735	8·013	0·743
32	8·03922	·05105	0·726	8·065	0·795
33	8·09027	·05041	0·716	8·115	0·845
34	8·14068	·05004	0·711	8·166	0·896
35	8·19072	·05000	0·711	8·216	0·946
36	8·24072	·05003	0·711	8·266	0·996
37	8·29075	·05006	0·712	8·316	1·046
38	8·34081	·04999	0·711	8·366	1·096
39	8·39080				

Position of Entry Plane: B_2 = 8·02 ± 0·01

Position of Exit Plane: B_1 = 7·27 ± 0·01

Undrawn Diameter = 1·1874/1·1871 in

Drawn Diameter = 1·0010/1·0007 in

Initial grid spacing (δ_2) = 0·050 in.

Final grid Spacing (δ_1) = 0·07036 in

Lubricant: OIL

TABLE NO. A78

(SEE SECTION 10.4)

grid no. n	A_n (in)	δ (in)	$\frac{v}{V}\left(=\frac{\delta}{\delta_1}\right)$	$A_n + \delta/2$	$A_n + \delta/2 - 10{\cdot}472$
1	9·91603	·07006	0·996	9·951	−0·521
2	9·98609	·06979	0·992	10·021	−0·451
3	10·05588	·07115	1·011	10·091	−0·381
4	10·12703	·06882	0·978	10·161	−0·311
5	10·19585	·07071	1·005	10·231	−0·241
6	10·26656	·07078	1·006	10·302	−0·170
7	10·33734	·06951	0·988	10·372	−0·100
8	10·40685	·06977	0·992	10·442	−0·030
9	10·47662	·06533	0·929	10·509	+0·037
10	10·54195	·06266	0·891	10·573	0·101
11	10·60461	·06121	0·870	10·635	0·163
12	10·66582	·06017	0·855	10·696	0·224
13	10·72599	·05919	0·841	10·756	0·284
14	10·78518	·05778	0·821	10·814	0·342
15	10·84296	·05752	0·818	10·872	0·400
16	10·90048	·05608	0·797	10·929	0·457
17	10·95656	·05547	0·788	10·984	0·512
18	11·01203	·05396	0·767	11·039	0·567
19	11·06599	·05402	0·768	11·093	0·621
20	11·12001	·05235	0·744	11·146	0·674
21	11·17236	·05182	0·736	11·198	0·726
22	11·22418	·05139	0·730	11·250	0·778
23	11·27557	·05075	0·721	11·301	0·829
24	11·32632	·05011	0·712	11·351	0·879
25	11·37643	·05003	0·711	11·401	0·929
26	11·42646	·05007	0·712	11·451	0·979
27	11·47653	·05010	0·712	11·502	1·030
28	11·52663	·04999	0·710	11·552	1·080
29	11·57662	·04993	0·710	11·602	1·130
30	11·62655				

Position of Entry Plane: A_2 = 11·224

Position of Exit Plane: A_1 = 10·472

grid no. n	B_n (in)	δ (in)	$\frac{v}{V}\left(=\frac{\delta}{\delta_1}\right)$	$B_n + \delta/2$	$B_n + \delta/2 - 10{\cdot}769$
1	10·23698	·07024	0·998	9·936	−0·497
2	10·30722	·07044	1·001	10·006	−0·427
3	10·37766	·07027	0·999	10·077	−0·356
4	10·44793	·06989	0·993	10·147	−0·286
5	10·51782	·07016	0·997	10·217	−0·216
6	10·58798	·07014	0·997	10·287	−0·146
7	10·65812	·07042	1·001	10·357	−0·076
8	10·72854	·06921	0·984	10·427	−0·006
9	10·79775	·06333	0·900	10·493	+0·060
10	10·86108	·06265	0·890	10·556	0·123
11	10·92373	·06098	0·867	10·618	0·185
12	10·98471	·05950	0·846	10·679	0·246
13	11·04421	·05884	0·836	10·738	0·305
14	11·10305	·05801	0·824	10·796	0·363
15	11·16106	·05684	0·808	10·854	0·421
16	11·21790	·05586	0·794	10·910	0·477
17	11·27376	·05505	0·782	10·965	0·532
18	11·32881	·05409	0·769	11·020	0·587
19	11·38290	·05302	0·754	11·073	0·640
20	11·43592	·05225	0·743	11·126	0·693
21	11·48817	·05158	0·733	11·178	0·745
22	11·53975	·05093	0·724	11·229	0·796
23	11·59072	·05054	0·718	11·280	0·847
24	11·64126	·04996	0·710	11·330	0·897
25	11·69122	·05011	0·712	11·380	0·947
26	11·74133	·05009	0·712	11·430	0·997
27	11·79142	·04990	0·709	11·480	1·047
28	11·84132	·05006	0·711	11·530	1·097
29	11·89138	·05006	0·711	11·580	1·147
30	11·94144				

Position of Entry Plane: B_2 = 11·525

Position of Exit Plane: B_1 = 10·769

Undrawn Diameter = 1.2473/1.2469 in
Drawn Diameter = 1.0010/1.0007 in
Initial grid spacing (δ_2) = 0.050 in.
Final grid spacing (δ_1) = 0.07763 in
Lubricant: SOAP

TABLE NO. A7.9

(SEE SECTION 10.4)

grid no. n	A_n (in)	δ (in)	$\frac{v}{V}\left(=\frac{\delta}{\delta_1}\right)$	$A_n + \delta/2$	$A_n + \delta/2 - 11.867$
1	11.13935	.07750	0.998	11.294	−0.573
5	11.44935	.07733	0.996	11.488	−0.379
6	11.52668	.07776	1.002	11.566	−0.301
7	11.60444	.07763	1.000	11.643	−0.224
8	11.68207	.07730	0.996	11.721	−0.146
9	11.75937	.07745	0.998	11.798	−0.069
10	11.83682	.07473	0.963	11.874	+0.007
11	11.91155	.07057	0.909	11.947	0.080
12	11.98212	.06859	0.884	12.016	0.149
13	12.05071	.06657	0.858	12.084	0.217
14	12.11728	.06578	0.847	12.150	0.283
15	12.18306	.06378	0.822	12.215	0.348
16	12.24684	.06293	0.811	12.278	0.411
17	12.30977	.06181	0.796	12.341	0.474
18	12.37158	.06027	0.776	12.402	0.535
19	12.43185	.05911	0.761	12.461	0.594
20	12.49096	.05802	0.747	12.520	0.653
21	12.54898	.05693	0.733	12.577	0.710
22	12.60591	.05596	0.721	12.634	0.767
23	12.66187	.05482	0.706	12.689	0.822
24	12.71669	.05376	0.693	12.744	0.877
25	12.77045	.05256	0.677	12.797	0.930
26	12.82301	.05184	0.668	12.849	0.982
27	12.87485	.05102	0.657	12.900	1.033
28	12.92587	.05043	0.650	12.951	1.084
29	12.97630	.05013	0.646	13.001	1.134
30	13.02643	.04996	0.644	13.051	1.184
31	13.07639	.05009	0.645	13.101	1.234
32	13.12648	.04997	0.644	13.151	1.284
33	13.17645	.04989	0.643	13.201	1.334
34	13.22634	.05015	0.646	13.251	1.384
35	13.27649				

Position of Entry Plane: A_2 = 12.875
Position of Exit Plane: A_1 = 11.867

grid no. n	B_n (in)	δ (in)	$\frac{v}{V}\left(=\frac{\delta}{\delta_1}\right)$	$B_n + \delta/2$	$B_n + \delta/2 - 11.874$
1	11.15140	.07747	0.998	11.306	−0.568
5	11.46128	.07759	0.999	11.500	−0.374
6	11.53887	.07749	0.998	11.578	−0.296
7	11.61636	.07759	0.999	11.655	−0.219
8	11.69395	.07710	0.993	11.732	−0.142
9	11.77105	.07754	0.999	11.810	−0.064
10	11.84859	.07415	0.955	11.886	+0.012
11	11.92274	.07030	0.906	11.958	0.084
12	11.99304	.06844	0.882	12.027	0.153
13	12.06148	.06641	0.855	12.095	0.221
14	12.12789	.06493	0.836	12.160	0.286
15	12.19282	.06414	0.826	12.225	0.351
16	12.25696	.06254	0.806	12.288	0.414
17	12.31950	.06142	0.791	12.350	0.476
18	12.38092	.05987	0.771	12.411	0.537
19	12.44079	.05913	0.762	12.470	0.596
20	12.49992	.05787	0.745	12.529	0.655
21	12.55779	.05670	0.730	12.586	0.712
22	12.61449	.05597	0.721	12.642	0.768
23	12.67046	.05465	0.704	12.698	0.824
24	12.72511	.05366	0.691	12.752	0.878
25	12.77877	.05297	0.682	12.805	0.931
26	12.83174	.05184	0.668	12.858	0.984
27	12.88358	.05114	0.659	12.909	1.035
28	12.93472	.05057	0.651	12.960	1.086
29	12.98529	.05003	0.644	13.010	1.136
30	13.03532	.05008	0.645	13.060	1.186-
31	13.08540	.05002	0.644	13.110	1.236
32	13.13542	.04991	0.643	13.160	1.286
33	13.18533	.05004	0.645	13.210	1.336
34	13.23537				

Position of Entry Plane: B_2 = 12.884
Position of Exit Plane: B_1 = 11.874

Undrawn Diameter = 1.3122/1.3118 in

Drawn Diameter = 1.0000/0.9998 in

Initial grid spacing (δ_2) = 0.050 in.

Final grid spacing (δ_1) = 0.08608 in

Lubricant: SOAP

TABLE NO. A7.10

(SEE SECTION 10.4)

grid no. n	A_n (in)	δ (in)	$\frac{v}{V}\left(=\frac{\delta}{\delta_1}\right)$	$A_n + \delta/2$	$A_n + \delta/2 - 12.016$	grid no. n	B_n (in)	δ (in)	$\frac{v}{V}\left(=\frac{\delta}{\delta_1}\right)$	$B_n + \delta/2$	$B_n + \delta/2 - 12.048$
5	11.53302	.08591	0.998	11.576	−0.440	5	11.58221	.08671	1.007	11.626	−0.422
6	11.61893	.08607	1.000	11.662	−0.354	6	11.66892	.08626	1.002	11.712	−0.336
7	11.70500	.08633	1.003	11.748	−0.268	7	11.75518	.08653	1.005	11.798	−0.250
8	11.79133	.08605	1.000	11.834	−0.182	8	11.84171	.08465	0.983	11.884	−0.164
9	11.87738	.08535	0.991	11.920	−0.096	9	11.92636	.08531	0.991	11.969	−0.079
10	11.96273	.08408	0.977	12.005	−0.011	10	12.01167	.08271	0.961	12.053	+0.005
11	12.04681	.07824	0.909	12.086	+0.070	11	12.09438	.07837	0.910	12.134	0.086
12	12.12505	.07613	0.884	12.163	0.147	12	12.17275	.07506	0.872	12.210	0.162
13	12.20118	.07347	0.853	12.238	0.222	13	12.24781	.07294	0.847	12.284	0.236
14	12.27465	.07243	0.841	12.311	0.295	14	12.32075	.07198	0.836	12.357	0.309
15	12.34708	.07019	0.815	12.382	0.366	15	12.39273	.07021	0.816	12.428	0.380
16	12.41727	.06902	0.802	12.452	0.436	16	12.46294	.06841	0.795	12.497	0.449
17	12.48629	.06689	0.777	12.520	0.504	17	12.53135	.06676	0.776	12.565	0.517
18	12.55318	.06531	0.759	12.586	0.570	18	12.59811	.06581	0.764	12.631	0.583
19	12.61849	.06377	0.741	12.650	0.634	19	12.66392	.06365	0.739	12.696	0.648
20	12.68226	.06243	0.725	12.713	0.697	20	12.72757	.06193	0.719	12.759	0.711
21	12.74469	.06087	0.707	12.775	0.759	21	12.78950	.06085	0.707	12.820	0.772
22	12.80556	.05937	0.690	12.835	0.819	22	12.85035	.05943	0.690	12.880	0.832
23	12.86493	.05803	0.674	12.894	0.878	23	12.90978	.05807	0.675	12.939	0.891
24	12.92296	.05706	0.663	12.951	0.935	24	12.96785	.05712	0.664	12.996	0.948
25	12.98002	.05614	0.652	13.008	0.992	25	13.02497	.05611	0.652	13.053	1.005
26	13.03616	.05516	0.641	13.064	1.048	26	13.08108	.05500	0.639	13.109	1.061
27	13.09132	.05395	0.627	13.118	1.102	27	13.13608	.05377	0.625	13.163	1.115
28	13.14527	.05305	0.616	13.172	1.156	28	13.18985	.05280	0.613	13.216	1.168
29	13.19832	.05194	0.603	13.224	1.208	29	13.24265	.05167	0.600	13.268	1.220
30	13.25026	.05109	0.593	13.276	1.260	30	13.29432	.05109	0.593	13.320	1.272
31	13.30135	.05065	0.588	13.327	1.311	31	1334541	.05039	0.585	13.371	1.323
32	13.35200	.04999	0.581	13.377	1.361	32	13.39580	.04996	0.580	13.421	1.373
33	13.40199	.05001	0.581	13.427	1.411	33	13.44576	.05012	0.582	13.471	1.423
34	13.45200	.05011	0.582	13.477	1.461	34	13.49588	.05004	0.581	13.521	1.473
35	13.50211	.04999	0.581	13.527	1.511	35	13.54592	.05008	0.582	13.571	1.523
36	13.55210	.05006	0.582	13.577	1.561	36	13.59600	.05000	0.581	13.621	1.573
37	13.60216					37	13.64600				

Position of Entry Plane: A_2 = 13.268

Position of Exit Plane: A_1 = 12.016

Position of Entry Plane: B_2 = 13.299

Position of Exit Plane: B_1 = 12.048

Nominal Diameter of Bar :- $1\frac{1}{16}$ in.

Lubricant :- Soap

Supply Voltage to Load-Cell :- 6.998/7.002 v (all tests)

TABLE No. A7.11

(see section 10.6.5)

Test no.	Galvanometer Deflections during Drawing Tests (in)														
	Rotational Speed			Drawing Speed				Torque				Drawing Force			
	R'	R''	R_d	$\hat{V}$	V'	V''	V_d	$\hat{T}$	T'	T''	T_d	P_c	P'	P_d	P_c
1	1.745 →		1.752	0.558	0.305 →			0.884	0.752 →		0.740	0.830	0.675	0.675	0.830
2	1.755 →		1.759	1.675	1.652 →		1.657		0.561 →		0.518	0.861	0.790	0.724	0.851
3	1.759 →		1.764	3.397 →					0.360 →		0.300	0.865	0.841	0.816	0.847
4	1.754 →		1.760	5.071 →					0.238 →		0.235	0.851	0.841	0.836	0.855
5	1.755 →		1.752	0.540	0.306 →			0.870	0.743 →		0.744	0.830	0.687	0.680	0.816
6	1.753 →		1.760	1.168	1.029 →				0.642 →		0.632	0.838	0.746	0.731	0.829
7	1.750 →		1.758	1.150	1.073 →			0.646	0.620 →		0.602	0.830	0.732	0.730	0.824
8	1.753 →		1.759	4.145 →			4.133		0.282 →		0.280	0.864	0.842	0.844	0.859
9	2.559 →		2.579	0.620	0.318 →			0.944	0.744 →		0.729	0.833	0.679	0.669	0.828
10	2.575 →		2.585	1.675	1.644 →			0.630	0.611 →		0.582	0.865	0.762	0.762	0.860
11	2.580 →		2.590	3.395 →			3.397		0.426 →		0.420	0.861	0.820	0.815	0.862
12	2.585 →		2.591	5.085 →			5.078		0.321 →		0.325	0.863	0.835	0.838	0.862
13	2.565 →		2.575	0.640	0.318 →		0.329	0.973	0.780 →		0.738	0.843	0.680	0.674	0.833
14	2.560 →		2.569	1.216	1.046 →			0.752	0.662 →		0.647	0.846	0.730	0.727	0.845
15	2.564 →		2.575	2.511	2.483 →		2.473		0.532 →		0.522	0.861	0.796	0.811	0.874
16	2.567 →		2.579	4.293	4.265 →		4.253		0.340 →		0.379	0.892	0.862	0.850	0.883
17	3.357 →		3.382	?	0.307 →			1.023	0.800 →		0.702	0.852	0.695	0.676	0.849
18	3.366 →		3.384	1.632	1.626 →			0.708	0.660 →		0.635	0.882	0.767	0.764	0.866
19	3.355 →		3.382	3.383	3.361 →		3.355	0.510	0.495 →		0.486	0.869	0.835	0.823	0.887
20	3.365 →		3.380	5.042 →			5.048		0.390 →		0.384	0.912	0.871	0.864	0.903
21	3.360 →		3.375	0.644	0.315 →			1.030	0.756 →		0.742	0.891	0.722	0.715	0.841
22	3.370 →		3.384	1.278	1.064 →			0.784	0.690 →		0.659	0.903	0.765	0.767	0.842
23	3.370 →		3.378	2.503	2.454 →				0.609 →		0.565	0.932	0.848	0.847	0.914
24	3.361 →		3.383	4.251	4.210 →				0.451 →		0.440	0.926	0.879	0.871	0.925
25	0.920 →		0.927	0.476	0.275 →			0.798	0.773 →		0.741	0.858	0.723	0.720	0.856
26	0.929 →		0.929	1.676 →					0.395 →		0.382	0.887	0.856	0.854	0.888
27	0.930 →		0.930	3.414 →					0.209 →		0.196	0.846	0.884	0.880	0.895
28	0.930 →		0.935	5.084 →					0.136 →		0.131	0.893 →		0.892	0.900
29	0.931 →		0.935	0.469	0.293 →			0.798	0.793 →		0.782	0.872	0.740	0.732	0.870
30	0.937 →		0.937	1.082	1.013 →				0.543 →		0.529	0.875	0.816	0.804	0.872
31	0.940 →		0.940	2.504 →					0.276 →		0.264	0.876	0.850	0.854	0.872
32	0.939 →		0.935	4.265 →			4.261		0.160 →		0.149	0.880	0.874	0.867	0.884
33	0.443 →		0.452	0.382	0.284 →				0.655 →		0.645	0.875	0.743	0.790	0.875
34	0.452 →		0.452	1.626 →					0.212 →		0.210	0.848	0.886	0.841	0.900
35	0.452 →		0.452	3.386 →					0.102 →		0.100	0.910 →		0.910	0.911
36	0.457 →		0.457	5.065 →					0.065 →		0.064	0.912 →		0.913	0.920
37	0.448 →		0.455	0.404	0.310 →				0.660 →		0.641	0.896	0.815	0.812	0.886
38	0.458 →		0.458	1.004 →					0.349 →		0.343	0.916	0.893	0.887	0.905
39	0.459 →		0.459	2.473 →					0.147 →		0.143	0.910 →		0.900	0.899
40	0.460 →		0.460	4.240 →			4.233		0.083 →		0.080	0.915 →		0.900	0.895

Galvanometer Deflections during Calibration (in) - Corrected to 7.000 volts

Rotational Speed	4.590 (tests no. 1 to 24)	Torque	4.194 (tests no. 1 to 24)
	4.584 (tests no. 25 to 40)		4.201 (tests no. 25 to 40)
Drawing Speed	4.530 (tests no. 1 to 24)	Drawing Force	4.076 (tests no. 1 to 24)
	4.533 (tests no. 25 to 40)		4.078 (tests no 25 to 40)

Nominal Diameter of Bar :- $1\frac{1}{8}$ in.	TABLE No. A7.12
Lubricant :- Soap	
Supply Voltage to Load-Cell :- 6.999/7.003 v (all tests)	(see section 10.6.5)

Test no.	Galvanometer Deflections during Drawing Tests (in)														
	Rotational Speed			Drawing Speed				Torque				Drawing Force			
	R'	R''	R_d	$\hat{V}$	V'	V''	V_d	$\hat{T}$	T'	T''	T_d	P_e	P'	P_d	P_c
161	1.024	→	1.024	0.436	0.259	→	→	0.988	0.952	0.900	0.884	1.481	1.333	1.324	1.474
162	1.024	→	1.027	1.595	→	→	1.584		0.571	→	0.557	1.527	1.485	1.481	1.531
163	1.026	→	1.026	3.356	→	→	→		0.326	→	0.318	1.562	1.541	1.533	1.545
164	1.027	→	1.027	5.046	→	→	→		0.211	→	0.207	1.558	1.541	1.532	1.553
165	1.018	→	1.023	0.489	0.277	→	→	0.991	0.965	0.916	0.900	1.472	1.321	1.315	1.451
166	1.022	→	1.022	1.081	0.982	→	0.993		0.719	→	0.715	1.497	1.422	1.413	1.486
167	1.031	→	1.031	2.487	2.449	→	→		0.405	→	0.395	1.515	1.481	1.480	1.506
168	1.031	→	1.031	4.242	→	→	4.234		0.256	→	0.256	1.524	1.512	1.511	1.505
169	2.708	→	2.715	0.901	0.662	→	→	1.169	0.943	0.909	0.878	1.501	1.326	1.324	1.483
170	2.714	→	2.721	1.655	1.581	→	→	0.901	0.840	0.837	0.830	1.517	1.399	1.398	1.520
171	2.711	→	2.721	3.394	3.384	→	3.369		0.656	→	0.639	1.542	1.484	1.473	1.541
172	2.720	→	2.728	5.049	→	→	→		0.502	→	0.486	1.547	1.511	1.499	1.538
173	2.701	→	2.715	0.939	0.678	→	→	1.135	0.927	0.906	0.859	1.475	1.320	1.307	1.464
174	2.705	→	2.710	1.212	1.027	→	→	0.985	0.882	0.862	0.838	1.488	1.350	1.335	1.491
175	2.707	→	2.715	2.523	2.426	→	→	0.762	0.749	→	0.733	1.513	1.422	1.423	1.504
176	2.707	→	2.720	4.254	4.240	→	4.220		0.554	→	0.540	1.515	1.468	1.460	1.507
177	0.443	→	0.461	0.411	0.305	→	→		0.765	→	0.762	1.462	1.381	1.374	1.463
178	0.466	→	0.466	1.569	→	→	1.561		0.304	→	0.300	1.506	1.496	1.496	1.508
179	0.470	→	0.470	3.338	→	→	→		0.152	→	0.148	1.536	→	1.534	1.526
180	0.469	→	0.469	5.031	→	→	→		0.094	→	0.091	1.544	→	1.535	1.532
181	0.456	→	0.462	0.414	0.330	→	0.324		0.859	→	0.853	1.456	1.367	1.362	1.447
182	0.464	→	0.464	1.111	→	→	1.002		0.427	→	0.421	1.480	1.444	1.440	1.469
183	0.470	→	0.467	2.405	→	→	2.395		0.205	→	0.201	1.498	→	1.487	1.482
184	0.472	→	0.472	4.211	→	→	→		0.119	→	0.110	1.496	→	1.484	1.490
185	1.735	→	1.748	0.579	0.335	→	→	1.084	0.940	0.887	0.859	1.456	1.303	1.291	1.449
186	1.746	→	1.756	1.617	1.554	→	1.532	0.774	0.751	→	0.728	1.503	1.418	1.410	1.497
187	1.756	→	1.756	3.312	→	→	→		0.496	→	0.485	1.527	1.494	1.488	1.518
188	1.760	→	1.760	5.010	→	→	→		0.355	→	0.349	1.534	1.519	1.512	1.533
189	1.738	→	1.750	0.604	0.351	→	→	1.115	0.960	0.921	0.888	1.461	1.300	1.290	1.455
190	1.746	→	1.752	1.116	1.025	→	→	0.865	0.841	0.828	0.815	1.495	1.378	1.372	1.480
191	1.750	→	1.750	2.408	2.385	→	2.364		0.610	→	0.600	1.506	1.457	1.451	1.504
192	1.757	→	1.757	4.168	→	→	4.174		0.408	→	0.406	1.525	1.494	1.490	1.504
193	4.375	4.395	4.410	0.971	0.676	→	0.669	1.258	1.020	0.868	0.842	1.476	1.294	1.284	1.462
194	4.392	→	4.418	1.652	1.542	→	→	1.047	0.874	0.861	0.820	1.499	1.349	1.347	1.497
195	4.401	→	4.417	4.407	3.329	→	3.318	0.807	0.768	→	0.745	1.520	1.421	1.418	1.521
196	4.408	→	4.420	5.078	5.024	→	5.015	0.660	0.635	→	0.633	1.530	1.455	1.461	1.526
197	4.397	4.410	4.423	0.988	0.704	→	0.704	1.267	0.926	0.874	0.831	1.472	1.300	1.276	1.462
198	4.405	→	4.423	1.311	1.038	→	→	1.146	0.905	0.867	0.819	1.477	1.313	1.300	1.463
199	4.414	→	4.425	2.520	2.410	→	2.421	0.894	0.806	→	0.776	1.495	1.370	1.363	1.489
200	4.417	→	4.427	4.290	4.223	→	4.213	0.704	0.677	→	0.678	1.501	1.421	1.415	?

Galvanometer Deflections during Calibration (in) - Corrected to 7.000 volts

Rotational Speed	4.585 (tests no. 161 to 168)	Torque	4.209 (tests no. 161 to 168)
	4.585 (tests no. 169 to 200)		4.204 (tests no. 169 to 200)
Drawing Speed	4.543 (tests no. 161 to 168)	Drawing Force	4.081 (tests no. 161 to 168)
	4.541 (tests no. 169 to 200)		4.083 (tests no. 169 to 200)

Nominal Diameter of Bar :- $1\frac{3}{16}$ in.

Lubricant :- Soap

Supply Voltage to Load-Cell :- 6·998/7·000 v (tests no. 41 to 56); 6·995 v (tests no. 57 to 80)

TABLE No. A7.13

(see section 10.6.5)

Galvanometer Deflections during Drawing Tests (in)

Test no.	Rotational Speed			Drawing Speed				Torque				Drawing Force			
	R'	R''	R_d	$\hat{V}$	V'	V''	V_d	$\hat{T}$	T'	T''	T_d	P_c	P'	P_d	P_e
41	0·998	→	1·004	0·590	0·355	→	0·348	1·529	1·490	1·456	1·482	2·095	1·865	1·854	2·080
42	1·010	→	1·015	1·602	→	→	1·587		0·922	→	0·868	2·134	2·056	2·032	2·132
43	1·021	→	1·021	3·313	→	→	→		0·528	→	0·528	2·138	2·118	2·104	2·157
44	1·020	→	1·020	4·999	→	→	→		0·380	→	0·353	2·154	→	2·141	2·152
45	1·004	→	1·004	0·598	0·338	→	→	1·563	1·504	1·476	1·438	2·078	1·862	1·840	2·084
46	1·005	→	1·010	1·888	1·095	→	→		1·231	→	1·126	2·143	2·012	1·985	2·095
47	1·015	→	1·015	2·385	→	→	2·382		0·730	→	0·705	2·120	2·078	2·069	2·113
48	1·018	→	1·021	4·213	→	→	4·210		0·459	→	0·437	2·140	2·120	2·100	2·126
49	2·735	2·745	2·750	0·730	0·307	→	→	1·851	1·412	1·345	1·415	2·034	1·782	1·730	2·010
50	2·739	→	2·743	1·702	1·561	→	1·575	1·342	1·259	1·246	1·312	2·082	1·913	1·916	2·084
51	2·743	→	2·754	3·357	3·339	→	3·305		1·062	→	1·005	2·145	2·037	2·023	2·134
52	2·763	→	2·767	5·037	4·994	→	4·987		0·827	→	0·810	2·155	2·096	2·091	2·161
53	2·710	2730	2·736	0·776	0·330	→	0·335	1·992	1·534	1·424	1·410	2·073	1·798	1·749	2·068
54	2·725	→	2·741	1·344	1·066	→	→	1·574	1·428	1·380	1·312	2·112	1·885	1·868	2·067
55	2·726	→	2·736	?	2·363	→	2·369	1·249	1·243	1·239	1·200	2·136	1·990	1·984	2·140
56	2·735	→	2·747	?	4·156	→	4·150		0·962	→	0·974	2·165	2·085	2·086	2·167
57	0·434	→	0·454	0·410	0·312	→	0·304		1·068	→	1·072	1·985	1·864	1·845	1·983
58	0·455	→	0·455	1·533	→	→	1·548		0·451	→	0·455	2·024	2·013	2·006	2·024
59	0·466	→	0·466	3·266	→	→	→		0·225	→	0·240	2·042	→	2·046	2·050
60	0·466	→	0·466	4·970	→	→	→		0·148	→	0·160	2·080	→	2·070	2·067
61	0·450	→	0·450	0·431	0·314	→	→		1·097	→	1·141	1·983	1·852	1·862	1·991
62	0·451	→	0·455	1·044	1·023	→	→		0·676	→	0·693	2·046	2·006	2·012	2·040
63	0·457	→	0·457	2·347	→	→	→		0·318	→	0·334	2·068	→	2·094	2·086
64	0·458	→	0·458	4·143	→	→	→		0·195	→	0·187	2·126	→	2·115	2·125
65	1·723	1·733	1·738	0·649	0·307	→	→	1·667	1·396	1·356	1·356	2·035	1·803	1·766	2·016
66	1·731	→	1·738	1·596	1·530	→	1·539		1·169	→	1·197	2·086	1·955	1·954	2·092
67	1·748	→	1·748	3·278	→	→	3·266		0·820	→	0·829	2·146	2·095	2·110	2·140
68	1·754	→	1·754	4·975	→	→	→		0·528	→	0·539	2·125	2·095	2·107	2·126
69	1·737	→	1·745	0·695	0·332	→	→	1·669	1·446	1·378	1·356	2·050	1·811	1·785	2·030
70	1·745	→	1·745	1·225	1·041	→	1·046	1·301	1·270	1·262	1·274	2·077	1·896	1·883	2·042
71	1·750	→	1·750	2·435	2·370	→	2·364		0·964	→	0·930	2·082	1·992	1·986	2·061
72	1·755	→	1·755	4·192	4·168	→	→		0·595	→	0·616	2·075	2·034	2·037	2·067
73	4·349	4·375	4·387	0·753	0·325	→	→	2·020	1·341	1·217	1·261	2·015	1·769	1·705	1·985
74	4·356	→	4·372	1·724	1·524	→	→	1·490	1·290	→	1·284	2·064	1·860	1·840	2·059
75	4·365	→	4·376	3·379	3·256	→	→		1·166	→	1·145	2·094	1·948	1·946	2·110
76	4·352	→	4·392	5·048	5·028	→	4·957		1·051	→	1·040	2·145	2·030	2·027	2·142
77	4·342	4·374	4·401	0·880	0·339	→	0·350	2·159	1·433	1·316	1·218	2·040	1·772	1·713	1·996
78	4·370	4·380	4·395	1·365	1·063	→	→	1·681	1·255	1·238	1·212	2·045	1·823	1·795	2·030
79	4·361	→	4·375	2·482	2·352	→	→	1·319	1·252	→	1·254	2·074	1·898	1·880	2·067
80	4·373	→	4·402	4·320	4·202	→	4·186		1·040	→	1·022	2·085	1·967	1·956	2·095

Galvanometer Deflections during Calibration (in) - Corrected to 7·000 volts

Rotational Speed :- 4·586 (all tests)	Torque :- 4·198 (all tests)
Drawing Speed :- 4·541 (all tests)	Drawing Force :- 4·093 (all tests)

Nominal Diameter of Bar :- $1\frac{1}{4}$ in.

Lubricant :- Soap

Supply Voltage to Load-Cell :- 6·999/7·002 v (all tests)

TABLE No. A7.14

(see section 10.6.5)

Galvanometer Deflections during Drawing Tests (in)

Test no.	Rotational Speed			Drawing Speed				Torque				Drawing Force			
	R'	R''	R_d	$\hat{V}$	V'	V''	V_d	$\hat{T}$	T'	T''	T_d	P_c	P'	P_d	P_e
81	1·046	→	1·053	0·588	0·312	→	→	1·965	1·870	1·834	1·765	2·788	2·516	2·488	2·767
82	1·060	→	1·060	1·640	1·605	→	1·584		1·199	→	1·220	2·842	2·747	2·750	2·835
83	1·068	→	1·068	3·266	→	→	→		0·739	→	0·741	2·885	2·852	2·852	2·894
84	1·076	→	1·081	4·959	→	→	→		0·538	→	0·520	2·915	2·894	2·875	2·894
85	1·053	→	1·053	0·681	0·365	→	0·356	1·968	1·862	1·834	1·838	2·802	2·534	2·504	2·792
86	1·057	→	1·057	1·445	1·070	→	1·084		1·573	→	1·546	2·842	2·676	2·666	2·834
87	1·067	→	1·067	2·383	→	→	→		1·009	→	0·975	2·868	2·802	2·790	2·850
88	1·076	→	1·076	4·152	→	→	4·147		0·615	→	0·619	2·880	2·843	2·854	2·884
89	2·685	→	2·685	1·335	0·746	→	0·774	2·145	1·814	→	1·900	2·812	2·495	2·475	2·812
90	2·695	→	2·695	1·797	1·593	→	1·584	1·842	1·754	→	1·815	2·870	2·603	2·603	2·874
91	2·696	→	2·685	3·352	3·327	→	3·266		1·467	→	1·480	2·920	2·768	2·763	2·908
92	2·722	→	2·722	?	4·968	→	→		1·203	→	1·191	2·946	2·852	2·845	2·962
93	2·686	→	2·686	1·270	0·778	→	0·770	2·340	1·912	→	2·016	2·866	2·538	2·510	2·856
94	2·686	→	2·694	1·453	1·151	→	1·135	2·195	1·981	→	2·010	2·913	2·685	2·576	2·894
95	2·678	→	2·686	?	2·380	→	2·364		1·834	→	1·786	2·952	2·731	2·732	2·932
96	2·712	→	2·712	4·226	4·188	→	4·154		1·399	→	1·388	2·974	2·854	2·852	2·954
97	0·423	→	0·430	0·433	0·329	→	→		1·745	→	1·841	2·894	2·686	2·677	2·886
98	0·445	→	0·452	1·583	→	→	→		0·745	→	0·760	2·966	2·930	2·932	2·964
99	0·452	→	0·462	3·263	→	→	→		0·395	→	0·371	3·010	2·995	2·985	2·992
100	0·458	→	0·458	4·949	→	→	4·959		0·246	→	0·247	3·031	→	2·999	3·026
101	0·434	→	0·434	0·477	0·360	→	→		1·736	→	1·762	2·918	2·727	2·716	2·908
102	0·437	→	0·437	1·108	1·073	→	→		1·030	→	1·009	2·960	2·898	2·896	2·954
103	0·443	→	0·443	2·332	→	→	2·326		0·535	→	0·536	2·994	2·980	2·985	2·972
104	0·447	→	0·447	4·130	→	→	→		0·305	→	0·306	3·019	→	3·004	3·008
105	1·736	→	1·745	0·915	0·375	→	→	2·271	2·028	2·003	2·107	2·898	2·545	2·510	2·884
106	1·755	→	1·748	1·650	1·546	→	1·526	1·814	1·779	→	1·837	2·968	2·750	2·752	2·950
107	1·775	→	1·775	3·296	3·235	→	→		1·272	→	1·284	2·988	2·894	2·895	2·982
108	1·786	→	1·792	4·953	4·946	→	→		0·948	→	0·936	3·025	2·966	2·956	3·009
109	1·750	→	1·757	0·857	0·405	→	→	2·347	2·050	2·018	2·150	2·879	2·550	2·520	2·875
110	1·750	→	1·750	1·404	1·125	→	1·134		1·920	→	2·004	2·928	2·676	2·677	2·936
111	1·759	→	1·759	2·405	2·333	→	2·322		1·595	→	1·583	2·989	2·838	2·835	2·982
112	1·774	→	1·785	4·178	4·120	→	→		1·081	→	1·056	2·997	2·930	2·924	2·990
113	4·326	→	4·343	1·306	0·786	→	0·780	2·293	1·698	→	1·716	2·779	2·449	2·406	2·753
114	4·305	→	4·337	1·780	1·563	→	1·556	2·060	1·804	→	1·789	2·830	2·518	2·504	2·832
115	4·330	→	4·350	3·462	3·290	→	3·244	1·689	1·657	→	1·601	2·877	2·662	2·653	2·856
116	4·350	→	4·386	5093	4·994	→	4·954		1·351	→	1·230	2·880	2·741	2·716	2·886
117	4·279	4·305	4·330	1·310	0·802	→	0·796	2·222	1·784	1·743	1·717	2·790	2·468	2·426	2·766
118	4·302	→	4·335	1·439	1·181	→	→	2·179	1·833	→	1·726	2·819	2·497	2·467	2·816
119	4·296	→	4·315	2·480	2·327	→	2·334	1·929	1·834	→	1·803	2·873	2·605	2·587	2·845
120	4·331	→	4·331	4·271	4·204	→	4·145		1·579	→	1·637	2·887	2·716	2·718	2·875

Galvanometer Deflections during Calibration (in) - Corrected to 7·000 volts

Rotational Speed :- 4·587 (all tests)	Torque :- 4·205 (all tests)
Drawing Speed :- 4·546 (all tests)	Drawing Force :- 4·095 (all tests)

Nominal Diameter of Bar :- $1\frac{5}{16}$ in.	TABLE No. A7.15
Lubricant :- Soap	(see section 10.6.5)
Supply Voltage to Load-Cell :- 7.000/7.002 v (all tests)	

Galvanometer Deflections during Drawing Tests (in)

Test no.	Rotational Speed			Drawing Speed				Torque				Drawing Force			
	R'	R''	R_d	$\hat{V}$	V'	V''	V_d	$\hat{T}$	T'	T''	T_d	P_c	P'	P_d	P_e
121	1.028	→	1.034	0.626	0.353	→	0.365	2.680	2.525	2.461	2.328	3.336	2.991	2.963	3.273
122	1.048	→	1.048	1.617	1.572	→	1.578		1.745	→	1.564	3.396	3.250	3.230	3.362
123	1.064	→	1.064	3.233	→	→	→		1.064	→	1.012	3.458	3.410	3.404	3.487
124	1.069	→	1.069	4.909	→	→	→		0.743	→	0.732	3.541	3.511	3.493	3.476
125	1.026	→	1.030	0.683	0.376	→	→	2.488	2.340	2.263	2.296	3.354	3.020	2.982	3.300
126	1.039	→	1.039	1.172	1.058	→	→		2.019	→	1.957	3.370	3.152	3.134	3.342
127	1.051	→	1.051	2.352	2.325	→	2.334		1.439	→	1.403	3.408	3.323	3.336	3.437
128	1.062	→	1.062	4.116	4.097	→	→		0.948	→	0.963	3.490	3.465	3.464	3.487
129	2.695	→	2.718	1.340	0.869	→	→	2.717	2.296	?	2.005	3.344	2.992	2.947	3.298
130	2.682	→	2.704	1.712	1.556	→	1.547	2.467	2.339	?	2.066	3.404	3.099	3.081	3.390
131	2.714	→	2.708	3.337	3.256	→	3.216		1.937	→	1.913	3.479	3.291	3.297	3.493
132	2.735	→	2.735	4.990	4.938	→	4.908		1.522	→	1.526	3.518	3.403	3.396	3.476
133	2.674	2.697	2.708	1.266	0.772	→	0.787	2.727	2.209	2.106	2.161	3.353	3.002	2.924	3.287
134	2.681	→	2.700	1.460	1.121	→	1.131	2.533	2.285	2.269	2.068	3.323	2.979	2.946	3.304
135	2.684	→	2.689	2.458	2.306	→	→		2.195	→	2.154	3.387	3.138	3.127	3.373
136	2.710	→	2.718	4.189	4.128	→	4.090		1.728	→	1.685	3.410	3.267	3.256	3.395
137	0.498	→	0.498	0.495	0.355	→	→		2.193	→	2.056	3.420	3.161	3.120	3.350
138	0.516	→	0.516	1.511	→	→	→		1.108	→	1.024	3.480	3.429	3.414	3.439
139	0.518	→	0.518	3.165	→	→	→		0.562	→	0.586	3.527	→	3.553	3.603
140	0.526	→	0.526	4.847	→	→	→		0.393	→	0.383	3.617	→	3.583	3.554
141	0.497	→	0.506	0.518	0.365	→	0.372	2.125	2.115	?	2.035	3.415	3.171	3.140	3.376
142	0.512	→	0.512	1.070	1.016	→	1.009		1.349	→	1.403	3.419	3.318	3.336	3.424
143	0.513	→	0.522	2.280	→	→	2.264		0.792	→	0.793	3.523	3.485	3.488	3.519
144	0.527	→	0.527	4.057	→	→	4.050		0.443	→	0.457	3.535	→	3.517	3.528
145	1.742	→	1.746	0.780	0.394	→	→	2.505	2.105	1.956	2.096	3.224	2.901	2.848	3.215
146	1.741	→	1.741	1.601	1.527	→	1.516	2.045	2.001	1.964	2.041	3.329	3.089	3.092	3.329
147	1.760	→	1.760	3.243	3.205	→	3.186		1.514	→	1.462	3.397	3.280	3.271	3.388
148	1.775	→	1.775	4.915	4.900	→	4.891		1.088	→	1.029	3.421	3.358	3.335	3.397
149	1.737	→	1.742	0.838	0.414	→	→	2.647	2.326	2.132	2.208	3.244	2.907	2.856	3.213
150	1.738	→	1.738	1.368	1.109	→	→	2.132	2.058	2.036	2.093	3.288	3.027	3.010	3.296
151	1.750	→	1.750	2.313	2.258	→	→		1.775	→	1.721	3.352	3.200	3.187	3.368
152	1.765	→	1.765	4.097	4.060	→	4.049		1.299	→	1.290	3.417	3.336	3.332	3.419
153	4.224	4.289	4.255	1.285	0.795	→	→	3.146	2.238	1.888	2.162	3.346	2.958	2.900	3.275
154	4.233	→	4.246	1.772	1.525	→	1.518	2.652	2.188	2.067	2.141	3.403	3.036	3.012	3.378
155	4.290	4.244	4.231	3.392	3.265	3.188	3.190	2.251	2.179	2.150	2.167	3.488	3.214	3.218	3.507
156	4.312	4.283	4.258	5.010	4.950	4.882	4.871	1.914	1.888	1.865	1.923	3.528	3.328	3.342	3.537
157	4.213	4.270	4.250	1.034	0.410	→	0.416	3.480	2.270	1.981	2.172	3.341	2.972	2.855	3.272
158	4.235	→	4.246	1.409	1.138	→	1.143	2.867	2.170	2.103	2.163	3.368	3.004	2.959	3.362
159	4.238	→	4.226	3.400	3.190	→	3.180	2.398	2.278	→	2.184	3.484	3.188	3.177	3.441
160	4.288	4.259	4.239	4.260	4.180	4.086	→	2.195	2.177	2.160	1.994	3.520	3.268	3.239	3.476

Galvanometer Deflections during Calibration (in) - Corrected to 7.000 volts

Rotational Speed :- 4.585 (all tests)	Torque :- 4.209 (all tests)
Drawing Speed :- 4.543 (all tests)	Drawing Force :- 4.081 (all tests)

Nominal Diameter of Bar :- $1\frac{1}{8}$ in.	TABLE No. A7.16
Lubricant :- Oil	(see section 10.6.5)
Supply Voltage to Load-Cell :- 7.001/7.003 v (all tests)	

Galvanometer Deflections during Drawing Tests (in)

Test no.	Rotational Speed			Drawing Speed				Torque				Drawing Force			
	R'	R''	R_d	$\hat{V}$	V'	V''	V_d	$\hat{T}$	T'	T''	T_d	P_c	P'	P_d	P_e
201.	0.455	→	0.460	0.448	0.348	→	→		1.495	→	1.449	1.670	1.491	1.479	1.667
202	0.472	→	0.474	1.598	→	→	→		0.600	→	0.580	1.728	1.711	1.696	1.701
203	0.474	→	0.474	3.347	→	→	3.354		0.295	→	0.288	1.749	1.741	1.736	1.749
204	0.471	→	0.474	5.043	→	→	5.031		0.190	→	0.192	1.755	1.752	1.741	1.757
205	0.455	→	0.461	0.504	0.388	→	0.378		1.557	→	1.505	1.722	1.529	1.513	1.703
206	0.462	→	0.465	1.120	1.099	→		0.840	0.826	→	0.806	1.745	1.682	1.671	1.718
207	0.469	→	0.475	2.406	→	→	2.414		0.420	→	0.410	1.747	1.732	1.723	1.738
208	0.474	→	0.474	4.209	→	→	4.216		0.233	→	0.228	1.730	1.724	1.714	1.723
209	1.015	→	1.015	0.662	0.373	→	→	1.771	1.729	1.677	1.638	1.652	1.351	1.333	1.622
210	1.031	→	1.032	1.611	→	→	1.619		1.140	→	1.075	1.705	1.612	1.591	1.694
211	1.036	→	1.042	3.375	→	→	→		0.624	→	0.610	1.731	1.696	1.686	1.726
212	1.037	→	1.037	5.049	→	→	→		0.422	→	0.406	1.740	1.722	1.715	1.728
213	1.010	→	1.015	0.695	0.393	→	→	1.853	1.815	1.729	1.625	1.681	1.385	1.372	1.675
214	1.018	→	1.026	1.240	1.112	→	1.119	1.371	1.345	→	1.352	1.714	1.565	1.569	1.717
215	1.030	→	1.030	2.449	2.431	→	→		0.836	→	0.793	1.752	1.693	1.679	1.733
216	1.041	→	1.041	4.236	→	→	→		0.499	→	0.494	1.742	1.727	1.718	1.739
217	1.726	→	1.735	0.781	0.375	→	→	1.982	1.844	1.666	1.557	1.682	1.343	1.321	1.672
218	1.728	→	1.728	1.672	1.571	→	→	1.534	1.501	1.435	1.403	1.737	1.552	1.537	1.713
219	1.753	→	1.753	3.399	3.355	→	3.336		0.951	→	0.947	1.750	1.671	1.672	1.744
220	1.754	→	1.759	5.030	→	→	→		0.673	→	0.672	1.753	1.703	1.705	1.734
221	1.705	→	1.720	0.887	0.409	→	→	1.985	1.885	1.725	1.637	1.684	1.334	1.314	1.683
222	1.720	→	1.728	1.420	1.152	→	→	1.654	1.613	1.588	1.538	1.722	1.481	1.465	1.705
223	1.744	→	1.744	2.456	2.396	→	2.393	1.210	1.188	1.163	1.153	1.728	1.607	1.602	1.713
224	1.754	→	1.754	4.212	4.202	→	4.194		0.795	→	0.776	1.712	1.673	1.662	1.712
225	2.650	2.659	2.659	1.203	0.727	→	→	1.967	1.716	1.606	1.601	1.727	1.381	1.367	1.723
226	2.650	→	2.670	1.721	1.571	→	→	1.788	1.655	1.634	1.548	1.771	1.500	1.483	1.752
227	2.670	→	2.681	3.423	3.352	3.334	→	1.306	1.286	1.268	1.264	1.779	1.640	1.635	1.768
228	2.688	→	2.693	5.061	5.035	→	5.008		0.991	→	0.996	1.789	1.702	1.704	1.760
229	2.660	2.669	2.670	1.274	0.762	→	→	1.950	1.716	1.576	1.625	1.724	1.373	1.353	1.695
230	2.655	→	2.670	1.446	1.153	→	→	1.893	1.740	1.675	1.597	1.749	1.422	1.406	1.723
231	2.664	→	2.681	2.561	2.429	→	2.437	1.532	1.484	1.452	1.424	1.753	1.557	1.540	1.743
232	2.688	→	2.696	4.282	4.253	4.232	4.225	1.056	1.048	1.026	1.007	1.740	1.637	1.622	1.719
233	4.330	4.368	4.375	1.250	0.743	→	→	2.170	1.582	1.381	1.316	1.691	1.312	1.292	1.671
234	4.327	?	4.362	1.852	1.555	→	→	1.953	1.620	?	1.462	1.727	1.387	1.379	1.714
235	4.327	4.349	4.357	3.535	3.439	3.330	→	1.556	1.532	1.452	1.419	1.746	1.531	1.525	1.740
236	4.338	4.358	4.374	5.116	5.094	5.052	5.019		1.313	1.296	1.238	1.758	1.612	1.586	1.724
237	4.322	4.350	4.365	1.301	0.774	→	→	2.164	1.581	1.458	1.395	1.698	1.312	1.290	1.700
238	4.325	4.330	4.355	1.493	1.182	→	→	2.047	1.612	1.564	1.489	1.732	1.355	1.342	1.706
239	4.328	4.340	4.355	2.625	2.411	→	2.419	1.739	1.576	1.558	1.503	1.735	1.450	1.436	1.714
240	4.353	→	4.369	4.352	4.276	→	4222	1.405	1.356	→	1.352	1.734	1.546	1.537	1.717

Galvanometer Deflections during Calibration (in) - Corrected to 7.000 volts

Rotational Speed	4.583 (tests no. 201 to 208)	Torque	4.203 (tests no. 201 to 208)
	4.590 (tests no. 209 to 240)		4.200 (tests no. 209 to 240)
Drawing Speed	4.537 (tests no. 201 to 208)	Drawing Force	4.080 (tests no. 201 to 208)
	4.544 (tests no. 209 to 240)		4.089 (tests no. 209 to 240)

Nominal Diameter of Bar :- $1\frac{3}{16}$ in.	TABLE No. A7.17
Lubricant :- Oil	(see section 10.6.5)
Supply Voltage to Load-Cell :- 7.000/7.003 v (all tests)	

Galvanometer Deflections during Drawing Tests (in)

Test no.	Rotational Speed			Drawing Speed				Torque				Drawing Force			
	R'	R''	R_d	$\hat{V}$	V'	V''	V_d	$\hat{T}$	T'	T''	T_d	P_c	P'	P_d	P_e
241	0.448	→	0.448	0.456	0.343	→	→		2.650	→	2.608	2.404	2.076	2.064	?
242	0.464	→	0.470	1.594	1.570	→	→		1.110	→	1.072	2.502	2.447	2.426	2.479
243	0.465	→	0.477	3.277	→	→	→		0.542	→	0.537	2.507	2.488	2.460	2.482
244	0.472	→	0.479	4.973	→	→	→		0.356	→	0.358	2.512	→	2.488	2.514
245	0.450	→	0.450	0.526	0.390	→	0.385		2.170	→	2.278	2.323	2.062	2.072	2.320
246	0.454	→	0.455	1.153	1.095	→	1.100		1.356	→	1.260	2.449	2.340	2.290	2.352
247	0.465	→	0.473	2.352	→	→	→		0.720	→	0.722	2.464	2.428	2.419	2.430
248	0.471	→	0.471	4.160	→	→	→		0.407	→	0.387	2.445	→	2.406	2.407
249	0.952	?	0.970	0.727	0.362	→	→	3.286	3.232	?	2.888	2.461	1.941	1.910	2.440
250	0.999	→	0.999	1.618	1.534	→	1.539		2.004	→	1.917	2.513	2.346	2.311	2.485
251	1.018	→	1.018	3.263	→	→	→		1.092	→	1.087	2.488	2.443	2.447	2.476
252	1.034	→	1.034	4.976	→	→	→		0.741	→	0.716	2.483	2.453	2.432	2.467
253	0.958	?	0.978	0.773	0.416	→	→	3.118	3.074	?	2.807	2.418	1.920	1.885	2.375
254	0.988	→	0.988	1.287	1.124	→	→	2.306	2.298	2.278	2.248	2.452	2.193	2.192	2.440
255	1.003	→	1.003	2.364	→	→	2.349		1.450	→	1.425	2.477	2.370	2.358	2.408
256	1.015	→	1.023	4.135	→	→	→		0.860	→	0.844	2.447	2.406	2.401	2.445
257	1.653	?	1.704	0.931	0.384	→	→	3.583	3.354	?	2.684	2.480	1.855	1.812	2.423
258	1.694	1.700	1.706	1.682	1.541	→	1.532		2.628	2.440	2.432	2.505	2.174	2.144	2.496
259	1.696	→	1.708	2.449	2.404	→	2.353		2.158	→	1.900	2.533	2.325	2.260	2.424
260	1.742	→	1.737	5.002	4.967	→	4.988		1.214	→	?	2.506	2.499	?	?
261	1.680	?	1.712	0.965	0.404	→	→	3.071	2.855	?	2.574	2.356	1.837	1.806	2.337
262	1.713	→	1.722	1.430	1.165	→	1.173	2.611	2.579	2.552	2.491	2.406	2.040	2.021	2.421
263	1.716	→	1.716	2.419	2.354	→	2.343	1.987	1.970	→	1.891	2.450	2.241	2.241	2.402
264	1.738	→	1.738	4.171	4.162	→	4.111		1.353	→	1.364	2.485	2.400	2.397	2.474
265	2.624	?	2.661	1.430	0.811	?	0.787	3.332	3.025	?	2.747	2.477	1.858	1.830	2.409
266	2.636	?	2.661	1.861	1.604	?	1.587	3.005	2.862	?	2.605	2.473	2.023	1.987	2.453
267	2.668	→	2.673	3.436	3.360	→	3.321		2.205	→	2.112	2.478	2.241	2.223	2.457
268	2.707	→	2.697	5.060	5.047	→	5.003		1.620	→	1.660	2.462	2.327	2.333	2.460
269	2.636	2.648	2.655	1.455	0.794	→	→	3.274	2.922	2.761	2.720	2.440	1.835	1.822	2.420
270	2.622	→	2.656	1.515	1.150	→	1.154	3.119	2.928	2.882	2.618	2.443	1.930	1.889	2.382
271	2.661	→	2.670	2.551	2.451	2.420	2.412	2.464	2.434	2.372	2.297	2.426	2.117	2.091	2.394
272	2.697	→	2.697	4.273	4.251	→	4.184		1.729	→	1.804	2.423	2.235	2.267	2.429
273	4.192	4.236	4.254	1.429	0.784	→	0.777	3.133	2.383	2.103	2.105	2.277	1.756	1.735	2.255
274	4.194	→	4.244	1.889	1.580	→	1.575	2.946	2.448	2.400	2.198	2.341	1.867	1.841	2.311
275	4.263	4.221	4.245	3.525	3.435	3.330	3.300	2.349	2.283	2.177	2.031	2.356	2.052	2.015	2.338
276	4.310	4.291	4.289	5.122	5.113	5.038	5.009		1.921	1.898	1.856	2.368	2.155	2.138	2.380
277	4.160	4.204	4.250	1.332	0.820	0.789	0.778	3.321	2.581	2.296	2.137	2.331	1.779	1.730	2.300
278	4.172	4.192	4.240	1.536	1.180	→	→	3.151	2.449	2.311	2.148	2.374	1.829	1.798	2.286
279	4.234	4.205	4.214	2.660	2.450	2.438	2.423	2.501	2.333	2.323	2.245	2.330	1.963	1.951	2.311
280	4.254	→	4.246	4.377	4.195	→	4.175		2.163	→	2.117	2.351	2.118	2.106	2.399
281	1.662	?	1.696	0.954	0.400	?	0.378	3.336	3.120	?	2.533	2.340	1.799	1.755	2.292
282	1.686	→	1.694	1.455	1.128	→	1.130	2.694	2.612	→	2.546	2.376	2.006	1.983	2.349
283	1.695	?	1.705	1.689	1.561	?	1.555		2.265	?	2.250	2.348	2.076	2.072	2.375
284	1.710	→	1.710	3.309	3.282	→	3.250		1.604	→	1.525	2.428	2.305	2.273	2.401
285	0.441	→	0.441	0.499	0.365	→	→		2.529	→	2.443	2.365	2.062	2.039	2.322
286	0.455	→	0.460	1.141	1.103	→	→		1.396	→	1.358	2.416	2.338	2.317	2.326
287	0.464	→	0.464	1.544	→	→	1.525		0.848	→	0.948	2.290	2.317	2.297	2.369

Galvanometer Deflections during Calibration (in) - Corrected to 7.000 volts

Rotational Speed	4.583 (tests no. 241 to 264)	Torque	4.198 (tests no. 241 to 264)
	4.589 (tests no. 265 to 287)		4.210 (tests no. 265 to 287)
Drawing Speed	4.543 (tests no. 241 to 264)	Drawing Force	4.089 (tests no. 241 to 264)
	4.538 (tests no. 265 to 287)		4.086 (tests no. 265 to 287)

Nominal Diameter of Bar :- 1¼ in.	TABLE No. A7.18
Lubricant :- Oil	(see section 10.6.5)
Supply Voltage to Load-Cell :- 7.000/7.002 v (all tests)	

Test no.	Galvanometer Deflections during Drawing Tests (in)														
	Rotational Speed			Drawing Speed				Torque				Drawing Force			
	R'	R''	R_d	$\hat{V}$	V'	V''	V_d	$\hat{T}$	T'	T''	T_d	P_c	P'	P_d	P_e
288	0.492	→	0.487	0.496	0.362	→	→		3.716	→	3.591	3.144	2.764	2.738	3.193
289	0.561	→	0.561	1.578	1.555	→	1.567		1.704	→	1.612	3.280	3.184	3.155	3.213
290	0.568	→	0.573	3.233	3.220	→	→		0.876	→	0.843	3.261	3.228	3.197	3.195
291	0.576	→	0.583	4.919	→	→	→		0.574	→	0.546	3.252	3.227	3.188	3.200
292	0.515	→	0.502	0.572	0.402	→	→		3.377	→	3.218	3.140	2.723	2.705	3.094
293	0.552	→	0.552	1.122	1.057	→	→		2.144	→	2.145	3.172	3.018	3.022	3.181
294	0.564	→	0.564	2.138	→	→	→		1.152	→	1.107	3.223	3.171	3.159	3.189
295	0.577	→	0.577	4.086	→	→	4.092		0.670	→	0.640	3.265	3.233	3.188	3.185
296	1.018	→	0.994	1.028	0.787	→	→		3.229	→	3.242	3.179	2.796	2.801	3.253
297	1.039	→	1.039	1.596	1.560	→	→		2.517	→	2.393	3.300	3.062	3.010	3.231
298	1.065	→	1.065	3.245	3.236	→	3.219		1.349	→	1.386	3.263	3.168	3.189	3.321
299	1.071	→	1.071	4.922	→	→	4.909		1.020	→	0.993	3.336	3.295	3.279	3.331
300	0.930	→	0.942	1.011	0.762	→	?		3.760	→	?	3.363	2.870	2.837	3.294
301	0.979	→	0.989	1.351	1.054	→	1.067		3.232	→	2.851	3.325	2.973	2.918	3.213
302	1.025	→	1.025	2.369	2.338	→	2.345		1.953	→	1.945	3.332	3.195	3.201	3.351
303	1.038	→	1.048	4.113	→	→	4.102		1.224	→	1.214	3.394	3.315	3.297	3.308
304	1.665	?	1.678	1.540	1.115	?	1.115	?	?	?	3.503	3.256	2.744	2.724	3.277
305	1.660	→	1.660	1.754	1.580	→	1.582	3.524	3.474	3.398	3.350	3.335	2.912	2.894	3.328
306	1.716	→	1.716	3.317	3.262	→	3.248		2.360	→	2.309	3.386	3.192	3.172	3.371
307	1.746	→	1.739	4.947	4.923	→	4.915		1.709	→	1.678	3.414	3.295	3.270	3.360
308	1.655	?	1.662	1.476	1.110	?	1.157	4.023	3.868	?	3.562	3.356	2.761	2.748	3.260
309	1.710	→	1.691	2.447	2.354	→	2.361	2.950	2.928	→	2.833	3.360	3.081	3.050	3.329
310	1.732	→	1.732	4.150	4.114	→	4.108		2.027	→	1.937	3.397	3.258	3.225	3.331
311	2.493	→	2.493	2.493	2.430	2.383	→	2.758	2.706	2.644	2.603	3.083	2.782	2.766	3.157
312	2.508	→	2.513	4.208	4.158	→	4.130		2.299	→	2.239	3.232	3.034	3.012	3.186
313	2.482	→	2.499	3.386	3.304	→	3.264		2.672	→	2.484	3.267	2.972	2.925	3.243
314	2.529	→	2.512	5.009	4.976	→	4.931		2.022	→	2046	3.256	3.093	3.090	3.228
315	2.443	→	2.468	2.509	2.409	2.383	2.379	3.176	3.094	3.088	2.899	3.206	2.824	2.791	3.196
316	2.500	→	2.488	4.225	4.166	→	4.145		2.430	→	2.380	3.248	3.045	3.040	3.257
317	2.462	→	2.459	3.374	3.288	→	3.258		2.704	→	2.760	3.308	3.015	2.978	3.273
318	2.504	→	2.512	5.011	4.964	→	4.926		2.199	→	2.159	3.322	3.140	3.124	3.296
319	3.136	?	3.136	2.570	2.430	?	2.382	3.803	3.729	?	3.639	3.319	2.800	2.761	3.291
320	3.233	3.201	3.190	4.246	4.162	4.118	→	2.992	2.992	2.913	2.852	3.345	3.028	3.000	3.297
321	3.191	?	3.165	3.467	3.310	?	3.267	3.212	3.173	?	2.966	3.321	2.914	2.878	3.253
322	3.270	→	3.239	5.075	4.988	→	4.941		2.598	→	2.482	3.322	3.080	3.063	3.260

Galvanometer Deflections during Calibration (in) - Corrected to 7.000 volts

Rotational Speed	4.584 (tests no. 288 to 303)	Torque	4.204 (tests no. 288 to 303)
	4.587 (tests no. 304 to 322)		4.205 (tests no. 304 to 322)
Drawing Speed	4.530 (tests no. 288 to 303)	Drawing Force	4.073 (tests no. 288 to 303)
	4.536 (tests no. 304 to 322)		4.085 (tests no. 304 to 322)

Nominal Diameter of Bar :- $1\frac{5}{16}$ *in.*

Lubricant :- Oil

Supply Voltage to Load-Cell :- 7.007 v (tests no. 323 to 326); 7.002/7.003 v (tests no. 327 to 347)

TABLE No. A7.19

(see section 10.6.5)

Galvanometer Deflections during Drawing Tests (in)

Test no.	Rotational Speed			Drawing Speed				Torque				Drawing Force			
	R'	R''	R_d	$\hat{V}$	V'	V''	V_d	$\hat{T}$	T'	T''	T_d	P_c	P'	P_d	P_c
323	0.501	→	0.494	0.930	0.885	→	0.891		2.793	→	2.647	3.898	3.676	3.646	3.852
324	0.520	→	0.520	1.595	→	→	1.580		1.721	→	1.738	3.894	3.792	3.789	3.801
325	0.526	→	0.526	3.209	→	→	3.202		0.877	→	0.862	3.878	3.842	3.823	3.872
326	0.434	→	0.544	4.843	→	→	→		0.543	→	0.558	3.840	3.804	3.808	3.844
327	0.510	→	0.494	1.011	0.938	→	0.913		2.370	→	2.499	3.749	3.571	3.603	3.832
328	0.522	→	0.528	2.338	→	→	2.344		1.278	→	1.269	3.941	3.889	3.872	3.913
329	0.524	→	0.532	4.040	→	→	→		0.767	→	0.773	3.964	3.948	3.940	3.874
330	0.867	→	0.862	1.125	0.962	→	→		3.660	→	3.664	3.839	3.456	3.450	3.833
331	0.900	→	0.890	1.637	1.546	→	→		3.022	→	2.928	3.947	3.698	3.692	3.949
332	0.943	→	0.943	3.205	3.182	→	→		1.790	→	1.673	4.051	3.929	3.893	4.011
333	0.866	→	0.861	1.123	0.971	→	→		3.599	→	3.671	3.827	3.459	3.463	3.855
334	0.936	→	0.941	2.305	→	→	→		2.302	→	2.232	3.979	3.824	3.774	3.922
335	0.949	→	0.955	4.046	→	→	4.056		1.401	→	1.360	4.020	3.946	3.900	3.920
336	1.653	→	1.653	2.460	2.408	→	2.421		3.103	→	3.091	3.890	3.616	3.619	3.944
337	1.691	→	1.686	4.141	4.115	→	4.092		2.172	→	2.177	3.988	3.822	3.818	3.914
338	1.671	→	1.681	3.312	3.242	→	→		2.543	→	2.521	3.951	3.732	3.714	3.862
339	1.707	→	1.707	4.933	4.888	→	→		1.645	→	1.667	3.836	3.730	3.733	3.832
340	2.476	→	2.499	2.488	2.425	→	2.410		3.697	?	3.225	3.855	3.429	3.370	3.885
341	2.492	→	2.507	4.225	4.188	→	4.164		2.957	→	2.847	3.983	3.721	3.669	3.962
342	2.490	→	2.490	3.390	3.268	→	→		3.365	→	3.341	3.964	3.599	3.572	3.894
343	2.534	→	2.544	?	4.905	→	4.900		2.543	→	2.484	3.939	3.736	3.707	3.909
344	3.216	?	3.202	3.468	3.440	?	3.278		3.503	?	3.151	3.834	3.410	3.389	3.849
345	3.254	→	3.220	4.969	4.931	→	4.922		3.076	→	2.843	3.907	3.642	3.602	3.870
346	3.214	→	3.198	4.281	4.197	→	4.123		3.313	3.186	3.227	3.927	3.571	3.557	3.837
347	3.177	→	3.188	3.472	3.375	→	3.259		3.372	?	3.164	3.827	3.412	3.363	3.700

Galvanometer Deflections during Calibration (in) - Corrected to 7.000 volts

Rotational Speed	4.587 (tests no. 323 to 335)	Torque	4.205 (tests no. 323 to 335)
	4.585 (tests no. 336 to 347)		4.205 (tests no. 336 to 347)
Drawing Speed	4.536 (tests no. 323 to 335)	Drawing Force	4.085 (tests no. 323 to 335)
	4.540 (tests no. 336 to 347)		4.085 (tests no. 336 to 347)

Nominal Diameter of Bar :- $1\frac{1}{16}$ in.

Lubricant :- Oil

Supply Voltage to Load-Cell :- 7.002 v (all tests)

TABLE No. A7.20

(see section 10.6.5)

Test no.	Galvanometer Deflections during Drawing Tests (in)														
	Rotational Speed			Drawing Speed				Torque				Drawing Force			
	R'	R''	R_d	$\hat{V}$	V'	V''	V_d	$\hat{T}$	T'	T''	T_d	P_c	P'	P_d	P_c
348	1.721 →		1.721	0.774	0.305 →			1.544	1.512	1.480	1.385	1.051	0.711	0.703	1.045
349	1.729 →		1.729	1.669	1.630 →			1.193	1.175 →		1.185	1.079	0.926	0.934	[illegible]
350	1.740 →		1.740	3.396 →					0.714 →		0.706	1.055	1.004	0.996	1.067
351	1.744 →		1.744	5.081 →					0.501 →		0.503	1.074	1.048	1.039	[illegible]
352	1.718 →		1.733	0.784	0.316 →			1.550	1.522	1.489	1.302	1.051	0.718	0.704	[illegible]
353	1.732 →		1.732	1.484	1.246 →		1.235	1.266	1.248 →		1.222	1.071	0.877	0.873	1.051
354	1.742 →		1.742	2.468 →					0.702 →		0.901	1.065	0.976	0.974	1.076
355	1.744 →		1.745	4.245 →					0.612 →		0.626	1.034	1.044	1.054	1.071

Galvanometer Deflections during Calibration (in) – corrected to [illegible]

Rotational Speed :- 4.585 (all tests)

Torque :- 4.205 (all tests)

Drawing Speed :- 4.540 (all tests)

Drawing Force :- 4.085 (all tests)

SERIES II DRAWING TESTS.

1.1/16 in. DIAMETER BAR LUBRICATED WITH SOAP

TABLE No. A7.21

(see sect. 10.6.5)

Ref. no. of Bar	Test no.		P (tonf)	R (rev/min)	V (ft/min)	$\frac{(P-P_R)}{P}$	$\left(\frac{T}{d_1 P}\right)$	ϕ	R_p (rev/min)	R_B/R	Θ_i (radians)
S1/5	33		4.83	5.00	0.852	0.095	0.100	–	0.059	0.012	1.01[illegible]
		37	4.95	5.06	0.929	0.091	0.098	–	0.064	0.014	0.[illegible]79
		38	5.06	5.17	3.010	0.026	0.051	0°40′	0.110	0.021	0.[illegible]
	34		4.96	5.10	4.897	0.014	0.032	0°30′	0.109	0.022	0.[illegible]77
		39	5.02	5.18	7.504	0.000	0.022	0°15′	0.117	0.023	0.186
	35		5.02	5.10	10.324	0.000	0.015	0°10′	0.115	0.024	0.134
		40	5.06	5.19	12.967	0.000	0.012	–	0.115	0.023	0.[illegible]
	36		5.04	5.16	15.518	0.000	0.009	0°10′	0.10[illegible]	[illegible]	[illegible]
S1/4	25		4.74	10.61	0.824	0.158	0.120	–	0.067	0.007	1.2[illegible]
		29	4.81	10.73	0.878	0.152	0.122	–	0.073	0.007	1.2[illegible]
		30	4.83	10.80	3.037	0.068	0.083	0°50′	0.172	0.017	0.771
	26		4.90	10.71	5.050	0.037	0.059	0°40′	0.20[illegible]	0.020	0.525
		31	4.84	10.84	7.600	0.031	0.042	0°15′	0.219	[illegible]	0.372
	27		4.95	10.72	10.412	0.014	0.031	0°15′	0.231	0.022	0.2[illegible]
		32	4.86	10.83	13.043	0.008	0.024	–	0.217	0.020	0.223
	28		4.93	10.72	15.576	0.000	0.020	0°[illegible]′	0.225	0.021	0.186
S1/1	1		4.58	20.30	0.915	0.188	0.121	–	0.072	0.003	1.407
		5	4.58	20.41	0.918	0.172	0.120	–	0.071	0.003	1.408
		6	4.63	20.39	3.088	0.110	0.102	0°55′	0.209	0.011	1.065
		7	4.5[illegible]	20.36	3.130	0.118	0.100	0°45′	0.205	0.010	1.058
	2		4.75	20.41	4.980	0.082	0.087	0°45′	0.293	0.015	0.8[illegible]
	3		4.78	20.46	10.367	0.029	0.056	0°40′	0.392	0.020	0.4[illegible]
		8	4.77	20.39	12.682	0.025	0.044	0°20′	0.380	0.019	0.414
	4		4.70	20.40	15.545	0.013	0.037	0°30′	0.380	0.019	0.34[illegible]
S1/2		13	4.65	30.07	0.954	0.194	0.124	–	0.078	0.003	1.455
	9		4.60	29.99	0.954	0.187	0.120	–	0.074	0.003	1.455
		14	4.67	30.01	3.139	0.137	0.105	1°5′	0.216	0.007	1.205
	10		4.78	30.19	4.956	0.121	0.095	1°00′	0.319	0.011	1.030
		15	4.75	30.06	7.541	0.076	0.083	–	0.419	0.014	0.82[illegible]
	11		4.75	30.24	10.361	0.046	0.066	0°45′	0.460	0.016	0.673
		16	4.93	30.09	13.051	0.034	0.058	–	0.536	0.012	0.5[illegible]
	12		4.77	30.31	15.588	0.034	0.050	0°30′	0.520	0.017	0.[illegible]
S1/3	17		4.70	39.59	0.921	0.185	0.126	–	0.073	0.002	1.4[illegible]
		21	4.92	39.62	0.944	0.191	0.114	–	0.074	0.002	1.4[illegible]
		22	4.99	39.74	3.194	0.154	0.102	1°00′	0.231	0.006	1.2[illegible]5
	18		4.90	39.69	4.900	0.137	0.100	1°10′	0.338	0.009	1.1[illegible]
		23	5.15	39.74	7.451	0.091	0.087	0°55′	0.480	0.012	0.969
	19		4.91	39.56	10.254	0.061	0.075	–	0.536	0.014	0.[illegible]
		24	5.12	39.63	12.882	0.053	0.065	0°45′	0.616	0.016	0.699
	20		5.04	39.68	15.457	0.046	0.057	0°40′	0.635	0.016	0.612

SERIES II DRAWING TESTS.

1.1/8 in. DIAMETER BAR LUBRICATED WITH SOAP

TABLE No. A7.22
(see section 10.6.5)

Ref. no. of Bar	Test no.		P (tonf)	R (rev/min)	V (ft/min)	$\frac{(P-P_R)}{P}$	$\left(\frac{T}{d_1 P}\right)$	ϕ	R_P (rev/min)	R_B/R	Θ_1 (radians)
S2/2	177		8·08	4·99	0·913	0·056	0·070	–	0·095	0·020	0·995
		181	8·05	5·15	0·987	0·061	0·079	–	0·115	0·023	0·974
		182	8·18	5·24	3·328	0·024	0·038	0°55'	0·192	0·038	0·418
	178		8·33	5·26	4·715	0·007	0·027	0°40'	0·194	0·038	0·305
		183	8·28	5·31	7·282	0·000	0·018	0°15'	0·202	0·040	0·203
	179		8·49	5·31	10·159	0·000	0·013	0°25'	0·214	0·041	0·146
		184	8·27	5·33	12·854	0·000	0·011	0°15'	0·214	0·041	0·116
	180		8·54	5·30	15·386	0·000	0·008	0°10'	0·188	0·036	0·097
S2/4	161		8·19	11·83	0·775	0·100	0·086	–	0·100	0·008	1·343
	"		"	"	"	"	0·081	–	0·095	"	"
		165	8·14	11·77	0·829	0·102	0·087	–	0·109	0·009	1·326
		"	"	"	"	"	0·083	–	0·103	"	"
		166	8·28	11·81	2·938	0·050	0·064	2°00'	0·287	0·025	0·848
	162		8·45	11·83	4·792	0·028	0·050	1°05'	0·372	0·032	0·608
		167	8·38	11·91	7·414	0·023	0·036	0°50'	0·403	0·034	0·426
	163		8·64	11·86	10·211	0·014	0·028	0°35'	0·453	0·039	0·317
		168	8·43	11·91	12·944	0·008	0·022	0°30'	0·446	0·039	0·254
	164		8·62	11·87	15·426	0·012	0·018	0°30'	0·445	0·038	0·214
S2/2	185		8·05	20·19	1·002	0·106	0·086	–	0·128	0·006	1·397
	"		"	"	"	"	0·081	–	0·120	"	"
		189	8·08	20·23	1·050	0·110	0·088	–	0·136	0·007	1·389
		"	"	"	"	"	0·084	–	0·132	"	"
		190	8·26	20·32	3·068	0·077	0·075	1°35'	0·351	0·017	1·079
		"	"	"	"	"	0·074	"	0·344	0·018	"
	186		8·31	20·33	4·669	0·057	0·067	1°35'	0·477	0·024	0·888
		191	8·33	20·37	7·220	0·034	0·054	1°00'	0·601	0·030	0·672
	187		8·44	20·45	10·079	0·021	0·043	1°05'	0·683	0·034	0·520
		192	8·43	20·46	12·722	0·020	0·036	1°00'	0·706	0·035	0·426
	188		8·48	20·49	15·321	0·009	0·031	0°35'	0·731	0·037	0·361
S2/3	169		8·30	31·82	1·980	0·117	0·084	–	0·253	0·008	1·354
	"		"	"	"	"	0·081	–	0·244	"	"
		173	8·15	31·73	2·028	0·104	0·084	–	0·255	0·008	1·348
		"	"	"	"	"	0·082	–	0·250	"	"
		174	8·23	31·78	3·074	0·094	0·079	1°50'	0·369	0·012	1·240
		"	"	"	"	"	0·077	"	0·358	"	"
	170		8·39	31·88	4·751	0·079	0·074	1°50'	0·538	0·017	1·085
	"		"	"	"	"	0·074	"	0·538	"	"
		175	8·36	31·81	7·347	0·060	0·066	1°30'	0·751	0·024	0·885
	171		8·52	31·85	10·301	0·038	0·057	1°25'	0·915	0·029	0·717
		176	8·38	31·81	12·944	0·031	0·049	1°00'	0·977	0·031	0·606
	172		8·55	31·96	15·442	0·023	0·043	1°05'	1·046	0·033	0·528
S2/1	193		8·16	51·88	2·022	0·124	0·092	–	0·281	0·006	1·434
	"		"	52·12	"	"	0·078	–	0·238	0·005	"
		197	8·14	52·15	2·105	0·117	0·084	–	0·264	0·005	1·429
		"	"	52·30	"	"	0·079	–	0·250	"	"
		198	8·17	52·24	3·108	0·111	0·082	1°45'	0·383	0·007	1·363
		"	"	"	"	"	0·078	"	0·366	"	"
	194		8·29	52·08	4·632	0·100	0·078	1°55'	0·550	0·011	1·265
	"		"	"	"	"	0·077	"	0·540	"	"
		199	8·26	52·35	7·298	0·084	0·072	1°35'	0·802	0·016	1·112
	195		8·40	52·19	10·132	0·064	0·067	1°35'	1·057	0·021	0·968
		200	8·30	52·39	12·892	0·053	0·060	1°30'	1·188	0·023	0·854
	196		8·46	52·28	15·364	0·050	0·055	1°30'	1·330	0·026	0·765

SERIES II DRAWING TESTS.

1.3/16 in. DIAMETER BAR LUBRICATED WITH SOAP

TABLE No. A7.23 (see section 10.6.5)

Ref. no. of Bar	Test no.		P (tonf)	R (rev/min)	V (ft/min)	$\frac{(P-P_R)}{P}$	$\left(\frac{T}{d_1 P}\right)$	ϕ	R_P (rev/min)	$R_B/R.$	θ_1 (radians)
S3/4		61	10·94	5·07	0·940	0·066	0·074	–	0·179	0·036	0·994
	57		10·95	4·89	0·934	0·060	0·072	–	0·172	0·037	0·980
		62	11·29	5·08	3·062	0·019	0·044	1°45′	0·357	0·071	0·442
	58		11·17	5·13	4·604	0·005	0·030	1°10′	0·358	0·070	0·307
		63	11·41	5·15	7·103	0·000	0·021	0°50′	0·386	0·076	0·204
	59		11·27	5·25	9·937	0·000	0·015	0°40′	0·387	0·074	0·149
		64	11·73	5·16	12·644	0·000	0·012	0°30′	0·421	0·083	0·116
	60		11·48	5·25	15·198	0·000	0·010	0°20′	0·389	0·076	0·098
S3/3		45	11·47	11·60	1·011	0·109	0·097	–	0·263	0·023	1·274
		"	"	"	"	"	0·095	–	0·259	0·022	"
	41		11·56	11·53	1·062	0·110	0·095	–	0·274	0·024	1·258
	"		"	"	"	"	0·093	–	0·267	0·023	"
		46	11·83	11·61	3·279	0·062	0·077	3°05′	0·696	0·061	0·790
	42		11·78	11·67	4·814	0·037	0·058	2°10′	0·765	0·067	0·604
		47	11·70	11·72	7·220	0·020	0·046	1°45′	0·914	0·079	0·433
	43		11·80	11·79	10·082	0·009	0·033	1°25′	0·918	0·079	0·322
		48	11·81	11·75	12·860	0·009	0·029	1°20′	1·014	0·088	0·255
	44		11·89	11·78	15·287	0·000	0·024	1°05′	1·002	0·087	0·216
S3/2	65		11·23	20·04	0·919	0·114	0·092	–	0·222	0·011	1·411
	"		"	20·16	"	"	0·089	–	0·216	"	1·412
		69	11·31	20·22	0·993	0·117	0·094	–	0·248	0·012	1·400
		"	"	"	"	"	0·090	–	0·236	"	"
		70	11·46	20·31	3·117	0·087	0·082	3°15′	0·683	0·034	1·077
		"	"	"	"	"	0·081	"	0·679	"	"
	66		11·51	20·14	4·596	0·063	0·075	3°10′	1·021	0·052	0·895
		71	11·49	20·37	7·174	0·044	0·062	2°30′	1·196	0·055	0·680
	67		11·84	20·35	9·974	0·024	0·051	2°20′	1·418	0·071	0·527
		72	11·45	20·43	12·722	0·019	0·038	1°25′	1·300	0·065	0·429
	68		11·73	20·41	15·213	0·014	0·033	1°15′	1·385	0·069	0·365
S3/5	49		11·23	32·13	0·919	0·125	0·093	–	0·225	0·007	1·471
	"		"	32·26	"	"	0·088	–	0·214	"	"
		53	11·44	31·83	0·987	0·133	0·099	–	0·262	0·008	1·462
		"	"	32·07	"	"	0·092	–	0·243	"	1·463
		54	11·66	32·01	3·192	0·108	0·090	3°25′	0·788	0·025	1·234
		"	"	"	"	"	0·087	"	0·763	0·024	"
	50		11·49	32·18	4·690	0·081	0·081	3°10′	1·022	0·032	1·098
	"		"	"	"	"	0·080	"	1·011	"	"
		55	11·79	32·03	7·152	0·069	0·078	3°10′	1·534	0·049	0·906
		"	"	"	"	"	0·078	"	1·534	"	"
	51		11·84	32·23	10·163	0·051	0·066	2°30′	1·863	0·059	0·735
		56	11·95	32·13	12·684	0·037	0·059	2°30′	2·114	0·067	0·625
	52		11·89	32·47	15·272	0·027	0·051	2°10′	2·188	0·068	0·545
S3/1	73		11·12	51·56	0·972	0·122	0·089	–	0·226	0·004	1·505
	"		"	51·87	"	"	0·081	–	0·204	"	"
		77	11·26	51·47	1·014	0·131	0·094	–	0·251	0·005	1·602
		"	"	51·86	"	"	0·086	–	0·231	"	"
		78	11·29	51·81	3·182	0·109	0·082	3°20′	0·690	0·014	1·358
		"	"	51·93	"	"	0·081	"	0·679	0·013	1·359
	74		11·39	51·64	4·577	0·099	0·084	3°20′	1·023	0·020	1·269
		79	11·45	51·70	7·118	0·086	0·081	3°15′	1·643	0·030	1·121
	75		11·56	51·75	9·906	0·070	0·074	2°55′	1·993	0·039	0·979
		80	11·51	51·84	12·827	0·056	0·067	2°45′	2·309	0·045	0·856
	76		11·84	51·59	15·377	0·054	0·066	2°40′	2·785	0·055	0·763

SERIES II DRAWING TESTS.

1.1/4 in. DIAMETER BAR LUBRICATED WITH SOAP

TABLE No. A7.24 (see section 10.6.5)

Ref. no. of Bar	Test no.		P (tonf)	R (rev/min)	V (ft/min)	$\frac{(P-P_R)}{P}$	$\left(\frac{T}{d_1 P}\right)$	ϕ	R_P (rev/min)	R_B/R	Θ_1 (radians)
S4/1	97		15.97	4.76	0.983	0.071	0.081	–	0.334	0.071	0.943
		101	16.11	4.89	1.076	0.066	0.079	–	0.364	0.076	0.912
		102	16.34	4.93	3.209	0.021	0.046	3°00'	0.642	0.132	0.412
	98		16.37	5.02	4.752	0.012	0.034	2°10'	0.687	0.139	0.292
		103	16.53	4.99	7.049	0.005	0.024	1°30'	0.736	0.150	0.199
	99		16.61	5.10	9.886	0.005	0.018	1°05'	0.758	0.151	0.146
		104	16.66	5.04	12.591	0.000	0.014	0°55'	0.741	0.149	0.113
	100		16.73	5.17	15.117	0.000	0.011	0°40'	0.722	0.141	0.097
S4/3	81		15.39	12.09	0.933	0.097	0.090	–	0.340	0.029	1.306
	"		"	"	"	"	0.088	–	0.334	0.028	1.306
		85	15.47	12.17	1.091	0.096	0.089	–	0.396	0.033	1.265
		"	"	"	"	"	0.087	–	0.390	0.033	1.265
		86	15.69	12.22	3.200	0.059	0.074	4°15'	0.980	0.081	0.826
	82		15.69	12.25	4.819	0.034	0.056	3°25'	1.126	0.093	0.626
		87	15.23	12.33	7.206	0.023	0.047	2°55'	1.418	0.117	0.453
	83		15.92	12.34	9.927	0.011	0.034	2°15'	1.423	0.117	0.340
		88	15.90	12.44	12.659	0.013	0.029	1°45'	1.519	0.124	0.272
	84		16.09	12.44	15.148	0.007	0.025	1°30'	1.582	0.129	0.229
S4/4	105		16.00	20.20	1.121	0.122	0.093	–	0.444	0.022	1.378
	"		"	"	"	"	0.092	–	0.439	0.022	1.378
		109	15.89	20.37	1.210	0.115	0.095	–	0.484	0.024	1.365
		"	"	"	"	"	0.094	–	0.476	0.024	1.365
		110	16.16	20.37	3.366	0.086	0.088	5°40'	1.260	0.063	1.044
	106		16.38	20.43	4.639	0.073	0.080	4°55'	1.607	0.080	0.897
		111	16.50	20.47	7.052	0.051	0.071	4°40'	2.191	0.108	0.690
	107		16.49	20.66	9.831	0.032	0.057	3°45'	2.439	0.120	0.538
		112	16.54	20.65	12.560	0.022	0.048	3°10'	2.640	0.130	0.437
	108		16.70	20.79	15.108	0.020	0.042	2°45'	2.788	0.136	0.373
S4/5	89		15.52	31.53	2.229	0.113	0.086	–	0.790	0.025	1.327
		93	15.82	31.54	2.324	0.114	0.089	–	0.868	0.028	1.317
		94	16.08	31.54	3.444	0.113	0.091	5°45'	1.332	0.043	1.204
	90		15.84	31.65	4.783	0.093	0.082	5°15'	1.636	0.052	1.082
		95	16.29	31.44	7.197	0.075	0.083	5°20'	2.574	0.083	0.893
	91		16.12	31.66	10.114	0.052	0.067	4°15'	2.893	0.093	0.727
		96	16.42	31.85	12.770	0.041	0.063	4°05'	3.482	0.111	0.617
	92		16.26	31.97	15.176	0.032	0.055	3°20'	3.561	0.113	0.540
S4/2	113		15.34	51.27	2.349	0.119	0.082	–	0.777	0.015	1.411
		117	15.40	50.72	2.396	0.116	0.085	–	0.833	0.017	1.406
		"	"	51.02	"	"	0.083	–	0.814	0.016	1.407
		118	15.56	50.98	3.534	0.114	0.087	5°10'	1.264	0.025	1.332
	114		15.62	51.02	4.691	0.110	0.085	5°15'	1.651	0.033	1.258
		119	15.86	50.91	7.034	0.093	0.085	5°10'	2.516	0.050	1.118
	115		15.88	51.32	10.001	0.075	0.077	4°30'	3.230	0.064	0.970
		120	15.94	51.33	12.819	0.060	0.073	4°35'	3.939	0.078	0.850
	116		15.90	51.56	15.256	0.048	0.063	3°45'	4.123	0.079	0.765

SERIES II DRAWING TESTS.

1.5/16 In. DIAMETER BAR LUBRICATED WITH SOAP

TABLE No. A7.25
(see section 10.6.5)

Ref. no. of Bar	Test no.		P (tonf)	R (rev/min)	V (ft/min)	$\frac{(P-P_R)}{P}$	$\left(\frac{T}{d_1 P}\right)$	ϕ	R_P (rev/min)	R_B/R	Θ_1 (radians)
S5/2	137		18.93	5.64	1.062	0.075	0.085	–	0.564	0.101	0.985
		141	18.90	5.63	1.091	0.071	0.082	–	0.558	0.099	0.972
		142	18.92	5.80	3.040	0.029	0.053	5°00′	0.990	0.172	0.496
	138		19.26	5.85	4.535	0.015	0.042	3°45′	1.208	0.209	0.351
		143	19.50	5.81	6.893	0.011	0.030	2°55′	1.313	0.229	0.235
	139		19.52	5.88	9.621	0.000	0.021	2°05′	1.296	0.223	0.172
		144	19.57	5.98	12.374	0.000	0.017	1°35′	1.322	0.224	0.136
	140		20.02	5.97	14.811	0.000	0.014	1°15′	1.401	0.238	0.114
S5/4	121		18.46	11.88	1.056	0.102	0.101	–	0.647	0.055	1.267
	"		"	"	"	"	0.098	–	0.630	0.054	"
		125	18.56	11.86	1.124	0.099	0.093	–	0.638	0.055	1.249
		"	"	"	"	"	0.090	–	0.616	0.052	"
		126	18.65	12.01	3.166	0.064	0.080	7°00′	1.544	0.130	0.823
	122		18.80	12.12	4.722	0.043	0.068	5°50′	1.989	0.166	0.630
		127	18.86	12.15	7.032	0.025	0.056	5°20′	2.441	0.203	0.456
	123		19.14	12.31	9.831	0.014	0.041	3°45′	2.520	0.207	0.342
		128	19.32	12.28	12.497	0.007	0.036	3°20′	2.854	0.235	0.272
	124		19.60	12.37	15.003	0.009	0.028	2°20′	2.690	0.220	0.230
S5/5	145		17.84	20.28	1.178	0.099	0.087	–	0.600	0.030	1.369
	"		"	"	"	"	0.081	–	0.557	0.028	"
		149	17.96	20.22	1.238	0.103	0.095	–	0.698	0.035	1.358
		"	"	"	"	"	0.087	–	0.639	0.032	"
		150	18.20	20.23	3.320	0.079	0.083	7°30′	1.654	0.083	1.047
		"	"	"	"	"	0.082	"	1.635	0.082	"
	146		18.43	20.26	4.584	0.072	0.080	7°10′	2.216	0.111	0.898
	"		"	"	"	"	0.079	"	2.179	0.109	"
		151	18.55	20.37	6.826	0.045	0.070	6°15′	2.929	0.145	0.703
	147		18.80	20.49	9.744	0.035	0.059	5°40′	3.557	0.176	0.538
		152	18.91	20.55	12.383	0.024	0.051	4°30′	3.881	0.191	0.440
	148		18.94	20.67	14.976	0.018	0.042	3°50′	3.922	0.192	0.374
S5/3		133	18.56	31.41	2.308	0.104	0.088	7°20′	1.233	0.040	1.318
		"	"	31.69	"	"	0.084	"	1.176	0.038	1.320
	129		18.51	31.66	2.599	0.104	0.091	7°20′	1.445	0.046	1.289
		134	18.39	31.49	3.356	0.102	0.092	8°20′	1.858	0.060	1.212
		"	"	"	"	"	0.091	"	1.843	0.059	"
	130		18.84	31.50	4.673	0.089	0.091	8°00′	2.651	0.085	1.089
		135	18.75	31.59	6.974	0.073	0.086	7°50′	3.702	0.119	0.910
	131		19.26	31.89	9.902	0.054	0.074	7°05′	4.640	0.147	0.741
		136	18.87	31.84	12.593	0.042	0.067	6°30′	5.262	0.167	0.623
	132		19.47	32.14	15.093	0.032	0.058	5°25′	5.543	0.175	0.544
S5/1		157	18.49	49.93	1.226	0.109	0.090	–	0.675	0.014	1.485
		"	"	50.61	"	"	0.079	–	0.587	0.012	1.486
	153		18.52	50.06	2.377	0.116	0.089	–	1.289	0.026	1.405
	"		"	50.84	"	"	0.075	–	1.084	0.022	1.408
		158	18.64	50.19	3.407	0.107	0.086	7°15′	1.789	0.036	1.336
		"	"	"	"	"	0.083	"	1.735	0.035	"
	154		18.84	50.17	4.578	0.107	0.086	7°30′	2.425	0.049	1.260
	"		"	"	"	"	0.081	"	2.290	0.046	"
		159	19.28	50.23	9.699	0.084	0.087	7°55′	5.347	0.108	0.974
	155		19.31	50.86	9.930	0.078	0.083	–	5.238	0.104	0.968
	"		"	50.30	9.692	"	0.082	–	5.047	0.102	0.975
		160	19.48	50.83	12.754	0.071	0.082	7°20′	6.727	0.134	0.847
		"	"	50.48	12.464	"	0.082	"	6.518	0.131	0.855
	156		19.53	51.12	15.130	0.056	0.071	6°30′	6.902	0.137	0.765
	"		"	50.77	14.920	"	0.070	"	6.722	0.134	0.768

SERIES II DRAWING TESTS.

1.1/8 in. DIAMETER BAR LUBRICATED WITH OIL

TABLE No. A7.26 (see section 10.6.5)

Ref. no. of Bar	Test no.		P (tonf)	R (rev/min)	V (ft/min)	$\frac{(P-P_R)}{P}$	$\left(\frac{T}{d_1 P}\right)$	ϕ	R_P (rev/min)	R_B/R	θ_1 (radians)
02/5	201		9·24	5·14	1·042	0·107	0·119	–	0·212	0·043	0·948
		205	9·53	5·14	1·162	0·112	0·121	–	0·245	0·049	0·895
		206	9·66	5·22	3·294	0·036	0·063	1°45'	0·369	0·073	0·420
	202		9·56	5·33	4·807	0·009	0·046	1°20'	0·390	0·075	0·303
		207	9·67	5·30	7·292	0·009	0·032	0°50'	0·413	0·079	0·202
	203		9·68	5·36	10·196	0·005	0·023	0°35'	0·407	0·078	0·147
		208	9·57	5·42	12·860	0·003	0·018	0°30'	0·400	0·076	0·118
	204		9·71	5·32	15·437	0·002	0·014	0°35'	0·395	0·075	0·097
02/2	209		9·12	11·72	1·115	0·182	0·140	–	0·263	0·023	1·246
	"		"	"	"	"	0·136	–	0·254	0·022	"
		213	9·28	11·66	1·174	0·176	0·144	–	0·290	0·026	1·228
		"	"	"	"	"	0·138	–	0·277	0·024	"
		214	9·46	11·75	3·328	0·087	0·105	2°40'	0·610	0·053	0·783
	210		9·41	11·90	4·839	0·054	0·089	2°10'	0·747	0·064	0·607
		215	9·67	11·89	7·357	0·033	0·064	1°40'	0·833	0·071	0·428
	211		9·56	11·96	10·267	0·021	0·048	1°15'	0·866	0·074	0·318
		216	9·62	12·02	12·923	0·008	0·038	1°10'	0·875	0·074	0·257
	212		9·61	11·97	15·432	0·010	0·032	0°40'	0·891	0·076	0·215
02/1	217		9·29	20·06	1·121	0·201	0·147	–	0·282	0·014	1·375
	"		"	"	"	"	0·132	–	0·254	0·013	"
		221	9·30	19·82	1·223	0·208	0·150	–	0·314	0·016	1·355
		"	"	"	"	"	0·137	–	0·287	0·015	"
		222	9·51	19·99	3·448	0·140	0·125	3°10'	0·755	0·039	1·022
		"	"	"	"	"	0·123	"	0·743	0·038	"
	218		9·59	20·09	4·718	0·106	0·116	3°00'	0·965	0·049	0·877
	"		"	"	"	"	0·110	"	0·923	0·047	"
		223	9·54	20·28	7·250	0·069	0·092	2°20'	1·168	0·059	0·668
		"	"	"	"	"	0·090	"	1·144	0·058	"
	219		9·66	20·39	10·205	0·045	0·073	1°55'	1·315	0·066	0·513
		224	9·45	20·40	12·819	0·022	0·062	1°40'	1·381	0·069	0·422
	220		9·68	20·40	15·373	0·029	0·051	1°20'	1·399	0·070	0·358
02/4	225		9·54	31·09	2·172	0·200	0·133	–	0·507	0·017	1·328
	"		"	31·19	"	"	0·124	–	0·476	0·016	1·329
		229	9·52	31·21	2·277	0·204	0·133	–	0·532	0·017	1·318
		"	"	31·31	"	"	0·122	–	0·488	0·016	1·319
		230	9·66	31·15	3·451	0·187	0·133	3°20'	0·817	0·027	1·197
		"	"	"	"	"	0·128	"	0·786	0·026	"
	226		9·78	31·09	4·718	0·153	0·125	3°15'	1·065	0·035	1·077
	"		"	"	"	"	0·123	"	1·049	0·034	"
		231	9·68	31·25	7·339	0·112	0·113	2°55'	1·484	0·048	0·877
		"	"	"	"	"	0·111	"	1·452	0·047	"
	227		9·82	31·33	10·196	0·078	0·097	2°35'	1·778	0·058	0·714
	"		"	"	10·141	"	0·095	"	1·746	0·057	0·717
		232	9·61	31·54	12·976	0·059	0·081	2°15'	1·845	0·060	0·601
		"	"	"	12·911	"	0·079	"	1·807	0·059	0·603
	228		9·88	31·54	15·389	0·049	0·074	2°00'	2·068	0·067	0·524
02/3	233		9·34	51·29	2·221	0·225	0·125	–	0·479	0·010	1·418
	"		"	51·75	"	"	0·109	–	0·417	0·008	1·420
		237	9·38	51·19	2·313	0·228	0·124	–	0·496	0·010	1·412
		"	"	51·53	"	"	0·115	–	0·458	0·009	1·413
		238	9·56	51·23	3·539	0·218	0·124	3°15'	0·775	0·015	1·331
		"	"	51·29	"	"	0·121	"	0·751	"	"
	234		9·54	51·25	4·669	0·197	0·125	3°05'	1·028	0·020	1·258
		239	9·58	51·26	7·296	0·164	0·121	3°10'	1·565	0·031	1·104
		"	"	51·41	"	"	0·120	"	1·549	"	1·105
	235		9·64	51·25	10·464	0·123	0·117	2°50'	2·186	0·044	0·944
	"		"	51·52	10·128	"	0·111	"	2·003	0·040	0·962
		240	9·57	51·56	13·047	0·108	0·105	2°40'	2·407	0·048	0·840
	236		9·71	51·38	15·571	0·083	0·100	2°45'	2·785	0·055	0·750
	"		"	51·62	15·441	"	0·099	"	2·727	0·054	0·756

SERIES II DRAWING TESTS.

1.3/16 in. DIAMETER BAR LUBRICATED WITH OIL

TABLE No. A7.27 (see section 10.6.5)

Ref. no. of Bar	Test no.		P (tonf)	R (rev/min)	V (ft/min)	$\frac{(P-P_R)}{P}$	$\left(\frac{T}{d_1 P}\right)$	ϕ	R_P (rev/min)	R_B/R	θ_1 (radians)
03/4	241		13·28	5·06	1·026	0·134	0·147	–	0·472	0·095	0·952
		245	12·84	5·08	1·166	0·111	0·125	–	0·438	0·089	0·893
		246	13·53	5·13	3·277	0·044	0·074	3°25'	0·769	0·152	0·419
	242		13·83	5·24	4·716	0·022	0·059	3°00'	0·907	0·176	0·307
		247	13·62	5·25	7·115	0·015	0·039	1°50'	0·885	0·171	0·207
	243		13·85	5·25	9·967	0·007	0·029	1°30'	0·930	0·181	0·149
		248	13·51	5·32	12·692	0·000	0·022	1°05'	0·888	0·169	0·119
	244		13·88	5·34	15·201	0·000	0·019	1°05'	0·929	0·176	0·100
03/6	285		13·08	4·97	1·093	0·126	0·142	–	0·478	0·099	0·913
	286		13·36	5·13	3·305	0·032	0·077	3°30'	0·794	0·158	0·416
	287		12·66	5·23	4·641	0·032	0·049	–	0·681	0·132	0·311
03/5	249		13·60	10·99	1·083	0·207	0·175	–	0·608	0·056	1·238
		253	13·36	11·06	1·244	0·202	0·170	–	0·665	0·061	1·195
		254	13·55	11·41	3·364	0·104	0·125	6°05'	1·339	0·119	0·768
		"	"	"	"	"	0·124	"	1·327	0·118	"
	250		13·89	11·54	4·606	0·066	0·107	5°10'	1·601	0·141	0·620
		255	13·69	11·59	7·152	0·043	0·078	3°40'	1·798	0·158	0·432
	251		13·75	11·77	9·924	0·018	0·059	2°50'	1·875	0·162	0·326
		256	13·52	11·73	12·614	0·016	0·047	2°10'	1·878	0·163	0·259
	252		13·72	11·95	15·210	0·012	0·040	1°50'	1·943	0·165	0·220
03/3	257		13·70	19·24	1·148	0·247	0·181	–	0·669	0·035	1·364
		261	13·02	19·56	1·208	0·217	0·162	–	0·599	0·031	1·357
		262	13·30	19·94	3·488	0·150	0·143	6°55'	1·560	0·080	1·020
		"	"	"	"	"	0·142	"	1·545	0·079	"
	258		13·84	19·72	4·627	0·130	0·140	6°35'	2·112	0·109	0·882
	"		"	19·79	"	"	0·130	"	1·956	0·101	0·884
		263	13·54	19·98	7·122	0·085	0·107	5°25'	2·427	0·124	0·674
	259		14·00	19·75	7·276	0·081	0·114	5°45'	2·724	0·140	0·658
		264	13·73	20·24	12·698	0·034	0·073	3°05'	2·965	0·149	0·426
	260		13·85	20·28	15·182	0·023	0·065	3°05'	3·191	0·160	0·364
03/6	281		12·94	19·32	1·454	0·227	0·178	–	0·787	0·041	1·313
	282		13·14	19·61	3·381	0·154	0·146	6°45'	1·528	0·079	1·027
	283		12·99	19·71	4·694	0·115	0·128	5°45'	1·836	0·095	0·874
	284		13·43	19·89	9·993	0·051	0·088	4°10'	2·769	0·141	0·516
03/2		269	13·49	30·92	2·377	0·245	0·160	–	1·203	0·039	1·307
		"	"	31·07	"	"	0·151	–	1·136	0·037	1·308
	265		13·70	30·77	2·427	0·247	0·163	–	1·272	0·042	1·301
		270	13·51	30·75	3·447	0·207	0·160	7°15'	1·748	0·058	1·196
		"	"	"	"	"	0·157	"	1·721	0·057	"
	266		13·68	30·92	4·824	0·179	0·154	7°10'	2·392	0·079	1·070
		271	13·42	31·22	7·429	0·127	0·134	6°20'	3·132	0·102	0·875
		"	"	"	7·333	"	0·130	"	3·009	0·098	0·881
	267		13·70	31·31	10·234	0·095	0·119	5°30'	3·900	0·126	0·717
		272	13·40	31·66	12·987	0·078	0·095	4°40'	3·874	0·124	0·607
	268		13·62	31·78	15·446	0·055	0·088	4°10'	4·313	0·138	0·530
03/1	273		12·59	49·63	2·347	0·227	0·139	–	0·968	0·020	1·406
	"		"	50·16	"	"	0·123	–	0·852	0·017	1·408
		277	12·89	49·25	2·454	0·234	0·147	–	1·095	0·023	1·398
		"	"	49·78	2·362	"	0·131	–	0·937	0·019	1·406
		278	13·13	49·39	3·537	0·228	0·137	6°05'	1·499	0·031	1·325
		"	"	49·63	"	"	0·130	"	1·411	0·029	1·326
	274		12·95	49·55	4·751	0·201	0·139	6°30'	2·013	0·041	1·246
	"		"	"	"	"	0·137	"	1·971	0·040	"
		279	12·89	50·14	7·426	0·157	0·133	5°55'	2·997	0·061	1·091
		"	"	49·79	7·389	"	0·133	"	2·965	0·060	"
	275		13·03	50·49	10·466	0·127	0·129	5°40'	4·130	0·083	0·942
	"		"	49·98	10·141	"	0·123	"	3·819	0·078	0·952
		280	13·00	50·38	12·814	0·098	0·123	5°30'	4·783	0·096	0·842
	276		13·10	51·06	15·649	0·090	0·108	5°00'	5·192	0·103	0·749
	"		"	50·83	15·418	"	0·107	"	5·047	0·101	0·754

SERIES II DRAWING TESTS.

1.1/4 in. DIAMETER BAR LUBRICATED WITH OIL

TABLE No. A7.28
(see section 10.6.5)

Ref. no. of Bar	Test no.		P (tonf)	R (rev/min)	V (ft/min)	$\frac{(P-P_R)}{P}$	$\left(\frac{T}{d_1 P}\right)$	ϕ	R_P (rev/min)	R_B/R	Θ_1 (radians)
04/2	288		17·74	5·57	1·086	0·131	0·154	–	0·793	0·144	0·970
		292	17·42	5·84	1·205	0·129	0·143	–	0·800	0·139	0·943
		293	17·59	6·28	3·172	0·048	0·090	6°20′	1·328	0·215	0·513
	289		18·19	6·38	4·683	0·029	0·069	4°50′	1·555	0·248	0·369
		294	17·88	6·42	6·474	0·016	0·048	3°20′	1·456	0·231	0·275
	290		18·09	6·47	9·819	0·010	0·036	2°35′	1·671	0·263	0·185
		295	18·11	6·57	12·499	0·010	0·027	1°55′	1·626	0·251	0·148
	291		18·04	6·56	15·076	0·008	0·023	1°50′	1·676	0·259	0·123
04/4		300	18·65	10·73	2·284	0·142	0·148	–	1·686	0·159	0·928
	296		17·63	11·77	2·360	0·117	0·135	–	1·496	0·129	0·956
		301	18·44	11·31	3·163	0·102	0·129	9°05′	2·005	0·179	0·794
	297		18·30	12·01	4·699	0·070	0·101	7°15′	2·311	0·195	0·628
		302	18·48	11·85	7·092	0·041	0·078	5°55′	2·705	0·231	0·443
	298		18·10	12·32	9·868	0·029	0·055	4°05′	2·593	0·213	0·341
		303	18·83	12·00	12·582	0·023	0·048	3°30′	2·997	0·253	0·265
	299		18·50	12·40	15·086	0·012	0·041	2°50′	3·005	0·246	0·230
04/1		308	18·56	19·24	3·328	0·172	0·153	–	2·530	0·134	1·024
	304		18·01	19·36	3·343	0·154	–	–	–	–	1·025
	305		18·44	19·30	4·753	0·123	0·139	10°05′	3·241	0·170	0·857
	"		"	"	"	"	0·136	"	3·171	0·167	"
		309	18·58	19·90	7·132	0·081	0·116	8°45′	4·098	0·209	0·671
	306		18·73	19·97	9·936	0·057	0·093	6°50′	4·584	0·233	0·519
		310	18·79	20·15	12·569	0·040	0·080	5°55′	4·978	0·251	0·428
	307		18·88	20·32	15·069	0·035	0·067	5°15′	5·022	0·250	0·366
04/3	311		17·05	29·22	7·367	0·096	0·117	8°05′	3·907	0·136	0·845
	"		"	"	7·222	"	0·114	"	3·740	0·130	0·855
		313	18·07	29·09	10·065	0·089	0·109	7°55′	5·269	0·184	0·688
	312		17·87	29·40	12·704	0·060	0·095	6°45′	5·704	0·197	0·582
		314	18·01	29·65	15·233	0·049	0·083	6°05′	6·017	0·206	0·505
04/5	315		17·73	28·62	7·303	0·116	0·129	9°10′	4·437	0·157	0·839
	"		"	"	7·222	"	0·128	"	4·380	0·155	0·845
		317	18·30	28·85	10·016	0·087	0·117	8°15′	5·699	0·200	0·686
	316		17·96	29·30	12·730	0·061	0·100	7°10′	6·045	0·209	0·579
		318	18·37	29·35	15·196	0·054	0·088	6°35′	6·532	0·226	0·502
04/5	319		18·36	36·95	7·367	0·152	0·149	10°30′	5·397	0·148	0·959
		321	18·37	37·61	10·084	0·120	0·127	9°10′	6·288	0·170	0·815
	320		18·50	38·12	12·717	0·092	0·119	8°40′	7·466	0·199	0·705
	"		"	37·73	12·581	"	0·116	"	7·186	0·193	"
		322	18·37	38·56	15·270	0·071	0·104	7°40′	7·770	0·204	0·623

SERIES II DRAWING TESTS.

1.5/16 in. DIAMETER BAR LUBRICATED WITH OIL

TABLE No. A7.29
(see section 10.6.5)

Ref. no. of Bar	Test no.		P (tonf)	R (rev/min)	V (ft/min)	$\frac{(P-P_R)}{P}$	$\left(\frac{T}{d_1 P}\right)$	ϕ	R_p (rev/min)	R_B/R_1	θ_1 (radians)
05/1	323		21.51	5.67	2.651	0.054	0.096	9°45'	1.804	0.323	0.546
		327	20.70	5.78	2.811	0.046	0.084	9°00'	1.620	0.284	0.528
	324		21.49	5.90	4.799	0.026	0.059	6°05'	1.998	0.342	0.336
		328	21.74	5.92	7.083	0.013	0.043	4°40'	2.193	0.375	0.233
	325		21.40	5.97	9.772	0.009	0.030	3°10'	2.073	0.352	0.172
		329	21.86	5.94	12.340	0.004	0.026	2°45'	2.286	0.389	0.136
	326		21.20	4.89	14.821	0.009	0.019	1°50'	1.951	0.403	0.093
05/2	330		21.19	9.99	2.882	0.095	0.127	14°05'	2.585	0.262	0.777
		333	21.12	9.98	2.909	0.091	0.125	14°55'	2.564	0.260	0.772
	331		21.77	10.37	4.649	0.060	0.102	11°10'	3.432	0.335	0.565
		334	21.94	10.79	6.981	0.037	0.077	8°20'	3.904	0.366	0.414
	332		22.34	10.88	9.689	0.018	0.059	6°20'	4.199	0.391	0.309
		335	22.16	10.94	12.359	0.018	0.047	5°05'	4.187	0.388	0.246
05/3	336		21.46	19.22	7.293	0.067	0.107	11°20'	5.528	0.291	0.642
		338	21.79	19.43	9.865	0.053	0.086	9°30'	6.103	0.318	0.510
	337		21.99	19.67	12.561	0.040	0.073	7°50'	6.624	0.341	0.418
		339	21.17	19.86	14.948	0.027	0.057	6°10'	5.956	0.304	0.361
05/3	340		21.28	28.43	7.345	0.105	0.128	13°00'	6.656	0.237	0.833
		342	21.86	29.20	9.946	0.087	0.113	12°25'	8.185	0.284	0.695
	341		21.96	29.22	12.786	0.062	0.099	10°30'	9.232	0.320	0.576
		343	21.73	29.72	15.001	0.050	0.086	9°10'	9.280	0.316	0.512
05/4		347	21.12	37.46	10.276	0.104	0.118	11°35'	8.481	0.229	0.803
	344		21.16	37.93	10.477	0.106	0.122	11°40'	8.990	0.240	0.799
		346	21.66	37.90	12.814	0.086	0.113	12°00'	10.381	0.277	0.699
		"	"	"	"	"	0.108	"	9.980	0.266	"
	345		21.56	38.38	15.081	0.064	0.105	11°15'	11.342	0.299	0.626

SERIES II DRAWING TESTS.

1.1/16 in. DIAMETER BAR LUBRICATED WITH OIL

TABLE No. A7.30
(see section 10.6.5)

Ref. no. of Bar	Test no.		P (tonf)	R (rev/min)	V (ft/min)	$\frac{(P-P_R)}{P}$	$\left(\frac{T}{d_1 P}\right)$	ϕ	R_p (rev/min)	R_B/R..	Θ_1 (radians)
01/2	348		5·80	20·03	0·913	0·326	0·192	—	0·144	0·007	1·406
	"		"	"	"	0·31	0·188	—	0·141	"	"
		352	5·80	20·00	0·946	0·319	0·194	—	0·150	0·007	1·399
		"	"	"	"		0·189	—	0·147	"	"
		353	5·91	20·16	3·734	0·183	0·156	1°55'	0·486	0·025	0·975
	349		5·95	20·13	4·901	0·143	0·146	1°55'	0·605	0·031	0·843
		354	5·87	20·28	7·478	0·085	0·113	1°20'	0·706	0·036	0·638
	350		5·82	20·25	10·341	0·048	0·090	1°10'	0·770	0·039	0·491
		355	5·98	20·30	12·962	0·037	0·075	0°40'	0·835	0·042	0·404
	351		5·92	20·30	15·544	0·024	0·062	0°50'	0·812	0·041	0·343

TABLE No. A7.31 (see section 10.6.6) — SERIES II - 1.1/16 in. DIAMETER BAR LUBRICATED WITH SOAP

		calculated from section 3.2 for $n = 1 \cdot 0$						from section [illegible]	
Test no.	θ_1 (radians)	$\frac{(l_1 - l_2)}{l_1}$	$P_{F(P)}/p$	μ_P	l_3/l_1	$P_{F(T)}/p$	μ_T	μ_P	μ_T
33	1·013	0·4862	0·1959	0·0279	3·8352	0·2261	0·0335	0·0277	0·0333
37	0·979	0·4574	0·1987	0·0285	3·7552	0·2270	0·0337	0·0283	0·0335
38	0·439	0·1008	0·2550	0·0393	1·9557	0·2255	0·0334	0·0386	0·0330
34	0·277	0·0408	0·3455	0·0605	1·2648	0·2164	0·0317	0·0592	0·0312
39	0·186	0·0185	—	—	0·8571	0·2184	0·0320	—	0·0316
35	0·134	0·0096	—	—	0·6188	0·2104	0·0306	—	0·0301
40	0·109	0·0064	—	—	0·5032	0·2081	0·0301	—	0·0297
36	0·091	0·0044	—	—	0·4192	0·1958	0·0279	—	0·0276
25	1·294	0·7373	0·2146	0·0313	4·3134	0·2417	0·0366	0·0313	0·0364
29	1·280	0·7241	0·2096	0·0304	4·2970	0·2453	0·0373	0·0304	0·0371
30	0·771	0·2962	0·2307	0·0344	3·1760	0·2264	0·0336	0·0341	0·0333
26	0·525	0·1429	0·2570	0·0397	2·3034	0·2237	0·0331	0·0391	0·0327
31	0·372	0·0728	0·4257	0·0850	1·6747	0·2175	0·0319	0·0831	0·0315
27	0·274	0·0399	0·3540	0·0629	1·2510	0·2161	0·0316	0·0614	0·0312
32	0·223	0·0266	0·3096	0·0514	1·0241	0·2059	0·0297	0·0504	0·0294
28	0·186	0·0185	—	—	0·8554	0·2063	0·0298	—	0·0294
1	1·407	0·8441	0·2224	0·0328	4·4158	0·2380	0·0358	0·0328	0·0357
5	1·408	0·8445	0·2043	0·0294	4·4160	0·2352	0·0353	0·0294	0·0351
6	1·065	0·5303	0·2077	0·0301	3·9467	0·2249	0·0333	0·0300	0·0331
7	1·058	0·5249	0·2246	0·0332	3·9337	0·2204	0·0324	0·0332	0·0323
2	0·842	0·3485	0·2356	0·0354	3·3916	0·2230	0·0329	0·0351	0·0327
3	0·495	0·1273	0·2301	0·0343	2·1828	0·2209	0·0325	0·0338	0·0322
8	0·414	0·0901	0·2792	0·0444	1·8565	0·2041	0·0294	[illegible]	0·0291
4	0·344	0·0628	0·2033	0·0293	1·5592	0·2079	0·0301	0·0289	0·0298
13	1·455	0·8897	0·2176	0·0319	4·4431	0·2418	0·0366	0·0319	0·0364
9	1·455	0·8894	0·2102	0·0305	4·4430	0·2331	0·0349	0·0305	0·0347
14	1·205	0·6556	0·2090	0·0303	4·1970	0·2162	0·0316	0·0303	0·0315
10	1·030	0·5004	0·2425	0·0367	3·8726	0·2114	0·0307	0·0366	0·0306
15	0·828	0·3382	0·2241	0·0331	3·3516	0·2140	0·0312	0·0329	0·0310
11	0·673	0·2301	0·2012	0·0289	2·8532	0·2011	0·0289	0·0287	0·0287
16	0·562	0·1631	0·2114	0·0308	2·4469	0·2071	0·0300	0·0304	[illegible]
12	0·488	0·1245	0·2695	0·0423	2·1599	0·1997	0·0286	0·0418	[illegible]
17	1·486	0·9189	0·2014	0·0289	4·4557	0·2447	0·0372	0·0289	0·0370
21	1·484	0·9169	0·2084	0·0302	4·4550	0·2209	0·0325	0·0302	0·0324
22	1·285	0·7289	0·2117	0·0308	4·3030	0·2058	0·0297	0·0308	0·0295
18	1·146	0·6024	0·2270	0·0337	4·1020	0·2103	0·0305	0·0336	0·0304
23	0·969	0·4497	0·2030	0·0292	3·7326	0·2030	0·0292	0·0291	0·0290
19	0·812	0·3262	0·1873	0·0264	3·3034	0·1955	0·0279	0·0263	0·0277
24	0·699	0·2469	0·2136	0·0311	2·9413	0·1918	0·0272	0·0309	0·0270
20	0·612	0·1919	0·2378	0·0358	2·6333	0·1882	0·0266	0·0354	[illegible]

TABLE No. A7.32 (see section 10.6.6)

SERIES II – 1.1/8 in. DIAMETER BAR LUBRICATED WITH SOAP

Test no.	θ_1 (radians)	calculated from section 3.2 for n=1·0: $\frac{(l_1-l_2)}{l_1}$	$P_{F(P)}/P$	μ_P	l_3/l_1	$P'_{F(T)}/P$	μ_T	from section 3.1: μ_P	μ_T
177	0.995	0.4969	0.1121	0.0150	3.8554	0.1515	0.0212	0.0150	0.0211
181	0.974	0.4788	0.1271	0.0173	3.8072	0.1724	0.0248	0.0173	0.0247
182	0.418	0.1025	0.2385	0.0372	1.9678	0.1636	0.0232	0.0365	0.0229
178	0.305	0.0557	0.1294	0.0176	1.4678	0.1533	0.0215	0.0174	0.0212
183	0.203	0.0249	–	–	0.9901	0.1544	0.0217	–	0.0214
179	0.146	0.0130	–	–	0.7177	0.1538	0.0216	–	0.0213
184	0.116	0.0083	–	–	0.5722	0.1555	0.0219	–	0.0215
180	0.097	0.0058	–	–	0.4780	0.1418	0.0196	–	0.0194
161	1.343	0.7969	0.1256	0.0171	4.3680	0.1640	0.0233	0.0171	0.0232
"	"	"	"	"	"	0.1550	0.0218	"	0.0217
165	1.326	0.7822	0.1304	0.0178	4.3539	0.1678	0.0239	0.0178	0.0238
"	"	"	"	"	"	0.1593	0.0225	"	0.0224
166	0.848	0.3787	0.1307	0.0179	3.4958	0.1530	0.0214	0.0178	0.0213
162	0.608	0.2086	0.1362	0.0187	2.7273	0.1527	0.0214	0.0186	0.0212
167	0.426	0.1064	0.2130	0.0321	2.0030	0.1486	0.0207	0.0317	0.0205
163	0.317	0.0599	0.2320	0.0359	1.5206	0.1529	0.0214	0.0352	0.0212
168	0.254	0.0389	0.2136	0.0322	1.2319	0.1518	0.0212	0.0317	0.0210
164	0.214	0.0277	0.4189	0.0856	1.0427	0.1446	0.0201	0.0837	0.0198
185	1.397	0.8449	0.1250	0.0170	4.4070	0.1635	0.0232	0.0170	0.0231
"	"	"	"	"	"	0.1542	0.0216	"	0.0215
189	1.389	0.8379	0.1315	0.0180	4.4020	0.1665	0.0237	0.0180	0.0236
"	"	"	"	"	"	0.1598	0.0226	"	0.0225
190	1.079	0.5674	0.1366	0.0188	4.0220	0.1561	0.0220	0.0188	0.0219
"	"	"	"	"	4.0218	0.1538	0.0216	"	0.0215
186	0.888	0.4094	0.1381	0.0190	3.6000	0.1549	0.0218	0.0190	0.0216
191	0.672	0.2506	0.1341	0.0184	2.9539	0.1530	0.0214	0.0183	0.0213
187	0.520	0.1556	0.1371	0.0189	2.3900	0.1516	0.0212	0.0187	0.0210
192	0.426	0.1066	0.1892	0.0277	2.0041	0.1490	0.0208	0.0274	0.0206
188	0.361	0.0773	0.1220	0.0165	1.7203	0.1503	0.0210	0.0163	0.0208
169	1.354	0.8067	0.1449	0.0201	4.3769	0.1602	0.0226	0.0201	0.0225
"	"	"	"	"	"	0.1544	0.0217	0.0 "	0.0216
173	1.348	0.8017	0.1301	0.0178	4.3724	0.1606	0.0227	0.0178	0.0226
"	"	"	"	"	"	0.1569	0.0221	"	0.0220
174	1.240	0.7067	0.1324	0.0181	4.2649	0.1550	0.0218	0.0181	0.0217
"	"	"	"	"	"	0.1515	0.0212	"	0.0211
170	1.085	0.5719	0.1375	0.0189	4.0317	0.1532	0.0215	0.0189	0.0214
"	"	"	"	"	"	0.1527	0.0214	"	0.0213
175	0.885	0.4072	0.1469	0.0204	3.5928	0.1538	0.0216	0.0204	0.0214
171	0.717	0.2816	0.1334	0.0183	3.1036	0.1531	0.0215	0.0182	0.0213
176	0.606	0.2074	0.1496	0.0209	2.7202	0.1499	0.0209	0.0207	0.0208
172	0.528	0.1605	0.1457	0.0202	2.4245	0.1494	0.0208	0.0200	0.0206
193	1.434	0.8777	0.1410	0.0195	4.4275	0.1742	0.0250	0.0195	0.0249
"	"	"	"	"	4.4278	0.1482	0.0207	"	0.0206
197	1.429	0.8734	0.1336	0.0183	4.4251	0.1586	0.0224	0.0183	0.0223
"	"	"	"	"	4.4253	0.1497	0.0209	"	0.0208
198	1.363	0.8150	0.1367	0.0188	4.3840	0.1559	0.0219	0.0188	0.0218
"	"	"	"	"	"	0.1493	0.0208	"	0.0207
194	1.265	0.7287	0.1374	0.0189	4.2937	0.1515	0.0212	0.0189	0.0211
"	"	"	"	"	"	0.1493	0.0208	"	0.0207
199	1.112	0.5952	0.1404	0.0194	4.0791	0.1476	0.0206	0.0194	0.0205
195	0.968	0.4744	0.1355	0.0186	3.7952	0.1487	0.0207	0.0186	0.0206
200	0.854	0.3832	0.1383	0.0191	3.5114	0.1434	0.0199	0.0190	0.0198
196	0.765	0.3163	0.1570	0.0221	3.2556	0.1422	0.0197	0.0220	0.0196

TABLE No. A7.33 (see section 10.6.6)		SERIES II - 1.3/16 in. DIAMETER BAR LUBRICATED WITH SOAP							
		calculated from section 3.2 for n=1·0						from section 3.1	
Test no.	θ_1 (radians)	$\frac{(l_1-l_2)}{l_1}$	$P_{F(P)}/p$	μ_P	l_3/l_1	$P_{F(T)}/p$	μ_T	μ_P	μ_T
61	0·994	0·5217	0·1261	0·0173	4·0107	0·1533	0·0217	0·0171	0·0214
57	0·980	0·5105	0·1181	0·0160	3·9824	0·1502	0·0211	0·0158	0·0209
62	0·442	0·1266	0·1539	0·0218	2·2246	0·1650	0·0236	0·0206	0·0229
58	0·307	0·0637	0·0843	0·0110	1·6046	0·1543	0·0218	0·0104	0·0211
63	0·204	0·0284	-	-	1·0808	0·1581	0·0225	-	0·0216
59	0·149	0·0154	-	-	0·7990	0·1531	0·0216	-	0·0208
64	0·116	0·0092	-	-	0·6177	0·1652	0·0237	-	0·0226
60	0·098	0·0067	-	-	0·5266	0·1507	0·0211	-	0·0203
45	1·274	0·7529	0·1448	0·0202	4·4255	0·1817	0·0265	0·0202	0·0264
"	"	"	"	"	4·4256	0·1783	0·0260	"	0·0258
41	1·258	0·7397	0·1485	0·0209	4·4097	0·1792	0·0261	0·0208	0·0259
"	"	"	"	"	4·4098	0·1751	0·0254	"	0·0252
46	0·790	0·3571	0·1728	0·0250	3·4984	0·1824	0·0267	0·0241	0·0262
42	0·604	0·2248	0·1623	0·0232	2·8857	0·1663	0·0239	0·0222	0·0233
47	0·433	0·1211	0·1623	0·0232	2·1794	0·1756	0·0255	0·0217	0·0246
43	0·322	0·0689	0·1354	0·0187	1·6658	0·1648	0·0236	0·0175	0·0227
48	0·255	0·0434	0·2148	0·0327	1·3308	0·1790	0·0261	0·0300	0·0249
44	0·216	0·0315	-	-	1·1374	0·1724	0·0249	-	0·0238
65	1·411	0·8677	0·1314	0·0181	4·5271	0·1684	0·0242	0·0181	0·0241
"	1·412	"	"	"	4·5276	0·1636	0·0234	"	0·0233
69	1·400	0·8584	0·1360	0·0188	4·5213	0·1734	0·0251	0·0188	0·0249
"	"	"	"	"	"	0·1652	0·0237	"	0·0235
70	1·077	0·5890	0·1482	0·0208	4·1634	0·1632	0·0233	0·0206	0·0231
"	"	"	"	"	"	0·1622	0·0232	"	0·0230
66	0·895	0·4403	0·1421	0·0198	3·7847	0·1645	0·0236	0·0194	0·0232
71	0·680	0·2787	0·1561	0·0221	3·1633	0·1626	0·0232	0·0214	0·0228
67	0·527	0·1750	0·1351	0·0187	2·5816	0·1645	0·0236	0·0178	0·0229
72	0·429	0·1208	0·1591	0·0226	2·1760	0·1464	0·0205	0·0216	0·0200
68	0·365	0·0887	0·1634	0·0234	1·8806	0·1468	0·0206	0·0221	0·0200
49	1·471	0·9172	0·1359	0·0188	4·5516	0·1694	0·0244	0·0188	0·0242
"	"	"	"	"	4·5518	0·1613	0·0230	"	0·0229
53	1·462	0·9102	0·1460	0·0204	4·5489	0·1808	0·0264	0·0204	0·0262
"	1·463	"	"	"	4·5492	0·1678	0·0241	"	0·0240
54	1·234	0·7197	0·1501	0·0211	4·3841	0·1713	0·0247	0·0210	0·0246
"	"	"	"	"	4·3842	0·1655	0·0237	"	0·0236
50	1·098	0·6066	0·1334	0·0184	4·1988	0·1600	0·0228	0·0182	0·0226
"	"	"	"	"	4·1989	0·1584	0·0225	"	0·0223
55	0·906	0·4492	0·1529	0·0216	3·8119	0·1696	0·0244	0·0211	0·0241
"	"	"	"	"	"	0·1691	0·0243	"	0·0240
51	0·735	0·3170	0·1599	0·0228	3·3361	0·1649	0·0236	0·0220	0·0232
56	0·625	0·2386	0·1543	0·0218	2·9610	0·1667	0·0239	0·0209	0·0233
52	0·545	0·1864	0·1444	0·0202	2·6560	0·1605	0·0229	0·0192	0·0233
73	1·505	0·9454	0·1294	0·0178	4·5605	0·1622	0·0231	0·0178	0·0230
"	"	"	"	"	4·5606	0·1472	0·0206	"	0·0205
77	1·502	0·9429	0·1394	0·0194	4·5599	0·1711	0·0247	0·0194	0·0246
"	"	"	"	"	4·5600	0·1571	0·0223	"	0·0222
78	1·358	0·8239	0·1322	0·0182	4·4959	0·1516	0·0214	0·0182	0·0212
"	1·359	"	"	"	4·4962	0·1492	0·0210	"	0·0209
74	1·269	0·7493	0·1324	0·0183	4·4214	0·1571	0·0223	0·0182	0·0221
79	1·121	0·6255	0·1368	0·0190	4·2347	0·1583	0·0225	0·0188	0·0223
75	0·979	0·5092	0·1376	0·0191	3·9791	0·1554	0·0220	0·0188	0·0218
80	0·856	0·4107	0·1375	0·0191	3·6897	0·1502	0·0211	0·0187	0·0209
76	0·763	0·3384	0·1597	0·0227	3·4247	0·1589	0·0226	0·0221	0·0222

TABLE No. A7.34 (see section 10.6.6)		SERIES II – 1.1/4 in. DIAMETER BAR LUBRICATED WITH SOAP							
		calculated from section 3.2 for n=1·0						from section 3.1	
Test no.	θ_1 (radians)	$\frac{(l_1-l_2)}{l_1}$	$P_{F(P)}/p$	μ_P	l_3/l_1	$P_{F(T)}/p$	μ_T	μ_P	μ_T
97	0·943	0·5014	0·1424	0·0199	4·0591	0·1641	0·0236	0·0191	0·0231
101	0·912	0·4768	0·1380	0·0192	3·9906	0·1646	0·0237	0·0184	0·0232
102	0·412	0·1194	0·1743	0·0254	2·2198	0·1731	0·0251	0·0219	0·0234
98	0·292	0·0618	0·1978	0·0296	1·6215	0·1712	0·0248	0·0249	0·0223
103	0·199	0·0289	0·1677	0·0242	1·1179	0·1766	0·0258	0·0200	0·0233
99	0·146	0·0156	0·3079	0·0534	0·8258	0·1754	0·0256	0·0425	0·0231
104	0·113	0·0095	–	–	0·6458	0·1729	0·0251	–	0·0227
100	0·097	0·0071	–	–	0·5561	0·1611	0·0231	–	0·0210
81	1·306	0·7933	0·1229	0·0168	4·5820	0·1617	0·0232	0·0167	0·0230
"	"	"	"	"	4·5821	0·1585	0·0226	"	0·0225
85	1·265	0·7613	0·1257	0·0173	4·5477	0·1614	0·0231	0·0171	0·0229
"	"	"	"	"	"	0·1589	0·0227	"	0·0225
86	0·826	0·4096	0·1432	0·0201	3·7795	0·1617	0·0232	0·0190	0·0226
82	0·626	0·2596	0·1301	0·0180	3·1479	0·1480	0·0209	0·0166	0·0200
87	0·453	0·1442	0·1577	0·0225	2·4236	0·1604	0·0229	0·0199	0·0216
83	0·340	0·0848	0·1334	0·0185	1·8875	0·1500	0·0212	0·0163	0·0198
88	0·272	0·0552	0·2392	0·0378	1·5351	0·1536	0·0218	0·0322	0·0202
84	0·229	0·0393	0·1898	0·0281	1·3004	0·1568	0·0223	0·0240	0·0206
105	1·378	0·8502	0·1433	0·0201	4·6305	0·1669	0·0241	0·0200	0·0239
"	"	"	"	"	"	0·1648	0·0237	"	0·0236
109	1·365	0·8398	0·1364	0·0190	4·6228	0·1701	0·0246	0·0188	0·0245
"	"	"	"	"	4·6229	0·1675	0·0242	"	0·0240
110	1·044	0·5829	0·1476	0·0208	4·2559	0·1702	0·0246	0·0201	0·0243
106	0·897	0·4640	0·1579	0·0225	3·9534	0·1674	0·0242	0·0214	0·0236
111	0·690	0·3019	0·1687	0·0244	3·3533	0·1758	0·0256	0·0222	0·0245
107	0·538	0·1961	0·1608	0·0230	2·7861	0·1688	0·0244	0·0205	0·0230
112	0·437	0·1336	0·1675	0·0242	2·3392	0·1704	0·0247	0·0210	0·0230
108	0·373	0·0988	0·2000	0·0300	2·0306	0·1704	0·0247	0·0256	0·0228
89	1·327	0·8103	0·1392	0·0194	4·5982	0·1549	0·0220	0·0193	0·0219
93	1·317	0·8023	0·1426	0·0200	4·5908	0·1605	0·0230	0·0198	0·0228
94	1·204	0·7120	0·1581	0·0226	4·4845	0·1675	0·0242	0·0222	0·0239
90	1·082	0·6146	0·1510	0·0214	4·3210	0·1562	0·0222	0·0208	0·0220
95	0·893	0·4603	0·1627	0·0233	3·9422	0·1741	0·0253	0·0221	0·0247
91	0·727	0·3325	0·1567	0·0223	3·4872	0·1591	0·0227	0·0207	0·0219
96	0·617	0·2498	0·1634	0·0234	3·0969	0·1677	0·0242	0·0212	0·0231
92	0·540	0·1980	0·1615	0·0231	2·7978	0·1612	0·0231	0·0207	0·0219
113	1·411	0·8763	0·1354	0·0188	4·6474	0·1452	0·0204	0·0187	0·0203
117	1·406	0·8724	0·1325	0·0183	4·6451	0·1520	0·0215	0·0183	0·0214
"	1·407	"	"	"	4·6456	0·1485	0·0209	"	0·0208
118	1·332	0·8138	0·1406	0·0196	4·6014	0·1561	0·0222	0·0195	0·0221
114	1·258	0·7555	0·1457	0·0205	4·5410	0·1551	0·0220	0·0202	0·0219
119	1·118	0·6435	0·1450	0·0204	4·3751	0·1611	0·0231	0·0199	0·0228
115	0·970	0·5243	0·1429	0·0200	4·1189	0·1544	0·0219	0·0193	0·0216
120	0·850	0·4283	0·1391	0·0194	3·8420	0·1572	0·0224	0·0184	0·0218
116	0·765	0·3639	0·1331	0·0184	3·6130	0·1434	0·0201	0·0174	0·0195

TABLE No. A7.35 (see section 10.6.6)		SERIES II - 1.5/16 in. DIAMETER BAR LUBRICATED WITH SOAP							
		calculated from section 3.2 for n=1·0						from section 3.1	
Test no.	θ_1 (radians)	$\frac{(l_1-l_2)}{l_1}$	$P_{F(P)}/p$	μ_P	l_3/l_1	$P_{F(T)}/p$	μ_T	μ_P	μ_T
137	0·985	0.5585	0.1343	0·0190	4·2535	0.1629	0·0238	0·0179	0·0232
141	0·972	0.5487	0.1292	0·0181	4·2303	0.1580	0·0230	0·0171	0·0224
142	0·496	0.1849	0.1572	0·0228	2·7472	0.1552	0·0225	0·0189	0·0205
138	0·351	0.0951	0.1528	0·0221	2·0203	0.1702	0·0251	0·0170	0·0220
143	0·235	0.0431	0·2498	0·0407	1·3791	0.1761	0·0261	0·0289	0·0222
139	0·172	0.0236	—	-	1·0261	0.1677	0·0246	—	0·0210
144	0·136	0.0150	—	-	0·8182	0·1654	0·0242	—	0·0206
140	0·114	0.0103	—	-	0·6788	0·1730	0·0256	-	0·0214
121	1·267	0·778	0·1309	0·0184	4·6229	0.1769	0·0263	0·0181	0·0260
"	"	"	"	"	4·6230	0.1724	0·0255	"	0·0252
125	1·249	0·7639	0·1291	0·0181	4·6073	0.1636	0·0239	0·0177	0·0237
"	"	"	"	"	4·6077	0.1582	0·0230	"	0·0227
126	0·823	0·4282	0·1503	0·0216	3·8893	0.1664	0·0244	0·0196	0·0234
122	0·630	0·2770	0·1555	0·0225	3·2762	0.1694	0·0249	0·0193	0·0232
127	0·456	0·1542	0·1616	0·0236	2·5311	0.1803	0·0269	0·0187	0·0240
123	0·342	0·0906	0·1557	0·0226	1·9735	0.1684	0·0248	0·0174	0·0217
128	0·272	0·0567	0·1278	0·0179	1·5763	0·1861	0·0280	0·0132	0·0237
124	0·230	0·0419	0·2069	0·0319	1·3599	0·1667	0·0245	0·0233	0·0210
145	1·369	0·8543	0·1161	0·0161	4·6912	0.1504	0·0217	0·0159	0·0215
"	"	"	"	"	4·6914	0.1397	0·0199	"	0·0197
149	1·358	0·8463	0·1217	0·0169	4·6854	0·1653	0·0242	0·0168	0·0240
"	"	"	"	"	4·6856	0.1515	0·0218	"	0·0217
150	1·047	0·6088	0·1291	0·0181	4·3626	0.1550	0·0224	0·0173	0·0220
"	"	"	"	"	4·3630	0.1533	0·0221	"	0·0217
146	0·898	0·4901	0·1462	0·0209	4·0776	0·1591	0·0231	0·0194	0·0224
"	"	"	"	"	4·0788	0.1562	0·0226	"	0·0219
151	0·703	0·3349	0·1352	0·0191	3·5405	0·1616	0·0236	0·0169	0·0223
147	0·538	0·2116	0·1634	0·0239	2·9177	0.1650	0·0242	0·0198	0·0221
152	0·440	0·1468	0·1621	0·0237	2·4742	0.1660	0·0243	0·0190	0·0219
148	0·374	0·1089	0·1698	0·0250	2·1525	0·1595	0·0232	0·0197	0·0207
133	1·318	0·8161	0·1274	0·0179	4·6608	0·1527	0·0220	0·0176	0·0218
"	1·320	"	"	"	4·6623	0.1455	0·0208	"	0·0207
129	1·289	0·7948	0·1312	0·0185	4·6407	0·1598	0·0233	0·0182	0·0230
134	1·212	0·7360	0·1389	0·0197	4·5730	0·1625	0·0237	0·0192	0·0234
"	"	"	"	"	4·5731	0.1613	0·0235	"	0·0232
130	1·089	0·6405	0·1384	0·0196	4·4238	0·1678	0·0247	0·0188	0·0242
135	0·910	0·4973	0·1469	0·0211	4·0982	0.1708	0·0252	0·0195	0·0244
131	0·741	0·3626	0·1487	0·0214	3·6531	0·1646	0·0241	0·0190	0·0228
136	0·623	0·2717	0·1541	0·0223	3·2494	0·1685	0·0248	0·0190	0·0230
132	0·514	0·2156	0·1501	0·0216	2·9415	0·1587	0·0231	0·0180	0·0212
157	1·485	0·9383	0·1164	0·0161	4·7331	0·1551	0·0224	0·0161	0·0223
"	1·486	"	"	"	4·7334	0·1353	0·0191	"	0·0190
153	1·405	0·8807	0·1312	0·0185	4·7081	0.1535	0·0222	0·0183	0·0220
"	1·408	"	"	"	4·7093	0.1295	0·0182	"	0·0181
158	1·336	0·8300	0·1293	0·0182	4·6727	0.1490	0·0214	0·0179	0·0212
"	"	"	"	"	4·6727	0·1443	0·0206	"	0·0205
154	1·260	0·7729	0·1387	0·0197	4·6175	0·1504	0·0216	0·0193	0·0214
"	"	"	"	"	4·6178	0·1421	0·0203	"	0·0201
159	0·974	0·5483	0·1533	0·0221	4·2294	0·1670	0·0245	0·0207	0·0239
155	0·968	0·5451	0·1435	0·0205	4·2216	0.1598	0·0233	0·0192	0·0227
"	0·975	"	"	"	4·2341	0·1572	0·0228	"	0·0222
160	0·847	0·4459	0·1589	0·0231	3·9466	0·1693	0·0249	0·0210	0·0239
"	0·855	"	"	"	3·9680	0.1671	0·0245	"	0·0236
156	0·765	0·3830	0·1471	0·0211	3·7307	0.1550	0·0224	0·0189	0·0214
"	0·768	"	"	"	3·7428	0·1526	0·0220	"	0·0210

TABLE No. A7.36 (see section 10.6.6)		SERIES II – 1.1/8 in. DIAMETER BAR LUBRICATED WITH OIL							
		calculated from section 3.2 for $n = 1\cdot0$						from section 3.1	
Test no.	θ_1 (radians)	$\frac{(l_1-l_2)}{l_1}$	$P_{F(P)}/P$	μ_P	l_3/l_1	$P_{F(T)}/P$	μ_T	μ_P	μ_T
201	0·948	0·4534	0·2363	0·0367	3·7359	0·2673	0·0433	0·0362	0·0428
205	0·895	0·4103	0·2736	0·0447	3·6033	0·2798	0·0461	0·0438	0·0455
206	0·420	0·1002	0·3615	0·0672	1·9471	0·2710	0·0441	0·0625	0·0426
202	0·303	0·0529	0·1779	0·0257	1·4326	0·2705	0·0440	0·0241	0·0423
207	0·202	0·0237	0·3927	0·0768	0·9659	0·2775	0·0456	0·0697	0·0436
203	0·147	0·0126	0·4091	0·0822	0·7069	0·2663	0·0431	0·0745	0·0412
208	0·118	0·0082	0·3825	0·0735	0·5702	0·2635	0·0425	0·0672	0·0407
204	0·097	0·0055	0·3741	0·0710	0·4677	0·2582	0·0413	0·0650	0·0396
209	1·246	0·7096	0·2565	0·0410	4·2688	0·2743	0·0449	0·0409	0·0446
"	"	"	"	"	4·2690	0·2660	0·0430	"	0·0427
213	1·228	0·6939	0·2531	0·0402	4·2468	0·2845	0·0472	0·0401	0·0469
"	"	"	"	"	4·2472	0·2709	0·0441	"	0·0438
214	0·783	0·3244	0·2672	0·0433	3·2894	0·2669	0·0432	0·0421	0·0425
210	0·607	0·2023	0·2679	0·0434	2·6907	0·2780	0·0457	0·0416	0·0446
215	0·428	0·1038	0·3189	0·0556	1·9794	0·2698	0·0439	0·0521	0·0424
211	0·318	0·0580	0·3605	0·0669	1·4981	0·2691	0·0437	0·0619	0·0420
216	0·257	0·0382	0·2178	0·0331	1·2213	0·2623	0·0422	0·0309	0·0405
212	0·215	0·0270	0·3860	0·0746	1·0292	0·2636	0·0425	0·0683	0·0407
217	1·375	0·8252	0·2439	0·0383	4·3923	0·2791	0·0459	0·0383	0·0457
"	"	"	"	"	4·3924	0·2521	0·0400	"	0·0398
221	1·355	0·8075	0·2570	0·0411	4·3776	0·2859	0·0475	0·0411	0·0472
"	"	"	"	"	4·3777	0·2617	0·0421	"	0·0418
222	1·022	0·5152	0·2714	0·0442	3·9019	0·2684	0·0436	0·0438	0·0431
"	"	"	"	"	3·9022	0·2643	0·0426	"	0·0422
218	0·877	0·3957	0·2688	0·0436	3·5548	0·2719	0·0443	0·0427	0·0437
"	"	"	"	"	3·5561	0·2599	0·0417	"	0·0411
223	0·668	0·2426	0·2851	0·0473	2·9135	0·2639	0·0426	0·0456	0·0417
"	"	"	"	"	2·9144	0·2583	0·0413	"	0·0405
219	0·513	0·1477	0·3014	0·0512	2·3340	0·2606	0·0418	0·0486	0·0406
224	0·422	0·1013	0·2194	0·0334	1·9571	0·2653	0·0429	0·0316	0·0415
220	0·358	0·0737	0·3925	0·0767	1·6814	0·2554	0·0407	0·0712	0·0393
225	1·328	0·7831	0·2557	0·0408	4·3548	0·2551	0·0407	0·0408	0·0404
"	1·329	"	"	"	4·3556	0·2387	0·0372	"	0·0370
229	1·318	0·7739	0·2633	0·0424	4·3455	0·2562	0·0409	0·0424	0·0406
"	1·319	"	"	"	4·3464	0·2352	0·0365	"	0·0363
230	1·197	0·6663	0·2812	0·0464	4·2054	0·2645	0·0427	0·0463	0·0424
"	"	"	"	"	4·2056	0·2546	0·0406	"	0·0403
226	1·077	0·5623	0·2728	0·0445	4·0111	0·2606	0·0418	0·0442	0·0415
"	"	"	"	"	4·0113	0·2572	0·0411	"	0·0408
231	0·877	0·3958	0·2819	0·0466	3·5550	0·2663	0·0431	0·0456	0·0425
"	"	"	"	"	3·5557	0·2605	0·0418	"	0·0413
227	0·714	0·2741	0·2861	0·0476	3·0686	0·2636	0·0425	0·0460	0·0417
"	0·717	"	"	"	3·0782	0·2591	0·0415	"	0·0407
232	0·601	0·1996	0·2972	0·0502	2·6748	0·2518	0·0399	0·0481	0·0390
"	0·603	"	"	"	2·6843	0·2457	0·0387	"	0·0378
228	0·524	0·1536	0·3164	0·0549	2·3761	0·2607	0·0419	0·0520	0·0407
233	1·418	0·8641	0·2602	0·0418	4·4196	0·2367	0·0368	0·0418	0·0366
"	1·420	"	"	"	4·4204	0·2066	0·0309	"	0·0307
237	1·412	0·8582	0·2658	0·0430	4·4160	0·2357	0·0366	0·0430	0·0364
"	1·413	"	"	"	4·4166	0·2173	0·0330	"	0·0328
238	1·331	0·7866	0·2770	0·0455	4·3573	0·2390	0·0373	0·0455	0·0371
"	"	"	"	"	4·3575	0·2318	0·0358	"	0·0356
234	1·258	0·7213	0·2732	0·0446	4·2843	0·2448	0·0385	0·0446	0·0382
239	1·104	0·5853	0·2800	0·0462	4·0594	0·2503	0·0396	0·0459	0·0393
"	1·105	"	"	"	4·0616	0·2473	0·0390	"	0·0387
235	0·944	0·4505	0·2740	0·0448	3·7275	0·2634	0·0424	0·0441	0·0420
"	0·962	"	"	"	3·7714	0·2466	0·0389	"	0·0385
240	0·840	0·3675	0·2929	0·0492	3·4557	0·2532	0·0402	0·0481	0·0397
236	0·750	0·2995	0·2786	0·0458	3·1839	0·2623	0·0422	0·0445	0·0414
"	0·756	"	"	"	3·2054	0·2571	0·0411	"	0·0404

TABLE No. A7.37 (see section 10.6.6)		SERIES II – 1.3/16 in. DIAMETER BAR LUBRICATED WITH OIL							
		calculated from section 3.2 for n=1.0						from section 3.1	
Test no.	θ_1 (radians)	$\frac{(l_1-l_2)}{l_1}$	$P_{F(P)}/P$	μ_P	l_3/l_1	$P_{F(T)}/P$	μ_T	μ_P	μ_T
241	0.952	0.4759	0.2816	0.0469	3.8903	0.3145	0.0517	0.0445	0.0535
245	0.893	0.4300	0.2590	0.0418	3.7533	0.2761	0.0456	0.0397	0.0445
246	0.419	0.1057	0.4194	0.0864	2.0455	0.3005	0.0514	0.0696	0.0468
242	0.307	0.0561	0.3992	0.0795	1.5104	0.3259	0.0578	0.0608	0.0510
247	0.207	0.0261	0.5622	0.1536	1.0381	0.3122	0.0543	0.1073	0.0478
243	0.149	0.0134	0.5385	0.1396	0.7462	0.3217	0.0567	0.0963	0.0493
248	0.119	0.0087	–	–	0.6013	0.3071	0.0530	–	0.0466
244	0.100	0.0061	–	–	0.5030	0.3127	0.0544	–	0.0475
285	0.913	0.4442	0.2840	0.0474	3.7974	0.3113	0.0541	0.0447	0.0526
286	0.416	0.1036	0.3108	0.0539	2.0257	0.3154	0.0551	0.0444	0.0499
287	0.311	0.0606	0.5210	0.1301	1.5675	0.2613	0.0423	0.1031	0.0390
249	1.238	0.7184	0.2886	0.0485	4.3826	0.3321	0.0595	0.0478	0.0589
253	1.195	0.6817	0.2964	0.0504	4.3299	0.3259	0.0578	0.0495	0.0572
254	0.768	0.3285	0.3167	0.0554	3.3857	0.3072	0.0530	0.0504	0.0507
"	"	"	"	"	3.3864	0.3044	0.0523	"	0.0501
250	0.620	0.2212	0.2962	0.0503	2.8662	0.3087	0.0534	0.0438	0.0499
255	0.432	0.1114	0.3870	0.0755	2.0962	0.3098	0.0537	0.0610	0.0487
251	0.326	0.0642	0.2831	0.0472	1.6120	0.3022	0.0518	0.0384	0.0465
256	0.259	0.0410	0.3971	0.0788	1.2952	0.3012	0.0515	0.0613	0.0460
252	0.220	0.0297	0.3927	0.0773	1.1059	0.2995	0.0511	0.0598	0.0454
257	1.364	0.8269	0.2993	0.0511	4.4983	0.3332	0.0598	0.0508	0.0593
261	1.357	0.8214	0.2646	0.0430	4.4938	0.2992	0.0511	0.0428	0.0507
262	1.020	0.5340	0.2816	0.0469	4.0414	0.2942	0.0499	0.0452	0.0489
"	"	"	"	"	4.0419	0.2911	0.0491	"	0.0482
258	0.882	0.4170	0.3119	0.0542	3.7117	0.3137	0.0547	0.0504	0.0529
"	0.884	"	"	"	3.7222	0.2904	0.0490	"	0.0475
263	0.674	0.2608	0.3257	0.0578	3.0773	0.2899	0.0488	0.0515	0.0463
259	0.658	0.2466	0.3302	0.0590	3.0048	0.3145	0.0549	0.0514	0.0515
264	0.426	0.1094	0.3130	0.0545	2.0785	0.2908	0.0490	0.0455	0.0449
260	0.364	0.0797	0.2900	0.0488	1.7881	0.3007	0.0514	0.0400	0.0464
281	1.313	0.7829	0.2902	0.0489	4.4584	0.3307	0.0591	0.0485	0.0586
282	1.027	0.5394	0.2850	0.0477	4.0542	0.2998	0.0512	0.0460	0.0503
283	0.874	0.4145	0.2767	0.0458	3.7032	0.2879	0.0484	0.0431	0.0470
284	0.516	0.1578	0.3208	0.0565	2.4642	0.2963	0.0504	0.0482	0.0467
269	1.307	0.7787	0.3141	0.0548	4.4540	0.2974	0.0506	0.0543	0.0502
"	1.308	"	"	"	4.4553	0.2809	0.0467	"	0.0464
265	1.301	0.7730	0.3192	0.0561	4.4480	0.3035	0.0521	0.0556	0.0517
270	1.196	0.6832	0.3033	0.0521	4.3322	0.3059	0.0527	0.0512	0.0521
"	"	"	"	"	4.3324	0.3010	0.0515	"	0.0510
266	1.070	0.5749	0.3115	0.0541	4.1343	0.3094	0.0536	0.0523	0.0527
271	0.875	0.4132	0.3065	0.0529	3.6992	0.2998	0.0512	0.0494	0.0497
"	0.881	"	"	"	3.7183	0.2906	0.0490	"	0.0476
267	0.717	0.2899	0.3273	0.0582	3.2171	0.3059	0.0527	0.0520	0.0501
272	0.607	0.2160	0.3593	0.0671	2.8366	0.2782	0.0461	0.0588	0.0435
268	0.530	0.1666	0.3305	0.0590	2.5258	0.2880	0.0484	0.0506	0.0450
273	1.406	0.8631	0.2632	0.0427	4.5243	0.2558	0.0411	0.0426	0.0480
"	1.408	"	"	"	4.5253	0.2257	0.0349	"	0.0347
277	1.398	0.8557	0.2738	0.0451	4.5195	0.2709	0.0444	0.0450	0.0441
"	1.406	"	"	"	4.5240	0.2407	0.0379	"	0.0377
278	1.325	0.7941	0.2868	0.0481	4.4694	0.2552	0.0410	0.0478	0.0407
"	1.326	"	"	"	4.4705	0.2408	0.0379	"	0.0377
274	1.246	0.7275	0.2760	0.0456	4.3944	0.2630	0.0427	0.0451	0.0423
"	"	"	"	"	4.3946	0.2579	0.0416	"	0.0412
279	1.091	0.5961	0.2629	0.0427	4.1782	0.2649	0.0431	0.0417	0.0425
"	"	"	"	"	4.1770	0.2638	0.0429	"	0.0423
275	0.942	0.4701	0.2710	0.0445	3.8737	0.2765	0.0457	0.0425	0.0447
"	0.952	"	"	"	3.8998	0.2620	0.0425	"	0.0416
280	0.842	0.3890	0.2531	0.0405	3.6163	0.2814	0.0468	0.0381	0.0454
276	0.749	0.3179	0.2834	0.0473	3.3406	0.2684	0.0439	0.0437	0.0423
"	0.754	"	"	"	3.3586	0.2637	0.0428		0.0413

TABLE No. A7.38 (see section 10.6.6)		SERIES II – 1.1/4 in. DIAMETER BAR LUBRICATED WITH OIL							
		calculated from section 3.2 for n=1·0						from section 3.1	
Test no.	θ_1 (radians)	$\frac{(l_1-l_2)}{l_1}$	$P_{F(P)}/P$	μ_P	l_3/l_1	$P_{F(T)}/P$	μ_T	μ_P	μ_T
288	0·970	0·5069	0·2591	0·0420	4·0753	0·3125	0·0546	0·0385	0·0527
292	0·943	0·4869	0·2653	0·0434	4·0207	0·2936	0·0499	0·0396	0·0481
293	0·513	0·1634	0·2923	0·0496	2·5683	0·2894	0·0489	0·0379	0·0431
289	0·369	0·0850	0·3428	0·0627	1·8923	0·3018	0·0519	0·0428	0·0434
294	0·275	0·0490	0·3311	0·0594	1·4502	0·2709	0·0446	0·0412	0·0375
290	0·185	0·0216	0·4614	0·1029	0·9692	0·3046	0·0526	0·0608	0·0422
295	0·148	0·0141	0·7038	0·2853	0·7857	0·2871	0·0484	0·1296	0·0393
291	0·123	0·0096	0·8057	0·4980	0·6497	0·2985	0·0511	0·1700	0·0410
300	0·928	0·4704	0·3009	0·0517	3·9739	0·3084	0·0536	0·0463	0·0513
296	0·956	0·4998	0·2349	0·0369	4·0559	0·2751	0·0456	0·0341	0·0441
301	0·794	0·3618	0·2833	0·0475	3·6073	0·2959	0·0505	0·0407	0·0473
297	0·628	0·2401	0·2935	0·0499	3·0472	0·2752	0·0456	0·0403	0·0415
302	0·443	0·1226	0·3355	0·0606	2·2498	0·2865	0·0482	0·0436	0·0415
298	0·341	0·0761	0·3850	0·0752	1·7940	0·2534	0·0408	0·0531	0·0352
303	0·265	0·0442	0·5288	0·1348	1·3792	0·2874	0·0484	0·0783	0·0397
299	0·230	0·0337	0·3525	0·0654	1·2083	0·2782	0·0463	0·0432	0·0381
308	1·024	0·5527	0·3120	0·0545	4·1892	0·3021	0·0520	0·0503	0·0505
304	1·025	0·5796	0·2654	0·0434	4·2476	–	–	0·0429	–
305	0·857	0·4122	0·2986	0·0511	3·7904	0·3025	0·0521	0·0447	0·0493
"	"	"	"	"	3·7933	0·2956	0·0504	-	0·0478
309	0·671	0·2658	0·3037	0·0524	3·1825	0·3019	0·0519	0·0420	0·0471
306	0·519	0·1640	0·3450	0·0633	2·5733	0·2985	0·0511	0·0463	0·0444
310	0·428	0·1119	0·3615	0·0680	2·1557	0·3051	0·0527	0·0466	0·0444
307	0·366	0·0832	0·4203	0·0871	1·8730	0·2946	0·0502	0·0567	0·0419
311	0·845	0·4115	0·2323	0·0363	3·7875	0·2555	0·0412	0·0329	0·0395
"	0·855	"	"	"	3·8175	0·2476	0·0395	-	0·0380
313	0·688	0·2836	0·3122	0·0545	3·2697	0·2757	0·0457	0·0451	0·0422
312	0·582	0·2092	0·2862	0·0481	2·8694	0·2733	0·0452	0·0384	0·0408
314	0·505	0·1607	0·3075	0·0533	2·5491	0·2685	0·0441	0·0410	0·0391
315	0·839	0·4018	0·2892	0·0489	3·7544	0·2834	0·0475	0·0431	0·0451
"	0·845	"	"	"	3·7709	0·2816	0·0471	"	0·0448
317	0·686	0·2786	0·3119	0·0544	3·2459	0·2981	0·0510	0·0441	0·0466
316	0·579	0·2052	0·2985	0·0511	2·8451	0·2899	0·0490	0·0400	0·0438
318	0·502	0·1554	0·3467	0·0637	2·5108	0·2906	0·0492	0·0468	0·0429
319	0·959	0·4976	0·3054	0·0528	4·0504	0·3048	0·0527	0·0479	0·0507
321	0·815	0·3800	0·3151	0·0553	3·6764	0·2864	0·0482	0·0477	0·0455
320	0·706	0·2929	0·3156	0·0554	3·3140	0·2975	0·0509	0·0452	0·0466
"	"	"	"	"	3·3205	0·2891	0·0488	-	0·0449
322	0·623	0·2343	0·3044	0·0525	3·0151	0·2859	0·0481	0·0418	0·0434

TABLE No. A7.39 (see section 10.6.6)

SERIES II – 1.5/16 in. DIAMETER BAR LUBRICATED WITH OIL

		calculated from section 3.2 for n = 1.0						from section 3.1	
Test no.	θ_1 (radians)	$\frac{(l_1 - l_2)}{l_1}$	$P_{F(P)}/P$	μ_P	l_3/l_1	$P_{F(T)}/P$	μ_T	μ_P	μ_T
323	0.546	0.1858	0.2928	0.0506	2.7580	0.2817	0.0480	0.0334	0.0397
327	0.528	0.1832	0.2505	0.0409	2.7402	0.2500	0.0408	0.0288	0.0347
324	0.336	0.0730	0.3572	0.0680	1.7824	0.2689	0.0450	0.0379	0.0346
328	0.233	0.0340	0.3783	0.0744	1.2301	0.2860	0.0490	0.0368	0.0354
325	0.172	0.0194	0.4587	0.1036	0.9310	0.2635	0.0438	0.0492	0.0322
329	0.136	0.0114	0.3202	0.0576	0.7169	0.2930	0.0507	0.0281	0.0353
326	0.093	0.0053	1.7828	-0.2785	0.4885	0.3138	0.0559	-11.979	0.0378
330	0.777	0.3609	0.2628	0.0436	3.6505	0.2824	0.0481	0.0345	0.0437
333	0.772	0.3578	0.2541	0.0417	3.6380	0.2797	0.0475	0.0331	0.0431
331	0.565	0.1948	0.3065	0.0540	2.8175	0.2949	0.0511	0.0351	0.0421
334	0.414	0.1050	0.3516	0.0663	2.1203	0.2961	0.0515	0.0368	0.0393
332	0.309	0.0576	0.3107	0.0551	1.5905	0.3015	0.0528	0.0286	0.0381
335	0.246	0.0372	0.4731	0.1098	1.2847	0.2945	0.0511	0.0486	0.0364
336	0.642	0.2562	0.2601	0.0430	3.1740	0.2726	0.0458	0.0313	0.0398
338	0.510	0.1652	0.3222	0.0581	2.6159	0.2670	0.0445	0.0374	0.0367
337	0.418	0.1112	0.3600	0.0688	2.1777	0.2715	0.0456	0.0399	0.0359
339	0.361	0.0883	0.3048	0.0536	1.9527	0.2381	0.0382	0.0335	0.0308
340	0.833	0.4094	0.2571	0.0423	3.8288	0.2708	0.0454	0.0350	0.0421
342	0.695	0.2949	0.2963	0.0515	3.3664	0.2733	0.0460	0.0381	0.0406
341	0.576	0.2051	0.3041	0.0535	2.8823	0.2796	0.0475	0.0357	0.0397
343	0.512	0.1670	0.2976	0.0518	2.6288	0.2664	0.0444	0.0339	0.0367
347	0.803	0.3886	0.2668	0.0445	3.7546	0.2541	0.0417	0.0366	0.0386
344	0.799	0.3832	0.2762	0.0467	3.7351	0.2648	0.0440	0.0379	0.0406
346	0.699	0.2992	0.2870	0.0492	3.3864	0.2700	0.0452	0.0369	0.0401
"	"	"	"	"	3.3987	0.2590	0.0428	"	0.0382
345	0.626	0.2429	0.2654	0.0442	3.1026	0.2752	0.0464	0.0316	0.0400

TABLE No. A7.40 (see section 10.6.6)		SERIES II – 1.1/16 in. DIAMETER BAR LUBRICATED WITH OIL							
		calculated from section 3.2 for $n = 1 \cdot 0$						from section 3.1	
Test no.	θ_1 (radians)	$\frac{(l_1 - l_2)}{l_1}$	$P_{F(P)}/P$	μ_P	l_3/l_1	$P_{F(T)}/P$	μ_T	μ_P	μ_T
348	1·406	0·8421	0·3870	0·0724	4·4144	0·3771	0·0694	0·0724	0·0690
"	"	"	"	"	"	0·3691	0·0671	"	0·0667
352	1·399	0·8363	0·3814	0·0707	4·4101	0·3801	0·0703	0·0707	0·0699
"	"	"	"	"	"	0·3717	0·0679	"	0·0675
353	0·975	0·4519	0·4044	0·0779	3·7391	0·3606	0·0647	0·0768	0·0641
349	0·843	0·3462	0·4127	0·0806	3·3826	0·3729	0·0682	0·0787	0·0672
354	0·638	0·2046	0·4163	0·0818	2·7098	0·3622	0·0651	0·0788	0·0638
350	0·491	0·1236	0·3893	0·0731	2·1528	0·3639	0·0656	0·0699	0·0639
355	0·404	0·0842	0·4368	0·0890	1·7959	0·3640	0·0657	0·0840	0·0637
351	0·343	0·0609	0·3881	0·0727	1·5369	0·3519	0·0623	0·0690	0·0605

TABLE No. A7.41 (see section 10.6.6)		SERIES II – 1.1/16 in. DIAMETER BAR LUBRICATED WITH SOAP							
		calculated for n = 0·25				calculated for n = 4·0			
Test no.	Θ_1 (radians)	$P^{0.25}_{F(P)}/P^{1.0}_{F(P)}$	$P_{F(P)}/P$	$P^{0.25}_{F(T)}/P^{1.0}_{F(T)}$	$P_{F(T)}/P$	$P^{4.0}_{F(P)}/P^{1.0}_{F(P)}$	$P_{F(P)}/P$	$P^{4.0}_{F(T)}/P^{1.0}_{F(T)}$	$P_{F(T)}/P$
33	1·013	1·0064	0·1971	1·0072	0·2277	0·9939	0·1947	0·9930	0·2245
37	0·979	1·0066	0·2001	1·0074	0·2286	0·9935	0·1975	[illegible]	[illegible]
38	0·439	1·0127	0·2581	1·0109	0·2279	0·9885	0·2519	[illegible]	0·2231
34	0·277	1·0123	0·3502	1·0117	0·2189	0·9858	0·3410	0·9887	[illegible]
39	0·186	1·0110	–	1·0118	0·2210	[illegible]	–	0·9886	0·2154
35	0·134	1·0111	–	1·0119	0·2129	0·9841	–	0·9884	0·2079
40	0·109	1·0215	–	1·0121	0·2106	0·9938	–	0·9885	0·2057
36	0·091	1·0130	–	1·0121	0·1982	0·9847	–	[illegible]	[illegible]
25	1·294	1·0029	0·2152	1·0056	0·2431	0·9972	0·2140	0·9945	[illegible]
29	1·280	1·0030	0·2102	1·0057	0·2467	0·9970	0·2090	0·9944	0·2433
30	0·771	1·0092	0·2328	1·0089	0·2284	0·9910	0·2286	0·9914	[illegible]
26	0·525	1·0114	0·2600	1·0105	0·2261	0·9883	0·2541	0·9898	0·2214
31	0·372	1·0128	0·4312	1·0113	0·2200	0·9874	0·4204	0·9891	0·2152
27	0·274	1·0122	0·3588	1·0116	0·2186	0·9860	0·3495	0·9888	0·2136
32	0·223	1·0146	0·3139	1·0120	0·2084	0·9869	0·3054	0·9884	0·2035
28	0·186	1·0155	–	1·0120	0·2088	0·9879	–	0·9884	0·2039
1	1·407	1·0016	0·2228	1·0053	0·2393	0·9983	0·2221	0·9948	0·2368
5	1·408	1·0016	0·2046	1·0052	0·2364	0·9984	0·2039	0·9948	0·2339
6	1·065	1·0057	0·2089	1·0069	0·2265	0·9944	0·2066	0·9933	0·2234
7	1·058	1·0058	0·2259	1·0069	0·2219	0·9943	0·2233	0·9932	0·2189
2	0·842	1·0085	0·2376	1·0084	0·2249	0·9917	0·2337	0·9918	0·2212
3	0·495	1·0122	0·2329	1·0107	0·2232	0·9884	0·2274	0·9895	0·2186
8	0·414	1·0130	0·2828	1·0112	0·2064	0·9876	0·2757	0·9891	0·2019
4	0·344	1·0137	0·2061	1·0116	0·2103	0·9871	0·2007	[illegible]	0·2056
13	1·455	1·0011	0·2178	1·0051	0·2431	0·9989	0·2173	0·9949	0·2406
9	1·455	1·0011	0·2104	1·0052	0·2343	0·9989	0·2100	0·9950	0·2319
14	1·205	1·0040	0·2099	1·0061	0·2175	0·9961	0·2082	0·9941	0·2149
10	1·030	1·0062	0·2440	1·0071	0·2129	0·9939	0·2410	0·9931	0·2099
15	0·828	1·0087	0·2260	1·0085	0·2158	0·9915	0·2222	0·9917	0·2122
11	0·673	1·0104	0·2034	1·0097	0·2031	0·9895	0·1992	0·9906	0·1993
16	0·562	1·0117	0·2139	1·0103	0·2092	[illegible]	0·2091	0·9900	0·2050
12	0·488	1·0129	0·2729	1·0109	0·2018	0·9883	0·2663	0·9894	0·1976
17	1·486	1·0009	0·2016	1·0051	0·2459	0·9992	0·2013	0·9950	0·2434
21	1·484	1·0008	0·2085	1·0051	0·2220	0·9991	0·2082	0·9950	0·2192
22	1·285	1·0031	0·2124	1·0057	0·2070	[illegible]	0·2111	0·9944	0·2047
18	1·146	1·0046	0·2280	1·0064	0·2116	0·9954	0·2259	[illegible]	0·2090
23	0·969	1·0070	0·2044	1·0075	0·2045	0·9933	0·2016	0·9927	0·2015
19	0·812	1·0090	0·1890	1·0087	0·1972	0·9913	0·1857	0·9916	0·1938
24	0·699	1·0102	0·2158	1·0095	0·1936	0·9900	0·2114	0·9903	0·1900
20	0·612	1·0114	0·2405	1·0101	0·1901	0·9892	[illegible]	0·9902	[illegible]

TABLE No. A7.42 (see section 10.6.6)		SERIES II – 1.1/8 in. DIAMETER BAR LUBRICATED WITH SOAP							
		calculated for n = 0·25				calculated for n = 4·0			
Test no.	Θ_1 (radians)	$P_{F(P)}^{0.25}/P_{F(P)}^{1.0}$	$P_{F(P)}/P$	$P_{F(T)}^{0.25}/P_{F(T)}^{1.0}$	$P_{F(T)}/P$	$P_{F(P)}^{4.0}/P_{F(P)}^{1.0}$	$P_{F(P)}/P$	$P_{F(T)}^{4.0}/P_{F(T)}^{1.0}$	$P_{F(T)}/P$
177	0·995	1·0166	0·1139	1·0169	0·1541	0·9842	0·1103	0·9840	0·1491
181	0·974	1·0173	0·1293	1·0172	0·1759	0·9838	0·1251	0·9837	0·1701
182	0·418	1·0347	0·2468	1·0278	0·1681	0·9680	0·2309	0·9742	0·1594
178	0·305	1·0384	0·1343	1·0296	0·1579	0·9664	0·1250	0·9727	0·1491
183	0·203	1·0380	–	1·0307	0·1592	0·9633	–	0·9718	0·1501
179	0·146	1·0380	–	1·0310	0·1586	0·9627	–	0·9715	0·1495
184	0·116	1·0455	–	1·0312	0·1603	0·4690	–	0·9714	0·1510
180	0·097	1·0494	–	1·0319	0·1463	0·9702	–	0·9707	0·1377
161	1·343	1·0056	0·1263	1·0122	0·1660	0·9946	0·1250	0·9883	0·1621
″	″	″	″	1·0122	0·1569	″	″	0·9883	0·1532
165	1·326	1·0060	0·1311	1·0123	0·1698	0·9941	0·1296	0·9882	0·1658
″	″	″	″	1·0123	0·1613	″	″	0·9882	0·1575
166	0·848	1·0217	0·1336	1·0197	0·1560	0·9794	0·1281	0·9815	0·1502
162	0·608	1·0298	0·1402	1·0245	0·1564	0·9725	0·1324	0·9772	0·1492
167	0·426	1·0349	0·2205	1·0280	0·1528	0·9674	0·2061	0·9741	0·1448
163	0·317	1·0378	0·2406	1·0293	0·1574	0·9665	0·2241	0·9728	0·1488
168	0·254	1·0394	0·2219	1·0302	0·1563	0·9657	0·2061	0·9721	0·1475
164	0·214	1·0397	0·4355	1·0307	0·1490	0·9645	0·4039	0·9716	0·1405
185	1·397	1·0041	0·1255	1·0118	0·1654	0·9959	0·1245	0·9887	0·1616
″	″	″	″	1·0118	0·1560	″	″	0·9887	0·1525
189	1·389	1·0043	0·1320	1·0119	0·1685	0·9957	0·1309	0·9887	0·1646
″	″	″	″	1·0119	0·1617	″	″	0·9887	0·1580
190	1·079	1·0138	0·1384	1·0155	0·1586	0·9869	0·1348	0·9853	0·1539
″	″	″	″	1·0155	0·1562	″	″	0·9853	0·1515
186	0·888	1·0204	0·1410	1·0189	0·1578	0·9808	0·1355	0·9822	0·1522
191	0·672	1·0278	0·1379	1·0232	0·1565	0·9742	0·1307	0·9783	0·1497
187	0·520	1·0326	0·1415	1·0262	0·1556	0·9703	0·1330	0·9757	0·1479
192	0·426	1·0355	0·1959	1·0279	0·1531	0·9682	0·1832	0·9741	0·1451
188	0·361	1·0364	0·1265	1·0289	0·1546	0·9664	0·1179	0·9733	0·1463
169	1·354	1·0053	0·1456	1·0121	0·1621	0·9948	0·1441	0·9884	0·1583
″	″	″	″	1·0121	0·1563	″	″	0·9884	0·1526
173	1·348	1·0055	0·1308	1·0122	0·1625	0·9947	0·1294	0·9884	0·1587
″	″	″	″	1·0122	0·1588	″	″	0·9884	0·1551
174	1·240	1·0086	0·1335	1·0132	0·1571	0·9917	0·1313	0·9874	0·1531
″	″	″	″	1·0132	0·1535	″	″	0·9874	0·1496
170	1·085	1·0135	0·1394	1·0154	0·1556	0·9869	0·1358	0·9854	0·1510
″	″	″	″	1·0154	0·1550	″	″	0·9854	0·1505
175	0·885	1·0205	0·1499	1·0189	0·1567	0·9807	0·1440	0·9821	0·1511
171	0·717	1·0261	0·1369	1·0223	0·1565	0·9754	0·1301	0·9791	0·1477
176	0·606	1·0301	0·1541	1·0246	0·1536	0·9724	0·1455	0·9771	0·1465
172	0·528	1·0320	0·1504	1·0261	0·1532	0·9701	0·1414	0·9758	0·1457
193	1·434	1·0032	0·1415	1·0116	0·1762	0·9969	0·1406	0·9889	0·1722
″	″	″	″	1·0116	0·1499	″	″	0·9889	0·1466
197	1·429	1·0033	0·1341	1·0116	0·1605	0·9968	0·1332	0·9889	0·1569
″	″	″	″	1·0116	0·1514	″	″	0·9889	0·1480
198	1·363	1·0051	0·1374	1·0121	0·1578	0·9952	0·1360	0·9885	0·1541
″	″	″	″	1·0121	0·1511	″	″	0·9885	0·1476
194	1·265	1·0079	0·1385	1·0130	0·1535	0·9125	0·1364	0·9877	0·1496
″	″	″	″	1·0130	0·1512	″	″	0·9877	0·1475
199	1·112	1·0128	0·1421	1·0150	0·1499	0·9879	0·1386	0·9858	0·1455
195	0·968	1·0176	0·1379	1·0174	0·1512	0·9833	0·1332	0·9836	0·1462
200	0·854	1·0218	0·1414	1·0196	0·1462	0·9796	0·1355	0·9815	0·1407
196	0·765	1·0248	0·1609	1·0214	0·1453	0·9768	0·1533	0·9799	0·1394

TABLE No. A7.43 (see section 10.6.6)		SERIES II – 1.3/16 in. DIAMETER BAR LUBRICATED WITH SOAP							
		calculated for n = 0·25				calculated for n = 4·0			
Test no.	θ_1 (radians)	$P_{F(P)}^{0.25}/P_{F(P)}^{1.0}$	$P_{F(P)}/P$	$P_{F(T)}^{0.25}/P_{F(T)}^{1.0}$	$P_{F(T)}/P$	$P_{F(P)}^{4.0}/P_{F(P)}^{1.0}$	$P_{F(P)}/P$	$P_{F(T)}^{4.0}/P_{F(T)}^{1.0}$	$P_{F(T)}/P$
61	0·994	1·0260	0·1294	1·0255	0·1572	0·9760	0·1231	0·9765	0·1497
57	0·980	1·0268	0·1212	1·0259	0·1541	0·9754	0·1152	0·9761	0·1466
62	0·442	1·0553	0·1624	1·0429	0·1721	0·9518	0·1465	0·9618	0·1587
58	0·307	1·0613	0·0895	1·0469	0·1615	0·9464	0·0798	0·9585	0·1479
63	0·204	1·0645	–	1·0486	0·1658	0·9453	–	0·9571	0·1513
59	0·149	1·0648	–	1·0496	0·1607	0·9427	–	0·9562	0·1464
64	0·116	1·0663	–	1·0490	0·1733	0·9465	–	0·9567	0·1581
60	0·098	1·0719	–	1·0501	0·1577	0·9482	–	0·9560	0·1436
45	1·274	1·0117	0·1464	1·0193	0·1852	0·9890	0·1422	0·9820	0·1784
"	"	"	"	1·0193	0·1817	"	"	0·9820	0·1751
41	1·258	1·0124	0·1504	1·0196	0·1827	0·9884	0·1468	0·9818	0·1759
"	"	"	"	1·0196	0·1786	"	"	0·9817	0·1719
46	0·790	1·0363	0·1791	1·0313	0·1881	0·9672	0·1671	0·9714	0·1772
42	0·604	1·0466	0·1699	1·0376	0·1725	0·9583	0·1556	0·9662	0·1606
47	0·433	1·0539	0·1711	1·0424	0·1830	0·9524	0·1546	0·9621	0·1689
43	0·322	1·0601	0·1434	1·0457	0·1723	0·9493	0·1284	0·9595	0·1581
48	0·255	1·0609	0·2277	1·0463	0·1873	0·9491	0·2037	0·9589	0·1716
44	0·216	1·0620	–	1·0473	0·1805	0·9477	–	0·9582	0·1652
65	1·411	1·0058	0·1321	1·0177	0·1714	0·9945	0·1306	0·9835	0·1656
"	1·412	"	"	1·0177	0·1665	"	"	0·9835	0·1609
69	1·400	1·0062	0·1368	1·0178	0·1764	0·9940	0·1351	0·9834	0·1705
"	"	"	"	1·0178	0·1682	"	"	0·9834	0·1625
70	1·077	1·0214	0·1513	1·0233	0·1670	0·9802	0·1452	0·9784	0·1597
"	"	"	"	1·0233	0·1660	"	"	0·9784	0·1587
66	0·895	1·0309	0·1465	1·0282	0·1692	0·9720	0·1381	0·9742	0·1603
71	0·680	1·0438	0·1630	1·0355	0·1684	0·9610	0·1501	0·9679	0·1574
67	0·527	1·0506	0·1420	1·0400	0·1711	0·9553	0·1291	0·9641	0·1586
72	0·429	1·0573	0·1682	1·0438	0·1528	0·9506	0·1512	0·9610	0·1407
68	0·365	1·0596	0·1731	1·0454	0·1535	0·9487	0·1550	0·9597	0·1409
49	1·471	1·0035	0·1364	1·0173	0·1723	0·9966	0·1355	0·9838	0·1666
"	"	"	"	1·0173	0·1641	"	"	0·9838	0·1587
53	1·462	1·0038	0·1465	1·0173	0·1839	0·9963	0·1454	0·9838	0·1778
"	1·463	"	"	1·0173	0·1707	"	"	0·9838	0·1651
54	1·234	1·0135	0·1522	1·0200	0·1747	0·9873	0·1482	0·9814	0·1681
"	"	"	"	1·0200	0·1688	"	"	0·9814	0·1624
50	1·098	1·0203	0·1361	1·0228	0·1637	0·9811	0·1309	0·9789	0·1566
"	"	"	"	1·0228	0·1620	"	"	0·9789	0·1551
55	0·906	1·0304	0·1576	1·0279	0·1744	0·9723	0·1487	0·9744	0·1653
"	"	"	"	1·0279	0·1738	"	"	0·9744	0·1647
51	0·735	1·0399	0·1662	1·0334	0·1704	0·9642	0·1541	0·9697	0·1599
56	0·625	1·0457	0·1614	1·0368	0·1729	0·9596	0·1481	0·9668	0·1612
52	0·545	1·0499	0·1516	1·0396	0·1669	0·9557	0·1380	0·9645	0·1548
73	1·505	1·0023	0·1297	1·0171	0·1649	0·9978	0·1291	0·9840	0·1596
"	"	"	"	1·0171	0·1497	"	"	0·9840	0·1448
77	1·502	1·0023	0·1397	1·0171	0·1741	0·9977	0·1391	0·9840	0·1684
"	"	"	"	1·0171	0·1598	"	"	0·9840	0·1546
78	1·358	1·0080	0·1333	1·0182	0·1543	0·9924	0·1312	0·9830	0·1490
"	1·359	"	"	1·0182	0·1520	"	"	0·9830	0·1467
74	1·269	1·0119	0·1340	1·0194	0·1601	0·9887	0·1309	0·9819	0·1542
79	1·121	1·0191	0·1394	1·0223	0·1618	0·9821	0·1344	0·9793	0·1550
75	0·979	1·0267	0·1413	1·0259	0·1594	0·9755	0·1342	0·9762	0·1517
80	0·856	1·0338	0·1422	1·0296	0·1546	0·9695	0·1333	0·9729	0·1461
76	0·763	1·0386	0·1659	1·0325	0·1641	0·9653	0·1542	0·9704	0·1542

TABLE No. A7.44 (see section 10.6.6)

SERIES II – 1.1/4 in. DIAMETER BAR LUBRICATED WITH SOAP

Test no.	Θ_1 (radians)	calculated for n = 0·25: $P_{F(P)}^{0.25}/P_{F(P)}^{1.0}$	$P_{F(P)}/P$	$P_{F(T)}^{0.25}/P_{F(T)}^{1.0}$	$P_{F(T)}/P$	calculated for n = 4·0: $P_{F(P)}^{4.0}/P_{F(P)}^{1.0}$	$P_{F(P)}/P$	$P_{F(T)}^{4.0}/P_{F(T)}^{1.0}$	$P_{F(T)}/P$
97	0·943	1·0368	0·1476	1·0348	0·1698	0·9672	0·1377	0·9688	0·1590
101	0·912	1·0389	0·1434	1·0359	0·1705	0·9654	0·1332	0·9679	0·1593
102	0·412	1·0722	0·1869	1·0561	0·1828	0·9400	0·1638	0·9516	0·1647
98	0·292	1·0779	0·2131	1·0600	0·1814	0·9359	0·1850	0·9486	0·1624
103	0·199	1·0805	0·1809	1·0614	0·1874	0·9356	0·1567	0·9475	0·1673
99	0·146	1·0777	0·3327	1·0624	0·1864	0·9307	0·2873	0·9467	0·1661
104	0·113	1·0776	–	1·0632	0·1838	0·9285	–	0·9461	0·1636
100	0·097	1·0899	–	1·0645	0·1715	0·9353	–	0·9453	0·1522
81	1·306	1·0132	0·1245	1·0247	0·1657	0·9877	0·1214	0·9775	0·1580
"	"	"	"	1·0247	0·1624	"	"	0·9775	0·1550
85	1·265	1·0156	0·1276	1·0254	0·1655	0·9856	0·1239	0·9768	0·1576
"	"	"	"	1·0254	0·1629	"	"	0·9768	0·1552
86	0·826	1·0455	0·1497	1·0395	0·1681	0·9600	0·1374	0·9649	0·1560
82	0·626	1·0612	0·1381	1·0486	0·1552	0·9473	0·1233	0·9575	0·1417
87	0·453	1·0714	0·1690	1·0556	0·1693	0·9394	0·1482	0·9520	0·1527
83	0·340	1·0801	0·1440	1·0605	0·1590	0·9342	0·1246	0·9482	0·1422
88	0·272	1·0821	0·2589	1·0623	0·1632	0·9321	0·2230	0·9468	0·1455
84	0·229	1·0833	0·2056	1·0630	0·1667	0·9318	0·1768	0·9462	0·1484
105	1·378	1·0092	0·1447	1·0236	0·1708	0·9914	0·1421	0·9784	0·1633
"	"	"	"	1·0236	0·1687	"	"	0·9784	0·1612
109	1·365	1·0099	0·1377	1·0237	0·1742	0·9907	0·1351	0·9783	0·1664
"	"	"	"	1·0238	0·1714	"	"	0·9783	0·1638
110	1·044	1·0295	0·1519	1·0312	0·1755	0·9734	0·1436	0·9718	0·1654
106	0·897	1·0398	0·1642	1·0364	0·1736	0·9646	0·1523	0·9674	0·1620
111	0·690	1·0542	0·1778	1·0448	0·1836	0·9534	0·1608	0·9606	0·1688
107	0·538	1·0647	0·1712	1·0514	0·1775	0·9450	0·1520	0·9553	0·1612
112	0·437	1·0708	0·1793	1·0552	0·1798	0·9410	0·1576	0·9523	0·1622
108	0·373	1·0737	0·2147	1·0573	0·1802	0·9386	0·1877	0·9506	0·1620
89	1·327	1·0120	0·1408	1·0243	0·1587	0·9888	0·1376	0·9778	0·1515
93	1·317	1·0125	0·1444	1·0245	0·1644	0·9883	0·1409	0·9776	0·1569
94	1·204	1·0192	0·1611	1·0267	0·1719	0·9824	0·1553	0·9757	0·1634
90	1·082	1·0272	0·1551	1·0301	0·1609	0·9753	0·1473	0·9728	0·1520
95	0·893	1·0400	0·1692	1·0365	0·1804	0·9647	0·1570	0·9673	0·1684
91	0·727	1·0526	0·1650	1·0437	0·1660	0·9541	0·1495	0·9615	0·1530
96	0·617	1·0598	0·1731	1·0481	0·1758	0·9488	0·1550	0·9579	0·1607
92	0·540	1·0658	0·1721	1·0518	0·1695	0·9443	0·1525	0·9550	0·1540
113	1·411	1·0075	0·1364	1·0232	0·1486	0·9929	0·1344	0·9788	0·1421
117	1·406	1·0077	0·1335	1·0232	0·1556	0·9927	0·1315	0·9787	0·1488
"	1·407	"	"	1·0232	0·1520	"	"	0·9787	0·1454
118	1·332	1·0117	0·1422	1·0242	0·1599	0·9890	0·1390	0·9778	0·1526
114	1·258	1·0159	0·1481	1·0256	0·1590	0·9851	0·1436	0·9767	0·1514
119	1·118	1·0247	0·1486	1·0290	0·1658	0·9775	0·1417	0·9737	0·1569
115	0·970	1·0351	0·1479	1·0339	0·1597	0·9686	0·1384	0·9696	0·1497
120	0·850	1·0437	0·1452	1·0385	0·1632	0·9613	0·1338	0·9657	0·1518
116	0·765	1·0509	0·1399	1·0423	0·1495	0·9557	0·1272	0·9626	0·1380

TABLE No. A7.45 (see section 10.6.6)		SERIES II – 1.5/16 in. DIAMETER BAR LUBRICATED WITH SOAP							
		calculated for n = 0·25				calculated for n = 4·0			
Test no.	Θ_1 (radians)	$P_{F(P)}^{0.25}/P_{F(P)}^{1.0}$	$P_{F(P)}/P$	$P_{F(T)}^{0.25}/P_{F(T)}^{1.0}$	$P_{F(T)}/P$	$P_{F(P)}^{4.0}/P_{F(P)}^{1.0}$	$P_{F(P)}/P$	$P_{F(T)}^{4.0}/P_{F(T)}^{1.0}$	$P_{F(T)}/P$
137	0·985	1·0409	0·1398	1·0405	0·1695	0·9640	0·1295	0·9644	0·1570
141	0·972	1·0422	0·1347	1·0412	0·1645	0·9629	0·1244	0·9639	0·1523
142	0·496	1·0855	0·1707	1·0663	0·1655	0·9307	0·1463	0·9443	0·1465
138	0·351	1·0912	0·1668	1·0715	0·1824	0·9257	0·1415	0·9405	0·1601
143	0·235	1·0943	0·2734	1·0741	0·1892	0·9238	0·2308	0·9385	0·1653
139	0·172	1·0979	–	1·0770	0·1806	0·9195	–	0·9365	0·1570
144	0·136	1·1035	–	1·0778	0·1783	0·9226	–	0·9360	0·1548
140	0·114	1·1009	–	1·0763	0·1862	0·9254	–	0·9371	0·1622
121	1·267	1·0186	0·1334	1·0312	0·1824	0·9831	0·1287	0·9721	0·1720
"	"	"	"	1·0312	0·1778	"	"	0·9721	0·1676
125	1·249	1·0200	0·1316	1·0317	0·1688	0·9818	0·1267	0·9717	0·1590
"	"	"	"	1·0317	0·1632	"	"	0·9717	0·1537
126	0·823	1·0553	0·1586	1·0482	0·1745	0·9525	0·1431	0·9582	0·1595
122	0·630	1·0721	0·1668	1·0583	0·1793	0·9398	0·1462	0·9503	0·1610
127	0·456	1·0839	0·1752	1·0663	0·1922	0·9320	0·1506	0·9443	0·1702
123	0·342	1·0932	0·1702	1·0721	0·1806	0·9257	0·1441	0·9401	0·1583
128	0·272	1·0905	0·1394	1·0720	0·1995	0·9267	0·1184	0·9402	0·1749
124	0·230	1·0971	0·2271	1·0755	0·1792	0·9221	0·1909	0·9376	0·1563
145	1·369	1·0118	0·1175	1·0293	0·1548	0·9891	0·1149	0·9737	0·1464
"	"	"	"	1·0293	0·1438	"	"	0·9737	0·1361
149	1·358	1·0125	0·1232	1·0295	0·1701	0·9885	0·1203	0·9736	0·1609
"	"	"	"	1·0295	0·1559	"	"	0·9736	0·1475
150	1·047	1·0361	0·1337	1·0381	0·1609	0·9681	0·1249	0·9663	0·1498
"	"	"	"	1·0381	0·1592	"	"	0·9663	0·1482
146	0·898	1·0491	0·1533	1·0446	0·1662	0·9577	0·1400	0·9611	0·1529
"	"	"	"	1·0446	0·1632	"	"	0·9611	0·1501
151	0·703	1·0666	0·1442	1·0547	0·1704	0·9438	0·1276	0·9531	0·1540
147	0·538	1·0803	0·1765	1·0634	0·1755	0·9339	0·1526	0·9465	0·1562
152	0·440	1·0877	0·1763	1·0682	0·1774	0·9292	0·1506	0·9429	0·1566
148	0·374	1·0940	0·1856	1·0720	0·1710	0·9253	0·1570	0·9402	0·1500
133	1·318	1·0152	0·1294	1·0302	0·1573	0·9860	0·1256	0·9730	0·1485
"	1·320	"	"	1·0301	0·1499	"	"	0·9730	0·1416
129	1·289	1·0171	0·1334	1·0308	0·1647	0·9843	0·1291	0·9725	0·1554
134	1·212	1·0227	0·1421	1·0326	0·1678	0·9794	0·1360	0·9709	0·1577
"	"	"	"	1·0326	0·1666	"	"	0·9709	0·1566
130	1·089	1·0322	0·1428	1·0365	0·1739	0·9714	0·1344	0·9677	0·1624
135	0·910	1·0472	0·1539	1·0439	0·1783	0·9589	0·1409	0·9617	0·1642
131	0·741	1·0626	0·1582	1·0524	0·1732	0·9473	0·1411	0·9549	0·1572
136	0·623	1·0729	0·1653	1·0587	0·1784	0·9396	0·1448	0·9500	0·1601
132	0·544	1·0802	0·1621	1·0632	0·1690	0·9344	0·1402	0·9467	0·1504
157	1·485	1·0047	0·1170	1·0280	0·1594	0·9955	0·1159	0·9748	0·1512
"	1·486	"	"	1·0280	0·1391	"	"	0·9748	0·1319
153	1·405	1·0095	0·1324	1·0288	0·1579	0·9912	0·1300	0·9742	0·1495
"	1·408	"	"	1·0288	0·1332	"	"	0·9742	0·1261
158	1·336	1·0140	0·1311	1·0298	0·1534	0·9872	0·1276	0·9733	0·1450
"	"	"	"	1·0298	0·1487	"	"	0·9733	0·1405
154	1·260	1·0193	0·1414	1·0314	0·1551	0·9825	0·1363	0·9719	0·1462
"	"	"	"	1·0314	0·1465	"	"	0·9719	0·1381
159	0·974	1·0418	0·1596	1·0410	0·1739	0·9635	0·1476	0·9640	0·1610
155	0·968	1·0424	0·1495	1·0413	0·1664	0·9629	0·1381	0·9638	0·1540
"	0·975	"	"	1·0410	0·1637	"	"	0·9640	0·1516
160	0·847	1·0525	0·1672	1·0468	0·1772	0·9548	0·1517	0·9593	0·1624
"	0·855	"	"	1·0464	0·1748	"	"	0·9596	0·1603
156	0·765	1·0610	0·1560	1·0513	0·1629	0·9483	0·1395	0·9558	0·1481
"	0·768	"	"	1·0512	0·1604	"	"	0·9559	0·1458

TABLE No. A7.46 (see section 10.6.6)		SERIES II – 1.1/8 in. DIAMETER BAR LUBRICATED WITH OIL							
		calculated for n = 0·25				calculated for n = 4·0			
Test no.	Θ_1 (radians)	$P^{0.25}_{F(P)}/P^{1.0}_{F(P)}$	$P_{F(P)}/P$	$P^{0.25}_{F(T)}/P^{1.0}_{F(T)}$	$P_{F(T)}/P$	$P^{4.0}_{F(P)}/P^{1.0}_{F(P)}$	$P_{F(P)}/P$	$P^{4.0}_{F(T)}/P^{1.0}_{F(T)}$	$P_{F(T)}/P$
201	0·948	1·0166	0·2402	1·0172	0·2719	0·9843	0·2326	0·9838	0·2630
205	0·895	1·0177	0·2785	1·0179	0·2848	0·9830	0·2690	0·9831	0·2751
206	0·420	1·0282	0·3718	1·0247	0·2777	0·9737	0·3521	0·9769	0·2648
202	0·303	1·0296	0·1832	1·0260	0·2775	0·9718	0·1729	0·9759	0·2640
207	0·202	1·0306	0·4047	1·0265	0·2848	0·9718	0·3816	0·9755	0·2707
203	0·147	1·0293	0·4219	1·0269	0·2735	0·9692	0·3973	0·9750	0·2597
208	0·118	1·0326	0·3948	1·0273	0·2707	0·9709	0·3712	0·9746	0·2568
204	0·097	1·0314	0·3862	1·0276	0·2653	0·9692	0·3630	0·9746	0·2517
209	1·246	1·0081	0·2586	1·0131	0·2778	0·9922	0·2545	0·9875	0·2708
"	"	"	"	1·0131	0·2695	"	"	0·9875	0·2627
213	1·228	1·0086	0·2553	1·0133	0·2883	0·9919	0·2511	0·9873	0·2809
"	"	"	"	1·0133	0·2745	"	"	0·9873	0·2675
214	0·783	1·0211	0·2728	1·0198	0·2722	0·9802	0·2619	0·9813	0·2619
210	0·607	1·0252	0·2747	1·0225	0·2843	0·9767	0·2617	0·9790	0·2722
215	0·428	1·0288	0·3280	1·0248	0·2765	0·9741	0·3106	0·9769	0·2636
211	0·318	1·0296	0·3714	1·0259	0·2761	0·9716	0·3505	0·9758	0·2626
216	0·257	1·0318	0·2246	1·0266	0·2692	0·9721	0·2116	0·9754	0·2558
212	0·215	1·0328	0·3980	1·0267	0·2706	0·9728	0·3749	0·9752	0·2570
217	1·375	1·0046	0·2450	1·0119	0·2824	0·9955	0·2428	0·9886	0·2759
"	"	"	"	1·0119	0·2552	"	"	0·9886	0·2493
221	1·355	1·0051	0·2583	1·0121	0·2894	0·9951	0·2557	0·9885	0·2826
"	"	"	"	1·0121	0·2649	"	"	0·9885	0·2587
222	1·022	1·0144	0·2754	1·0160	0·2727	0·9862	0·2677	0·9848	0·2643
"	"	"	"	1·0160	0·2685	"	"	0·9848	0·2603
218	0·877	1·0184	0·2737	1·0183	0·2769	0·9825	0·2641	0·9828	0·2672
"	"	"	"	1·0183	0·2646	"	"	0·9827	0·2554
223	0·668	1·0239	0·2920	1·0217	0·2696	0·9775	0·2787	0·9797	0·2585
"	"	"	"	1·0217	0·2639	"	"	0·9796	0·2530
219	0·513	1·0273	0·3096	1·0239	0·2668	0·9746	0·2937	0·9777	0·2547
224	0·422	1·0289	0·2257	1·0251	0·2720	0·9732	0·2135	0·9767	0·2592
220	0·358	1·0301	0·4043	1·0258	0·2620	0·9722	0·3816	0·9760	0·2493
225	1·328	1·0058	0·2571	1·0123	0·2583	0·9943	0·2542	0·9882	0·2521
"	1·329	"	"	1·0123	0·2417	"	"	0·9883	0·2357
229	1·318	1·0061	0·2649	1·0124	0·2594	0·9940	0·2617	0·9882	0·2532
"	1·319	"	"	1·0124	0·2381	"	"	0·9882	0·2324
230	1·197	1·0094	0·2839	1·0137	0·2681	0·9909	0·2787	0·9870	0·2611
"	"	"	"	1·0137	0·2581	"	"	0·9870	0·2513
226	1·077	1·0129	0·2763	1·0152	0·2645	0·9878	0·2694	0·9856	0·2568
"	"	"	"	1·0152	0·2611	"	"	0·9856	0·2535
231	0·877	1·0185	0·2871	1·0183	0·2712	0·9825	0·2770	0·9827	0·2617
"	"	"	"	1·0183	0·2653	"	"	0·9827	0·2560
227	0·714	1·0229	0·2926	1·0209	0·2691	0·9789	0·2800	0·9804	0·2584
"	0·717	"	"	1·0209	0·2645	"	"	0·9804	0·2540
232	0·601	1·0259	0·3049	1·0228	0·2575	0·9759	0·2900	0·9786	0·2464
"	0·603	"	"	1·0229	0·2513	"	"	0·9786	0·2404
228	0·524	1·0271	0·3249	1·0237	0·2669	0·9753	0·3085	0·9779	0·2550
233	1·418	1·0036	0·2611	1·0117	0·2394	0·9966	0·2593	0·9888	0·2340
"	1·420	"	"	1·0117	0·2090	"	"	0·9889	0·2043
237	1·412	1·0036	0·2668	1·0117	0·2384	0·9964	0·2649	0·9888	0·2330
"	1·413	"	"	1·0117	0·2199	"	"	0·9888	0·2149
238	1·331	1·0058	0·2786	1·0123	0·2420	0·9944	0·2754	0·9883	0·2362
"	"	"	"	1·0123	0·2347	"	"	0·9883	0·2291
234	1·258	1·0078	0·2753	1·0130	0·2480	0·9925	0·2712	0·9876	0·2418
239	1·104	1·0122	0·2834	1·0149	0·2540	0·9884	0·2767	0·9859	0·2467
"	1·105	"	"	1·0148	0·2510	"	"	0·9859	0·2439
235	0·944	1·0166	0·2786	1·0172	0·2679	0·9842	0·2697	0·9837	0·2591
"	0·962	"	"	1·0170	0·2508	"	"	0·9839	0·2427
240	0·840	1·0198	0·2987	1·0190	0·2580	0·9814	0·2874	0·9821	0·2487
236	0·750	1·0221	0·2847	1·0203	0·2676	0·9796	0·2729	0·9809	0·2572
"	0·756	"	"	1·0203	0·2624	"	"	0·9809	0·2522

TABLE No. A7.47 (see section 10.6.6)		SERIES II - 1.3/16 in. DIAMETER BAR LUBRICATED WITH OIL							
		calculated for n = 0·25				calculated for n = 4·0			
Test no.	Θ_1 (radians)	$P^{0.25}_{F(P)}/P^{1.0}_{F(P)}$	$P_{F(P)}/P$	$P^{0.25}_{F(T)}/P^{1.0}_{F(T)}$	$P_{F(T)}/P$	$P^{4.0}_{F(P)}/P^{1.0}_{F(P)}$	$P_{F(P)}/P$	$P^{4.0}_{F(T)}/P^{1.0}_{F(T)}$	$P_{F(T)}/P$
241	0·952	1·0241	0·2884	1·0254	0·3225	0·9777	0·2754	0·9766	0·3071
245	0·893	1·0278	0·2662	1·0272	0·2836	0·9745	0·2524	0·9750	0·2692
246	0·419	1·0401	0·4364	1·0362	0·3114	0·9636	0·4043	0·9673	0·2907
242	0·307	1·0373	0·4145	1·0358	0·3376	0·9647	0·3855	0·9677	0·3154
247	0·207	1·0405	0·5854	1·0375	0·3239	0·9625	0·5415	0·9662	0·3016
243	0·149	1·0390	0·5599	1·0369	0·3335	0·9640	0·5194	0·9668	0·3110
248	0·119	1·0447	-	1·0386	0·3187	0·9634	-	0·9654	0·2964
244	0·100	1·0465	-	1·0378	0·3245	0·9678	-	0·9660	0·3020
285	0·913	1·0259	0·2913	1·0263	0·3195	0·9763	0·2773	0·9758	0·3038
286	0·416	1·0397	0·3230	1·0357	0·3267	0·9652	0·2998	0·9677	0·3052
287	0·311	1·0474	0·5461	1·0405	0·2719	0·9567	0·4988	0·9637	0·2518
249	1·238	1·0123	0·2922	1·0198	0·3387	0·9883	0·2852	0·9816	0·3260
253	1·195	1·0141	0·3006	1·0205	0·3325	0·9867	0·2925	0·9810	0·3197
254	0·768	1·0309	0·3265	1·0296	0·3162	0·9717	0·3078	0·9730	0·2988
"	"	"	"	1·0296	0·3134	"	"	0·9729	0·2962
250	0·620	1·0349	0·3065	1·0323	0·3187	0·9688	0·2869	0·9706	0·2996
255	0·432	1·0391	0·4020	1·0354	0·3208	0·9655	0·3735	0·9680	0·2999
251	0·326	1·0403	0·2946	1·0370	0·3133	0·9629	0·2727	0·9667	0·2921
256	0·259	1·0430	0·4139	1·0379	0·3126	0·9628	0·3821	0·9658	0·2909
252	0·220	1·0427	0·4094	1·0382	0·3109	0·9620	0·3777	0·9657	0·2892
257	1·364	1·0074	0·3015	1·0181	0·3392	0·9930	0·2972	0·9831	0·3275
261	1·357	1·0078	0·2667	1·0182	0·3047	0·9927	0·2627	0·9830	0·2941
262	1·020	1·0218	0·2877	1·0240	0·3013	0·9798	0·2759	0·9778	0·2877
"	"	"	"	1·0241	0·2981	"	"	0·9778	0·2846
258	0·882	1·0264	0·3201	1·0269	0·3221	0·9756	0·3043	0·9753	0·3059
"	0·884	"	"	1·0271	0·2983	"	"	0·9751	0·2832
263	0·674	1·0349	0·3370	1·0320	0·2992	0·9684	0·3154	0·9709	0·2814
259	0·658	1·0332	0·3412	1·0314	0·3244	0·9699	0·3203	0·9714	0·3055
264	0·426	1·0410	0·3257	1·0364	0·3014	0·9636	0·3015	0·9671	0·2812
260	0·364	1·0407	0·3017	1·0366	0·3116	0·9640	0·2795	0·9670	0·2907
281	1·313	1·0094	0·2929	1·0187	0·3368	0·9910	0·2876	0·9825	0·3249
282	1·027	1·0215	0·2911	1·0239	0·3069	0·9801	0·2793	0·9779	0·2932
283	0·874	1·0282	0·2845	1·0275	0·2958	0·9742	0·2696	0·9747	0·2806
284	0·516	1·0389	0·3333	1·0350	0·3067	0·9649	0·3096	0·9683	0·2869
269	1·307	1·0097	0·3172	1·0188	0·3030	0·9908	0·3113	0·9825	0·2922
"	1·308	"	"	1·0188	0·2862	"	"	0·9825	0·2760
265	1·301	1·0100	0·3234	1·0189	0·3093	0·9906	0·3162	0·9824	0·2982
270	1·196	1·0141	0·3076	1·0205	0·3122	0·9866	0·2993	0·9810	0·3001
"	"	"	"	1·0205	0·3072	"	"	0·9810	0·2953
266	1·070	1·0193	0·3175	1·0229	0·3165	0·9820	0·3059	0·9788	0·3029
271	0·875	1·0274	0·3150	1·0273	0·3080	0·9747	0·2988	0·9749	0·2922
"	0·881	"	"	1·0272	0·2985	"	"	0·9750	0·2834
267	0·771	1·0325	0·3380	1·0306	0·3153	0·9705	0·3177	0·9720	0·2974
272	0·607	1·0379	0·3729	1·0338	0·2876	0·9658	0·3470	0·9693	0·2696
268	0·530	1·0390	0·3434	1·0349	0·2980	0·9649	0·3189	0·9684	0·2789
273	1·406	1·0059	0·2648	1·0177	0·2603	0·9944	0·2617	0·9834	0·2515
"	1·408	"	"	1·0177	0·2297	"	"	0·9835	0·2220
277	1·398	1·0062	0·2755	1·0178	0·2757	0·9941	0·2722	0·9834	0·2664
"	1·406	"	"	1·0177	0·2450	"	"	0·9834	0·2368
278	1·325	1·0092	0·2894	1·0186	0·2599	0·9914	0·2843	0·9827	0·2507
"	1·326	"	"	1·0186	0·2452	"	"	0·9827	0·2366
274	1·246	1·0124	0·2794	1·0197	0·2682	0·9883	0·2727	0·9816	0·2582
"	"	"	"	1·0197	0·2630	"	"	0·9816	0·2532
279	1·091	1·0193	0·2680	1·0226	0·2709	0·9821	0·2582	0·9791	0·2593
"	"	"	"	1·0227	0·2698	"	"	0·9790	0·2582
275	0·942	1·0257	0·2780	1·0260	0·2836	0·9764	0·2646	0·9761	0·2698
"	0·952	"	"	1·0258	0·2688	"	"	0·9762	0·2557
280	0·842	1·0297	0·2606	1·0284	0·2894	0·9728	0·2462	0·9740	0·2740
276	0·749	1·0340	0·2930	1·0309	0·2767	0·9694	0·2747	0·9718	0·2608
"	0·754	"	"	1·0308	0·2719	"	"	0·9719	0·2563

TABLE No. A7.48 (see section 10.6.6)		SERIES II - 1.1/4 in. DIAMETER BAR LUBRICATED WITH OIL							
		calculated for n = 0·25				calculated for n = 4·0			
Test no.	Θ_1 (radians)	$P^{0.25}_{F(P)}/P^{1.0}_{F(P)}$	$P_{F(P)}/P$	$P^{0.25}_{F(T)}/P^{1.0}_{F(T)}$	$P_{F(T)}/P$	$P^{4.0}_{F(P)}/P^{1.0}_{F(P)}$	$P_{F(P)}/P$	$P^{4.0}_{F(T)}/P^{1.0}_{F(T)}$	$P_{F(T)}/P$
288	0·970	1·0298	0·2668	1·0324	0·3226	0·9730	0·2521	0·9708	0·3034
292	0·943	1·0319	0·2737	1·0334	0·3034	0·9712	0·2576	0·9700	0·2848
293	0·513	1·0494	0·3067	1·0450	0·3024	0·9572	0·2798	0·9604	0·2779
289	0·369	1·0483	0·3594	1·0457	0·3156	0·9580	0·3284	0·9598	0·2897
294	0·275	1·0561	0·3496	1·0499	0·2844	0·9521	0·3151	0·9565	0·2591
290	0·185	1·0507	0·4840	1·0470	0·3189	0·9585	0·4416	0·9688	0·2921
295	0·148	1·0514	0·7412	1·0490	0·3012	0·9524	0·6713	0·9571	0·2748
291	0·123	1·0477	0·8469	1·0482	0·3129	0·9523	0·7698	0·9579	0·2860
300	0·928	1·0313	0·3103	1·0334	0·3187	0·9717	0·2924	0·9700	0·2992
296	0·956	1·0318	0·2424	1·0331	0·2842	0·9714	0·2282	0·9702	0·2669
301	0·794	1·0381	0·2941	1·0374	0·3070	0·9663	0·2737	0·9666	0·2860
297	0·628	1·0461	0·3071	1·0426	0·2869	0·9592	0·2816	0·9624	0·2648
302	0·443	1·0493	0·3520	1·0456	0·2995	0·9572	0·3211	0·9599	0·2750
298	0·341	1·0583	0·4072	1·0503	0·2661	0·9509	0·3659	0·9561	0·2422
303	0·265	1·0502	0·5552	1·0471	0·3009	0·9566	0·5057	0·9587	0·2755
299	0·230	1·0518	0·3712	1·0487	0·2918	0·9531	0·3363	0·9575	0·2664
308	1·024	1·0270	0·3204	1·0308	0·3114	0·9756	0·3043	0·9721	0·2937
304	1·025	1·0340	0·2744	1·0326	—	0·9696	0·2573	0·9707	—
305	0·857	1·0349	0·3091	1·0355	0·3132	0·9687	0·2893	0·9682	0·2929
"	"	"	"	1·0356	0·3062	"	"	0·9681	0·2862
309	0·671	1·0415	0·3163	1·0402	0·3140	0·9633	0·2926	0·9644	0·2911
306	0·519	1·0450	0·3606	1·0432	0·3114	0·9600	0·3313	0·9618	0·2871
310	0·428	1·0455	0·3779	1·0439	0·3185	0·9603	0·3471	0·9612	0·2932
307	0·366	1·0479	0·4403	1·0454	0·3080	0·9586	0·4028	0·9601	0·2829
311	0·845	1·0390	0·2414	1·0370	0·2649	0·9651	0·2242	0·9669	0·2470
"	0·855	"	"	1·0368	0·2567	"	"	0·9671	0·2395
313	0·688	1·0443	0·3260	1·0411	0·2870	0·9610	0·3000	0·9636	0·2657
312	0·582	1·0486	0·3001	1·0441	0·2854	0·9573	0·2740	0·9611	0·2627
314	0·505	1·0513	0·3233	1·0461	0·2809	0·9551	0·2937	0·9595	0·2567
315	0·839	1·0373	0·3000	1·0365	0·2937	0·9666	0·2795	0·9673	0·2741
"	0·845	"	"	1·0364	0·2918	"	"	0·9674	0·2724
317	0·686	1·0419	0·3249	1·0402	0·3100	0·9629	0·3003	0·9644	0·2874
316	0·579	1·0467	0·3124	1·0433	0·3025	0·9571	0·2863	0·9618	0·2787
318	0·502	1·0473	0·3632	1·0444	0·3035	0·9582	0·3323	0·9609	0·2793
319	0·959	1·0301	0·3146	1·0326	0·3147	0·9727	0·2970	0·9706	0·2958
321	0·815	1·0376	0·3270	1·0370	0·2970	0·9663	0·3045	0·9670	0·2770
320	0·706	1·0411	0·3286	1·0396	0·3093	0·9638	0·3042	0·9648	0·2870
"	"	"	"	1·0399	0·3006	"	"	0·9646	0·2789
322	0·623	1·0450	0·3181	1·0421	0·2980	0·9604	0·2923	0·9627	0·2753

TABLE No. A7.49 (see section 10.6.6)		SERIES II – 1.5/16 in. DIAMETER BAR LUBRICATED WITH SOAP							
		calculated for n = 0·25				calculated for n = 4·0			
Test no.	Θ_1 (radians)	$P_{F(P)}^{0.25} / P_{F(P)}^{1.0}$	$P_{F(P)} / P$	$P_{F(T)}^{0.25} / P_{F(T)}^{1.0}$	$P_{F(T)} / P$	$P_{F(P)}^{4.0} / P_{F(P)}^{1.0}$	$P_{F(P)} / P$	$P_{F(T)}^{4.0} / P_{F(T)}^{1.0}$	$P_{F(T)} / P$
323	0·546	1·0520	0·3080	1·0514	0·2962	0·9555	0·2797	0·9557	0·2693
327	0·528	1·0612	0·2658	1·0557	0·2639	0·9478	0·2374	0·9523	0·2381
324	0·336	1·0581	0·3777	1·0558	0·2839	0·9516	0·3397	0·9522	0·2561
328	0·233	1·0490	0·3974	1·0530	0·3012	0·9552	0·3618	0·9544	0·2730
325	0·172	1·0621	0·4861	1·0577	0·2787	0·9515	0·4355	0·9507	0·2505
329	0·136	1·0448	0·3354	1·0519	0·3081	0·9565	0·3071	0·9554	0·2799
326	0·093	1·0444	1·8589	1·0495	0·3294	0·9641	1·7161	0·9571	0·3004
330	0·777	1·0459	0·2749	1·0460	0·2954	0·9599	0·2523	0·9600	0·2711
333	0·772	1·0407	0·2659	1·0463	0·2927	0·9594	0·2438	0·9597	0·2685
331	0·565	1·0479	0·3212	1·0496	0·3095	0·9581	0·2937	0·9571	0·2822
334	0·414	1·0473	0·3682	1·0506	0·3111	0·9587	0·3371	0·9563	0·2832
332	0·309	1·0429	0·3242	1·0493	0·3164	0·9617	0·2989	0·9574	0·2887
335	0·246	1·0460	0·4948	1·0507	0·3094	0·9601	0·4542	0·9562	0·2816
336	0·642	1·0517	0·2735	1·0502	0·2863	0·9553	0·2485	0·9566	0·2608
338	0·510	1·0550	0·3400	1·0532	0·2812	0·9526	0·3070	0·9543	0·2548
337	0·418	1·0547	0·3796	1·0537	0·2861	0·9538	0·3433	0·9539	0·2590
339	0·361	1·0669	0·3253	1·0602	0·2525	0·9433	0·2876	0·9489	0·2260
340	0·833	1·0446	0·2686	1·0446	0·2829	0·9612	0·2471	0·9611	0·2603
342	0·695	1·0494	0·3109	1·0484	0·2865	0·9575	0·2837	0·9580	0·2618
341	0·576	1·0506	0·3196	1·0506	0·2937	0·9561	0·2908	0·9563	0·2674
343	0·512	1·0552	0·3140	1·0533	0·2806	0·9524	0·2835	0·9542	0·2542
347	0·803	1·0478	0·2796	1·0462	0·2659	0·9584	0·2557	0·9598	0·2439
344	0·799	1·0468	0·2892	1·0460	0·2770	0·9591	0·2649	0·9600	0·2542
346	0·699	1·0501	0·3014	1·0487	0·2831	0·9570	0·2747	0·9579	0·2586
"	"	"	"	1·0493	0·2718	"	"	0·9574	0·2480
345	0·626	1·0515	0·2791	1·0503	0·2891	0·9555	0·2536	0·9566	0·2633

TABLE No. A7.50 (see section 10.6.6)		SERIES II - 1.1/16 in. DIAMETER BAR LUBRICATED WITH OIL							
		calculated for n = 0·25				calculated for n = 4·0			
Test no.	Θ_1 (radians)	$P_{F(P)}^{0.25}/P_{F(P)}^{1.0}$	$P_{F(P)}/P$	$P_{F(T)}^{0.25}/P_{F(T)}^{1.0}$	$P_{F(T)}/P$	$P_{F(P)}^{4.0}/P_{F(P)}^{1.0}$	$P_{F(P)}/P$	$P_{F(T)}^{4.0}/P_{F(T)}^{1.0}$	$P_{F(T)}/P$
348	1·406	1·0015	0·3876	1·0053	0·3791	0·9984	0·3864	0·9949	0·3752
"	"	"	"	1·0053	0·3711	"	"	0·9949	0·3672
352	1·399	1·0016	0·3820	1·0053	0·3821	0·9984	0·3808	0·9948	0·3781
"	"	"	"	1·0053	0·3737	"	"	0·9948	0·3698
353	0·975	1·0059	0·4068	1·0071	0·3632	0·9944	0·4021	0·9931	0·3581
349	0·843	1·0068	0·4154	1·0077	0·3758	0·9935	0·4100	0·9925	0·3701
354	0·638	1·0079	0·4196	1·0086	0·3653	0·9920	0·4130	0·9916	0·3592
350	0·491	1·0091	0·3928	1·0092	0·3672	0·9917	0·3860	0·9911	0·3606
355	0·404	1·0085	0·4406	1·0093	0·3674	0·9912	0·4331	0·9910	0·3608
351	0·343	1·0087	0·3917	1·0096	0·3553	0·9902	0·3845	0·9907	0·3486

TENSILE TESTS ON SERIES II MATERIAL.

1.1/16 in. DIAMETER BARSTOCK.

TABLE No. A7.51

(SEE SECTION 10.8)

Ref. no. of Bar	ϵ true strain	$\bar{\dot{\epsilon}}$ ($\times 10^{-3}$ sec^{-1})	σ (tonf/in^2)	σ^* (tonf/in^2)	Ref. no. of Bar	ϵ true strain	$\bar{\dot{\epsilon}}$ ($\times 10^{-3}$ sec^{-1})	σ (tonf/in^2)	σ^* (tonf/in^2)
S1/1	0		18·5	18·5					
	0·0353		21·43	21·43					
	0·0526	2·0	24·23	24·23					
	0·0808	2·5	27·41	27·41					
	0·1070	2·3	29·42	29·42					
	0·1562	2·0	31·97	31·97					
S1/2	0		18·6	18·6					
	0·0296		20·72	20·72					
	0·0498	2·0	24·16	24·16					
	0·1005	2·1	29·22	29·22					
	0·1596	2·1	32·35	32·35					
	0·2477	3·0	35·55	35·55					
S1/3	0		18·6	18·6					
	0·0217		21·10	21·10					
	0·0498	2·0	25·93	25·93					
	0·1053	2·2	30·59	30·59					
	0·1810	2·6	33·79	33·79					
	0·2927	4·7	37·34	37·24					
S1/4	0		18·4	18·4					
	0·0274		19·98	19·98					
	0·0488	1·8	24·01	24·01					
	0·0962	1·9	28·96	28·96					
	0·1519	1·9	32·08	32·08					
	0·2255	1·5	34·66	34·66					
S1/5	0		17·7	17·7					
	0·0265		20·01	20·01					
	0·0507	2·0	24·11	24·11					
	0·1061	2·0	29·32	29·32					
	0·1733	2·2	32·51	32·51					
	0·2183	1·9	34·00	34·00					
O1/2	0		18·3	18·3					
	0·0334		21·31	21·31					
	0·0497	1·8	24·07	24·07					
	0·0998	2·0	29·10	29·10					
	0·1604	2·0	32·27	32·27					
	0·2343	1·6	34·73	34·73					

TENSILE TESTS ON SERIES II MATERIAL.

1.1/8 in. DIAMETER BARSTOCK.

TABLE No. A7.52

(SEE SECTION 10.8)

Ref. no. of Bar	ϵ true strain	$\bar{\dot{\epsilon}}$ ($\times 10^{-3}$ sec^{-1})	σ (tonf/in^2)	σ^{*} (tonf/in^2)
S2/1	0		19·7	19·7
	0·0246		20·97	20·97
	0·0478	1·9	25·69	25·69
	0·1070	2·0	31·80	31·80
	0·1707	2·1	35·00	35·00
	0·2159	1·5	36·60	36·60
	0·3192	2·0	39·74	39·56
S2/2	0		20·1	20·1
	0·0246		21·20	21·20
	0·0411	1·8	25·08	25·08
	0·0988	2·1	31·65	31·65
	0·1562	2·0	34·83	34·83
	0·2175	1·9	37·22	37·22
	0·3163	2·2	40·20	40·03
S2/3	0		19·4	19·4
	0·0236		20·98	20·98
	0·0488	1·9	26·16	26·16
	0·1031	2·1	31·83	31·83
	0·1596	2·1	34·86	34·86
	0·2586	3·0	38·51	38·45
	0·3236	5·6	40·81	40·61
S2/4	0		19·8	19·8
	0·0246		20·90	20·90
	0·0478	1·7	26·15	26·15
	0·1005	2·1	31·76	31·76
	0·1614	2·1	35·00	35·00
	0·2247	2·3	37·42	37·42
	0·3127	2·1	40·18	40·03
S2/5	0		19·7	19·7
	0·0255		21·09	21·09
	0·0488	1·8	26·11	26·11
	0·1053	2·1	31·82	31·82
	0·1631	2·1	34·92	34·92
	0·2207	2·0	37·00	37·00
	0·3142	2·0	39·79	39·63

Ref. no. of Bar	ϵ true strain	$\bar{\dot{\epsilon}}$ ($\times 10^{-3}$ sec^{-1})	σ (tonf/in^2)	σ^{*} (tonf/in^2)
02/1	0		19·7	19·7
	0·0247		21·13	21·13
	0·0459	1·9	25·77	25·77
	0·1008	2·1	31·75	31·75
	0·1604	2·0	35·05	35·05
	0·2367	2·1	37·80	37·80
	0·3214	2·0	40·31	40·12
02/2	0		19·4	19·4
	0·0236		20·80	20·80
	0·0468	1·9	25·54	25·54
	0·1005	2·0	31·46	31·46
	0·1501	1·9	34·25	34·25
	0·1997	2·0	36·34	36·34
	0·2646	2·3	38·54	38·54
	0·3170	1·7	39·89	39·71
02/3	0		19·5	19·5
	0·0227		20·94	20·94
	0·0497	1·9	26·35	26·35
	0·1008	2·0	31·68	31·68
	0·1604	2·0	34·94	39·94
	0·2437	2·2	37·85	37·85
	0·3206	2·0	40·04	39·85
02/4	0		19·9	19·9
	0·0227		20·94	20·94
	0·0440	1·9	25·68	25·68
	0·1017	2·0	32·06	32·06
	0·1579	2·0	35·11	35·11
	0·2311	2·0	37·80	37·80
	0·3141	1·8	40·23	40·06
02/5	0		19·3	19·3
	0·0257		21·46	21·46
	0·0497	1·8	26·27	26·27
	0·1008	2·0	31·73	31·73
	0·1664	2·0	35·19	35·19
	0·2351	2·2	37·58	37·58
	0·3228	1·9	40·01	39·82

TENSILE TESTS ON SERIES II MATERIAL. TABLE No. A7.53

1.3/16 in. DIAMETER BARSTOCK. (SEE SECTION 10.8)

Ref. no. of Bar	ε true strain	$\bar{\dot{\varepsilon}}$ ($\times 10^{-3}$ sec^{-1})	σ (tonf/in^2)	σ^* (tonf/in^2)
S3/1	0		18.9	18.9
	0.0306		21.62	21.62
	0.0449	2.1	24.32	24.32
	0.1023	2.1	30.31	30.31
	0.1810	2.1	34.08	34.08
	0.2722	1.5	36.88	36.80
	0.7262	–	48.36	44.77
S3/2	0		18.6	18.6
	0.0306		21.15	21.15
	0.0536	2.1	25.01	25.01
	0.1105	2.1	30.35	30.35
	0.2037	2.6	34.12	34.12
	0.2896	2.6	36.71	36.59
	0.3941	1.7	39.27	38.75
	0.4311	3.0	40.47	39.74
S3/3	0		17.7	17.7
	0.0296		20.67	20.67
	0.0526	2.1	24.52	24.52
	0.1053	2.2	29.39	29.39
	0.2021	2.6	33.61	33.61
	0.2776	2.9	36.01	35.92
	0.3888	1.1	38.63	38.15
S3/4	0		19.0	19.0
	0.0208		20.48	20.48
	0.0449	2.2	24.78	24.78
	0.1031	2.3	30.31	30.31
	0.2151	2.9	34.92	34.92
	0.2798	3.6	36.90	36.80
	0.3853	1.5	39.52	39.04
S3/5	0		19.0	19.0
	0.0246		20.54	20.54
	0.0459	1.8	24.80	24.80
	0.0948	2.1	30.02	30.02
	0.1733	2.1	33.95	33.95
	0.2791	1.8	37.14	37.04
	0.3988	1.5	40.37	39.80

Ref. no. of Bar	ε true strain	$\bar{\dot{\varepsilon}}$ ($\times 10^{-3}$ sec^{-1})	σ (tonf/in^2)	σ^* (tonf/in^2)
03/1	0		18.2	18.2
	0.0276		20.61	20.61
	0.0526	2.1	24.96	24.96
	0.1062	2.1	30.10	30.10
	0.1840	2.2	33.73	33.73
	0.2912	2.3	37.05	36.96
	0.3893	0.8	39.40	38.92
03/2	0		18.4	18.4
	0.0237		20.02	20.02
	0.0497	1.9	24.86	24.86
	0.1053	2.1	30.09	30.09
	0.1756	2.1	33.27	33.27
	0.2738	1.7	36.35	36.30
	0.3954	1.7	39.56	39.04
03/3	0		19.4	19.4
	0.0169		20.45	20.45
	0.0497	2.1	26.28	26.28
	0.1035	2.1	30.96	30.96
	0.1798	2.2	34.18	34.18
	0.3988	3.3	39.80	39.26
03/4	0		17.9	17.9
	0.0257		20.09	20.09
	0.0469	1.9	24.06	24.06
	0.1035	2.1	29.70	29.70
	0.1748	2.2	33.18	33.18
	0.2761	1.9	36.38	36.31
	0.3947	1.8	39.47	38.96
03/5	0		17.8	17.8
	0.0247		20.06	20.06
	0.0507	2.0	24.62	24.62
	0.1053	2.1	29.63	29.63
	0.1740	2.2	32.83	32.83
	0.2776	1.9	36.06	36.00
	0.3947	2.2	39.06	38.55
03/6	0		17.6	17.6
	0.0257		20.10	20.10
	0.0478	2.0	24.10	24.10
	0.1017	2.0	29.24	29.24
	0.1790	2.1	32.89	32.89
	0.2807	1.9	35.94	35.87
	0.3994	2.2	39.09	38.56

TENSILE TESTS ON SERIES II MATERIAL. 1.1/4 in. DIAMETER BARSTOCK.

TABLE No. A7.54 (SEE SECTION 10.8)

Ref. no. of Bar	ϵ true strain	$\bar{\dot{\epsilon}}$ ($\times 10^{-3}$ sec^{-1})	σ (tonf/in^2)	σ^* (tonf/in^2)
S4/1	0		22.9	22.9
	0.0198		24.42	24.42
	0.0468	2.0	29.41	29.41
	0.1096	2.4	34.55	34.55
	0.2509	5.5	39.76	39.76
	0.3548	2.1	42.49	42.14
	0.4860	0.5	45.90	44.64
S4/2	0		19.3	19.3
	0.0255		22.03	22.03
	0.0449	1.9	25.92	25.92
	0.1023	2.1	32.03	32.03
	0.1614	1.7	35.04	35.04
	0.2624	2.1	38.54	38.47
	0.3548	1.5	41.10	40.76
	0.4898	2.1	45.02	43.74
S4/3	0		19.3	19.3
	0.0246		21.60	21.60
	0.0459	1.9	25.95	25.95
	0.1014	2.0	32.01	32.01
	0.1614	1.7	35.13	35.13
	0.2586	1.6	38.51	38.45
	0.3591	1.8	41.32	40.96
	0.4977	2.4	45.29	43.95
S4/4	0		21.2	21.2
	0.0185		22.73	22.73
	0.0440	1.9	28.08	28.08
	0.1005	2.1	33.46	33.46
	0.1725	2.4	36.71	36.71
	0.2691	3.0	39.92	39.84
	0.3514	1.5	42.09	41.76
	0.4910	1.8	45.99	44.68
S4/5	0		21.3	21.3
	0.0198		22.76	22.76
	0.0459	1.9	28.13	28.13
	0.1023	2.1	33.32	33.32
	0.1631	2.1	36.09	36.09
	0.2744	2.5	39.80	39.71
	0.3584	2.6	41.87	41.50
	0.4977	2.0	46.09	44.74

Ref. no. of Bar	ϵ true strain	$\bar{\dot{\epsilon}}$ ($\times 10^{-3}$ sec^{-1})	σ (tonf/in^2)	σ^* (tonf/in^2)
04/1	0		21.4	21.4
	0.0188		23.14	23.14
	0.0469	1.9	28.54	28.54
	0.1089	2.2	33.89	33.89
	0.1647	2.2	36.33	36.33
	0.2662	2.5	39.54	39.54
	0.3556	1.5	41.94	41.60
	0.4929	2.3	45.83	44.52
04/2	0		19.5	19.5
	0.0218		21.62	21.62
	0.0488	1.9	26.89	26.89
	0.0998	2.0	31.94	31.94
	0.1621	1.5	35.07	35.07
	0.2662	1.6	38.44	38.44
	0.3653	1.6	41.28	40.90
	0.5020	2.6	45.15	43.77
04/3	0		20.2	20.2
	0.0257		22.10	22.10
	0.0450	1.9	26.15	26.15
	0.0935	1.8	31.63	31.63
	0.1873	2.1	35.83	35.83
	0.2647	2.2	38.39	38.39
	0.3941	1.8	41.85	41.31
04/4	0		22.9	22.9
	0.0198		24.44	24.44
	0.0469	1.9	29.44	29.44
	0.1062	2.2	34.36	34.36
	0.1980	2.8	37.96	37.96
	0.2731	3.8	40.29	40.29
	0.3612	2.0	42.68	42.30
	0.4935	2.0	46.29	44.96
04/5	0		20.2	20.2
	0.0198		21.89	21.89
	0.0488	1.8	27.74	27.74
	0.1026	2.1	32.74	32.74
	0.1622	1.7	35.53	35.53
	0.2677	2.1	39.06	39.06
	0.3598	1.8	41.65	41.28
	0.4935	1.9	45.43	44.13

TENSILE TESTS ON SERIES II MATERIAL.

1.5/16 in. DIAMETER BARSTOCK.

TABLE No. A7.55

(SEE SECTION 10.3)

Ref. No. of Bar	ϵ true strain	$\bar{\dot{\epsilon}}$ ($\times 10^{-3}\,sec^{-1}$)	σ ($tonf/in^2$)	σ^* ($tonf/in^2$)	Ref. No. of Bar	ϵ true strain	$\bar{\dot{\epsilon}}$ ($\times 10^{-3}\,sec^{-1}$)	σ ($tonf/in^2$)	σ^* ($tonf/in^2$)
S5/1	0		21.2	21.2	05/1	0		23.8	23.8
	0.0217		22.91	22.91		0.0218		25.87	25.87
	0.0421	2.0	26.49	26.49		0.0545	1.9	30.50	30.50
	0.1070	2.4	31.54	31.54		0.1142	2.4	33.72	33.72
	0.1766	2.8	34.15	34.15		0.2054	2.7	36.17	36.17
	0.2882	2.5	37.18	37.06		0.2919	2.5	38.34	38.24
	0.3975	2.9	40.14	39.59		0.4068	1.8	?	?
	0.5510	2.7	43.97	42.24		0.5545	1.7	44.96	43.17
S5/2	0		21.4	21.4	05/2	0		23.6	23.6
	0.0185		22.77	22.77		0.0218		25.85	25.85
	0.0430	1.7	27.22	27.22		0.0488	1.8	29.86	29.86
	0.1257	2.8	32.27	32.27		0.1115	2.4	33.24	33.24
	0.1855	2.5	34.25	34.25		0.1823	2.1	35.44	35.44
	0.2752	1.3	36.41	36.33		0.2829	2.2	38.00	37.92
	0.4016	2.0	39.74	39.22		0.4021	2.0	41.03	40.46
	0.5532	1.7	43.57	41.84		0.5625	2.5	45.17	43.30
S5/3	0		19.5	19.5	05/3	0		23.8	23.8
	0.0274		21.46	21.46		0.0198		25.82	25.82
	0.0478	1.9	25.12	25.12		0.0507	1.9	30.48	30.48
	0.0979	2.0	29.53	29.53		0.1213	2.7	33.93	33.93
	0.1818	1.4	32.67	32.67		0.2111	2.7	36.56	36.56
	0.2896	1.0	35.80	35.69		0.2859	2.0	38.34	38.26
	0.4061	2.3	39.00	38.45		0.4081	2.0	41.52	40.90
	0.5515	2.5	42.66	40.98		0.5630	2.1	45.50	43.61
S5/4	0		20.8	20.8	05/4	0		23.3	23.3
	0.0236		22.88	22.88		0.0237		25.55	25.55
	0.0449	1.9	26.50	26.50		0.0459	2.0	28.87	28.87
	0.1031	2.2	31.04	31.04		0.1080	2.4	32.77	32.77
	0.1757	2.1	33.74	33.74		0.1972	2.6	35.56	35.56
	0.2942	1.6	36.82	36.70		0.2769	1.9	37.53	37.46
	0.4036	2.5	39.87	39.32		0.4061	2.1	40.94	40.34
	0.5545	1.7	43.63	41.93		0.5647	2.3	44.94	43.06
S5/5	0		19.6	19.6					
	0.0274		22.22	22.22					
	0.0468	2.0	25.39	25.39					
	0.0997	2.0	30.08	30.08					
	0.1801	1.9	33.28	33.28					
	0.2859	1.5	36.32	36.21					
	0.4081	2.3	39.59	39.02					
	0.5487	2.0	43.24	41.56					

CALIBRATION OF NEEDLE VALVE

(SEE APPENDIX 2)

TABLE No. A7.56

Setting of Relief Valve (lbf/in^2)	Setting of Needle Valve (no. of turns open)	Speed of Ram (ft/min)	Setting of Relief Valve (lbf/in^2)	Setting of Needle Valve (no. of turns open)	Speed of Ram (ft/min)
100	1	0·23	100	½	0·04
	2	0·86		1½	0·41
	3	1·41	200	1½	0·95
	4	1·89		½	0·07
200	4	3·30	400	½	0·22
	3	2·39		1½	1·70
	2	1·52	600	1½	2·23
	1	0·45		½	0·38
300	1	0·78	800	½	0·66
	2	2·06		1	1·76
	3	3·05		1½	2·73
	4	4·13	1,000	1½	3·15
400	4	4·91		1	2·08
	3	3·69		½	0·83
	2	2·45	1,200	½	1·00
	1	1·01		1	2·24
600	1	1·49		1½	3·48
	2	3·07			
	3	4·64			
	4	5·02			
800	3	4·88			
	2	3·67			
	1	1·78			
1,000	1	2·06			
	2	4·08			
	3	4·81			

APPENDIX 8

Change in Die-Pressure due to Die-Rotation

It is necessary for the satisfactory usage of the rotating-die technique that the relevant parameters, die-pressure and shear stress, be not significantly changed from their non-rotational values by the introduction of die-rotation. Several mechanisms have been suggested by which die-rotation could alter those parameters, but although it was not found to be possible to make quantitative assessments of their effects, it was argued that they would be either insignificant or separable by suitable selection of the experimental data (Section 10.6.4). One possibility which was considered and dismissed as having negligible influence (page 109), was that the die-pressure necessary to maintain yielding might be different under the stress system with die-rotation to that without rotation. This mechanism was originally thought of as having a purely local effect in that die-rotation, by virtue of its introduction of a shear stress into the circumferential direction at the surface of the die, caused a rotation of the principal axes, and only the slight reduction of die-pressure which could be expected to accompany that rotation was considered.

However, subsequently to the completion of the main body of this thesis it was realised that die-rotation would also have a macroscopic effect on the stress system, arising from the reduction of drawing force. As drawn bar deforms under the combined influence of the tensile drawing stress and compressive die-pressure, a reduction in the former should be accompanied by an increase in the latter. Although the arguments already presented (Section 10.6.4) suggest that this effect will not be large, it is clear that as die-rotation caused reductions of drawing force of up to 25%, it could nevertheless be significant.

In the following evaluation of the magnitude of the effect, the prefix δ denotes a disturbance of a quantity resulting from the change in die-pressure. Typical values of non-rotational drawing force P, and coefficient of friction μ_T are listed in Table A8.1. Values of P_F/P were calculated from Equation 2.8, which also led indirectly to the mean die-preesure, $\bar{\sigma}$, using the additional relationships

$$\bar{\sigma} = Q/A_s \quad \text{and} \quad Q = P_O \sin\alpha$$

The maximum reduction in drawing force due to die-rotation occurs at $\theta = 90^{o}$, and is given by P_F. The accompanying disturbance in the drawing stress, $\hat{\delta p}$, was derived by assuming that the longitudinal stress is always uniformly distributed across the cross-section. This assumption is used in the equilibrium theory of drawing (Section 2.1.2), and if the model of yielding behaviour assumed in that theory is also adopted here, then the associated disturbance of die-pressure, $\hat{\delta\sigma}$, follows directly.

$$\hat{\delta\sigma} = -\hat{\delta p}$$

This value of $\hat{\delta\sigma}$ relates only to the die-exit section, where the full reduction of longitudinal stress occurs, and $\hat{\delta\sigma}$ will in fact fall monotonically to zero at die-entry. If the decrease is assumed linear with longitudinal distance, then the mean disturbance $\bar{\delta\sigma}$ may be calculated from

$$\bar{\delta\sigma} = \hat{\delta\sigma}.\frac{(d_2+2d_1)}{3(d_2+d_1)}$$

where $\bar{\delta\sigma}$ is defined as $\delta Q/A_s$. The deviation of this value from $\hat{\delta\sigma}/2$ is small and arises from the change in diameter through the die.

If Coulomb friction obtains, then

$$\text{Torque}(T) \propto \bar{\sigma}$$

and as $$P_{F(T)}/P \propto T$$

the effect of the increase in die-pressure on $P_{F(T)}/P$ is proportional to $\bar{\delta\sigma}$. To a first approximation $\mu_T \propto P_{F(T)}/P$ (from Equation 2.8), and the error $\delta\mu_T$, introduced into the calculation of μ_T may therefore be calculated from

$$\delta\mu_T/\mu_T \doteq \bar{\delta\sigma}/\bar{\sigma}$$

It will be recalled that the values given for $\hat{\delta p}$ and $\bar{\delta\sigma}$ relate to $\theta = 90^{o}$, and although this condition, which produces the greatest disturbance of die-pressure, may also be intuitively supposed to give the greatest disturbance of $P_{F(T)}/P$ and μ_T, this is not necessarily the case. The condition for this situation is that $\delta T/T$ should be a maximum. To confirm that this does occur at $\theta = 90^{o}$ it is noted that

$$\begin{aligned}\delta\sigma &= -\delta p \\ &\propto P-P_R\end{aligned}$$

The approximate analysis of Section 3.1 shows that

$$P-P_R \propto 1-\cos\theta$$

and $$T \propto \sin\theta \ .$$

Then $$\delta T/T \propto (1-\cos\theta)/\sin\theta$$

and in the range $0 \leq \theta \leq 90^{\circ}$ the maximum value does occur at $\theta = 90^{\circ}$, and $\delta T/T \rightarrow 0$ as $\theta \rightarrow 0^{\circ}$. Thus the effect of the increase in die-pressure is to produce overestimates of μ_T which vary from zero at $\theta = 0$ up to $\bar{\delta\sigma}/\bar{\sigma}$ at $\theta = 90^{\circ}$, and on this basis the corrected values of μ_T have been listed in Table A8.1.

As evaluation of μ from measurements of reduction in drawing force has already been discarded as unreliable, the effect of the change in die-pressure on μ_P has not been considered, except to note that whereas an increase in die-pressure leads to overestimates of μ_T, it causes $P_{F(P)}/P$ and μ_P to be underestimated. The mechanism discussed in this Appendix cannot therefore be used to explain either the behaviour of the torque parameter at the onset of die-rotation (Section 10.6.4) or the unrealistically high values of $P_{F(P)}/P$ calculated at low values of θ (Section 10.7.6).

Although the analysis presented here is based on several questionable assumptions, it shows that the consequences of the change in die-pressure caused by die-rotation are not serious for the calculation of μ_T, particularly at low values of θ, but that the effect is significant in relation to the method suggested for deduction of distribution of shear stress. As allowance for the effect must utilise either some theoretical model as here, or an independent method of measuring die-pressure with and without die-rotation, this must finally destroy any hope that distribution of shear stress could be deduced by the rotating-die technique.

LUBRICANT	DIAMETER OF BAR (in)	P (tonf)	μ_T	P_F/P	$\bar{\sigma}$ (tonf/in^2)	$\hat{\delta}_P$ (tonf/in^2)	$\bar{\delta}_\sigma$ (tonf/in^2)	$\bar{\delta}_\sigma/\bar{\sigma}$ (%)	μ_T (corrected values from Table 10.7)
SOAP	1.1/16	4·8	0·032	0·206	41·7	1·3	0·64	1·5	0·030/0·034
	1.1/8	8·3	0·023	0·158	34·2	1·7	0·83	2·4	0·020/0·023
	1.3/16	11·4	0·023	0·158	29·9	2·3	1·12	3·7	0·021/0·025
	1.1/4	16·0	0·023	0·158	31·1	3·2	1·54	5·0	0·020/0·026
	1.5/16	18·8	0·023	0·158	28·0	3·8	1·81	6·5	0·020/0·025
OIL	1.1/16	5·9	0·070	0·363	41·3	2·5	1·24	3·0	0·066/0·072
	1.1/8	9·5	0·050	0·289	33·0	3·5	1·72	5·2	0·041/0·048
	1.3/16	13·3	0·050	0·289	29·5	4·9	2·38	8·1	0·050/0·058
	1.1/4	18·2	0·050	0·289	29·5	6·7	3·23	11·0	0·045/0·054
	1.5/16	21·5	0·050	0·289	27·0	7·9	3·77	14·0	0·040/0·053

TABLE No. A8.1

REFERENCES

1) J.E. Hockett : Int. J. Mech. Sci. 1967, 9, 233-236
2) J.G. Wistreich : Met. Rev. 1958, 3, (10), 97-142.
3) G.D.S. MacLellan : J. Iron Steel Inst. 1948, 158, 347-356.
4) W. Johnson and R. Sowerby : Wire Ind. 1969, 36, 137-144, 249-256.
5) A.P. Green : Proc. Instn. Mech. Engrs. 1960, 174 (31), 847-864
6) E. Siebel : Stahl u. Eisen, 1947, 66/67, 171-180. B.I.S.I.T.S. 334
7) O. Pawelski : Arch. f. d. Eisenh. 1961, 32, 513-520. B.I.S.I.T.S. 2499
8) G. Sachs and K.R. Van Horn : 'Practical Metallurgy', A.S.M. 1940
9) G. Sachs : Z. ang. Math. Mech. 1927, 7, (3), 235-236
10) E.A. Davis and S.J. Dokos : J. Appl. Mech. 1944, 11, A193-A198
11) A.G. Atkins and R.M. Caddell : Int. J. Mech. Sci. 1968, 10, 15-28
12) F. Körber and A. Eichinger : Mitt. K.W.I. Eisenf. 1940, 22, (5), 57-79
13) R. Hill : 'Mathematical Theory of Plasticity', O.U.P. 1950
14) J. Halling : Engineer, 1959, 207, 250-254
15) W. Prager : Trans. Roy. Inst. Tech. Stockholm, 1953, no. 65
16) R. Hill and S.J. Tupper : J. Iron Steel Inst. 1948, 159, 353-359
17) J.G. Wistreich : Proc. Instn. Mech. Engrs. 1955, 169, 654-665
18) A.P. Green and R. Hill : J. Mech. Phys. Solids, 1952, 1, 31-36
19) R.T. Shield : Proc. Roy. Soc. A. 233, 267-287
20) Z. Mróz : Z. ang. Math. Phys. 1967, 18, (2), 219-236
21) O. Richmond and H.L. Morrison : J. Mech. Phys. Solids, 1967, 15, 195-203
22) R. Hill : J. Mech. Phys. Solids, 1967, 15, 223-227
23) W. Johnson and P.B. Mellor : 'Plasticity for Mechanical Engineers', Van Norstrand, 1962
24) E.G. Thomsen, C.T. Yang and S. Kobayashi : 'Mechanics of Plastic Deformation in Metal Processing', Macmillan, 1965
25) B. Avitzur : 'Metal Forming : Processes and Analysis', McGraw-Hill, 1968
26) P. Oxley : Int. J. Mech. Sci. 1963, 5, 183-184
27) I.F. Collins : J. Mech. Phys. Solids, 1969, 17, 323-338
28) R.T. Shield : J. Mech. Phys. Solids, 1955, 3, 246-258
29) H. Ford and J.M. Alexander : 'Advanced Mechanics of Materials', Longmans, 1963

30) P.J. Thompson : University of Aston in Birmingham, M.Sc. thesis 196
31) P.W. Whitton : J. Inst. Met. 1957/8, 86, 417-421
32) W.M. Mair : J. Strain Anal. 1967, 2, (3), 188-195
33) A.G. Atkins : J. Inst. Met. 1969, 97, 289-298
34) R.W. Johnson and G.W. Rowe : J. Inst. Met. 1968, 96, 97-105. Discussion. ibid 383-384
35) R.M. Caddell and A.G. Atkins : Trans. A.S.M.E. 1968, B90, (2), 411-419
36) G.D.S. MacLellan : J. Inst. Met. 1952/3, 81, 1-13
37) C.T. Yang : Trans. A.S.M.E. 1961, B83, 523-530
38) G.W. Rowe: 'Principles of Metalworking', Edward Arnold, 1965
39) A.F. Gerds and F.W. Boulger : 'Metal Deformation Processing II', 1966, D.M.I.C. Rep.no. 226, 78-124
40) Summary by J.M. Capus : J. Inst. Met. 1966, 94, 429-432
41) F.P. Bowden and D. Tabor : 'The Friction and Lubrication of Metals', Part I 1954, Part II 1964, O.U.P.
42) A.S. Akhmatov : 'Molecular Physics of Boundary Friction', Israel Programme for Translations 1966
43) P.R. Lancaster and G.W. Rowe : Wear 1958/9, 2 , 428-437
44) P.R. Lancaster and G.W. Rowe : Proc. Instn. Mech. Engrs. 1963/4, 178, (3), 69-89
45) M.S. Shaw, W.H. Stableford and D.H. Sansome : Int. J. Mach. Tool Des. Res. 1970, 10, -
46) W.A. Glaeser : 'Metal Deformation Processing II', 1966, D.M.I.C. Rep. no. 226, 67-77
47) R.L. Jentgen : 'Metal Formation Processing III', 1967, D.M.I.C. Rep. no. 243, 74-103
48) M.C. Shaw : Wear, 1963, 6, 140-158
49) F.F. Ling and M.B. Peterson : 'Conference on Manufacturing Technology' 1967, 1181-1192
50) D.G. Christopherson and H. Naylor : Proc. Instn. Mech. Engrs. 1955, 169, 643-653
51) W. Schroeder and D.A. Webster : J. Appl. Mech. 1949, 16, 289-294

52) R. Hill : Phil. Mag. 1950, 41, 733
53) A.T. Male and M.G. Cockroft : J. Inst. Met. 1964, 93, 38-46
54) A.T. Male : J. Inst. Met. 1966, 94, 121-125
55) A. Shutt : Int. J. Mech. Sci. 1966, 8, 509-511
56) V.F. Verschchagin, V.A. Shapochkin and Ye. V. Zubova : Phys. Met. Metallog. 1960, 10, (1), 123-126
57) P.W. Bridgeman : 'Studies in Large Plastic Flow and Fracture', McGraw-Hill, 1952
58) J. Boyd and B.P. Robertson : Trans. A.S.M.E. 1945, 67, 51
59) R. Lauterbach, F. Lira and E.G. Thomsen : Wear, 1967, 10, (6), 469-482
60) M.C. Shaw, A. Ber and P.A. Mamin : Trans. A.S.M.E. 1960, D82, (2), 342-346
61) G.W. Pearsall and W.A. Backofen : Trans. A.S.M.E. 1963, B85, 68-76
62) H.G. Baron and F.C. Thompson : J. Inst. Met. 1950, 78, 415-462
63) W. Lueg and K.H. Treptow : Stahl u. Eisen, 1952, 72, 399-412
64) H. Kuntze and A. Pomp : Stahl u. Eisen, 1954, 74, 1325-1334
65) W. Lueg and K.H. Treptow : Stahl u. Eisen, 1956, 76, 1107-1116
66) A.F. Gerds and C.B. Ogle : Wire Wire Prod. 1963, 38, 1696-1700, 1755-1756
67) O. Pawelski and W. Lueg : Stahl u. Eisen, 1961, 81, 1729-1739. B.I.S.I.T.S. 2894
68) T.A. Trozera : Trans. A.S.M. 1964, 57, 309-323
69) W. Evans and B. Avitzur : Trans. A.S.M.E. 1968, F90, 72-80
70) O. Pawelski and O. Armstroff : Archiv. f.d. Eisenh. 1967, 38, (12), 899-904
71) J. Wells : M. Sc. Thesis, University of Leeds, 1962
72) R.W. Lunt and G.D.S. MacLellan : J. Inst. Met. 1946, 72, 65
73) Likhtman, Shchukin and Rebinder : Israel Programme for Scientific Translations, Oldbourne Press, 1964
74) H.C. Rogers and L.F. Coffin : 'Conference on Manufacturing Technology', 1967, 1137-1156
75) O. Pawelski : Stahl u. Eisen, 1964, 84, 1233-1243, B.I.S.I.T.S. 4095

76) H. Majors : Trans. A.S.M.E. 1955, 78, 79-87

77) T.Z. Blazynski and I.M. Cole : Proc. Instn. Mech. Engrs. 1960, 174, (28), 797-812

78) Applied Mechanics Reviews, 1966, p. 213

79) Kanaev and Ya Veiler : Sov. Phys. Doklady, 1964, 9, (6), 495-497

80) B. Kenny : J. Strain. Anal. 1967, 2, (2), 134-136

81) G.G. Moore and J.F. Wallace : J. Mech. Eng. Sci. 1965, 7, (3), 279-282

82) W. Linicus and G. Sachs : Mitt. Dt. Mater. Anst. 'Spanlose Formung der Metalle', 1931, 16, 38-67

83) H. Greenwood and F.C. Thompson : Nature, 1931, 128, (3221), p. 152

84) E.L. Francis, H. Greenwood and F.C. Thompson : Carnegie Schol. Mem. I.S.I. 1933, 22, 15-30

85) C.O. von Hofsten and E. Lindstrand : Jernkont. Ann. 1958, 142, (3), 128-164. B.I.S.I.T.S. 1331

86) A.R. Goreham and S. Harper : Private communication

87) K.D. Lietzmann and K.R. Eichner : Neve Hütte, 1969, 14, (8), 458-463

88) T. Nishihara, M. Kakuzen and H. Nakamura : Tech. Rep. Eng. Inst. Kyoto Univ. 1955, 5, Rep. no. 22, 75

89) D. Rothman and D.H. Sansome : Int. J. Mach. Tool Des. Res. 1970 10, 179-192

90) P.M. Cook and J.G. Wistreich : Brit. J. Appl. Physics, 1952, 3, 159-165

91) Ohashi and Nishikiori : Exp. Mech. 1966, 6, 171-176

92) Veys : Ph.D.Thesis, University of Sheffield, 1961

93) I. Gokyu, T. Kishi and T. Ninomiya : Nippon Kink. Gakk. 1967, 31, (1), 83-89

94) O. Pawelski and O. Armstroff : Archiv. f.d. Eisenh. 1967, 38, (7), 527-534

95) P.W. Bridgman : Trans. A.S.M. 1944, 32, 553-574

96) N.N. Davidenkov and N.I. Spiridonova : Proc. A.S.T.M. 1946, 46, 1147-1158

97) B.O. Peirce and R.M. Foster : 'A Short Table of Integrals', Blaisdell, 1956

98) B.S. 1134, 1961 : 'Centre-Line-Average Height Method for Assessment of Surface Texture'

99) C.C. Perry and H.R. Lissner : 'The Strain Gauge Primer', McGraw-Hill

100) R.C. Brewer and J.M. Alexander : J. Mech. Phys. Solids, 1960, 8, 76-78